

Conceptual Model Report: Minor Aquifers in Llano Uplift Region of Texas



Report By:

Jianyou (Jerry) Shi, Ph.D., P.G.

Radu Boghici, P.G.

William Kohlrenken

and

William Hutchison, Ph.D., P.E., P. G.

Independent Groundwater Consultant

Texas Water Development Board

P.O. Box 13231

Austin, Texas 78711-3231

March 7, 2016

03/07/2016

3/7/2016

3/7/16

3/7/16

3/7/16

This document is released under the authority of Jianyou (Jerry) Shi, P.G. 11113, Radu Boghici, P.G. 482, William Hutchison, P.E. 96287, P.G. 286, and Cynthia Ridgeway, P.G. 471 on March 7, 2016.

This page is intentionally blank.

Table of Contents

EXECUTIVE SUMMARY:	1
1.0 INTRODUCTION	3
2.0 STUDY AREA	8
2.1 PHYSIOGRAPHY AND CLIMATE	16
2.2 GEOLOGY	36
2.2.1. <i>Structural Setting</i>	36
2.2.2. <i>Geologic History</i>	36
2.2.3. <i>Structure and Texture</i>	47
2.2.4. <i>Surface Geology</i>	48
3.0 PREVIOUS INVESTIGATIONS	57
3.1 RECONNAISSANCE INVESTIGATIONS	57
3.2 MULTIPLE COUNTY STUDIES	57
3.3 SINGLE COUNTY STUDIES	61
3.4 LOCAL STUDIES	65
3.5 GROUNDWATER FLOW MODELING STUDIES	65
4.0 HYDROLOGIC SETTING	69
4.1 HYDROSTRATIGRAPHY	69
4.1.1. <i>Hydrostratigraphic Layer Structure</i>	69
4.2. GROUNDWATER LEVELS AND FLOWS	87
4.2.1. <i>Distribution of Water Level Measurements</i>	87
4.2.2. <i>Pre-development Water Levels</i>	87
4.2.3. <i>Post-development Water Levels</i>	88
4.2.4. <i>Transient Water-Level Data (Hydrographs)</i>	89
4.3 RECHARGE	110
4.4 RIVERS, STREAMS, LAKES, AND SPRINGS	130
4.4.1. <i>Gain or Loss of Rivers and Streams</i>	130
4.4.2. <i>Lakes and Reservoirs</i>	131
4.4.3. <i>Springs</i>	132
4.5 HYDRAULIC PROPERTIES	150
4.5.1 <i>Transmissivity and Hydraulic Conductivity</i>	152
4.5.2 <i>Storativity, Specific Storage, and Specific Yield</i>	153
4.6 AQUIFER DISCHARGE	169
4.6.1. <i>Evapotranspiration</i>	169
4.6.2. <i>Aquifer Discharge through Pumping</i>	170
4.7 GROUNDWATER QUALITY	184

4.7.1	<i>Marble Falls Aquifer</i>	184
4.7.2	<i>Ellenburger-San Saba Aquifer</i>	185
4.7.3	<i>Hickory Aquifer</i>	186
5.0	CONCEPTUAL GROUNDWATER FLOW MODEL FOR THE LLANO UPLIFT MINOR AQUIFERS	212
5.1	PRE-DEVELOPMENT CONDITIONS (STEADY STATE)	213
5.2	POST-DEVELOPMENT CONDITIONS (TRANSIENT STATE)	214
5.3	IMPLEMENTATION OF GROUNDWATER RECHARGE AND FAULTS	215
6.0	FUTURE IMPROVEMENTS	218
	ACKNOWLEDGEMENTS	219
	REFERENCES	220
	APPENDIX A	229

List of Figures and Tables

Figure 1.0.1	Location of major aquifers in Texas (revised from TWDB, 2013a).....	5
Figure 1.0.2	Location of minor aquifers in Texas (revised from TWDB, 2013b).	6
Figure 1.0.3	Location of minor aquifers in Llano Uplift region (based on TWDB (2013b)) ...	7
Figure 2.0.1	Locations of highways, cities, and towns in Llano Uplift region (based on Texas Natural Resources Information System datasets (TNRIS, 2014)).....	9
Figure 2.0.2	Locations of river basins and surface water bodies in Llano Uplift region (based on Texas Natural Resources Information System datasets (TNRIS, 2014)).	10
Figure 2.0.3	Texas River Authorities in study area (based on TWDB (2013c)).	11
Figure 2.0.4	Texas Regional Water Planning Areas in study area (labelled by letters) (based on TWDB (2013d)).	12
Figure 2.0.5	Texas Groundwater Conservation Districts (GCDs) in study area (based on TWDB (2013e)).....	13
Figure 2.0.6	Texas Groundwater Management Areas in study area (labelled by numbers) (based on TWDB (2013f)).....	14
Figure 2.0.7	Texas Priority Groundwater Management Areas in study area (based on TWDB (2013g)).	15
Figure 2.1.1	Physiographic provinces in study area (Wermund, 1996)	18
Figure 2.1.2	Level III ecological regions in study area (U.S. Environmental Protection Agency, 2013).	19
Figure 2.1.3	Topographic map of study area showing land surface elevation in feet above mean sea level. Elevation data are from U.S. Geological Survey Digital Elevation Model with a resolution of 30 meters by 30 meters.	20
Figure 2.1.4	Climate classifications of study area (based on Larkin and Bomar, 1983).....	21
Figure 2.1.5	Climate classifications of study area (based on National Weather Service, 2013).	22
Figure 2.1.6	Average annual air temperature in degrees Fahrenheit for study area. Temperature data are from Parameter-elevation Regressions on Independent Slopes Model (PRISM) temperature dataset from Oregon State University (PRISM Climate Group, 2013).....	23
Figure 2.1.7	Average annual precipitation in study area for time period 1981 to 2010 from Parameter-elevation Relationships on Independent Slopes Model (PRISM) (PRISM Climate Group, 2013).....	24
Figure 2.1.8	Measured annual precipitation at stations in Blanco, Brown (Brownwood), Burnet, Coleman, and Concho (Paint Rock) counties (National Climatic Data Center, 2014).	25

Figure 2.1.9	Measured annual precipitation at stations in Gillespie (Fredericksburg), Hays (San Marcos), Kendall (Boerne), Kerr (Kerrville), and Kimble (Junction) counties (National Climatic Data Center, 2014).	26
Figure 2.1.10	Measured annual precipitation at stations in Lampasas, Llano, Mason, McCulloch (Brady), and Menard counties (National Climatic Data Center, 2014).....	27
Figure 2.1.11	Measured annual precipitation at stations in Mills (Goldthwaite), San Saba (Red Bluff Crossing), Travis (Austin), and Williamson (Jarrell) counties (National Climatic Data Center, 2014).....	28
Figure 2.1.12	Measured average monthly precipitation at stations in Blanco, Brown (Brownwood), Burnet, Coleman, and Concho (Paint Rock) counties (National Climatic Data Center, 2014).....	29
Figure 2.1.13	Measured average monthly precipitation at stations in Gillespie (Fredericksburg), Hays (San Marcos), Kendall (Boerne), Kerr (Kerrville), and Kimble (Junction) counties (National Climatic Data Center, 2014).	30
Figure 2.1.14	Measured average monthly precipitation at stations in Lampasas, Llano, Mason, McCulloch (Brady), and Menard counties (National Climatic Data Center, 2014).....	31
Figure 2.1.15	Measured average monthly precipitation at stations in Mills (Goldthwaite), San Saba (Red Bluff Crossing), Travis (Austin), and Williamson (Jarrell) counties (National Climatic Data Center, 2014).....	32
Figure 2.1.16	Average annual net pan evaporation rate (inch per year) between 1954 and 2012 at selected quadrangles in study area (TWDB, 2013h).	33
Figure 2.1.17	Average monthly lake surface evaporation between 1954 and 2012 at selected quadrangles 608, 609, 610, and 710 in study area (TWDB, 2013h).	34
Figure 2.1.18	Average monthly lake surface evaporation between 1954 and 2012 at selected quadrangles 708, 709, 808, and 809 in study area (TWDB, 2013h)	35
Figure 2.2.1	Schematic locations of major geologic structures in Llano Uplift region and surrounding areas. Surface geology of Llano Uplift region is based on Geologic Atlas of Texas (Bureau of Economic Geology, 2013).	49
Figure 2.2.2	Schematic cross section of major geologic structure in Llano Uplift region and surrounding areas (Standen and Ruggiero, 2007).	50
Figure 2.2.3	Location of major geologic structures in Llano Uplift region and surrounding areas (arches are after Ewing, 2004; Fredericksburg High is after Bluntzer, 1992).....	51
Figure 2.2.4	Simplified Surface geology of Llano Uplift region and surrounding areas (Bureau of Economic Geology, 2013).....	52
Figure 2.2.5	Distribution of faults in Llano Uplift region and surrounding areas. Surface geology of Llano Uplift region is based on Geologic Atlas of Texas (GAT) (Bureau of Economic Geology, 2013). Faults are modified from geodatabase by Standen and Ruggiero (2007) with reference to Johnson (2004).	53

Figure 2.2.6	Distribution of faults along a cross section in Gillespie County (Tybor, 1993; imported from Standen and Ruggiero (2007)).....	54
Figure 2.2.7	Detailed Surface geology of study area (based on Bureau of Economic Geology, 2013).....	55
Table 2.2.1.	Stratigraphy and hydrogeologic classification of geologic units in study area.	56
Figure 3.5.1	Areal coverage of previous groundwater flow models.	68
Figure 4.1.1	Interpreted ground surface or top elevation of Layer 1 (Cretaceous and younger units) based on U.S. Geological Survey's Digital Elevation Model (DEM).....	72
Figure 4.1.2	Interpreted bottom elevation of Layer 1 (Cretaceous and younger units).....	73
Figure 4.1.3	Interpreted thickness of Layer 1 (Cretaceous and younger units).....	74
Figure 4.1.4	Interpreted top elevation of Layer 3 (Marble Falls Aquifer).	75
Figure 4.1.5	Interpreted bottom elevation of Layer 3 (Marble Falls Aquifer).	76
Figure 4.1.6	Interpreted thickness of Layer 3 (Marble Falls Aquifer).	77
Figure 4.1.7	Interpreted top of Layer 5 (Ellenburger-San Saba Aquifer).	78
Figure 4.1.8	Interpreted bottom of Layer 5 (Ellenburger-San Saba Aquifer).	79
Figure 4.1.9	Interpreted thickness of Layer 5 (Ellenburger-San Saba Aquifer).....	80
Figure 4.1.10	Interpreted top of Layer 7 (Hickory Aquifer).	81
Figure 4.1.11	Interpreted bottom of Layer 7 (Hickory Aquifer).	82
Figure 4.1.12	Interpreted thickness of Layer 7 (Hickory Aquifer).....	83
Figure 4.1.13	Location of hydrostratigraphic cross sections. Surface geology is based on Geologic Atlas of Texas (Bureau of Economic Geology, 2013). Faults are based on Standen and Ruggiero (2007).....	84
Figure 4.1.14	Hydrostratigraphic cross section along northwest-southeast direction. Vertical exaggeration relative to horizontal direction is 50. Location of cross section is shown in Figure 4.2.13.	85
Table 4.2. 1	Summary of groundwater level measurements by decade in Cretaceous, Marble Falls, Ellenburger-San Saba, and Hickory aquifers between 1930 and 2014. ...	90
Figure 4.2.1	Location of wells with water level measurements in Cretaceous aquifers.	91
Figure 4.2.2	Location of wells with water level measurements in Marble Falls Aquifer.	92
Figure 4.2.3	Location of wells with water level measurements in Ellenburger-San Saba Aquifer.....	93
Figure 4.2.4	Location of wells with water level measurements in Hickory Aquifer.....	94
Figure 4.2.5	Pre-development potentiometric surface map of Cretaceous aquifers.....	95
Figure 4.2.6	Pre-development water levels in Ellenburger-San Saba Aquifer.....	96
Figure 4.2.7	Pre-development water levels in Hickory Aquifer.....	97
Figure 4.2.8	Water levels in Cretaceous aquifers (1950).	98

Figure 4.2.9	Potentiometric surface map of Cretaceous aquifers (1980).	99
Figure 4.2.10	Potentiometric surface map of Cretaceous aquifers (2010).	100
Figure 4.2.11	Water levels in Marble Falls Aquifer (1980).	101
Figure 4.2.12	Water levels in Ellenburger-San Saba Aquifer (1950).....	102
Figure 4.2.13	Water levels in Ellenburger-San Saba Aquifer (1980).....	103
Figure 4.2.14	Water levels in Ellenburger-San Saba Aquifer (2010).....	104
Figure 4.2.15	Water levels in Hickory Aquifer (1980).	105
Figure 4.2.16	Water levels in Hickory Aquifer (2010).	106
Figure 4.2.17	Water level hydrographs at selected wells in Cretaceous aquifers.....	107
Figure 4.2.18	Water level hydrographs at selected wells in Ellenburger-San Saba Aquifer...	108
Figure 4.2.19	Water level hydrographs at selected wells in Hickory Aquifer.	109
Figure 4.3.1	Average infiltration distribution due to precipitation between 1960 and 2009 in study area (annual infiltration rates from Kirk and others (2012)).	113
Figure 4.3.2	Infiltration distribution due to precipitation for 2005, a dry year with low precipitation (annual infiltration rates from Kirk and others (2012)).....	114
Figure 4.3.3	Infiltration distribution due to precipitation for 2007, a wet year with high precipitation (annual infiltration rates from Kirk and others (2012)).....	115
Figure 4.3.4	Locations of U.S. Geological Survey’s stream gages and catchment basins used for estimating effective groundwater recharge. Catchment basins are colored and numbered. Catchment basins across study area boundary may not be completely shown.....	116
Figure 4.3.5	Variations of annual groundwater recharge rates associated with catchment basins 0, 2, 5, 29, and 30 calculated from stream baseflow. Catchment basins are colored and numbered.	117
Figure 4.3.6	Variations of annual groundwater recharge rates associated with catchment basins 3, 13, 14, 17, and 19 calculated from stream baseflow. Catchment basins are colored and numbered.	118
Figure 4.3.7	Variations of annual groundwater recharge rates associated with catchment basins 1, 4, 6, 8, and 20 calculated from stream baseflow. Catchment basins are colored and numbered.	119
Figure 4.3.8	Variations of annual groundwater recharge rates associated with catchment basins 11, 12, 15, 21, and 22 calculated from stream baseflow. Catchment basins are colored and numbered.	120
Figure 4.3.9	Variations of annual groundwater recharge rates associated with catchment basins 9, 10, 16, and 25 calculated from stream baseflow. Catchment basins are colored and numbered.	121

Figure 4.3.10	Variations of annual groundwater recharge rates associated with catchment basins 26, 27, and 28 calculated from stream baseflow. Catchment basins are colored and numbered.	122
Figure 4.3.11	Distribution of average annual groundwater recharge calculated from stream baseflow in study area.	123
Figure 4.3.12	Variations of minimum, maximum, and average monthly groundwater recharge rates associated with catchment basins 0, 2, 5, 29, and 30 calculated from stream baseflow. Catchment basins are colored and numbered.	124
Figure 4.3.13	Variations of minimum, maximum, and average monthly groundwater recharge rates associated with catchment basins 3, 13, 14, 17, and 19 calculated from stream baseflow. Catchment basins are colored and numbered.	125
Figure 4.3.14	Variations of minimum, maximum, and average monthly groundwater recharge rates associated with catchment basins 1, 4, 6, 8, and 20 calculated from stream baseflow. Catchment basins are colored and numbered.	126
Figure 4.3.15	Variations of minimum, maximum, and average monthly groundwater recharge rates associated with catchment basins 11, 12, 15, 21, and 22 calculated from stream baseflow. Catchment basins are colored and numbered.	127
Figure 4.3.16	Variations of minimum, maximum, and average monthly groundwater recharge rates associated with catchment basins 9, 10, 16, and 25 calculated from stream baseflow. Catchment basins are colored and numbered.	128
Figure 4.3.17	Variations of minimum, maximum, and average monthly groundwater recharge rates associated with catchment basins 26, 27, and 28 calculated from stream baseflow. Catchment basins are colored and numbered.	129
Figure 4.4.1	River flux hydrographs for selected gages located on Colorado and Guadalupe rivers. River monthly flux data are downloaded from U.S. Geological Survey (2014).	134
Figure 4.4.2	Stream gain (positive value) or loss (negative value) results in cubic feet per second per mile of stream channel (cfsm) (based on data compiled by Slade and others (2002)).	135
Figure 4.4.3	Variations of annual stream gain or loss for stream segments associated with catchment basins 0, 2, 5, 29, and 30 (acre-feet per year per square mile). Catchment basins are colored and numbered.	136
Figure 4.4.4	Variations of annual stream gain or loss for stream segments associated with catchment basins 3, 13, 14, 17, and 19 (acre-feet per year per square mile). Catchment basins are colored and numbered.	137
Figure 4.4.5	Variations of annual stream gain or loss for stream segments associated with catchment basins 1, 4, 6, 8, and 20 (acre-feet per year per square mile). Catchment basins are colored and numbered.	138
Figure 4.4.6	Variations of annual stream gain or loss for stream segments associated with catchment basins 11, 12, 15, 21, and 22 (acre-feet per year per square mile). Catchment basins are colored and numbered.	139

Figure 4.4.7	Variations of annual stream gain or loss for stream segments associated with catchment basins 9, 10, 16, and 25 (acre-feet per year per square mile). Catchment basins are colored and numbered.	140
Figure 4.4.8	Variations of annual stream gain or loss for stream segments associated with catchment basins 26, 27, and 28 (acre-feet per year per square mile). Catchment basins are colored and numbered.	141
Figure 4.4.9	Variations of minimum, maximum, and average monthly stream gain or loss for stream segments associated with catchment basins 0, 2, 5, 29, and 30 (acre-feet per month per square mile). Catchment basins are colored and numbered.	142
Figure 4.4.10	Variations of minimum, maximum, and average monthly stream gain or loss for stream segments associated with catchment basins 3, 13, 14, 17, and 19 (acre-feet per month per square mile). Catchment basins are colored and numbered.	143
Figure 4.4.11	Variations of minimum, maximum, and average monthly stream gain or loss for stream segments associated with catchment basins 1, 4, 6, 8, and 20 (acre-feet per month per square mile). Catchment basins are colored and numbered.	144
Figure 4.4.12	Variations of minimum, maximum, and average monthly stream gain or loss for stream segments associated with catchment basins 11, 12, 15, 21, and 22 (acre-feet per month per square mile). Catchment basins are colored and numbered.	145
Figure 4.4.13	Variations of minimum, maximum, and average monthly stream gain or loss for stream segments associated with catchment basins 9, 10, 16, and 25 (acre-feet per month per square mile). Catchment basins are colored and numbered.	146
Figure 4.4.14	Variations of minimum, maximum, and average monthly stream gain or loss for stream segments associated with catchment basins 26, 27, and 28 (acre-feet per month per square mile). Catchment basins are colored and numbered.	147
Figure 4.4.15	Water level hydrographs of O. H. Ivie Reservoir, Brady Creek Reservoir, Lake Buchanan, Inks Lake, Lyndon B. Johnson (LBJ) Lake, and Lake Marble Falls.	148
Figure 4.4.16	Flow hydrographs of selected springs originating from minor aquifers in Llano Uplift region.	149
Figure 4.5.1	Histogram of logarithmic transmissivity of Cretaceous aquifers.	155
Figure 4.5.2	Histogram of logarithmic hydraulic conductivity of Cretaceous aquifers.	156
Figure 4.5.3	Distribution of transmissivity of Cretaceous aquifers (Edwards and Trinity). .	157
Figure 4.5.4	Distribution of hydraulic conductivity of Cretaceous aquifers (Edwards and Trinity).	158
Figure 4.5.5	Distribution of transmissivity of Marble Falls Aquifer.	159
Figure 4.5.6	Distribution of hydraulic conductivity of Marble Falls Aquifer.	160
Figure 4.5.7	Histogram of logarithmic transmissivity of Ellenburger-San Saba Aquifer.	161

Figure 4.5.8	Histogram of logarithmic hydraulic conductivity of Ellenburger-San Saba Aquifer.....	162
Figure 4.5.9	Distribution of transmissivity of Ellenburger-San Saba Aquifer.	163
Figure 4.5.10	Distribution of hydraulic conductivity of Ellenburger-San Saba Aquifer.	164
Figure 4.5.11	Histogram of logarithmic transmissivity of Hickory Aquifer.....	165
Figure 4.5.12	Histogram of logarithmic hydraulic conductivity of Hickory Aquifer.	166
Figure 4.5.13	Distribution of transmissivity of Hickory Aquifer.....	167
Figure 4.5.14	Distribution of hydraulic conductivity of Hickory Aquifer.	168
Figure 4.6.1	Vegetation type in study area (McMahan and others, 1984).	172
Table 4.6.1	Depth of plant roots (Schenk and Jackson, 2003).	173
Figure 4.6.2	Estimated average annual groundwater evapotranspiration distribution between 1960 and 2009 in study area (annual evapotranspiration rates from Kirk and others (2012)).	174
Figure 4.6.3	Estimated annual groundwater evapotranspiration distribution for 2005, a dry year with low precipitation (data from Kirk and others (2012)).	175
Figure 4.6.4	Estimated annual groundwater evapotranspiration distribution for 2007, a wet year with high precipitation (data from Kirk and others (2012)).	176
Figure 4.6.5	Maximum groundwater evapotranspiration distribution (data from Deeds and Kelley in Scanlon and others (2005)).	177
Figure 4.6.6	Annual groundwater pumping between 1984 and 2011 in Blanco, Brown, Burnet, Coleman, and Concho counties (pumping data from TWDB water use survey).	178
Figure 4.6.7	Annual groundwater pumping between 1984 and 2011 in Gillespie, Hays, Kendall, Kerr, and Kimble counties (pumping data from TWDB water use survey).	179
Figure 4.6.8	Annual groundwater pumping between 1984 and 2011 in Lampasas, Llano, Mason, McCulloch, and Menard counties (pumping data from TWDB water use survey).	180
Figure 4.6.9	Annual groundwater pumping between 1984 and 2011 in Mills, San Saba, Travis, and Williamson counties (pumping data from TWDB water use survey).	181
Table 4.6.2	Groundwater use in 2011 by category.	182
Figure 4.6.10	Population density in study area (data from the U. S. Census Bureau (2010)).	183
Figure 4.7.1	Nitrate concentrations in groundwater samples collected from Marble Falls Aquifer.....	188
Figure 4.7.2	Total dissolved solids concentrations in groundwater samples collected from Marble Falls Aquifer.	189

Figure 4.7.3	Chloride concentrations in groundwater samples collected from Marble Falls Aquifer.....	190
Figure 4.7.4	Sulfate concentrations in groundwater samples collected from Marble Falls Aquifer.....	191
Figure 4.7.5	Piper diagram of groundwater samples collected from Marble Falls Aquifer (TDS = Total Dissolved Solids and mg/l = milligrams per liter).	192
Figure 4.7.6	Stable and radiogenic isotopes in a groundwater sample collected from Marble Falls Aquifer.....	193
Figure 4.7.7	Nitrate concentrations in groundwater samples collected from Ellenburger-San Saba Aquifer.....	194
Figure 4.7.8	Fluoride concentrations in groundwater samples collected from Ellenburger-San Saba Aquifer.....	195
Figure 4.7.9	Gross alpha radiation in groundwater samples collected from Ellenburger-San Saba Aquifer.....	196
Figure 4.7.10	Total dissolved solids concentrations in groundwater samples collected from Ellenburger-San Saba Aquifer.....	197
Figure 4.7.11	Chloride concentrations in groundwater samples collected from Ellenburger-San Saba Aquifer.....	198
Figure 4.7.12	Piper diagram of groundwater samples collected from Ellenburger-San Saba Aquifer (TDS = Total Dissolved Solids and mg/l = milligrams per liter).	199
Figure 4.7.13	Carbon-14 activities in groundwater samples collected from Ellenburger-San Saba Aquifer.....	200
Figure 4.7.14	Tritium activities in groundwater samples collected from Ellenburger-San Saba Aquifer.....	201
Figure 4.7.15	Nitrate concentrations of groundwater samples collected from Hickory Aquifer.	202
Figure 4.7.16	Fluoride concentrations of groundwater samples collected from Hickory Aquifer.	203
Figure 4.7.17	Radium 226/228 activities of groundwater samples collected from Hickory Aquifer.....	204
Figure 4.7.18	Gross alpha radiation of groundwater samples collected from Hickory Aquifer.	205
Figure 4.7.19	Total dissolved solids concentrations in groundwater samples collected from Hickory Aquifer.....	206
Figure 4.7.20	Chloride concentrations in groundwater samples collected from Hickory Aquifer.	207
Figure 4.7.21	Sulfate concentrations in groundwater samples collected from Hickory Aquifer.	208

Figure 4.7.22	Piper diagram of groundwater samples collected from Hickory Aquifer (TDS = Total Dissolved Solids and mg/l = milligrams per liter).	209
Figure 4.7.23	Carbon-14 activities in groundwater samples collected from Hickory Aquifer.	210
Figure 4.7.24	Tritium activities in groundwater samples collected from Hickory Aquifer. ...	211
Figure 5.1.1	Schematic hydrogeologic cross section and groundwater flow of pre-development conditions.	216
Figure 5.1.2	Schematic hydrogeologic cross section and groundwater flow of post-development conditions.	217
Table A.1	Summary of springs in study area with at least one measurement (based on Heitmuller and Reece (2003)).....	230
Table A.2	Summary of aquifer transmissivity and horizontal hydraulic conductivity values for Cretaceous, Marble Falls, Ellenburger-San Saba, and Hickory aquifers in study area.	239
Table A.3	Summary of aquifer storativity values from hydraulic tests.	289

EXECUTIVE SUMMARY:

The Texas State legislature mandated that the Texas Water Development Board (TWDB) obtain or develop groundwater availability models for all major and minor aquifers in Texas. To develop a groundwater availability model (also known as a numerical groundwater flow model), a conceptual groundwater model must be constructed first and lays the foundation for the groundwater availability model to be built upon. A conceptual model is a simplified version of the “real world”, which the groundwater availability model can handle through a computer program.

This report summarizes a groundwater conceptual model developed for the minor aquifers (the Hickory, Ellenburger-San Saba, and Marble Falls) in the Llano Uplift region. The minor aquifers defined by the TWDB in the study area occupy an area of 8,764 square miles in nineteen counties: Blanco, Brown, Burnet, Coleman, Concho, Gillespie, Hays, Kendall, Kerr, Kimble, Lampasas, Llano, Mason, McCulloch, Menard, Mills, San Saba, Travis, and Williamson. Both the Hickory Aquifer and Ellenburger-San Saba Aquifer contain outcrop and downdip portions, while only the outcrop portion of the Marble Falls Formation was defined as official aquifer by the TWDB.

This conceptual model provides the geologic framework and interpretation of the groundwater flow system within in the study area. This initial evaluation includes information concerning climate, physiography, geology, previous studies, hydrostratigraphy, water levels and groundwater flow, recharge, surface water features, hydraulic properties of the aquifers, discharge (such as pumping from wells), and water quality.

The conceptual flow model for the Llano Uplift region contains seven hydrostratigraphic units including four aquifers (from top to bottom): the Cretaceous aquifers, Marble Falls Aquifer, Ellenburger-San Saba Aquifer, and Hickory Aquifer. Separating the aquifers are three confining units. All seven units are discontinuous. The top and bottom of the conceptual model domain are the ground surface and the top of the Precambrian strata, respectively. In this model domain, the interaction with the underlying Precambrian units is assumed to be zero due to the low permeability of the Precambrian units in the study area. The lateral extent of the conceptual flow model is bounded by the Ouachita Thrust Fault to the east and southeast and the official Hickory Aquifer boundary plus five miles for the rest. The groundwater flow through the lateral boundary is also assumed to be zero. This assumption is based on the following reasoning: the fault wall is assumed to act as a flow barrier and the groundwater along the rest of the model domain lateral boundary may very likely be brackish, which may hinder the groundwater movement due to the higher density of the brackish water. Thus, a no-flow condition is likely justified and can be maintained as long as no significant groundwater withdrawal occurs near the lateral boundary.

The conceptual flow model includes two hydrogeologic conditions: the pre-development conditions prior to 1950 and the post-development conditions after 1950. Because of limited groundwater withdrawal prior to 1950, the aquifers in the Llano Uplift region were under long-term dynamic equilibrium. During the pre-development conditions, groundwater levels and flows fluctuated over time due to seasonal and annual changes in precipitation. However, the natural discharge such as spring flow and baseflow to rivers was balanced by the natural recharge such

as infiltration due to precipitation. As a result, the water levels and storage in the aquifers showed little long-term variation.

After 1950, the groundwater pumping had changed the aquifer system in the study area. These changes included falling water level or aquifer storage, reducing discharge to rivers and springs, and increasing groundwater recharge. Aquifer overdraft could also reduce the groundwater flow to the deep (downdip) portions of the aquifers.

In summary, this conceptual model identifies the unique hydrostratigraphic units and the associated structures, characteristics of the groundwater flow, and factors that control the flow. The information from the conceptual model will be used to construct a numerical groundwater flow model or groundwater availability model for the minor aquifers in the Llano Uplift region. Although the TWDB has made the best efforts during the development of this conceptual model, uncertainties still exist due to the lack of data for certain areas and the complexity of the study area. These uncertainties include, but not limited to, the hydrostratigraphic structure to the east and downdip areas, the interaction between the groundwater and lakes/reservoirs, and the characteristics of faults. The TWDB will update the conceptual model if warranted by additional information through the continued stakeholder process and the development of the numerical model. If this occurs, the TWDB will inform the stakeholders.

1.0 INTRODUCTION

The Texas Water Development Board (TWDB) has designated nine major and twenty-one minor aquifers in Texas (Figures 1.0.1 and 1.0.2). The characteristics of these aquifers are discussed by George and others (2011). Major aquifers supply large quantities of water over large areas and minor aquifer supply relatively small quantities of water over large areas or supply large quantities of water over small areas.

This report documents the development of a conceptual groundwater model for the minor aquifers in the Llano Uplift region. This conceptual model lays the foundation for a numerical groundwater availability model that will be developed and documented in a separate report.

There are two major aquifers, the Edwards-Trinity (Plateau) and the Trinity, that occur in the Llano Uplift region. The Llano Uplift region also contains three minor aquifers: Hickory, Ellenburger-San Saba, and Marble Falls (Figures 1.0.3). According to the water use survey conducted by the TWDB in 2013, the major groundwater uses in the Llano Uplift region were for municipal, irrigation, mining, livestock, and manufacturing purposes. The 2012 State Water Plan indicated a total groundwater use of approximately 84,000 acre-feet per year, with approximately 343,000 acre-feet per year available from the three minor aquifers in the Llano Uplift region.

Senate Bill 2 passed by the Texas Senate in 2001 mandated that the TWDB, in coordination with Groundwater Conservation Districts and Regional Water Planning Groups, obtain or develop groundwater availability models for all major and minor aquifers in Texas. As a result, the TWDB has developed or adopted groundwater availability models for all the major aquifers and the majority of the minor aquifers in Texas. In the Llano Uplift region, the Hill Country portion of the Trinity Aquifer was included in the groundwater flow models by Mace and others (2000) and Jones and others (2009). The groundwater flow in Trinity Aquifer to the north and east of the Llano Uplift region was simulated in a groundwater availability model by R.W. Harden & Associates, Inc. and others (2004). The Edwards-Trinity (Plateau) Aquifer was covered in the groundwater flow models by Anaya and Jones (2009) and Hutchison and others (2011).

Groundwater availability models provide a tool for assessing groundwater availability and the effects of water management strategies during different climatic conditions. A groundwater availability model is a numerical representation of the aquifer system capable of simulating historical conditions and predicting future aquifer conditions using various climatic and pumping scenarios.

To fulfill the legislature mandate and help the groundwater conservation districts in the study area manage their groundwater resources, the TWDB is developing a groundwater availability model for the minor aquifers in the Llano Uplift region. The precursor of such a groundwater availability model is the development of a conceptual groundwater model. A conceptual groundwater model is a simplified version of the “real world”, which the groundwater availability model can handle through a computer code.

To help the conceptual model development, the TWDB contracted a study of the structure and stratigraphy of the minor aquifers in the Llano Uplift region and the study results were summarized in a report by Standen and Ruggiero (2007). This report and its associated database provided the fundamental geologic framework, structure, and extent of the minor aquifers in the study area.

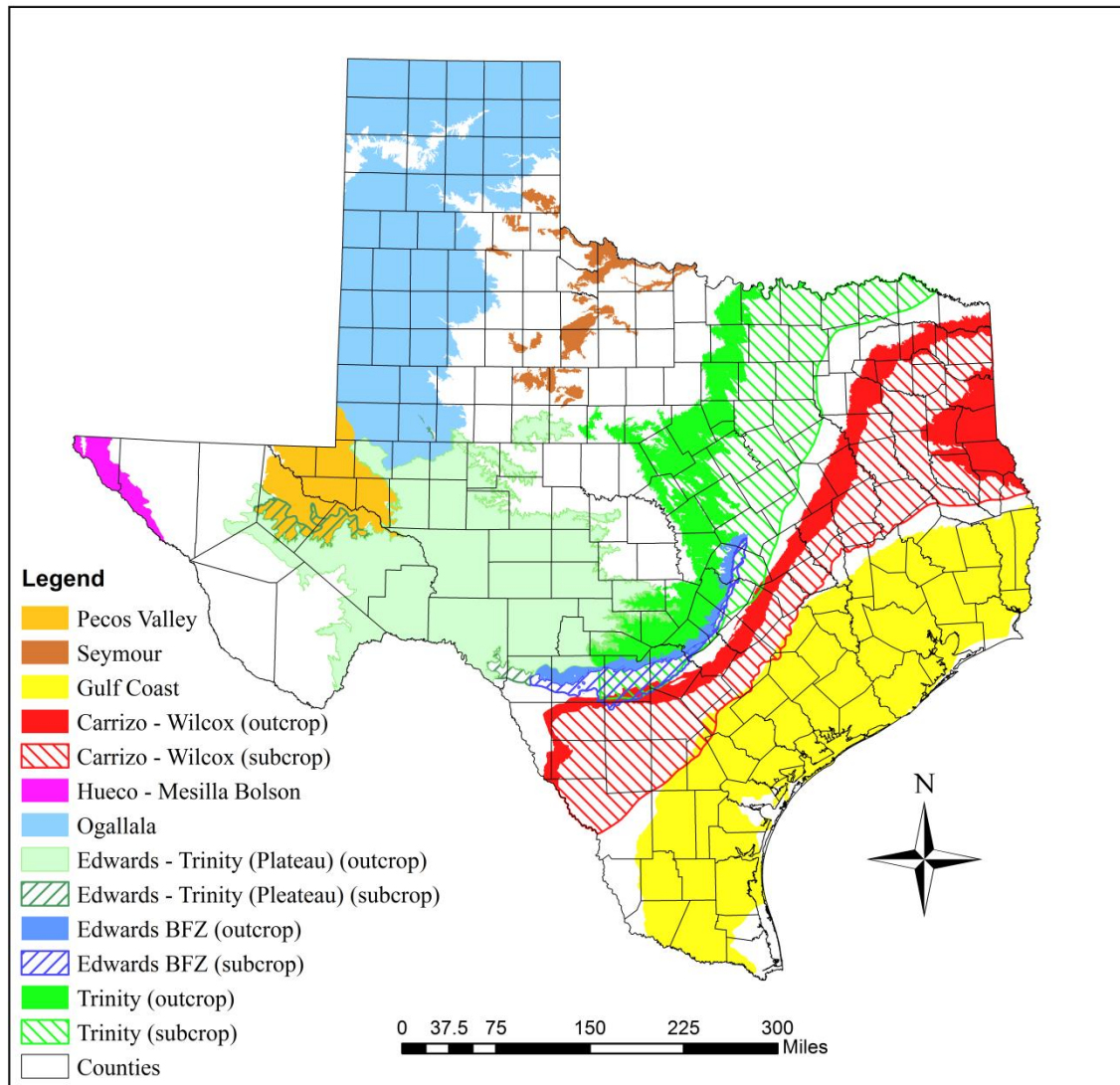


Figure 1.0.1 Location of major aquifers in Texas (revised from TWDB, 2013a).

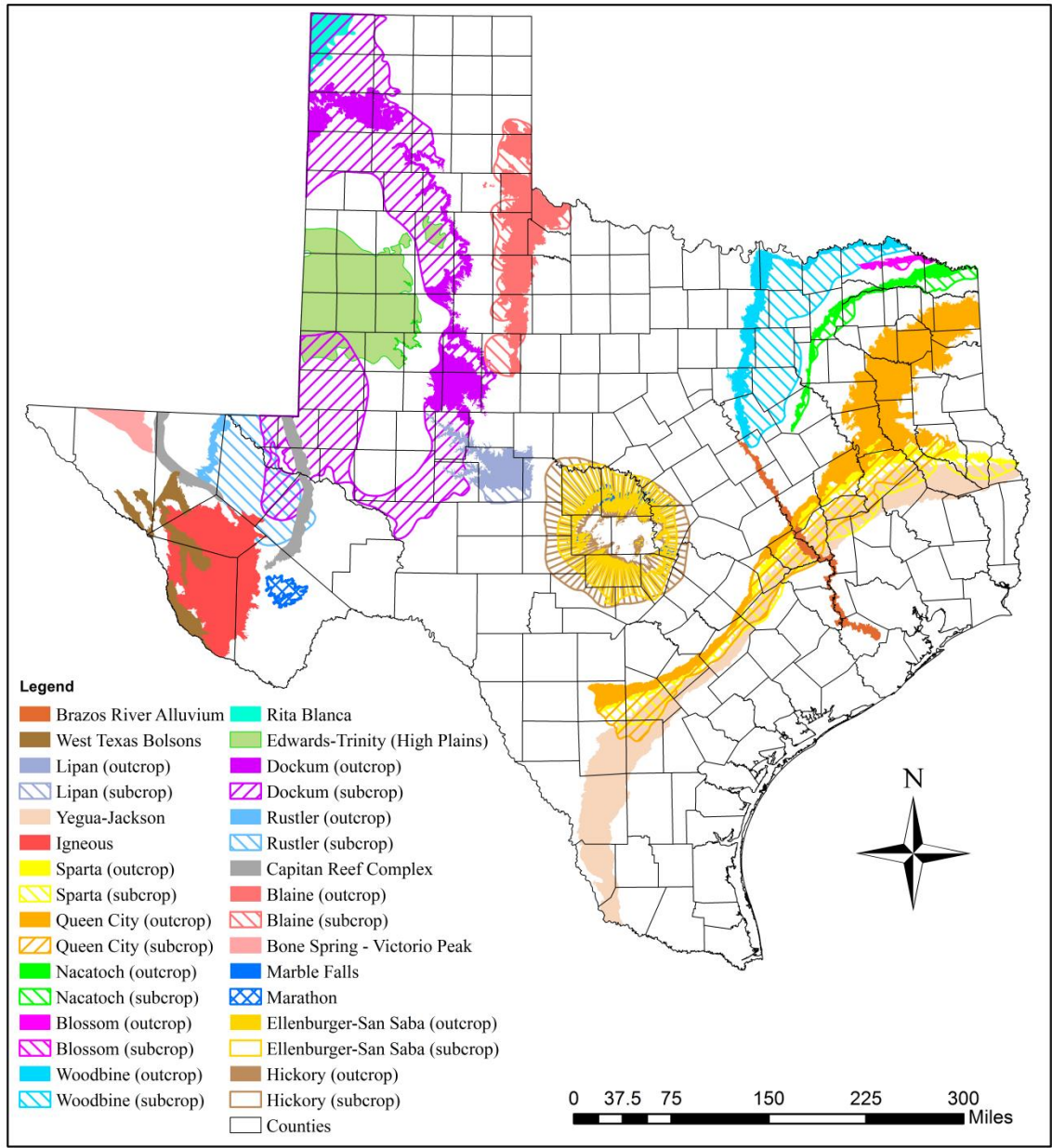


Figure 1.0.2 Location of minor aquifers in Texas (revised from TWDB, 2013b).

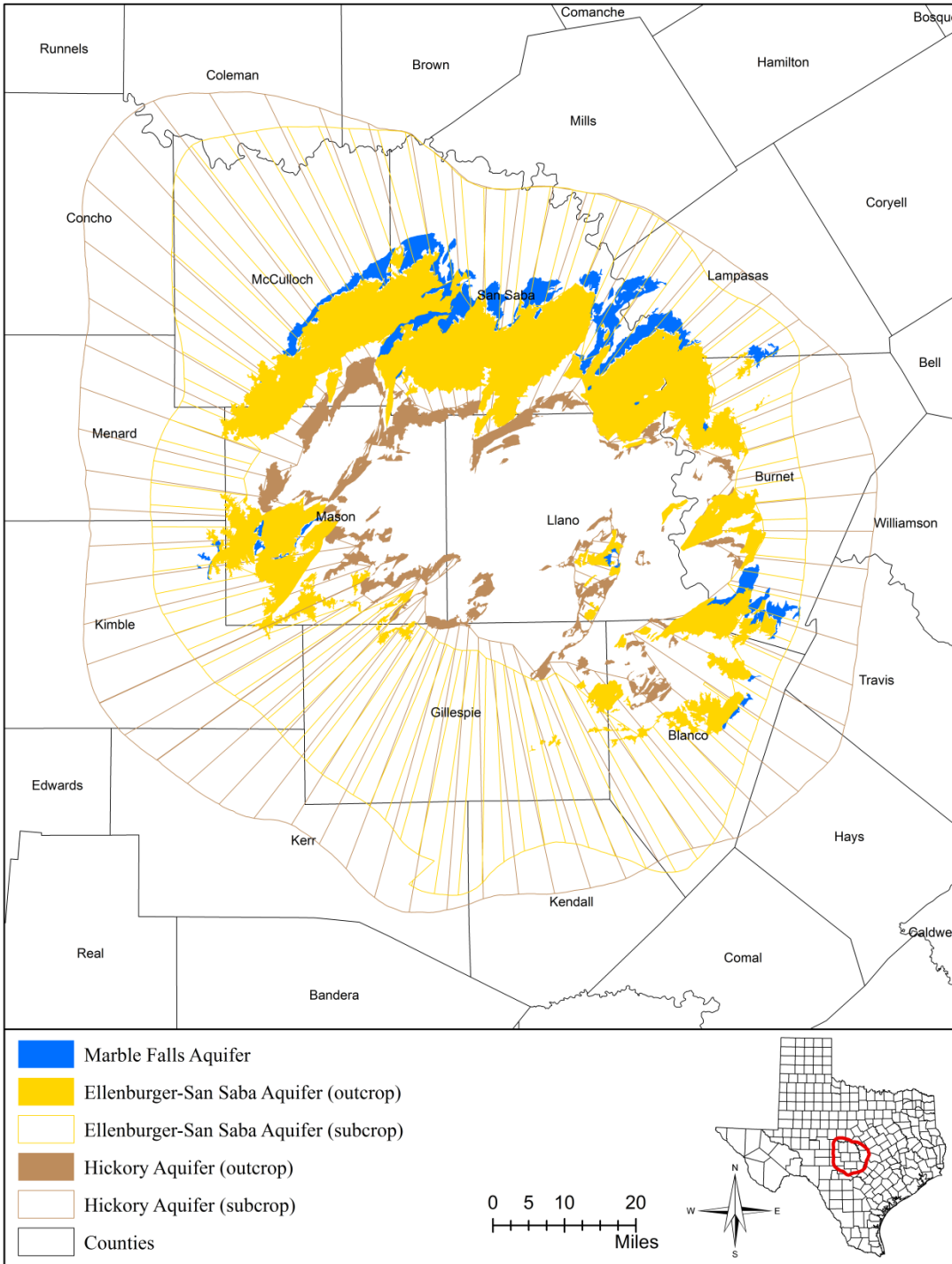


Figure 1.0.3 Location of minor aquifers in Llano Uplift region (based on TWDB (2013b))

2.0 STUDY AREA

The minor aquifers defined by the TWDB in the study area occupy 8,764 square miles in nineteen counties: Blanco, Brown, Burnet, Coleman, Concho, Gillespie, Hays, Kendall, Kerr, Kimble, Lampasas, Llano, Mason, McCulloch, Menard, Mills, San Saba, Travis, and Williamson. Both the Hickory Aquifer and Ellenburger-San Saba Aquifer contain outcrop and downdip portions, while only the outcrop portion of the Marble Falls Formation was defined as official aquifer by the TWDB (Figure 1.0.3). The outcrops of the minor aquifers in the study area exist as bands or remnants around the Llano Uplift, a structural dome or high, and the downdip portions slope away from the dome.

Figure 2.0.1 shows the counties, roadways, cities, and towns in the study area. The study area contains rivers, streams, lakes, and reservoirs in four river basins: the Brazos River Basin, the Colorado River Basin, the Guadalupe River Basin, and the San Antonio River Basin (Figure 2.0.2). The two major rivers in the study area are the Colorado River and the Guadalupe River. Major lakes or reservoirs are O. H. Ivie Reservoir to the north and Lake Buchanan to the east. Figure 2.0.3 shows the river authorities associated with the study area: Upper Colorado River Authority, Central Colorado River Authority, Lower Colorado River Authority, Brazos River Authority, Upper Guadalupe River Authority, and Guadalupe-Blanco River Authority. The study area falls into the Regional Water Planning Areas F, G, K, J, and L (Figure 2.0.4). The study area includes whole or part of the following groundwater conservation districts: Blanco-Pedernales Groundwater Conservation District, Bandera County River Authority & Ground Water District, Central Texas Groundwater Conservation District, Cow Creek Groundwater Conservation District, Hays Trinity Groundwater Conservation District, Headwaters Groundwater Conservation District, Hickory Underground Water Conservation District No. 1, Hill Country Underground Water Conservation District, Kimble County Groundwater Conservation District, Lipan-Kickapoo Water Conservation District, Menard County Underground Water District, Real-Edwards Conservation and Reclamation District, and Saratoga Underground Water Conservation District (Figure 2.0.5).

The study area intersects Texas Groundwater Management Areas 7, 8, and 9 (Figure 2.0.6) and Hill Country Priority Groundwater Management Area (Figure 2.0.7). A priority groundwater management area is an area designated and delineated by the Texas Commission on Environmental Quality that is experiencing, or is expected to experience, within 50 years, critical groundwater problems including shortages of surface water or groundwater, land subsidence resulting from groundwater withdrawal, and contamination of groundwater supplies. The priority groundwater management area ensures the management of groundwater in the area with critical groundwater problems.



Figure 2.0.1 Locations of highways, cities, and towns in Llano Uplift region (based on Texas Natural Resources Information System datasets (TNRIS, 2014)).

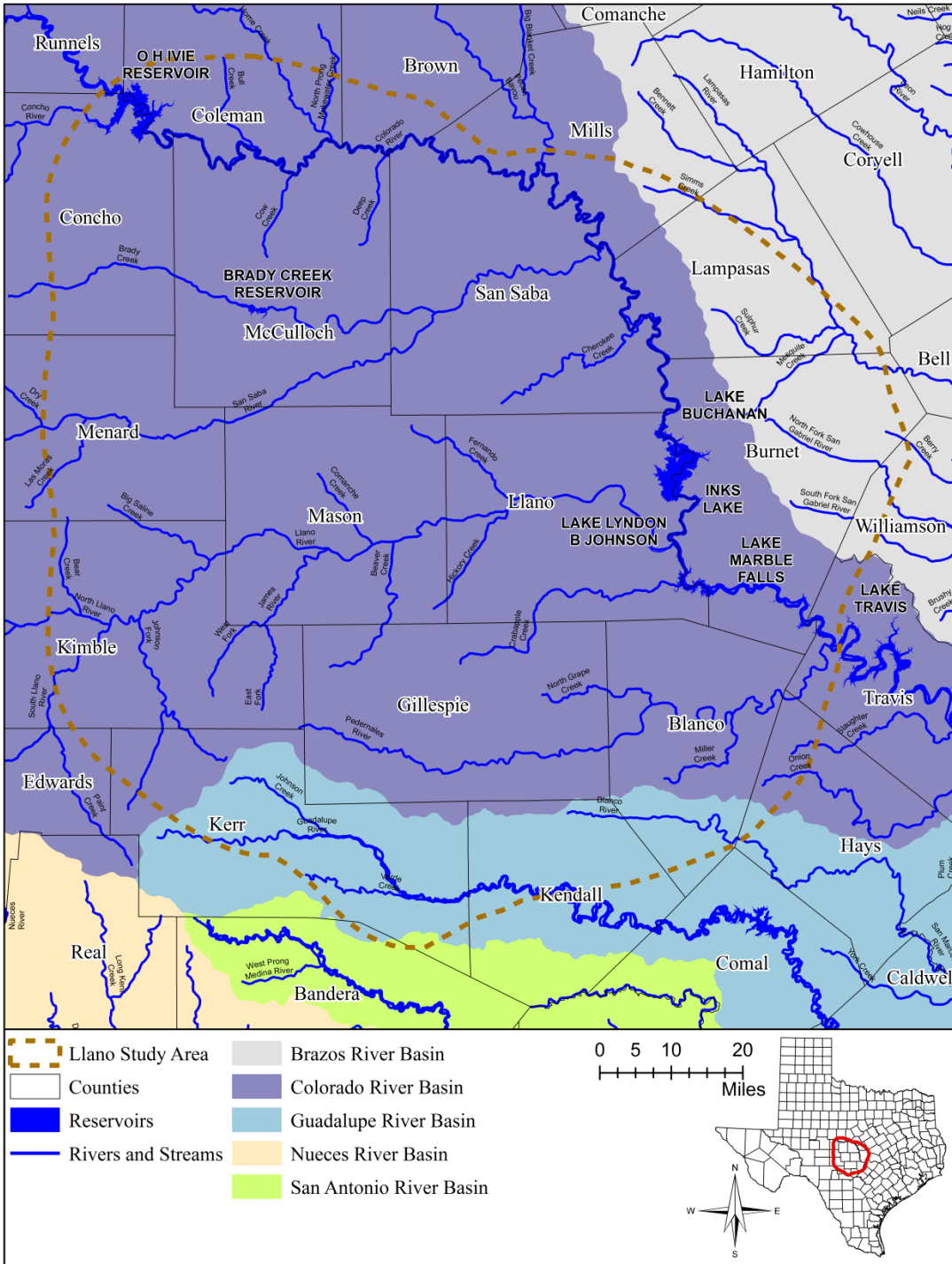


Figure 2.0.2 Locations of river basins and surface water bodies in Llano Uplift region (based on Texas Natural Resources Information System datasets (TNRIS, 2014)).

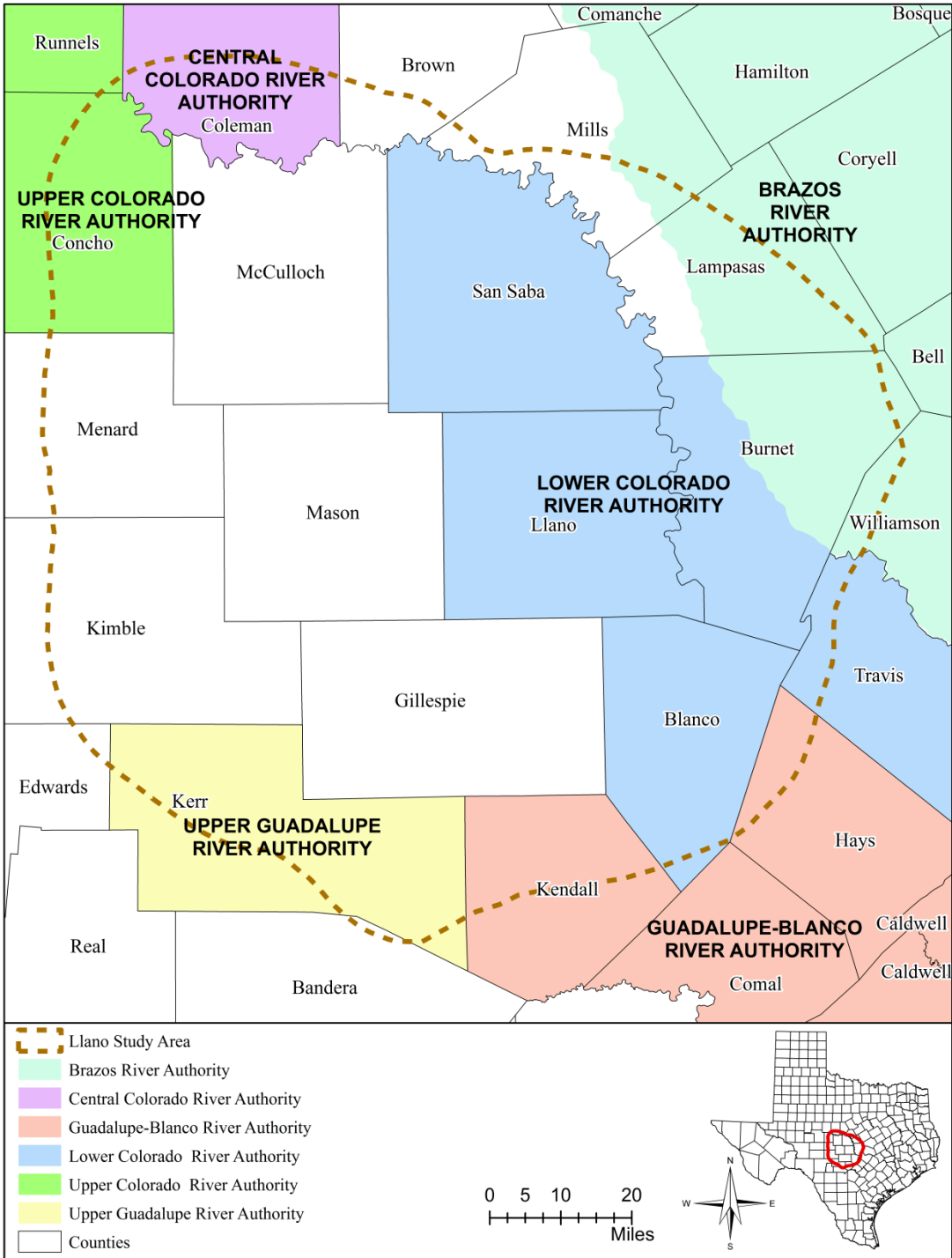


Figure 2.0.3 Texas River Authorities in study area (based on TWDB (2013c)).

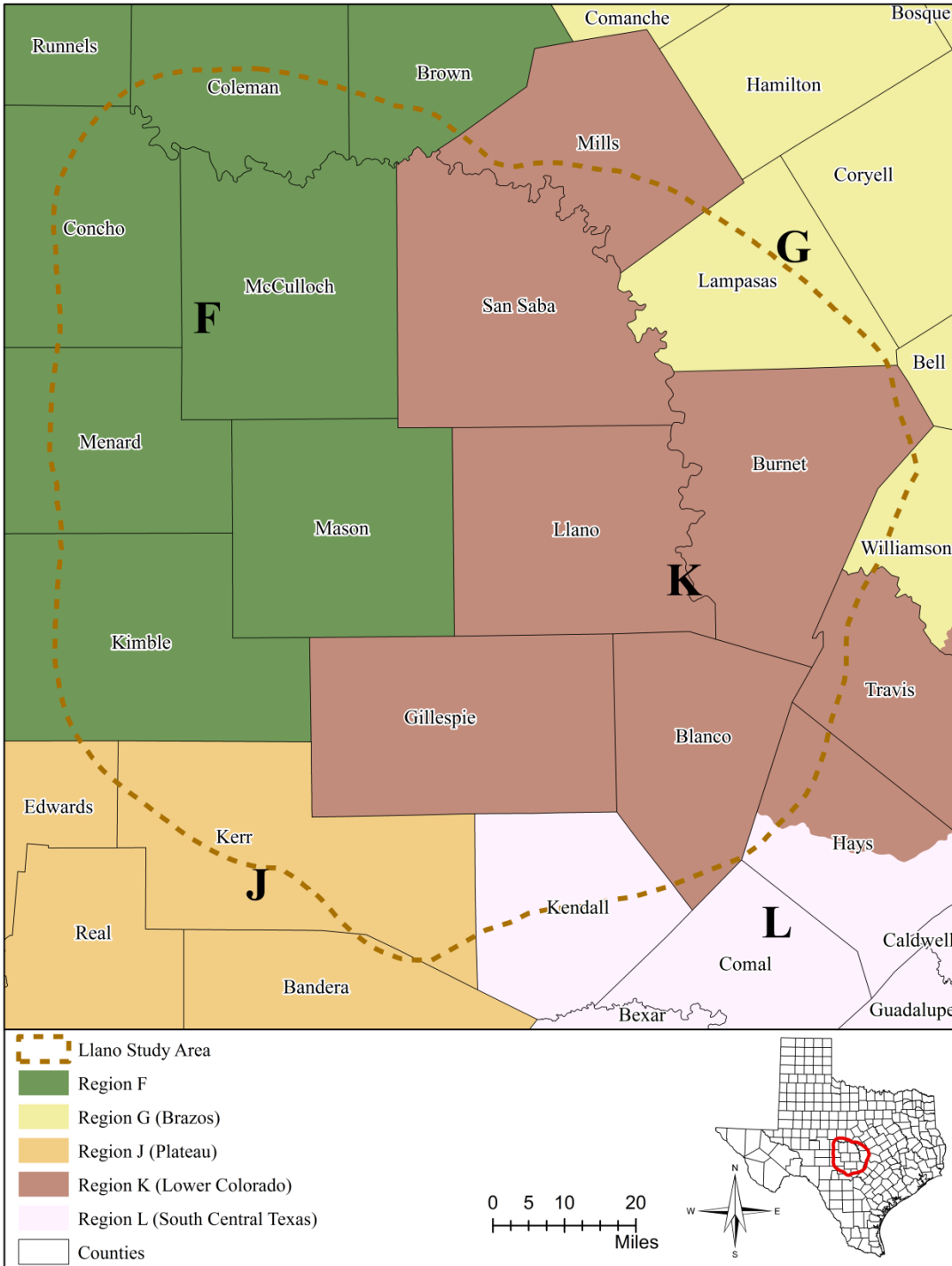


Figure 2.0.4 Texas Regional Water Planning Areas in study area (labelled by letters) (based on TWDB (2013d)).

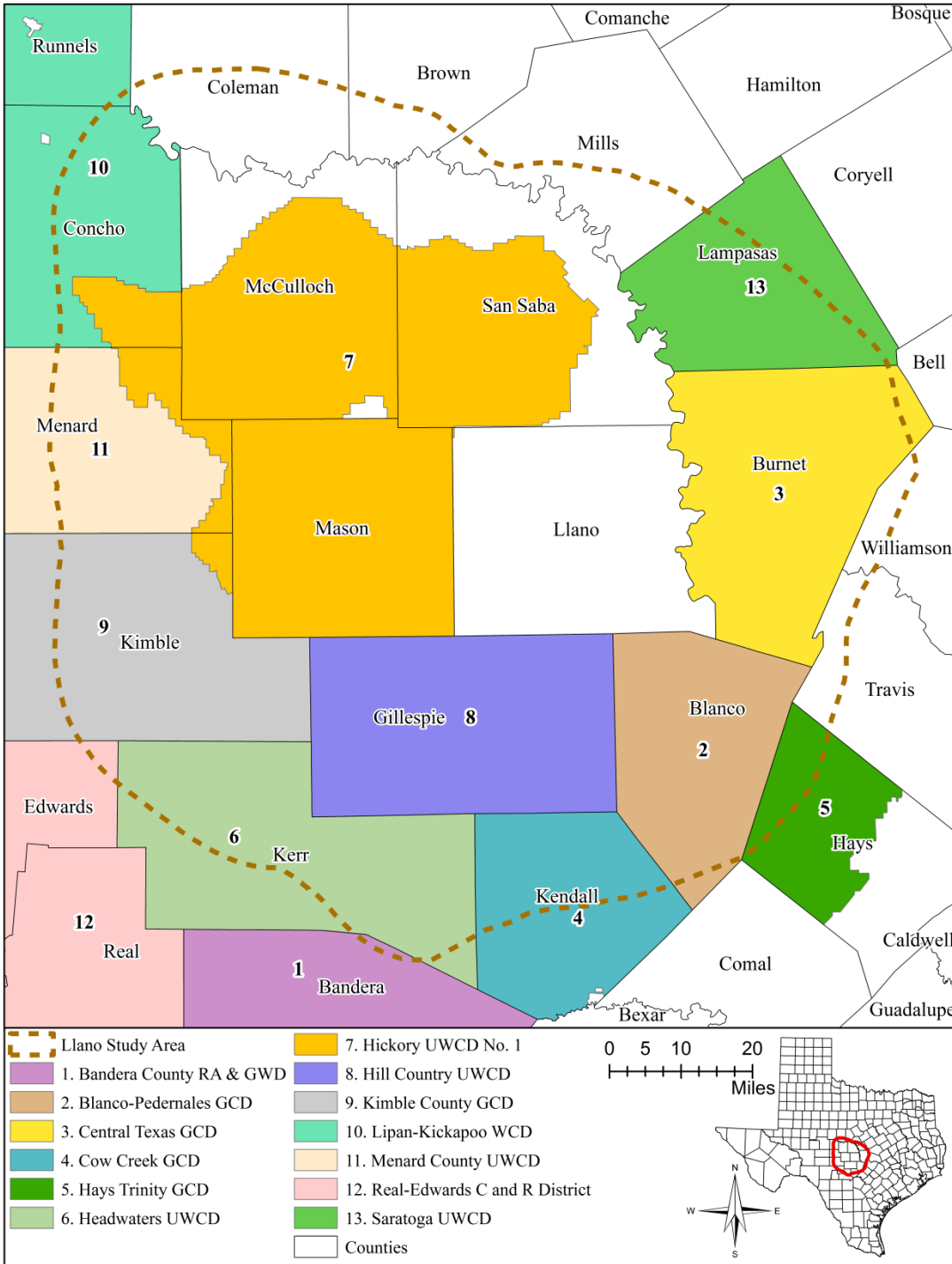


Figure 2.0.5 Texas Groundwater Conservation Districts (GCDs) in study area (based on TWDB (2013e)).

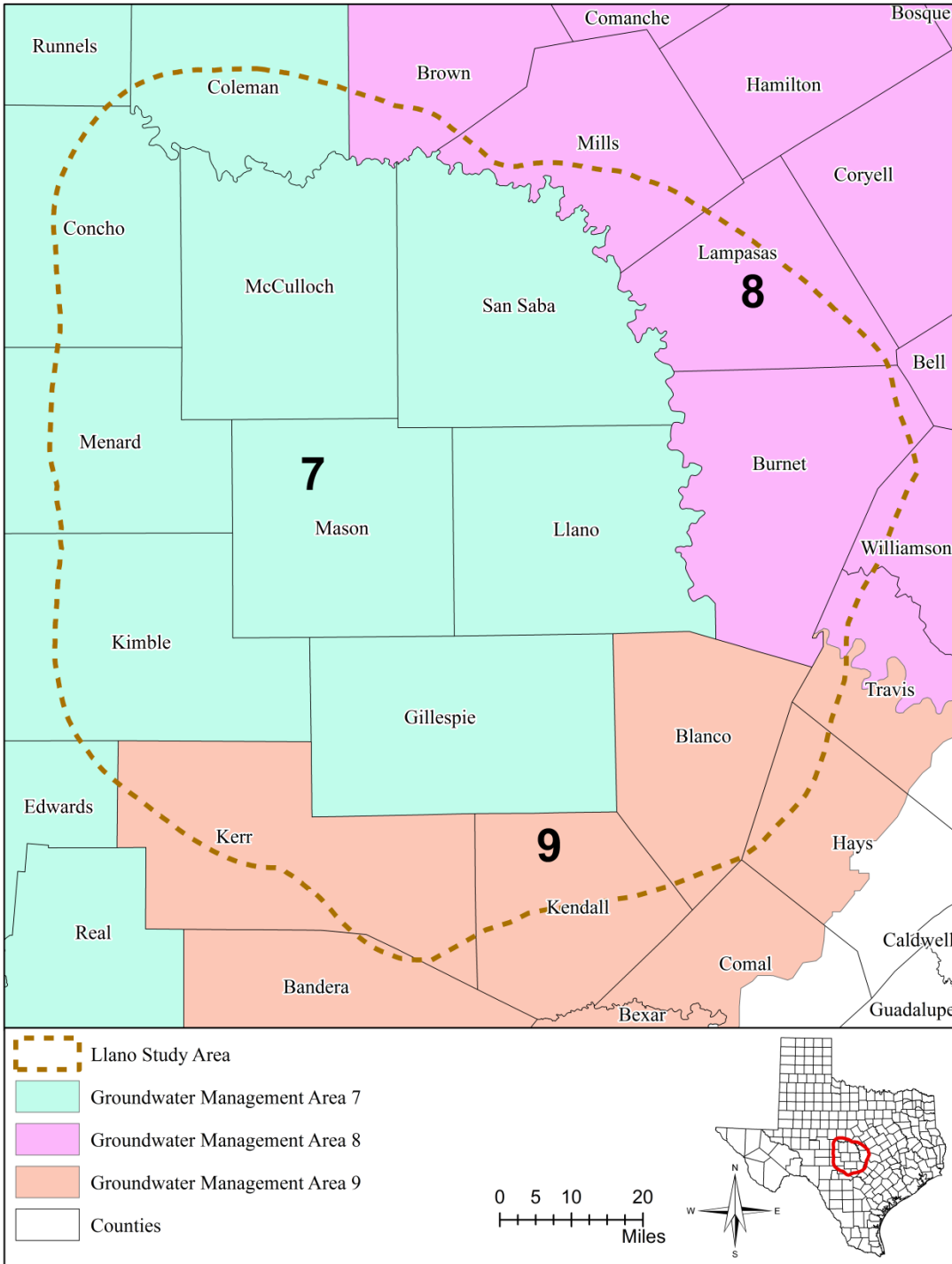


Figure 2.0.6 Texas Groundwater Management Areas in study area (labelled by numbers) (based on TWDB (2013f)).

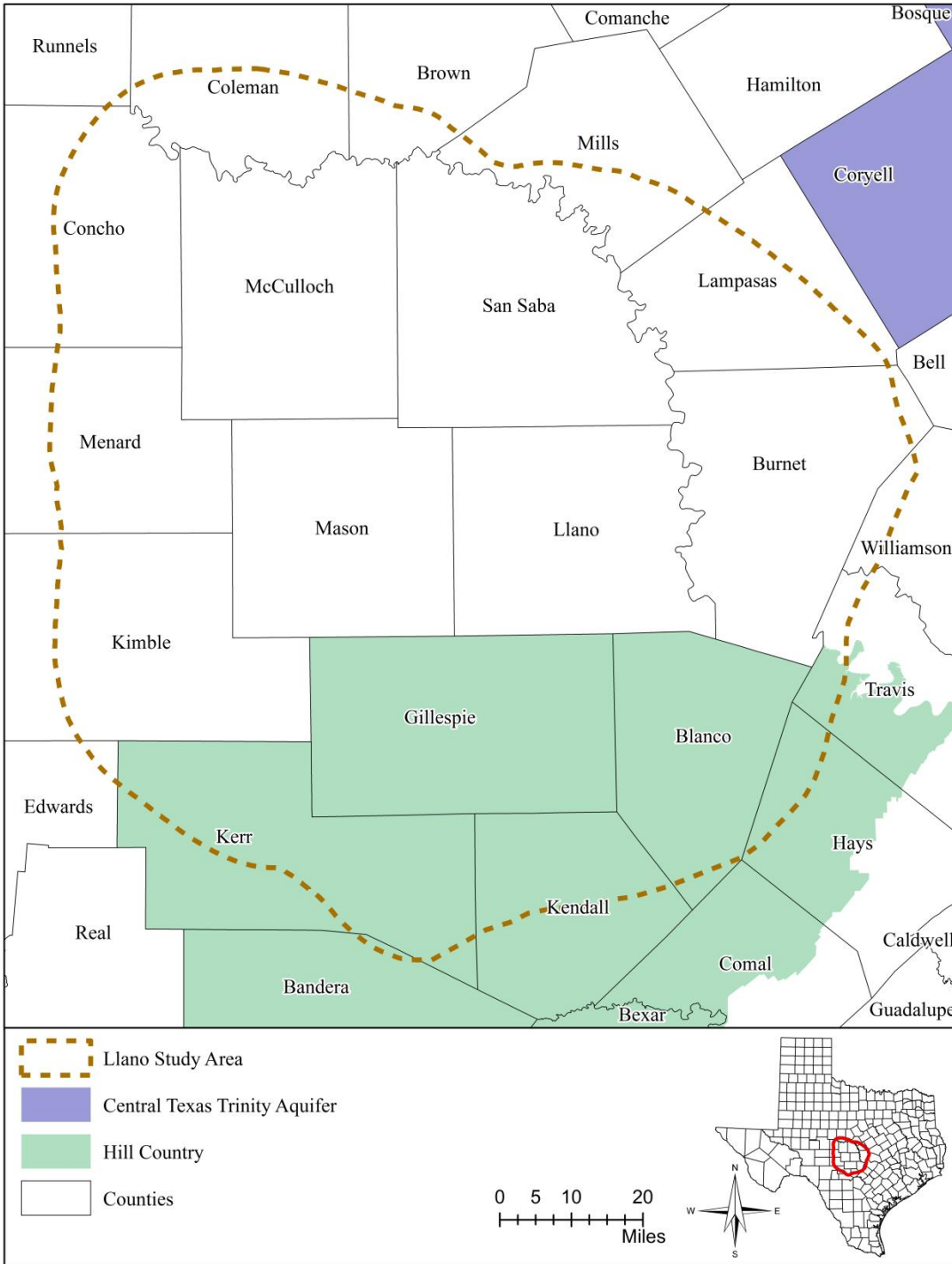


Figure 2.0.7 Texas Priority Groundwater Management Areas in study area (based on TWDB (2013g)).

2.1 Physiography and Climate

The study area sits on three physiographic provinces: the Central Texas Uplift at the middle, the North Central Plain to the north, and the Edwards Plateau to the east, south, and west (Figure 2.1.1). According to Wermund (1996), the Central Texas Uplift Physiographic Province has a central basin with a rolling floor and rounded granite hills with relieves of 400 to 600 feet (for example, the Enchanted Rock granite dome). The rocks exposed at the basin floor and the granite are more than one billion years old. The basin is surrounded by a rim composed of more resistant Paleozoic rocks. The central basin is vegetated with live oak and mesquite, while live oak and ashe juniper mainly occupy the rim region.

Farther east, south, and west from Central Texas Uplift Physiographic Province is the Edwards Plateau Physiographic Province. Wermund (1996) described the Edwards Plateau as full of escarpments capped by hard Cretaceous limestone. Streams and caverns have been developed along the weak parts of the limestone. The central interior of the province is represented by stair step topography due to alternating beds of hard and soft limestone. The vegetation is mainly mesquite and juniper brush in the study area.

To the north of the study area is the North Central Plains Physiographic Province. Erosion has removed the younger rocks and left the Upper Paleozoic Formations in the province. Areas with shale bedrock are often flat forming prairie, while hills and rolling plains dominate the areas with hard rocks. Live oak and ashe juniper are the main vegetation in the study area.

The study area is located predominately in the Edwards Plateau Level III ecological region (Figure 2.1.2). This region consists of sharp fault lines and limited perennial streams. The land is now mainly grassland with sparsely distributed juniper, mesquite, and oak used for ranching and hunting. North and northeast of the study area are classified as Central Great Plains and Cross Timbers Level III ecological regions (U.S. Environmental Protection Agency, 2013) (Figure 2.1.2). The Central Great Plains, once grassland, is now mainly cropland. Once with transitional “cross-timbers” as the native vegetation, the Cross Timbers Level III ecological region is now mainly rangeland and pastureland.

Structurally, the Llano Uplift region is a dome with Precambrian rocks pushed upward around Llano and Mason counties. The Precambrian rocks were less resistant to weathering and erosion than younger geological units. As a result, a topographic depression exists at the central portion of the study area in addition to a regional ground elevation decreasing from west to east (Figure 2.1.3). Locally, the rivers and streams have cut in the bedrock and formed narrow valleys. The elevation of the ground surface varies from over 2,000 feet above mean sea level in southwest of the study area to less than 700 feet above mean sea level at the Colorado River near the border between Burnet and Travis counties.

The climate in the study area is classified as Subtropical Subhumid represented by hot summers and dry winters (Larkin and Bomer, 1983) (Figure 2.1.4). According to the National Weather Service (2013), the majority of the study area falls in the Edwards Plateau Climate Division (Figure 2.1.5). According to Thornwaite (1931), the Edwards Plateau has a meso-thermal, semiarid to arid climate. The average annual temperature in the study area ranges from

approximately 62 degrees Fahrenheit to the southwest in Gillespie, Kerr, and Kimble counties to about 69 degrees Fahrenheit to the east in Burnet, Blanco, and Travis counties (Figure 2.1.6). In general, the temperature is higher in valleys and lower along mountain ridges.

Based on the Parameter-elevation Regressions on Independent Slopes Model (PRISM) precipitation dataset from Oregon State University (PRISM Climate Group, 2013), the average annual precipitation across the study area based on the period from 1981 to 2010 ranges from about 24 inches in central Kimble County to about 36 inches in central Kendall County and decreases from east to west (Figure 2.1.7). Data collected from the study area and its vicinity between 1950 and 2010 show that precipitation could -varies significantly from year to year (Figures 2.1.8 through 2.1.11). Please note that the annual precipitation data were calculated using monthly data and any years without the complete 12-month data were not used for the annual precipitation calculation. The average monthly precipitation calculated from the same dataset shows bimodal distribution with two relatively high precipitation periods: May through June and August through September (Figures 2.1.12 through 2.1.15).

The average annual net pan evaporation rate between 1954 and 2012 increases from east to west, ranging from 53 to 65 inches per year (Figure 2.1.16). The annual pan evaporation rate significantly exceeds the annual average rainfall, with the deficit increasing from east to west. Average monthly variations in lake surface evaporation between 1954 and 2012 are shown in Figures 2.1.17 and 2.1.18 for eight quadrangles in the study area. As shown in Figures 2.1.17 and 2.1.18, the average lake evaporation is highest in July and lowest in January and December.

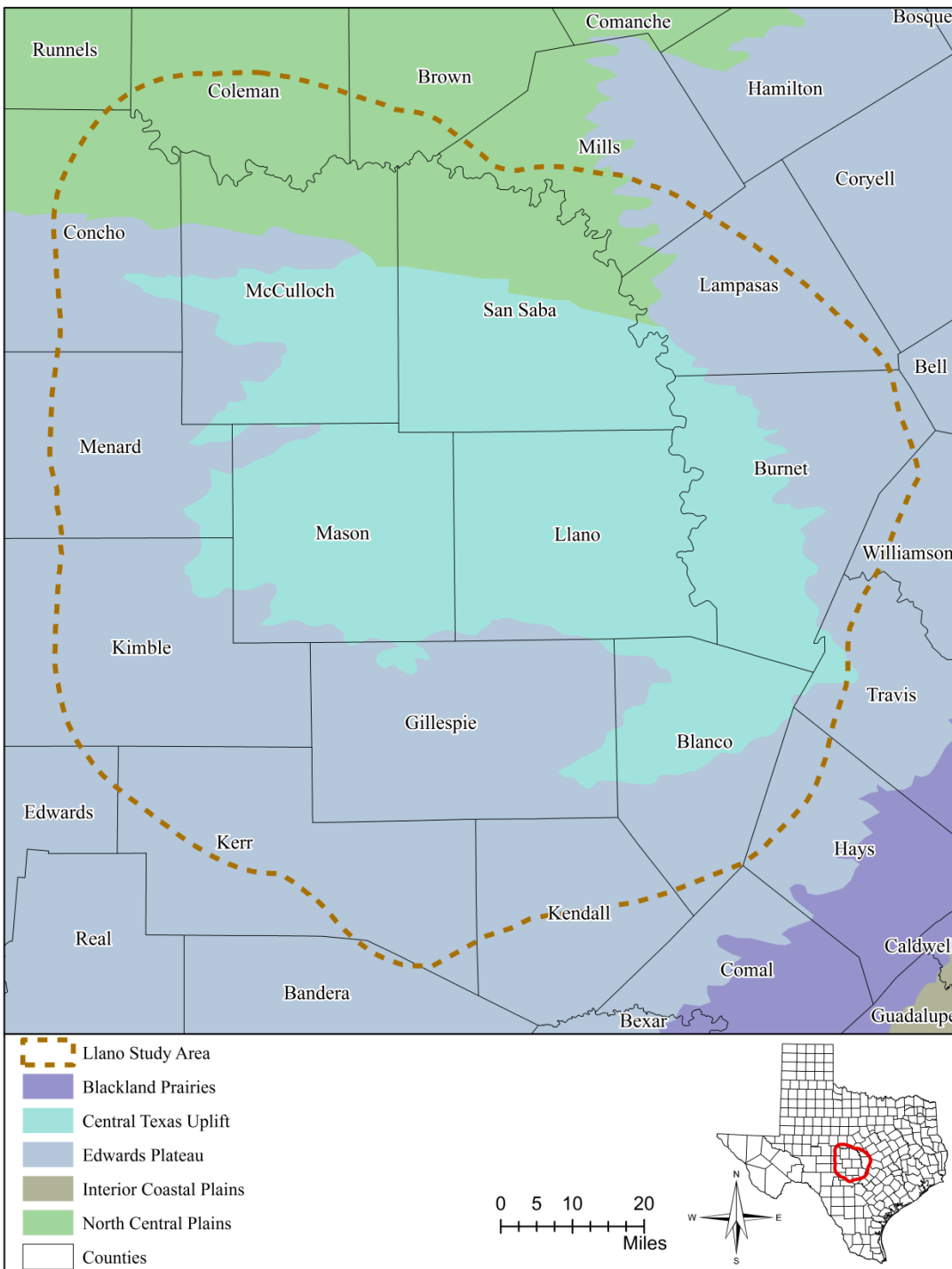


Figure 2.1.1 Physiographic provinces in study area (Wermund, 1996)

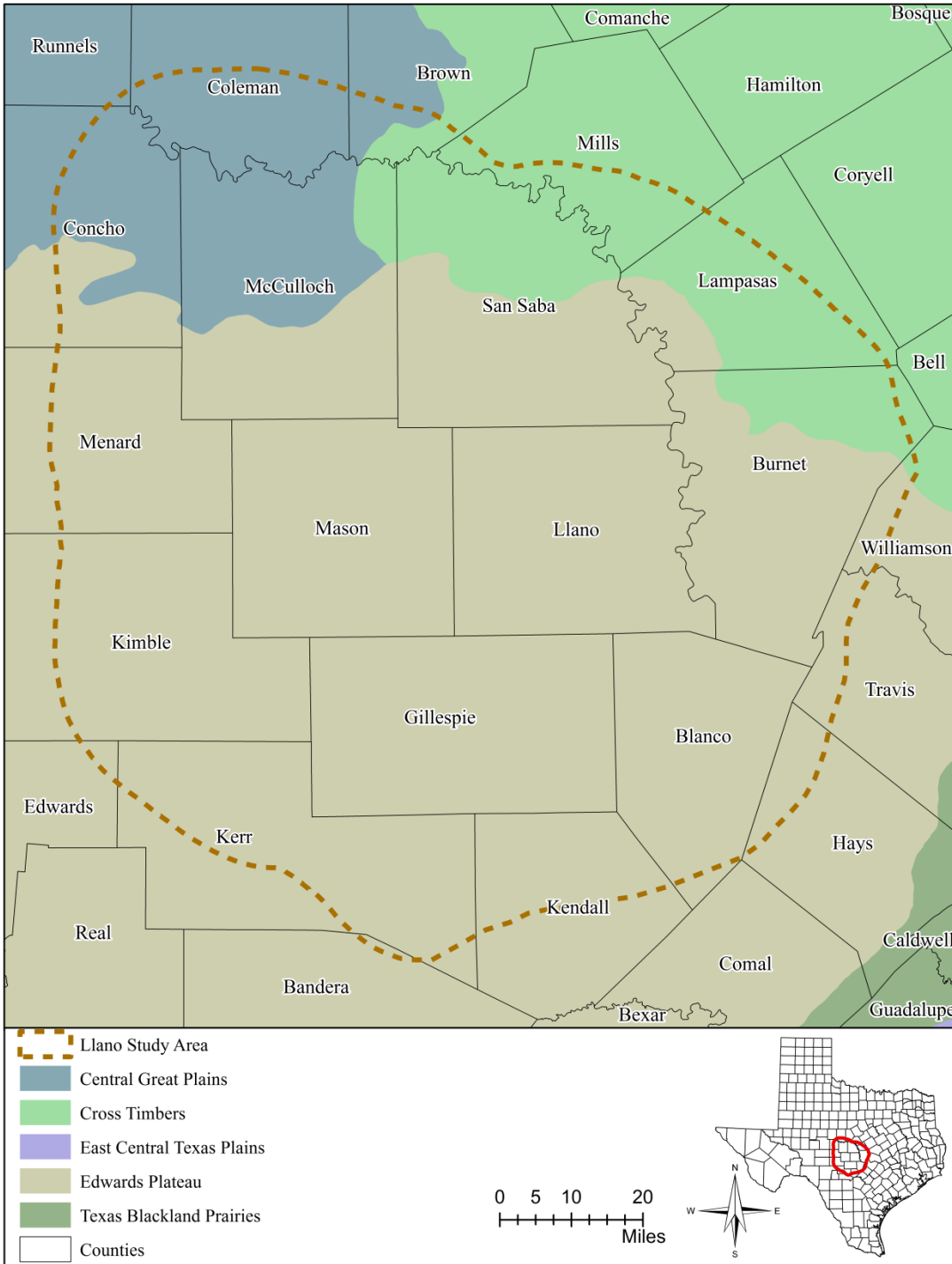


Figure 2.1.2 Level III ecological regions in study area (U.S. Environmental Protection Agency, 2013).

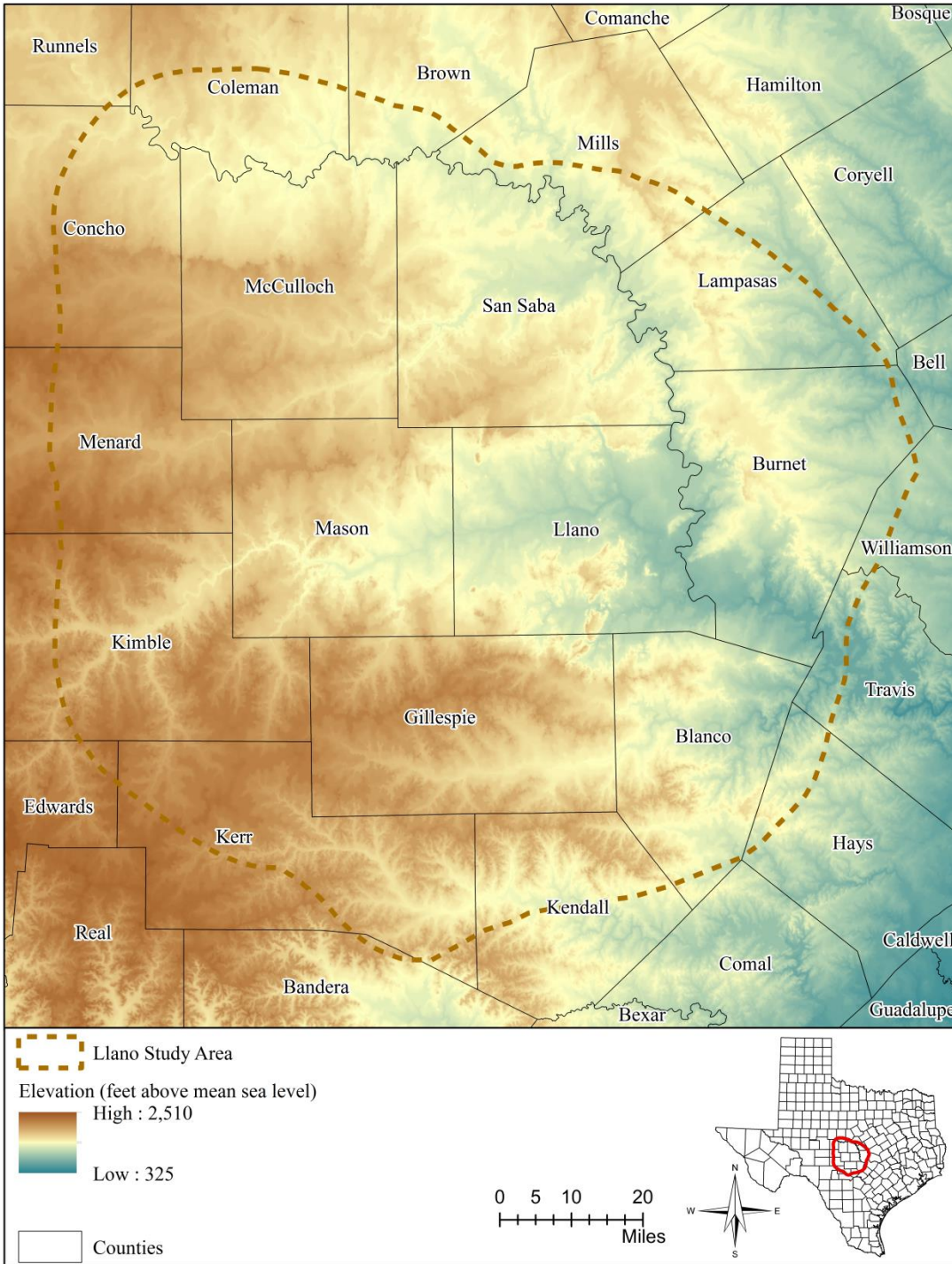


Figure 2.1.3 Topographic map of study area showing land surface elevation in feet above mean sea level. Elevation data are from U.S. Geological Survey Digital Elevation Model with a resolution of 30 meters by 30 meters.

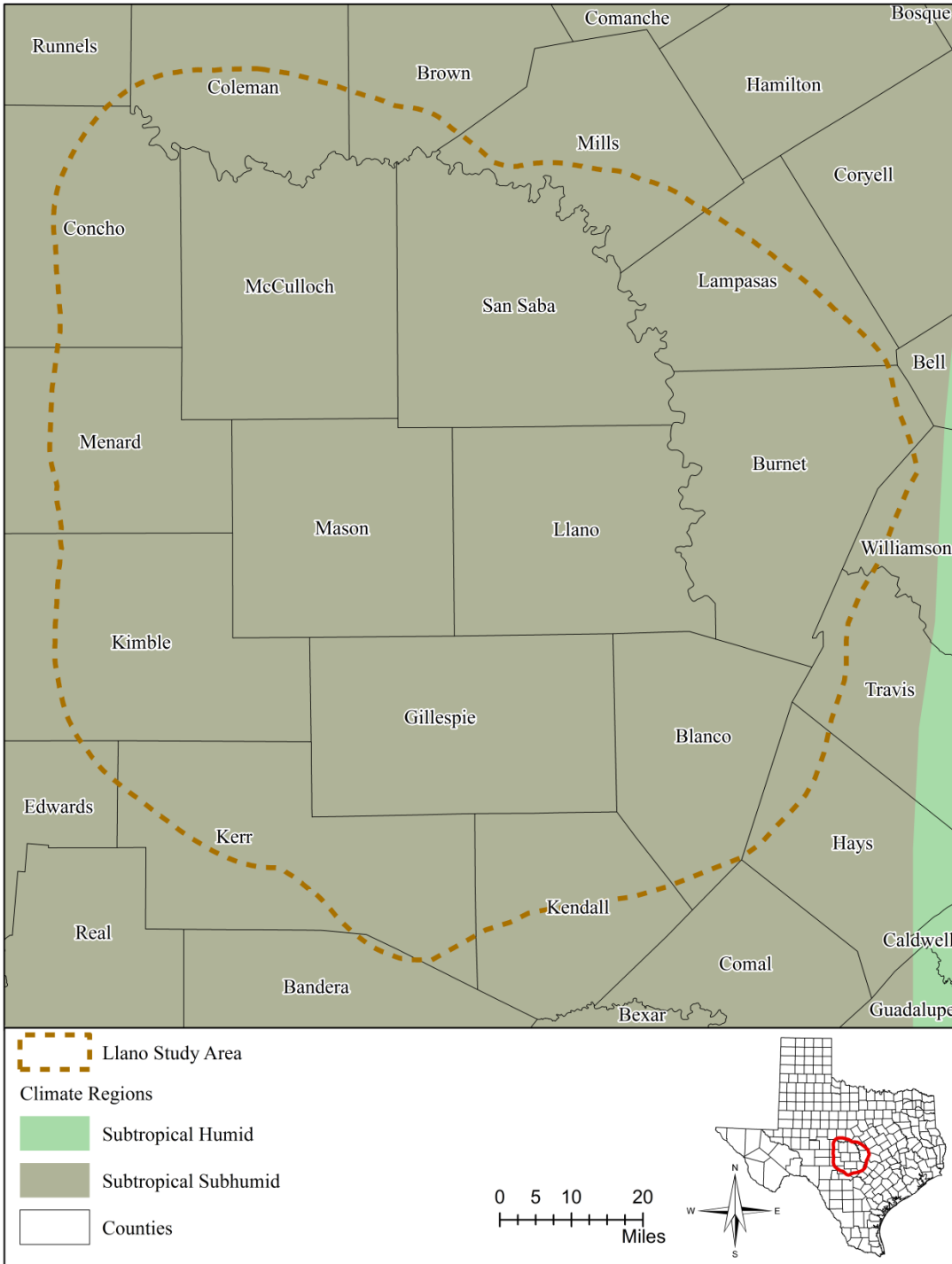


Figure 2.1.4 Climate classifications of study area (based on Larkin and Bomar, 1983).

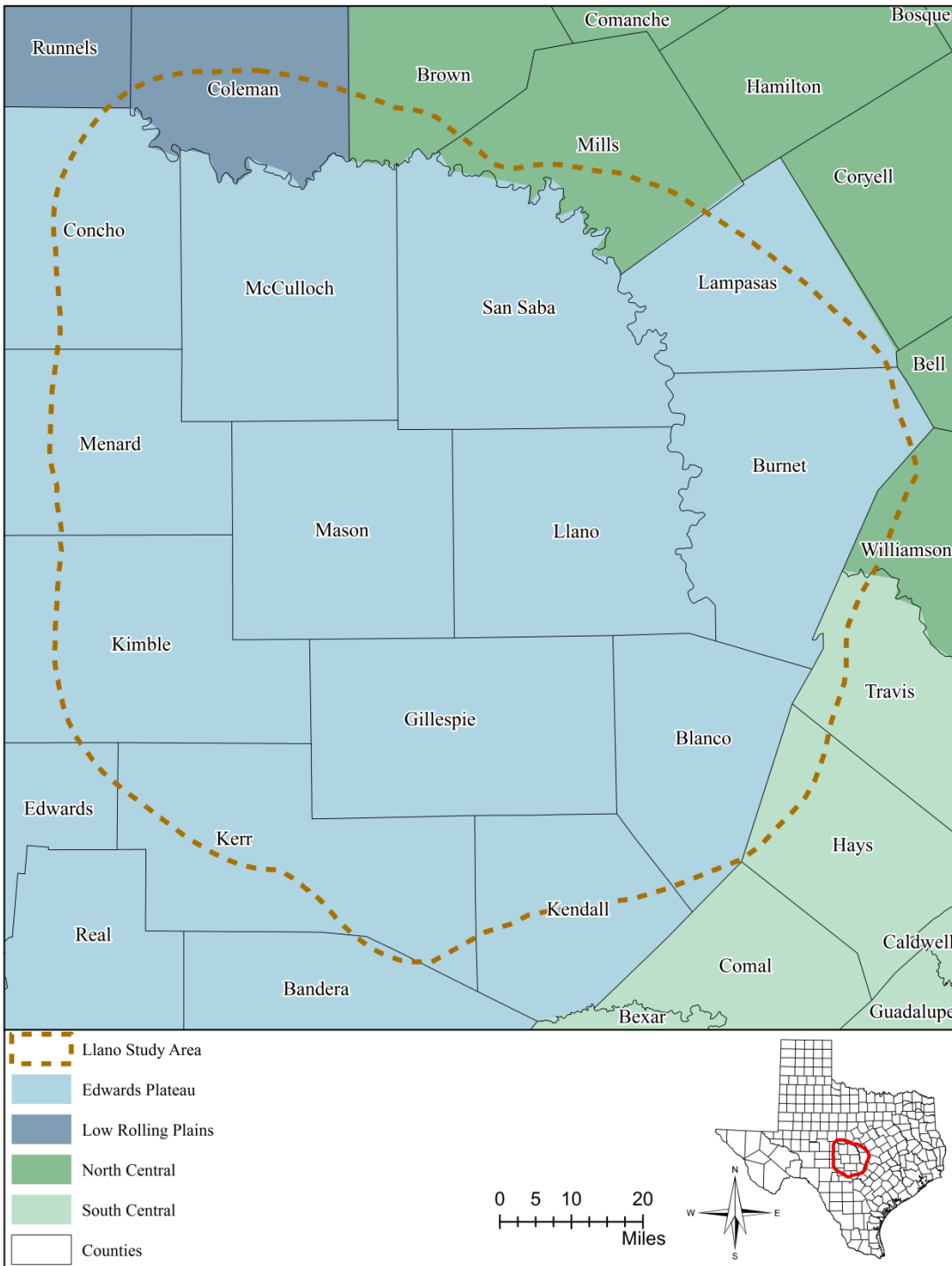


Figure 2.1.5 Climate classifications of study area (based on National Weather Service, 2013).

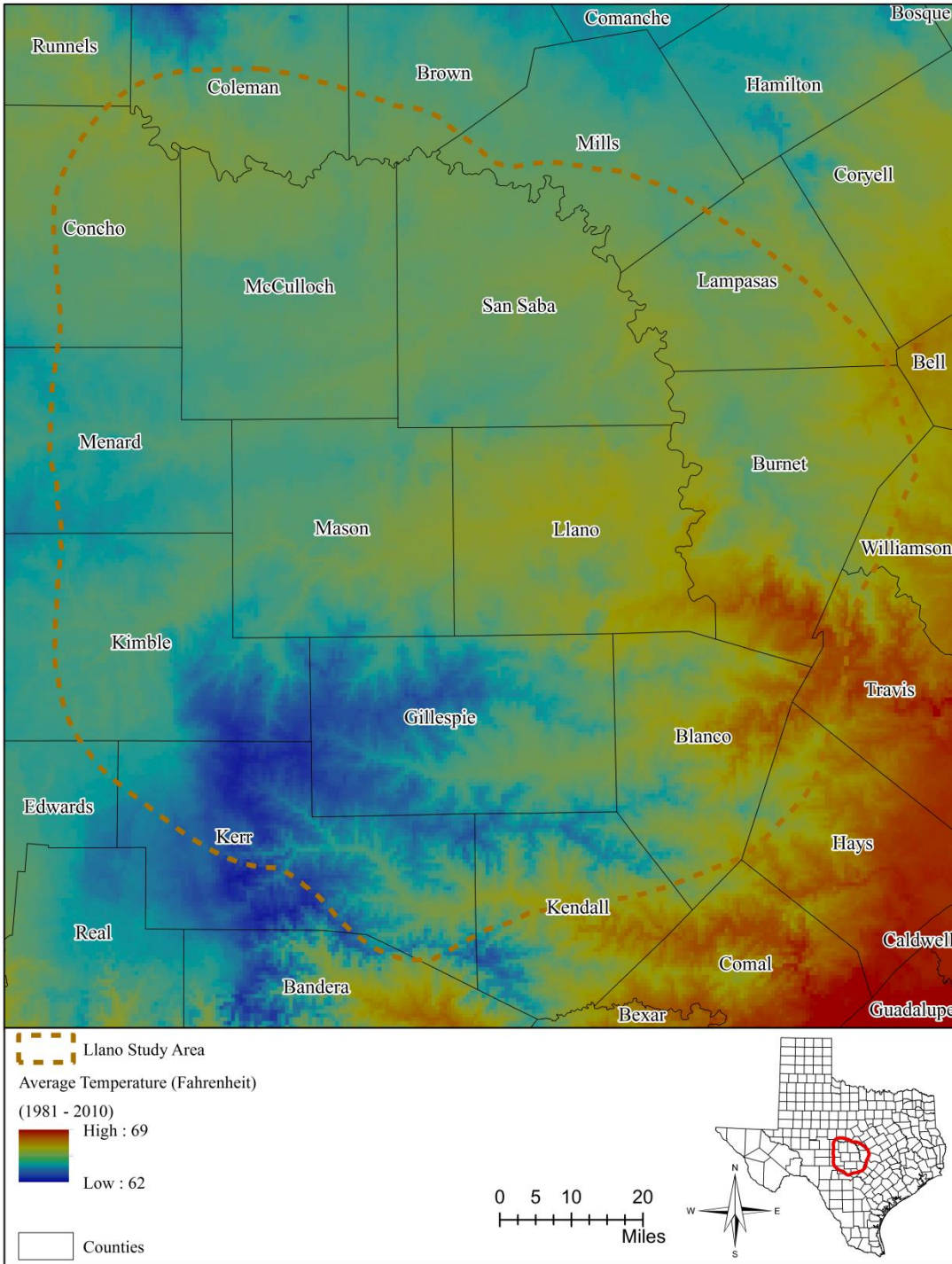


Figure 2.1.6 Average annual air temperature in degrees Fahrenheit for study area. Temperature data are from Parameter-elevation Regressions on Independent Slopes Model (PRISM) temperature dataset from Oregon State University (PRISM Climate Group, 2013).

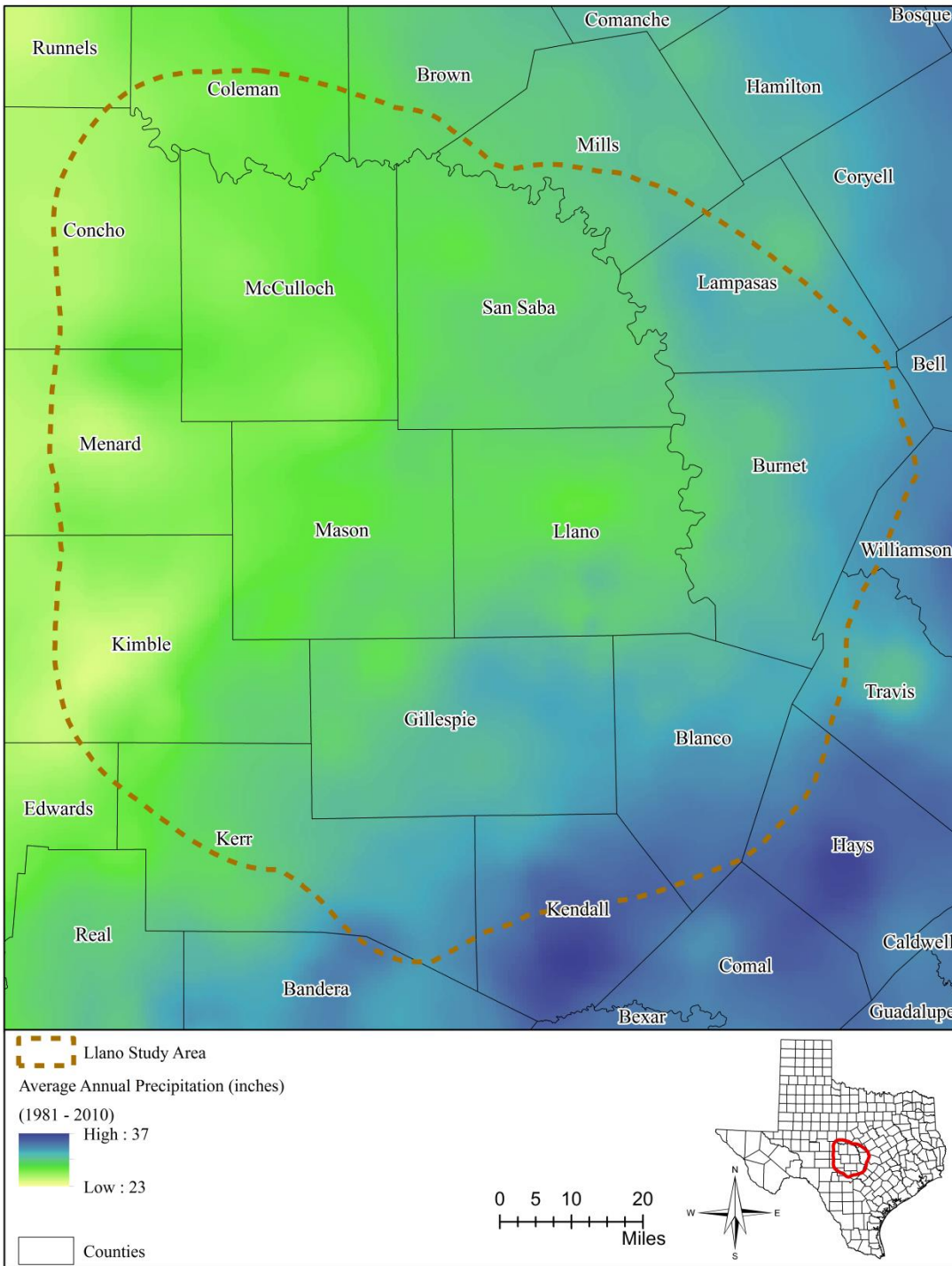


Figure 2.1.7 Average annual precipitation in study area for time period 1981 to 2010 from Parameter-elevation Relationships on Independent Slopes Model (PRISM) (PRISM Climate Group, 2013).

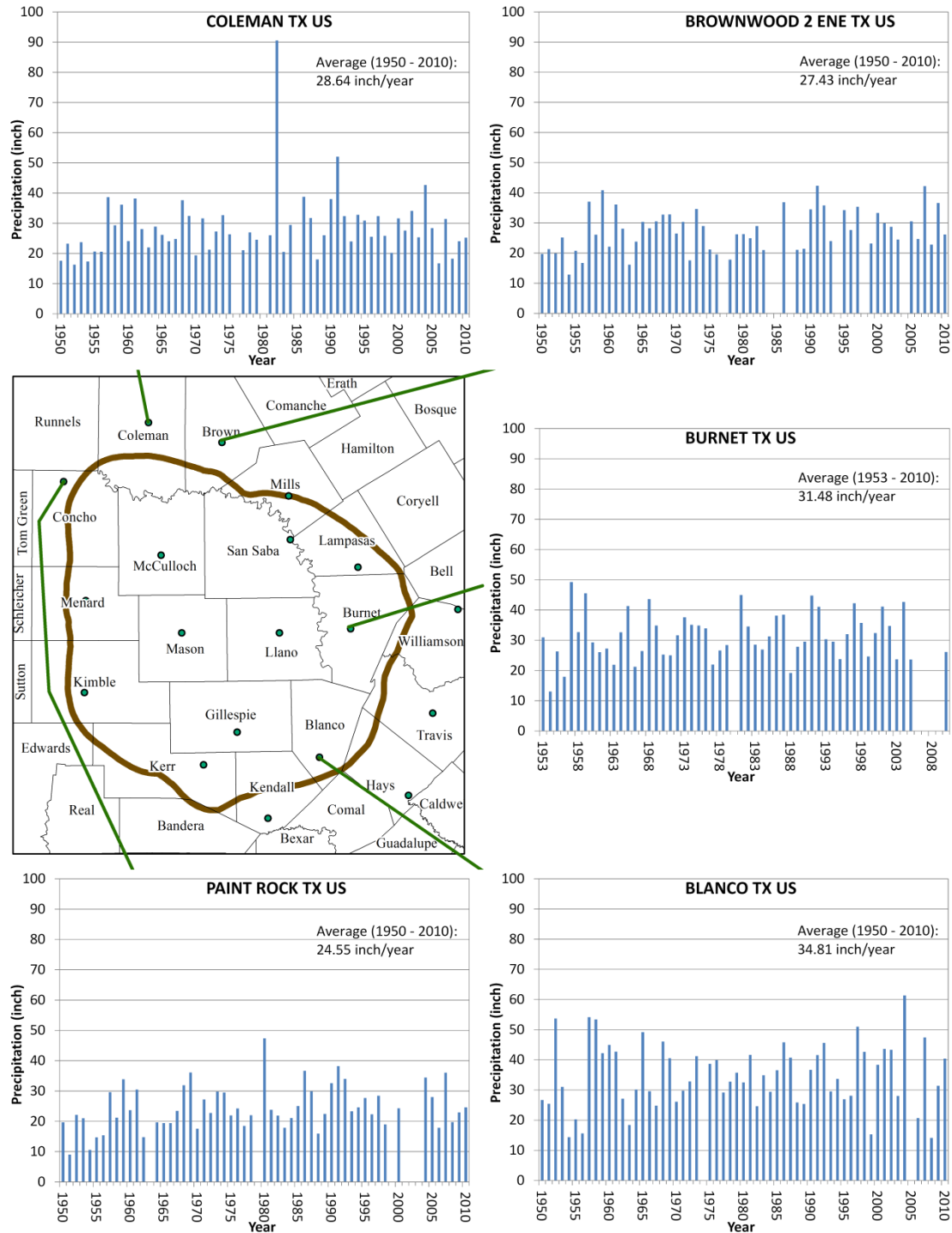


Figure 2.1.8 Measured annual precipitation at stations in Blanco, Brown (Brownwood), Burnet, Coleman, and Concho (Paint Rock) counties (National Climatic Data Center, 2014).

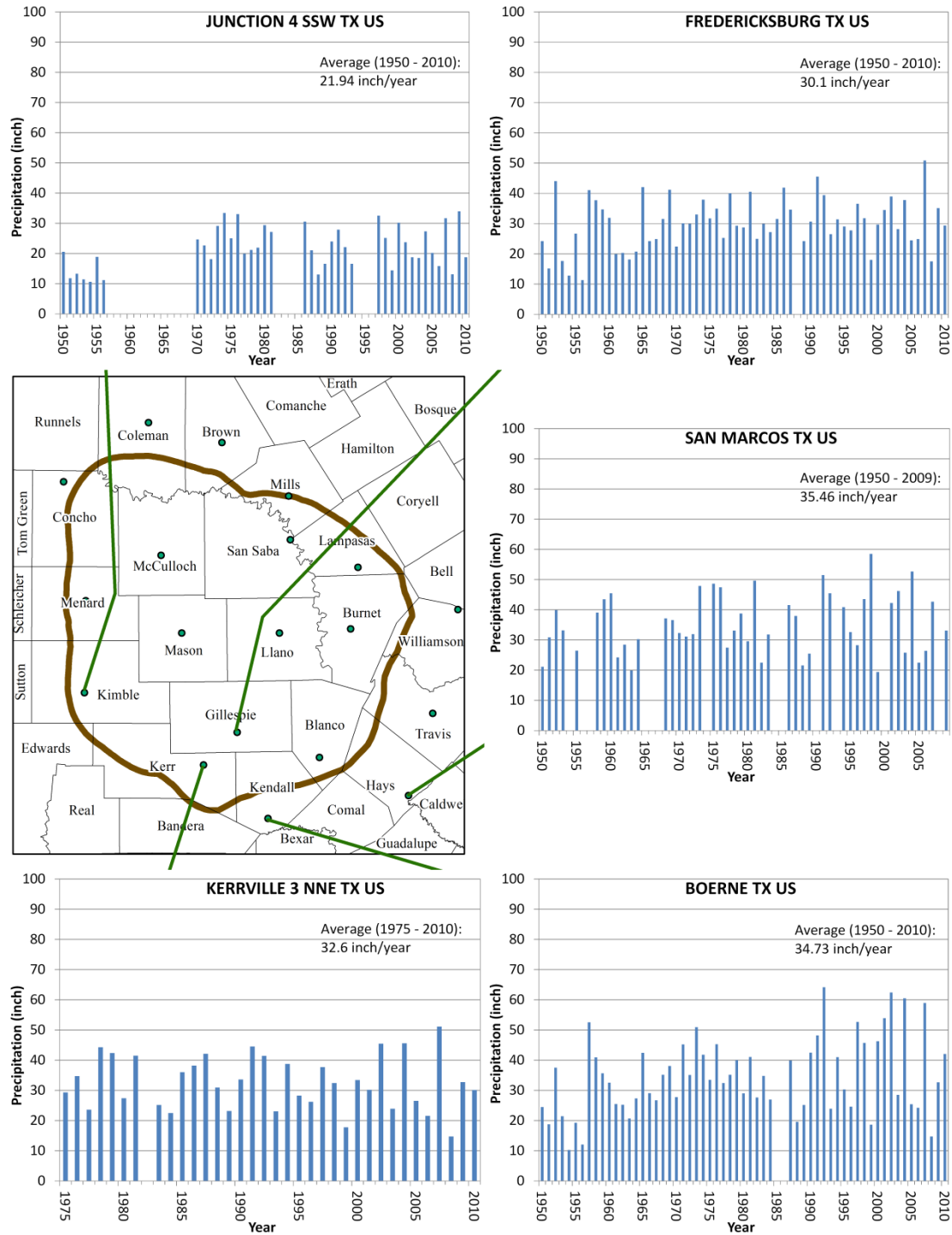


Figure 2.1.9 Measured annual precipitation at stations in Gillespie (Fredericksburg), Hays (San Marcos), Kendall (Boerne), Kerr (Kerrville), and Kimble (Junction) counties (National Climatic Data Center, 2014).

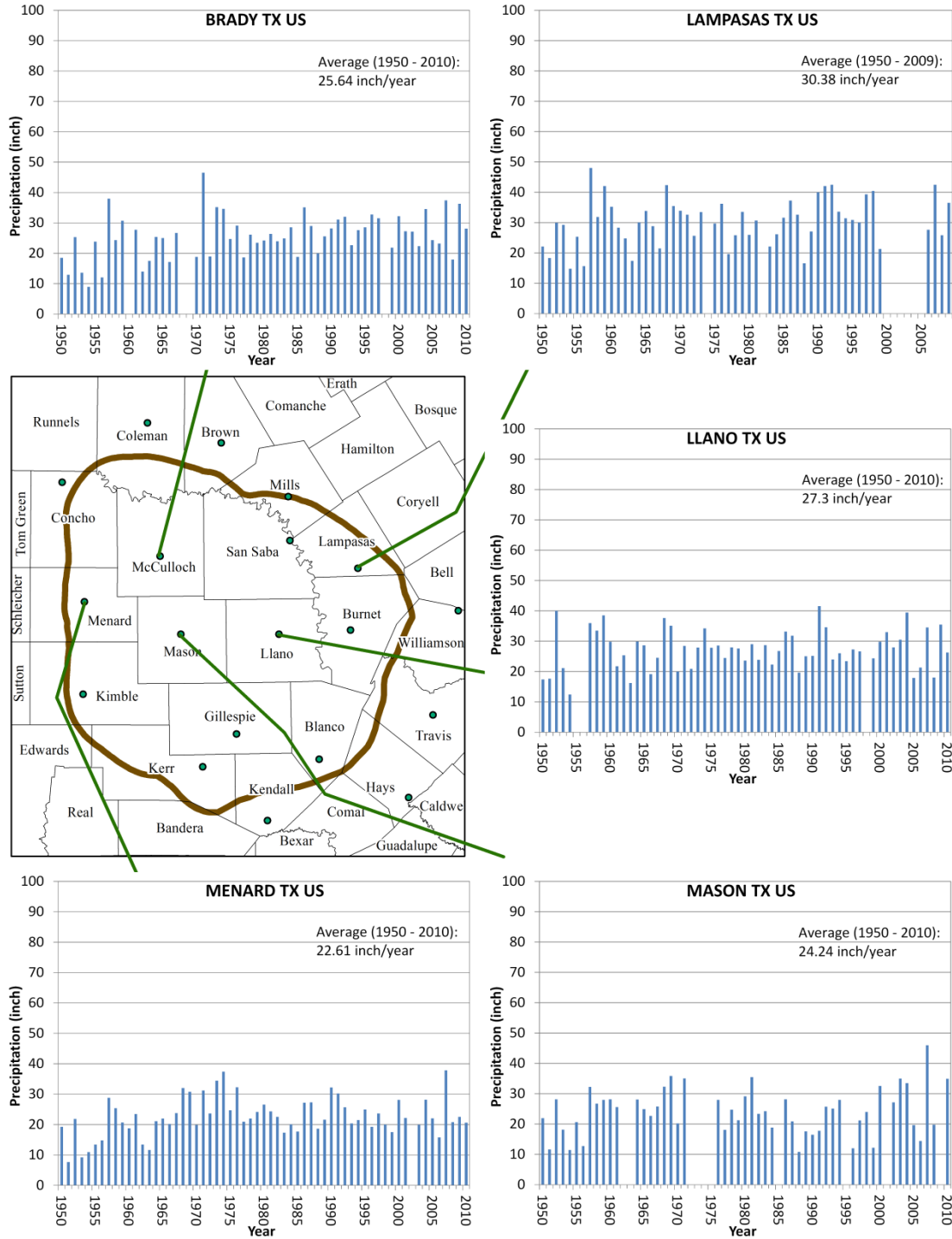


Figure 2.1.10 Measured annual precipitation at stations in Lampasas, Llano, Mason, McCulloch (Brady), and Menard counties (National Climatic Data Center, 2014).

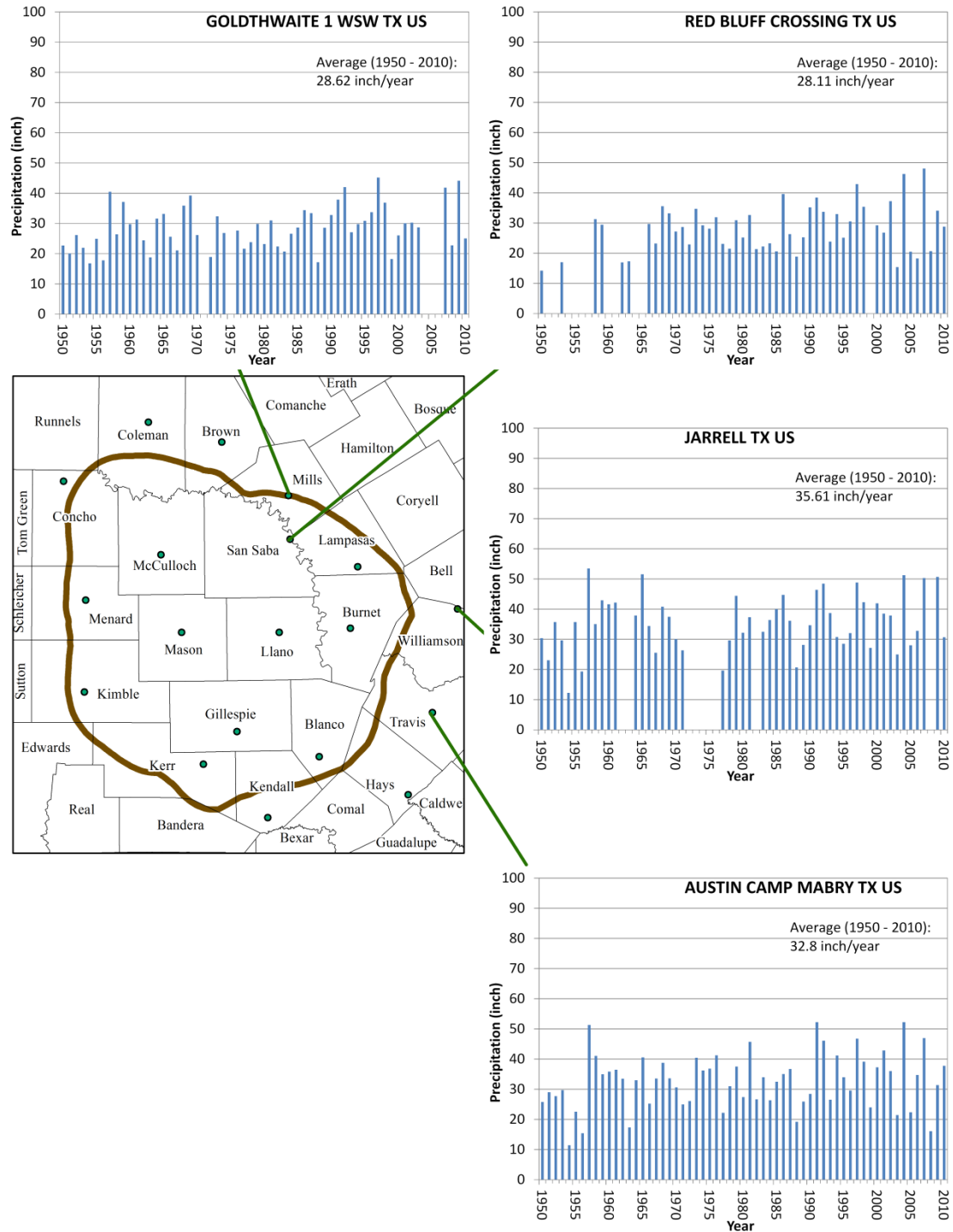


Figure 2.1.11 Measured annual precipitation at stations in Mills (Goldthwaite), San Saba (Red Bluff Crossing), Travis (Austin), and Williamson (Jarrell) counties (National Climatic Data Center, 2014).

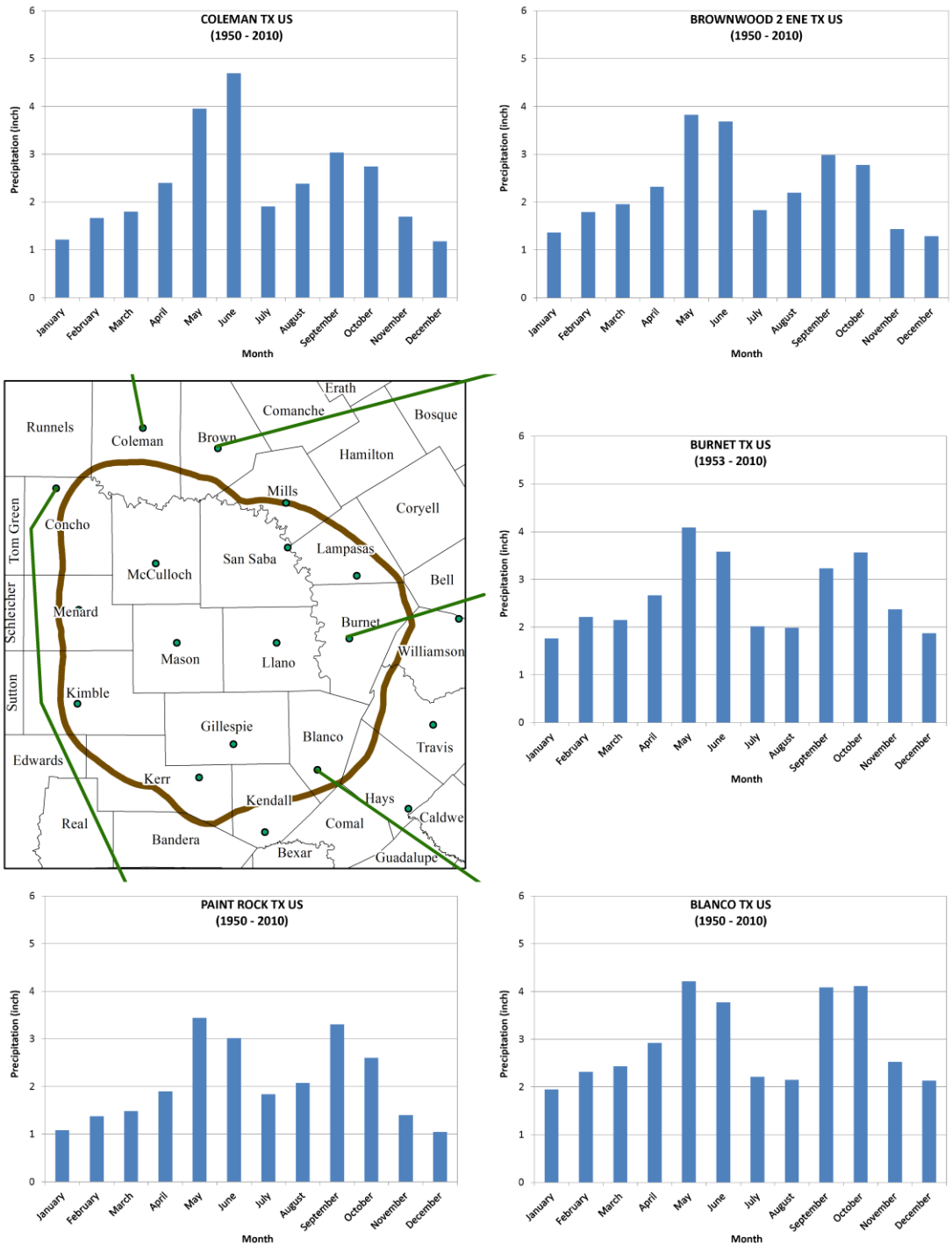


Figure 2.1.12 Measured average monthly precipitation at stations in Blanco, Brown (Brownwood), Burnet, Coleman, and Concho (Paint Rock) counties (National Climatic Data Center, 2014).

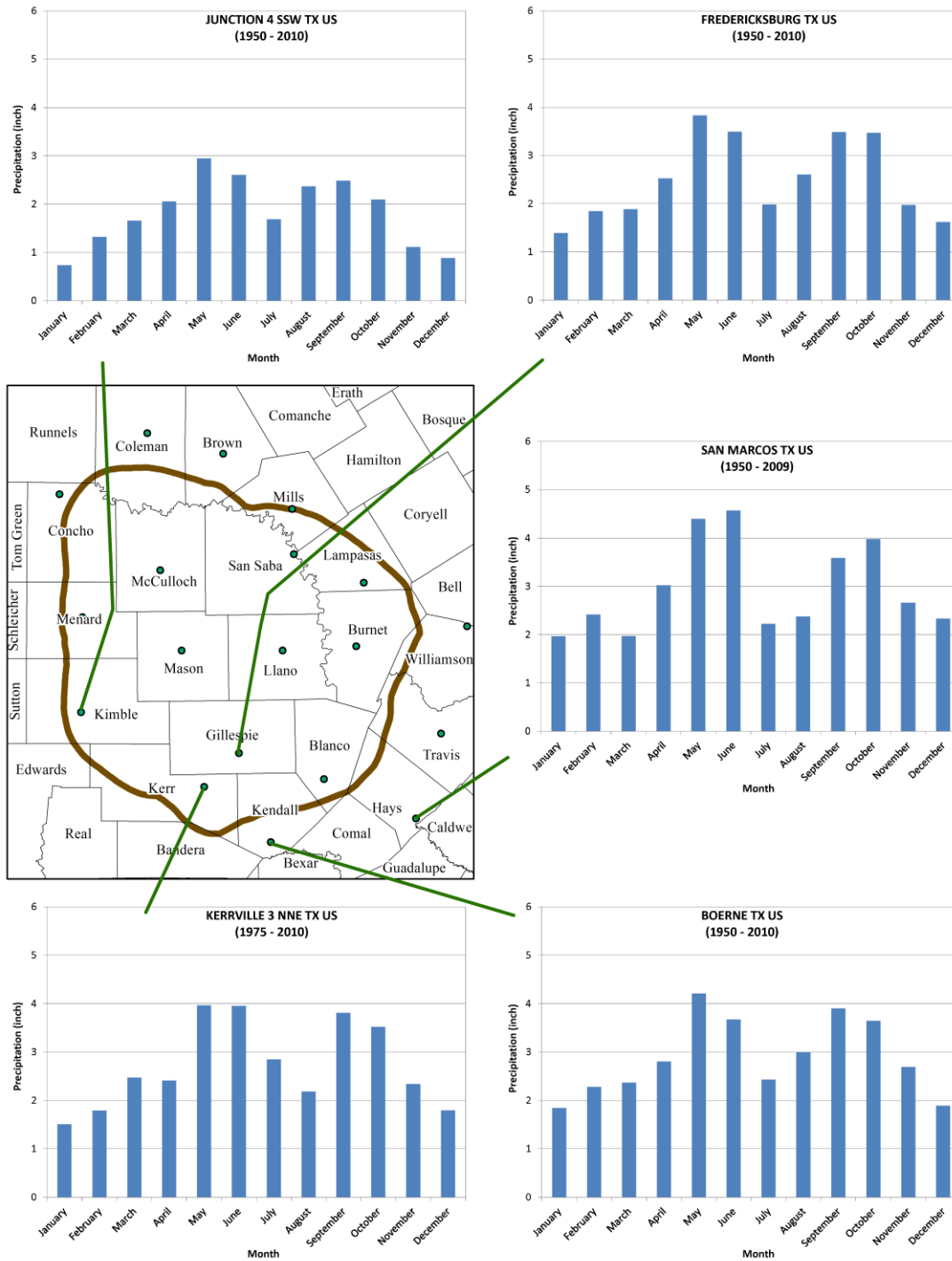


Figure 2.1.13 Measured average monthly precipitation at stations in Gillespie (Fredericksburg), Hays (San Marcos), Kendall (Boerne), Kerr (Kerrville), and Kimble (Junction) counties (National Climatic Data Center, 2014).

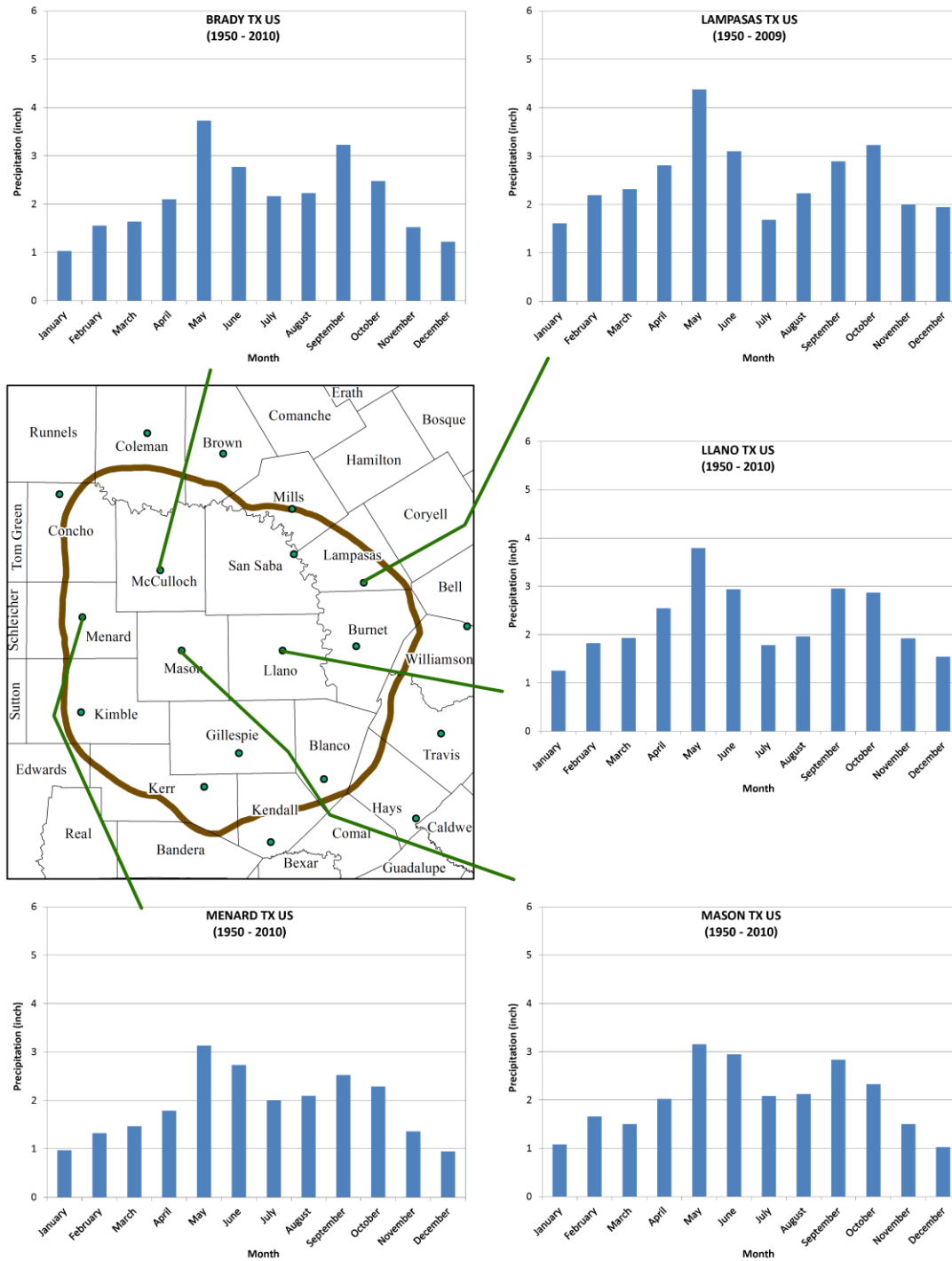


Figure 2.1.14 Measured average monthly precipitation at stations in Lampasas, Llano, Mason, McCulloch (Brady), and Menard counties (National Climatic Data Center, 2014).

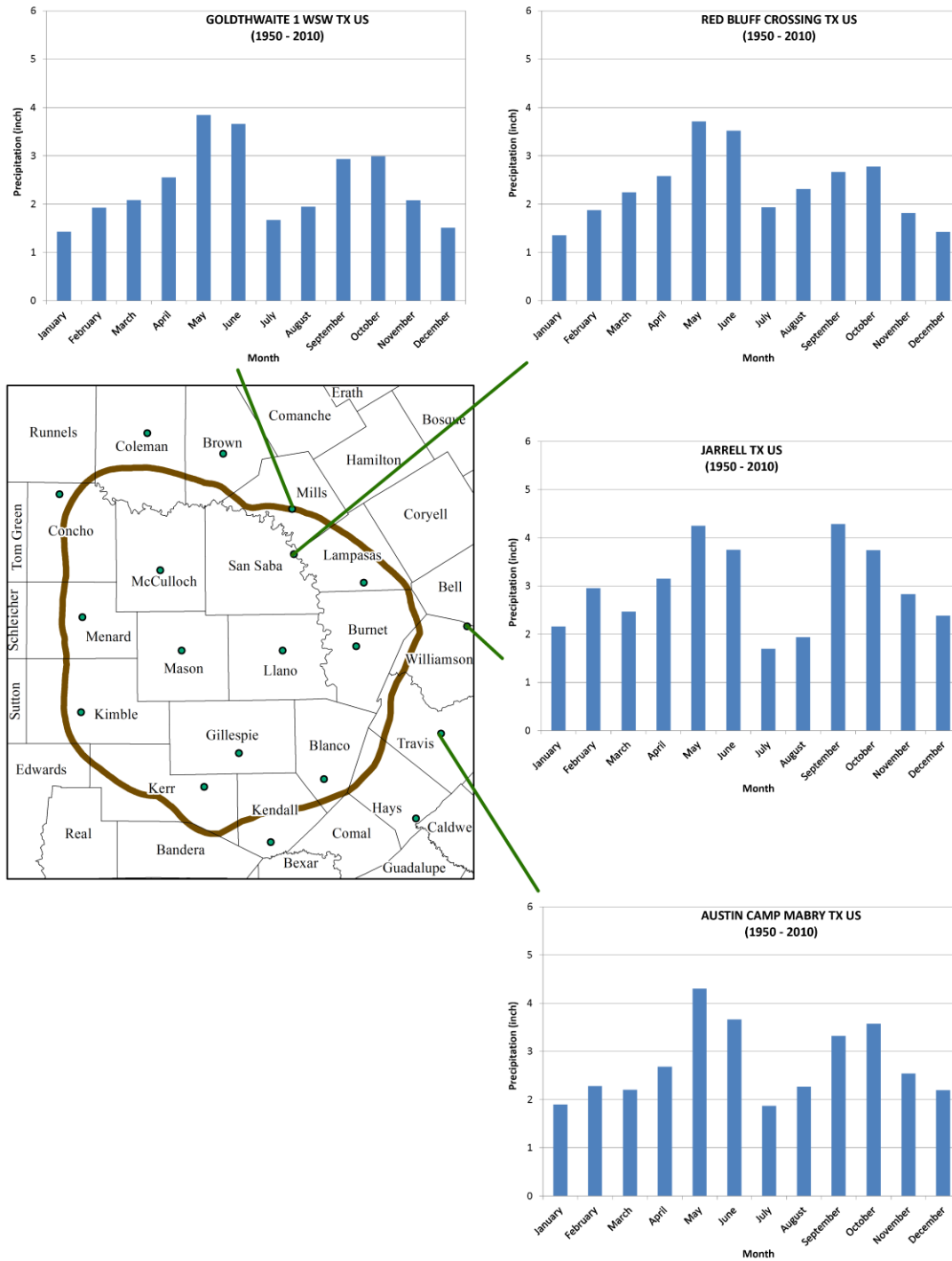


Figure 2.1.15 Measured average monthly precipitation at stations in Mills (Goldthwaite), San Saba (Red Bluff Crossing), Travis (Austin), and Williamson (Jarrell) counties (National Climatic Data Center, 2014).

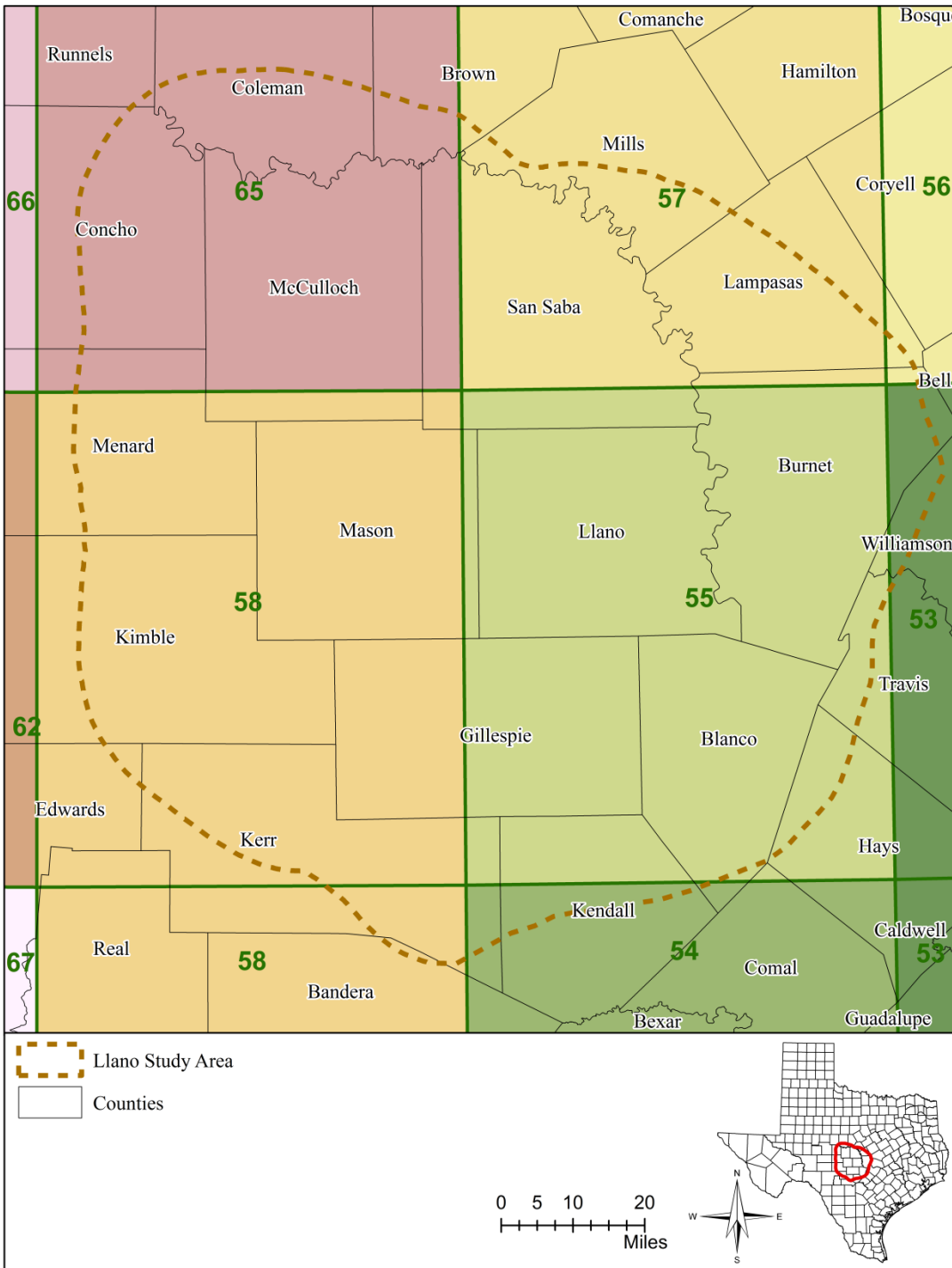


Figure 2.1.16 Average annual net pan evaporation rate (inch per year) between 1954 and 2012 at selected quadrangles in study area (TWDB, 2013h).

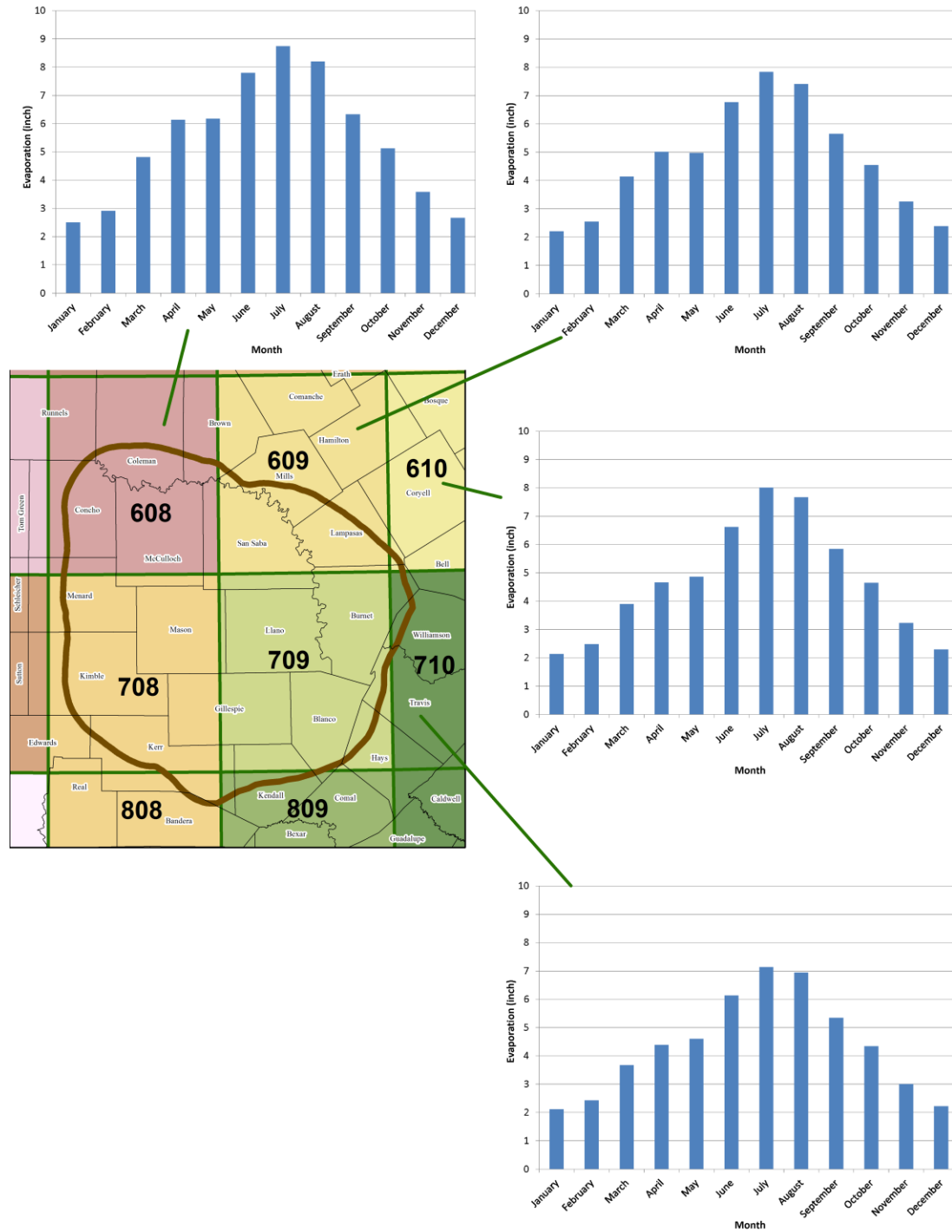


Figure 2.1.17 Average monthly lake surface evaporation between 1954 and 2012 at selected quadrangles 608, 609, 610, and 710 in study area (TWDB, 2013h).

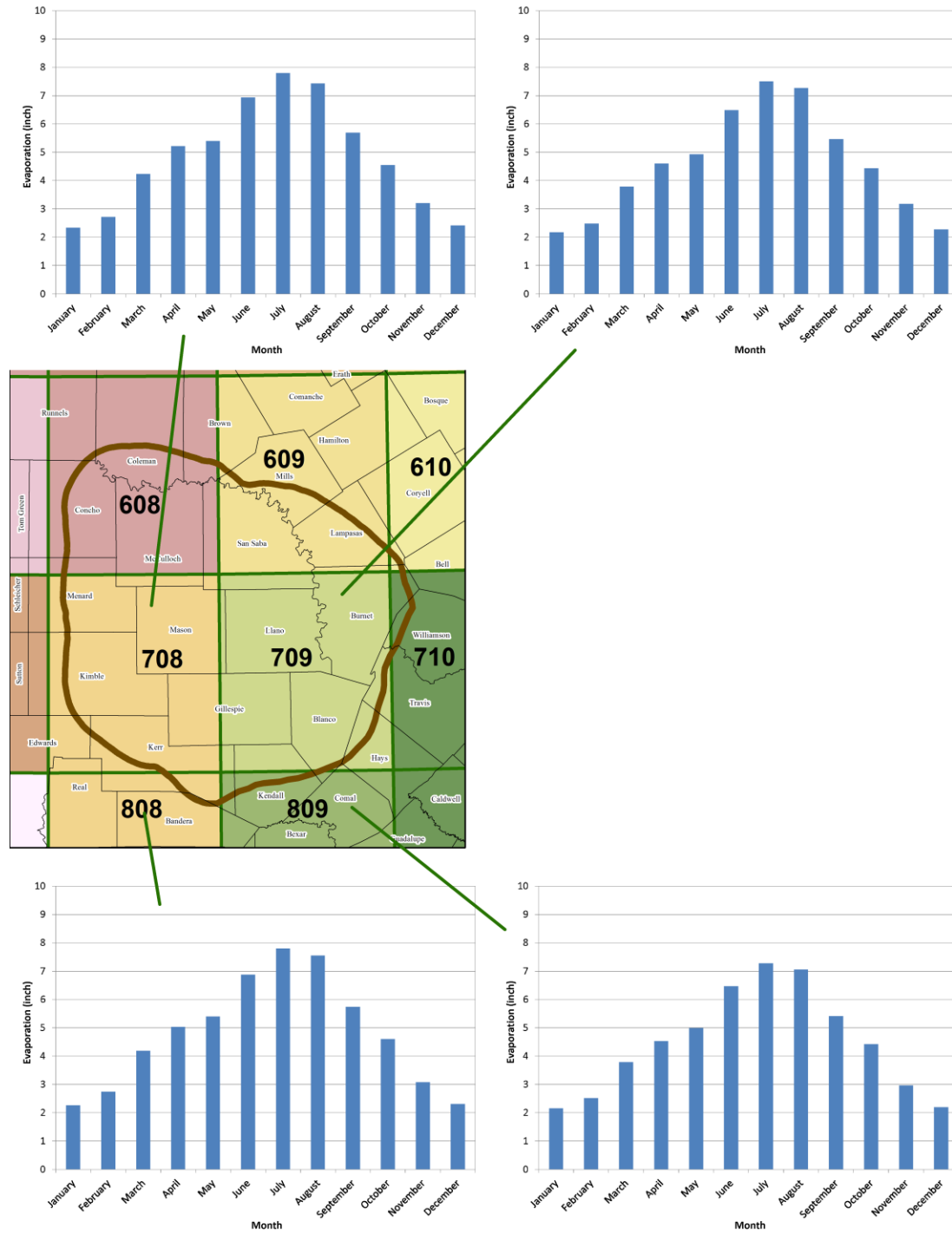


Figure 2.1.18 Average monthly lake surface evaporation between 1954 and 2012 at selected quadrangles 708, 709, 808, and 809 in study area (TWDB, 2013h)

2.2 Geology

This section provides a brief discussion of the geology of the study area. The discussion is divided into the structural setting, geologic history, structure and texture, and surface geology through the study area.

2.2.1. Structural Setting

The Llano Uplift is a structural high with 2 to 3 kilometers of relief relative to the equivalent geologic units in the Fort Worth and Kerr basins to the northeast and southwest, respectively (Johnson (2004) (Figure 2.2.1). Kier and others (1979) concluded that this structural high or dome, along with the Fort Worth and Kerr basins, was formed by the Ouachita Orogeny during the early to middle Pennsylvanian. The Ouachita Orogeny also left numerous normal faults with grabens and horsts in the Llano Uplift region. In general, the dome area has been experiencing greater erosion, due to the rising of the area and lesser resistance of the older rock units to weathering, than the Cretaceous rocks on the flanks of the uplift. As a result, the Llano Uplift region is, in fact, topographically low at the middle. The Balcones Fault Zone (formed during the Mesozoic Era) is located farther to the southeast and outside of the study area. These main geologic structures are schematically shown in Figures 2.2.1 and 2.2.2.

2.2.2. Geologic History

The study area includes a variety of sedimentary, igneous, and metamorphic rocks ranging from the Precambrian to modern ages and is believed to be the most structurally and stratigraphically complex area in Texas. The complexity of the stratigraphy originates from the dynamic transitions through geologic time among the sedimentary, metamorphic, and igneous rocks that was further enhanced by a series of tectonic events over space and time. The following sections summarize the theories and findings that may explain how the study area has evolved and became what it is today. The stratigraphy and its hydrogeologic classification of the study area are presented in Table 2.2.1.

2.2.2.1 Precambrian Era

The Precambrian rocks exposed in the Llano Uplift region consist of older metamorphic (gneisses, amphibolites, and schists) and younger intrusive igneous (granites) rocks (Barnes and Bell, 1977; McGhee, 1963), which were formed along the southern margin of the North American Craton (Laurentia) due to the Grenville Orogeny over 1.3 to 1.1 billion years ago (Hoh and Hunt, 2004). According to Mosher (2004), the Grenville Orogeny lasted more than 300 million years.

For the next 0.6 billion years, these Precambrian rocks experienced uplift and significant erosion (Long, 2004); however, the timings of these events are unknown (Ewing, 2004). Fracture sets and faults of multiple orientations are common in these basement rocks and some evidence favors pre-Pennsylvanian origin (Johnson, 2004). The erosion and faulting created a Precambrian paleotopographic relief up to 800 feet (Barnes and Bell, 1977), which controlled the depositional patterns of the Late Cambrian Riley Formation (including the Hickory, Cap Mountain, and Lion Mountain members) (Krause, 1996). Bluntzer (1992) believed that some of the Precambrian granite highs or knobs had penetrated both the Paleozoic and Cretaceous rocks in Gillespie and Blanco counties. Though some wells are completed in Precambrian crystalline rocks, they are not included in this study due to their low groundwater production.

2.2.2.2 Cambrian Period

From the late Cambrian Period to the early Ordovician Period, nearly all of Texas had generally undergone subsidence. The Cambrian sea encroached from the south with the deposition of the Moore Hollow Group. The Moore Hollow Group includes the older Riley and younger Wilberns formations.

2.2.2.2.1 Riley Formation

The Riley Formation consists of three members: the Hickory, Cap Mountain, and Lion Mountain Members, as discussed below.

Hickory Member - The Hickory Member, the oldest member of the Riley Formation, was deposited directly on the Precambrian irregular surface around the Precambrian knobs (Long, 2004). The Hickory Member is a mixture of terrestrial and marine sandstones, siltstones, and mudstones (Krause, 1996) deposited in a variety of environments including alluvial fans, braided streams, eolian dunes, shallow marine shelf, and minor lagoons (Cornish, 1975; Krause, 1996; McBride and others, 2002). The deposition of the Hickory Member was the result of a transgressing sea from south to north with a similar pace between the deposition and subsidence (Watson, 1980). The source area was believed to be at north or northwest. Wilson (1962) and Black (1988) divided the Hickory Member into three units based on sedimentary characteristics: rounded to sub-rounded quartz sand in lower unit, silty or argillaceous sand in middle unit, and hematite-cemented well-rounded sand in upper unit. Locally, the lower unit may consist of medium to coarse sandstone and conglomerates (Cornish, 1975; Daniel B. Stephens & Associates, Inc., 2005). The lithofacies are gradational both upward and southward within the Cap Mountain Limestone Member (Wilson, 1962; Watson, 1980; Krause, 1996). As a result, the upper Hickory can be equivalent to the lower Cap Mountain. According to Standen and Ruggiero (2007), the average dip of the Hickory Member is approximately 1.5 degrees, but varies throughout the study area; the Hickory Member pinches out on the central portion of the Llano Uplift region and generally thickens away in all directions. However, this radial distribution of the Hickory Member thickness is probably related to the erosion rather than the original deposition. In general, the Hickory Member thickens from north to south ranging from zero feet at the Llano Uplift or Precambrian knobs to about 1,000 feet in Kerr County to the south in the study area. The top and base of the Hickory Member are strong geophysical log correlation surfaces (Standen and Ruggiero, 2007) with relatively high gamma readings. The Hickory Member is considered the primary aquifer in the Central portion of the Llano Uplift region and “provides moderate to large amounts of good-quality water to wells down to the depths in excess of 3,000 feet” (Preston and others, 1996).

Cap Mountain Member - The Cap Mountain Member can be divided into three units: interbeds of sandstone, siltstone and impure limestone at the bottom; siltstone at the middle; and glauconitic limestone at the top (Watson, 1980; Krause, 1996). The lower unit represents a deepening marine shelf environment; the middle (silt) unit was deposited when the subsidence exceeded the rate of sedimentation; and the upper unit indicated a similar pace between the subsidence and sedimentation (Watson, 1980). Locally the Cap Mountain Member was directly deposited on the Precambrian rocks where the Hickory Member is absent (Preston and others, 1996; Standen and Ruggiero, 2007). This often occurs at the Precambrian knobs or farther north relative to the Hickory Member. Because the relief along the top of the Hickory Member is not as great as the Precambrian surface, the thickness of the Cap Mountain Member is more evenly

distributed than the Hickory Member (Krause, 1996). The Cap Mountain Member also thins towards the Precambrian knobs and the Central portion of the Llano Uplift region, and thickens toward the south or southwest. Thickness of this unit ranges from zero to 650 feet in the study area (Preston and others, 1996; Standen and Ruggiero, 2007). This member is considered to be a confining unit or aquitard.

Lion Mountain Member - The Lion Mountain Member consists of glauconitic sandstone, sandy limestone with minor shale, and limestone (Barnes, 1963; Barnes and Bell, 1977). Siltstone, shale, and limestone with burrows mainly exist at the lower part, while the upper part is predominantly crossbedded sandstone (Dekker, 1966). The glauconitic sandstone is characterized by green to olive green color and crossbedding, while the limestone often exists as white lenses of glauconitic trilobite coquinite (Dekker, 1966; Watson, 1980). The crossbeds in the Lion Mountain sandstone show bimodal dip directions: northeast and southwest (Dekker, 1966). The sand unit of the Lion Mountain Member was deposited in shallow marine environment during a regressive phase (Krause, 1996) with strong tidal influence (Dekker, 1966). Based on the mineral character, Dekker (1966) concluded that the terrigenous source materials of the Lion Mountain Member were from the north or northwest where granite was the source rock. The siltstone, shale, and limestone were deposited in a low to moderate energy environment such as a bay or estuarine setting (Dekker, 1966). The thickness of the Lion Mountain Member ranges from about 70 feet in McCulloch County to less than 50 feet in Burnet and Blanco counties; it pinches out against the Llano Uplift Precambrian basement rocks (Dekker, 1966). Locally, the Lion Mountain Member could also directly overlay the Precambrian rocks around the Precambrian knobs where the Hickory and Cap Mountain members are missing. The Lion Mountain Member thins toward the east and southeast and may cease to exist under the Ouachita fold belt (Barnes and Bell, 1977). In the Llano Uplift region, the Lion Mountain Member is overlain by the glauconite-poor Welge Member with a traceable unconformity; but the contact between the Lion Mountain and Welge members may become gradational farther to the south and southeast from the Llano Uplift region (Barnes and Bell, 1977). No matter what the contact could be, the Lion Mountain Member is hydraulically connected with the overlying Welge Member (Standen and Ruggiero, 2007). As a result, Bluntzer (1992), Preston and others (1996), and Carrell (2000) combined these two members into a single aquifer.

2.2.2.2 Wilberns Formation

The Wilberns Formation consists of four members (from the oldest to the youngest): the Welge, Morgan Creek, Point Peak, and San Saba, as described below.

Welge Member - The Welge Member is a medium- to coarse-grained, yellowish-brown, mature quartz sandstone (Dekker, 1966; Barnes and Bell, 1977). The sandstone generally does not contain glauconite (Watson, 1980), and lacks of sedimentary structures except some small-scale crossbeds (Dekker, 1966). However, glauconite content increases toward the southeast from the Llano Uplift region and the Welge Member sandstone becomes a greensand and indistinguishable from the underlying Lion Mountain Member (Barnes and Bell, 1977). The bimodal crossbedding structure in the Welge Member sandstone indicated tidal influence which was interpreted as a near-shore depositional environment by Dekker (1966). The thickness of the Welge Member ranges from zero to about 30 feet (Dekker, 1966; Watson, 1980) and decreases toward the southeast (Preston and others, 1996). The combined thickness of the Lion Mountain

Member and the Welge Sandstone Member ranges from 15 to 220 feet in the study area (Standen and Ruggiero, 2007). The Welge Member grades upward to the Morgan Creek Member.

As described by Bluntzer (1992) and Carrell (2000), the Lion Mountain and Welge members are combined into a single aquifer in this study due to their hydrogeologic similarity. This aquifer is called Lion Mountain-Welge Aquifer in the following sections.

Morgan Creek Member - According to Watson (1980), the Morgan Creek Member consists of granular, green to olive gray, glauconitic limestone. The limestone bedding at the lower part is thick but thins upward. The lower part is often sandy with reddish to pinkish color where it grades downward to the Welge Member (Kier, 1988). The middle part of the Morgan Creek Member contains thin to medium bedded, coarse-grained limestone with dark, silty, argillaceous, wave bedded, fine-grained limestone (Watson, 1980; Kier, 1988). The upper part of the member contains interbeds of coarse-grained limestone and dark, silty, fine-grained limestone. In the Llano Uplift region, the Morgan Creek Member displays relatively consistent sedimentary structure except farther south in the study area where the limestone grades to siltstone and becomes indistinguishable from the overlying Point Peak Member (Watson, 1980). Oolites and trilobites are common throughout the member. Watson (1980) stated that the Morgan Creek Member was deposited in a uniform calcitic marine environment. The Morgan Creek Member is absent at the central part of the Llano Uplift region, but its thickness may be as great as 220 feet at other locations in the study area (Standen and Ruggiero, 2007). The Morgan Creek Member generally thins to the southeast (Preston and others, 1996). The Morgan Creek Member is considered a confining unit or aquitard due to its relatively low permeability.

Point Peak Member - The Point Peak Member contains argillaceous and glauconitic siltstone and limestone with shale layers (Barnes and Bell, 1977; Watson, 1980; Carrell, 2000); the lower half of the member consists of predominately thinly bedded siltstone with an increasing amount of fine-grained limestone upward (Watson, 1980). Intraformational conglomerate and stromatolitic, light green, microcrystalline limestone are common in the upper half of the member. The siltstone of the Point Peak Member was deposited in a very shallow marine environment with the fine-grained materials carried by wind from the north or northwest (Watson, 1980). The limestone portion of the member is believed to be from a marine shelf (reef zone) environment with limited terrigenous input. The abundance of glauconite may suggest a low energy environment during the deposition of the Point Peak Member. The boundary between the Point Peak Member and the overlying San Saba Member is gradational where the upper half of the Point Peak Member is stromatolitic limestone, or unconformable where the Point Peak Member siltstone is overlain by the San Saba Member limestone or dolomite. The Point Peak Member thins to the northeast while the San Saba Member thickens. The thickness of the Point Peak Member ranges from zero to 265 feet in the study area (Standen and Ruggiero, 2007). The Point Peak Member is considered a confining unit or aquitard due to its low permeability.

San Saba Member - The San Saba Member consists of limestone and dolomite. The limestone is mostly fine- to medium-grained, thinly- to thickly-bedded, gray, and glauconitic; the dolomite is either fine-grained and medium-bedded or medium- to coarse-grained and thickly-bedded (Watson, 1980; Kier, 1988). The dolomite facies can be gray, pink, red, or purple, and contains a significant amount of cherts. The contact between the limestone and dolomite is gradational both

vertically and horizontally; dolomite, whenever it exists, is often on the top of the limestone. Stromatolites are common in the western part of the Llano Uplift region, which is a continuation of the same sedimentary process that led to the deposition of the Point Peak Member stromatolitic limestone (Watson, 1980; Kier, 1988). In the western part of the Llano Uplift region, the San Saba Member may contain a 55- to 70-foot thick sand layer (Kier, 1988), which is confirmed by the geophysical logs in this study. Barnes (1959) pointed out that there might be a north-south trending reef barrier along western Mason County, which separates the sandy San Saba to the west from the calcitic San Saba to the east. Farther east from the reef barrier, the marine depositional environment was deeper and of lower energy. As a result, the limestone in the San Saba Member becomes finer toward the east. However, a shallower marine environment was active toward the end of the San Saba geologic time, which caused the deposition of an intraformational conglomerate in the upper part of the San Saba Member; this depositional environment continued into the early Ellenburger Group geologic time (Watson, 1980). The San Saba Member thickens to the south and may reach a maximum thickness of 850 feet (Preston and others, 1996).

Since the San Saba Member and the overlying Ellenburger Group are hydraulically connected, the two units are combined as a single aquifer in this study.

2.2.2.3 Ordovician Period

In general, the marine sedimentary environment continued from the late Cambrian (the San Saba time) to the early Ordovician (the Ellenburger time). However, after the Ellenburger time, the region experienced an uplift related to the Concho (Texas) Arch (Figure 2.2.3) which extends from the Texas Panhandle to southwest of the Llano Uplift region; the lack of widespread middle Ordovician through Devonian rocks in the study area is related to the uplift of the Concho Arch (Ewing, 2004).

Ellenburger Group - The Ellenburger Group is comprised of, in ascending order, the Tanyard, Gorman, and Honeycut formations. The Tanyard Formation contains a lower member, Treadgill, and an upper member, Staendebach. The Treadgill Member consists of gray, medium- to coarse-grained dolomite to the east of the Llano Uplift region and grades to thinly-bedded, gray, silty, argillaceous limestone to the west (Watson, 1980). Farther to the west, the Treadgill Member becomes indistinguishable from the underlying San Saba Member (Kier, 1988). The Staendebach Member consists of gray, fine- to medium-grained dolomite and grades northeast to gray limestone on the top part; dolomitic cherts are common in this member (Watson, 1980). The Gorman Formation consists of pink, fine-grained dolomite at the lower part and thinly- to thickly-bedded, gray, microcrystalline limestone at the upper part (Watson, 1980; Kier, 1988). Well rounded quartz sand grains are common in the Gorman Formation. The Honeycut Formation contains three units: nearly equal thickness of gray limestone and gray, fine- to medium-grained dolomite at the bottom; predominantly brown, very fine grained dolomite at the middle; and gray limestone on the top (Watson, 1980; Kier, 1988). According to Watson (1980), the Ellenburger Group was deposited in a shallow marine environment with little terrigenous material except the Gorman Formation which may have received the quartz sand from land to the east and south. This land emergence coincides with the development of the Concho Arch as described by Ewing (2004). The depositional environment and erosion afterwards control the distribution and thickness of the Ellenburger Group. In general, the Ellenburger Group was not deposited or eroded away at the central portion of the Llano Uplift region and thickens outward

especially to west and east. The thickness of the Ellenburger Group ranges from zero to more than 2,000 feet. In geophysical logs, this group is represented by a very low, but smooth gamma reading. The Ellenburger Group has various degrees of karstification. Some of karst structures have developed to very large caves (such as the Longhorn Cavern in the Gorman Formation). The abundance of secondary porosity has made the Ellenburger Group an important oil/gas reservoir or groundwater aquifer.

Burnam Limestone - According to Watson (1980), the Ellenburger Group in the Llano Uplift region had undergone the greatest erosion during the middle Ordovician to pre-Devonian periods. The only upper Ordovician rock, the Burnam Limestone, was found in a collapse structure in the Honeycut Formation of the Ellenburger Group located in southern Burnet County (Barnes, Cloud, and Duncan, 1953). Due to its limited presence, the Burnam limestone is not considered as a separate geologic unit in this modeling study.

2.2.2.4 Silurian, Devonian, and Mississippian Periods

Silurian and Devonian Formations – The erosion that began during the early Ordovician continued throughout the Silurian Period. This pre-Devonian erosion also left little Silurian strata in the study area (the Silurian strata were either not deposited or truncated away) (Watson, 1980). After this pre-Devonian truncation, the Llano Uplift region was invaded from the east by a transgressive marine environment followed by a series of regressions and transgressions; truncation continued at the emergent land areas (Watson, 1980). As a result, the Devonian rocks only exist as remnants above the depressions or in collapse structures in the Ellenburger Group. These Devonian rocks include the Pillar Bluff limestone, the Stribling Formation, an unnamed limestone, the Bear Spring Formation, and the Houy Formation (Watson, 1980). Due to their restricted distribution, the Silurian and Devonian rocks are not considered separate geologic units in this study. Preston and others (1996) called these units (as well as the Chappel and Barnett formations which are discussed below) as “generally non-water bearing”.

Early Mississippian Chappel Formation - During the Mississippian Period, the study area was again inundated and became a marine shelf or basin environment. Two Mississippian formations are found in the study area: Chappel from early Mississippian and Barnett from late Mississippian (Watson, 1980). The Chappel Formation is mainly comprised of gray to brown, fine to coarse-grained biosparite and biomicrite (Kier, 1988). This formation differs from other formations in the region due to its high content of crinoids and its crystalline characteristics (Watson, 1980). The Chappel Formation was deposited in a marine margin over an uneven Ellenburger or Devonian rock surface during transgression. Erosion may have truncated the top portion of the Chappel Formation before deposition of the Barnett Formation. As a result, its distribution is discontinuous (Watson, 1980). The Chappel Formation crops out in several isolated areas in the eastern, northern, and western Llano Uplift region (McFarland, 1984). The thickness of this formation is often less than two feet except in the low areas (depressions), sinks, or collapse structures in the Ellenburger Group where it could be over 50 feet (Watson, 1980; Kier, 1988). Due to its restricted distribution and thickness, the Chappel Formation is not considered a separate geologic unit in this study.

Late Mississippian Barnett Formation - In eastern San Saba County, the Barnett Formation consists of soft shale with limestone near the top and, locally, a thin, calcareous siltstone near the bottom (Watson, 1980). Farther west, limestone replaces part of the Barnett shale. The Barnett

shale is more brownish and contains more plants than the overlying Marble Falls shale (Kier, 1980; Watson, 1980). The Barnett shale is petroliferous and microsparite concretions are common (Watson, 1980; Kier, 1988). Near the town of Marble Falls in Burnet County, the Barnett shale has a light color (Kier, 1980; Kier, 1988). In comparison with the Chappel Formation, the Barnett Formation was deposited in a deeper and quieter marine environment with a very low accumulation rate (Watson, 1980). The Barnett Formation thickens outward from the Central portion of the Llano Uplift region. Its thickness could reach more than 100 feet in the northern study area (Watson, 1980). In southern Coleman and Brown counties of the conceptual model study area, its thickness was about 50 feet (see Figure 10 in Bruner and Smosna (2011)). Due to its low permeable nature, the Barnett Formation is considered a confining unit or aquitard in this study.

2.2.2.5 Pennsylvanian Period

During early to middle Pennsylvanian Period, central Texas endured the most significant tectonic event, the Ouachita Orogeny, which was related to the collision between the South American continent (part of Gondwana) and the North American continent (Laurentia). The Ouachita Orogeny created the Ouachita Mountains (as well as the Ouachita thrust fault), Fort Worth Basin, Bend Arch, and Kerr Basin (Figure 2.2.3). The Bend Arch was the western limit of the Fort Worth Basin during the early Pennsylvanian Period and the eastern limit of the West Texas (Midland) Basin during the middle Pennsylvanian and Permian periods; it was a topographic high but not an active uplift (Ewing, 2004). As a result, deposition of marine platform facies continued over the Llano Uplift region during this period of time. The Llano Uplift was located at the southern end of the Bend Arch. According to Bluntzer (1992), there is also a narrow structure bridge, the Fredericksburg High, from Gillespie County southwest to Bandera County associated with the late Paleozoic uplifting (Figure 2.2.3). The Cretaceous geologic units directly overlay the Precambrian rocks at the north portion of the structure. These regional geologic features controlled the source area and the deposition environment of the study area.

The geologic groups deposited in the study area during the Pennsylvanian Period include the Bend (consisting of the Marble Falls and Smithwick formations), Strawn, Canyon, and Cisco. The Cisco Group straddles the Pennsylvanian and Permian periods.

Marble Falls Formation - The Marble Falls Formation exhibits varying lithology throughout the study area. In McCulloch, San Saba, and Lampasas counties, this formation contains limestone separated by a shale unit at the middle; the lithologic difference was due to the water depth with shale being deposited in a deeper outer marine shelf (Watson, 1980). The limestone near the town of Marble Falls was deposited at basin platform, basin fill, and broad embayment (Namy, 1969). A variety of carbonate rocks were found in fault blocks in Mason and Kimble counties; these rocks were deposited in different marine environments ranging from strandline to shelf (Winston, 1963). Based on geophysical logs, the Marble Falls Formation appears to extend far downdip from these three isolated areas, with a thickness ranging from zero to more than 200 feet (Standen and Ruggiero, 2007). Preston and others (1996) described the thickness of this formation ranging from 385 to 460 feet. The geologic contacts with the underlying Barnett Formation and the overlying Smithwick Formation are most likely conformable (Kier, 1988). In this study, only the carbonate-dominated intervals of the Marble Falls Formation were correlated with geophysical logs and treated as an aquifer.

Smithwick Formation - The Marble Falls Formation grades both vertically and laterally to the Smithwick Formation (Kier, 1980). The Smithwick Formation is mainly soft, fossil-poor, black shale with limestone, siltstone, and sandstone layers; limestone is mainly at the bottom; siltstone and sandstone increase upward (Watson, 1980; Kier, 1988). The Smithwick Formation was deposited in a starved prodelta and deltafront environment (Kier and others, 1979; Kier, 1988). This formation thickens to south, east, and north from the central portion of the Llano Uplift region. To the west of the Llano Uplift, the Smithwick Formation is relatively thin and grades to the Strawn sandstone in western San Saba County (Watson, 1980). Its thickness could be several hundred feet or more to the east of the Llano Uplift region (Watson, 1980). The Smithwick Formation is considered to be a confining unit (Morey, 1955; Carrell, 2000).

Strawn Group - According to Watson (1980), the Strawn Group consists of thin-bedded to massive, yellowish-brown sandstone, mudstone, and silty shale with abundant small plant fragments; contains a limestone layer at the bottom when it overlies directly on the Marble Falls limestone; and supersedes the Smithwick and Marble Falls formations to the west of the Llano Uplift region. The Strawn Group was deposited in river mouth bars and flood basin facies of deltaic environment that filled the Fort Worth Basin to the north of the Llano Uplift region with a westward progradation (Kier, 1980; Kier, 1988). As a result, the Strawn Group thickens northward, ranging from about 75 feet in central McCulloch County and 140 feet in San Saba County to approximately 600 feet to farther north (Plummer, 1950). An equivalent geologic unit may very likely exist to the south of the Llano Uplift region. However, its lithology is not identified in the geophysical logs. The Strawn Group is mostly combined with the Smithwick as a confining unit in this study.

Canyon Group - The Canyon Group, conformably overlying the Strawn Group, consists of limestone alternating with shale and much less sandstone than the Strawn Group below and Cisco Group above (Sellards and others, 1932; Kier and others, 1979). The Canyon Group was deposited on an open marine shelf over a subsiding delta platform in the Fort Worth Basin with a reduction of terrigenous clastic sediments from the Ouachita Mountains to the east (Kier and others, 1979). According to Sellards and others (1932), the group is distributed in a 10 to 20 mile wide belt from Wise County (north and out of the study area) southwest to McCulloch County (in the study area). The Canyon Group is predominantly limestone and crops out along the Colorado River Valley in the study area (Kier and others, 1979). Its thickness could reach about 300 to 400 feet along the Colorado River Valley (Kier and others, 1979), and increases towards north and northeast. An equivalent geologic unit may very likely exist to the south of the Llano Uplift region; however, its lithology is not identified in the geophysical logs. The Canyon Group is considered a confining unit in this study.

Cisco Group - According to Kier and others (1979), the Cisco Group mainly consists of terrigenous clastic and carbonate rocks. The much higher content of sandstone and conglomerate in the Cisco Group than the underlying Strawn Group indicates an increased sediment input from the east to the Fort Worth Basin due to rejuvenated uplift of the source area along the Ouachita foldbelt. The Cisco Group can be found in a 20 to 40 mile wide belt extending from the Red River south and southwest to McCulloch County (Sellards and others, 1932). The thickness of Cisco Group along the Colorado River Valley is about 900 feet (Kier and others, 1979). An equivalent geologic unit may very likely exist to the south of the Llano Uplift region; however,

its lithology is not identified in the geophysical logs. The Cisco Group is combined with the Canyon Group and is treated as a confining unit in this study. The geologic contact between the Cisco Group and the underlying Canyon Group is conformable. The boundary between the Pennsylvanian and Permian is within the Cisco Group (Kier and others, 1979). Therefore, the younger formations of the Cisco Group could belong to the Permian Period.

2.2.2.6 Permian Period

By the Permian Period, the inland seas were gradually withdrawing from the central Texas, which, coupled with sediment filling, left behind shallow basins rimmed by extensive tidal flats. In central and north-central Texas, the Permian formations are dominated by marine shelf carbonate and tidal-flat evaporate deposited in a restricted environment where terrigenous clastic input from the Ouachita foldbelt to the east was reduced in comparison with the underlying Cisco Group (Smith, 1974; Kier and others, 1979). The reduction of the terrigenous clastic input was due to the dry climate, which reduced the precipitation and stream flow, and lower relief of the Ouachita foldbelt, which reduced the source. The Permian rocks crop out at the northwestern corner of the study area (Figure 2.2.4). The Permian rocks in this area primarily contain two groups: the Cisco at the bottom and the Wichita Albany on top. The Permian rocks are considered a confining unit due to its relative low permeability in this study area.

2.2.2.7 Triassic and Jurassic Periods

During the early Mesozoic Era, Texas tilted to southeast (Brown, 1980). This was likely related to the separation of the South American continent (part of the Gondwana) from the North American continent (the Laurentia). By the end of the Paleozoic Era, the Permian sea retreated from the study area until early Cretaceous. Concurrent with the sea retreat there was a regional uplifting. Ewing (2004) called this uplift the Llano Arch (Figure 2.2.3). As a result, neither Triassic nor Jurassic strata were found in the study area except for some locally-distributed gravels along the eastern side of the Llano Uplift region (Damon, 1940). During the same time, erosion diminished the older topographic relief and created the low-relief Wichita paleoplain (Hill, 1901) upon which the Cretaceous strata were deposited with an angular unconformity (Preston and others, 1996).

2.2.2.8 Cretaceous Period

By the early Cretaceous Period, the shallow Mesozoic sea returned from the southeast, and covered the whole study area by the middle of the Cretaceous time (Brown, 1980). As a result, Cretaceous formations were deposited across the entire region. However, the Cretaceous units (such as Travis Peak Formation) over the Llano Arch and its extension, the San Marcos Arch (Figure 2.2.3), are not very thick (Bluntzer, 1992). Post-Cretaceous uplifting and erosion removed the Cretaceous and younger formations in most of the study area. Today, the Cretaceous strata can only be found near the exterior edge (east, south, and west) of the study area. Different nomenclatures have been used to describe the Cretaceous strata in central Texas. In this study, the Cretaceous strata contain the Trinity and Fredericksburg groups to the east of the Llano Uplift; to the south and west of the Llano Uplift, the Cretaceous Strata is comprised of the Trinity and Edwards groups. In the latter case, the Edwards Group includes strata deposited during most of the Fredericksburg and Washita time (Brown, 1980).

Trinity Group – The Trinity Group consists of the Travis Peak Formation at the bottom and the Glen Rose and Paluxy formations at the top. In southern Burnet and Travis counties, the Travis Peak Formation can be further divided into five members in the study area (from the oldest to the

youngest): Sycamore/Hosston, Hammett, Cow Creek, and Hensell (Preston and others, 1996). The Sycamore Member contains gravels and sands deposited in the drainage systems on the Wichita paleoplain (Ledbetter, 1976). To the southeast, the Hosston Member was deposited in a shallow marine shelf environment (Brown, 1980). The Hosston Member contains interbedded sandstone, siltstone, claystone, shale, dolomite, limestone, and a basal conglomerate with a thickness ranging from zero to 350 feet (Preston and others, 1996). However, this basal conglomerate probably is also part of the Sycamore Member. The Hosston Member extends northwest (outside of the study area) and overlies the Sycamore Member as the transgression continued. Thus, the Sycamore and Hosston members belong to a marine transgression series with time overlaps. The lower Trinity members (Sycamore and Hosston) can only be found southeast of the Llano Uplift (Brown, 1980).

As the transgression continued during the middle Trinity time, the Hammett Member was deposited in a deeper, restricted environment. The Hammett Member is a dark to buff shale and grades upward and laterally to the Cow Creek Member (Brown, 1980). The Cow Creek Member contains coarse grained, sandy limestone and dolomite limestone. Like the lower Trinity members, the Hammett and Cow Creek members only exist to the southeast of the Llano Uplift with a combined thickness ranging from 0 to 160 feet (Preston and others, 1996). Above the Cow Creek Member is the Hensell Member. Preston and others (1996) described the Hensell (and Bexar) members as follows:

“The Hensell Member consists of interbedded red to gray clay, silt, sand, sandstone, conglomerate, and thin limestone. The thickest sands and sandstones are immediately adjacent to the south and east parts of the Llano Uplift. On the south side of the study area, the Hensell grades downdip into the Bexar Shale Member, which consists of a relatively thin sequence of silty dolomite, marl, calcareous shale, and shaly limestone. The Hensell/Bexar Member ranges from 10 to about 300 feet in thickness, thinning to the east and south.”

To the north, northeast, and west of the Llano Uplift, the members of the Travis Peak Formation are not discernable and, thus, the term, Travis Peak, is used collectively to describe a sequence of a basal conglomerate overlain by sand, silt, limestone, and clay; the upper part of the Travis Peak Formation grades vertically and laterally to the Glen Rose Formation (Fisher and Rodda, 1966). Due to the high relief of the Wichita paleoplain, the thickness of the Travis Peak Formation may change significantly from place to place ranging from zero to more than 200 feet.

In the northwestern portion of the study area (McCulloch, Concho, and Coleman c

The Glen Rose Formation is the thickest and most widely exposed Trinity formation. It consists of a lower member and an upper member separated by a thin clam (Corbula) bed. The lower member contains limestone, shale, and limestone reef; the upper member is comprised of interbedded limestone, dolomite, marl, and evaporites (Preston and others, 1996). The Glen Rose Formation was formed in a shoreline or shelf environment and grades northward and upward to a marginal marine siliciclastics, the Paluxy Member. The Glen Rose Formation pinches out against the Llano Uplift and increases in thickness southward to about 1,000 feet in the study area.

The Paluxy Formation only exists only to the north of the Colorado River and crops out along the valley walls in Burnet, Lampasas, and Mills counties in the northeastern portion of the study

area. According to Caughey (1977), the Paluxy Formation consists of sandstone interbedded with shale deposited in a strandplain environment with a net sand thickness of up to 150 feet. The Paluxy Formation grades south to marl and limestone of the Walnut Formation in the study area.

Fredericksburg Group – The Fredericksburg Group contains, in ascending order, the Walnut, Comanche Peak, and Edwards formations (Brown, 1980). The Walnut Formation consists of interbedded limestone and marls, and increases in thickness from Blanco to eastern Burnet and southern Lampasas counties in the study area. The Comanche Peak Formation, a limestone, exists locally in Burnet County and north in the study area. The distribution of the Edwards Formation is similar to that of the Walnut Formation, but its thickness decreases from south to north in the study area.

Edwards Group – The Edwards Group is used to represent a thick sequence of carbonate rocks in the south and west of the study area. The Edwards Group contains two formations: the Terrett Formation at the bottom and the Segovia Formation at the top. The Terrett Formation is comprised of limestone, dolomite, and evaporite and thickens to the southwest. The Segovia Formation contains similar rocks as the Terrett Formation and thickens southward to about 400 feet (Brown, 1980).

The Cretaceous rocks are hydraulically connected to the older geologic units in the Llano Uplift region and are included as a combined hydrogeologic unit in this study.

2.2.2.9 Cenozoic Era

The uplift and erosion continued in the Llano Uplift region during the Cenozoic Era. At the same time, sinking and deposition to the southeast significantly increased the loading in the Gulf Coast basin. These two forces destabilized the old, weak Ouachita fault zone and created a band of northeast-southwest oriented, dip-slipped normal faults to the south and southeast, the Balcones Fault Zone. The uplifting and faulting enhanced the erosion and tilted the existing geologic units. Today, most of the post-Cretaceous rocks have been removed from the central portion of the Llano Uplift region and the Quaternary deposits are mainly found in river valleys. Due to this reason, the Cenozoic formations are not considered a separate unit in this study. However, the Cenozoic formations, where they exist, will be included in the Cretaceous rocks in a single group and used to evaluate the surface water-groundwater interaction and groundwater recharge.

2.2.2.10 Summary

Based on their distribution and hydrogeologic properties, the following geologic units (from the oldest to the youngest) are considered groundwater aquifers in this study: the Hickory Member, Lion Mountain Member, Welge Member, San Saba Member, Ellenburger Group, Marble Falls Formation, and Cretaceous/Cenozoic units. As shown in [Table 2.2.1](#), the Lion Mountain and Welge members are lumped together as a single aquifer; the San Saba Member and Ellenburger Group are lumped together as a single aquifer; the Cretaceous and younger units are lumped together as a single aquifer. All of the other units are considered confining units due to their limited distribution and low permeability.

2.2.3. Structure and Texture

The groundwater flow and aquifer storage are influenced by not only the thickness of each formation but also by its bedding orientation and porosity. In principle, groundwater flow often follows relatively permeable units confined by low permeable units and, in carbonate rocks, the secondary porosity or fractures or karst features. Faults can act as groundwater flow conduits (flow through the fault faces) or barriers (flow perpendicular to the fault faces).

2.2.3.1 Faults

In the study area, the pre-Cretaceous rocks are extensively faulted. Though some of the faults may have existed before the Pennsylvanian Period (Johnson, 2004), the majority of the faults in the study area are related to the Ouachita Orogeny, a major Pennsylvanian tectonic event. The Ouachita Orogeny created the Ouachita Mountains, Fort Worth Basin, Bend Arch, and a diversity of faults dominated by the high angle normal faults with northeast-southwest trend and dip slip (Figure 2.2.5). The faulting activity was initiated during the early Pennsylvanian and penetrated the Paleozoic rocks through the Strawn Group (Johnson, 2004). The diversity as well as intensity of the faults were likely controlled by a southeast-northwest extension force and the strength of the underlying rocks. The faults with different strikes (other than the ones with northeast-southwest trend) may be related to older faults or other weak lithologic zones such as the edge of the granitic intrusion (Johnson, 2004). The faults that developed during the Pennsylvanian Period vertically displaced the Paleozoic rocks up to 3,000 feet (Standen and Ruggiero, 2007) and juxtaposed the younger against older units (Figure 2.2.6). The apparent lateral displacement ranges from a few feet to several miles (Bluntzer, 1992). The Cretaceous and younger rocks were also faulted during the Cenozoic Era. These faults, part of the Balcones Fault Zone, are also predominantly normal faults with northeast to southwest trended strikes and high angles; however, most of the faults are likely located to the southeast outside the study area. In addition, smaller-scale faults such as step and en echelon faults also occur throughout the study area (Carrell, 2000).

2.2.3.2 Tilted Beddings

Faults and Precambrian knobs also tilted and impacted the rock beddings. While the Precambrian knobs controlled the beddings during sedimentation, the faulting modified the then-existing rock beddings. The dip in Paleozoic rocks varies from a few tens of feet per mile to several hundred feet per mile (Barnes and Bell, 1977). In general, the Paleozoic rocks have greater dips than the Cretaceous rocks (Paige, 1912; Figure 2.2.6). Dips of 400 to 900 feet per mile in the Paleozoic rocks, generally to the south and southeast, are common with the steepest dipping beds near the faults and Precambrian knobs. The regional strike of these rocks generally follows the Precambrian dome in the Llano Uplift region (Bluntzer, 1992). The dip of Cretaceous rocks ranges from 10 to 15 feet per mile in the northern and western part of the study area to about 100 feet per mile in east and southeast part of the study area (Bluntzer, 1992). Greater dip often occurs near the Balcones Fault Zone and the Precambrian knobs.

2.2.3.3 Karst Conditions

The San Saba, Ellenburger, Glen Rose, and Edwards carbonate rocks in the study area contain caves of different sizes and shapes (Bluntzer, 1992). Some of these caves, such as the Longhorn Cavern in the Gorman Member of the Ellenburger Group, are large and extend over great distances. Some of the caves collapsed and served as traps for younger geological units. Many of

these collapse structures can be identified by evaluating the topography of the top of the Ellenburger Group.

Collapse of the carbonate rocks to the ground surface form sinkholes and expedite groundwater recharge. Caves or fractures can discharge groundwater as springs when the water level in the formations is greater than the elevation of the discharge point of the spring. In addition, caves and fractures provide preferential pathways for contaminant migration.

Dissolution of carbonate rocks by slightly acidic groundwater can change the landscape, too. In the study area, many river valleys follow the large fractures and fault zones. Preferential dissolution along the fractures and evaporite sections has modified the Edwards limestone into large blocks.

The abundance of dissolution cavities (or cave features) and fractures in the San Saba, Ellenburger, and Cretaceous carbonate rocks significantly enhance the rock permeability and storage. Many groundwater wells in the study area are screened in these formations for this reason.

2.2.4. Surface Geology

The surface geology of the study area is presented in [Figure 2.2.7](#). Please note that, as described in Section 2.2.2, the Washita Group exposed in the southwestern portion of the study area in [Figure 2.2.7](#) has been incorporated into the Edwards Group; in the far northern portion of the study area the Antlers Group is the equivalent of the Trinity Group where the Trinity Group is not distinguishable.

Precambrian rocks occupy the central portion of the study area surrounded by Cambrian rocks (Hickory, Cap Mountain, Lion Mountain, Welge, Morgan Creek, Point Peak, and San Saba members)([Figure 2.2.7](#)). Farther outward to the west, north, and southeast is the Ordovician Ellenburger Group. The Pennsylvanian Marble Falls Formation crops out farther to the north and southeast. The Smithwick Formation overlies and is exposed next to the outcropping of the Marble Falls but occupies a smaller area. Farther to the north, the study area is covered by the low-permeability Pennsylvanian Strawn Group with similarly low permeable Pennsylvanian Canyon and Cisco groups to the farther west. The low-permeability Permian formations are only found at the northwestern corner of the study area. Near the eastern and southeastern perimeter of the study area is the Cretaceous Trinity Group and the low-permeability Walnut and Comanche formations of the Fredericksburg Group. The Edwards Group occupies near the western and southwestern perimeter of the study area with the Hensell Member of the Trinity Group cropping out along river valleys. Along the bottom of the river valleys are the youngest deposits of the Quaternary Period.

The surface geology will be incorporated into hydrogeologic unit configuration, groundwater recharge, and groundwater-surface water interaction during the conceptual and numerical model constructions.

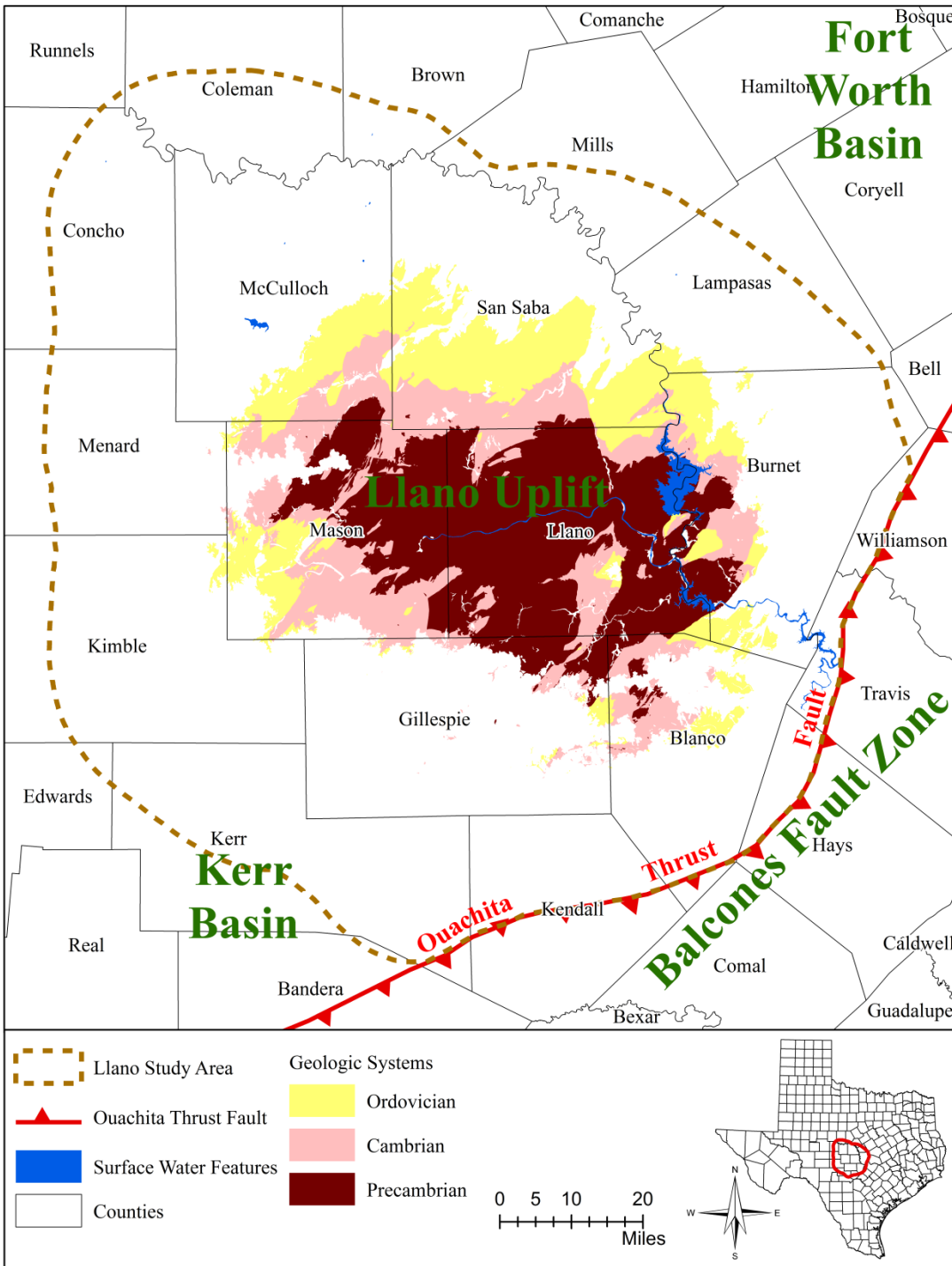


Figure 2.2.1 Schematic locations of major geologic structures in Llano Uplift region and surrounding areas. Surface geology of Llano Uplift region is based on Geologic Atlas of Texas (Bureau of Economic Geology, 2013).

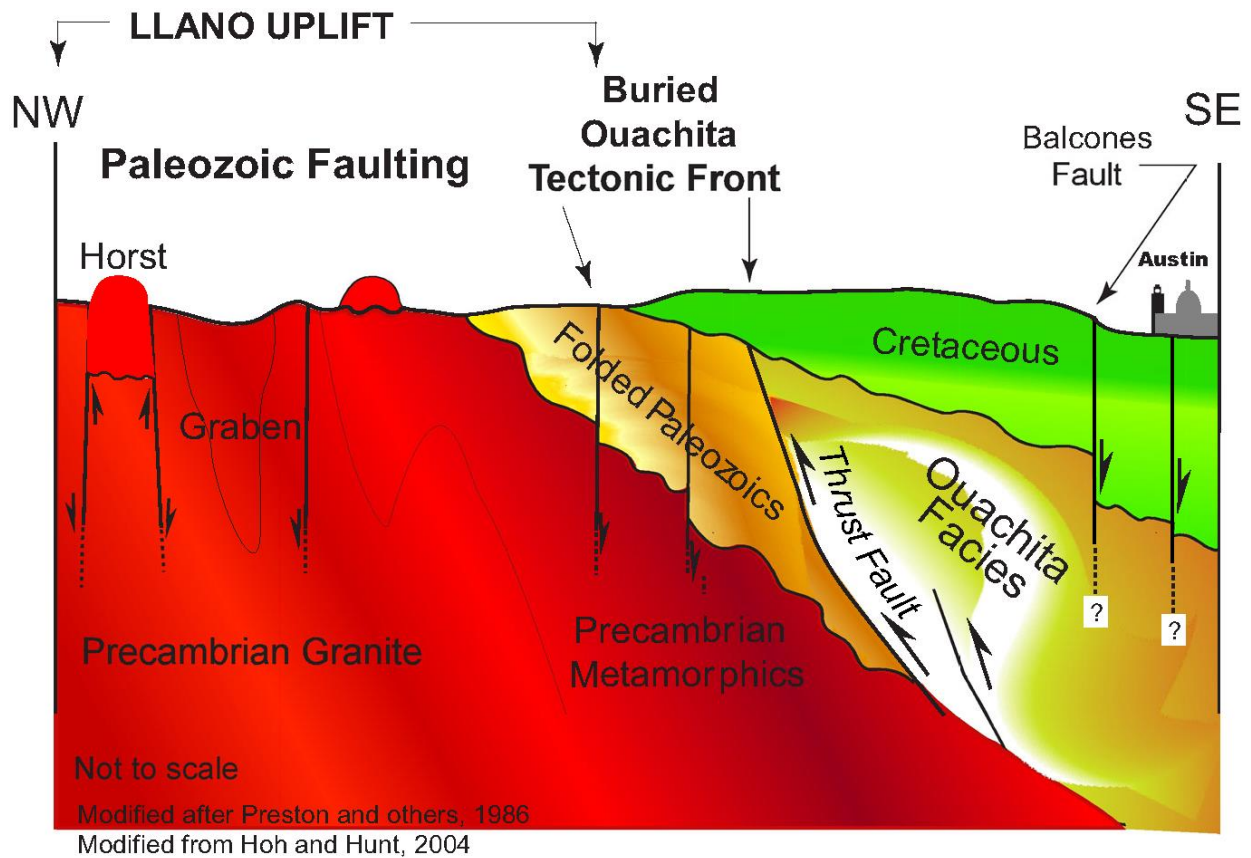


Figure 2.2.2 Schematic cross section of major geologic structure in Llano Uplift region and surrounding areas (Standen and Ruggiero, 2007).

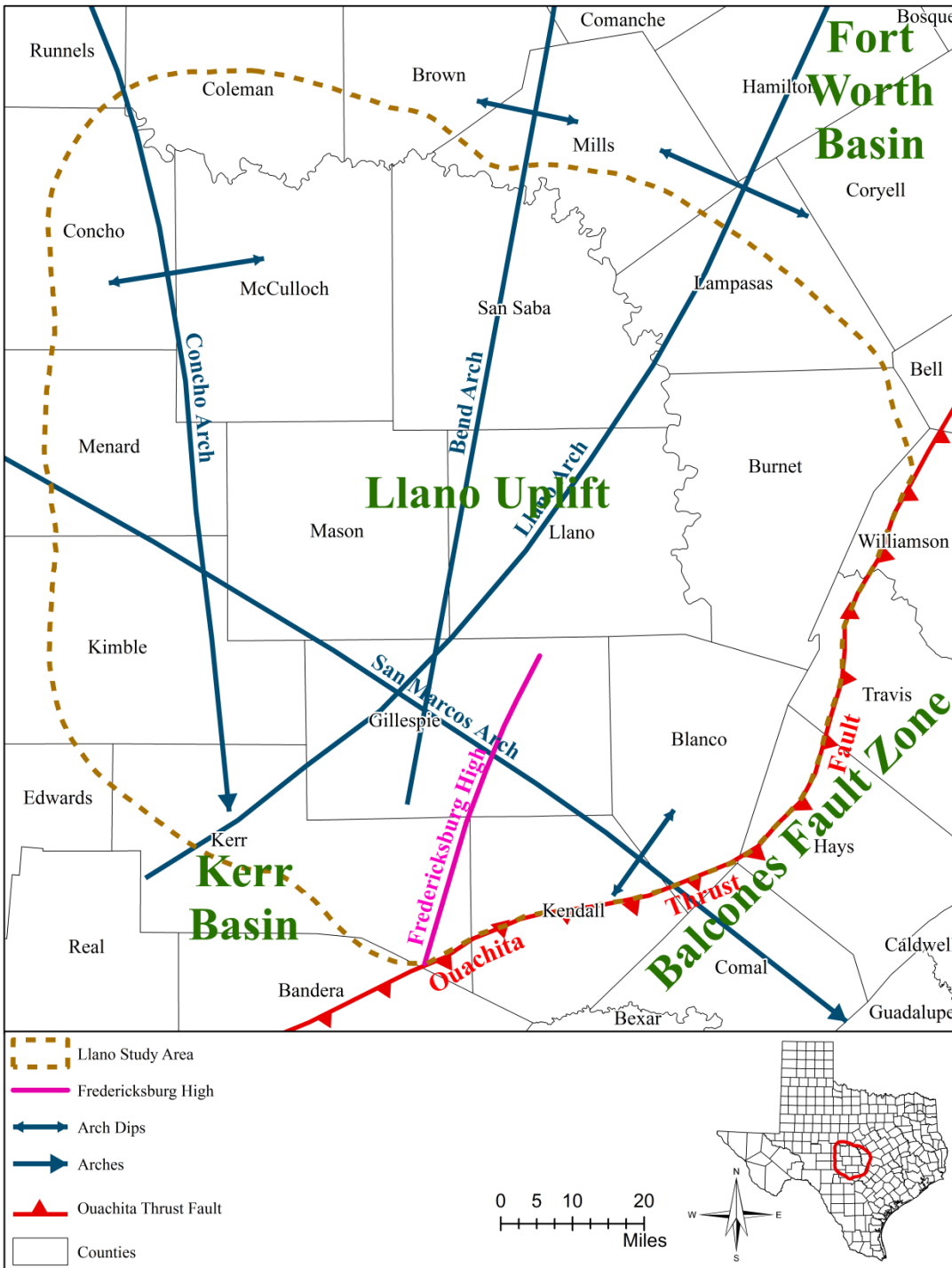


Figure 2.2.3 Location of major geologic structures in Llano Uplift region and surrounding areas (arches are after Ewing, 2004; Fredericksburg High is after Bluntzer, 1992).

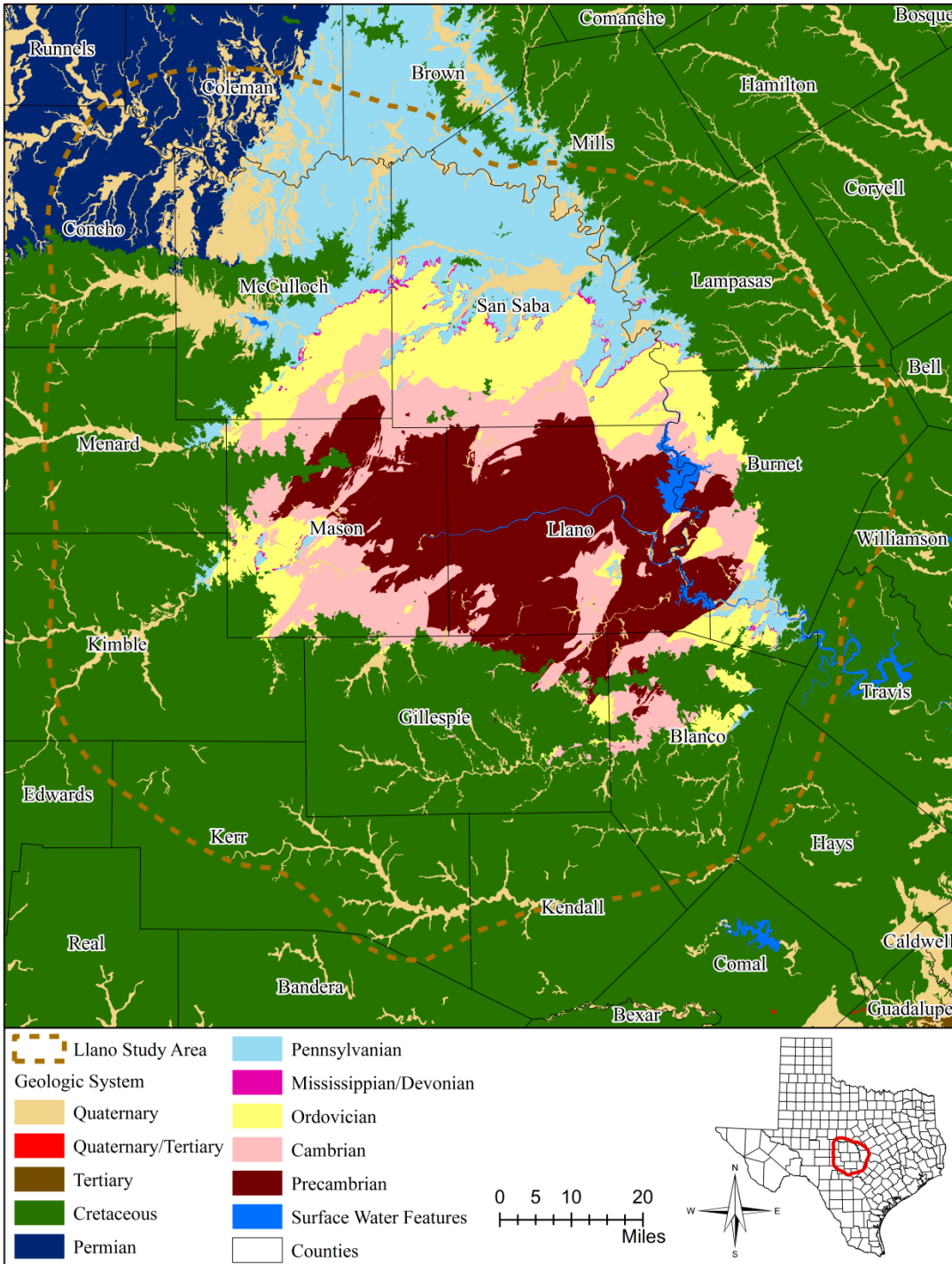


Figure 2.2.4 Simplified Surface geology of Llano Uplift region and surrounding areas (Bureau of Economic Geology, 2013).

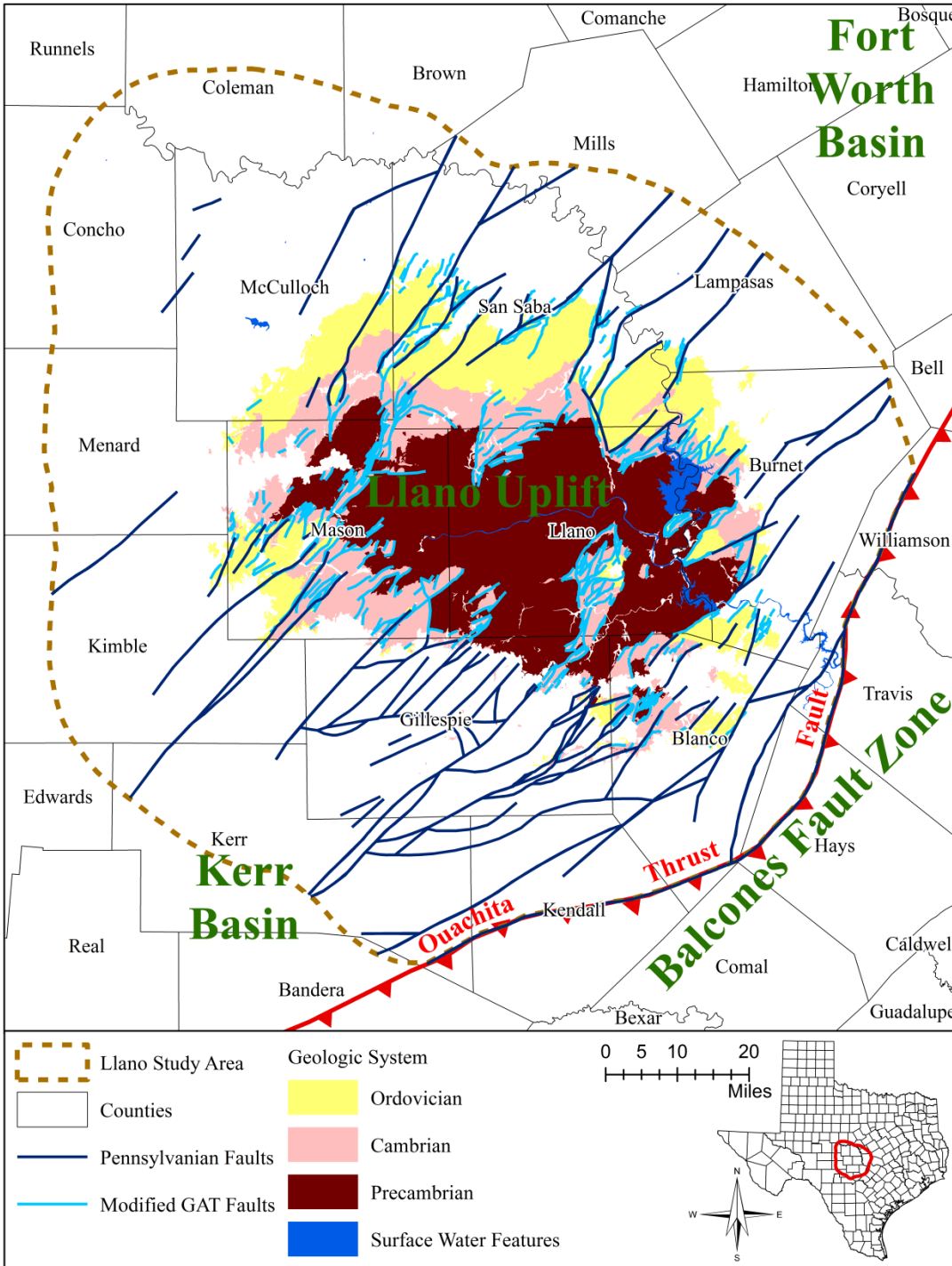


Figure 2.2.5 Distribution of faults in Llano Uplift region and surrounding areas. Surface geology of Llano Uplift region is based on Geologic Atlas of Texas (GAT) (Bureau of Economic Geology, 2013). Faults are modified from geodatabase by Standen and Ruggiero (2007) with reference to Johnson (2004).

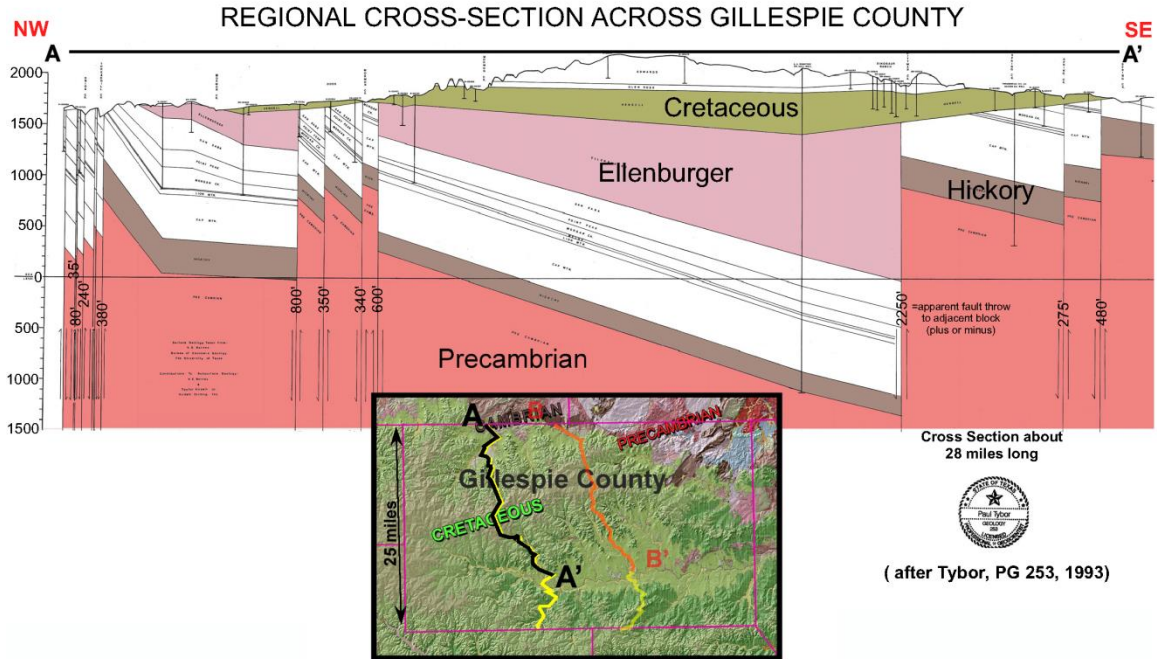


Figure 2.2.6 Distribution of faults along a cross section in Gillespie County (Tybor, 1993; imported from Standen and Ruggiero (2007).

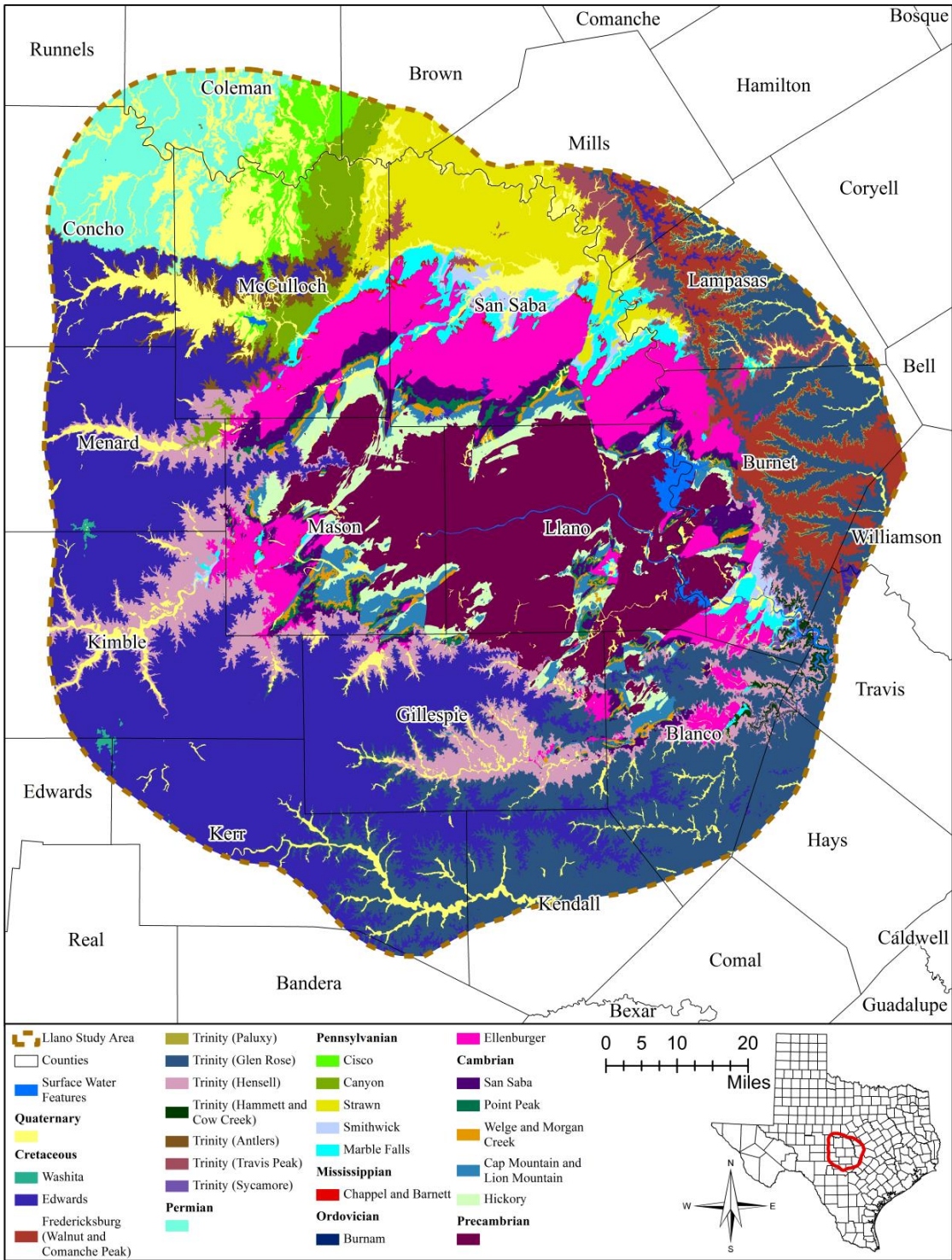


Figure 2.2.7 Detailed Surface geology of study area (based on Bureau of Economic Geology, 2013).

Table 2.2.1. Stratigraphy and hydrogeologic classification of geologic units in study area.

		Geologic Units					Hydrogeologic Units			
Era	System	North and East of Study Area			South and West of Study Area					
		Group	Formation	Member	Formation	Member				
Cenozoic	Quaternary	Loose sediments at river valley bottoms					Cretaceous Aquifer			
Mesozoic	Cretaceous	Washita	Buda, Del Rio							
			Georgetown							
			Kiamichi							
		Fredericksburg	Edwards			Edwards Group		Segovia		
			Comanche Peak							
			Walnut							
		Trinity	Antlers	Paluxy				Absent		
				Glen Rose				Glen Rose		
				Travis Peak	Hensell				Travis Peak	Hensell
					Cow Creek/Hammett					Cow Creek/Hammett
		Sycamore/Hosston			Sycamore/Hosston					
	Jurassic	Absent								
	Triassic	Absent								
Paleozoic	Permian	Wichita Albany	Undivided			Absent				
		Cisco	Undivided			Absent				
	Pennsylvanian	Canyon	Undivided			Undivided	Confining Layer			
		Strawn	Undivided			Undivided				
		Bend	Smithwick	Undivided	Undivided	Smithwick		Undivided		
			Marble Falls	Undivided	Undivided	Marble Falls		Undivided		
	Mississippian	Barnett			Barnett		Confining Layer			
		Chappel			Chappel					
		Devonian	Exists in collapses only							
		Silurian	Absent							
		Ordovician	Burnam	Exists in collapses only						
			Ellenburger	Honeycut	Undivided	Honeycut	Undivided	Ellenburger-San Saba Aquifer		
		Gorman		Undivided	Gorman	Undivided				
		Tanyard		Staendebach		Tanyard	Staendebach			
			Threadgill			Threadgill				
		Cambrian	Moore Hollow	Wilberns	San Saba		Wilberns	San Saba	Confining Layer	
Point Peak							Point Peak			
Morgan Creek							Morgan Creek			
Welge							Welge			
Riley			Lion Mountain			Lion Mountain	Welge-Lion Mountain Aquifer			
	Cap Mountain				Cap Mountain	Confining Layer				
		Hickory			Hickory	Hickory Aquifer				
Precambrian	Metamorphic (gneisses, amphibolites, and schists) and intrusive igneous (granites) rocks					Confining Layer				

3.0 Previous Investigations

This section focuses on previous hydrogeologic investigations in the study area. Other previous geologic studies are discussed in Section 2.2. The previous studies are organized as reconnaissance investigations, multiple county studies, single county studies, local studies, and groundwater flow modeling studies.

3.1 Reconnaissance Investigations

Reconnaissance investigations are the first phase of water resources planning. Some of the previous reconnaissance investigations covered parts of the study area, such as the Guadalupe River basin by Alexander and others (1964), the Colorado River basin by Mount and others (1967), and the Brazos River basin by Cronin and others (1973) (see [Figure 2.0.2](#) for the location of the river basins). These reconnaissance investigations only determined general groundwater quality, first-order estimate of water availability, existing water use, and areas for further studies of major water-bearing units.

3.2 Multiple County Studies

The summary of the multiple county studies is arranged from the earliest to the most recent and described as follows:

Using spring and flowing well data, Hill (1901) gave a detailed description of the Cretaceous units and its artesian conditions in the Black and Grand Prairies of Texas. This study covers the southeast, east, and northeast portion of the conceptual model study area. Sundstrom and others (1949) summarized water user information, well information, driller logs, water supply source, pumping rate, and water quality for each of the communities located in central and north-central Texas which covers the northern portion of the conceptual model study area. Follett (1956) compiled the groundwater levels from 1937 through 1956 in Hays, Travis, and Williamson Counties. Drapper (1959) studied the Hickory sandstone aquifer at parts of Llano, Mason, San Saba, and McCulloch counties.

Holland and Mendieta (1965) investigated the water quality of the Llano River and its interaction with groundwater below the town of Junction in 1962 when evapotranspiration was not important and no runoff-producing rains were observed for 66 days prior to the investigation so that the river was dominated by baseflow. This segment of the Llano River was located in Kimble, Mason, and Llano counties. The study showed that the river gained water from the alluvium deposit and then lost it to groundwater. The study also compared the results with previous studies performed in 1918, 1925, and 1952. The comparison indicated that the 1962 study was similar to that from 1918 and 1925, but different from the study in 1952 when the extreme drought almost reduced the river flow to zero.

The study by Evans (1974) focused on how the total dissolved solids of the groundwater in the Trinity and Fredericksburg groups correlated to the stratigraphy, structure, property, and groundwater development of the water-bearing units in Williamson and Eastern Burnet counties. The study concluded that the shallow groundwater and groundwater at outcrop area had lower total dissolved solids due to shorter residence time and prior leaching of the rocks at the recharge zone. At the recharge area, the groundwater was dominated by calcium, magnesium, and

bicarbonate. Nitrate was also high in the recharge area mainly due to contamination. In the downdip portion, sodium, sulfate, and chloride were much higher.

Klemt and others (1975) studied the groundwater occurrence, quality, availability, recharge, discharge, movement, and usage of the groundwater in the Precambrian rocks and the Antlers Formation, Travis Peak Formation, Glen Rose Formation, Paluxy Formation, and Edwards and associated rocks of the Cretaceous age in all or parts of Brown, Burnet, Lampasas, Mills, Travis, and Williamson counties. The study showed that the principal aquifers were the Antlers and Travis Peak formations. Other important aquifers in the Llano Uplift area are the Glen Rose Formation, Paluxy Formation, and Edwards and associated limestones. Groundwater from the Travis Peak Formation was fresh or slightly saline with a total dissolved solids concentration of 300 to 3,000 milligram per liter. The total dissolved solids increased with depth.

The Hill Country covers all or parts of the following counties in the conceptual model study area: Bandera, Blanco, Gillespie, Hays, Kendall, Kerr, and Medina. Ashworth (1983) evaluated the hydraulic characteristics of the Trinity Aquifer and the quality and quantity of groundwater in the Hill Country. The study divided the Trinity Aquifer into three parts: the Hosston and Sligo members of the lower part, the Cow Creek and Hensell members of the middle part, and the Glen Rose Formation of the upper part. The lower part could yield small amounts of good quality groundwater from Kerrville (Kerr County) to Bandera County. The quality of groundwater in the lower part in the rest of the study area was saline. Wells completed in the middle Trinity, the most widely used aquifer in the Hill Country, could produce small to moderate amounts of fresh to slightly saline water. The upper Trinity often had low permeability and, thus, produced little water. The water quality of the upper Trinity was also poor due to dissolution of the evaporites. The study also concluded that the annual recharge and discharge of the Trinity Aquifer was small.

A field study by Sharp and others (1985) in June 1985 showed that the Katemcy Creek in Mason and McCulloch counties recharged the Hickory Aquifer along its entire length.

Black (1988) concluded that the groundwater flow in the Hickory Aquifer in Mason and McCulloch counties was more complicated than the study results from Mason (1961) which indicated a uniform flow pattern from the outcrop area to the downdip portion. Black (1988) suggested that the faults impeded the groundwater lateral flow through a reduced area into the subsurface. However, faults could significantly enhance the interaction between the groundwater and surface water. The Hickory Aquifer could gain from or lose water to rivers, though the San Saba in the study area was a gaining river. The groundwater at the outcrop and shallow confined portion was dominated by calcium-bicarbonate in an active flow regime. The groundwater moved fast in the outcrop portion and moved to the adjacent rivers within 40 years. The study also found that the water level at the outcrop area was declining. The deep portion of the aquifer was stagnant and had higher sulfate and chloride concentrations. The travel time from the outcrop to the deep confined portion was over 30,000 years. Only a small portion of recharge at the outcrop area reached the downdip portion, so the source for the deep confined portion of the aquifer was small. Since most of the groundwater production is in the outcrop area, aquifer recharge and pumping greatly affect each other, and control the total groundwater availability. Overdraft of groundwater at the downdip portion may occur due to low recharge to that zone

and, as a result, which may cause the intrusion of saline water. The study also showed that the impoundments had little effect on aquifer recharge.

Kuniansky (1989) estimated the groundwater recharge in eastern portion of the Edwards-Trinity Plateau ranging from 0.12 to 2.24 inches per year.

Baker and others (1990) studied the northern and eastern portion of the Llano Uplift area where the Trinity Group was the major water-bearing unit. Their study indicated that in 1985 the total groundwater withdrawal from all aquifers was about 81,000 acre-feet with 77,000 acre-feet from the Trinity Aquifer. Groundwater pumping had reduced the artesian pressure and created pumping cone of depressions in the Trinity Aquifer due to low transmissivity and restricted recharge of the aquifer. The study suggested that potential methods to increase the aquifer recharge could include runoff control in the outcrop area and injection wells in the downdip portion.

Duffin and Musick (1991) and Ridgeway and Petrini (1999) investigated the Edwards and Trinity aquifers in portions of Bastrop, Bell, Burnet, Lee, Milam, Travis, and Williamson counties. The study was bounded by the Colorado River to south, the border between Burnet and Lampasas counties to north, the outcrop of the Travis Peak Formation to west, and the total dissolved solids of 3,000 parts per million in groundwater to east. Groundwater availability, quality, and existing pumping were evaluated. Ridgeway and Petrini (1999) concluded that pumping had caused water level decline in the Trinity Aquifer and suggested that the future water demand could be met by conversion to surface water and conservation.

The U.S. Geological Survey performed a series of hydrogeologic studies on the Edwards-Trinity Aquifer and its contiguous hydraulically-connected units in west-central Texas, which covered the western portion and Hill Country portion of the conceptual model study area. The study by Lurry and Pavlicek (1991) focused on the groundwater withdrawal and category of groundwater usage. Barker and Ardis (1992) summarized the hydraulic test results from previous investigations. Based on groundwater levels and structure, Barker and Ardis (1992) concluded that the Hickory, Ellenburger-San Saba, and Marble Falls aquifers were hydraulically connected to the Cretaceous aquifers in the Llano Uplift region. In general, most of the underlying Paleozoic rocks provide a relatively impermeable base for the Edwards-Trinity Aquifer system. Ardis and Barker (1993) calculated and mapped the saturated thickness of the Edwards-Trinity Aquifer based on the water level and aquifer base. A historical groundwater level comparison was investigated by Bush and others (1993) using the groundwater level data collected between December 1915 and November 1969. They pointed out that the early water levels reflected the pre-development conditions.

Another study of the Edward-Trinity Aquifer in west-central Texas by the U.S. Geological Survey (Barker and others, 1994) indicated that the major aquifer in the Hill Country was the Trinity Aquifer. Streams in the Hill Country received flows from the shallow aquifers. The vertical flow component to the regional flow system was limited by lower permeability units within the Trinity Aquifer and the overall transmissivity of the Trinity Aquifer was generally low. The outcrop section often was more permeable than the downdip portion. The transmissivity of the Edwards-Trinity Aquifer ranged from less than 1,000 to 50,000 square feet

per day with an average of about 5,000 square feet per day. The vertical head difference over low permeable units was often high. The Trinity Aquifer received its recharge from the overlying Edwards limestone, recharge at the outcrop, or leakage from surface water. Water levels could vary greatly over short periods such as between summer (low water level) and winter (high water level). In eastern Edwards-Trinity (Plateau) region, the transmissivity values of the Edwards-Trinity Aquifer were less than 5,000 square feet per day (Barker and Ardis, 1996). Except for karstified areas, the average hydraulic conductivity of the Edwards-Trinity rocks was about 10 feet per day.

Eight Paleozoic and Cretaceous aquifers in the Hill Country were investigated by Bluntzer (1992). These aquifers were the Hickory, Lion Mountain and Welge, Ellenburger and San Saba, Marble Falls, lower Trinity, middle Trinity, upper Trinity, and Edwards (Plateau). The study indicated that the aquifers were hydraulically connected due to faults and stratigraphic positioning, and contributed to the river base flows. The sustainable yield was believed to be relatively small due to low storage and low transmissivity of the aquifers.

Bush and others (1994) concluded that the groundwater from the Edwards and Trinity aquifers in the Hill Country was predominately of bicarbonate facies, and the average water quality was good.

Preston and others (1996) expanded the study area by Bluntzer (1992) to the Central Texas which covered the whole conceptual model study area. This expanded study, however, focused on only the Paleozoic aquifers. These Paleozoic aquifers were the Hickory, Lion Mountain and Welge, Ellenburger and San Saba, and Marble Falls. The study showed that faulting had compartmentalized the aquifers especially near the outcrop area, which, in turn, restricted the lateral flow. Therefore, pumping had greater impacts in the compartmentalized area. Recharge to the unconfined portion was mainly from precipitation, while recharge to the downdip portion was small and restricted. The baseflow of the major rivers was from Edwards-Trinity (Plateau) Aquifer. The interaction between the surface water and groundwater was enhanced by faults.

As part of the National Water-Quality Assessment Program, Ging and others (1997) investigated the volatile organic compounds in the groundwater collected from the Edwards limestone aquifer in south-central Texas which covered Kerr, Kendall, Bandera, parts of Gillespie, Blanco, and Hays counties in the conceptual model study area. The study indicated that twenty eight volatile organic compounds related to site development were detected at 89 wells.

Ashworth and others (2001) studied the Hosston and Sligo members of the lower Trinity Group in Bandera and Kerr counties. Their study indicated that the lower Trinity Aquifer produced good quality water though sodium, potassium, sulfate, and chloride concentration were higher in the downdip portion of the aquifer. The confined portion of the lower Trinity Aquifer in Kerrville area seemed more permeable (with a transmissivity of 15,000 to 46,000 gallon per day per foot and storativity value of 10^{-4} to 10^{-5}) than other areas. The aquifer received most of its recharge from the overlying middle Trinity units, which could be increased when the Hammett shale was missing. The groundwater in the aquifer moved south and southeast. Significant water level decline due to overdraft had been observed at Kerrville, Kerr County (about 250 feet between 1920s and 1980s) and in Bandera County (as much as 400 feet). Based on the confined

storage and a recoverable specific yield of 0.3 percents, the groundwater availability was estimated 421,500 acre-feet in Bandera County and 160,500 acre-feet in Kerr County.

Chapter 8 in Mace and others (2004) described that the Edwards-Trinity aquifer near the Llano Uplift was hydraulically connected with the Paleozoic aquifers. Chapter 9 in Mace and others (2004) concluded that the groundwater in the Hickory Aquifer declined more in Gillespie and Mason counties.

A hydrogeologic atlas of the Hill Country Trinity Aquifer was published by Wierman, Broun, and Hunt (2010). This atlas covered Blanco, Hays, and Travis counties in the Hill Country. The atlas included structure and isopach contour maps of the Lower Trinity (Hosston and Sligo members), Hammett and Cow Creek members of middle Trinity, and Hensell Member and lower Glen Rose Formation of the upper Trinity. The groundwater recharge, flow direction, interaction between surface water and groundwater, springs, and water quality were also included in the atlas.

Using the remote sensing technologies, Kirk and others (2012) estimated the effective groundwater recharge for almost all of the study area. In their study, the effective groundwater recharge was calculated, using a mass balance method, as the difference between the precipitation infiltration and effective evapotranspiration. The infiltration was defined as precipitation minus stream discharge. Thus, the precipitation infiltration was equivalent to the total groundwater recharge. The stream discharge was related to precipitation, reference evapotranspiration, and soil permeability, and was calibrated to measured stream flows.

State-wide groundwater data were also provided by the U.S. Geological Survey and Texas Water Development Board. Myers (1969) and Christian and Wuerch (2012) calculated and compiled the transmissivity data based on aquifer tests for the state of Texas. Some of the data pertain to the conceptual model study area. Between 1998 and 2005, the U.S. Geological Survey has annually published water resources data of Texas for every water year (<http://pubs.usgs.gov/wdr/#TX>). These reports included groundwater level and water quality data collected at wells. Over the years, the TWDB has been maintaining a groundwater database at its website (http://wiid.twdb.texas.gov/ims/www_drl/viewer.htm?). The database includes groundwater levels, well logs, driller reports, pumping tests if available, and well records, among others.

3.3 Single County Studies

The single county studies are arranged by alphabetic order of the county names and described as follows:

3.3.1 Bandera County

Reeves and Lee (1962) concluded that the aquifers in Bandera County included the Hosston and Sligo members, the Cow Creek and Hensell members of the Pearsall Formation, the Glen Rose Formation, and limestones of the Fredericksburg and Washita groups. The Hosston and Sligo members, the oldest aquifers in the county, were under artesian conditions and produced small to large quantities of water. The Hensell sand in the northern part of the county could yield moderate to large amount of water. The Glen Rose limestone only yielded small amount of water due to its low permeability. The Fredericksburg and Washita groups yielded small to moderate

amount of water in much of the western part of Bandera County. In general, the groundwater quality in Bandera County was good except for the high sulfate concentration from the upper Trinity Aquifer. The total groundwater use in 1958 was estimated 900 acre-feet. The study indicated that a large amount of groundwater was available for development.

3.3.2 Blanco County

According to Follett (1973), the aquifers in Blanco County that could yield moderate to large quantity of fresh to slightly saline groundwater were, in the order of importance, the Ellenburger-San Saba, Pearsall, lower Glen Rose, and Hickory. A total of about 1,400 acre-feet of groundwater were pumped mainly for domestic use with approximately 26,000 acre-feet available for development in 1968. Most of the existing wells had yields of 10 to 25 gallons per minute. In general, the groundwater, though usually hard, met the drinking water quality standards. Aquifers got recharge from precipitation and surrounding countries. The general groundwater flow direction was to the south and southeast. Groundwater discharged at seeps, springs, and pumping wells. Some flowing wells were perennial.

Wet Rock Groundwater Services, L.L.C. (2013) performed three pumping tests at a 237-acre parcel located in Blanco County to determine the hydraulic property of the Trinity Aquifer. Each test contained a pumping well and an observation well. The hydraulic conductivity values from the pumping tests ranged from 0.09 to 1.9 feet per day. Water quality from three pumping wells all met the Texas Commission on Environmental Quality Maximum Contaminant Levels (MCL) and Secondary Standards, except for two samples which contained iron concentration higher than the two standards.

3.3.3 Burnet County

Based on the data collected in 1988, Lower Colorado River Authority (1992) investigated the total groundwater withdrawal and availability of the Hickory, Ellenburger, Marble Falls, and Trinity aquifers in Burnet County. In general, the groundwater quality was good except for two wells with the total dissolved solids over the standards.

3.3.4 Gillespie County

Ruggiero (2014) developed two 3-dimensional stratigraphic structure models for the Hill Country Underground Water Conservation District. One model covers only Gillespie County and the other includes Gillespie County and adjacent areas to its south and west. These models contain all of the major hydrogeologic units in 3-dimensional view (from Precambrian to Edwards).

3.3.5 Hays County

According to DeCook (1960), the Edwards and Trinity aquifers were the principal aquifers in Hays County. Water levels, flow directions, location of aquifers, and groundwater quality were evaluated using well and spring data. The study indicated that much of the groundwater in the county was from the recharge at the outcrop and regional flow was parallel to the Balcones Fault Zone. The quality of the groundwater in the aquifers was generally good. However, some wells in the Glen Rose Formation might have total dissolved solids concentration greater than 1,000 parts per million.

3.3.6 Kendall County

According to Reeves (1967), the principal water-bearing units in Kendall County were the Hosston and Sligo members, Cow Creek and Hensell members, and the lower Glen Rose

Formation of the Trinity Group. Most existing wells in these aquifers yielded several gallons per minute to 425 gallons per minute. In general, the water quality was good, however the water hardness was elevated. The total water use in 1965 was 1,000 acre-feet and the total groundwater availability of the Trinity Aquifer was estimated around 50,000 acre-feet per year. The study recommended that new wells be placed with enough distance to overcome overlapping of pumping depressions due to low permeability of the Trinity Aquifer.

3.3.7 Kerr County

Reeves (1969) concluded that the major groundwater-bearing units in Kerr County were Hosston and Sligo members, Hensell Member, and Edwards and associated limestones. In 1966, the county pumped a total of 3,600 acre-feet of groundwater. Additional groundwater was available in the southern portion of the county where the Hosston, Sligo, and Hensell were the thickest. Springs and seeps received about 52,000 acre-feet of groundwater per year from the Edwards and associated limestones and about 6,000 acre-feet per year from the upper Glen Rose limestone. The groundwater quality, in general, was good except for the upper Glen Rose where the groundwater contained high sulfate concentration due to the dissolution of evaporites.

The vertical recharge to the Hensell sand was controlled by the overlying units. The Hensell sand was expected to receive more vertical recharge when being overlain by relatively permeable Edwards limestone than the upper Glen Rose Formation (Wilson, 2008). The groundwater movement in the Hensell sand was very slow with an average residence time of 24,000 to 28,000 years. Most wells in the Edwards limestone yielded two to five gallons per minute. Wells in the Hensell sand yielded higher at about 15 to 25 gallons per minute. The recharge to the Edwards limestone and Hensell sand were estimated to be 83,700 and 8,708 acre-feet per year, respectively. Other water-bearing units such as lower Glen Rose Formation, Cow Creek Member, and Hosston and Sligo members received much less recharge.

3.3.8 Kimble County

According to Alexander and Patman (1969), the Edwards and associated limestones were the most extensive aquifers for fresh groundwater, although the “alluvium aquifer” provided groundwater for more than half of the wells in the county. Total groundwater withdrawal was about 1,900 acre-feet for the whole county in 1964 with about 33,000 acre-feet of groundwater available for development. The groundwater availability value was based on the base flow of the Llano River at the town of Junction.

3.3.9 McCulloch County

Mason (1961) focused on the Hickory sandstone which extended almost across all of McCulloch County. Based on evaluation of pumping test results, the transmissivity of the Hickory Aquifer was estimated to be about 20,000 and 30,000 gallon per day per foot at the confined (downdip) portion and the outcrop area, respectively. The aquifer storativity (storage coefficient) was calculated as 0.0001 at the town of Brady. The recharge to the Hickory was mainly due to precipitation at the outcrop area in southeast of McCulloch County and Mason County to the south. The water levels indicated that the groundwater in the aquifer was confined by the low permeable Cap Mountain Member and moved uniformly from the outcrop area to the north and northwest. About 1,000,000 acre-feet of groundwater in the Hickory sandstone may be available to withdraw assuming a 500-foot drawdown in water levels. In general, the water quality in the Hickory Aquifer met the standards.

Clement and others (1985) concluded that the San Saba River in southeastern McCulloch County did not gain from or lose water to the Hickory Aquifer though locally the river could.

3.3.10 Menard County

Baker and others (1965) pointed out that no known wells were screened in the Precambrian, Hickory, and San Saba rocks in Menard County. In addition, the groundwater in the Ellenburger, Pennsylvanian, and Permian rocks may be too saline for most use. Due to the high amount of clay and silt, the well production in the Trinity rocks was often low with poor water quality. However, the Edwards and associated rocks cropped out in most of the county except at the southeast along the San Saba River and supplied quality groundwater to most of the wells in the county. The Quaternary deposits in the river valleys are another main water-bearing unit.

The recharge to the Paleozoic and Edwards rocks was mainly in the outcrop areas. The Trinity rocks received recharge from the outcrop area as well as from the overlying Edwards rock. The Quaternary deposits are recharged by the surrounding rocks.

3.3.11 San Saba County

According to Pettigrew, Jr. (1991), the thickness of the Hickory Aquifer in San Saba County varies due to Precambrian relief. Unlike Mason (1961), this study indicated that the groundwater flow in the Hickory Aquifer was controlled by structure, which resulted in non-uniform flow. Locally, faults can change the groundwater flow direction away from the downdip. Regional groundwater flow from the Hickory Member across faults to the juxtaposed Welge Member and Ellenburger Group occurred due to relatively high permeability among the three geologic units. However, the groundwater flow stopped at the faults when the Hickory Aquifer juxtaposed low permeable units. The groundwater facies changed from calcium-bicarbonate at the crop area to sodium-bicarbonate at the downdip. The Hickory Aquifer in the downdip portion had lower total dissolved solids and was classified as sodium bicarbonate, whereas the overlying unit was sodium chloride. The difference indicated a lack of vertical leakage in the central and northern portion of San Saba County. A sharp increase in chloride concentration in northern San Saba County indicated that the groundwater flow in the Hickory Aquifer became very slow due to limited recharge through the overlying Smithwick and Strawn shales.

3.3.12 Travis County

Brune and Duffin (1983) investigated the Edwards and associated limestones and the Trinity Group in Travis County. They divided the Trinity Group to three parts: the Hosston and Sligo members of the lower Trinity; the Hensell Member, Cow Creek Member, and the lower Glen Rose Formation of the middle Trinity; and the upper Glen Rose and Paluxy formations of the upper Trinity. The lower part of the Trinity Group was characterized by low permeability, small to moderate pumping rates, declining groundwater levels, and slightly saline water quality. The middle part of the Trinity Group generally had very low hydraulic conductivity, slightly saline water quality, and high sulfate concentration from gypsum beds. The upper part of the Trinity Group was also tight, but groundwater was fresh. In 1976, Travis County got most of its water needs from surface water. There was groundwater available (about 20,200 acre-feet) for development at the time.

3.4 Local Studies

Local studies cover relatively small areas such as cities or towns. Two of the studies were for the town of Burnet, Burnet County (Mount, 1962) and the town of Fredericksburg, Gillespie County (Mount, 1963). Near the town of Burnet, the principal water-bearing units were, in the order of importance, the San Saba Member, the Gorman Formation of the Ellenburger Group, the Hensell Sand of the Trinity Group, and the Hickory Sandstone. The wells and springs with the largest flows and good water quality were often from the San Saba Member. Most existing wells were completed in the Hensell Sand and could easily go dry because of the low aquifer thickness. Very few wells tapped the Hickory Sandstone due to its depth in the study area. At the town of Fredericksburg, Mount (1963) studied the following principal water-bearing rocks: Edwards and Comanche limestones, Hensell Sand, carbonates of the Ellenburger Group, and Hickory Sandstone. He concluded that up to 5,000 acre-feet of groundwater could be developed from these rocks with the Ellenburger Group having the greatest potential. His study indicated that the Ellenburger Group received its recharge from the overlying Hensell Sand, which in turn received its own recharge at the outcrop area. Both the Ellenburger Group and Hensell Sand yielded good quality water. Though most wells for domestic, irrigation, and livestock use were in the Hensell Sand, its low permeability restricted further development. The Hickory Sandstone likely received recharge from the Edwards and Comanche limestones and further development of the groundwater in the Hickory rock was also restricted due to limited recharge. In addition, groundwater resources were also evaluated in aquifers at the town of Melvin, McCulloch County (Sundstrom and George, 1942), at the town of San Saba, San Saba County (George, 1944), and at the town of Mason, Mason County (George, 1947).

3.5 Groundwater Flow Modeling Studies

The following list discusses the various modeling studies conducted in the study area:

- 1) Klemt and others (1975) mentioned that the TWDB contracted Dames and Moore to develop a computer model in 1968 to evaluate the impacts of projected pumping on groundwater level declines in the Hensell and Hosston members in 1975, 1990, and 2020. The model contained two layers representing the Hensell and Hosston members, respectively. The model had a grid dimension of 7.5 (east-west) by 8.5 (north-south) miles. This model covered only the northeastern portion of the conceptual model study area. Information regarding this model can be found in Klemt and others (1975) (http://www.twdb.texas.gov/publications/reports/numbered_reports/doc/R195/Report195.asp)
- 2) The U.S. Geological Survey developed a one-layer, steady state, finite element flow model for the Edwards-Trinity Aquifer and its contiguous hydraulically connected units in west-central Texas (Kuniansky and Holligan, 1994). The modeled area covered the western and Hill Country portions of the conceptual model study area. The model was calibrated to the water levels collected between 1974 and 1975. The pre-development conditions were assessed using a separate simulation. The authors, however, pointed out that this model may not be used for

the Hill Country due to its simplification of a complex system. The modeling report can be downloaded from <http://pubs.usgs.gov/wri/1993/4039/report.pdf>.

- 3) Mace and others (2000) developed a 3-dimensional MODFLOW model to simulate the groundwater flow in the Trinity Aquifer in the Hill Country which covers the southern portion of our conceptual model study area. The hydraulic units included in the model were the Edwards (Plateau), upper Trinity, and middle Trinity. The model was calibrated to the steady-state conditions in 1975 and transient conditions of 1996 to 1997. During the model calibration, the groundwater recharge, aquifer hydraulic conductivity, specific storage of the confined aquifer, and specific yield of the unconfined portion were adjusted to match the modeled hydraulic conditions to the observed values. The calibrated model was then used to predict the influence of groundwater pumping under drought conditions through 2050. The modeling report can be found from http://www.twdb.texas.gov/publications/reports/numbered_reports/doc/R353/Report353.pdf.
- 4) R.W. Harden & Associates, Inc. and others (2004) developed a MODFLOW model for the northern Trinity and Woodbine aquifers in Groundwater Management Area 8. The model contained seven numerical layers representing the Woodbine Aquifer and subunits of the Trinity Aquifer. The model included a three-phase calibration. Phase 1 involved a model from 1880 through 1980 and was calibrated to the water levels and stream baseflow in 1980. Phases 2 involved a transient period of 1980 through 1989 with the initial heads from the last time period (1980) of the Phase 1 model and were calibrated to aquifer conditions observed during the same time period. Phase 3 involved model verification to the water levels and stream flow between 1990 and 2000. After the calibrations, the model was used to predict aquifer responses with projected pumping scenarios under average and drought-of-record precipitation conditions. The modeling report can be downloaded from http://www.twdb.texas.gov/groundwater/models/gam/trnt_n/TRNT_N_Model_Report.pdf
- 5) LBG-Guyton Associates (2007) developed a 3-dimensional groundwater flow model for the Hill Country Underground Water Conservation District and the City of Fredericksburg. This MODFLOW model approximately covers the southeastern quarter of the Gillespie County and contains two numerical layers representing the Hensell Sand as Layer 1 and the Ellenburger Group as Layer 2. The model was calibrated to groundwater levels and stream flows from 1940s through 2004. After the calibration, the model was used to predict the Ellenburger Aquifer response to potential groundwater pumping. The model report can be downloaded from <http://www.hcuwcd.org/Ellenburger%20Model%20Report%20May142007.pdf>.
- 6) Jones and others (2009) updated the groundwater flow model developed by Mace and others (2000). In the updated model, the lower Trinity unit was added to the bottom of the original model as a separate model layer. The updated model was calibrated to the steady-state water levels and river discharge for 1980 and the transient conditions between 1981 and 1997. During the calibration, recharge due

to precipitation and groundwater pumping were adjusted. The calibrated model was then used to evaluate the groundwater availability under varied future hydraulic conditions. The modeling report can be downloaded from http://www.twdb.texas.gov/groundwater/models/gam/trnt_h/TRNT_H_2009_Update_Model_Report.pdf.

- 7) Anaya and Jones (2009) developed a MODFLOW flow model for the Edwards-Trinity (Plateau) and Pecos Valley aquifers which included the Edwards-Trinity (Plateau) and Hill Country portion of the Trinity aquifers located in our conceptual model study area. This model contained two active numerical layers representing Edwards/Pecos Valley and Trinity aquifers, respectively. This model was calibrated to the steady-state water levels in 1980 and transient water levels from 1980 through 2000. The modeling report can be downloaded from http://www.twdb.texas.gov/groundwater/models/gam/eddt_p/ET-Plateau_Full.pdf.
- 8) Using the parameter estimate program, PEST (Doherty, 2009), Young and others (2010) recalibrated the groundwater availability model for the Edwards-Trinity (Plateau) and Pecos Valley aquifers by Anaya and Jones (2009). The recalibrated model extended the simulation time to 1930 through 2000. During the recalibration process, aquifer hydraulic conductivity and model boundary conditions were adjusted by PEST to match the modeled to measured water levels.
- 9) Hutchison and others (2011) updated the model for Edwards-Trinity (Plateau) and Pecos Valley aquifers by Anaya and Jones (2009). The updated model merged the two layers in the original model to a single layer. The input parameters of the model were also revised as necessary to improve the water level calibration in Reagan and Glasscock counties. The updated model was calibrated to water level from 1930 to 2005. The modeling report can be found at http://www.twdb.texas.gov/groundwater/models/alt/eddt_p_2011/ETP_PV_One_Layer_Model.pdf.
- 10) Kelley and others (2014) updated the groundwater flow model by R.W. Harden & Associates, Inc. and others (2004) for the Trinity and Woodbine aquifers in Groundwater Management Area 8. This updated model contains eight numerical layers representing hydrogeologic units from ground surface to the bottom of the Trinity Group.

The areal coverage of the previous groundwater flow models are presented in [Figure 3.5.1](#). Please note that this figure only shows the coverage within or near the conceptual model study area. Please also note that the coverage only represents the model domains which may contain inactive or non-simulated areas.

In summary, most of the existing groundwater flow models that extended to the conceptual model study area simulated only the Cretaceous aquifers. One or two models may have contained some of the Paleozoic hydrogeologic units, but their lateral coverage was limited to local scale.

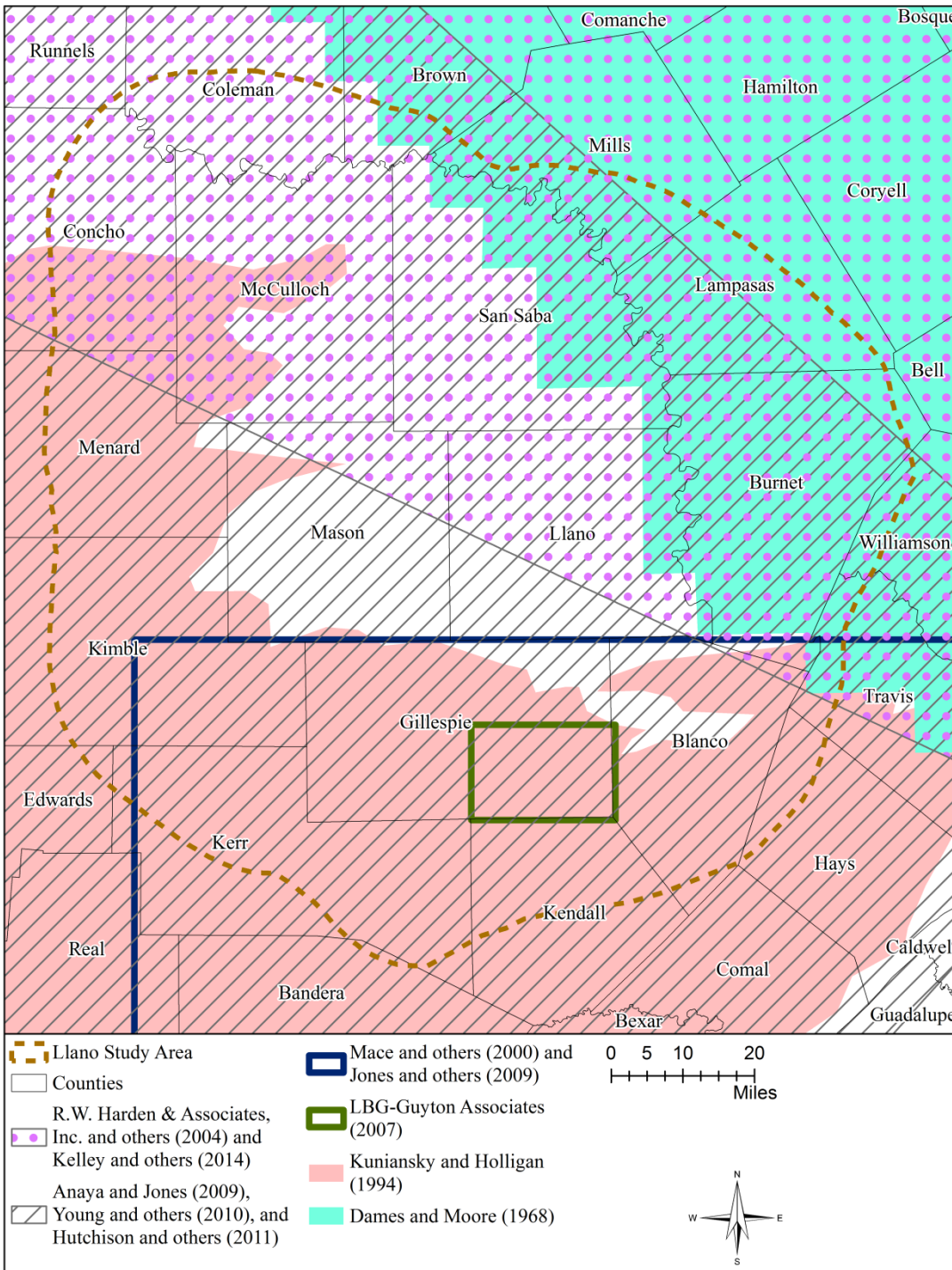


Figure 3.5.1 Areal coverage of previous groundwater flow models.

4.0 Hydrologic Setting

This section summarizes the information needed for the development of the conceptual groundwater flow model. Specifically, this section includes the layering framework, water levels, recharge, surface water-aquifer interaction, discharge, hydraulic properties, and water quality of the aquifer.

4.1 Hydrostratigraphy

Hydrostratigraphy involves dividing the same geologic unit with clear heterogeneous properties or lumping geologic units with similar hydrogeologic properties. The classification of the hydrostratigraphy is also related to the purpose of the numerical model, data availability, and understanding of the groundwater flow system. Due to a lack of groundwater usage information, water level data, and limited formation distribution, the Lion Mountain and Welge members are lumped together with the Morgan Creek and Point Peak members located above these geologic units and the Cap Mountain Member located below. As a result, the geologic units in the Llano Uplift region have been organized into the following hydrostratigraphic layers (from top to bottom): the Cretaceous and younger units as Layer 1, all the geologic units between the Cretaceous and Marble Falls Aquifer as Layer 2, the Marble Falls Aquifer as Layer 3, all the geologic units between the Marble Falls Aquifer and Ellenburger-San Saba Aquifer as Layer 4, the Ellenburger-San Saba Aquifer as Layer 5, all the geological units between the Ellenburger-San Saba Aquifer and Hickory Aquifer as Layer 6, and the Hickory Aquifer as Layer 7. Details of the hydrogeologic units in the study area are presented in [Table 2.2.1](#).

4.1.1 Hydrostratigraphic Layer Structure

The hydrostratigraphic layer structure involves the definition of the top and bottom of each hydrostratigraphic layer. To help develop this conceptual model, Standen and Ruggiero (2007) produced the bottom elevations for the Marble Falls Aquifer, the top elevations for the Welge Sandstone, and the top and bottom elevations for the Ellenburger-San Saba and Hickory aquifers. In the same study, Standen and Ruggiero (2007) also developed the faulting structure in the Marble Falls Formation and older geologic units. Their study provided the foundation for TWDB to evaluate additional data to fill the gaps in certain areas (mainly downdip or subcrop). The new data included geophysical logs, driller logs, water well reports, and point data from previous studies. The geophysical logs are from the Brackish Resources Aquifer Characterization System (BRACS) database (TWDB, 2012b); the driller logs and water well reports are from the TWDB groundwater database (TWDB, 2014a); more recent driller logs and geophysical logs are from the Hill Country Underground Water Conservation District, the Blanco-Pedernales Groundwater Conservation District, and the Central Texas Groundwater Conservation District. In addition, the surface geology from the Bureau of Economic Geology of The University of Texas at Austin (TWDB, 2014b) was also extracted using ArcGIS 10.1 to obtain the location and elevation of the layer top and bottom in the outcrop areas.

As described in Section 2, the complexity of the Llano Uplift geology had been the product of the original depositional environments and post-depositional tectonic activities. The paucity of borehole logs and extensive faulting limited the use of automatic graphing tools. As a result, the final layer structures were mainly drawn by hand except the ground surface which was defined using the U. S. Geological Survey's Digital Elevation Model (DEM). During the process, our understanding of the regional geology was incorporated into the drawings as much as possible.

In general, the process involved creating the preliminary structure contours using SURFER, comparing the contours with log data, determining the trend and variation of the structures, and comparing the structure contours with the ones above and below. Inconsistency and errors were evaluated and minimized by adding control points. Using this approach, the top and bottom structures of the Marble Falls, Ellenburger-San Saba, and Hickory aquifers were generated. As a final quality control, the thicknesses for each of these layers was calculated and mapped, and compared with the log data and the TWDB aquifer designation map. This process was repeated until the structures were consistent with the log data and our understanding of the regional geology and hydrogeology.

Figure 4.1.1 shows the ground surface elevation or the top of Layer 1 (Cretaceous and younger units) which ranges from 2,367 feet above mean sea level in the western portion to a low of 673 feet above mean sea level in the east. The interpreted bottom and thickness of Layer 1 are presented in Figures 4.1.2 and 4.1.3, respectively. Figure 4.1.2 indicates that the bottom of Layer 1 is over 1,500 feet above mean sea level at the northwestern and central portions of the study area and decreases to less than 500 feet above mean sea level to the southeast near the edge of the study area. The thickness of Layer 1 is the greatest in Kerr County; thins in west, east, and southeast; and is absent to the north in McCulloch and San Saba counties (Figure 4.1.3). This thickness distribution is consistent with the boring logs and surface geology from the Bureau of Economic Geology of The University of Texas at Austin.

Figures 4.1.4, 4.1.5, and 4.1.6 are the interpreted top elevation, bottom elevation, and thickness of Layer 3 (Marble Falls Aquifer), respectively. Both the top and bottom of Layer 3 show a circular pattern with a decreasing elevation from the central portion of the Llano Uplift to the study area boundary. The thickness of Marble Falls Aquifer changes significantly from non-existence in central and southwestern parts to more than 300 feet in some of the far down dip parts of the study area (Figures 4.1.6). This distribution is consistent with the boring logs and surface geology. The structure and, in a lesser degree, the thickness of the Marble Falls Aquifer appear to be controlled by the faults.

Figures 4.1.7, 4.1.8, and 4.1.9 represent the interpreted top elevation, bottom elevation, and thickness of Layer 5 (Ellenburger-San Saba Aquifer), respectively. Like the Marble Falls Aquifer, both the top and bottom of Ellenburger-San Saba Aquifer show a circular pattern with a decreasing elevation from the central portion of the Llano Uplift to the study area boundary. The thickness of Layer 5 is over 100 feet for most of the study area with the greatest thicknesses of over 2,000 feet in northwestern Williamson and eastern Burnet counties (Figures 4.1.9). The impact of faulting is also clearly seen in the layer structure: tilting of the stratigraphic units and abrupt change of unit thickness across faults.

The interpreted top elevation, bottom elevation, and thickness of Layer 7 (Hickory Aquifer) are shown in Figures 4.1.10, 4.1.11, and 4.1.12, respectively. Again, both the top and bottom of Layer 7 show a circular pattern with a decreasing elevation from the central portion of the Llano Uplift to the study area boundary. The thickness of Layer 7 is over 300 feet for most of the study area. This is more evident in McCulloch, Menard, Kimble, and Gillespie counties where the thickness data from logs are available (Figure 4.1.12). Like the Ellenburger -San Saba Aquifer, the Hickory Aquifer structure is also greatly influenced by faults.

To show the variation of layer structure and relationship among layers as well as the impacts of faults and fault density, two cross sections are presented in [Figures 4.1.14](#) and [4.1.15](#), with the cross section locations shown in [Figure 4.1.13](#). The cross-sections were intentionally oriented either approximately perpendicular to ([Figures 4.1.14](#)) or parallel with ([Figures 4.1.15](#)) the dominant faulting direction. Both cross sections indicate significant layer structure change and fault impacts which have caused lateral disconnection within the same hydrostratigraphic unit and connection between different hydrostratigraphic layers.

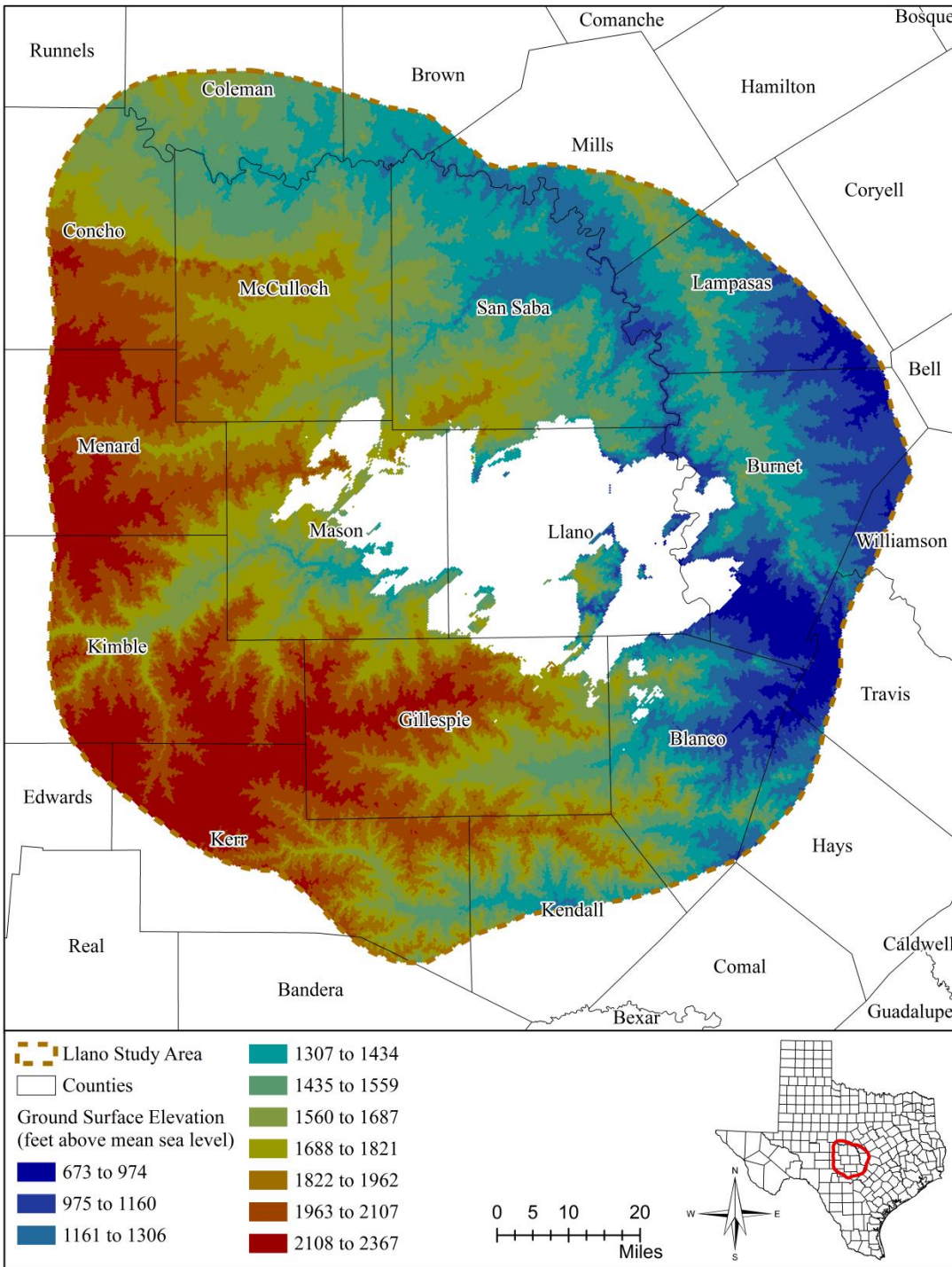


Figure 4.1.1 Interpreted ground surface or top elevation of Layer 1 (Cretaceous and younger units) based on U.S. Geological Survey’s Digital Elevation Model (DEM).

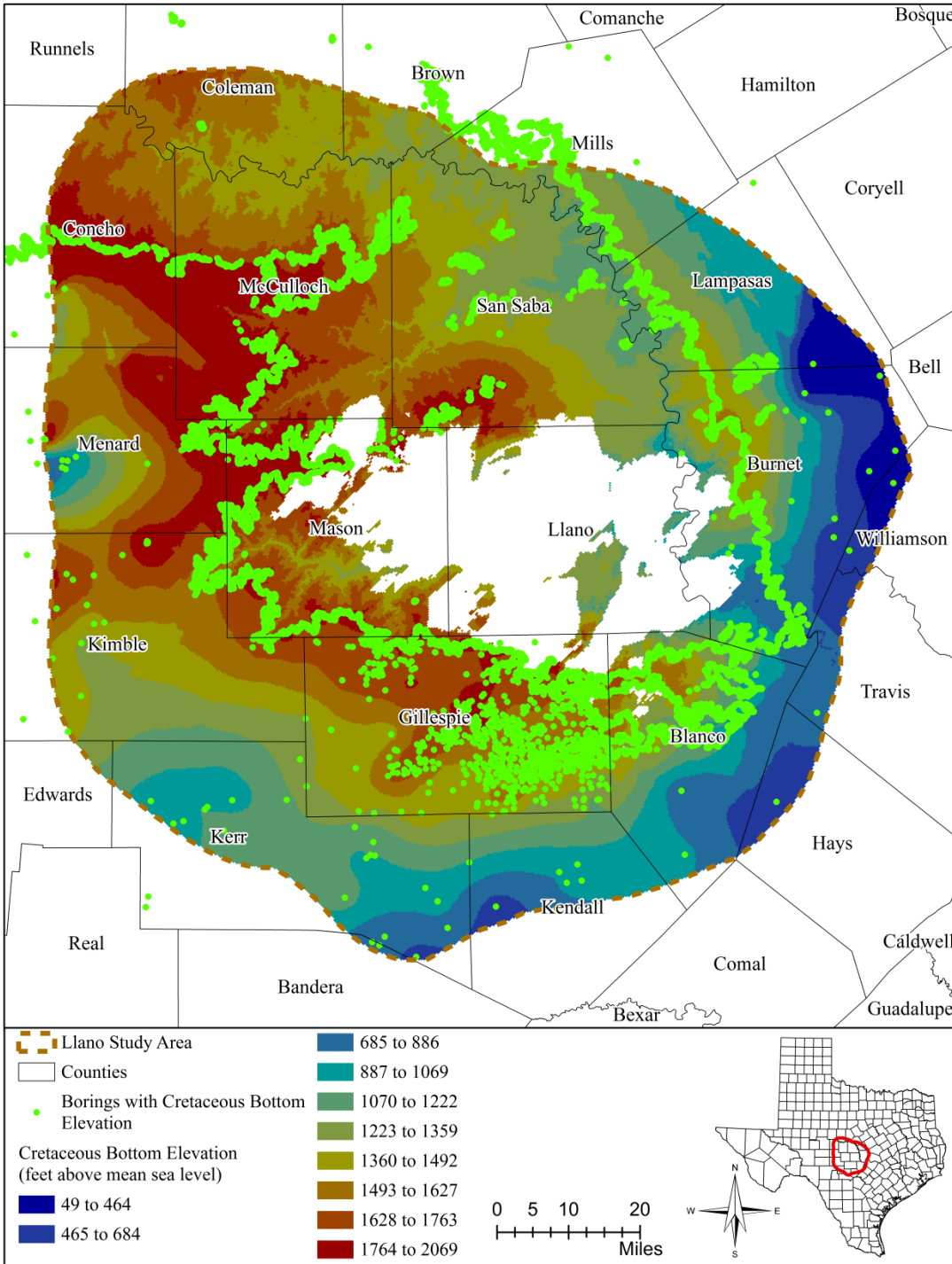


Figure 4.1.2 Interpreted bottom elevation of Layer 1 (Cretaceous and younger units).

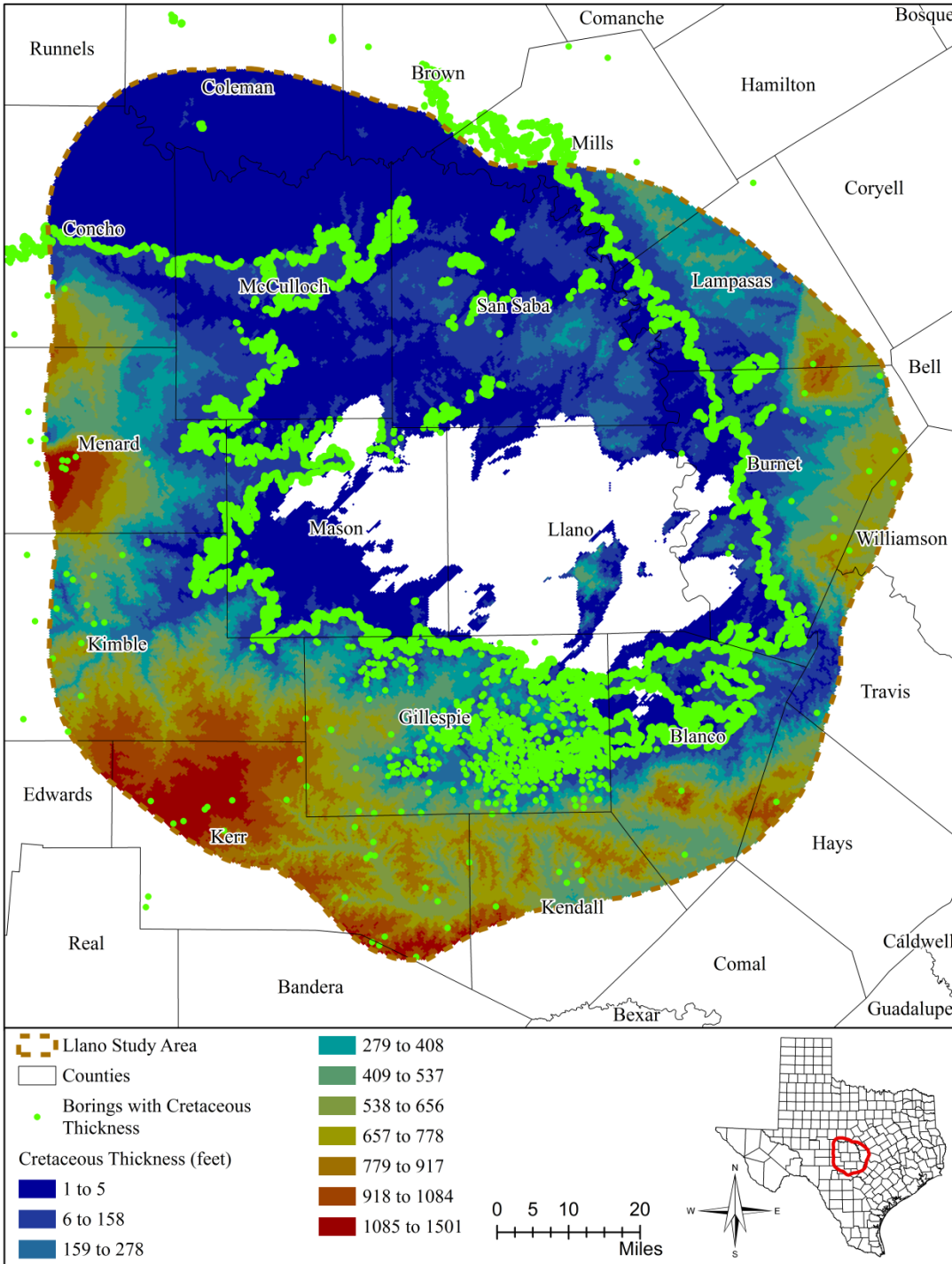


Figure 4.1.3 Interpreted thickness of Layer 1 (Cretaceous and younger units).

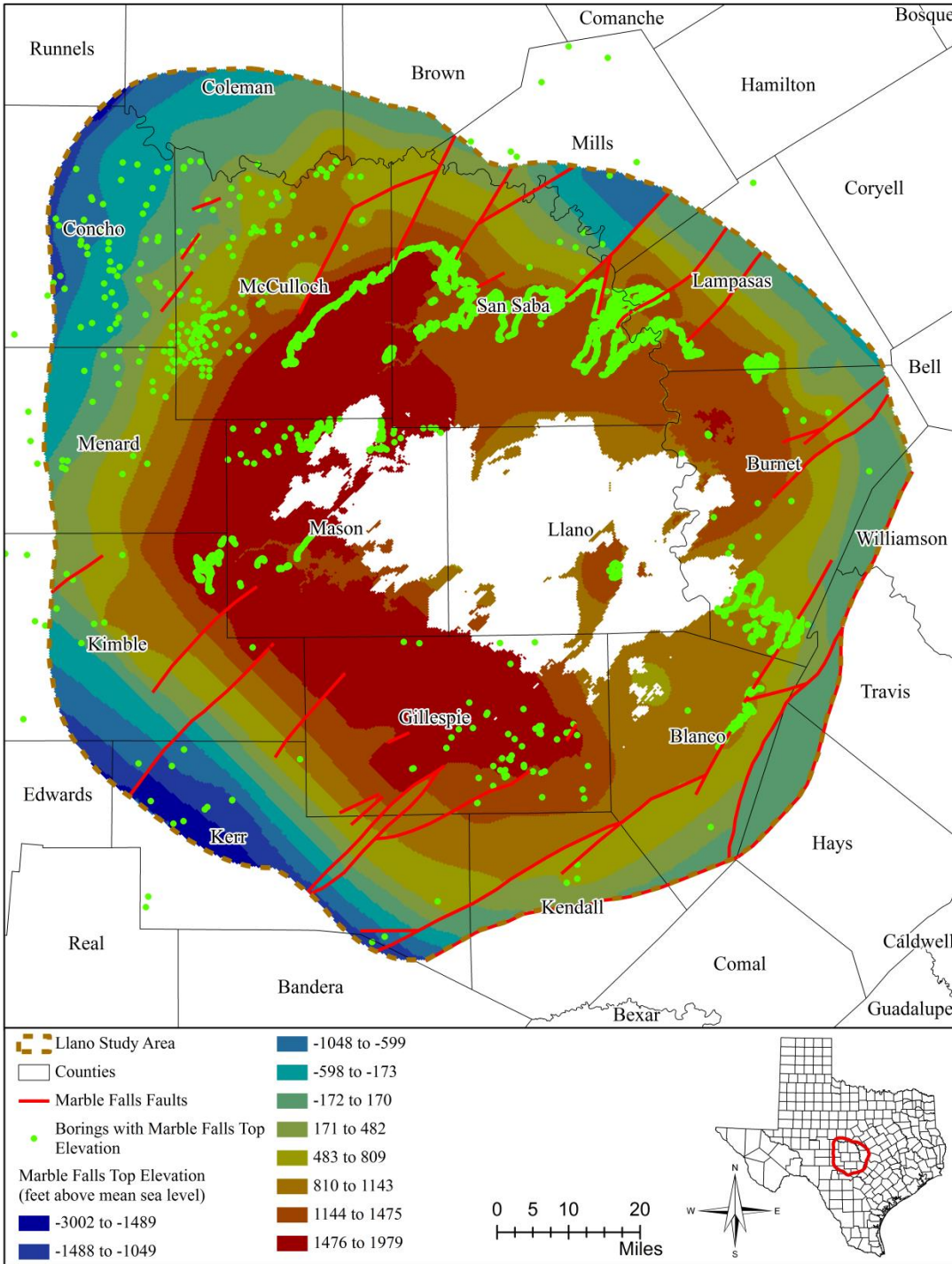


Figure 4.1.4 Interpreted top elevation of Layer 3 (Marble Falls Aquifer).

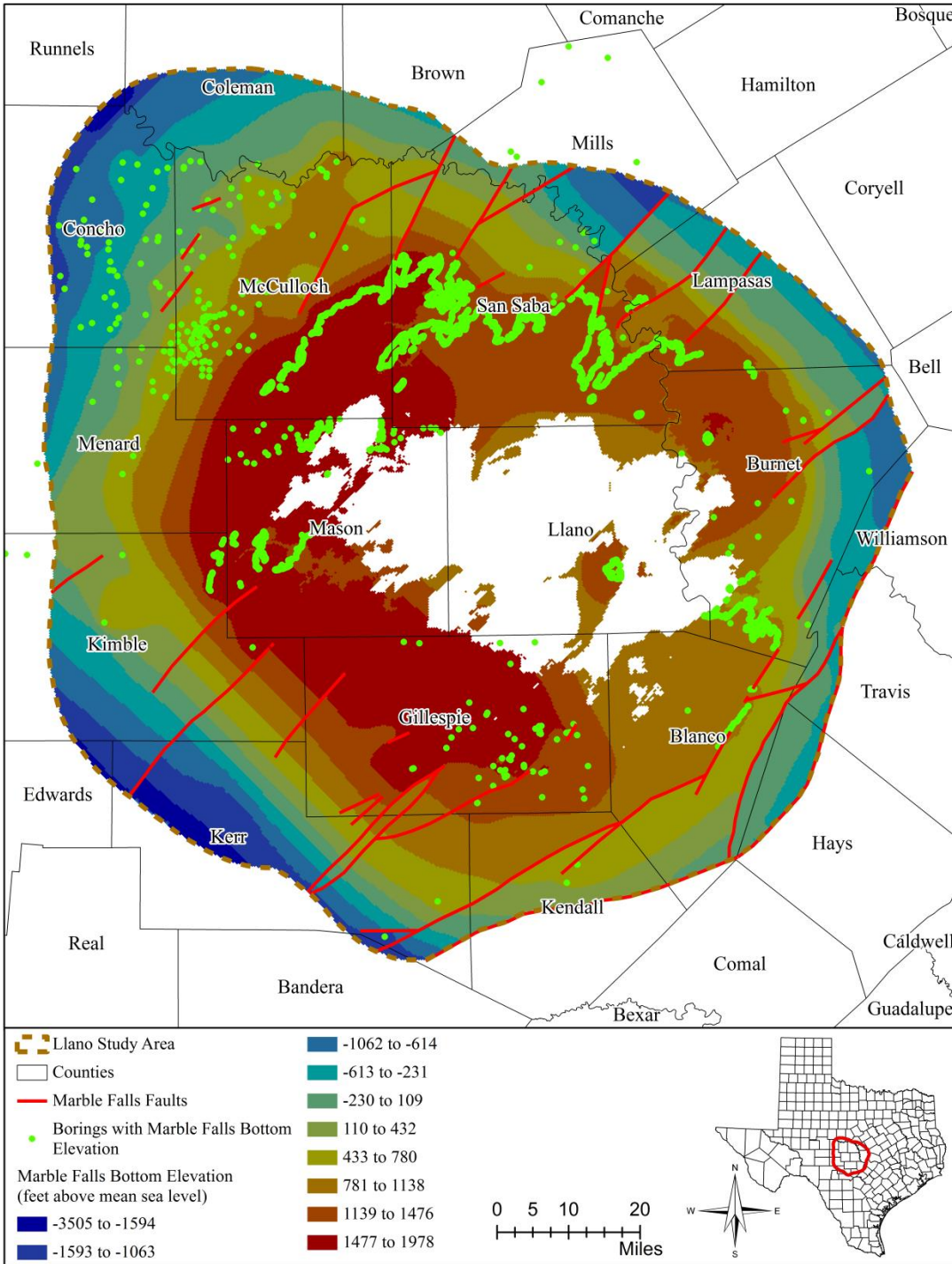


Figure 4.1.5 Interpreted bottom elevation of Layer 3 (Marble Falls Aquifer).

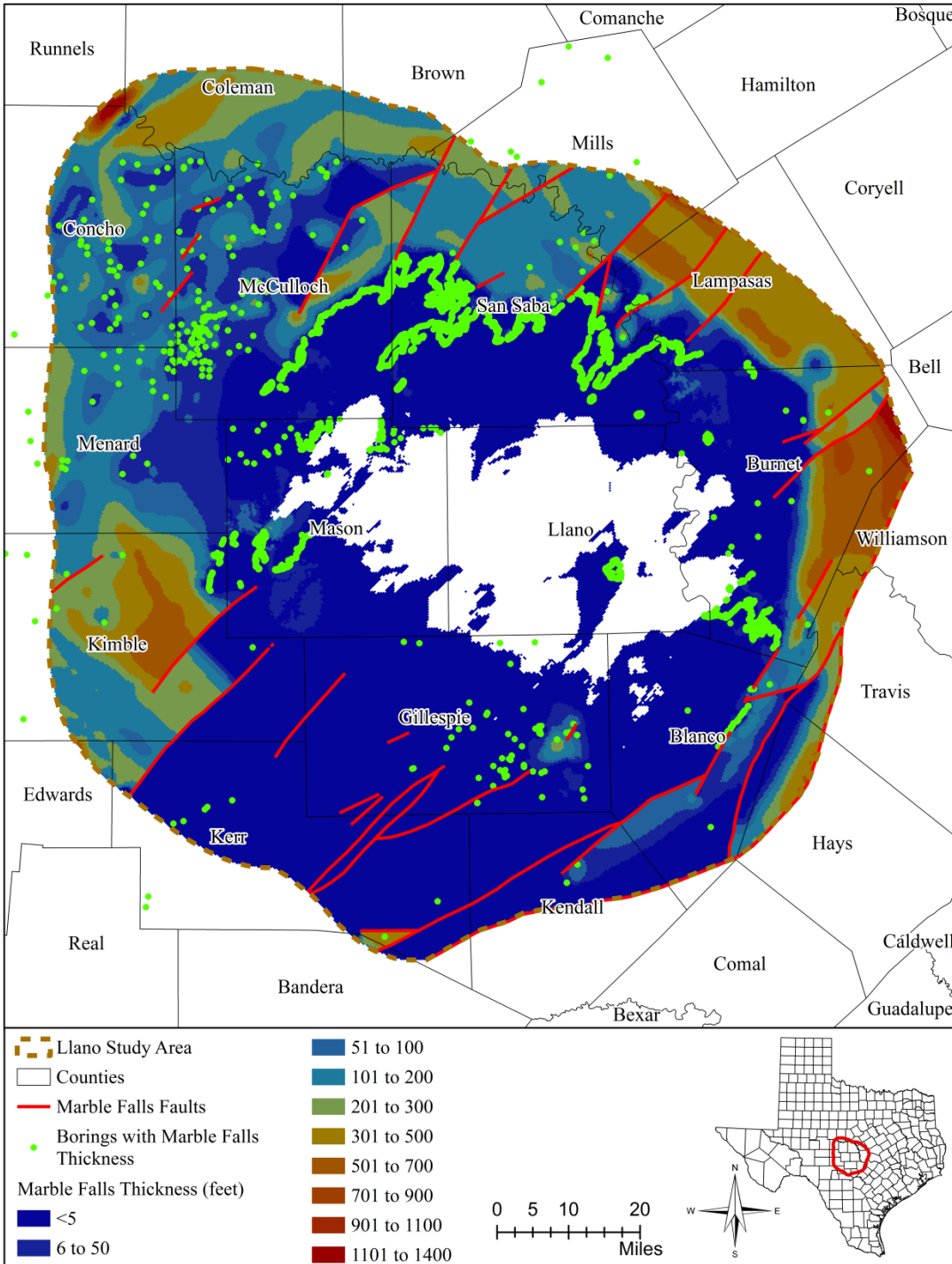


Figure 4.1.6 Interpreted thickness of Layer 3 (Marble Falls Aquifer).

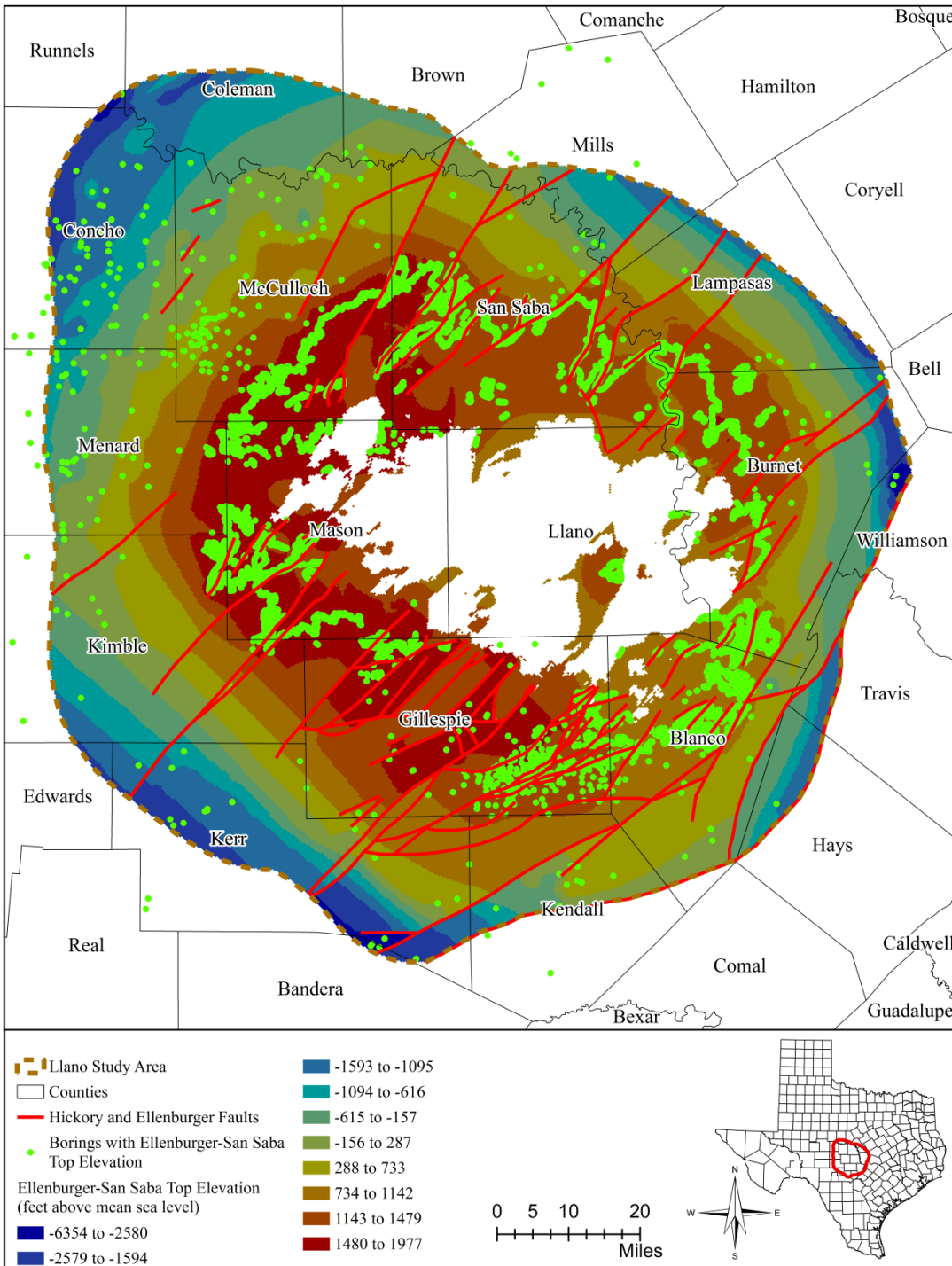


Figure 4.1.7 Interpreted top of Layer 5 (Ellenburger-San Saba Aquifer).

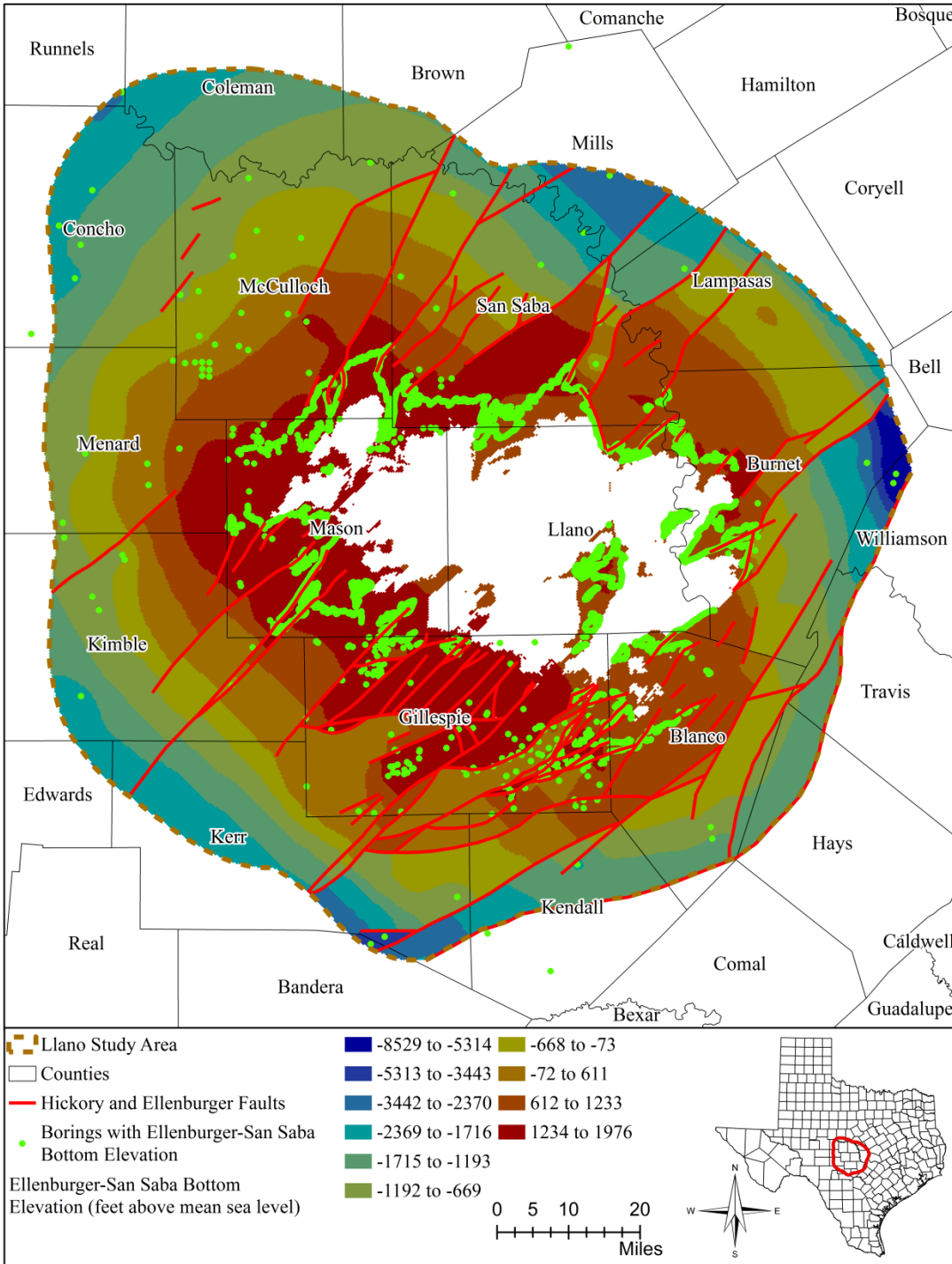


Figure 4.1.8 Interpreted bottom of Layer 5 (Ellenburger-San Saba Aquifer).

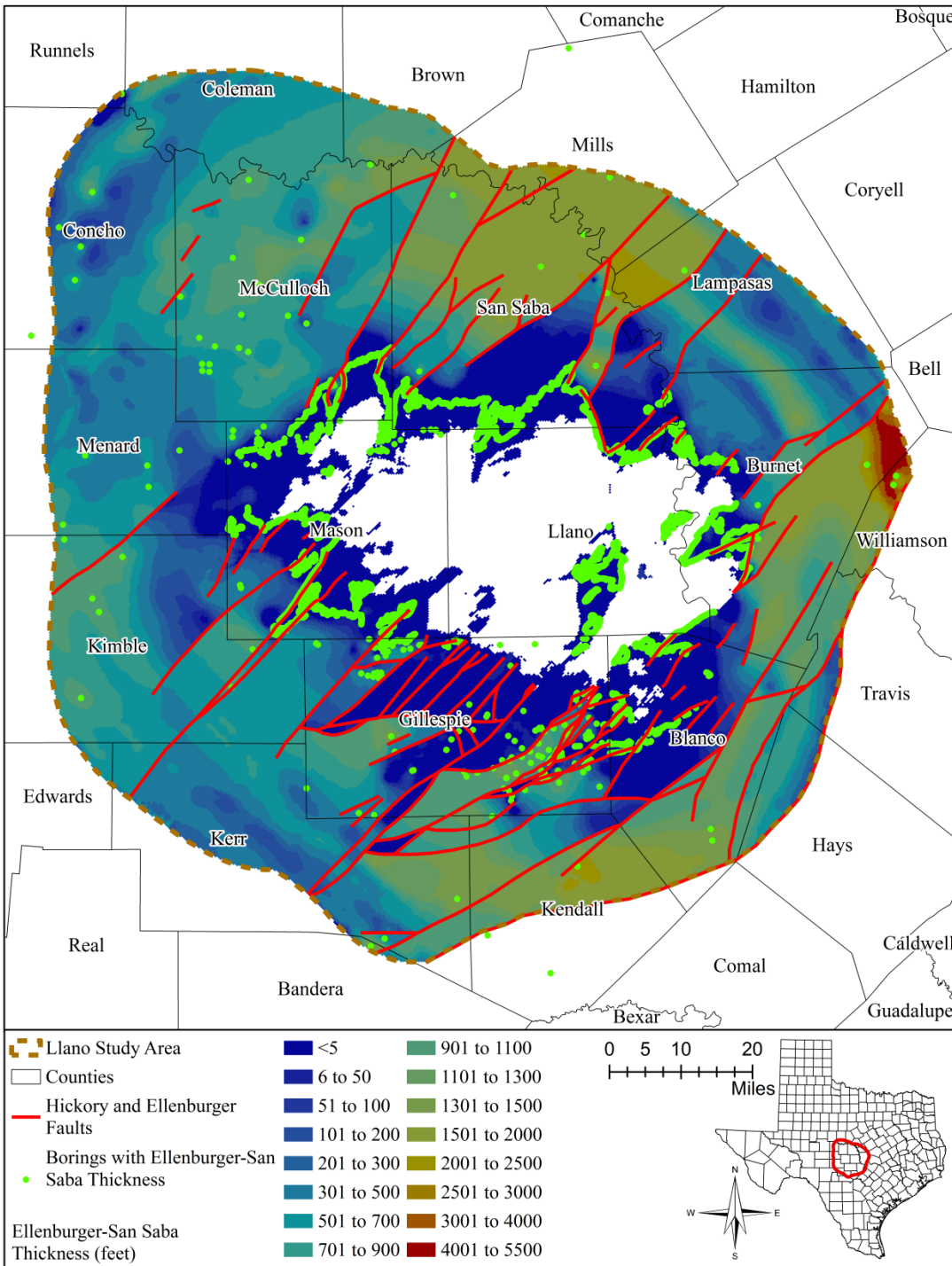


Figure 4.1.9 Interpreted thickness of Layer 5 (Ellenburger-San Saba Aquifer).

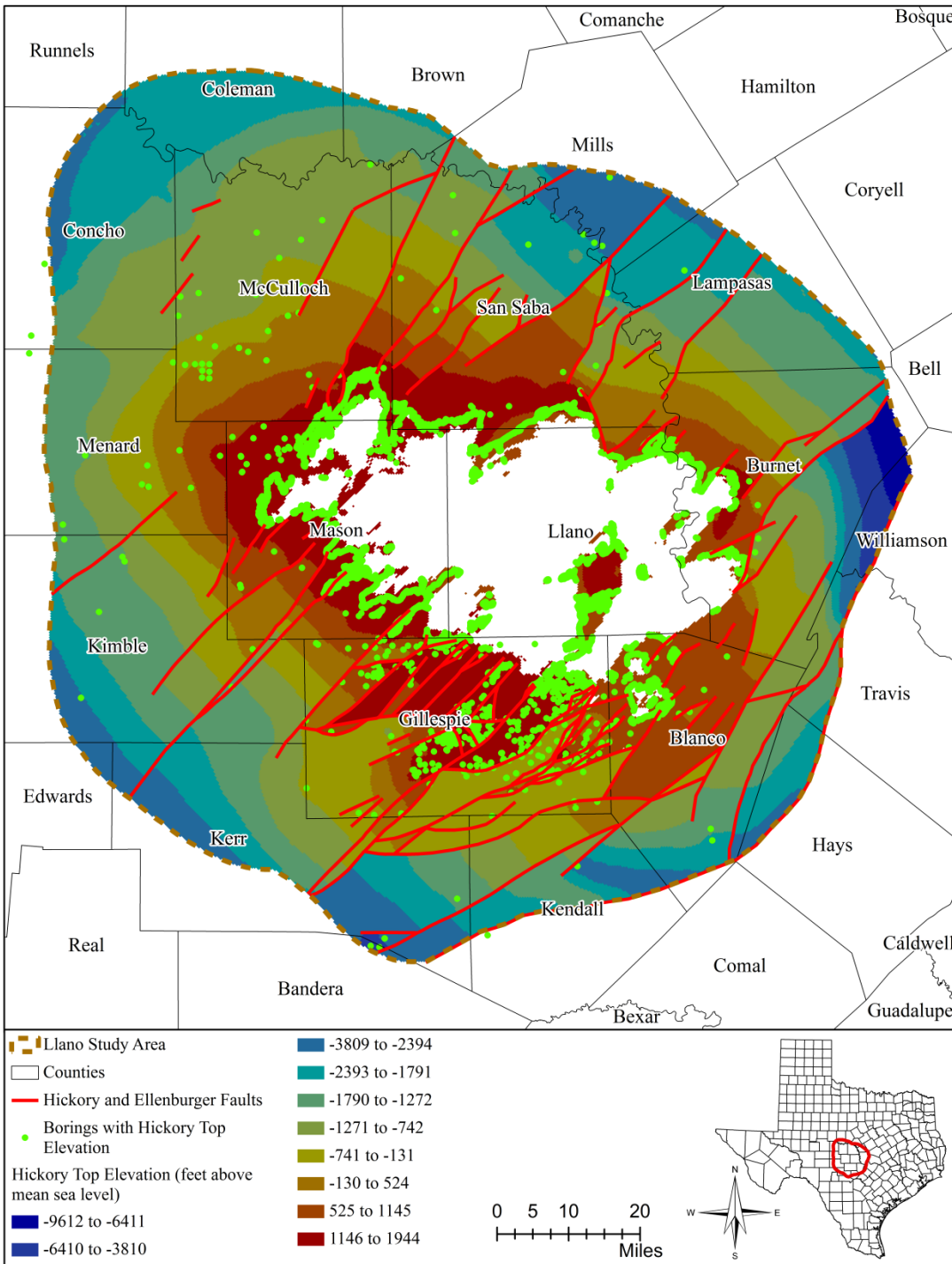


Figure 4.1.10 Interpreted top of Layer 7 (Hickory Aquifer).

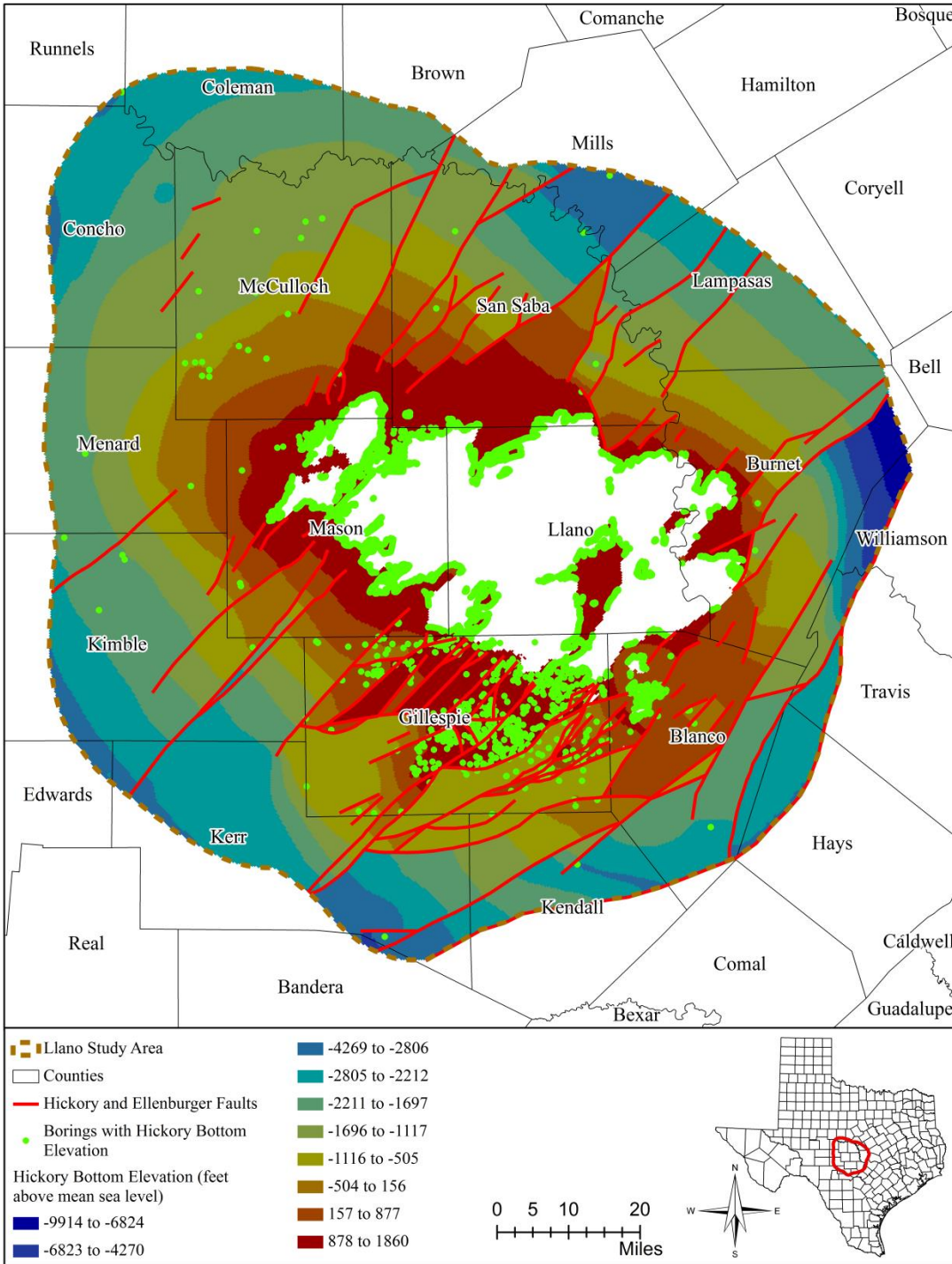


Figure 4.1.11 Interpreted bottom of Layer 7 (Hickory Aquifer).

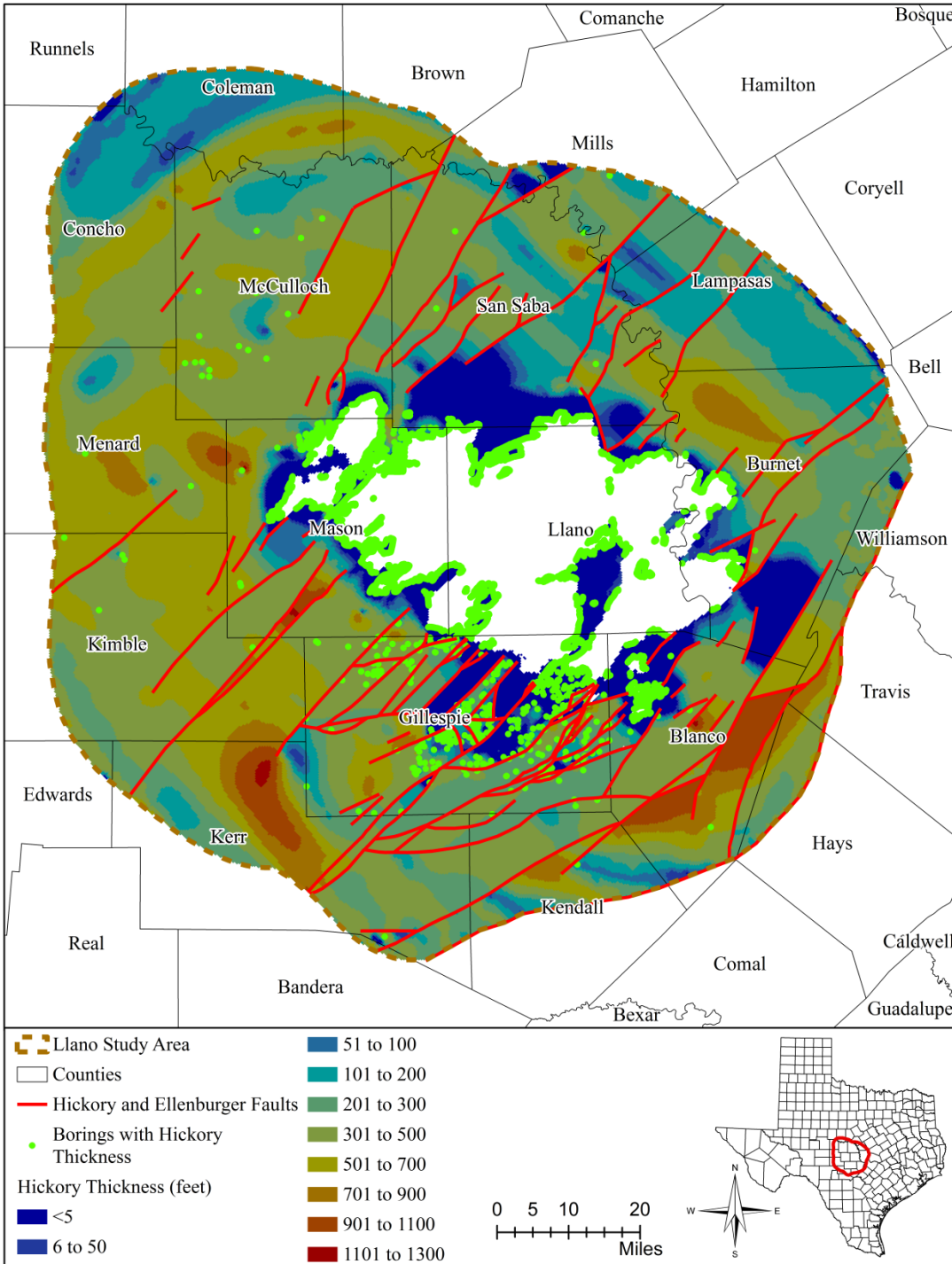


Figure 4.1.12 Interpreted thickness of Layer 7 (Hickory Aquifer).

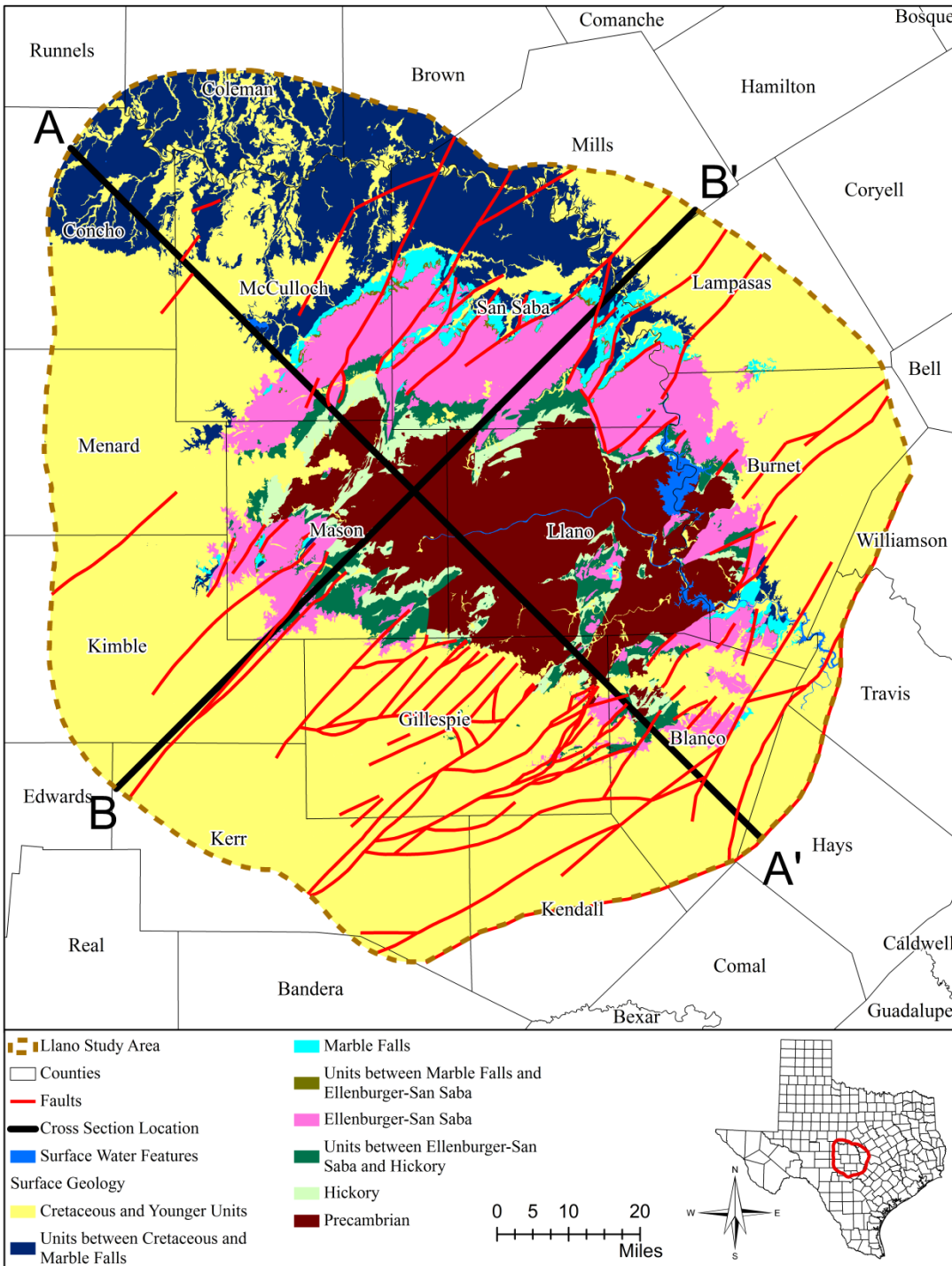
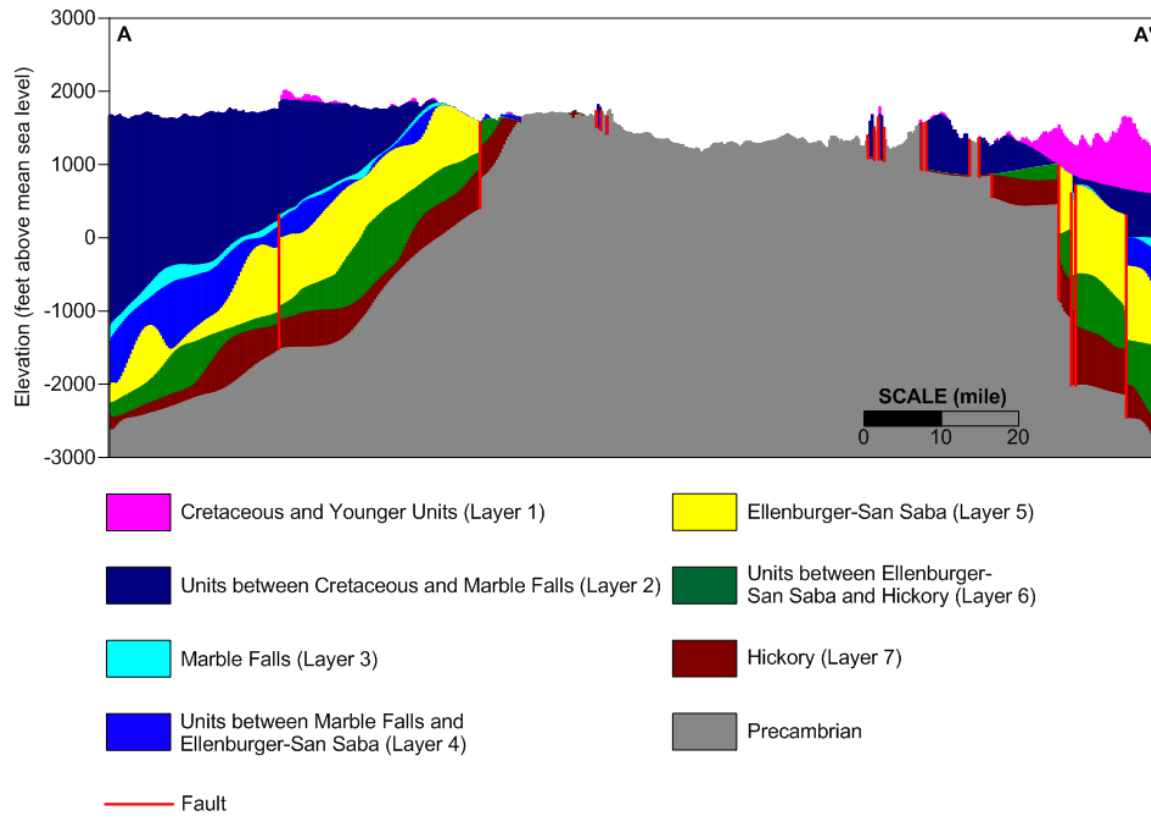


Figure 4.1.13 Location of hydrostratigraphic cross sections. Surface geology is based on *Geologic Atlas of Texas* (Bureau of Economic Geology, 2013). Faults are based on Standen and Ruggiero (2007).



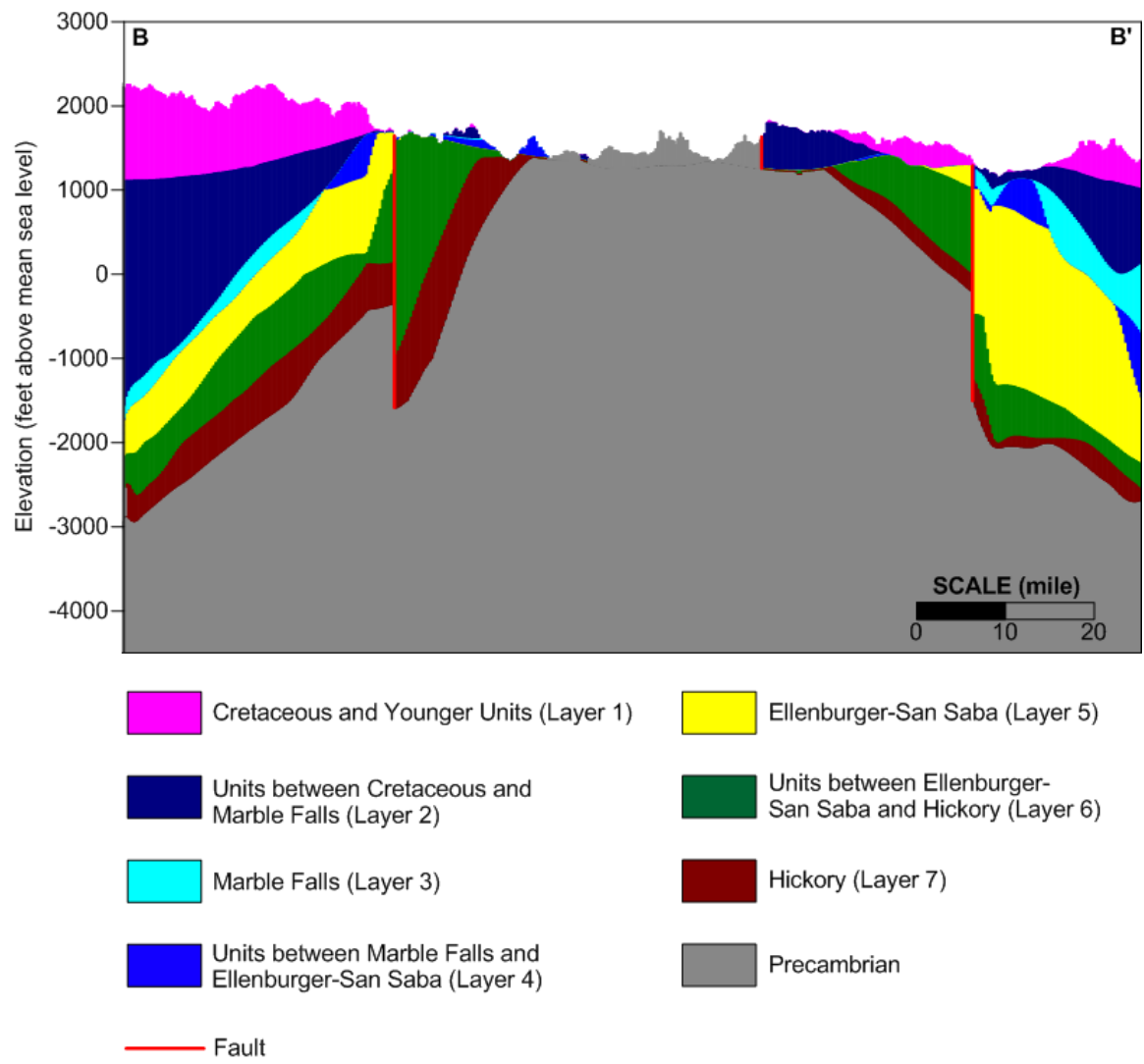


Figure 4.1.15 Hydrostratigraphic cross section along southwest-northeast direction. Vertical exaggeration relative to horizontal direction is 50. Location of cross section is shown in Figure 4.2.13.

4.2. Groundwater Levels and Flows

Groundwater level data from the TWDB groundwater database (TWDB, 2014a) were used to evaluate pre- and post-development groundwater flow and identify water level targets for the numerical flow model. The following subsection summarizes the estimate of pre-development water levels, groundwater level changes over time, and possible cross-formation flow patterns between aquifers.

4.2.1. Distribution of Water Level Measurements

The TWDB groundwater database (TWDB, 2014a) generated 4,389 wells with water level measurements in the study area. Screen information was available at 2,343 wells. The well screen information was then compared with the hydrostratigraphic structure to determine which hydrogeologic unit(s) these wells belong to. This analysis generated 1,388 wells completed in a single hydrogeologic unit. Of these wells, 673 wells were screened in the Cretaceous aquifers, 14 in the Marble Falls Aquifer, 133 in the Ellenburger-San Saba Aquifer, and 126 in the Hickory Aquifer. These wells contain 14,991 groundwater level measurements between 1930 and 2014. The water level measurements were broken down by decade and summarized in [Table 4.2.1](#). As the table shows, the numbers of groundwater level measurements have steadily increased over the last several decades with the Cretaceous aquifers having the most measurements and the Marble Falls Aquifer the fewest. The greatest jump occurred between 1970s and 1980s.

The spatial distributions of wells completed in the Cretaceous, Marble Falls, Ellenburger-San Saba, and Hickory aquifers are presented in [Figures 4.2.1, 4.2.2, 4.2.3, and 4.2.4](#) respectively. Most of the wells in the Cretaceous aquifers are located to the south of the study area where this unit is relatively thick ([Figures 4.1.3 and 4.2.1](#)). Very few wells are in the Marble Falls Aquifer ([Figure 4.2.2](#)). Wells in the Ellenburger-San Saba Aquifer are mainly located in Burnet, McCulloch, and San Saba counties and southeastern Gillespie County ([Figure 4.2.3](#)). Most of the Hickory Aquifer wells are located at or near the outcrop areas in Burnet, Gillespie, Mason, and McCulloch counties ([Figure 4.2.4](#)).

4.2.2. Pre-development Water Levels

Before large-scale groundwater withdrawals by pumping occurred, the aquifers in the study area were under relatively long-term steady state conditions. Seasonal fluctuation of water levels and recharge/discharge were mainly influenced by natural cycles. Under the steady-state conditions, the aquifer discharge such as by springs was balanced out by recharge such as precipitation infiltration.

Prior to the 1950s drought, groundwater use in the study area was relatively small (TWDB, 2012a). Thus, the measured water level data from wells recorded before 1950 were used to approximate the pre-development conditions in this analysis. Pre-development water level for the Marble Falls Aquifer was unsuccessful because no water level measurements were noted in the TWDB groundwater database prior to 1950. In addition, due to lack of data (especially in the downdip areas), water levels were also challenging for the Ellenburger-San Saba and Hickory aquifers. In addition to using measured water levels in wells, spring orifice elevations were also used to approximate the pre-development groundwater levels. The information of spring

locations and associated aquifers is from Heitmuller and Reece (2003). The spring orifice elevations were determined by intercepting the spring location with the U.S. Geological Survey's Digital Elevation Model. The following sections describe the "pseudo" pre-development water levels developed for the Cretaceous, Ellenburger-San Saba, and Hickory aquifers in the study area.

4.2.2.1 Cretaceous Aquifers

Figure 4.2.5 shows the estimated pre-development water level contours for the Cretaceous aquifers. This figure indicates that, prior to the large-scale groundwater development, the groundwater in the Cretaceous aquifers generally flowed from west to east in the study area. In Kerr and Kendall counties the groundwater in the downdip portion flowed to south as well. The highest water levels are expected to be about 2,000 feet above mean sea level in Gillespie and Kimble counties. The eastern portions of Burnet and Blanco counties had the lowest pre-development water levels around 900 feet above mean sea level.

4.2.2.2 Ellenburger-San Saba Aquifer

The pre-development measured water levels at wells and the estimated elevations at spring orifices associated with the Ellenburger-San Saba Aquifer are posted in Figure 4.2.6. In general, the well and spring data show the pre-development water level decreasing from more than 1,600 feet above mean sea level in the western counties to about 1,200 feet above mean sea level in the eastern counties.

4.2.2.3 Hickory Aquifer

The measured water levels and estimated spring orifice elevations associated with the Hickory Aquifer are posted in Figure 4.2.7. As the figure shows, the data locations are all located in the outcrop area. Therefore, it is impossible to give a correct evaluation of the pre-development water level conditions in the whole aquifer within the study area. However, these data do show higher water levels to the west and lower values to the east.

4.2.3. *Post-development Water Levels*

Groundwater withdrawal since 1950 has modified the aquifers in the study area. The impacts include reducing spring flow and declining groundwater level. To illustrate this change across the study area over time, measured groundwater levels from 1950, 1980, and 2010 are presented in Figures 4.2.8, 4.2.9, and 4.2.10 for the Cretaceous aquifers. No enough water level measurements are available for the Marble Falls Aquifer to evaluate the change of the post-development conditions. The water level measurements from 1980 are shown in Figure 4.2.11. Figures 4.2.12, 4.2.13, and 4.2.14 show the water level measurement for the Ellenburger-San Saba Aquifer in 1950, 1980, and 2010, respectively. No measured water levels were found in the TWDB groundwater database 1950 for the Hickory Aquifer. Figures 4.2.15 and 4.2.16 show the water levels in 1980 and 2010, respectively, for the Hickory Aquifer.

In the Cretaceous aquifers, it is impossible to compare the water levels in 1950 with another time due to lack of data during that year. The water level differences between 1980 and 2010 are also not obvious. However, the groundwater level shows a decline in southern Gillespie, northern Kerr, and northern Kendall counties from pre-development (Figure 4.2.5) to 1980 (Figure 4.2.9). For the Ellenburger-San Saba and Hickory aquifers, the post-development water levels are concentrated in small zones of the outcrop areas. It is impossible to make an aquifer-wide

assessment of groundwater level changes. However, the Hickory Aquifer shows 20 to 100 feet water level decline from 1980 (Figure 4.2.15) to 2010 (Figure 4.2.16) in southwestern and eastern McCulloch County.

4.2.4. Transient Water-Level Data (Hydrographs)

In this section, the groundwater level change over time is evaluated using transient water level measurements collected from wells. Only those wells screened in a single hydrogeologic unit were assessed to create the water level hydrographs. The wells were selected based on the following criteria:

- A well must have at least 40 water level measurements from different dates;
- The earliest water level at the well must be taken before 1990; and
- The latest water level at the well must be taken after 2010.

Of 1,388 wells screened in a single aquifer, 62 wells meet the criteria. Of them, 24 wells are in the Cretaceous aquifers, 13 in the Ellenburger-San Saba Aquifer, and 12 in the Hickory Aquifer. No wells were found in the Marble Falls Aquifer to satisfy the criteria.

4.2.4.1 Cretaceous Aquifers

Water level hydrographs at selected wells completed in the Cretaceous aquifers are presented in Figure 4.2.17. As the figure shows, water levels at Wells 57-15-601 (Burnet County), 57-55-301 (Hays County), 57-58-706 (Kendall County), and 56-63-920 (Kerr County) have been declining for the last 10 to 30 years ranging from about 20 to over 100 feet. The water levels at Well 41-64-604 (Lampasas County) has been relatively stable at about 835 feet above mean sea level since late 1960s. Well 57-41-903 (Gillespie County) experienced an increase in water levels during the late 1980s and early 1990s and has been stable since then.

4.2.4.2 Ellenburger-San Saba Aquifer

Figure 4.2.18 shows the water level hydrographs at selected wells completed in the Ellenburger-San Saba Aquifer. In comparison with the Cretaceous aquifers, the water level in the Ellenburger-San Saba Aquifer shows a smaller fluctuation. In general, the water level in the Ellenburger-San Saba Aquifer has been relative stable except the three wells in Gillespie County which experienced a water level declining for the last 5 to 10 years.

4.2.4.3 Hickory Aquifer

Figure 4.2.19 shows the water level hydrographs at selected wells completed in the Hickory Aquifer. Similar to the Ellenburger-San Saba Aquifer, the water level at Well 42-63-916 (McCulloch County), Wells 56-08-403 and 56-06-613 (Mason County), Well 57-05-702 (Llano County) in the Hickory Aquifer has been relatively stable with small fluctuation. Well 57-41-502 (Gillespie County) experienced a slight water level increase over the last 5 to 10 years. Water level at Well 42-60-902 in McCulloch County has been declining for about 50 feet since middle 1970s.

Table 4.2. 1 Summary of groundwater level measurements by decade in Cretaceous, Marble Falls, Ellenburger-San Saba, and Hickory aquifers between 1930 and 2014.

Decade	Cretaceous	Marble Falls	Ellenburger-San Saba	Hickory	Total
1930 to 1940	53	0	2	0	55
1941 to 1950	30	0	4	2	36
1951 to 1960	36	0	40	53	129
1961 to 1970	374	0	180	12	566
1971 to 1980	297	5	107	283	692
1981 to 1990	475	6	157	578	1,216
1991 to 2000	2,101	6	609	873	3,589
2001 to 2010	3,976	4	794	787	5,561
2011 to 2014	2,232	0	697	218	3,147
Total	9,574	21	2,590	2,806	14,991

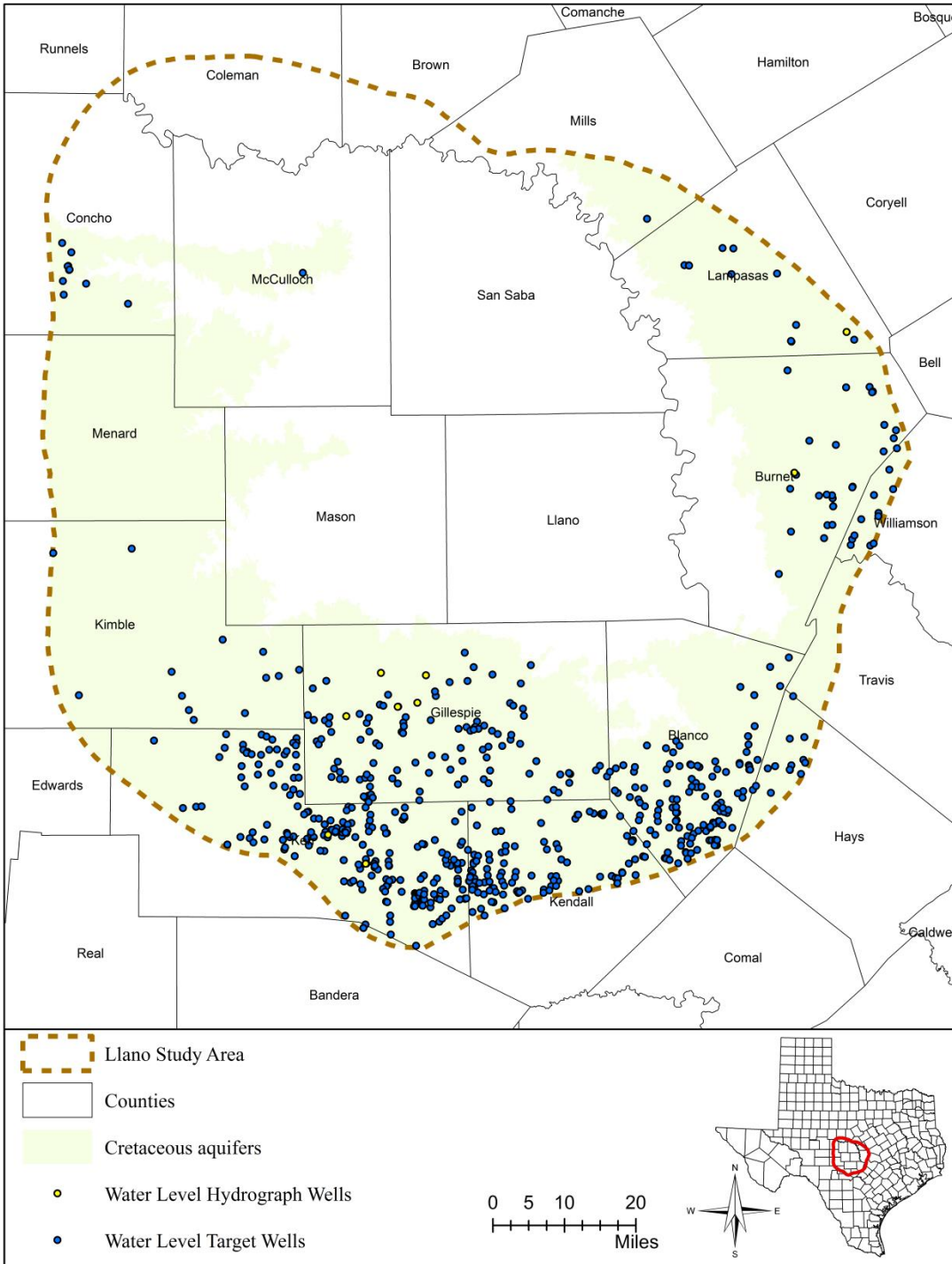


Figure 4.2.1 Location of wells with water level measurements in Cretaceous aquifers.

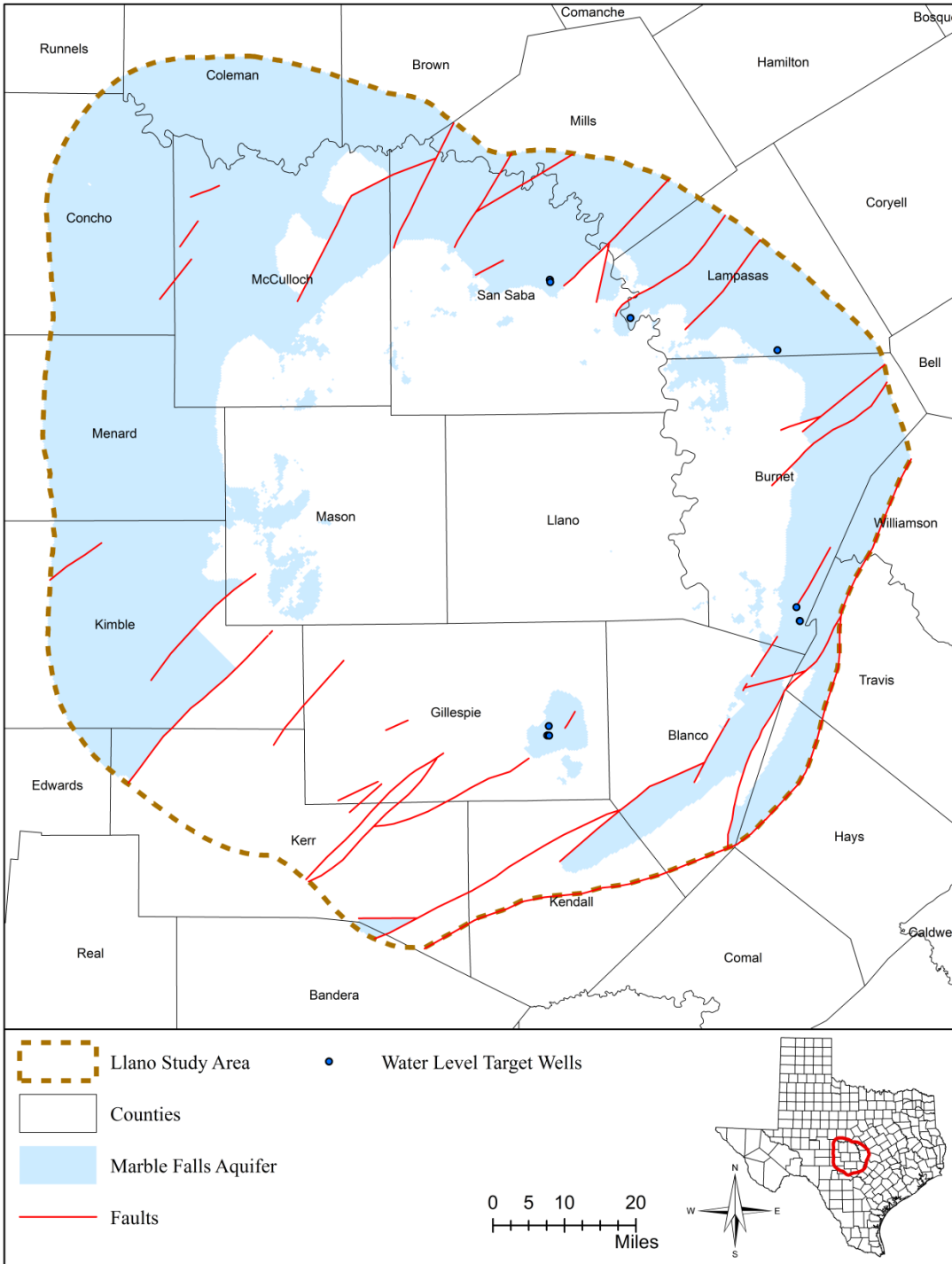


Figure 4.2.2 Location of wells with water level measurements in Marble Falls Aquifer.

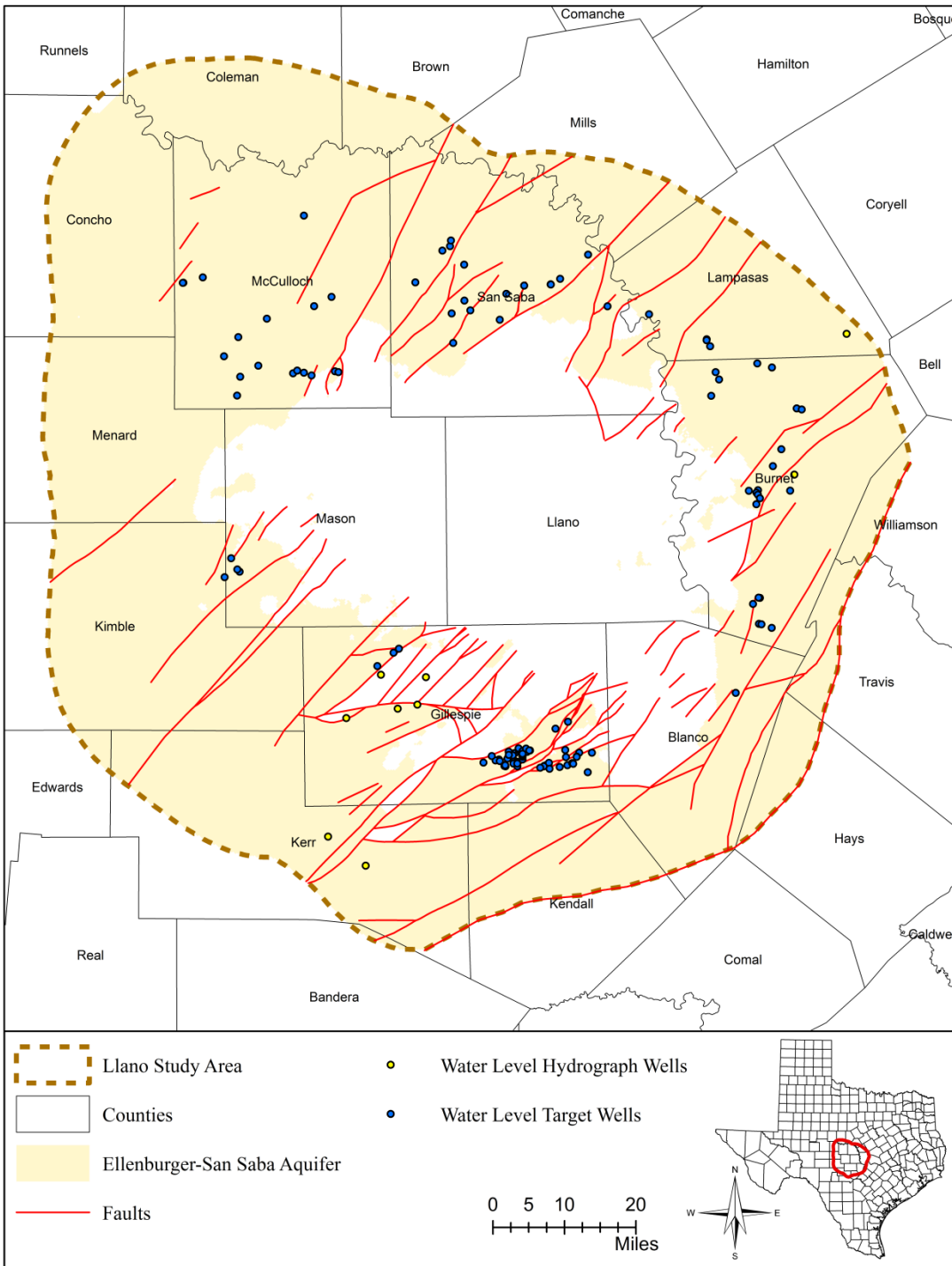


Figure 4.2.3 Location of wells with water level measurements in Ellenburger-San Saba Aquifer.

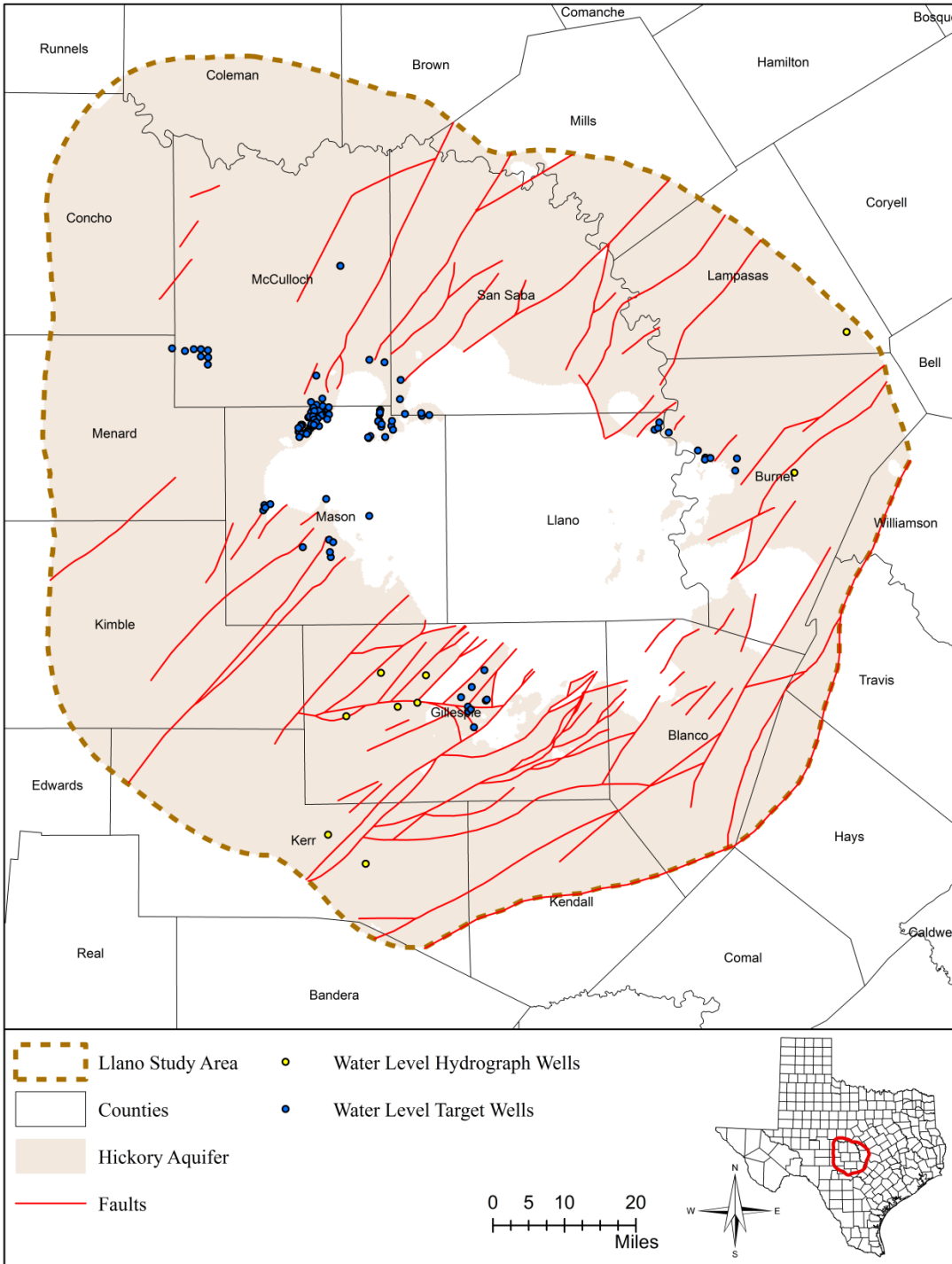


Figure 4.2.4 Location of wells with water level measurements in Hickory Aquifer.

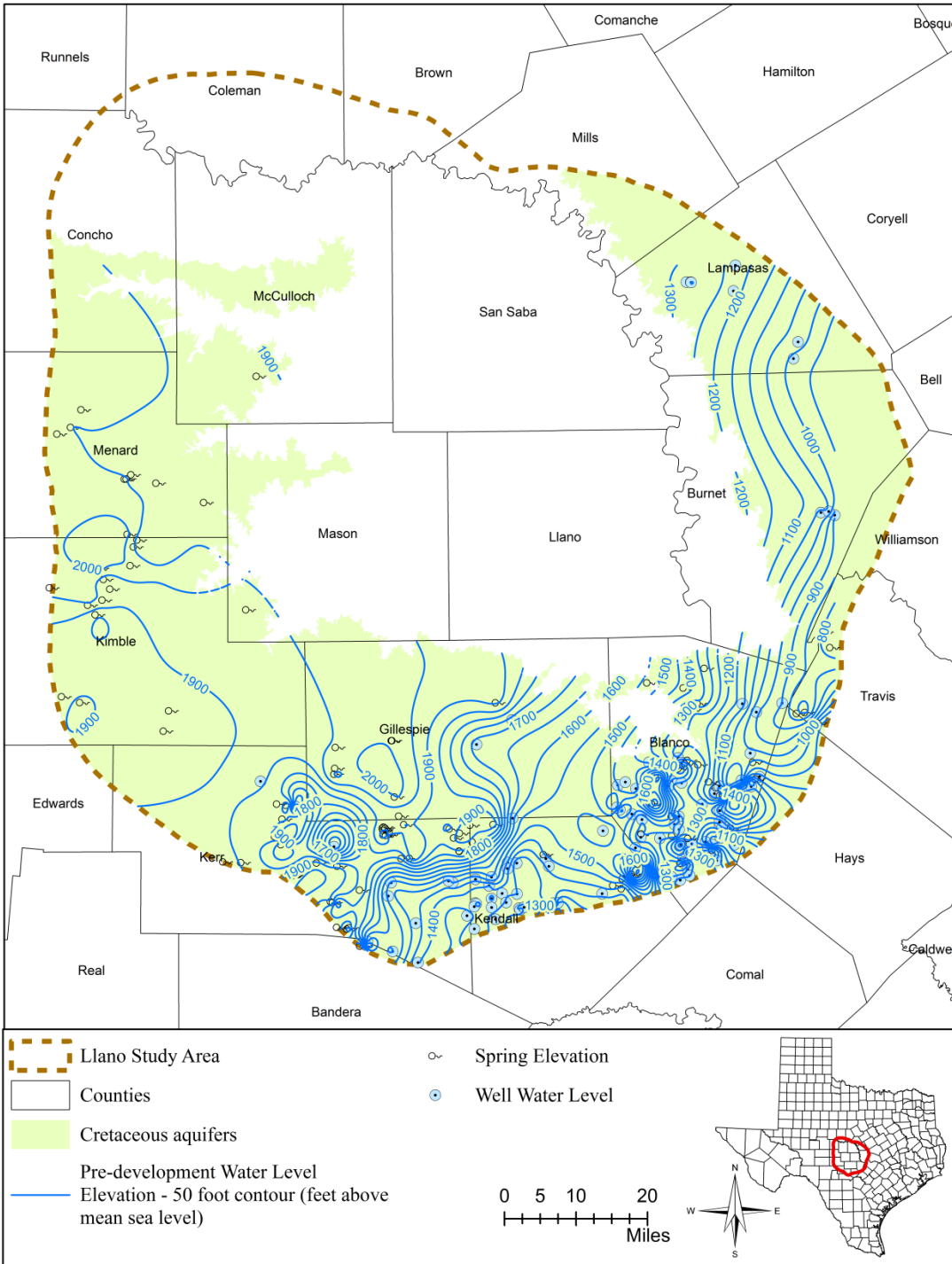


Figure 4.2.5 Pre-development potentiometric surface map of Cretaceous aquifers.

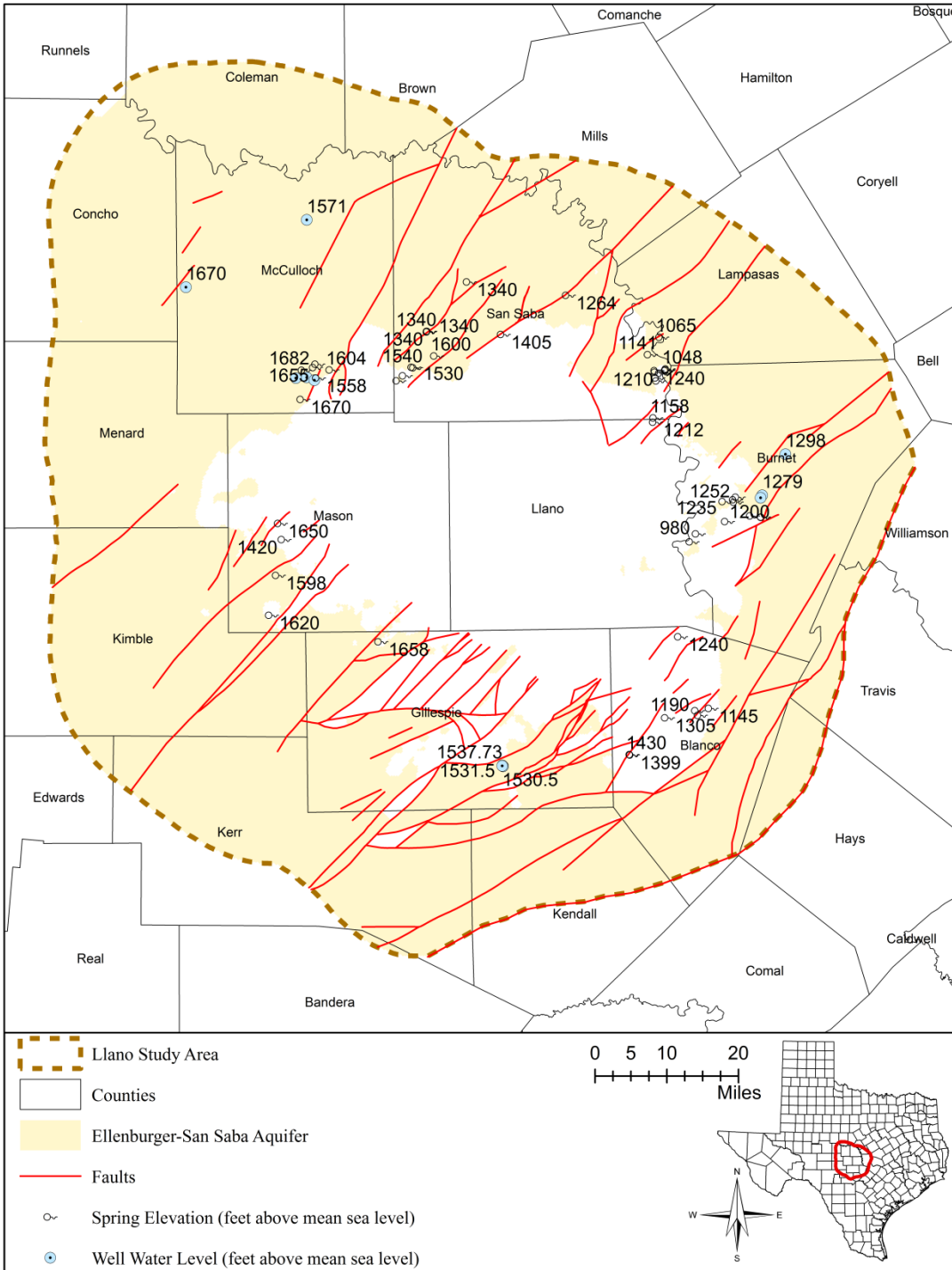


Figure 4.2.6 Pre-development water levels in Ellenburger-San Saba Aquifer.

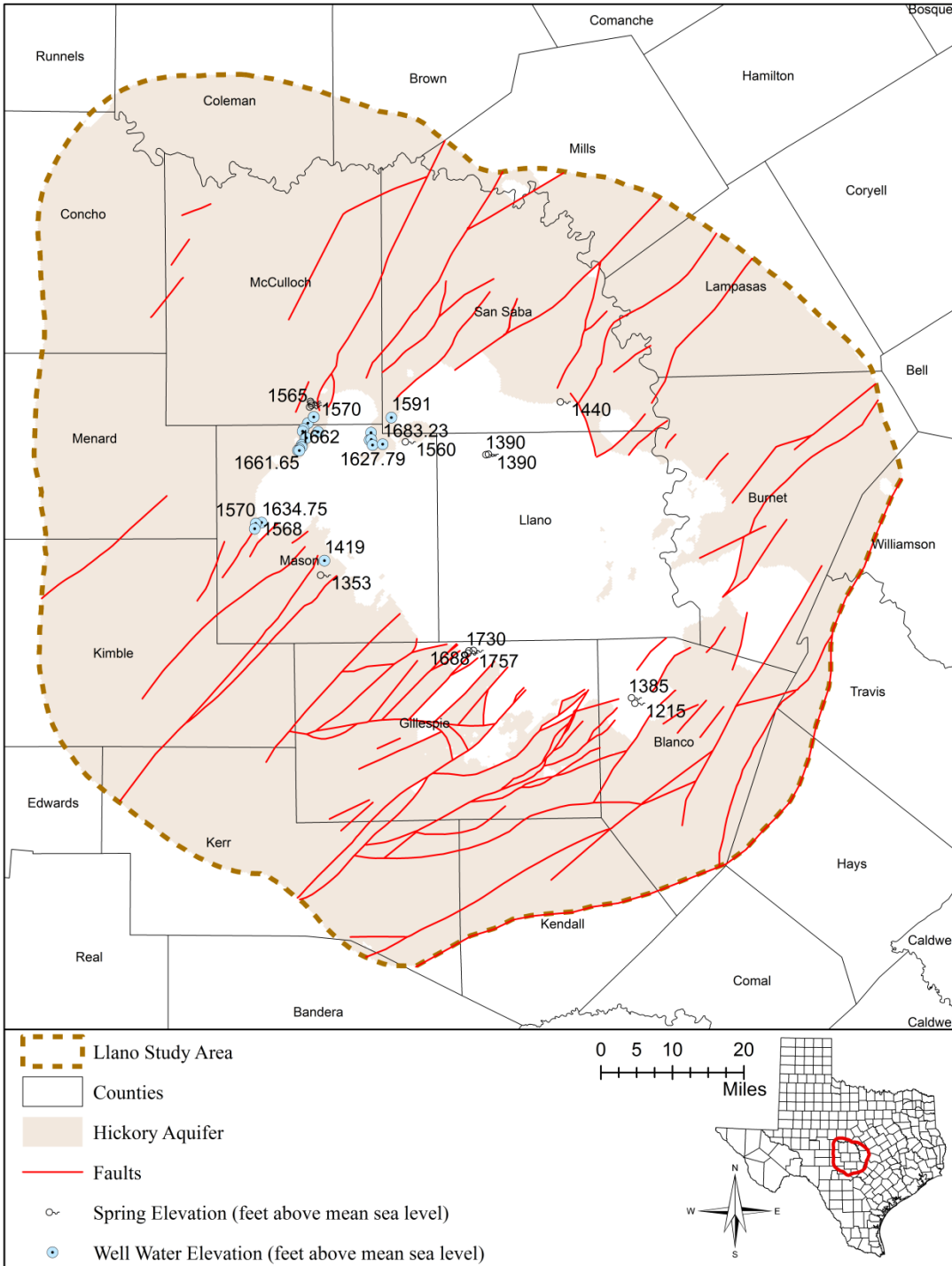


Figure 4.2.7 Pre-development water levels in Hickory Aquifer.

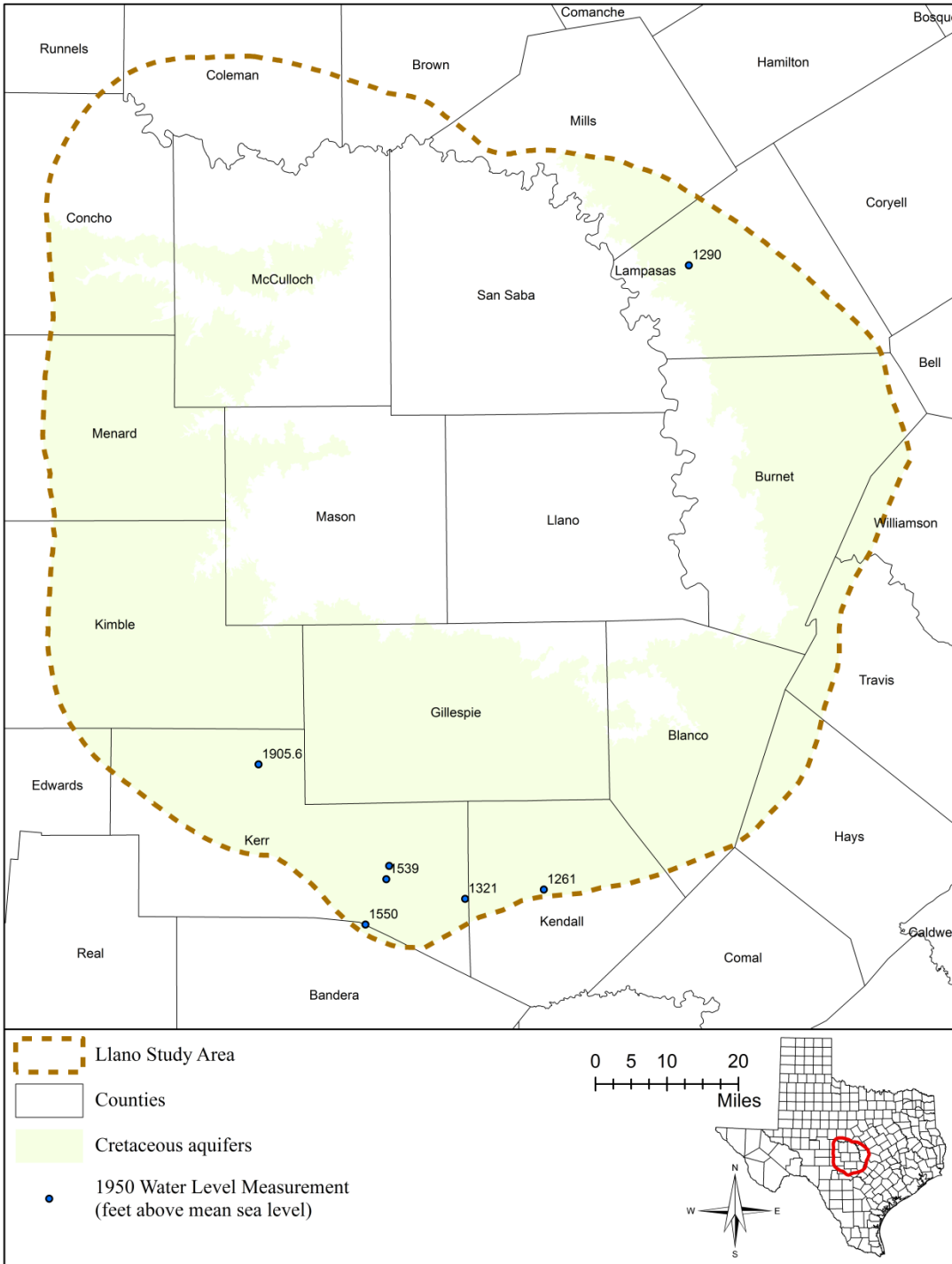


Figure 4.2.8 Water levels in Cretaceous aquifers (1950).

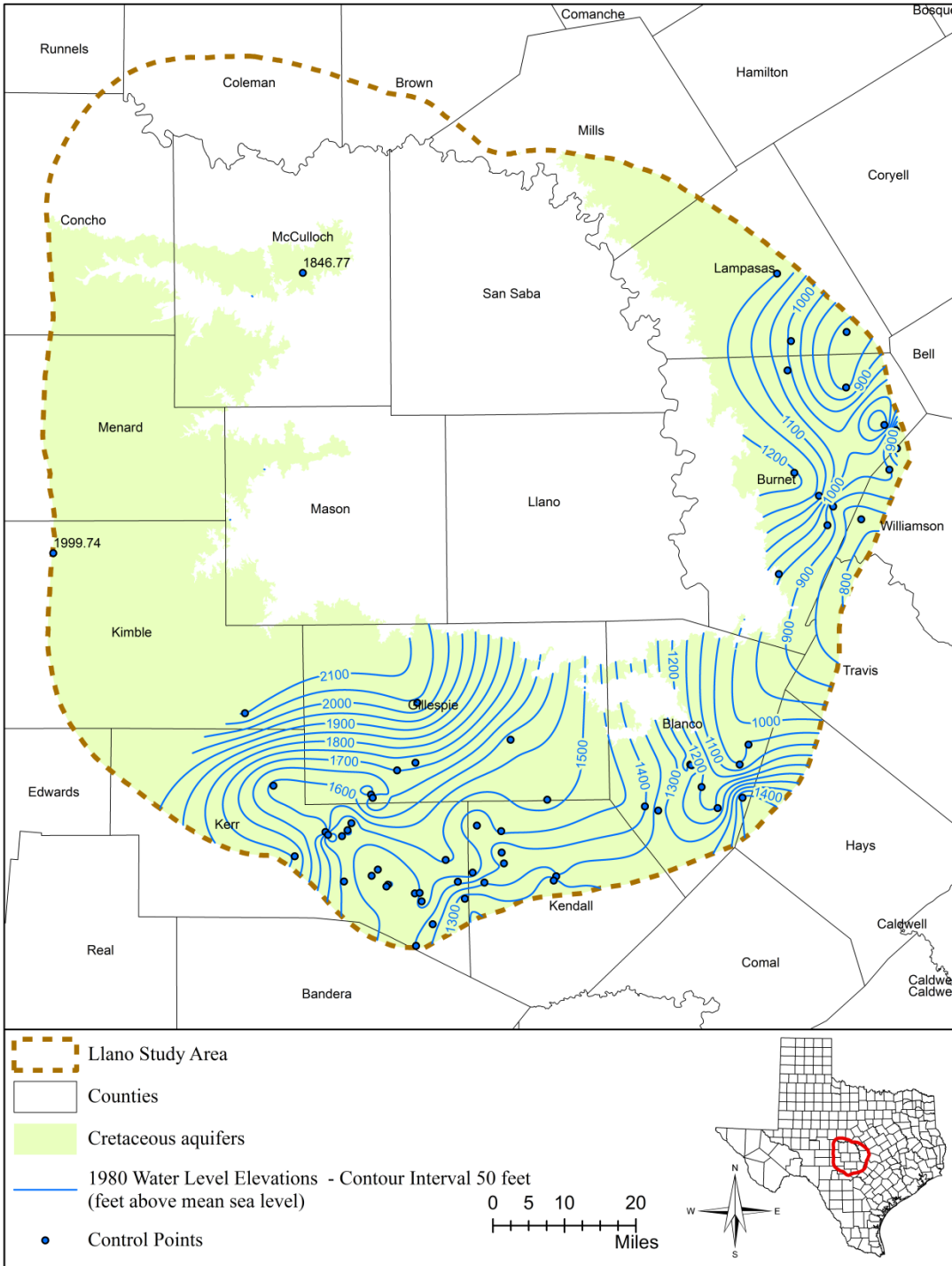


Figure 4.2.9 Potentiometric surface map of Cretaceous aquifers (1980).

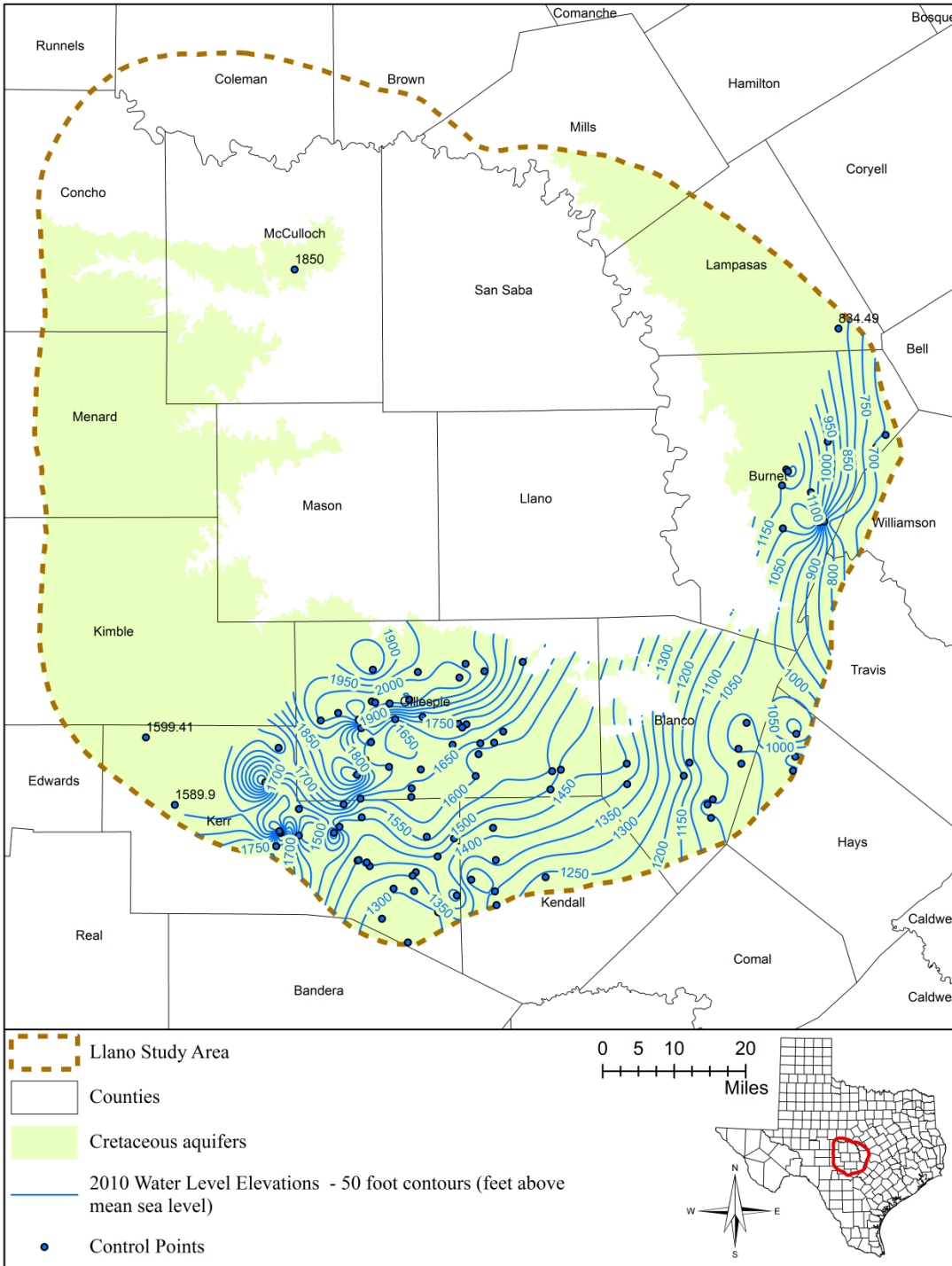


Figure 4.2.10 Potentiometric surface map of Cretaceous aquifers (2010).

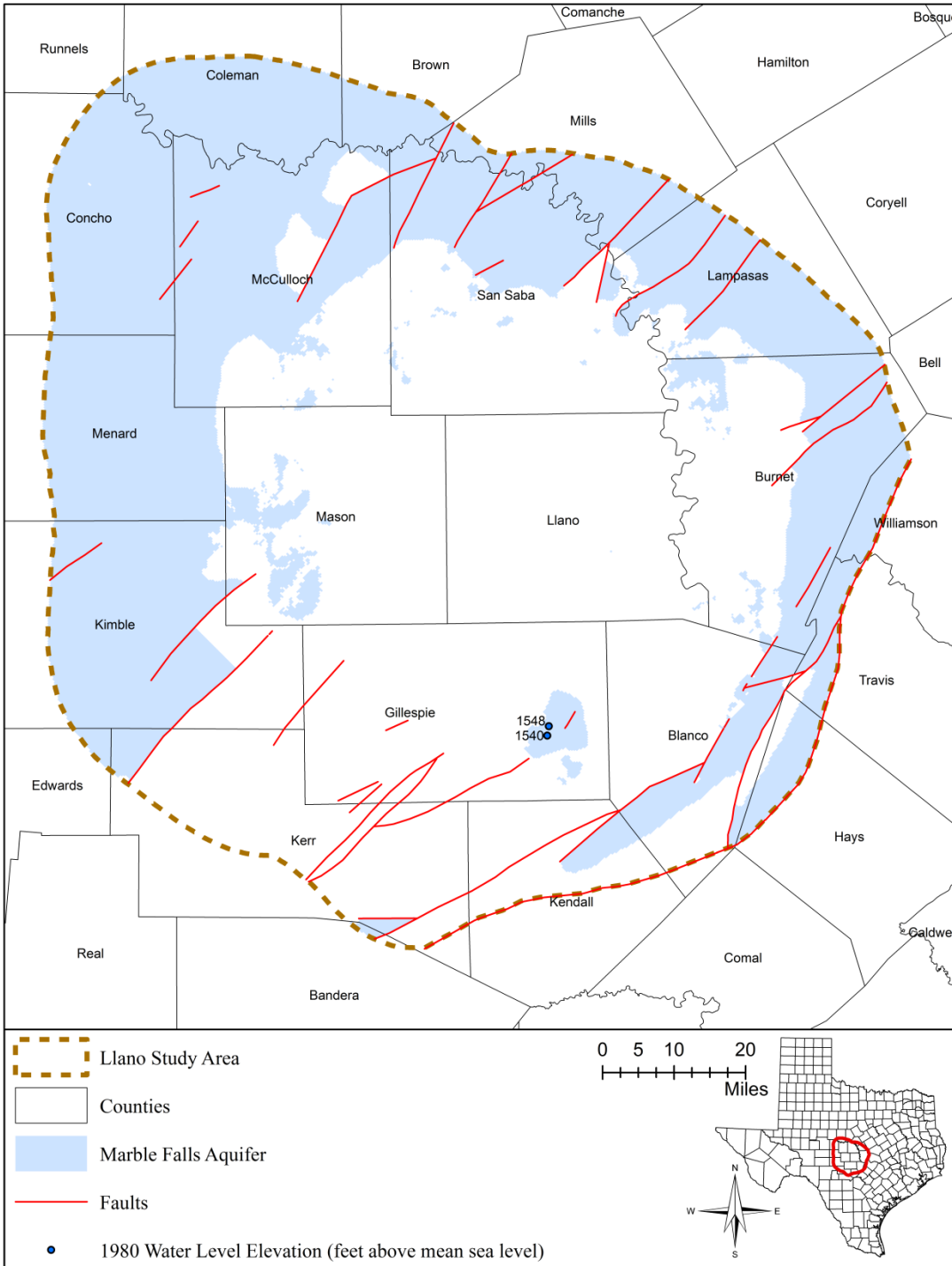


Figure 4.2.11 Water levels in Marble Falls Aquifer (1980).

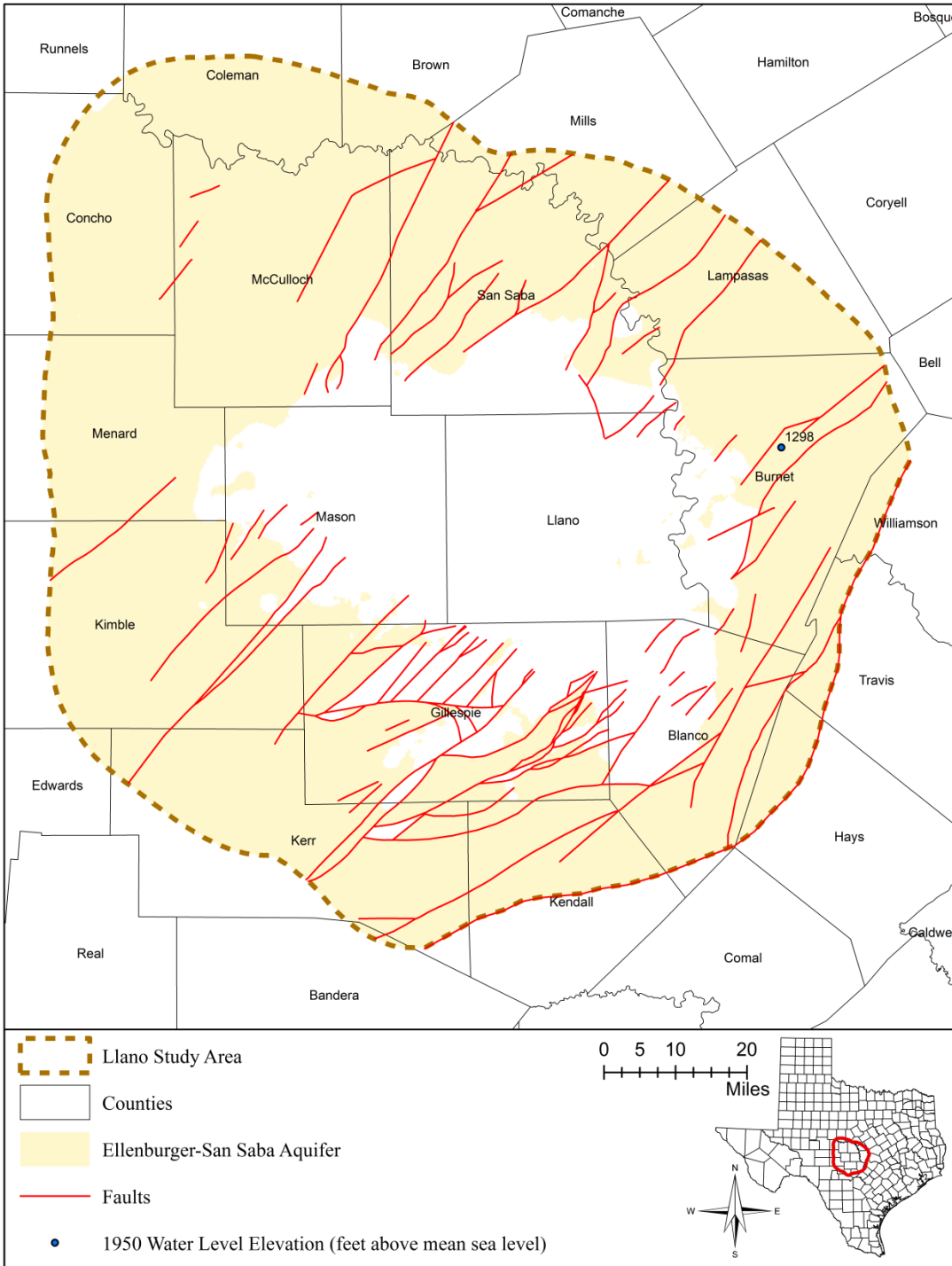


Figure 4.2.12 Water levels in Ellenburger-San Saba Aquifer (1950).

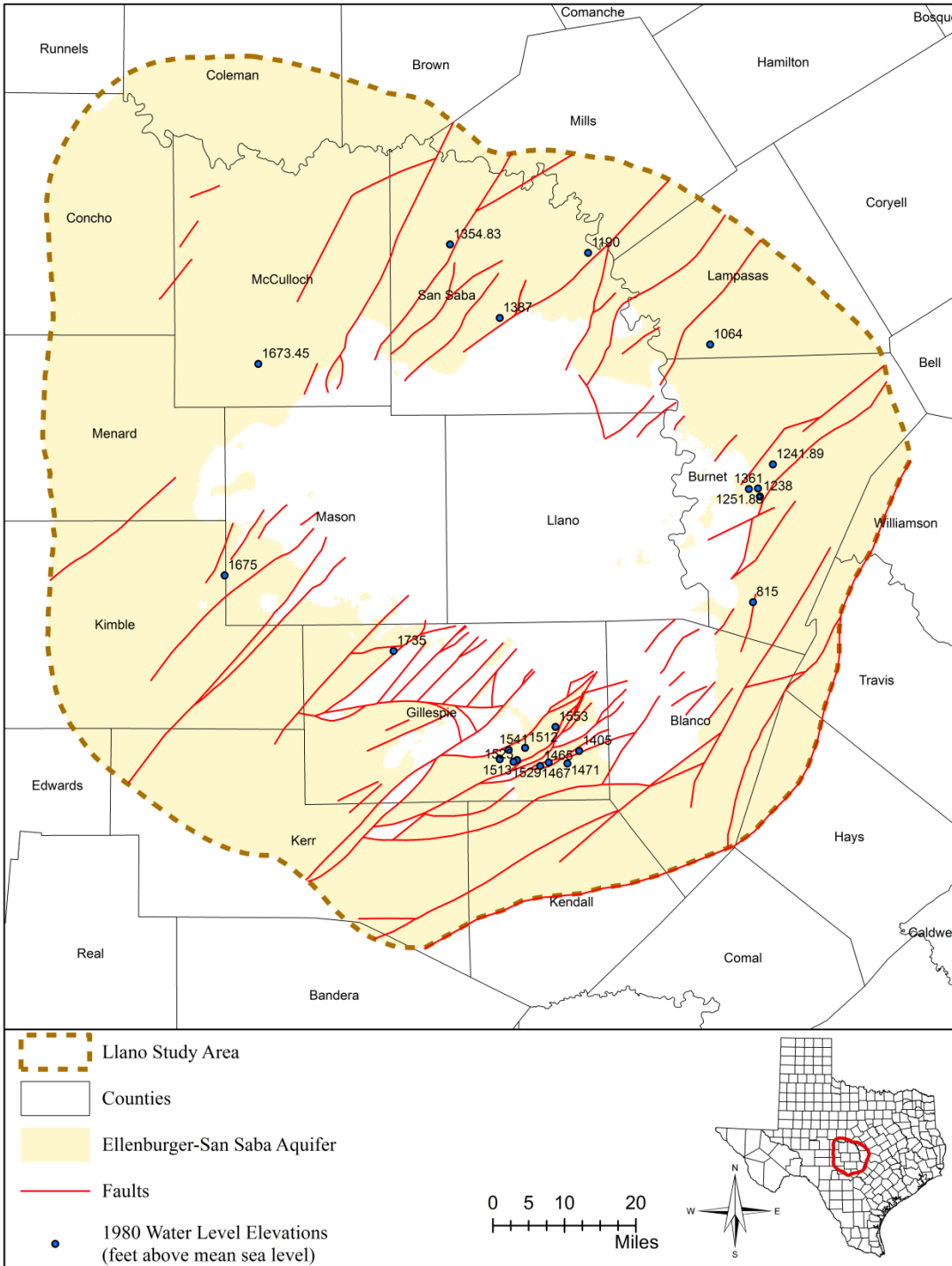


Figure 4.2.13 Water levels in Ellenburger-San Saba Aquifer (1980).

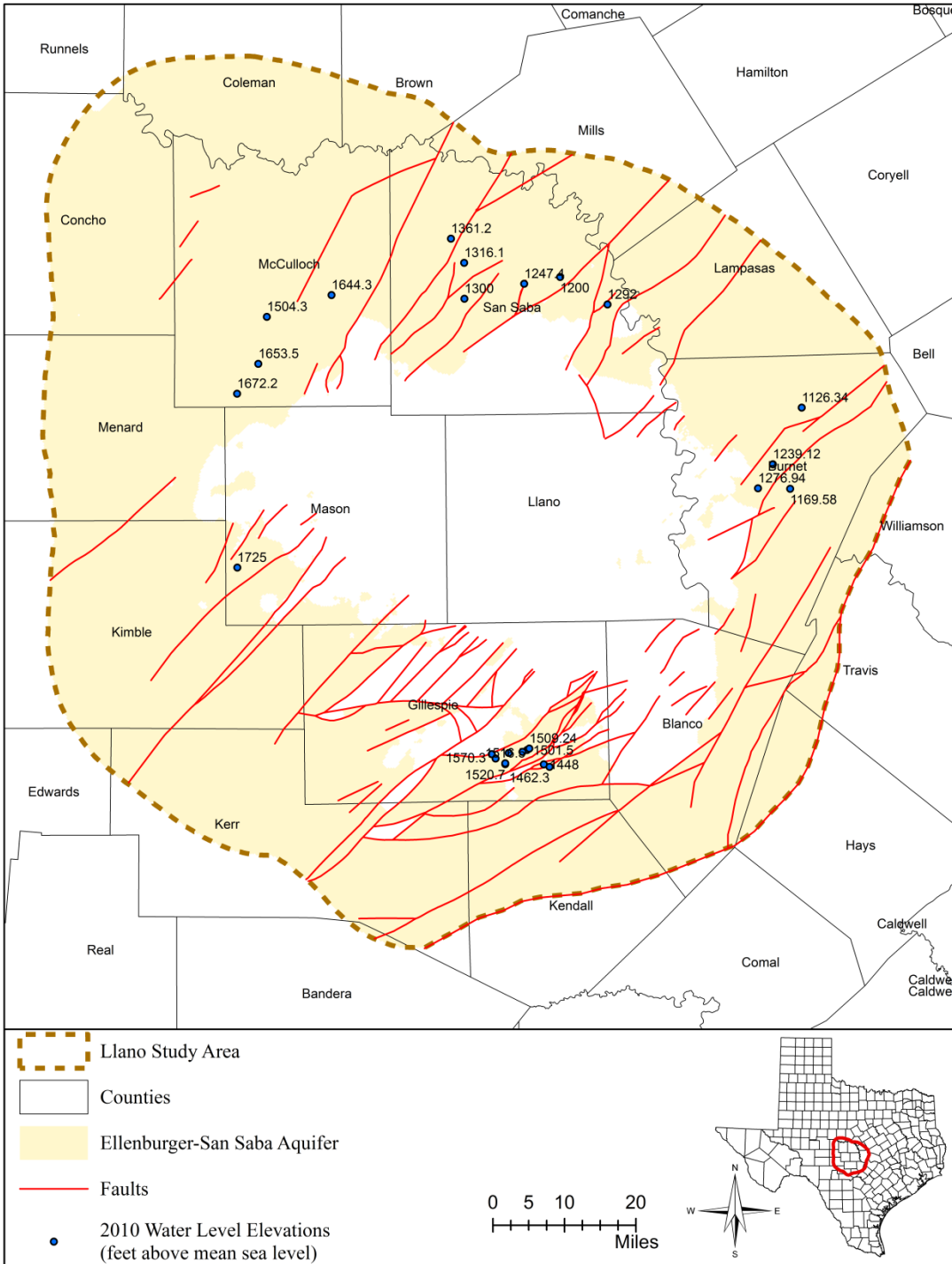


Figure 4.2.14 Water levels in Ellenburger-San Saba Aquifer (2010).

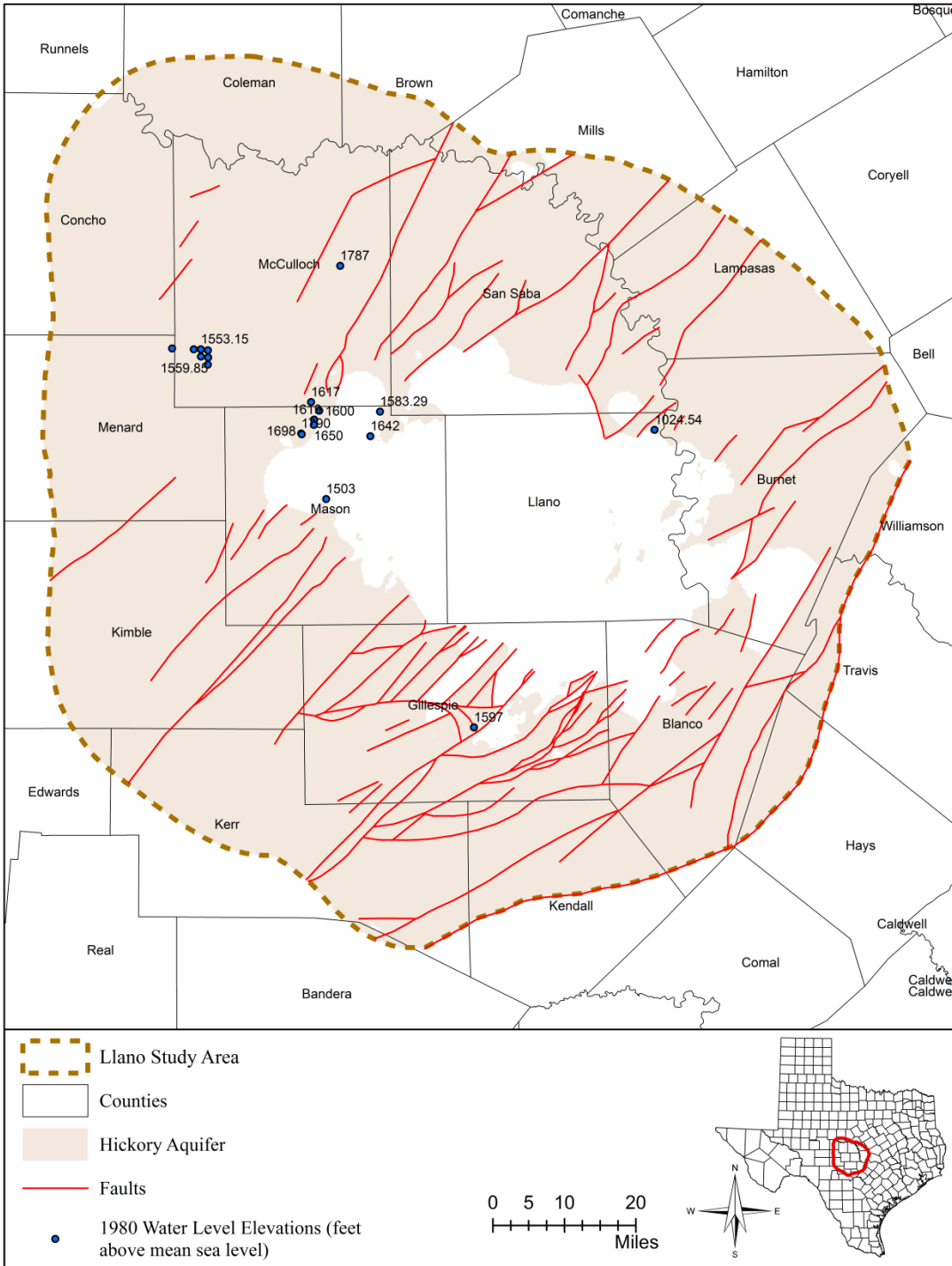


Figure 4.2.15 Water levels in Hickory Aquifer (1980).

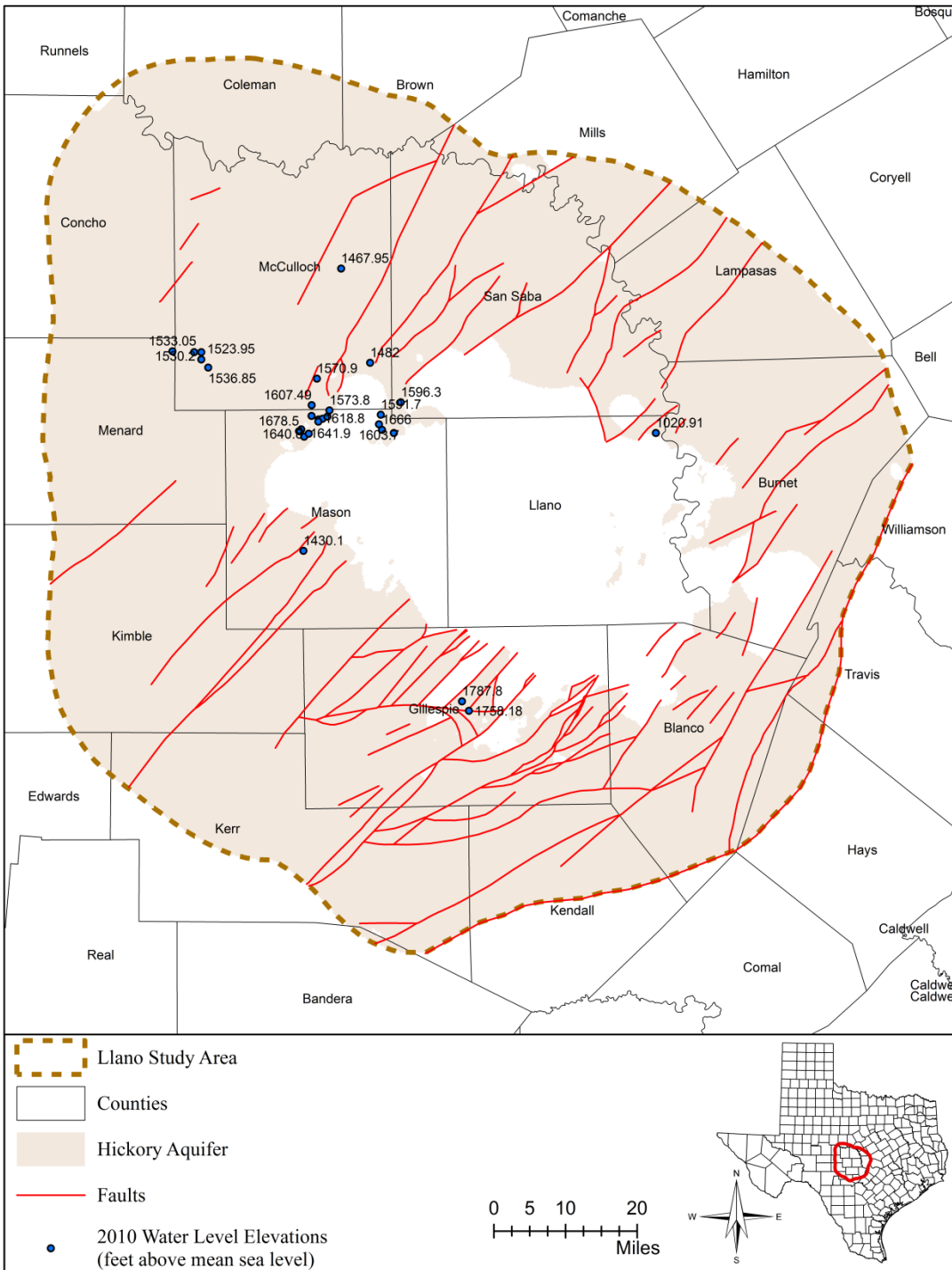


Figure 4.2.16 Water levels in Hickory Aquifer (2010).

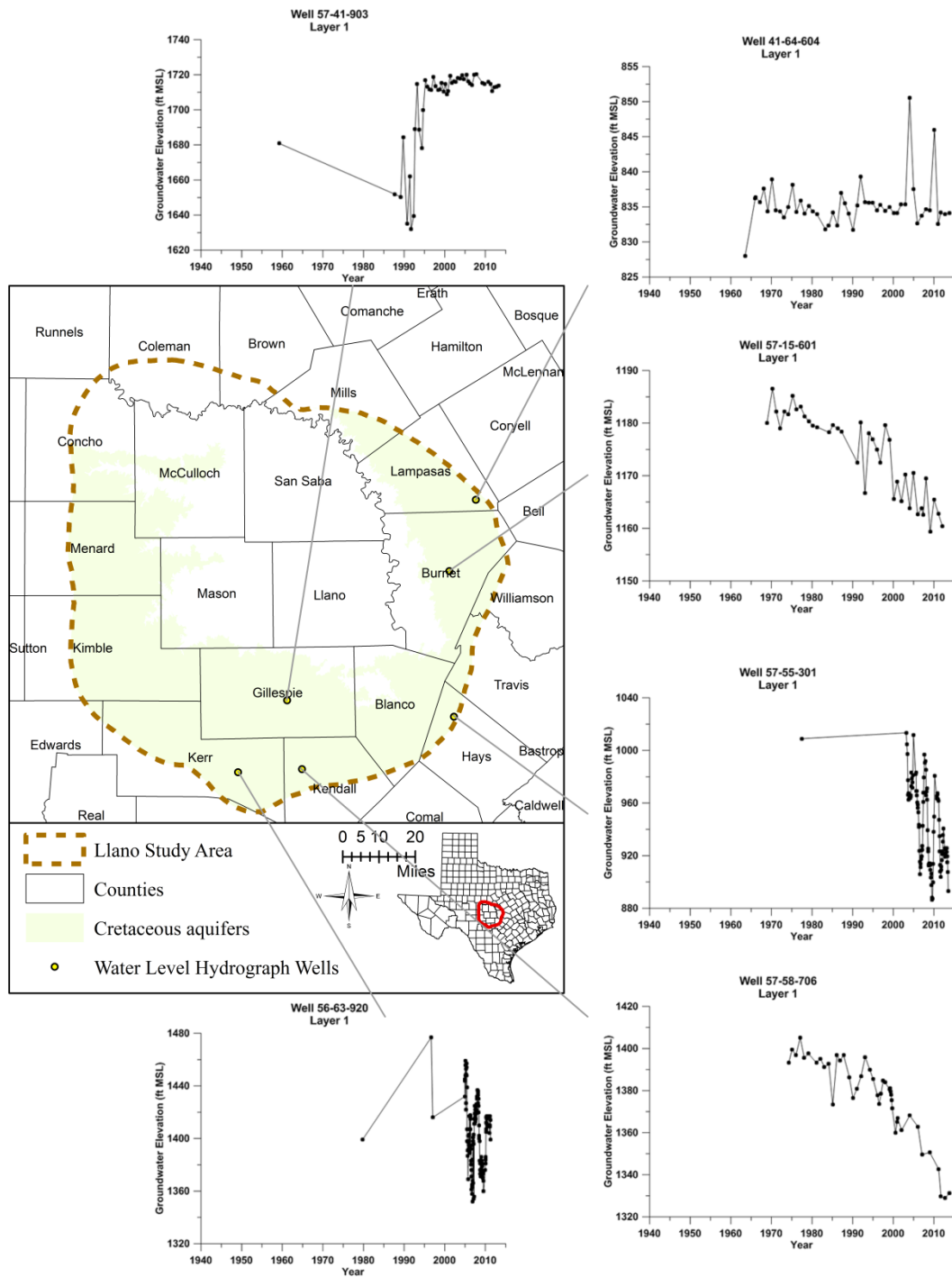


Figure 4.2.17 Water level hydrographs at selected wells in Cretaceous aquifers.

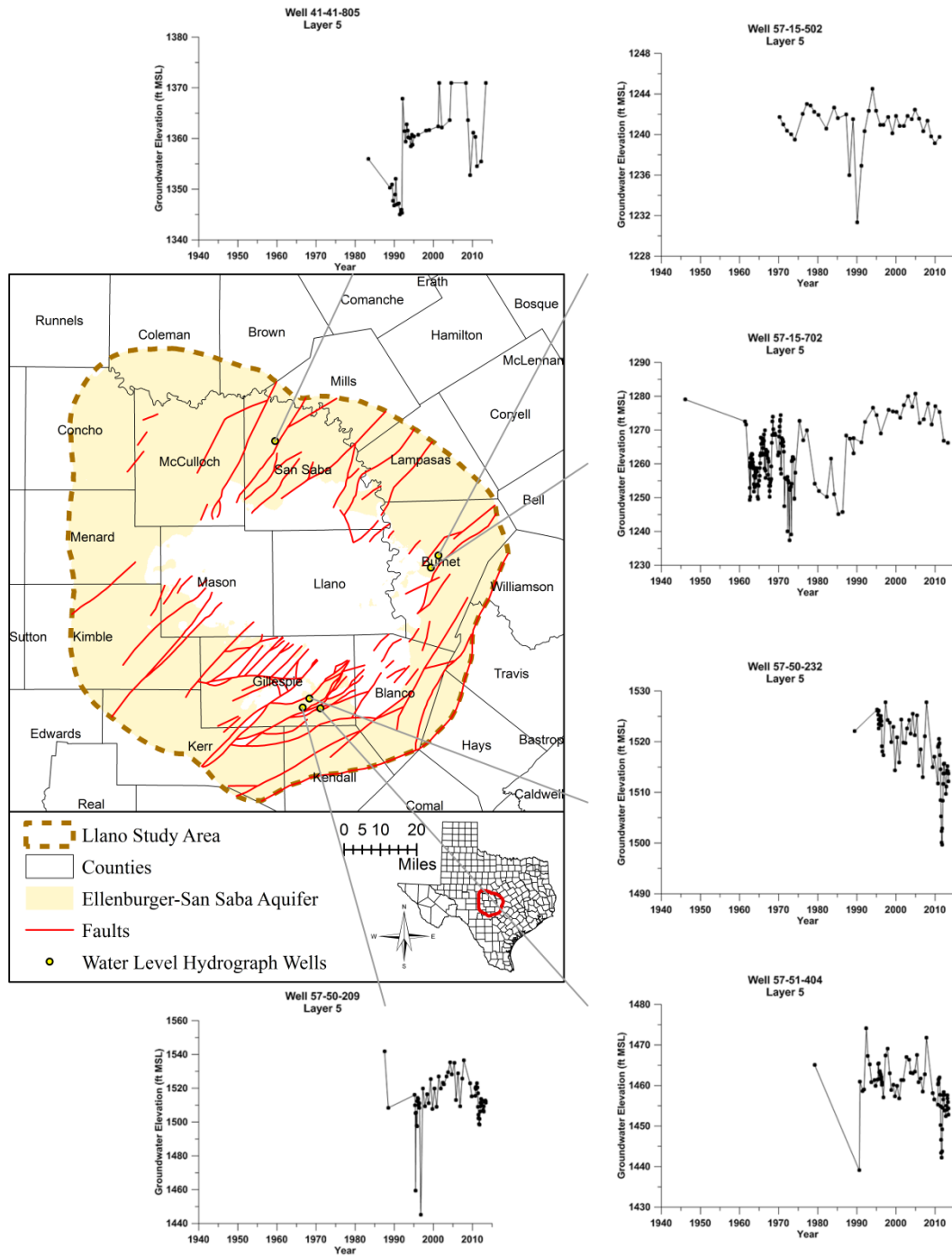


Figure 4.2.18 Water level hydrographs at selected wells in Ellenburger-San Saba Aquifer.

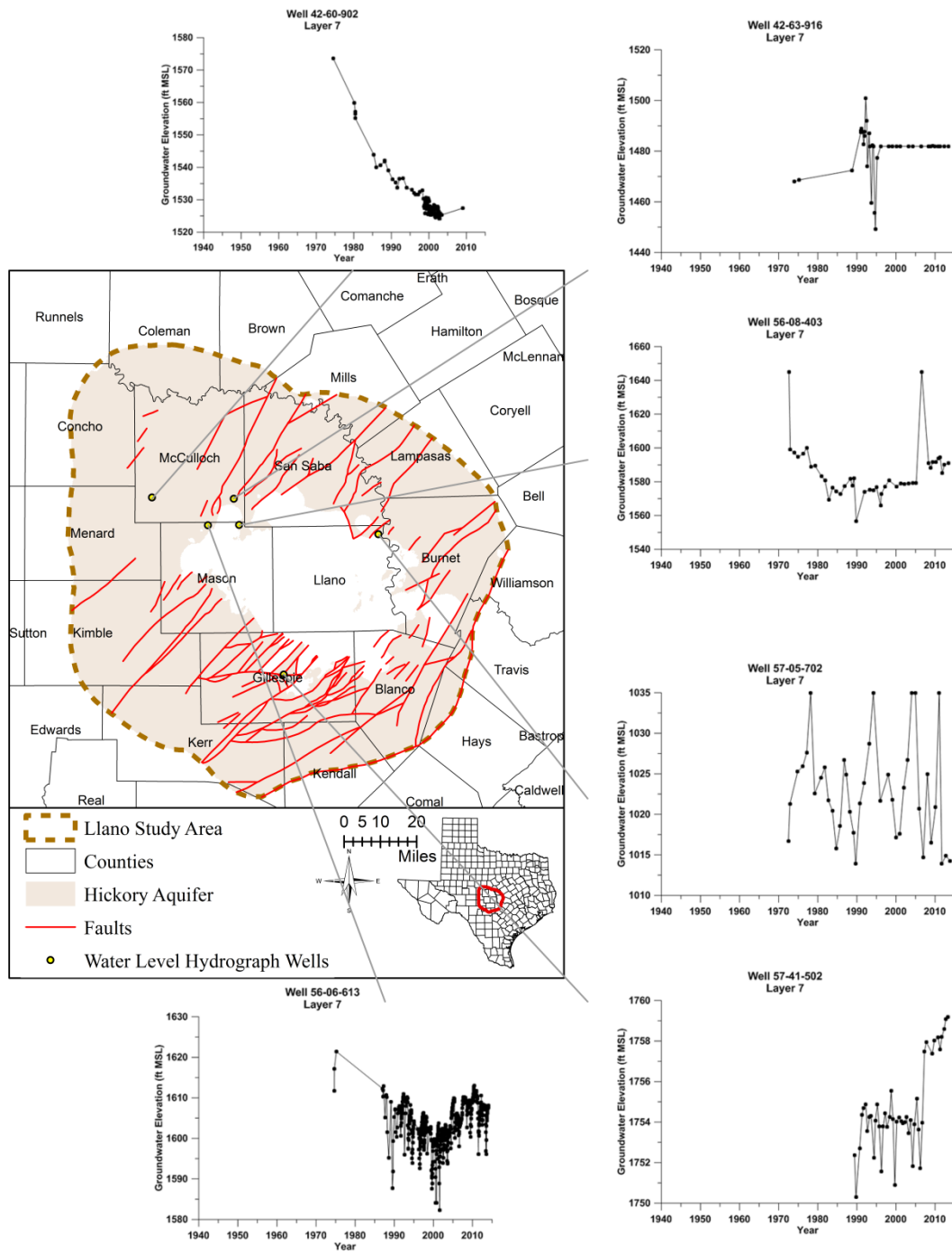


Figure 4.2.19 Water level hydrographs at selected wells in Hickory Aquifer.

4.3 Recharge

Total groundwater recharge is the water that reaches the aquifer. Total groundwater recharge could be derived from precipitation, irrigation return flow, or leakage of surface waters.

Kirk and others (2012) estimated the annual precipitation infiltration between 1960 and 2009 in the study area. The precipitation infiltration in their study was defined as the precipitation minus the surface runoff. Because part of the infiltration may stay in the unsaturated zone, the precipitation infiltration was expected to be higher than the groundwater recharge. As a result, the precipitation infiltration can be considered the upper limit of the groundwater recharge.

Based on the annual precipitation infiltration between 1960 and 2009 (Kirk and others, 2012), an average annual infiltration was calculated and presented in [Figure 4.3.1](#). As shown in [Figure 4.3.1](#), the average annual infiltration decreased from about 31 inches per year in the east to about 15 inches per year to the west of the study area. As expected, the precipitation infiltration was positively correlated to precipitation. [Figures 4.3.2](#) and [4.3.3](#) show the annual precipitation infiltration for a dry year (2005) and a wet year (2007), respectively. Please note that the precipitation infiltration for 2005 may have been over-estimated in the northwestern portion of the study area (Concho, McCulloch, and Menard counties) ([Figure 4.3.2](#)).

Effective groundwater recharge is the total groundwater recharge minus the evapotranspiration. Some of the total recharge may move over a relative shallow flow system in a short period of time and discharge to streams as baseflow. As a result, the groundwater recharge estimated from stream baseflow is often less than the total groundwater recharge. In addition, once stream baseflow and evapotranspiration are subtracted from the total recharge the remainder is assumed to be the water that enters the deep groundwater flow system. The general procedure to estimate the groundwater recharge using the stream baseflow is as follows:

- 1) estimate the stream baseflow index at a gage (that is, the ratio of baseflow to total flow);
- 2) calculate the stream total flow difference between this gage and an upstream gage;
- 3) convert the total flow difference to baseflow difference by multiplying the baseflow index (a positive baseflow difference indicates a gaining stream segment and a negative baseflow difference represents a losing stream segment);
- 4) estimate the catchment basin area of the stream segment; and
- 5) divide the baseflow difference by the catchment basin area to calculate the average effective groundwater recharge rate for the catchment basin between the two gages.

This method was used to estimate both annual and monthly groundwater recharge rates. To minimize bias, only adjacent gages sharing at least 8-year complete datasets were used for this calculation. If a nearby upstream gage did not meet this criterion, a farther upstream gage was

used. A complete year means that it contains 12 complete months without any missing stream flow measurement. A total of 27 gages were selected for the groundwater recharge evaluation (Figure 4.3.4). The monthly flow measurements and baseflow index values were downloaded in May 2014 from the U.S. Geological Survey's websites, <http://waterdata.usgs.gov/nwis/> and <http://water.usgs.gov/GIS/metadata/usgswrd/XML/bfi48grd.xml>, respectively. The catchment basin areas were delineated using SURFER on a 30 meter by 30-meter U.S. Geological Survey's Digital Elevation Model. Figure 4.3.4 shows the locations of the gages and related catchment basins in the study area. When a catchment basin was completely defined by this method, its area was calculated using ArcGIS 10.2. Due to a technical limitation of the software used for the catchment basin analysis not all catchment basins were completely defined using this approach. The area for the remaining catchment basins (all located near the study area boundary) were calculated as the total catchment basin area related to the downstream gage minus the area(s) related to the upstream gage(s) using from the U.S. Geological Survey (<http://water.usgs.gov/GIS/metadata/usgswrd/XML/bfi48grd.xml>).

The variations of annual groundwater recharge rates for the associated catchment basins are presented in Figures 4.3.5 through 4.3.10. Please note that the calculation for catchment basin 3 may be inaccurate due to the impounding of the O. H. Ivie Reservoir in 1990. As shown in these figures, the groundwater recharge rates from the stream baseflow could change by more than an order of magnitude from year to year. For certain years, a stream segment may lose water to the adjacent groundwater system which is reflected in the graphs as negative annual groundwater recharge rate (see catchment basin 29 in Figure 4.3.5 and catchment basin 28 in Figure 4.3.10). The annual variation could be driven by precipitation (intensity and frequency); increased pumping or pumping near the stream (Domenico and Schwartz, 1997); vegetation growth (evapotranspiration) or brush control; or some combination.

Spatial variation can also be seen across the study area. The lowest average annual groundwater recharge estimated from the stream baseflow is found in the northwest portion of the study area with a value less than 0.20 inches per year (Figure 4.3.11). This is the area where the low permeable Permian units crop out or the Cretaceous units are thin (such as southern Concho County) and the precipitation rate is low. Another area where the estimated average groundwater recharge values are low (from 0.2 to 0.5 inches per year) is located between Brown, Mills, and San Saba counties where the Pennsylvanian units (excluding the Marble Falls) are prominent. In the central portion of the study area where the older Paleozoic and Precambrian units crop out, the average annual groundwater recharge rates ranges from about 0.5 to 1.0 inches per year. In contrast, the Cretaceous outcrop areas have the highest estimated average annual groundwater recharge rates: ranging from about 1.0 to more than 2 inches per year (Figure 4.3.11). The average annual groundwater recharge values appear to correlate well with the hydrostratigraphy.

To evaluate the seasonal change, the minimum, maximum, and average monthly estimated groundwater recharge rates are presented in Figures 4.3.12 through 4.3.17. As expected, the areas with the lowest annual recharge rates, such as the northwestern portion of the study area, have the lowest minimum, maximum, and average monthly recharge rates. This area also shows higher monthly estimated groundwater recharge rates in May and October (the two months with

the average highest precipitation; see [Figures 2.1.15 through 2.1.18](#)) than other months. This monthly groundwater recharge pattern is not clear for the rest of the study area.

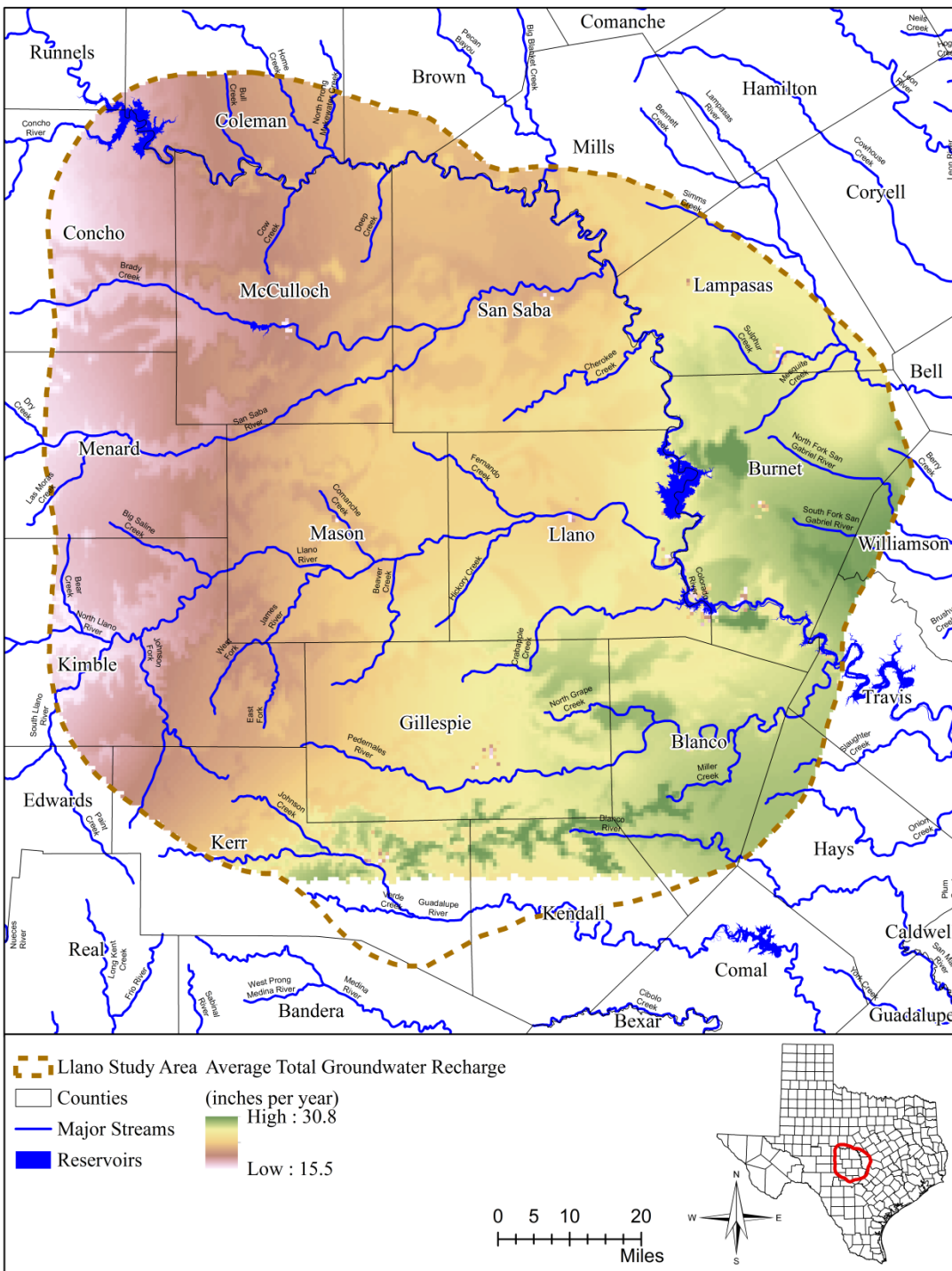


Figure 4.3.1 Average infiltration distribution due to precipitation between 1960 and 2009 in study area (annual infiltration rates from Kirk and others (2012)).

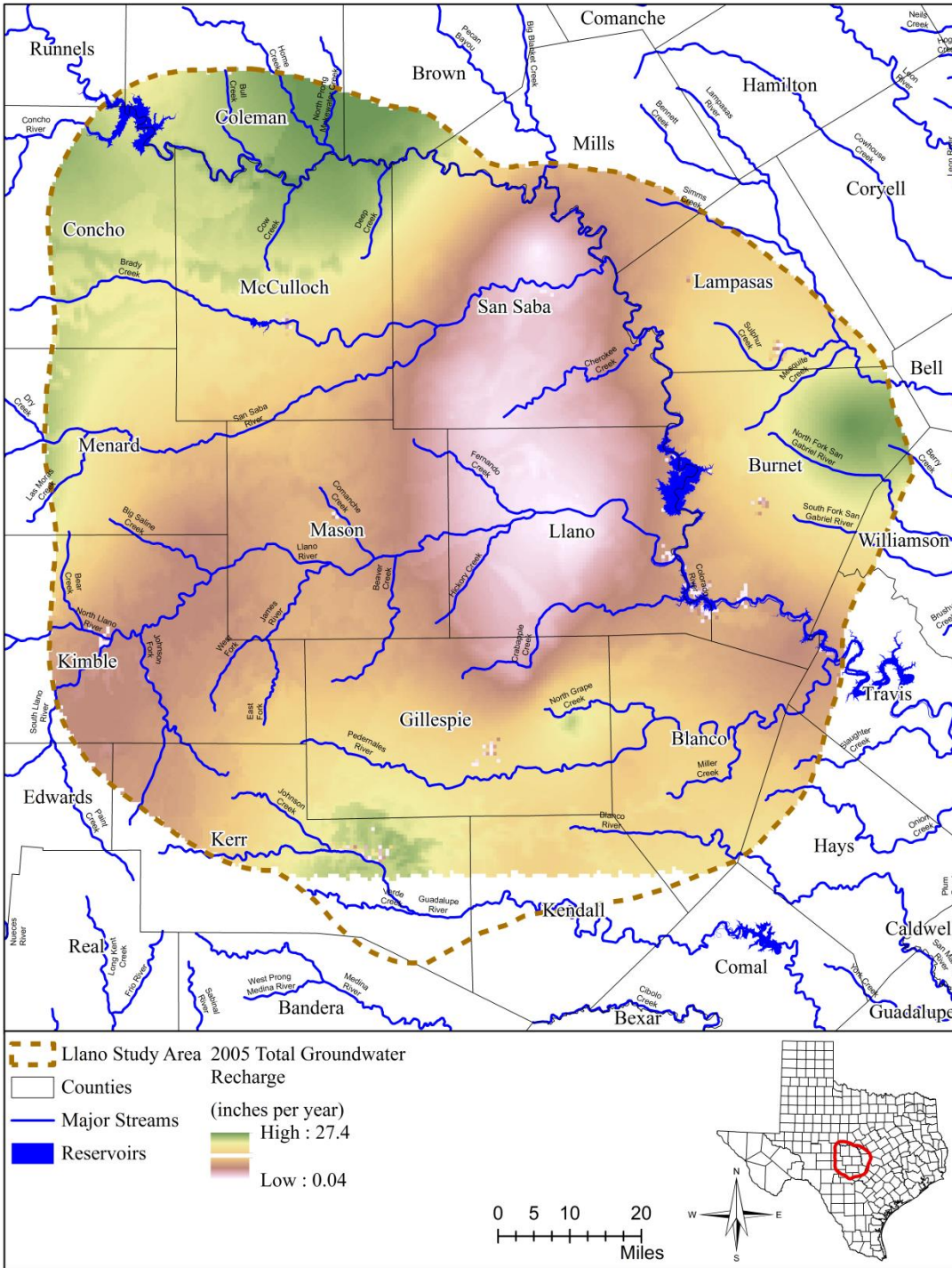


Figure 4.3.2 Infiltration distribution due to precipitation for 2005, a dry year with low precipitation (annual infiltration rates from Kirk and others (2012)).

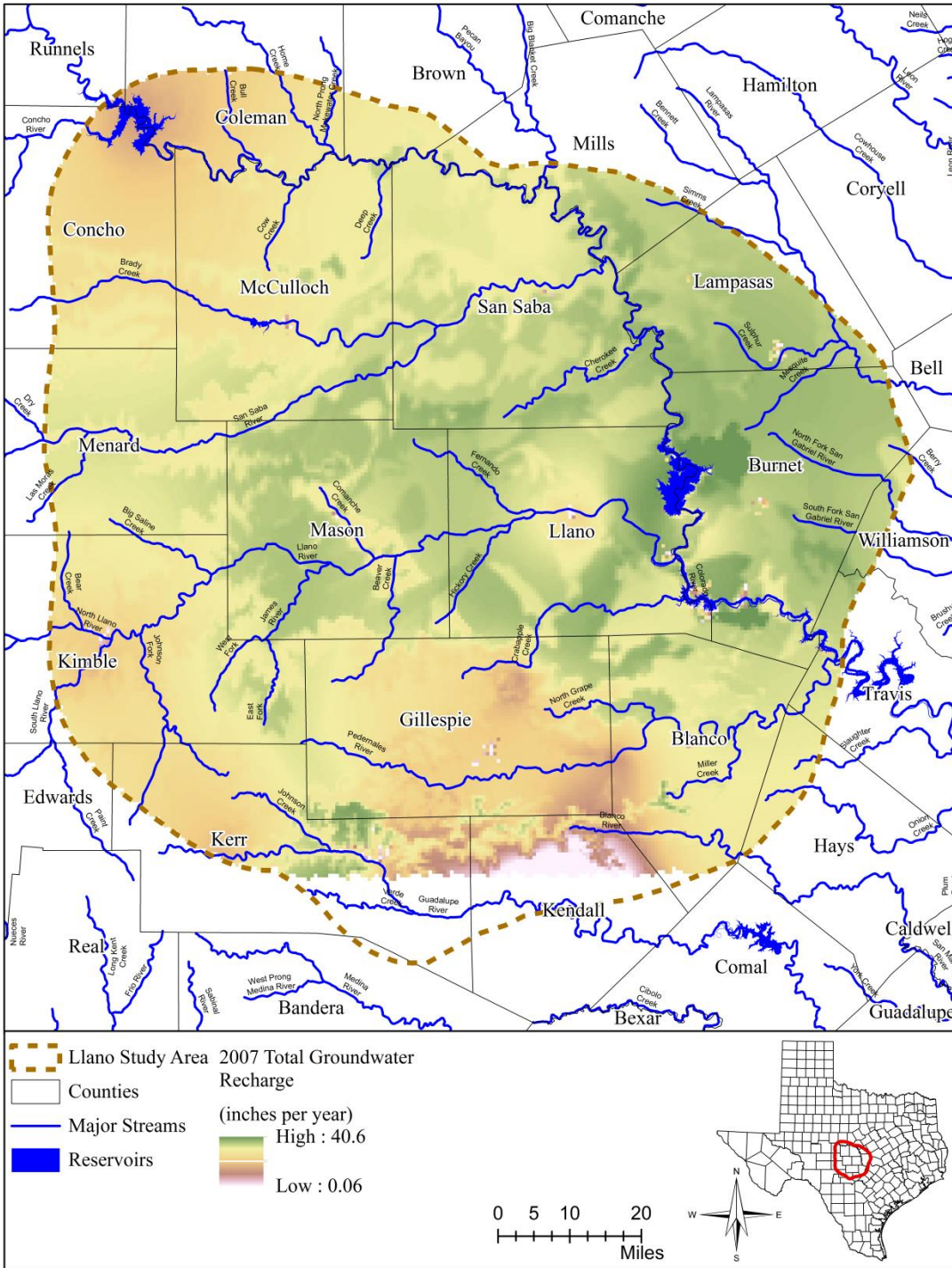


Figure 4.3.3 Infiltration distribution due to precipitation for 2007, a wet year with high precipitation (annual infiltration rates from Kirk and others (2012)).

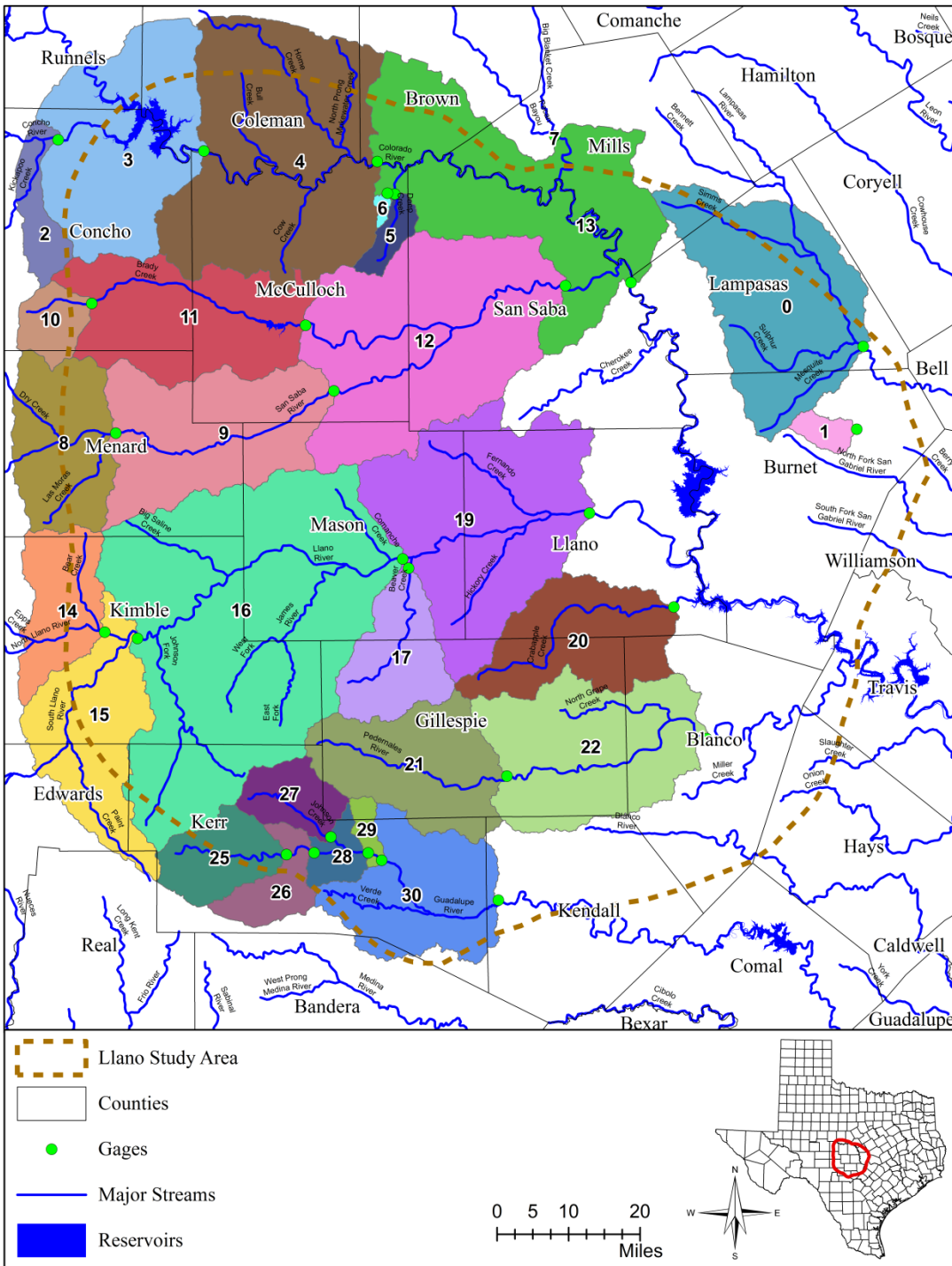


Figure 4.3.4 Locations of U.S. Geological Survey’s stream gages and catchment basins used for estimating effective groundwater recharge. Catchment basins are colored and numbered. Catchment basins across study area boundary may not be completely shown.

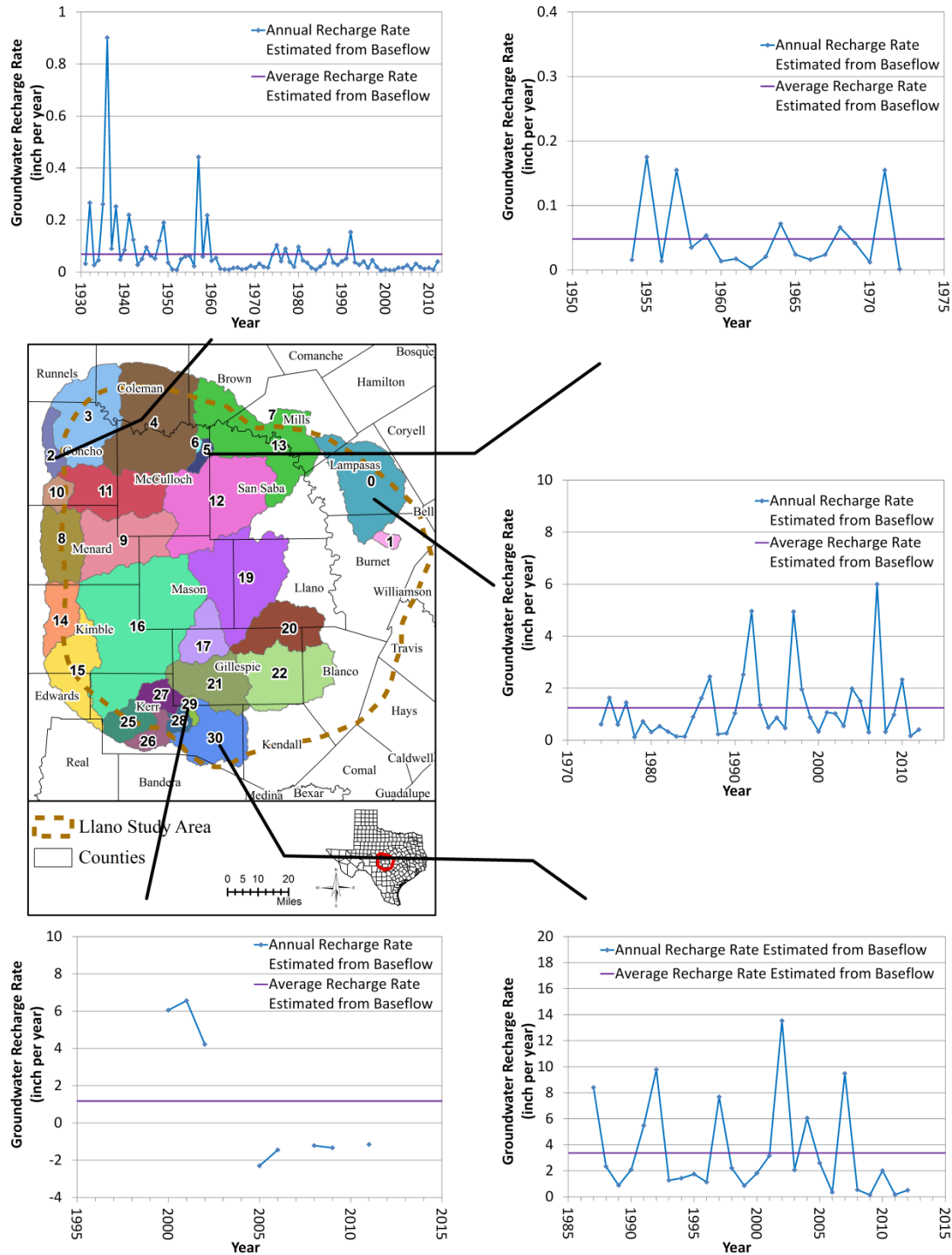


Figure 4.3.5 Variations of annual groundwater recharge rates associated with catchment basins 0, 2, 5, 29, and 30 calculated from stream baseflow. Catchment basins are colored and numbered.

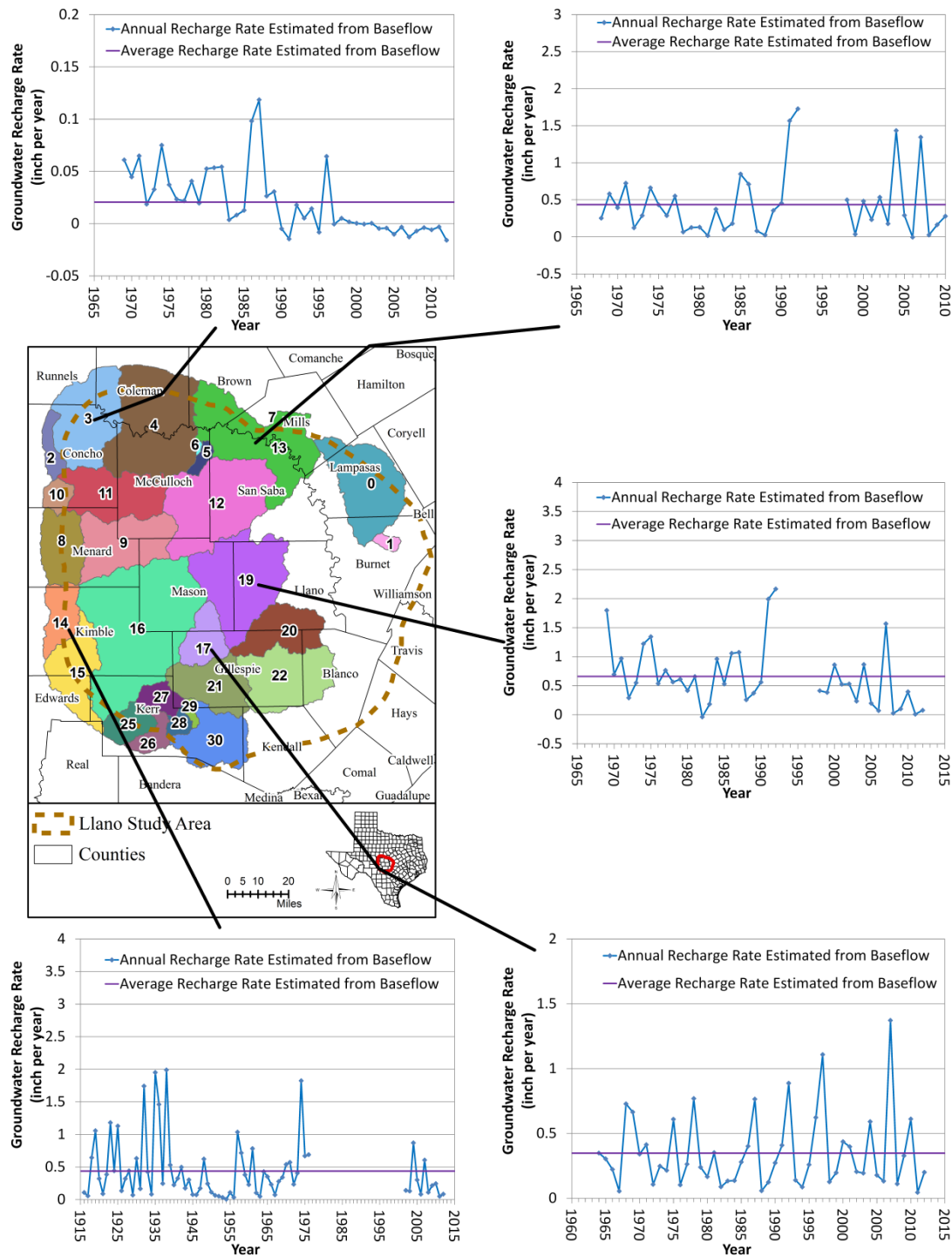


Figure 4.3.6 Variations of annual groundwater recharge rates associated with catchment basins 3, 13, 14, 17, and 19 calculated from stream baseflow. Catchment basins are colored and numbered.

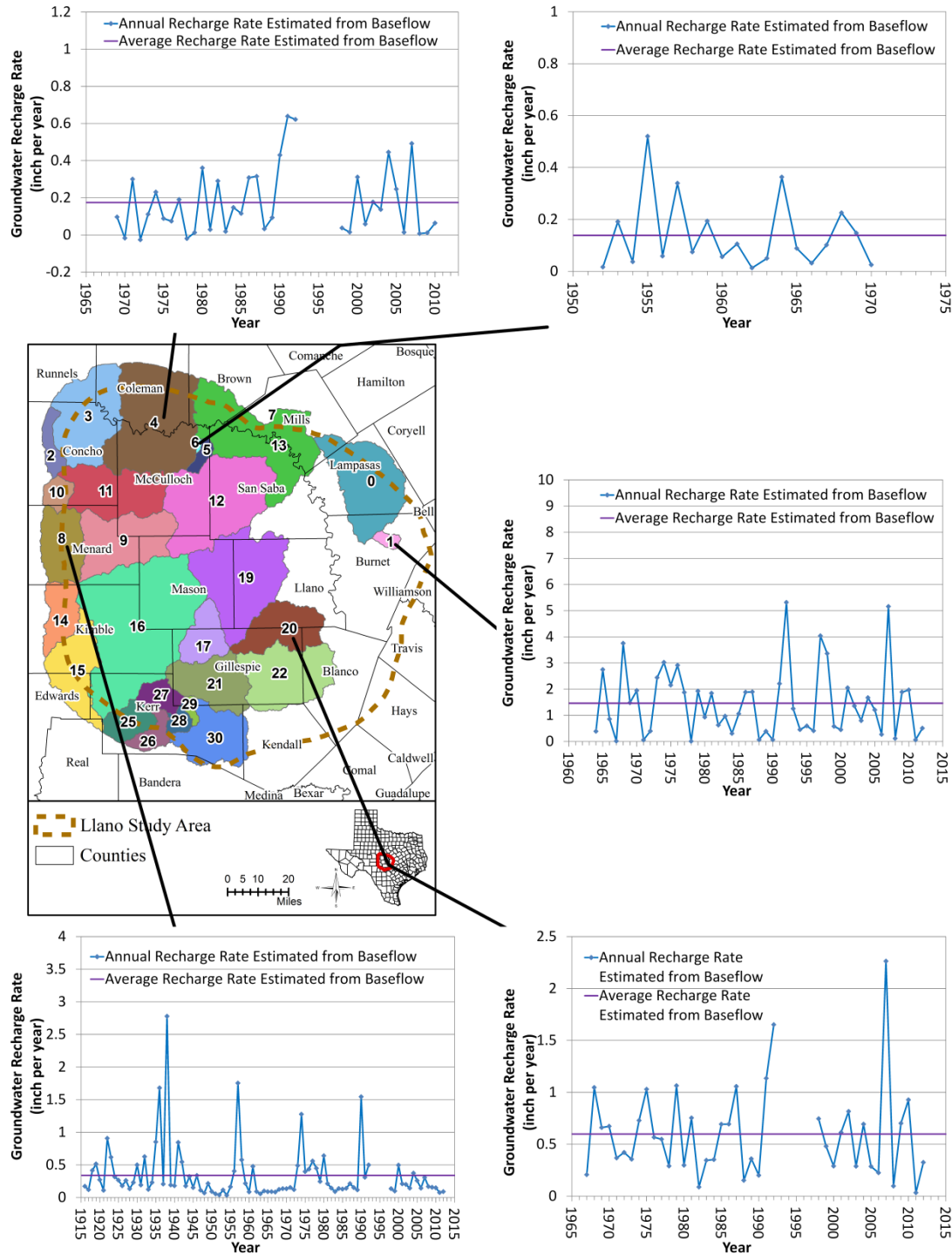


Figure 4.3.7 Variations of annual groundwater recharge rates associated with catchment basins 1, 4, 6, 8, and 20 calculated from stream baseflow. Catchment basins are colored and numbered.

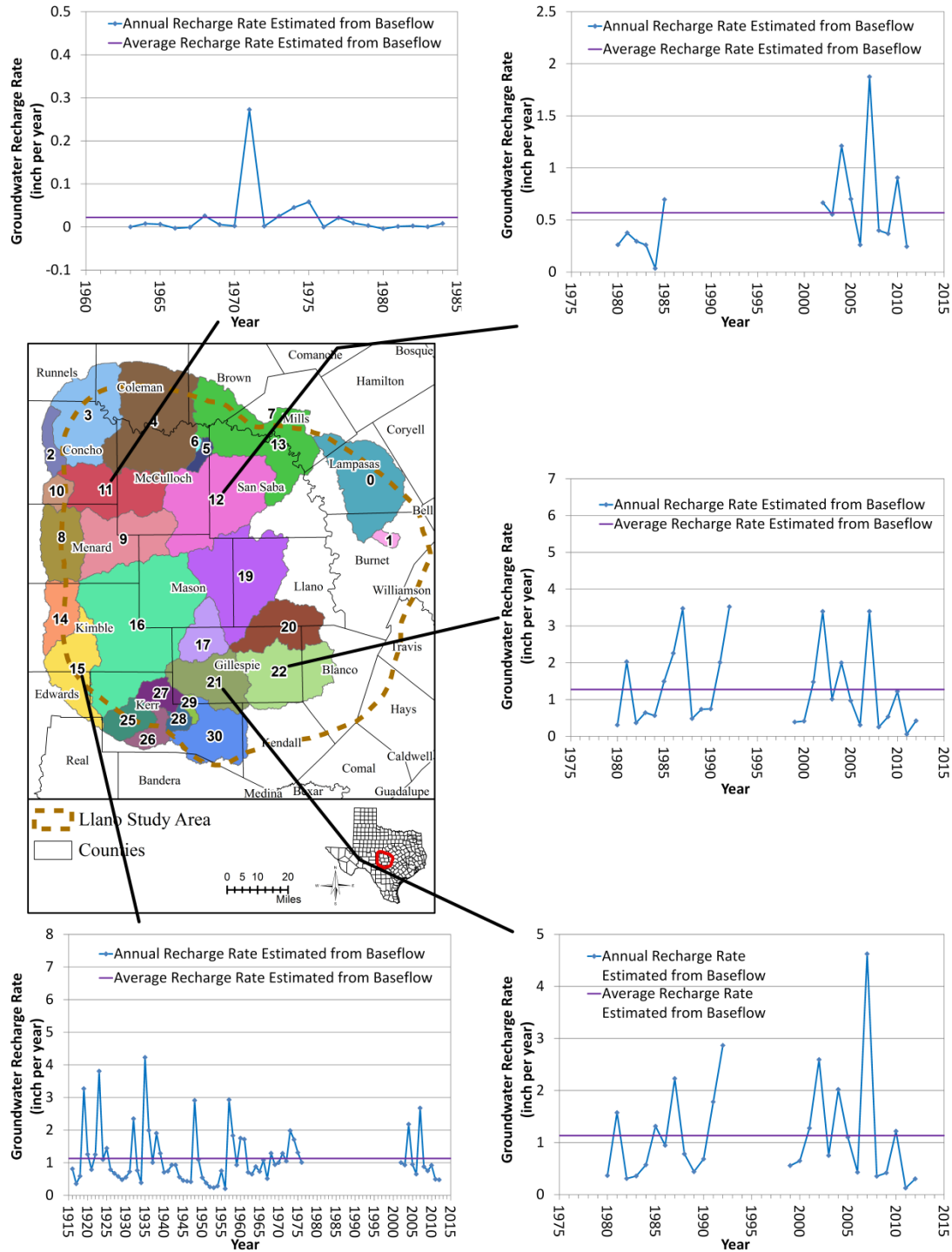


Figure 4.3.8 Variations of annual groundwater recharge rates associated with catchment basins 11, 12, 15, 21, and 22 calculated from stream baseflow. Catchment basins are colored and numbered.

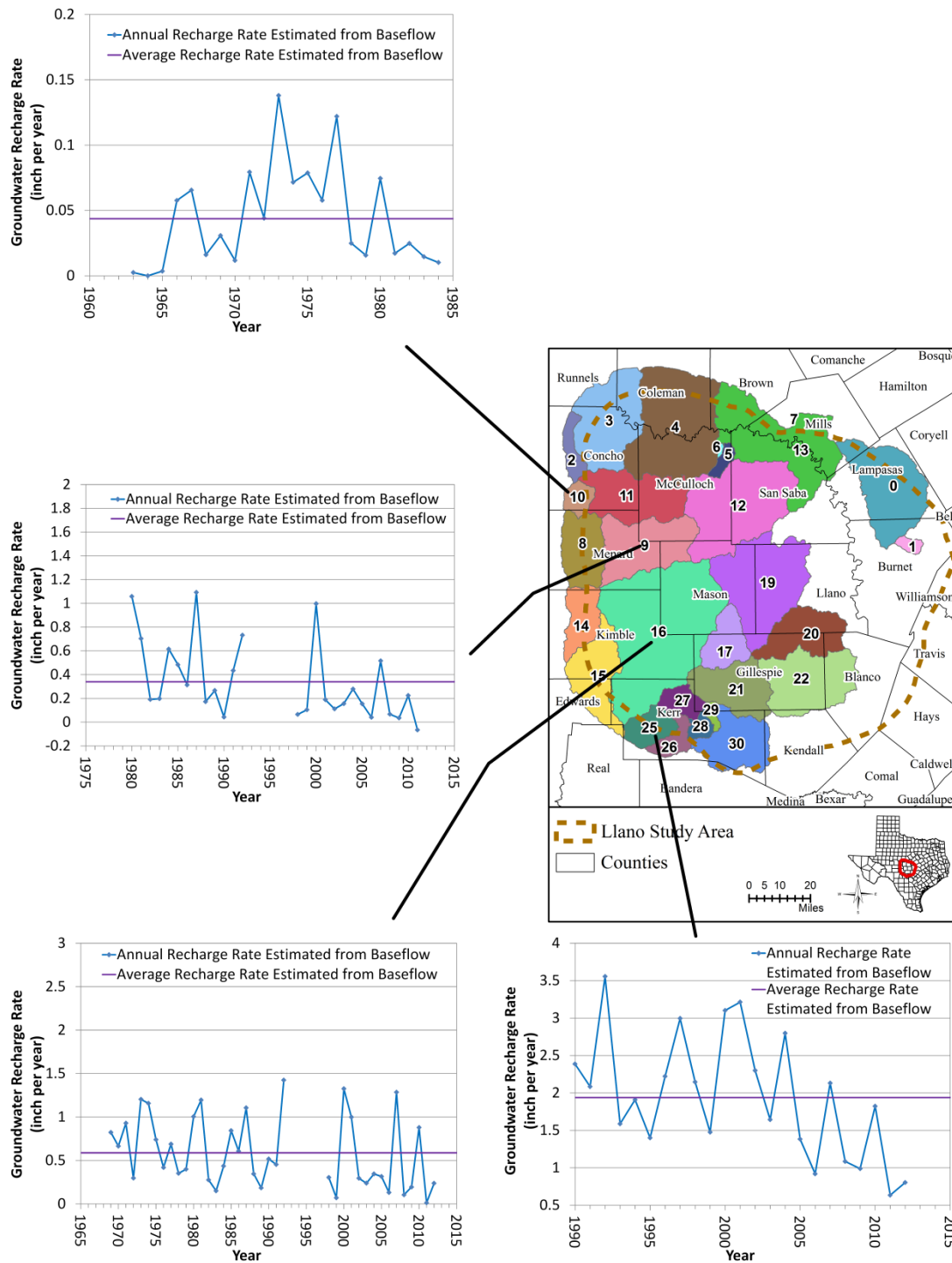


Figure 4.3.9 Variations of annual groundwater recharge rates associated with catchment basins 9, 10, 16, and 25 calculated from stream baseflow. Catchment basins are colored and numbered.

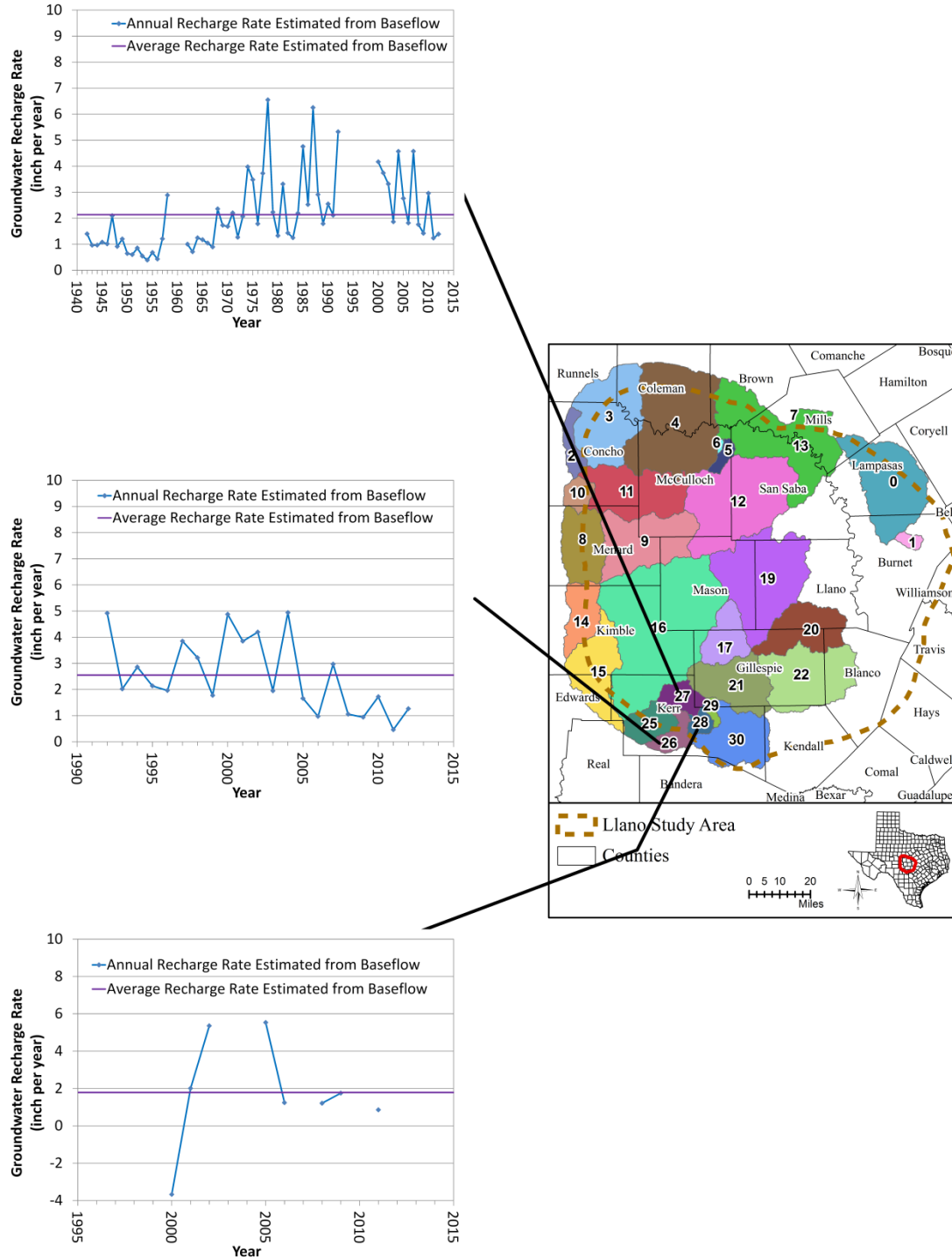


Figure 4.3.10 Variations of annual groundwater recharge rates associated with catchment basins 26, 27, and 28 calculated from stream baseflow. Catchment basins are colored and numbered.

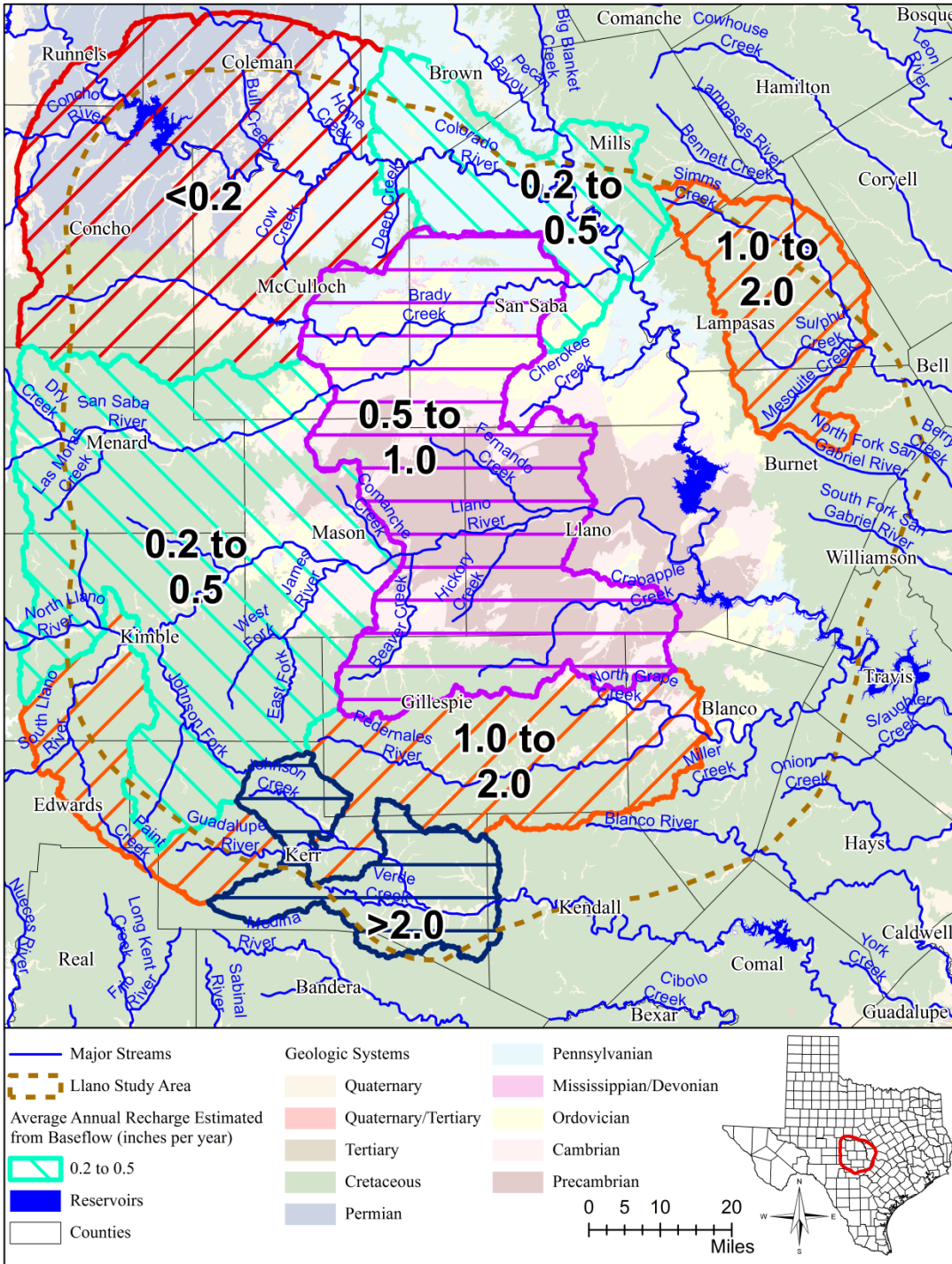


Figure 4.3.11 Distribution of average annual groundwater recharge calculated from stream baseflow in study area.

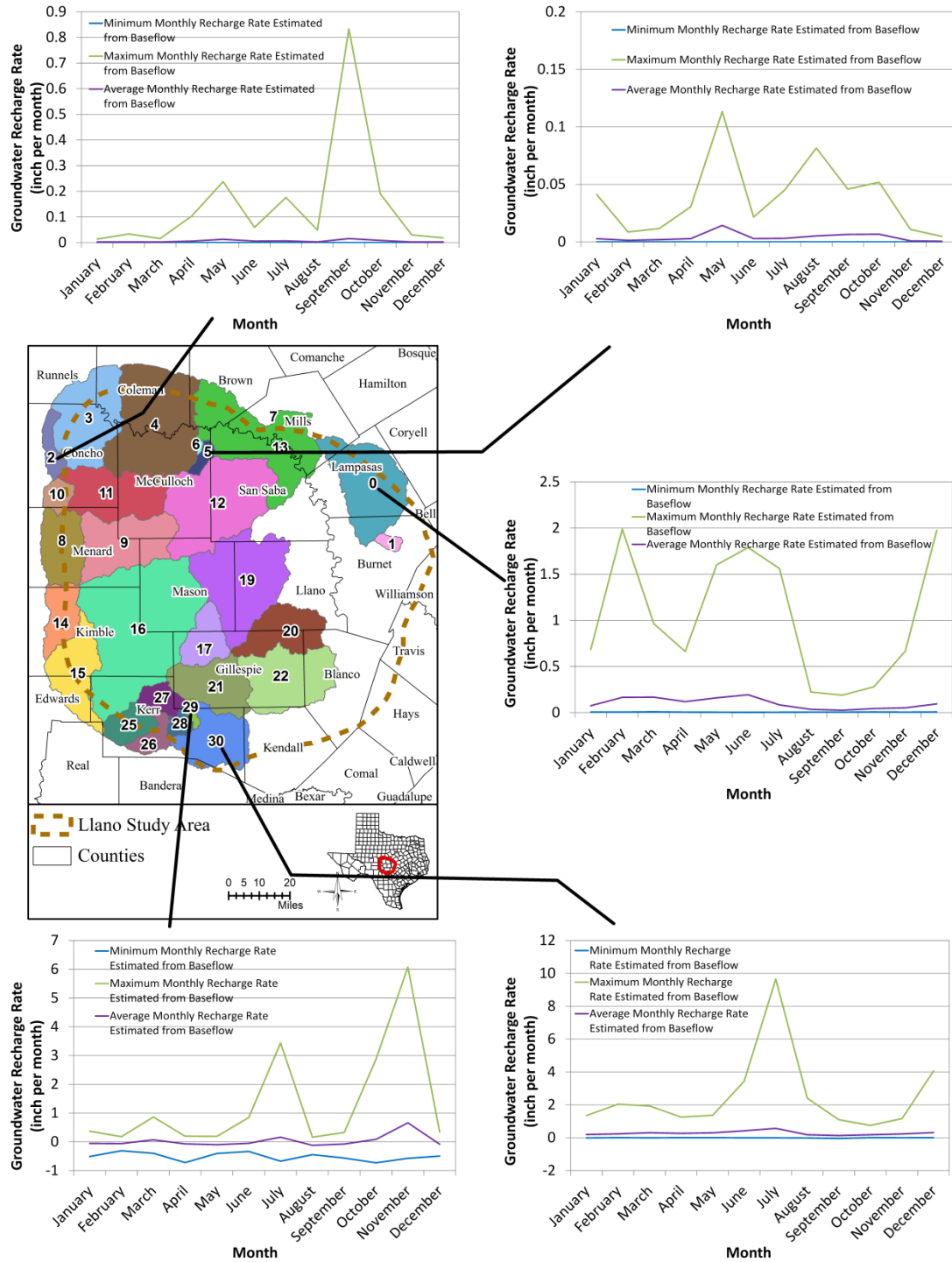


Figure 4.3.12 Variations of minimum, maximum, and average monthly groundwater recharge rates associated with catchment basins 0, 2, 5, 29, and 30 calculated from stream baseflow. Catchment basins are colored and numbered.

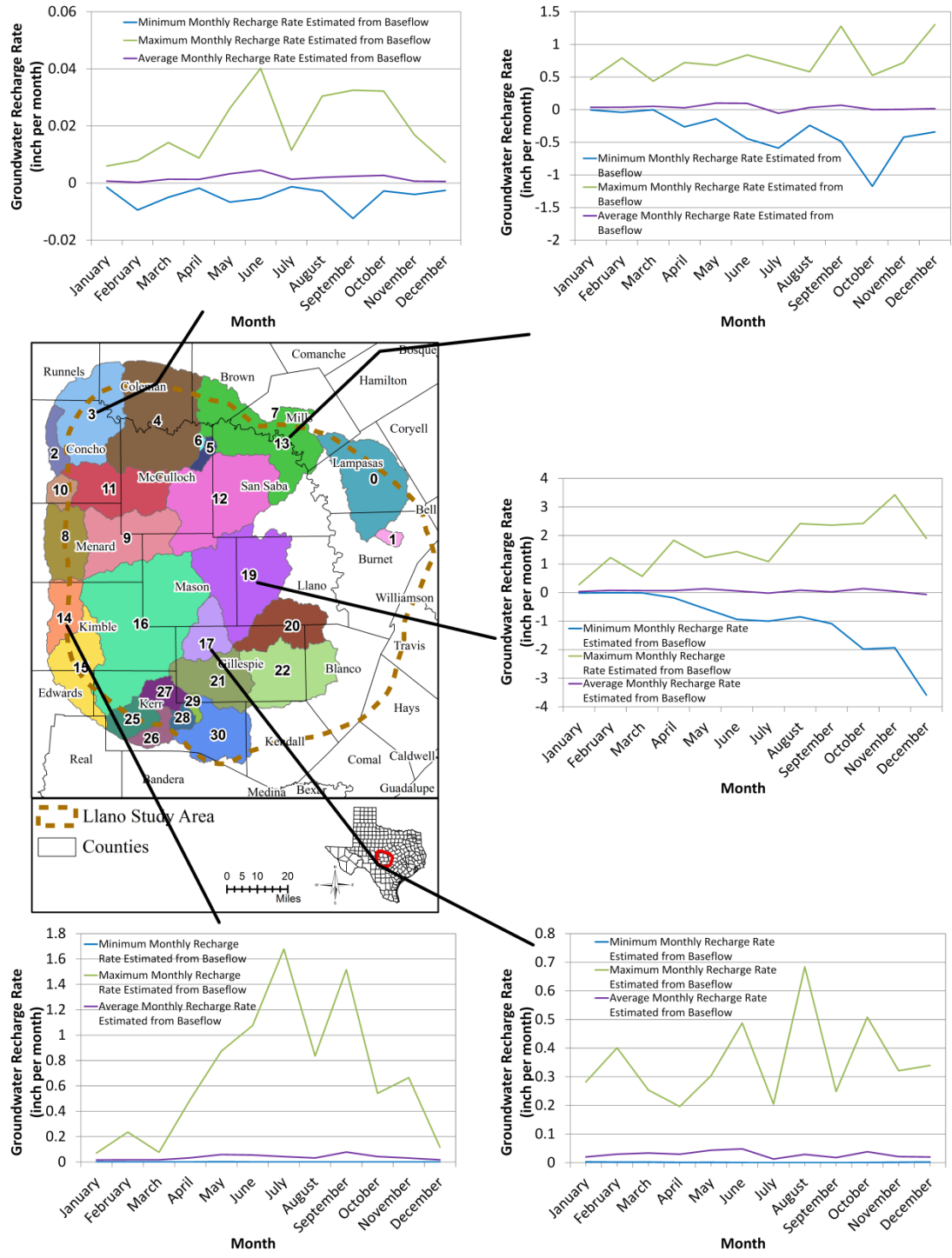


Figure 4.3.13 Variations of minimum, maximum, and average monthly groundwater recharge rates associated with catchment basins 3, 13, 14, 17, and 19 calculated from stream baseflow. Catchment basins are colored and numbered.

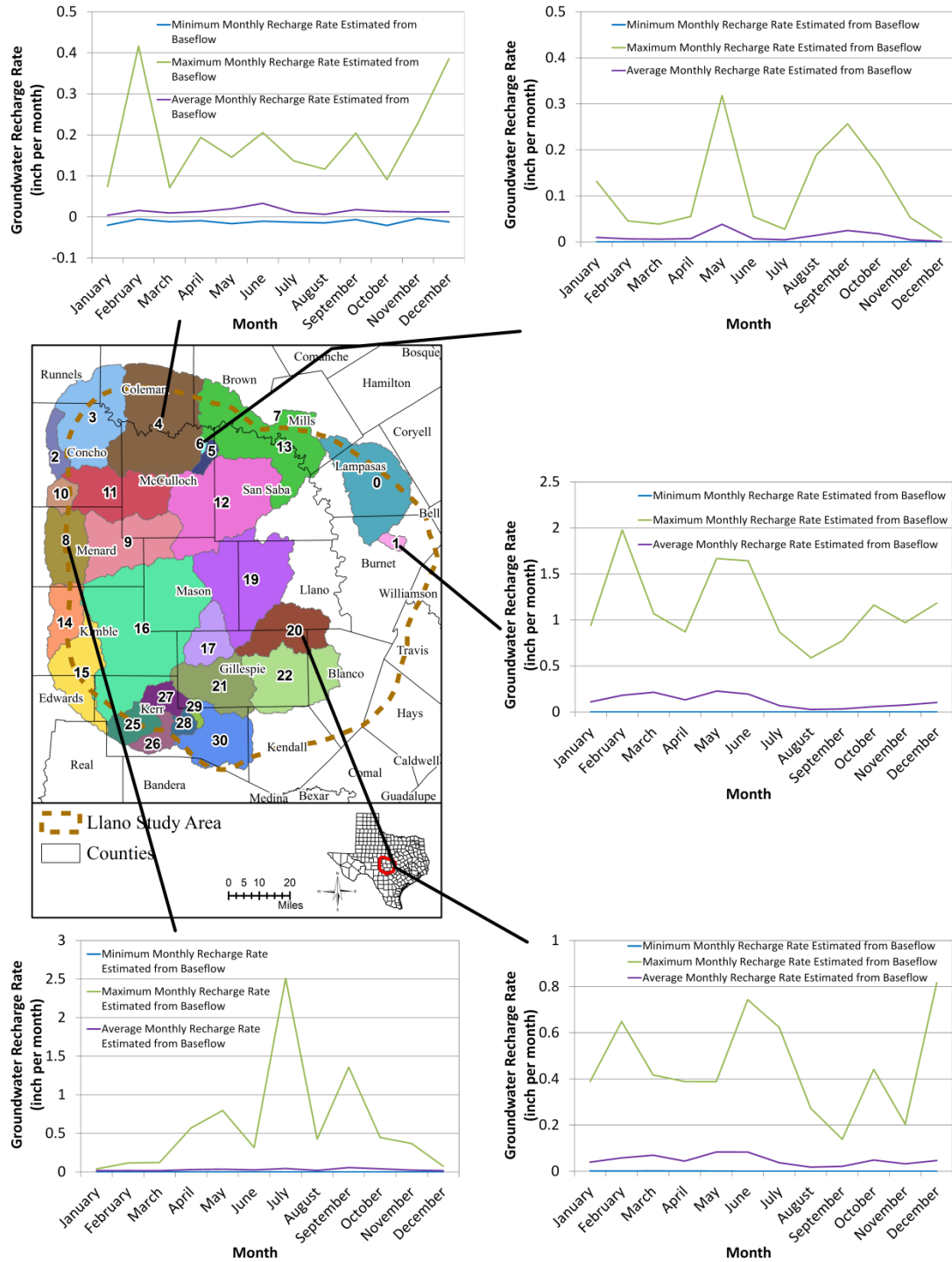


Figure 4.3.14 Variations of minimum, maximum, and average monthly groundwater recharge rates associated with catchment basins 1, 4, 6, 8, and 20 calculated from stream baseflow. Catchment basins are colored and numbered.

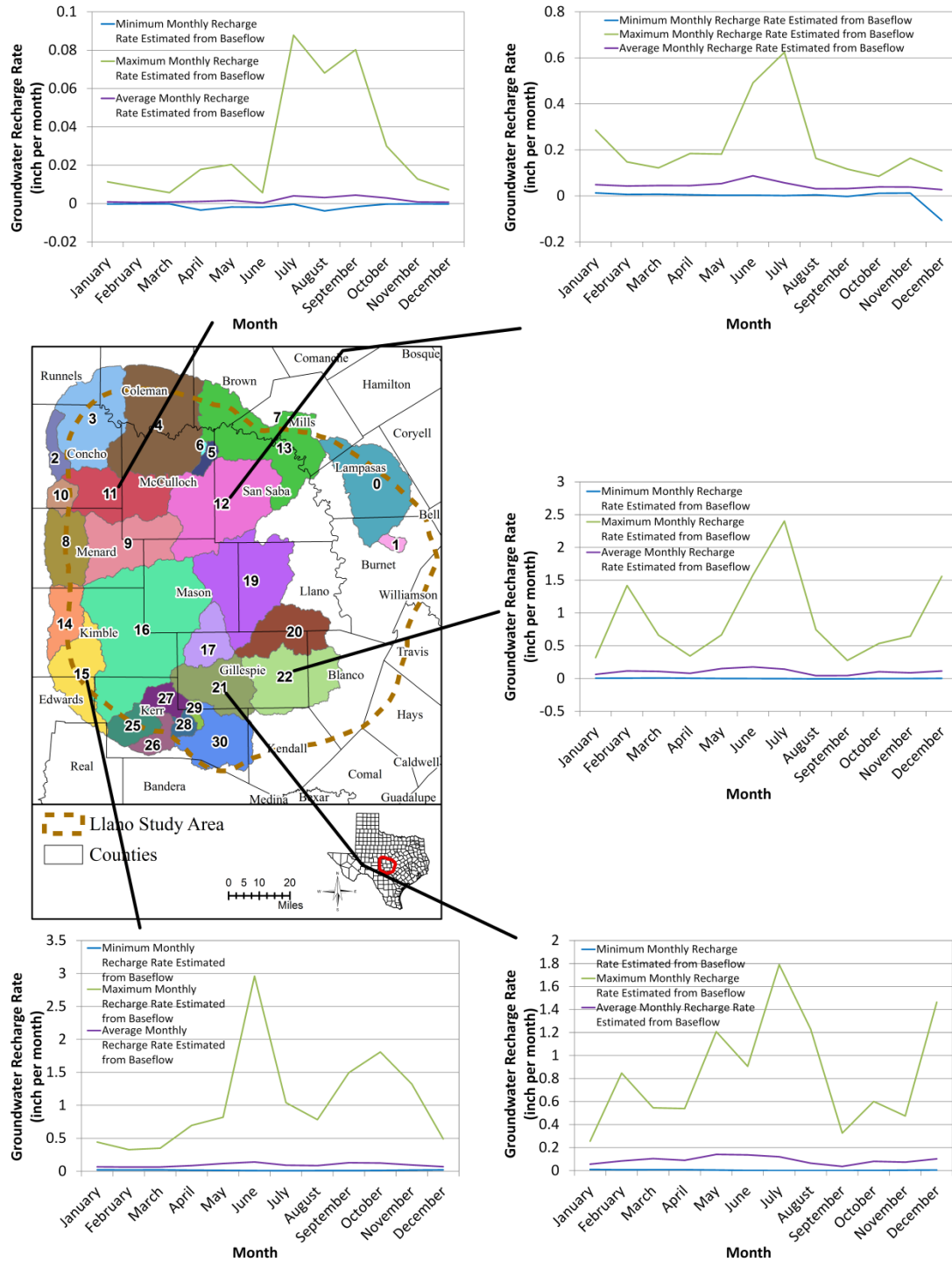


Figure 4.3.15 Variations of minimum, maximum, and average monthly groundwater recharge rates associated with catchment basins 11, 12, 15, 21, and 22 calculated from stream baseflow. Catchment basins are colored and numbered.

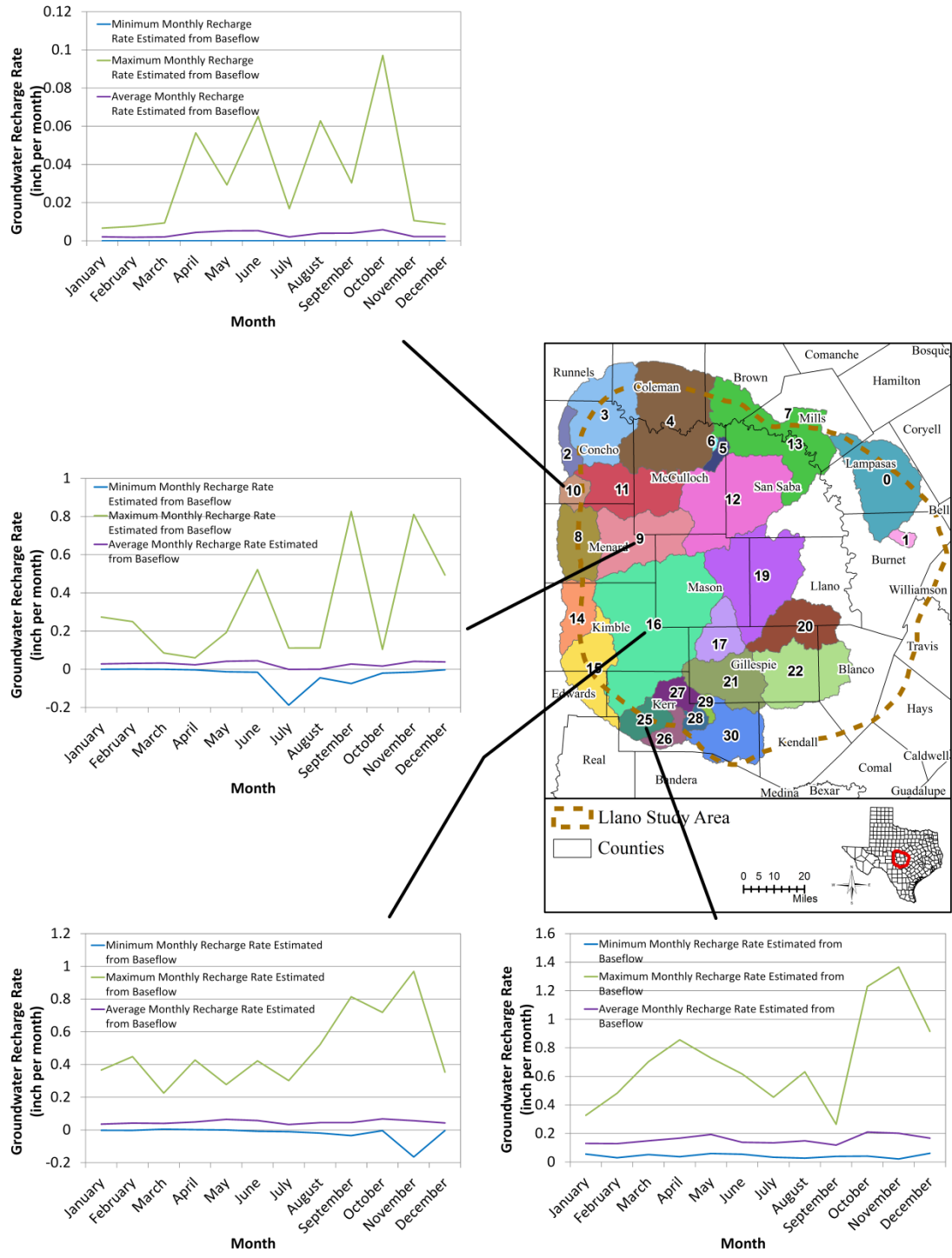


Figure 4.3.16 Variations of minimum, maximum, and average monthly groundwater recharge rates associated with catchment basins 9, 10, 16, and 25 calculated from stream baseflow. Catchment basins are colored and numbered.

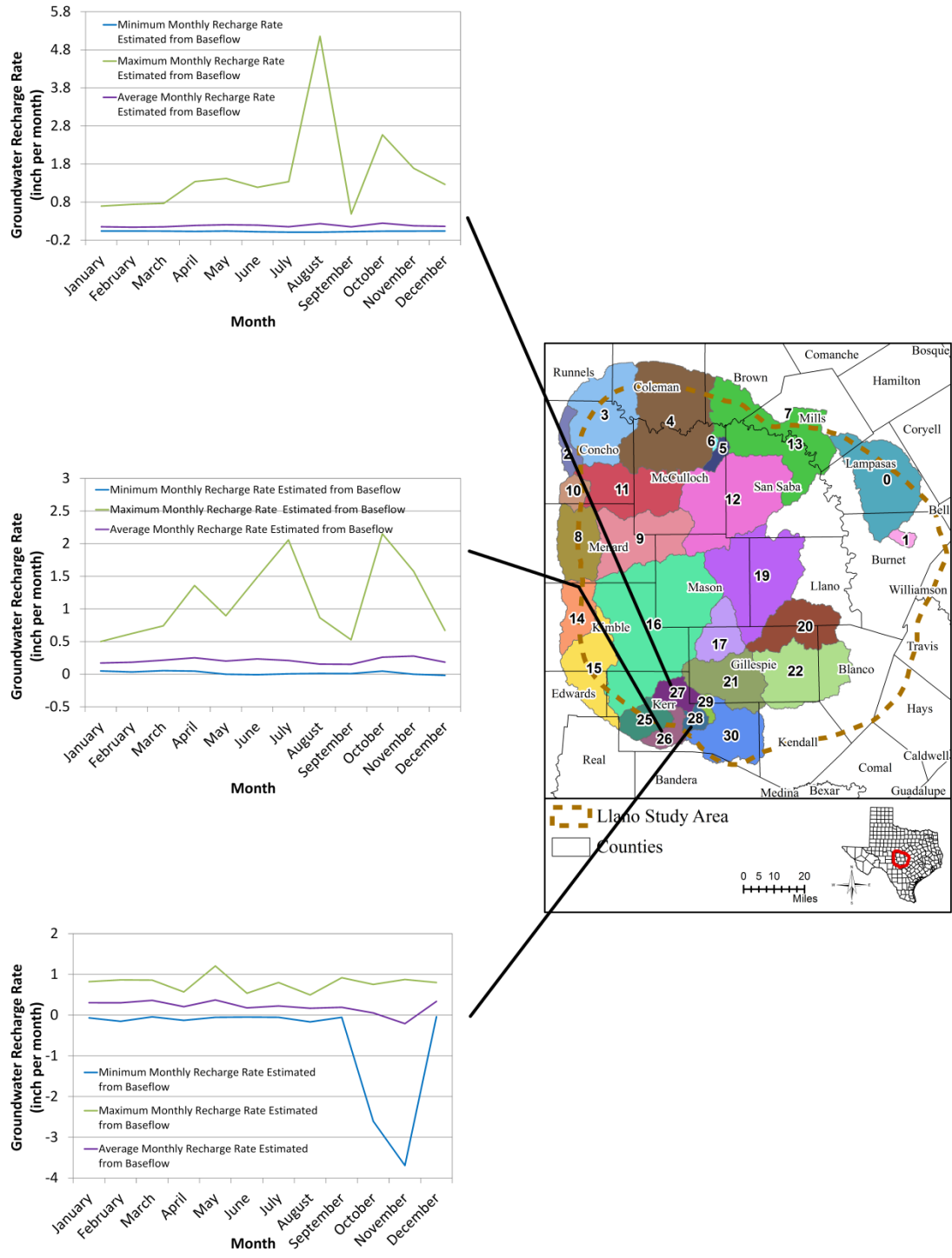


Figure 4.3.17 Variations of minimum, maximum, and average monthly groundwater recharge rates associated with catchment basins 26, 27, and 28 calculated from stream baseflow. Catchment basins are colored and numbered.

4.4 Rivers, Streams, Lakes, and Springs

Groundwater can interact with surface waters such as rivers, streams, and lakes. Such interactions could involve gaining water from, or losing water to, the surface water bodies. In a numerical groundwater flow model, surface water bodies are often defined as boundary conditions. In this section, the interaction between groundwater and surface water is evaluated and, if possible, quantified. The information from this analysis will be used for the numerical model development.

4.4.1 Gain or Loss of Rivers and Streams

The interaction between groundwater and surface water is often treated as a calibration criterion during the numerical model development. The interaction is quantified as stream gain or loss. When the water level in an aquifer is higher than the riverbed, the groundwater flows into the river. In this case, the river gains water from the aquifer. The opposite could happen when the water level in an aquifer is lower than the riverbed. In this case, the river loses water to the aquifer. A river flux measured at a stream gage often represents the total flow at that station. This total flow includes flow from upstream including any releases from reservoirs or surface water right permits, baseflow, and runoff. Runoff is the flow above land surface that usually occurs during and after rainfall events. Baseflow is the flow from groundwater to a river or vice versa. Thus, the analysis of baseflow is typically used to evaluate stream gains or losses with respect to groundwater.

Two major rivers cross the study area: the Colorado River to the north and the Guadalupe River to the south (Figure 2.0.2). There are three major tributaries associated with the Colorado River in the study area: the San Saba, Llano, and Pedernales rivers. A few small tributaries of the Guadalupe River are located in Kerr County. Several tributaries in Burnet and Lampasas counties merge into the Brazos River. However, the Colorado River and its tributaries drain most of the study area.

River flux hydrographs from selected gages located on the Colorado and Guadalupe rivers in the study area are shown in Figure 4.4.1. The blue line represents monthly average river flux calculated from daily measurements and downloaded from the U.S. Geological Survey's website, http://waterdata.usgs.gov/nwis/uv/?referred_module=sw. The annual flux is calculated from the monthly values and presented as a red line. Figure 4.4.1 shows that discharge in the Colorado River is almost 10 times greater than the discharge in the Guadalupe River in terms of flow. It also shows that the river flux can vary more than one order of magnitude from one month to another. The 1950s' drought may have impacted the Guadalupe River more than the Colorado River. In addition, both rivers show a reduction in flow for the last five or so years.

To evaluate the groundwater/surface water interaction, Slade and others (2002) compiled all of the previous stream gain/loss studies in the state of Texas. Most of the studies were performed during the winter months when the volume of pumping from the aquifers is typically low and stream losses from evapotranspiration are also low. The stream flow measurements from these studies approximated the baseflow values that could be used to estimate the groundwater gains or losses within of a stream segment. However, these studies were performed before the manmade lakes and reservoirs were constructed. As a result, the stream gain/loss data may not reflect current conditions. In addition, most of stream gages (246 out of 270) only had one gain/loss

calculation based on one round of stream flow measurements. It is recommended that caution should be taken with this type of data. Multiple gain/loss calculations from different dates existed at twenty-four gages. For these gages, the average gain/loss values were used to evaluate the groundwater/surface water interaction. Since the gain/loss calculations from Slade and others (2002) were based on stream segments with different lengths, the values were normalized by dividing the stream segment lengths and the normalized stream gain/loss results are shown in [Figure 4.4.2](#). Almost all of the streams show an alternative gain or loss pattern over its course. Also, stream gain or loss slightly increases from the northwestern to south and from smaller (such as Pedernales River) to larger rivers (such as San Saba, Llano, and Guadalupe rivers). For smaller streams, the normalized gain/loss is often less than 0.1 cubic feet per second over a mile of stream segment, while the larger streams have more segments with the normalized gain or loss more than 0.1 cubic feet per second over a mile of stream segment.

To evaluate the streams gains and losses, especially the long-term variation and seasonal changes, the baseflow data used for the groundwater recharge calculations in the previous section are presented here. These data represent the stream gain/loss for a stream segment intercepted by a catchment basin. To minimize any bias associated with the variation of the basin sizes, the total groundwater gain (positive) or loss (negative) were normalized. [Figures 4.4.3](#) through [4.4.8](#) are the annual average gain or loss and [Figures 4.4.9](#) through [4.4.14](#) are the monthly average gain or loss. As the groundwater recharge rate (see [Figure 4.3.11](#)), the groundwater gain or loss is the lowest in the catchment basins dominated by the Permian outcrops, highest in the Cretaceous outcrop areas, and intermediate in the Precambrian outcrop area; the annual stream flow gain or loss in a catchment basin also change significantly from year to year ([Figures 4.4.3](#) through [4.4.8](#)) and from month to month ([Figures 4.4.9](#) through [4.4.14](#)). On average, all of the stream segments in the study area gain water from aquifers on an annual basis ([Figures 4.4.3](#) through [4.4.8](#)). In addition, for certain stream segments, the stream can lose water in certain months and gain water in the others (see catchment basin 29 in [Figure 4.4.9](#), catchment basin 13 in [Figure 4.4.10](#), and catchment basin 28 in [Figure 4.4.14](#)). These stream segments happen to be in smaller catchment basins. This indicates that the stream gain or loss is also related to the selected (measured) stream length.

4.4.2 Lakes and Reservoirs

In the study area, there are five manmade lakes or reservoirs along the Colorado River (from upstream to downstream): O. H. Ivie Reservoir (impounded in March 1990), Lake Buchanan (impounded in May 1937), Inks Lake (impounded in June 1938), Lyndon B. Johnson Lake (impounded in May 1951), and Lake Marble Falls (impounded in July 1951). Another relatively small reservoir, the Brady Creek Reservoir, was impounded in January 1963 along the Brady Creek near the town of Brady in McCulloch County. The lake/reservoir level hydrographs as well as their locations are presented in [Figure 4.4.15](#). The water levels at the O. H. Ivie and Brady Creek reservoirs are from the U. S. Geological Survey (http://waterdata.usgs.gov/nwis/uv/?referred_module=sw). The water levels for the other lakes are from the Lower Colorado River Authority (<http://www.lcra.org/water/river-and-weather/pages/historical-lake-levels.aspx>).

As [Figure 4.4.15](#) shows, water levels for the O. H. Ivie and Brady Creek reservoirs are only available since about 2000 and the reservoir level at the Brady Creek Reservoir has been declining since 2005. The Lower Colorado River Authority (LCRA) operates the Highland

Lakes System that includes Buchanan, Inks, LBJ, Marble Falls, Travis, and Austin. Please note that Travis and Austin lakes are located outside of the study area. The maximum water levels at Inks, LBJ, and Marble Falls lakes have been relatively steady, which is reasonable since they are operated as “constant” lakes in the Highland Lakes System. Lake Buchanan, the uppermost lake of the Highland Lakes System, shows recent declines since 2007 due to the drought and water demands.

The O. H. Ivie Reservoir is likely sitting on the low permeable Permian units. Thus, its interaction with the groundwater is expected to be minimal. The bottom of the Brady Creek Reservoir is likely Quaternary deposits underlain by the Cretaceous units. Thus, some interaction between the groundwater in the Cretaceous and the reservoir likely exists. However, this interaction is also limited by the reservoir size. All or the majority of the other four lakes (Buchanan, LBJ, Inks, and Marble Falls) are sitting on the Precambrian rock. Thus, interaction between these lakes and groundwater in the aquifers of interests are restricted to the areas where the lakes are in contact with the aquifers, such as the northern end of Lake Buchanan. The construction of lakes and reservoirs appear to have influenced groundwater flow patterns through time. From the surface water point view, the groundwater flow patterns are impacted by the size and water level of the lakes and reservoirs. Larger surface water bodies with greater impounded water level are expected to have greater impacts on the groundwater flow. However, the impacts are most likely restricted in the areas adjacent to the surface water bodies. At the regional scale, this should not significantly change the overall relation between the groundwater and surface water. As a result, it is expected that the lakes and reservoirs, in general, are still receiving groundwater from the surrounding aquifers.

4.4.3 Springs

When the water level in an aquifer is above the ground, it can discharge to the surface as springs. Springs often follow faults, fractures, or sedimentary rock beddings. Springs typically occur in topographically low areas such as river valleys or the outcrop areas where hydrogeologic conditions preferentially reject recharge. Along with groundwater levels and stream gain/loss data, the spring flow information can be used as calibration targets during the numerical model development. The spring information for this analysis was taken from the TWDB groundwater database (TWDB, 2014a).

In the study area, there are 264 springs with at least one flow measurement (Table A.1 of Appendix A). Of these springs, 113 springs originate from the Cretaceous aquifers, 9 from the Marble Falls Aquifer, 47 from the Ellenburger-San Saba Aquifer, 6 from the Hickory Aquifer, 17 from the Marble Falls and Ellenburger aquifers, and 1 from the Hickory and associated Cambrian rocks. The aquifer association for the rest of the 71 springs is unknown and not documented.

In the study area, there are also 101 springs without any flow measurements. Of these springs, 15 originate from the Cretaceous aquifers, 1 from the Marble Falls Aquifer, 12 from the Ellenburger-San Saba Aquifer, 9 from the Hickory Aquifer, 1 from the Hickory and Ellenburger aquifers, and 1 from the Hickory and associated Cambrian rocks. The aquifer association for the rest of the 62 springs is unknown and not documented.

The springs with known aquifer associations (including springs without flow measurements) are shown in [Figure 4.4.16](#). This figure also contains flow hydrographs of selected springs originating in the minor aquifers with the most flow measurements available. As the figure shows, spring flow measurements are sparse and all but the San Saba Springs had measurements terminated during or before 1990s. However, [Figure 4.4.16](#) does indicate the drought during the 1950s reduced the flows by more than half for most of the springs in the study area. The flow reduction was not observed at the Gorman Springs most likely due to lack of data during 1950s. The San Saba Springs have the most flow measurements, almost 2005. Though the average flow at the San Saba Springs remains almost unchanged, the fluctuation appears less obvious for the last 5 years.

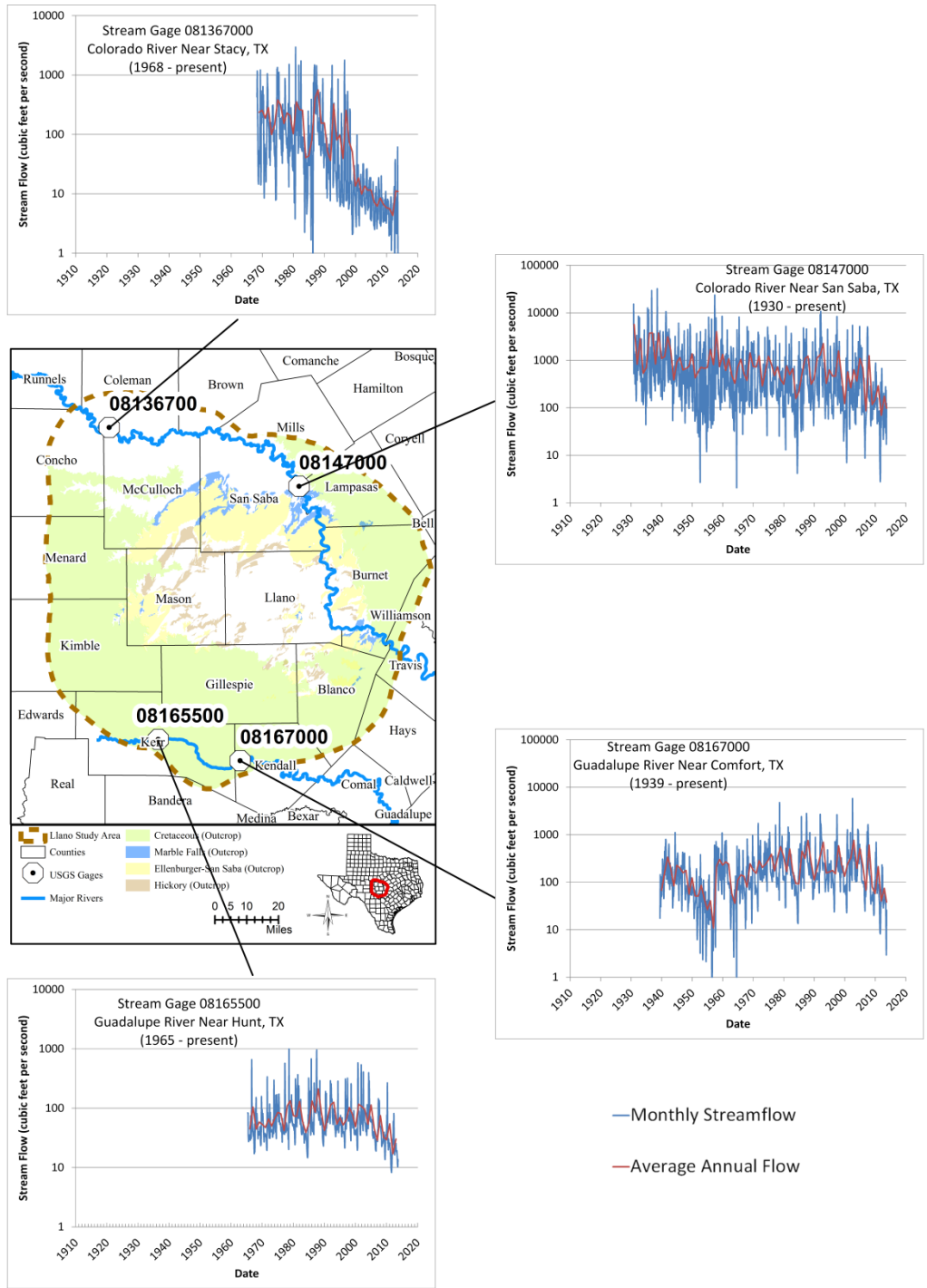


Figure 4.4.1 River flux hydrographs for selected gages located on Colorado and Guadalupe rivers. River monthly flux data are downloaded from U.S. Geological Survey (2014).

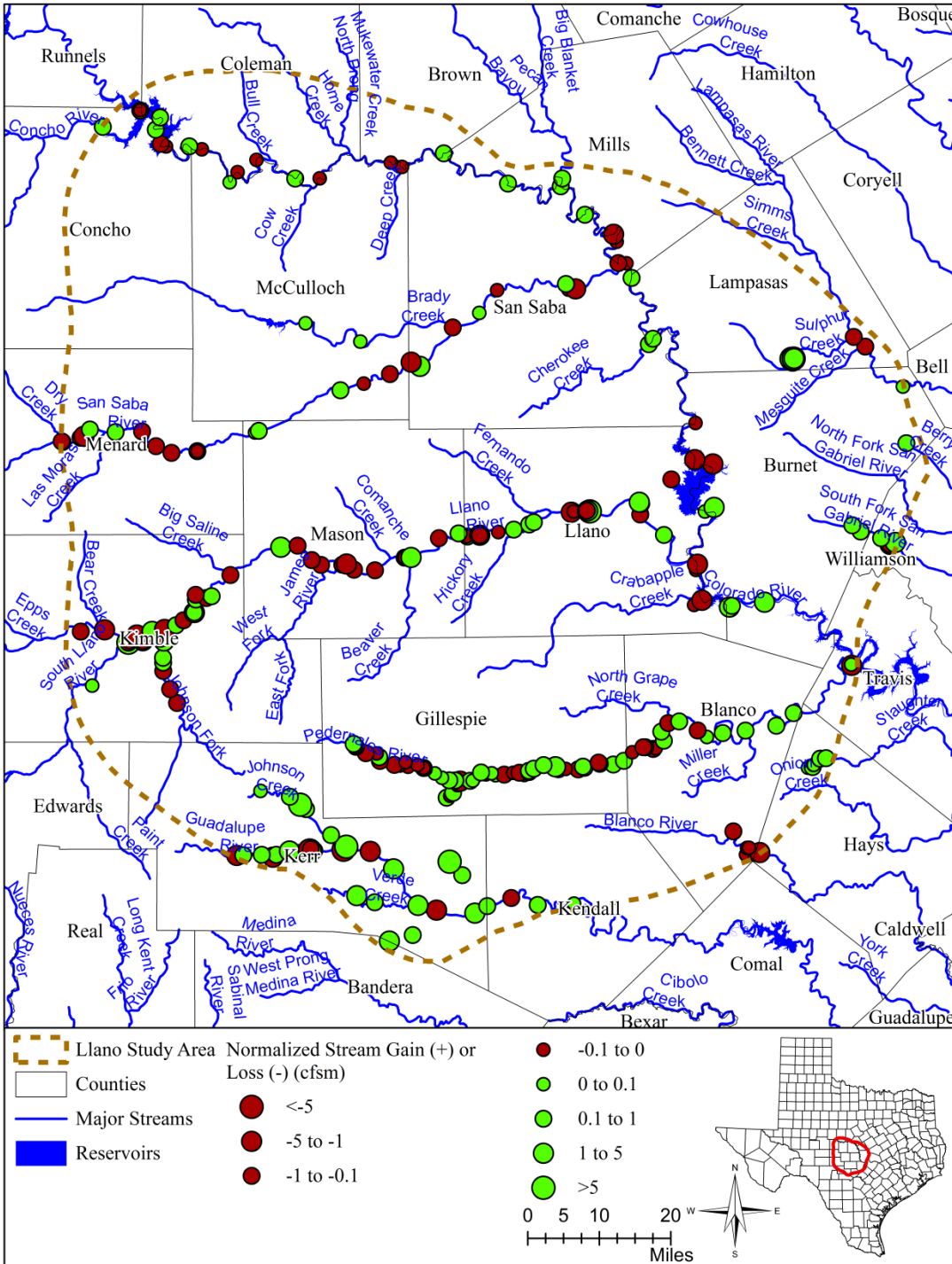


Figure 4.4.2 Stream gain (positive value) or loss (negative value) results in cubic feet per second per mile of stream channel (cfsm) (based on data compiled by Slade and others (2002)).

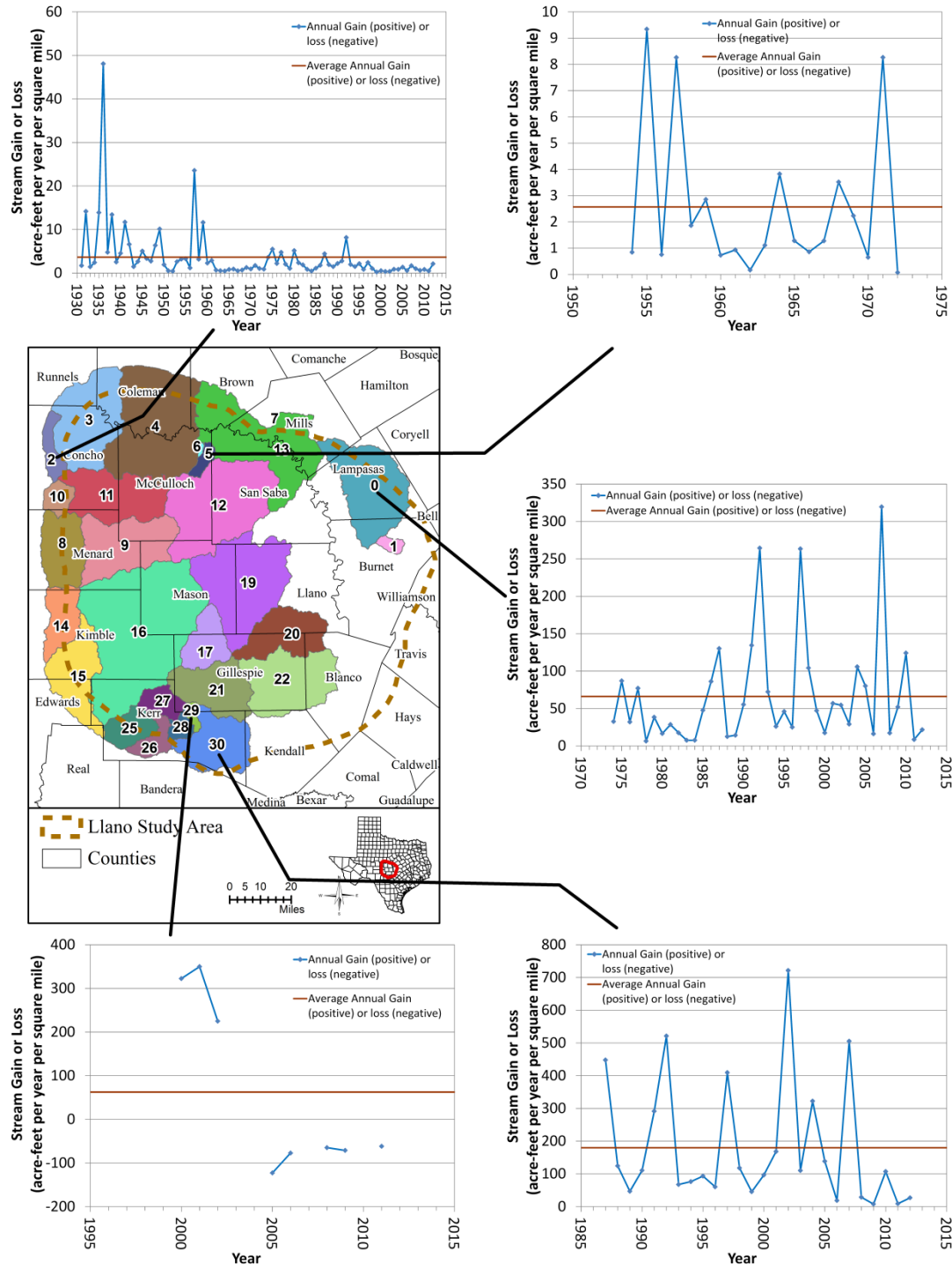


Figure 4.4.3 Variations of annual stream gain or loss for stream segments associated with catchment basins 0, 2, 5, 29, and 30 (acre-feet per year per square mile). Catchment basins are colored and numbered.

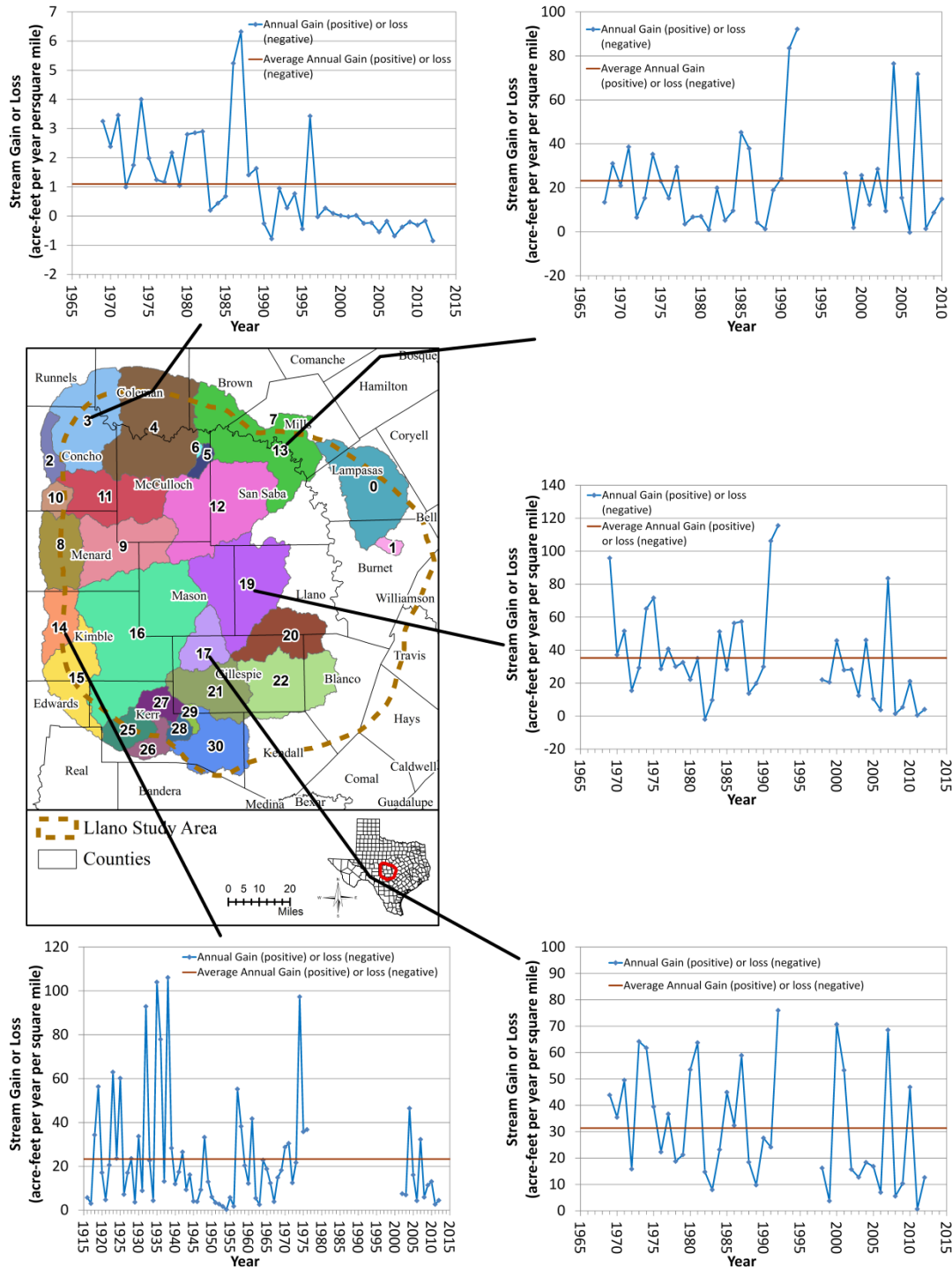


Figure 4.4.4 Variations of annual stream gain or loss for stream segments associated with catchment basins 3, 13, 14, 17, and 19 (acre-feet per year per square mile). Catchment basins are colored and numbered.

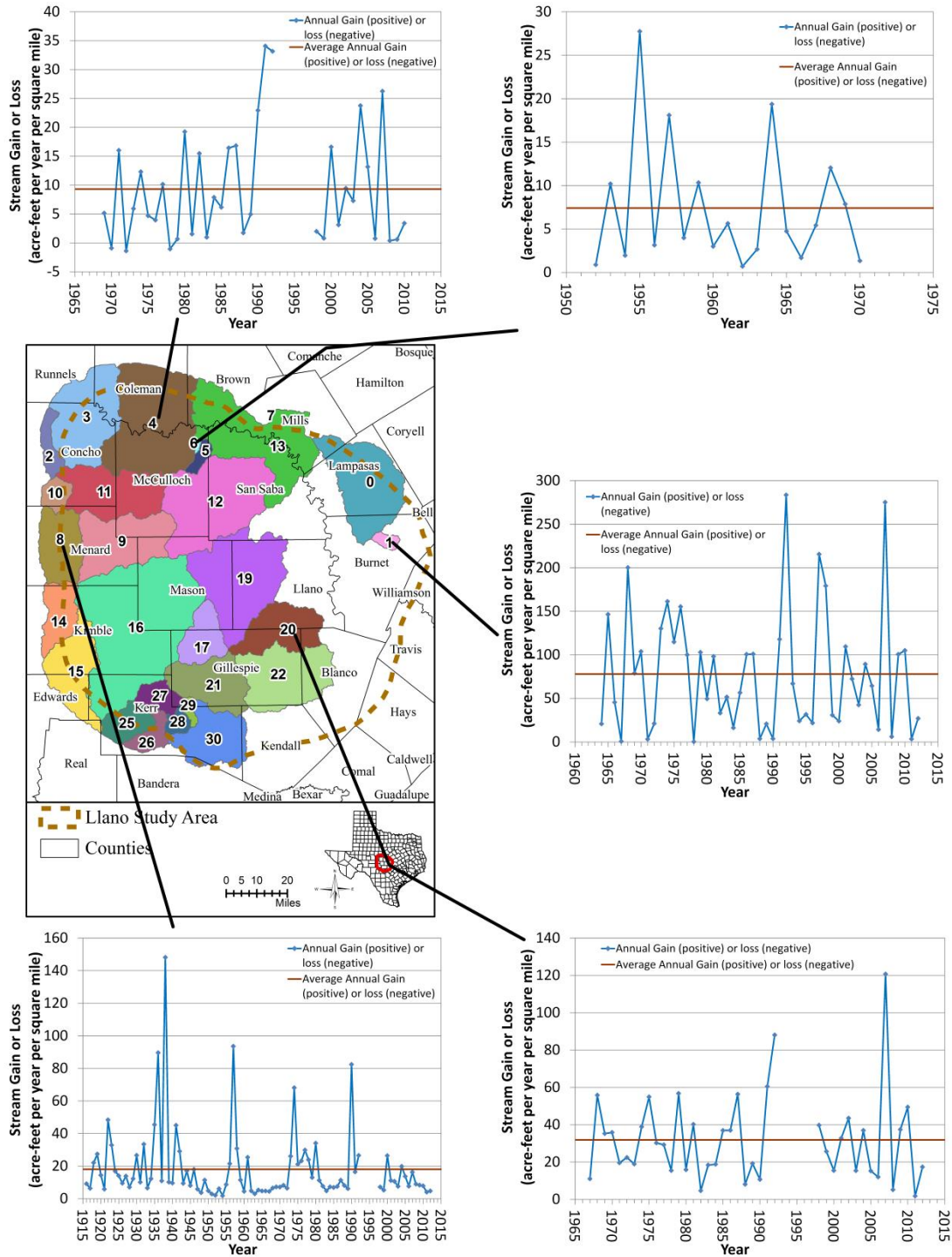


Figure 4.4.5 Variations of annual stream gain or loss for stream segments associated with catchment basins 1, 4, 6, 8, and 20 (acre-feet per year per square mile). Catchment basins are colored and numbered.

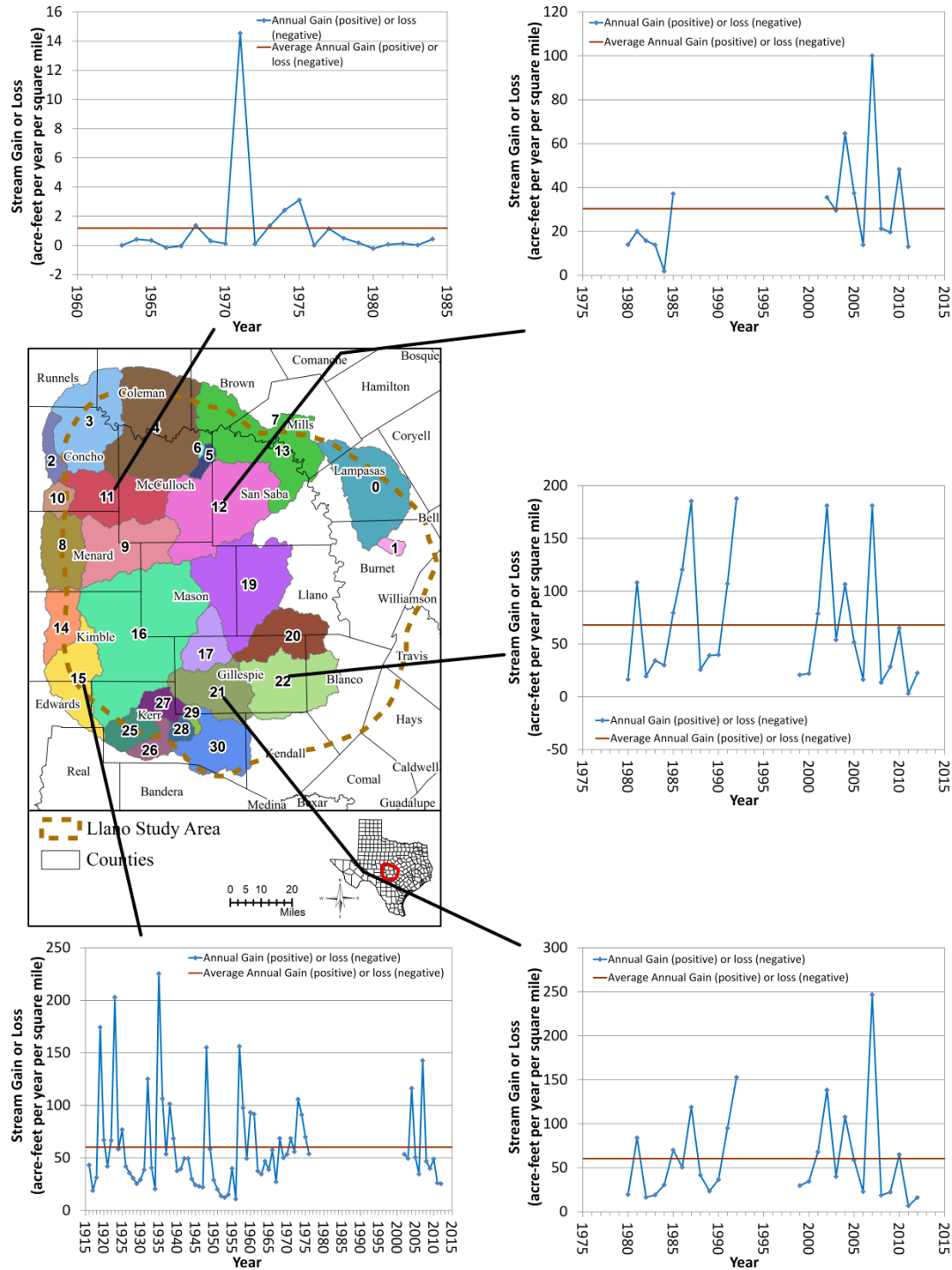


Figure 4.4.6 Variations of annual stream gain or loss for stream segments associated with catchment basins 11, 12, 15, 21, and 22 (acre-feet per year per square mile). Catchment basins are colored and numbered.

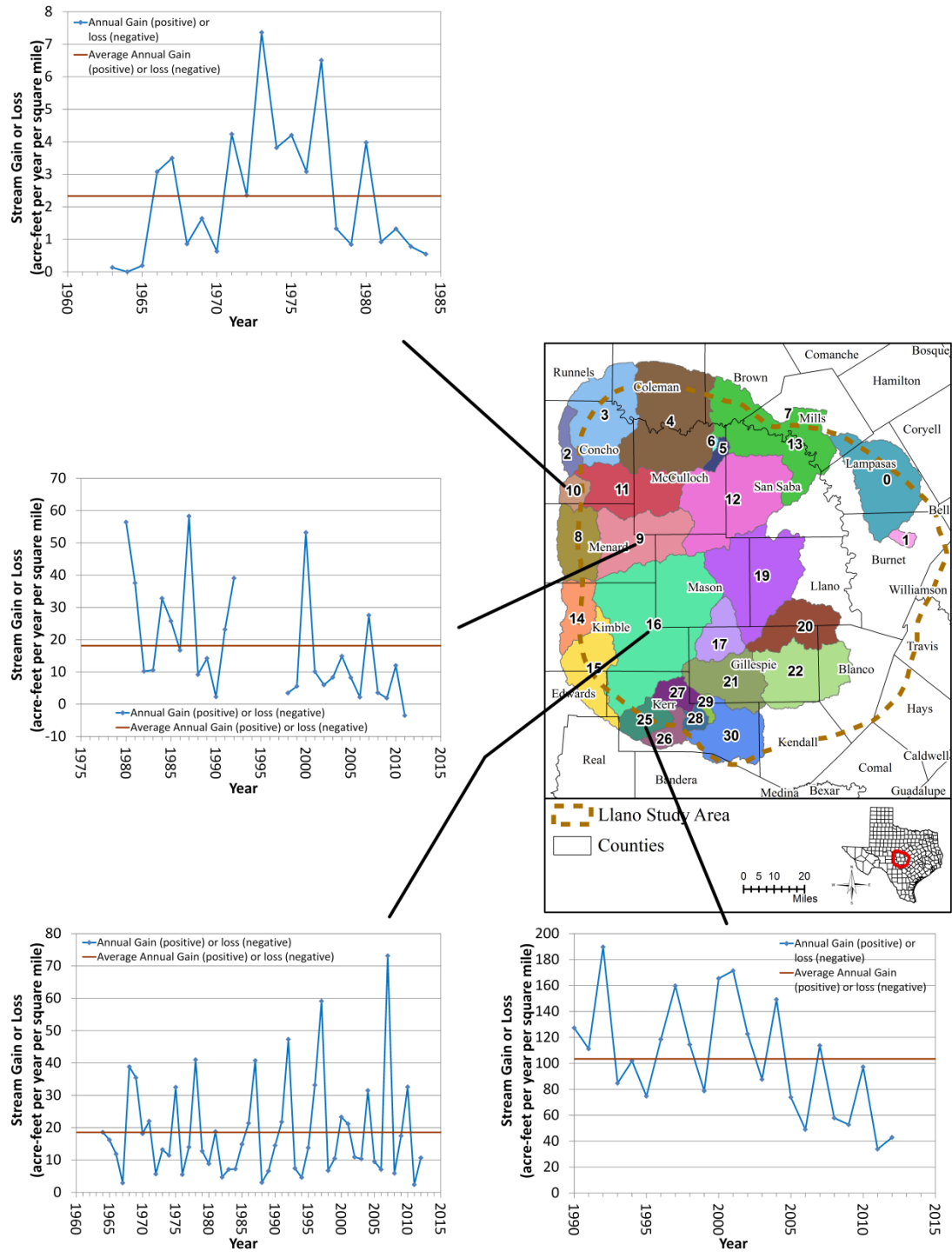


Figure 4.4.7 Variations of annual stream gain or loss for stream segments associated with catchment basins 9, 10, 16, and 25 (acre-feet per year per square mile). Catchment basins are colored and numbered.

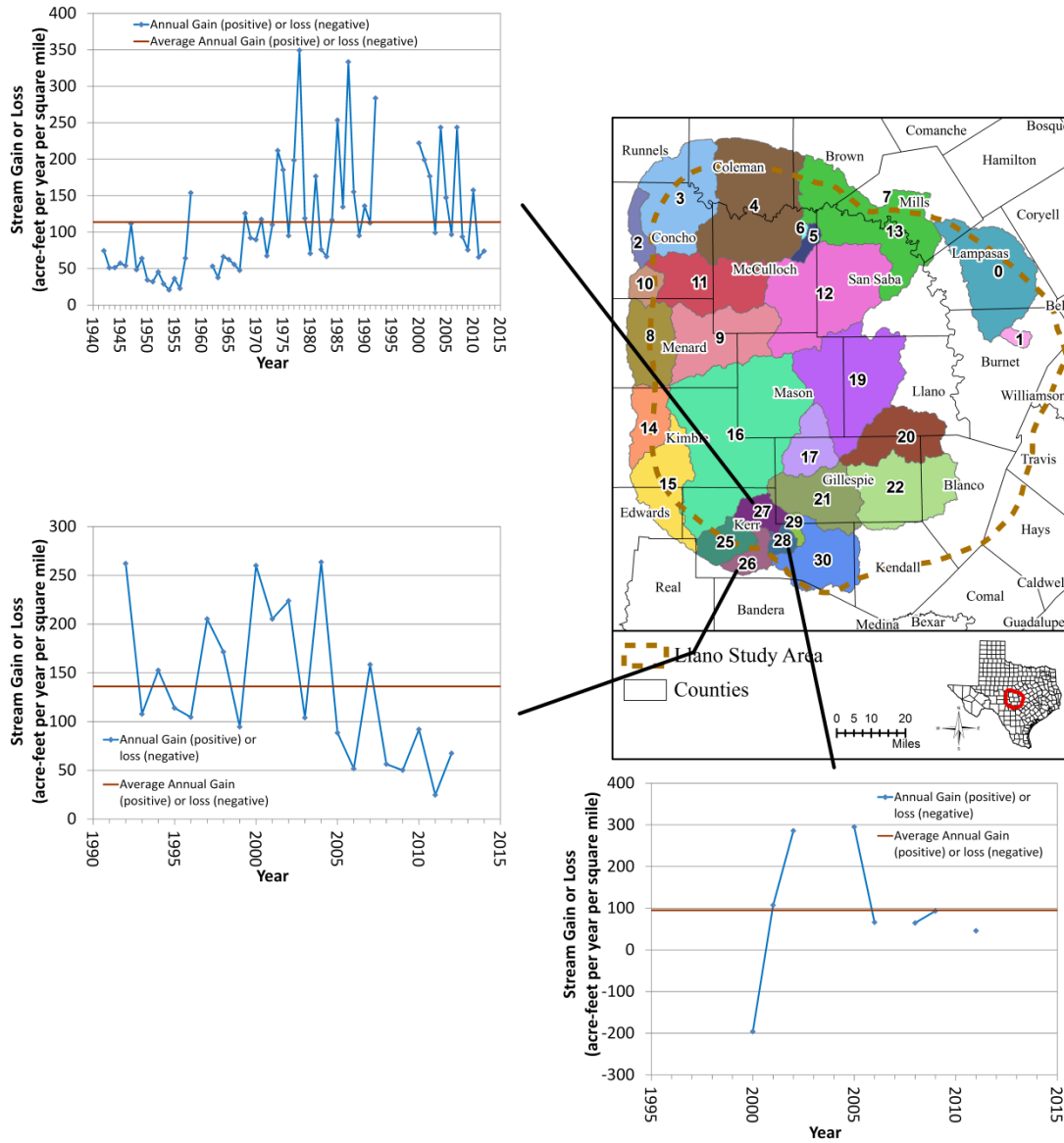


Figure 4.4.8 Variations of annual stream gain or loss for stream segments associated with catchment basins 26, 27, and 28 (acre-feet per year per square mile). Catchment basins are colored and numbered.

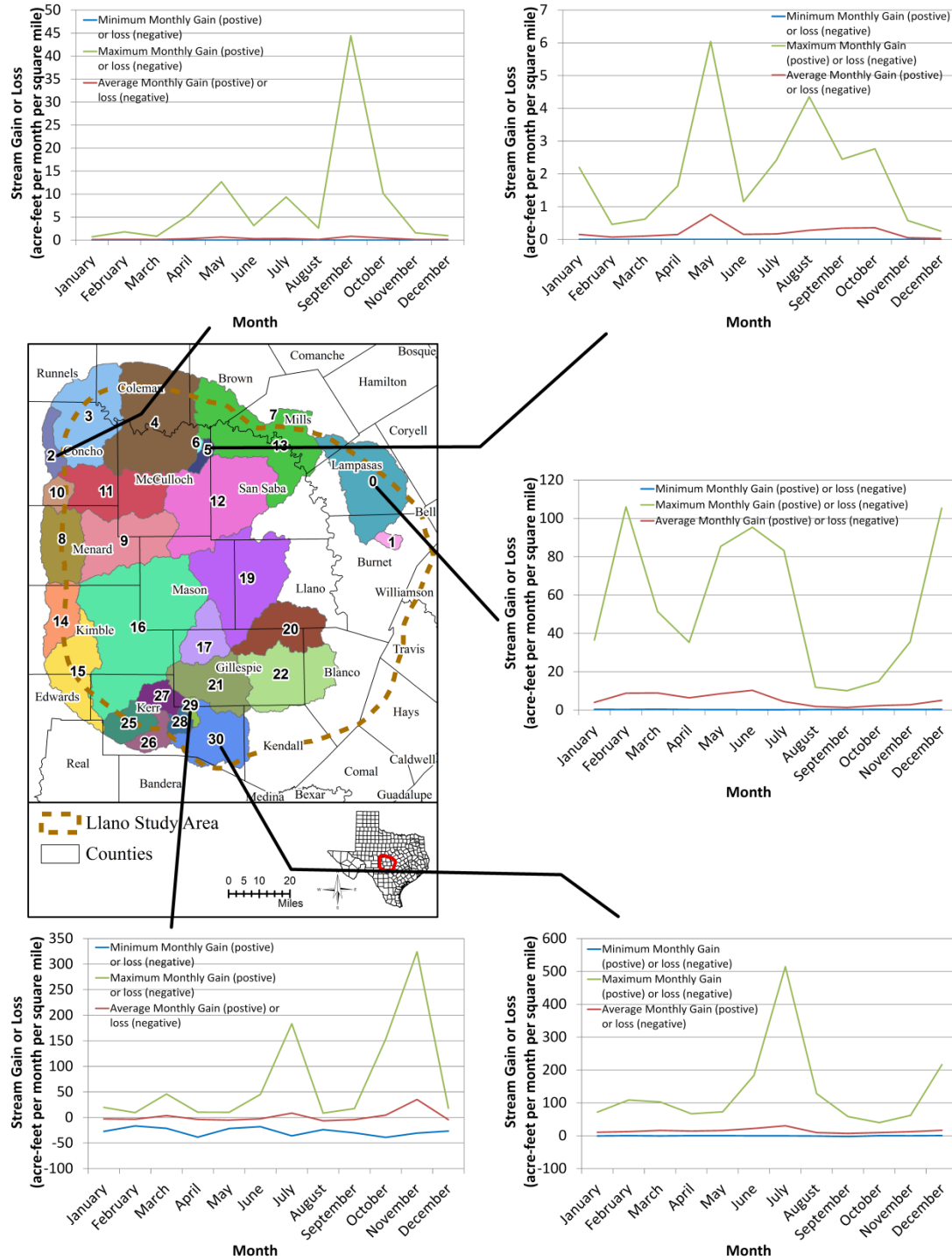


Figure 4.4.9 Variations of minimum, maximum, and average monthly stream gain or loss for stream segments associated with catchment basins 0, 2, 5, 29, and 30 (acre-feet per month per square mile). Catchment basins are colored and numbered.

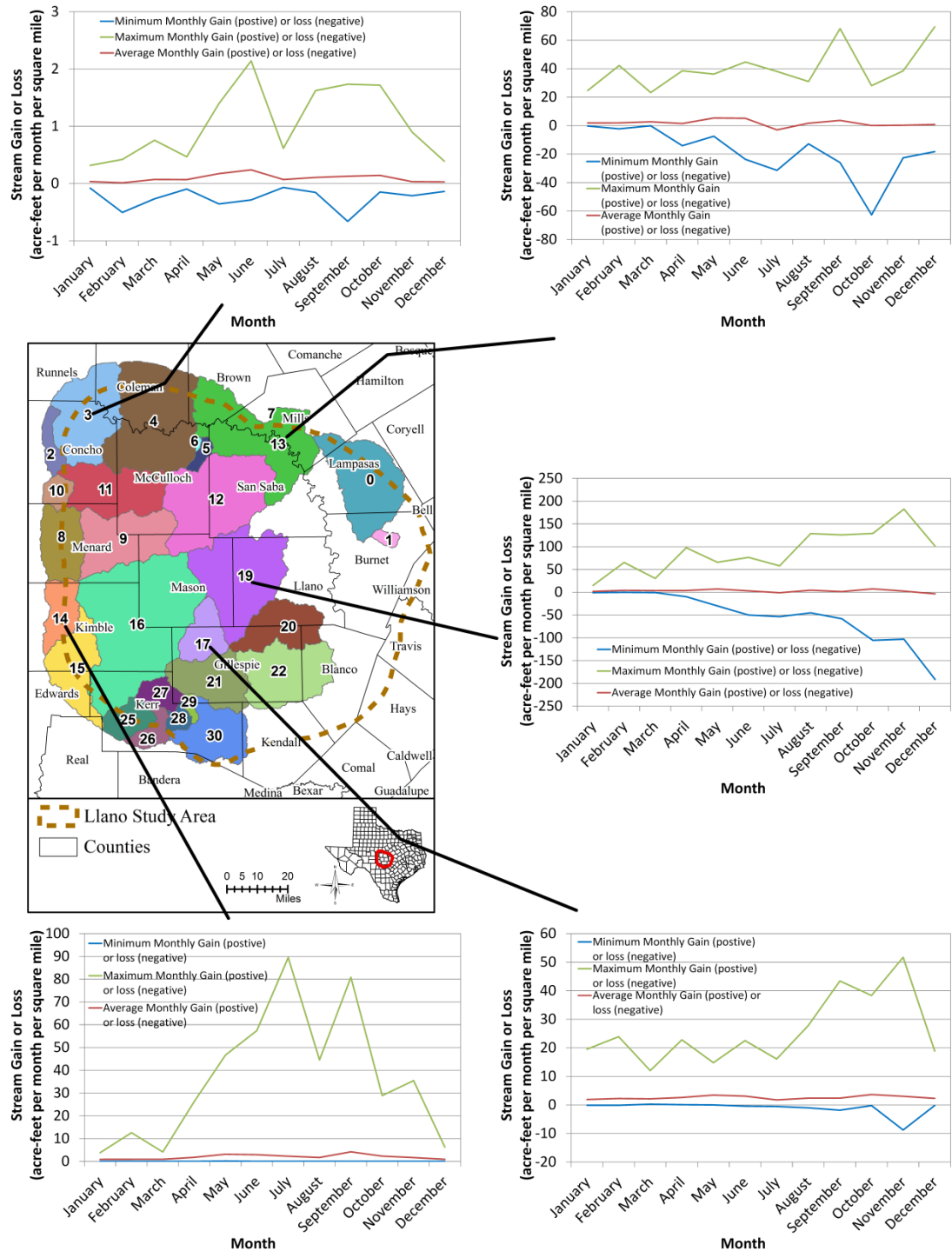


Figure 4.4.10 Variations of minimum, maximum, and average monthly stream gain or loss for stream segments associated with catchment basins 3, 13, 14, 17, and 19 (acre-feet per month per square mile). Catchment basins are colored and numbered.

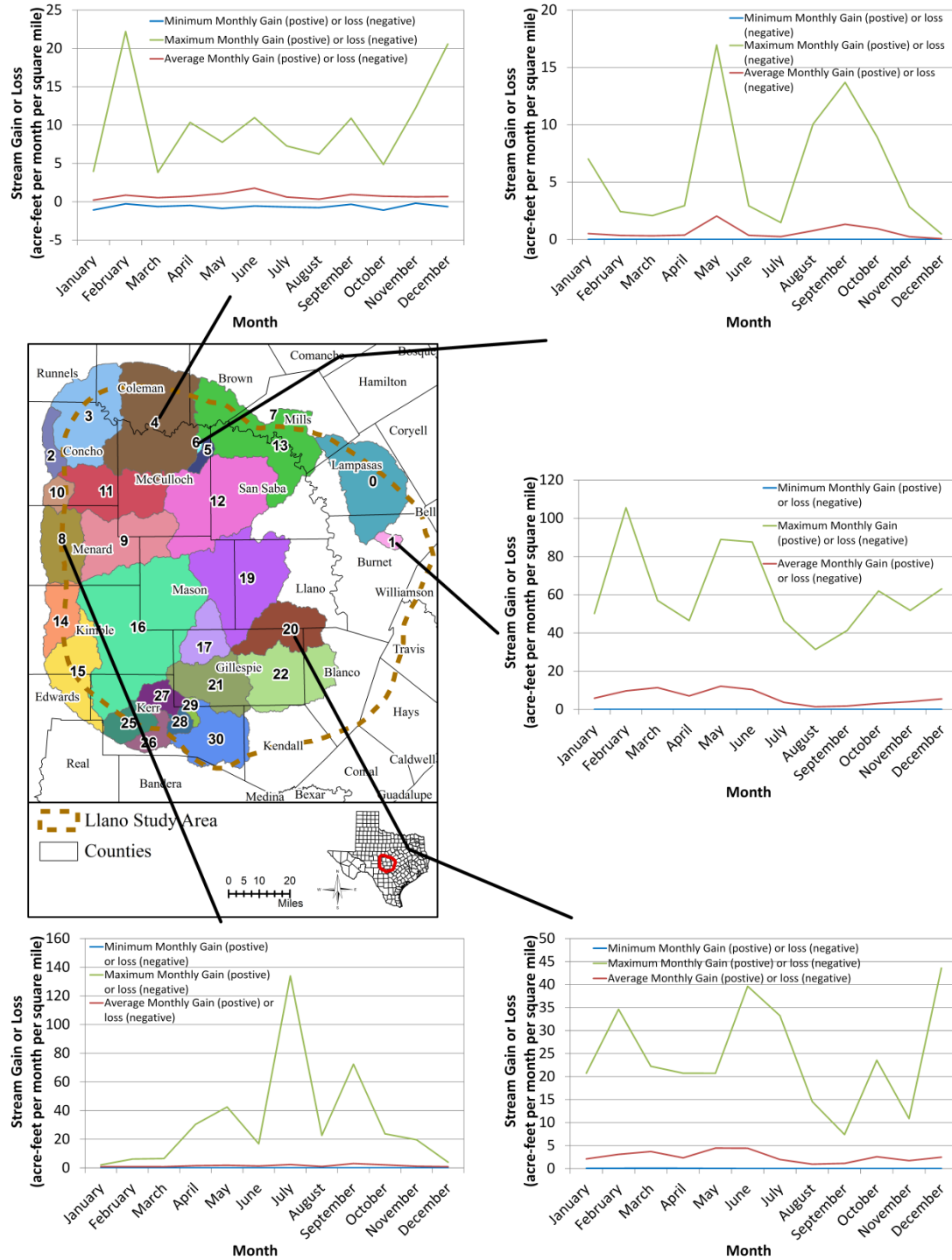


Figure 4.4.11 Variations of minimum, maximum, and average monthly stream gain or loss for stream segments associated with catchment basins 1, 4, 6, 8, and 20 (acre-feet per month per square mile). Catchment basins are colored and numbered.

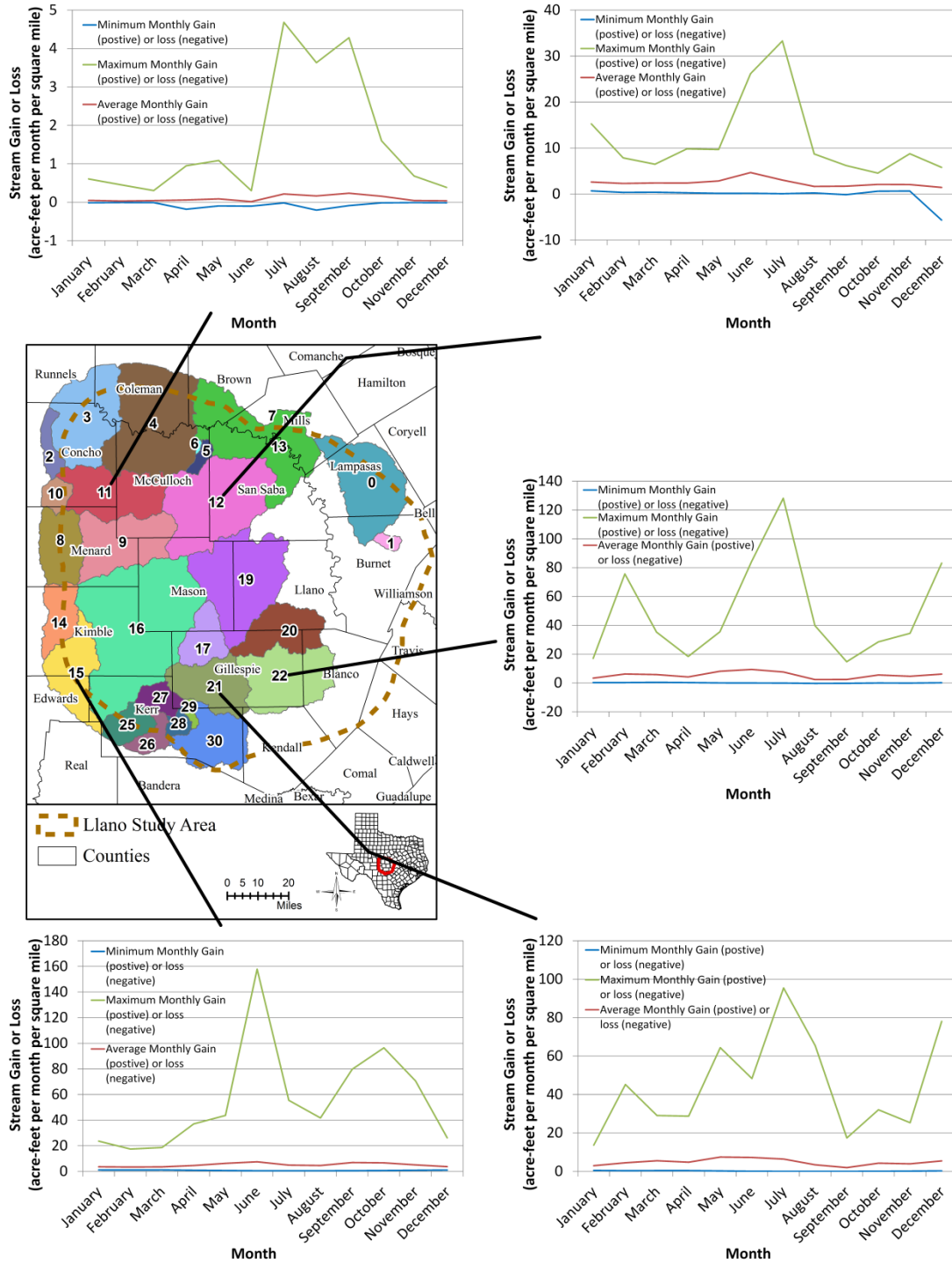


Figure 4.4.12 Variations of minimum, maximum, and average monthly stream gain or loss for stream segments associated with catchment basins 11, 12, 15, 21, and 22 (acre-feet per month per square mile). Catchment basins are colored and numbered.

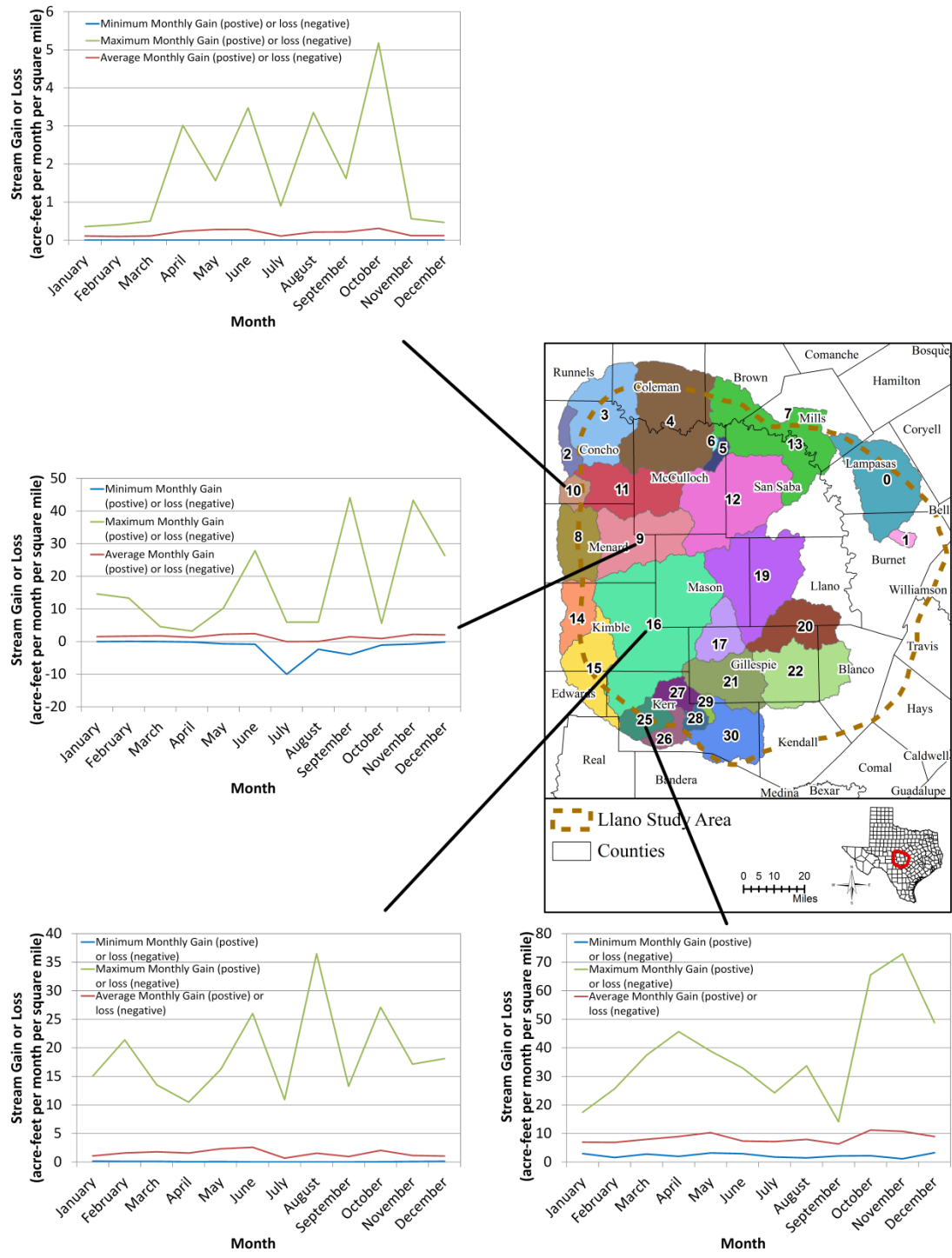


Figure 4.4.13 Variations of minimum, maximum, and average monthly stream gain or loss for stream segments associated with catchment basins 9, 10, 16, and 25 (acre-feet per month per square mile). Catchment basins are colored and numbered.

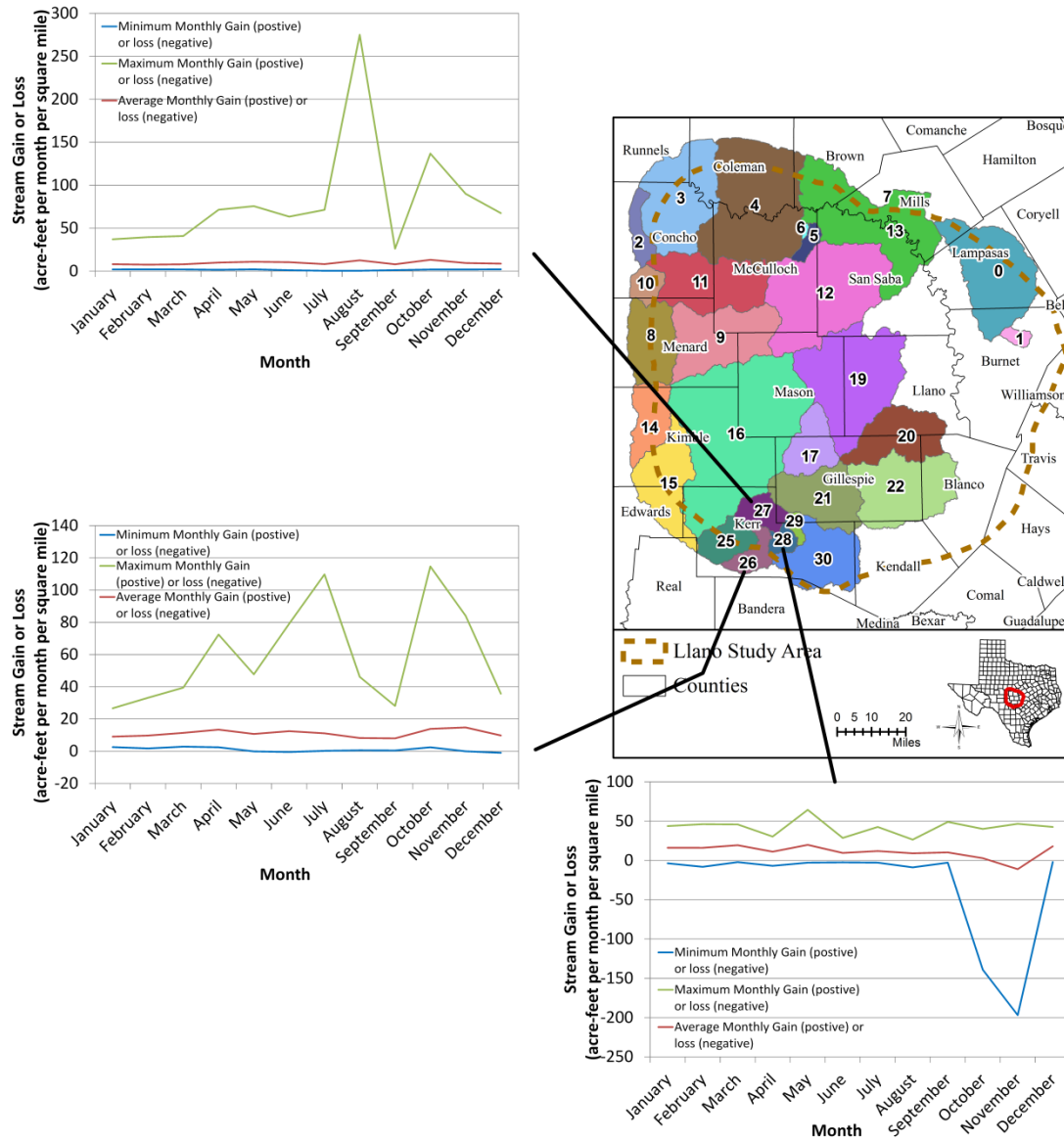


Figure 4.4.14 Variations of minimum, maximum, and average monthly stream gain or loss for stream segments associated with catchment basins 26, 27, and 28 (acre-feet per month per square mile). Catchment basins are colored and numbered.

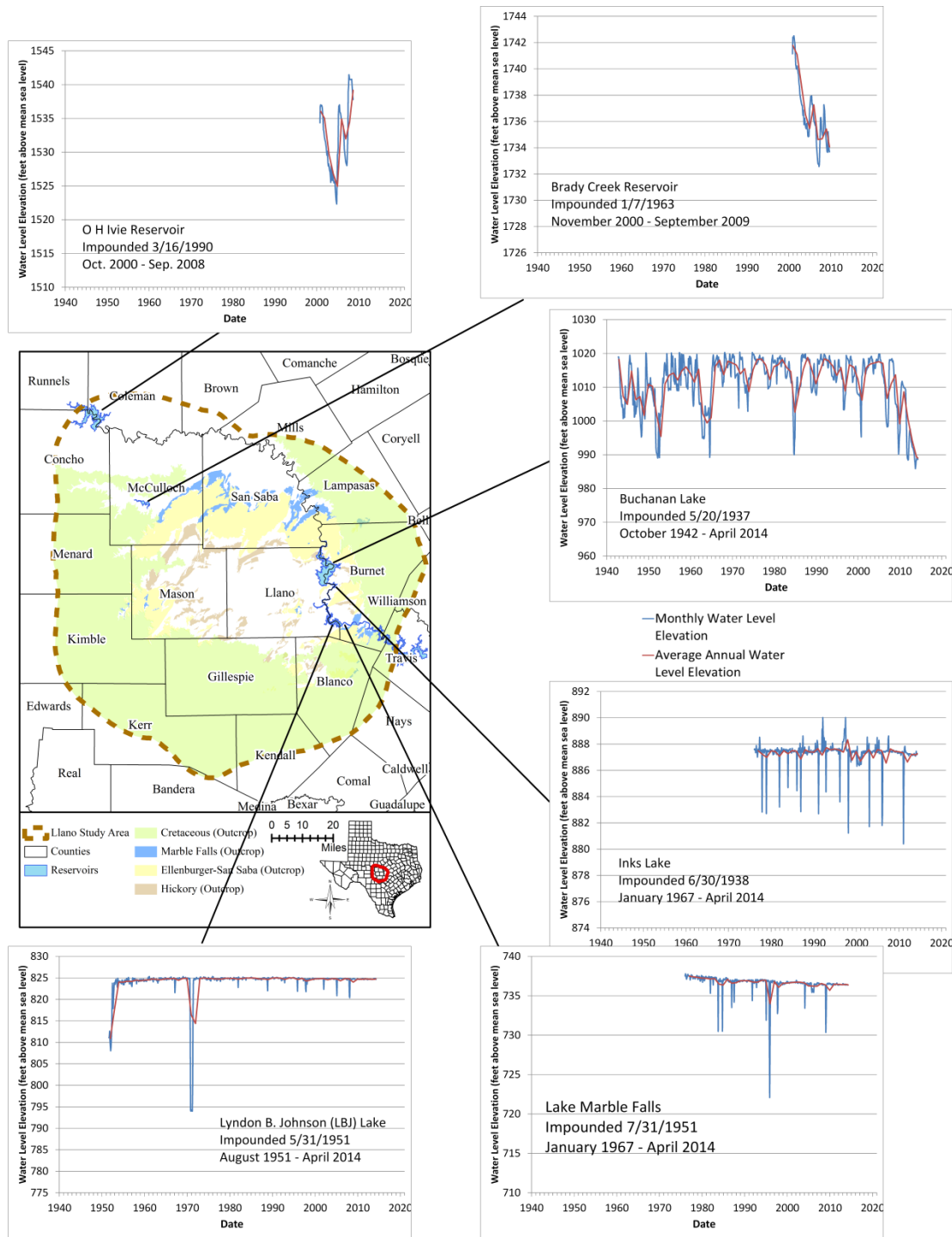


Figure 4.4.15 Water level hydrographs of O. H. Ivie Reservoir, Brady Creek Reservoir, Lake Buchanan, Inks Lake, Lyndon B. Johnson (LBJ) Lake, and Lake Marble Falls.

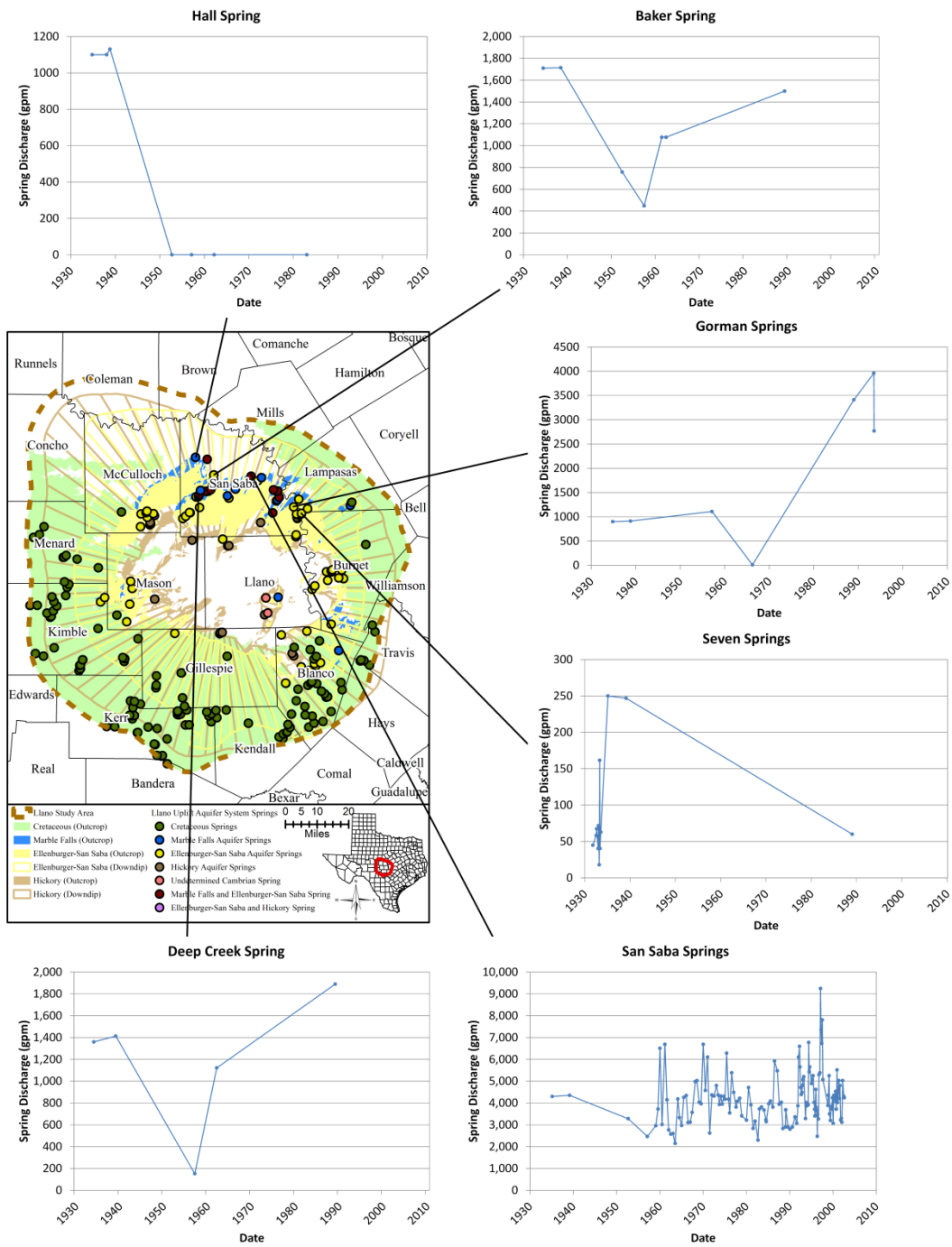


Figure 4.4.16 Flow hydrographs of selected springs originating from minor aquifers in Llano Uplift region.

4.5 Hydraulic Properties

The ability of an aquifer to transmit groundwater is influenced by aquifer lithology, fracturing, karstification, structural deformation, and proximity to surface water bodies. Several hydraulic parameters are used to describe aquifer properties including hydraulic conductivity, transmissivity, specific yield, storativity, and specific capacity. Each of these terms is briefly described below.

Hydraulic Conductivity (K) is a parameter representing how easily groundwater can flow through an aquifer. A higher hydraulic conductivity value means that the groundwater can flow through the aquifer more easily than an aquifer with lower hydraulic conductivity. Units for hydraulic conductivity may be expressed in feet per day or gallons per day per square foot.

Transmissivity (T) is the product of the hydraulic conductivity and the saturated aquifer thickness. Transmissivity is a measure of groundwater flow through the entire thickness of an aquifer. An aquifer with a higher transmissivity tends to transmit more water than an aquifer with lower transmissivity. Units for transmissivity may be expressed in square feet per day or gallons per day per foot.

Specific Yield (S_y), also called drainable porosity, is the volume of water released per unit volume of aquifer under the force of gravity. It approximates the effective porosity when the voids in the aquifer are large and well connected. For aquifers with finer materials, the specific yield is usually less than the effective porosity. The unit of specific yield is dimensionless.

Storativity (S), also called coefficient of storage, is the volume of water released per unit area of aquifer when the water level in the aquifer is lowered by a unit of length. In a confined (or artesian) aquifer, storativity can be used to calculate aquifer specific storage by dividing the aquifer thickness. In an unconfined (water table) aquifer, storativity is essentially equal to the specific yield. The storativity of a confined aquifer is often lower than the specific yield of an unconfined aquifer; given both aquifers contain the same materials. As a result, for the same aquifer, the outcrop area yields more water than downdip portion with the same head loss or drawdown. Storativity is dimensionless. Specific storage has a unit of one over length such as 1/foot or foot⁻¹.

Specific Capacity (S_c), the discharge of a well divided by the drawdown, is a measure of well yield. Specific capacity depends on aquifer property, well construction, and pumping rate. Specific capacity increases with increasing aquifer transmissivity and well diameter. Well specific capacity is often hindered by poor well design and construction as well as increasing pumping rate, which reduces well efficiency. Specific capacity may be expressed in gallons per minute per foot of drawdown in the well.

Previous studies and additional calculations using well specific capacity data were used to develop the hydraulic properties for the Hickory, Ellenburger-San Saba, Marble Falls, and Cretaceous aquifers in the study area. The previous studies included Myers (1969), Bluntzer (1992), Preston and others (1996), Christian and Wuerch (2012), Daniel B. Stephens and Associates (2006), Hunt and others (2010), and Young and others (2012).

These previous studies yielded 13 hydraulic property values for the Hickory Aquifer. Of the 13 data, eight were derived from single well tests and five were from time-drawdown or distance-drawdown tests. For the Ellenburger-San Saba Aquifer, four hydraulic property values were estimated from single well tests and eight were from time-drawdown or distance-drawdown tests. For the Cretaceous aquifers, 21 transmissivity and hydraulic conductivity values were estimated from single well tests and 27 were based on time-drawdown or distance-drawdown tests.

Additional specific capacity data were investigated and used to estimate the transmissivity values of the aquifers. Well specific capacity tests are often performed by driller once a new well is installed and developed. Many of these tests have been reported in drillers' reports and stored in the TWDB's groundwater database.

The aquifer transmissivity values were calculated using an EXCEL spreadsheet program developed by Michael Cobb (http://www.geology.wisc.edu/~hydro/cobbm_research.html) following the method of Bradbury and Rothschild (1985). The method applies the Cooper-Jacob approximation of the Theis equation with a correction for partial penetration and well loss. The well loss was assumed to be zero during our calculation. The equations are listed below:

$$T = \frac{Q}{4\pi s_m} \left[\ln \left(\frac{2.25Tt}{r_w^2 S} \right) + 2s_p \right] \quad (4.5.1)$$

$$s_p = \frac{1-L/b}{L/b} \left(\ln \frac{b}{r_w} - G(L/b) \right) \quad (4.5.2)$$

$$G(L/b) = 2.948 - 7.363(L/b) + 11.447(L/b)^2 - 4.675(L/b)^3 \quad (4.5.3)$$

Where:

b = aquifer thickness	s_m = measured drawdown
L = screen length	s_p = partial penetration parameter
Q = mean pumping rate	S = storativity
r_w = effective radius	T = transmissivity
t = pumping duration	

For a given specific capacity (Q/s_m), transmissivity can be solved iteratively. The transmissivity is then converted to hydraulic conductivity by dividing the well screen length. During our calculation, the aquifer storativity was assumed 0.0005.

Following the methodology described above, the aquifer transmissivity and hydraulic property values were estimated for 43 Hickory Aquifer wells, 41 Ellenburger-San Saba Aquifer wells, two Marble Falls Aquifer wells, and 177 Cretaceous Aquifer wells.

4.5.1 Transmissivity and Hydraulic Conductivity

The aquifer transmissivity and hydraulic conductivity values from previous studies and our calculations are summarized in Appendix A (Table A.2) and briefly discussed below.

Cretaceous Aquifers - The transmissivity values range from 3 to about 80,000 square feet per day with a geometric mean value of 193 square feet per day. The hydraulic conductivity values range from 0.02 to 884.97 feet per day with a geometric mean value of 1.70 feet per day. Both transmissivity and conductivity show a logarithmic normal distribution (Figures 4.5.1 and 4.5.2). Spatially, lower transmissivity and conductivity values are located throughout the study area; however, the highest values are only found in the southern counties (Figures 4.5.3 and 4.5.4).

Marble Falls Aquifer – There are only two transmissivity values, 63 and 2,366 square feet per day, both in Burnet County (Figure 4.5.5). The associated hydraulic conductivity values were calculated as 6.29 and 197.20 feet per day (Figure 4.5.6). The data are hardly enough to draw any conclusion regarding the Marble Falls Aquifer. However, in comparison with the other limestone aquifers in the study area, the geometric mean hydraulic conductivity for the Marble Falls Aquifer, 35.22 feet per day, is likely over-estimated.

Ellenburger-San Saba Aquifer - The transmissivity values of the Ellenburger-San Saba Aquifer range from 7 to 31,968 square feet per day with a geometric mean value of 495 square feet per day. The hydraulic conductivity values range from 0.01 to 224.64 feet per day with a geometric mean value of 2.81 feet per day. Most of the transmissivity values are more than 100 square feet per day. The hydraulic conductivity values are evenly spread. The histograms of common logarithmic transmissivity and conductivity values, however, do not show a normal distribution (Figures 4.5.7 and 4.5.8). The lowest transmissivity and conductivity values are located in Blanco County (Figures 4.5.9 and 4.5.10).

Hickory Aquifer - The transmissivity values of the Hickory Aquifer range from 15 to 10,368 square feet per day with a geometric mean value of 957 square feet per day and the hydraulic conductivity values range from 0.03 to 155.52 feet per day with a geometric mean value of 3.09 feet per day. Most of the transmissivity values fall between 1,000 and 10,000 square feet per day. Most of the hydraulic conductivity values are less than 5 feet per day. Both common logarithmic transmissivity and conductivity values show normal distribution (Figures 4.5.11 and 4.5.12). Spatially, Gillespie County has the highest transmissivity and conductivity values, while San Saba County has the lowest ones (Figures 4.5.13 and 4.5.14).

In summary, the horizontal hydraulic conductivity values for the Cretaceous, Ellenburger-San Saba, and Hickory aquifers span several orders of magnitudes with a geometric mean about 2 to 3 feet per day (Table A.2 of Appendix A). The highly variable hydraulic conductivity values suggest strong heterogeneity within the aquifers. The two values for the Marble Falls Aquifer were hardly enough to represent the whole aquifer and, very likely, over-estimated the aquifer overall hydraulic conductivity. No vertical hydraulic conductivity data are available for any of

the aquifers. However, it is well known that the vertical conductivity is often lower than its counterpart horizontal hydraulic conductivity due to horizontal beddings. A tight unit such as shale could significantly reduce the vertical hydraulic conductivity by an order of magnitude or more. However, unique cases do exist, such as vertical fractures which can enhance the vertical hydraulic connection. In this case, the vertical hydraulic conductivity could be much higher than the horizontal one.

In addition, the aquifer hydraulic test data are unevenly distributed in the study area. For the Hickory, Ellenburger-San Saba, and Marble Falls aquifers, most of the hydraulic test data in McCulloch, Gillespie, and Blanco counties are located at towns of Brady, Fredericksburg, and Blanco with most municipal groundwater users. For the Cretaceous aquifers, most of the hydraulic test data are within Kerr, Kendall, and Gillespie counties where the Cretaceous water-bearing units (such as the Glen Rose Formation, Hensell Member, and Hosston Member) are thicker and more productive, and have better water quality. The histograms of the Hickory and Cretaceous aquifers (normal distribution) may indicate a single predominant control over aquifer permeability such as the effect of aquifer matrix in the Hickory Aquifer and the fracturing in the Cretaceous aquifers.

4.5.2 *Storativity, Specific Storage, and Specific Yield*

Aquifer storage properties are directly related to aquifer porosity in the unconfined portions of an aquifer and aquifer porosity and matrix compressibility in the confined portions of the aquifer. Using the data from previous studies and laboratory results, Bluntzer (1992) gave ranges of aquifer porosity and storativity values for the Cretaceous and Paleozoic aquifers in the Hill County. For the Trinity Aquifer, the porosity and storativity ranged from 0.01 to 0.38 and from 0.0000008 to 0.00005, respectively. The Ellenburger-San Saba Aquifer had a porosity ranging from 0.01 to 0.17 and the Ellenburger had a storativity of 0.0022. The porosity and storativity of the Hickory Aquifer ranged from 0.03 to 0.42 and from 0.00004 to 0.0001, respectively. Please note that the aquifer porosity is usually higher than its specific yield.

In the groundwater availability model for the Edwards-Trinity (Plateau) and Pecos Valley aquifers, Anaya and Jones (2009) used specific yield values of 0.0005 to 0.005 for the Edwards Aquifer and 0.003 to 0.03 for the Trinity Aquifer in the Llano Uplift region. The specific storage in that model was from 5×10^{-7} to 5×10^{-4} foot⁻¹ for the Edwards Aquifer and 10^{-6} to 10^{-5} foot⁻¹ for the Trinity Aquifer in the Llano Uplift region. In the Hill Country portion of the Trinity Aquifer groundwater availability model, Jones and others (2009) calibrated the numerical model using specific storage values of 10^{-7} to 10^{-5} foot⁻¹ and specific yield ranging from 0.0005 to 0.008.

Table A.3 (Appendix A) lists the storativity values for the Cretaceous, Ellenburger-San Saba, and Hickory aquifers from hydraulic tests. For the Cretaceous aquifers, the aquifer storativity values range from 0.0000008 to 0.055 with a geometric mean of about 0.00018. The Ellenburger-San Saba Aquifer has storativity values ranging from 0.00008 to 0.0017 with a geometric mean of about 0.00023. For the Hickory Aquifer, only three field test values are available ranging from 0.000037 to 0.0001 with a geometric mean of 0.000069. Although all of the values are called storativity, the high-end values are more likely specific yield values.

No storativity and specific yield data are available for the Marble Falls Aquifer and confining units. Based on its texture, the Marble Falls Aquifer may have similar storativity values as the Cretaceous aquifers. For the confining units, it is common to assume that its storativity and specific yield may be about one order magnitude lower than the aquifers.

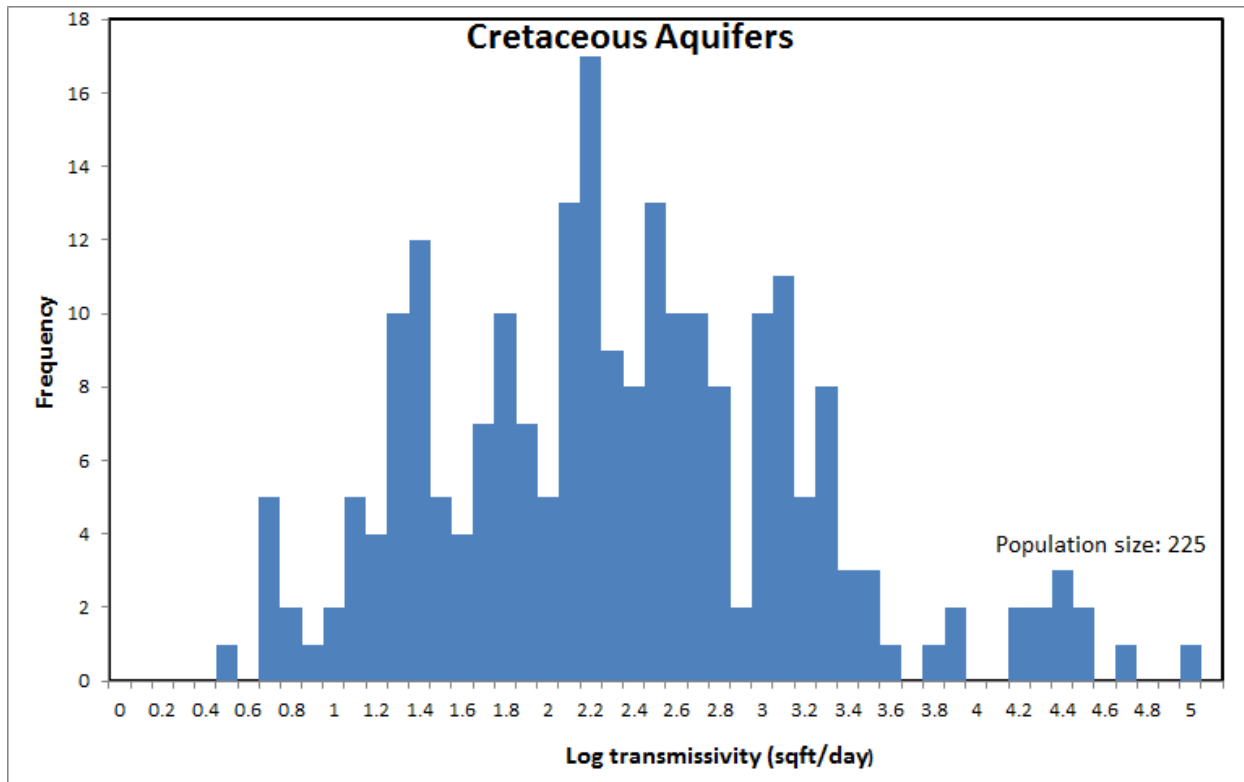


Figure 4.5.1 Histogram of logarithmic transmissivity of Cretaceous aquifers.

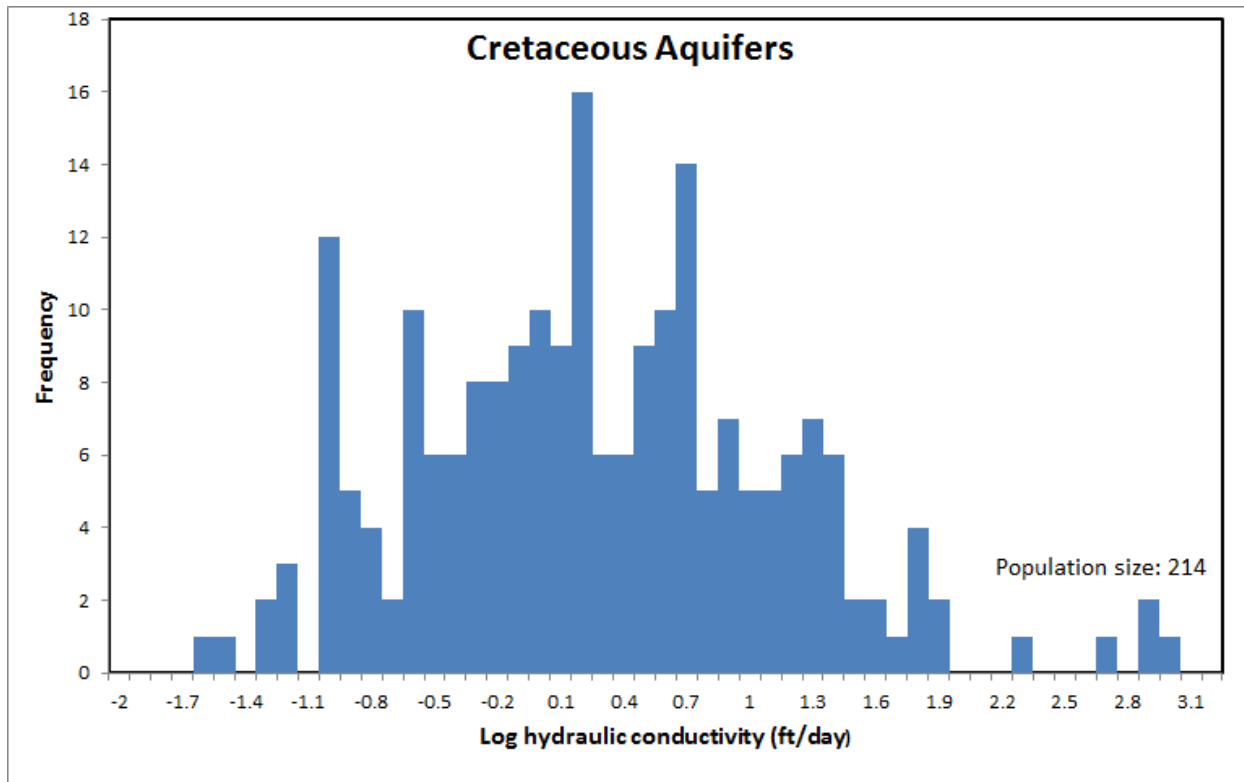


Figure 4.5.2 Histogram of logarithmic hydraulic conductivity of Cretaceous aquifers.

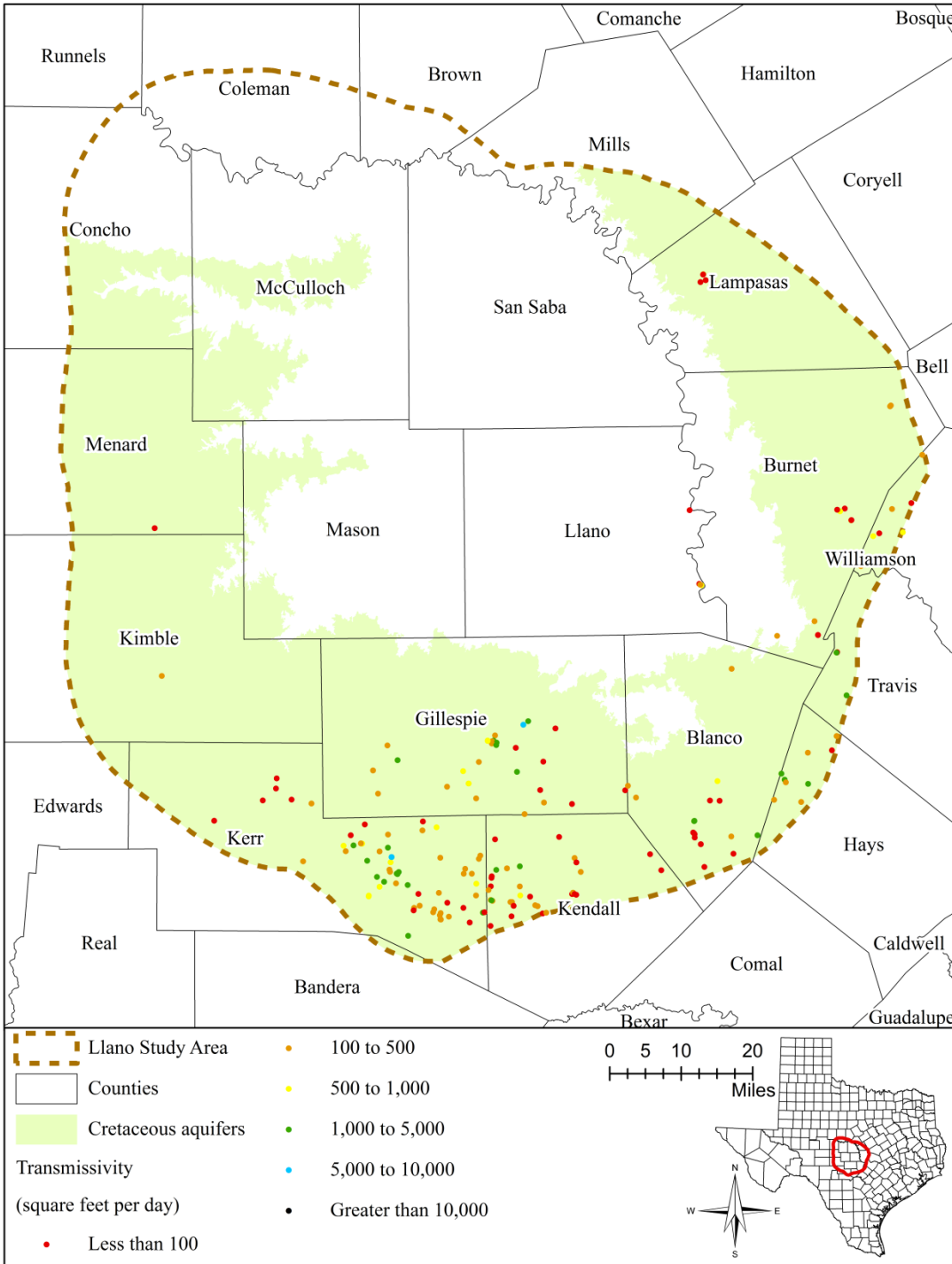


Figure 4.5.3 Distribution of transmissivity of Cretaceous aquifers (Edwards and Trinity).

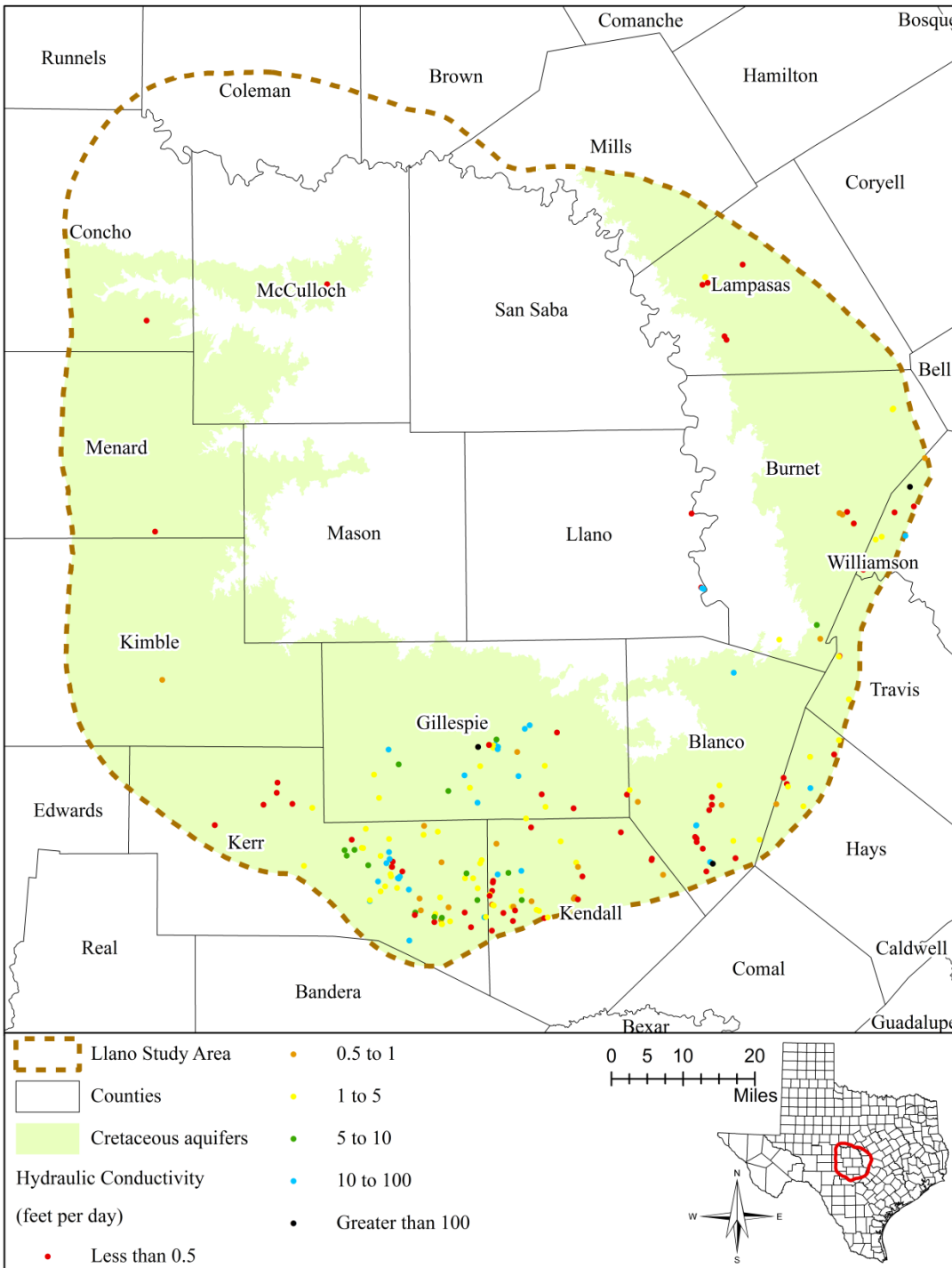


Figure 4.5.4 Distribution of hydraulic conductivity of Cretaceous aquifers (Edwards and Trinity).

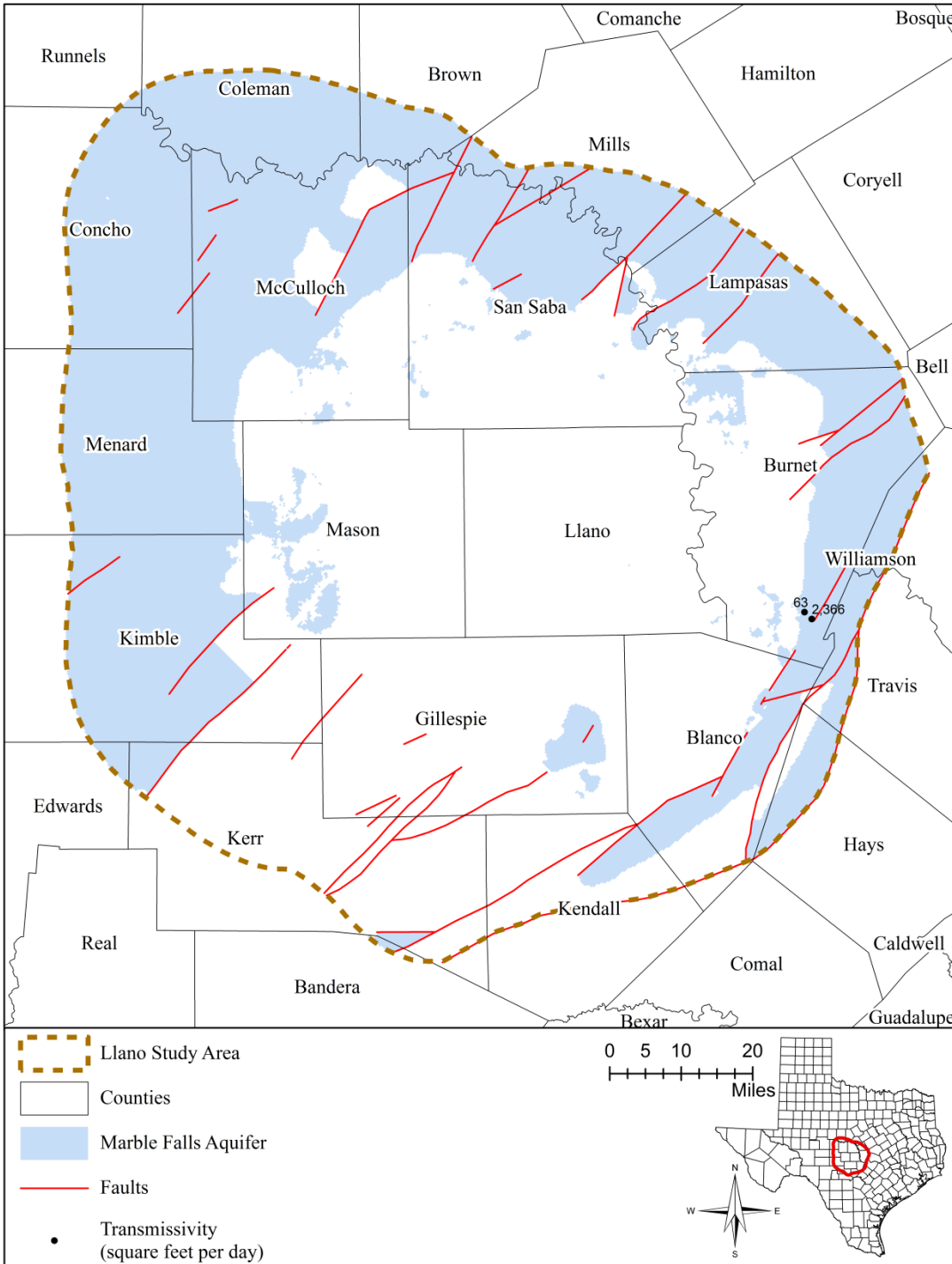


Figure 4.5.5 Distribution of transmissivity of Marble Falls Aquifer.

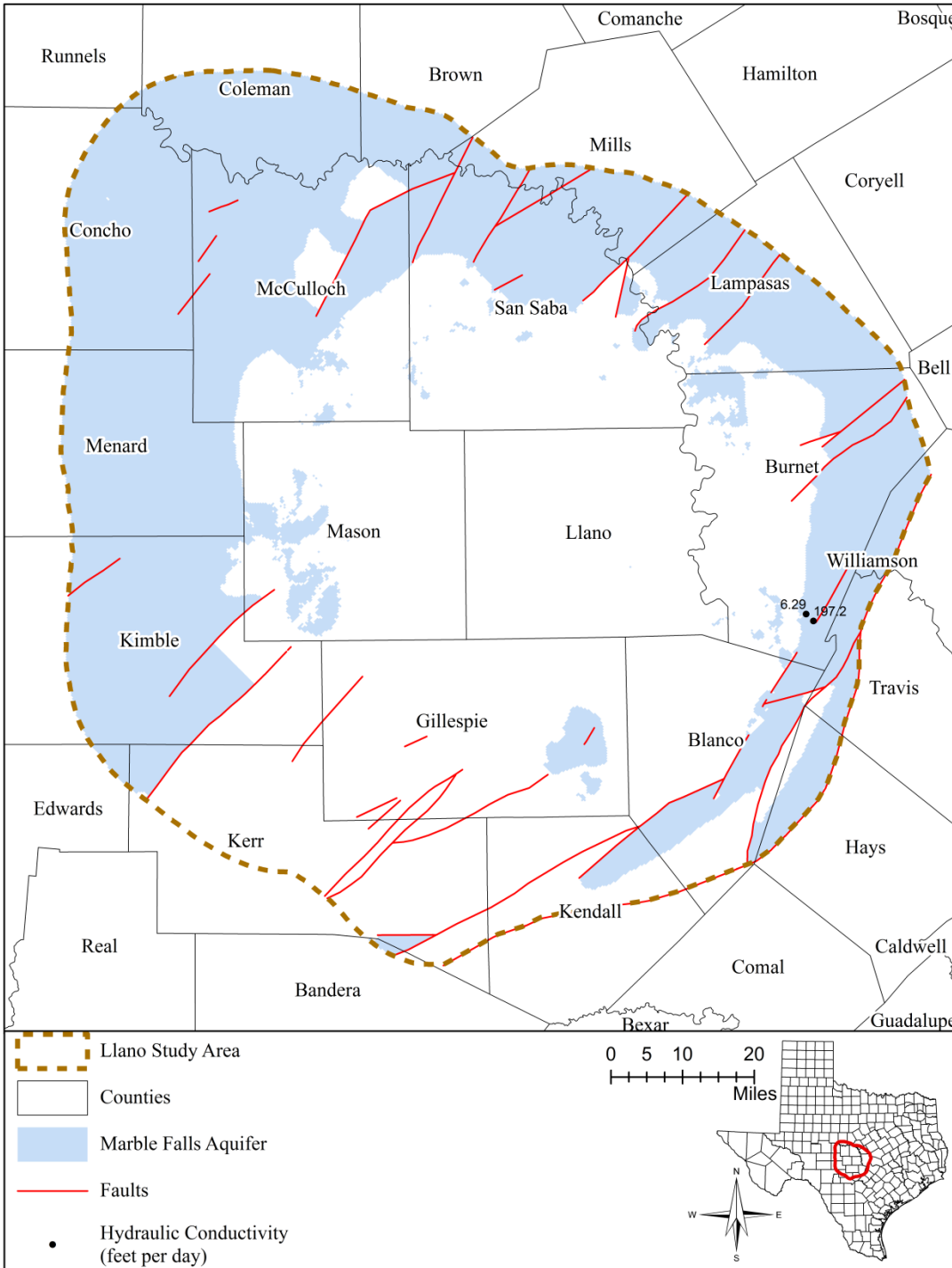


Figure 4.5.6 Distribution of hydraulic conductivity of Marble Falls Aquifer.

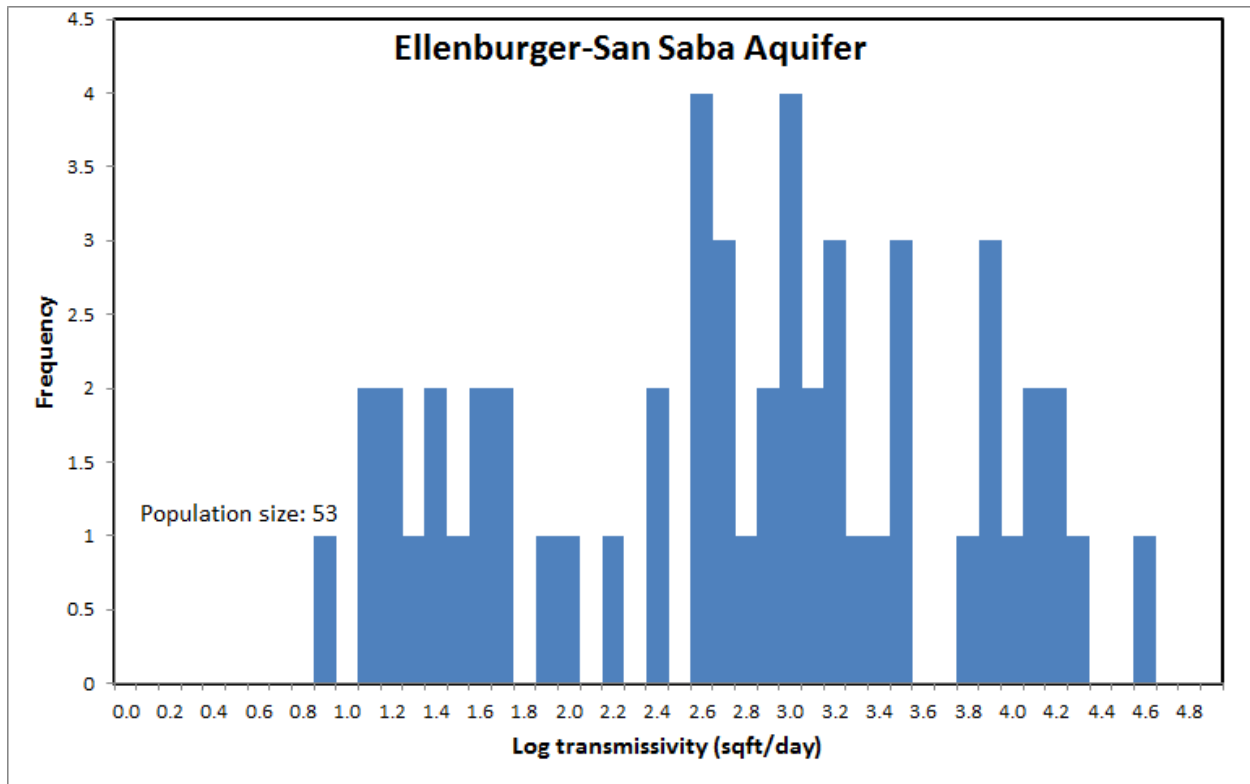


Figure 4.5.7 Histogram of logarithmic transmissivity of Ellenburger-San Saba Aquifer.

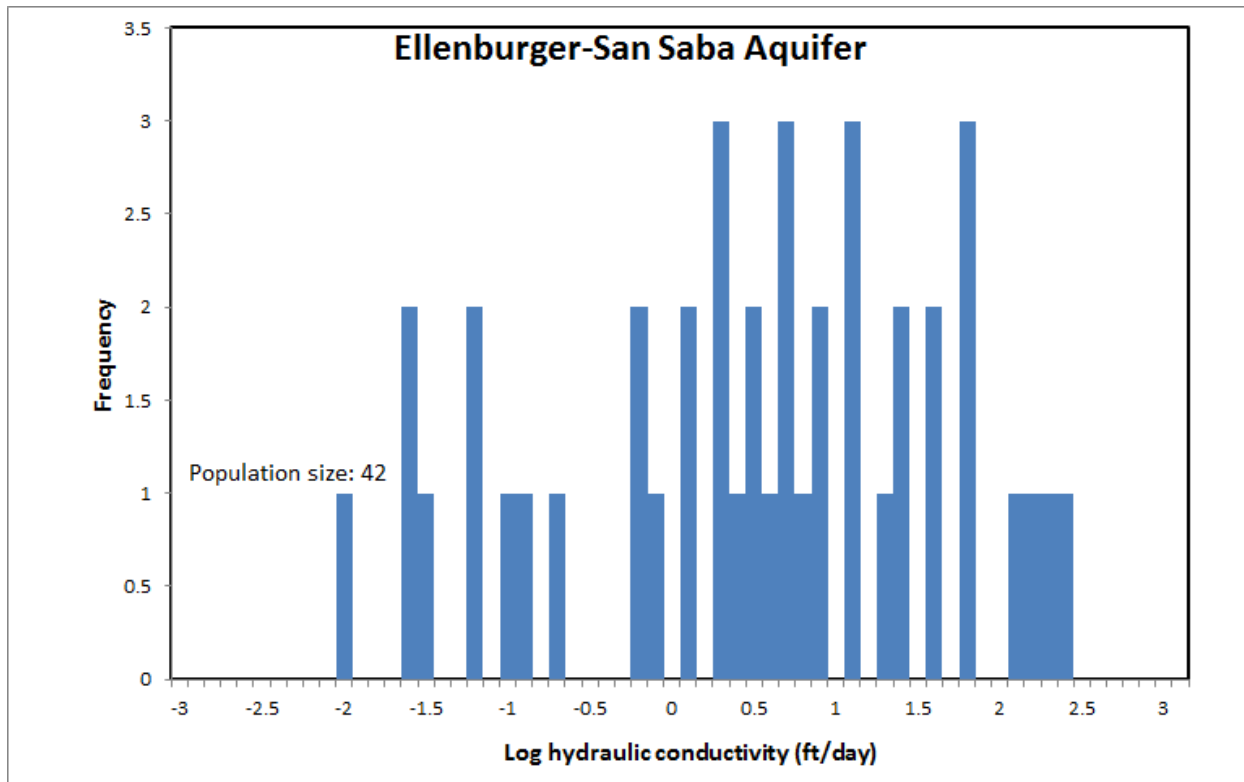


Figure 4.5.8 Histogram of logarithmic hydraulic conductivity of Ellenburger-San Saba Aquifer.

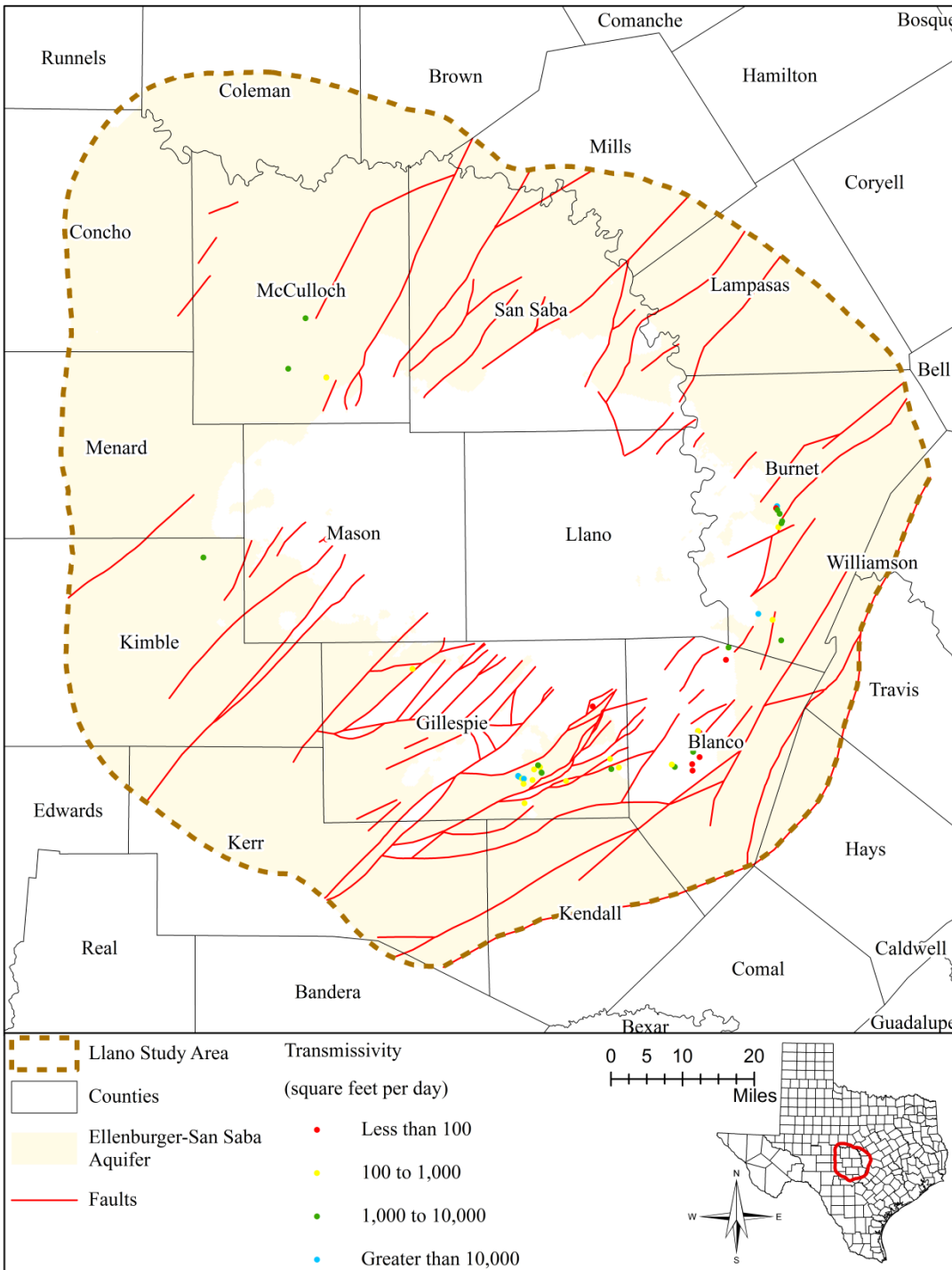


Figure 4.5.9 Distribution of transmissivity of Ellenburger-San Saba Aquifer.

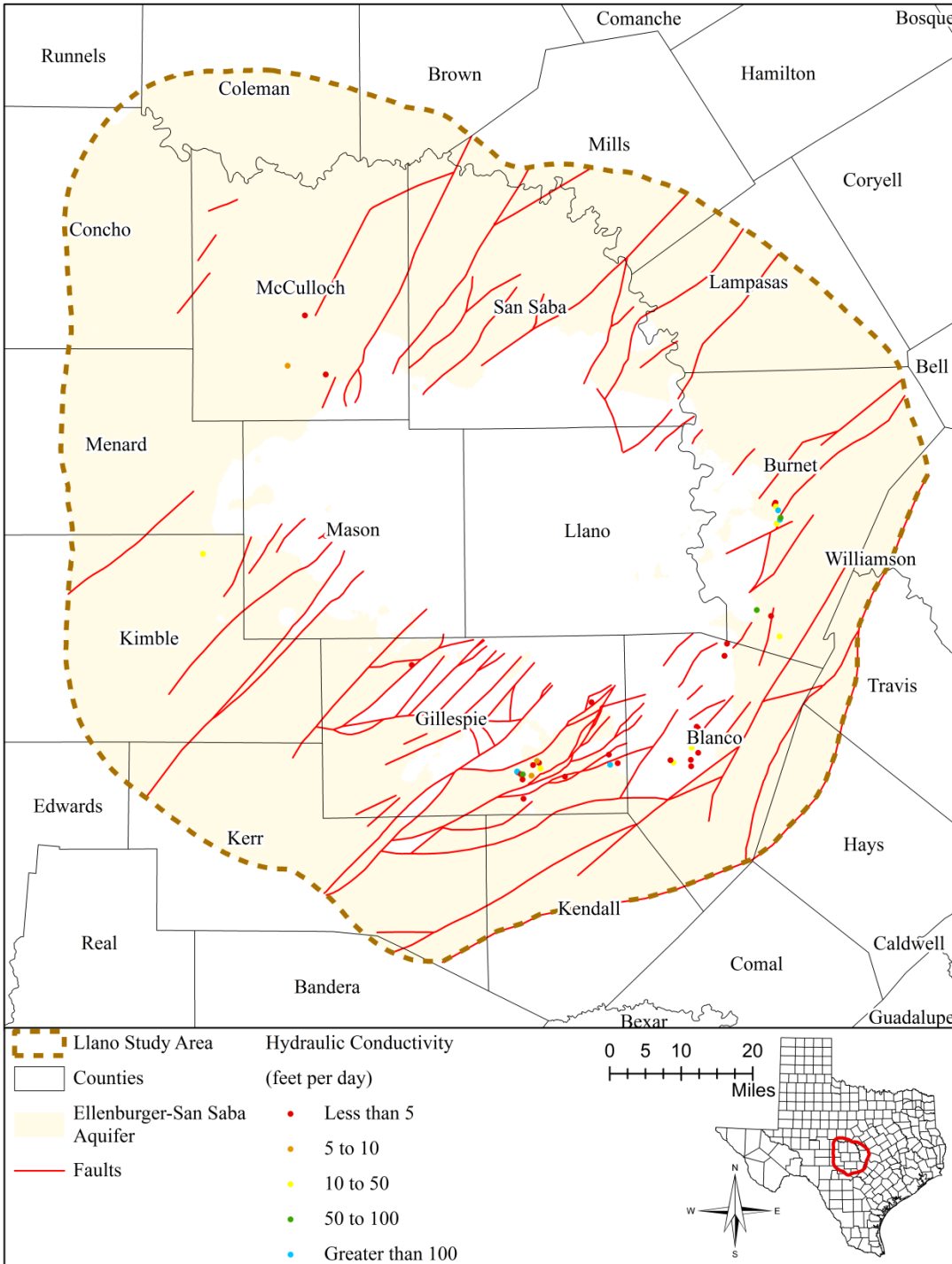


Figure 4.5.10 Distribution of hydraulic conductivity of Ellenburger-San Saba Aquifer.

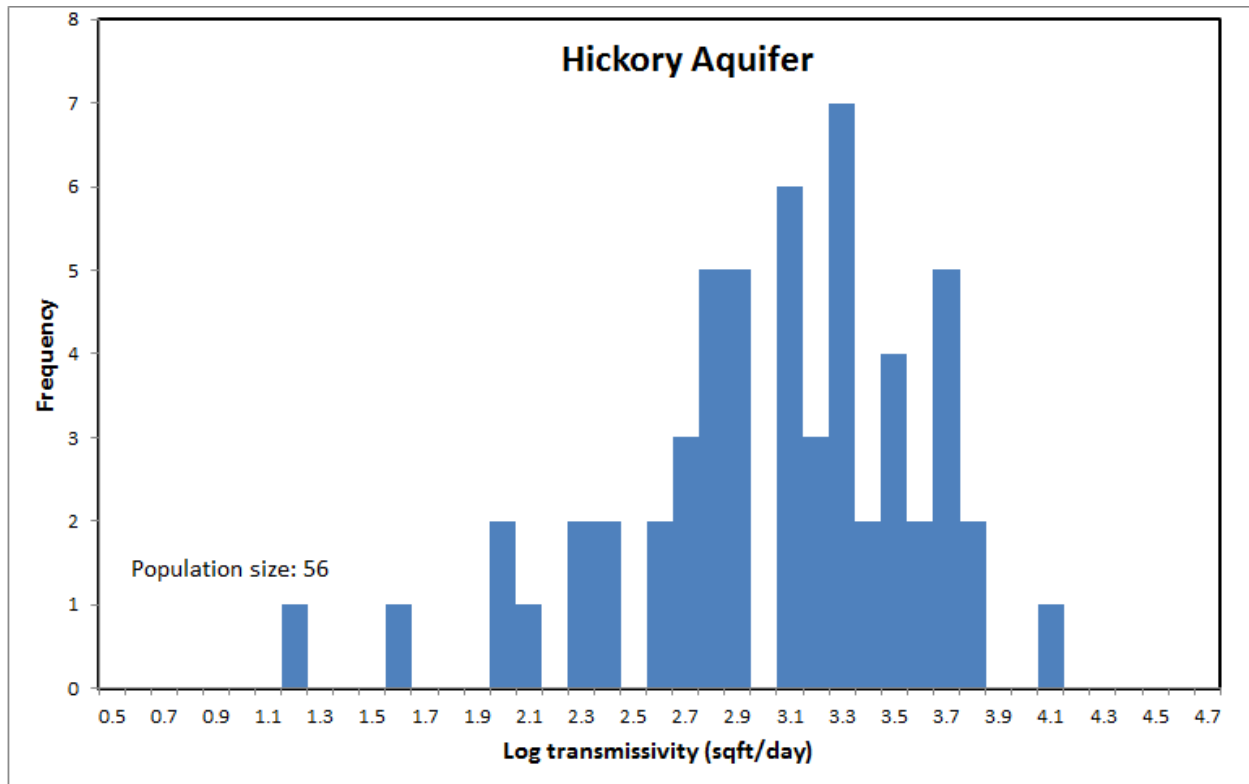


Figure 4.5.11 Histogram of logarithmic transmissivity of Hickory Aquifer.

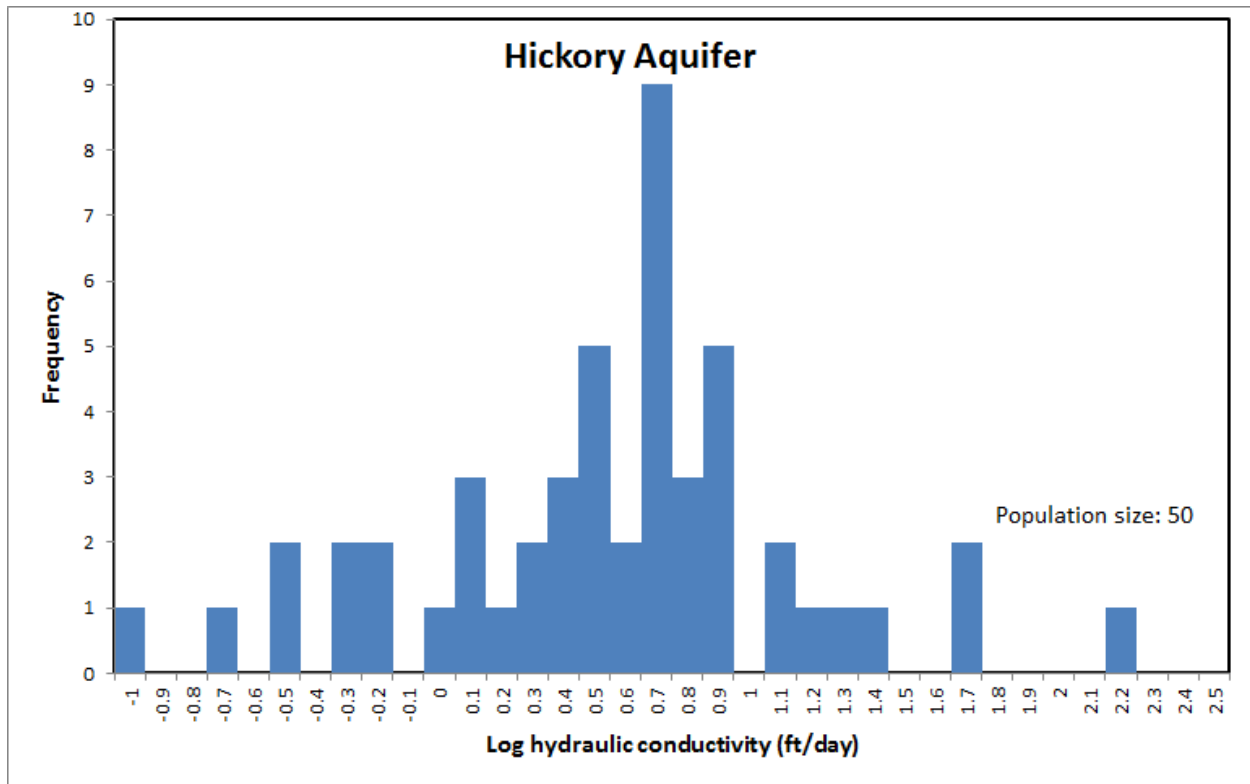


Figure 4.5.12 Histogram of logarithmic hydraulic conductivity of Hickory Aquifer.

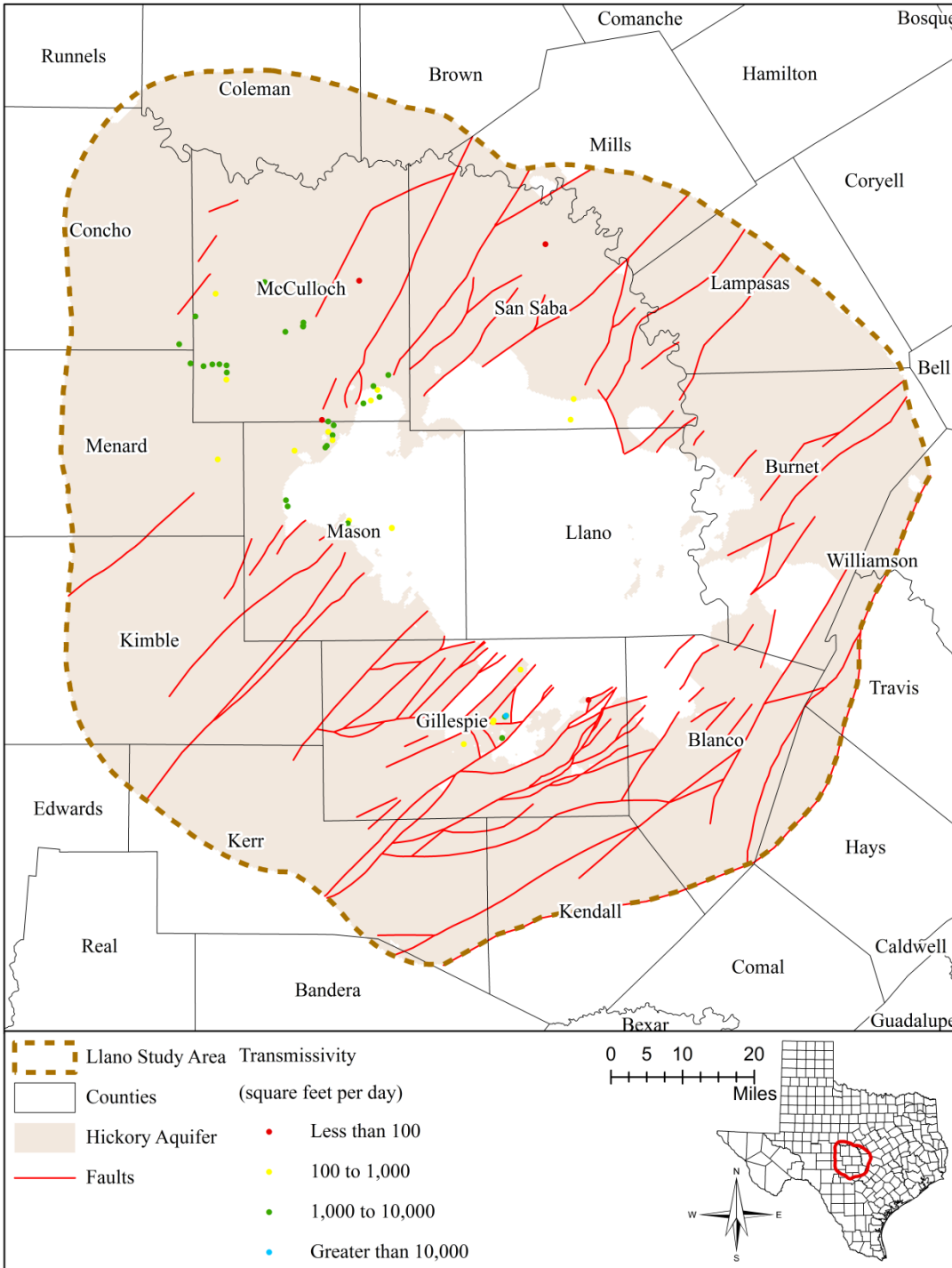


Figure 4.5.13 Distribution of transmissivity of Hickory Aquifer.

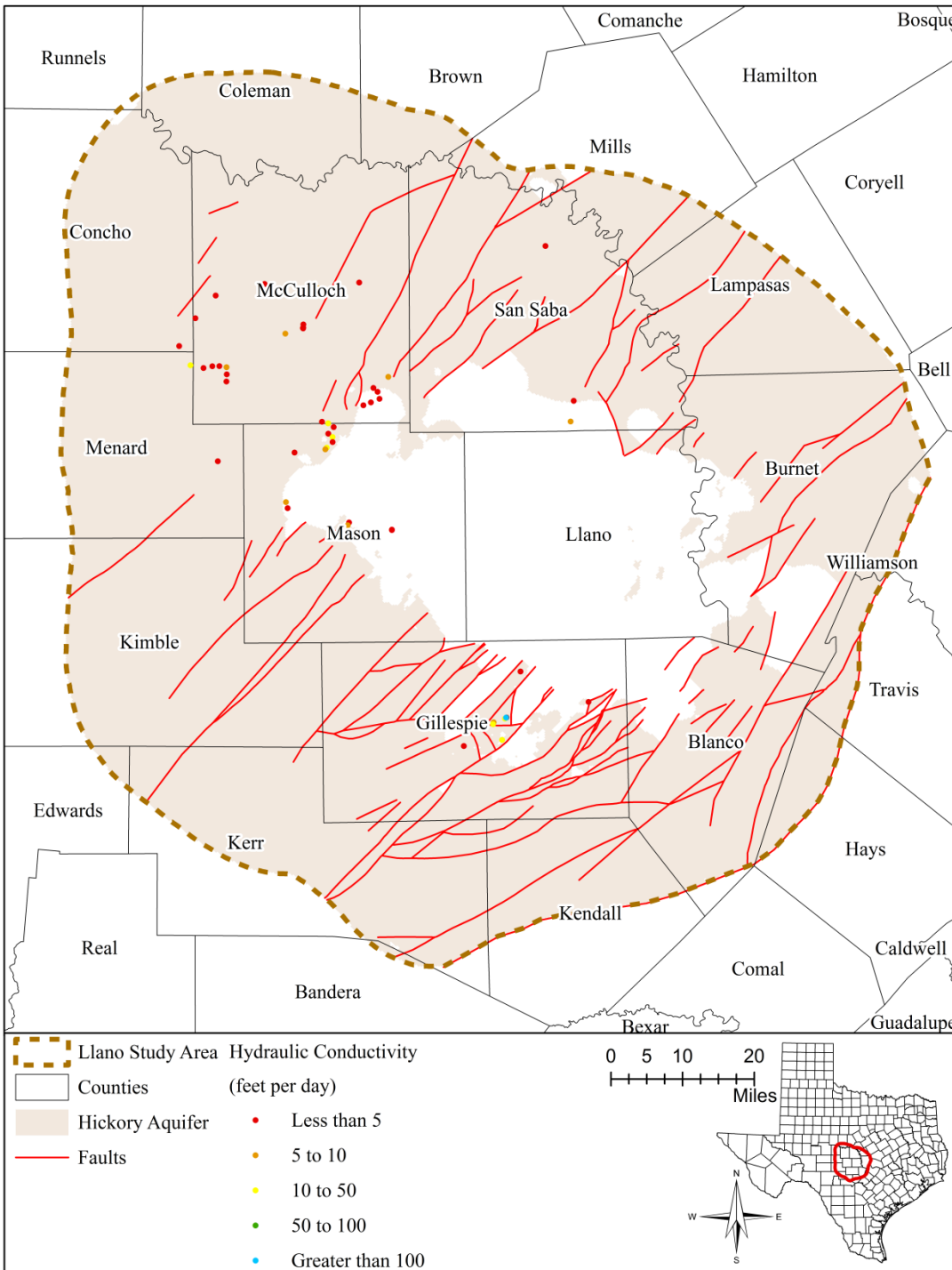


Figure 4.5.14 Distribution of hydraulic conductivity of Hickory Aquifer.

4.6 Aquifer Discharge

Discharge refers to the groundwater leaving a groundwater system by flow to surface water, to land surface, or to atmosphere. Groundwater discharge can occur naturally through flow to springs, streams, lakes, reservoirs, and evapotranspiration. Groundwater can also be removed from the groundwater system by pumping. For information on groundwater discharge through springs, streams, lakes, and reservoirs please refer to Section 4.4 entitled “Rivers, Streams, Lakes, and Springs”. The following sections will discuss natural discharge through evapotranspiration and groundwater pumping through anthropogenic means.

4.6.1. *Evapotranspiration*

Evapotranspiration is the total amount of groundwater removed by evaporation and transpiration of plants. Evapotranspiration is controlled by the depth of water table, soil texture, and vegetation such as the density, root depth, and type of plants. Greater density and root depth enhance evapotranspiration. Conifer forests tend to remove more groundwater than deciduous forests.

In the study area, live oak and mesquite trees dominate the central portion, while more ashe juniper trees are found toward the study area boundary (Figure 4.6.1; McMahan and others, 1984). Scanlon and others (2005) extracted the non-crop root depth data in Texas and crop root depth data in various locations from a global database developed by Schenk and Jackson (2003). The data indicate that the root depth increases from grassland and crops to trees (Table 4.6.1).

Using remote sensing calibrated against measured data, Kirk and others (2012) estimated the annual groundwater evapotranspiration from 1960 through 2009. Using their data, an average annual groundwater evapotranspiration rate between 1960 and 2009 was calculated (Figure 4.6.2). As shown in the figure, the average annual groundwater evapotranspiration is higher to the east of Lake Buchanan, in river valleys, and in areas with thicker vegetation. The whole study area shows a decreasing trend from east to west ranging from about 30 to 18 inches per year. The groundwater evapotranspiration also changes from year to year. During a very dry year like 2005, the evapotranspiration rates, in general, were low ranging from about 18 to 29 inches per year (Figure 4.6.3). However, the rates near the northwestern portion of the study area might have been overestimated. A very wet year like 2007 shows relative high evapotranspiration rates ranging from about 19 to 55 inches per year (Figure 4.6.4).

In a study presented to the TWDB by Scanlon and others (2005), Deeds and Kelley estimated long-term maximum evapotranspiration rates across Texas. In general, the maximum groundwater evapotranspiration rates are the total amount of water lost to evaporation and transpiration when the groundwater table reaches the ground surface. In the numerical flow model, the maximum evapotranspiration rates can be used to estimate the groundwater evapotranspiration when the water table fluctuates. As shown in Figure 4.6.5, the maximum groundwater evapotranspiration rates are lower in the middle (at lower 20s inches per year) and increase towards north and west of the study area. The highest values are expected at the largest surface water bodies (about 50 inches per year).

4.6.2. Aquifer Discharge through Pumping

Since 1984, Texas Water Development Board has conducted an annual historical water use survey. The TWDB staff associated with this annual survey collects raw data and develops estimates of use data in six categories: municipal, manufacturing, steam-electric generation, irrigation, mining, and livestock. Water use estimates for municipal, manufacturing, and steam-electric power categories come from an annual survey of public water suppliers, major manufacturing and power entities. Response to this survey is mandatory (Section 16.012(m) of the Texas Water Code, as amended by the 78th Texas Legislature in 2003). Water use for mining is based on the annual water-use survey and estimated from water use in secondary processes for oil and gas recovery. Water use for livestock is derived from annual livestock population estimates produced by the Texas Agricultural Statistics Service. Estimated water use per animal unit is based on research conducted by the Texas Agricultural Experiment Station. Irrigated agriculture water-use estimates are based on annual crop acreage from the Natural Resources Conservation Service (prior to 2001) and the Farm Service Administration (2001 and later). Irrigation rates per acre are estimated based on potential evapotranspiration, with final estimates reviewed by local authorities.

The annual groundwater use for all six categories between 1984 and 2011 from different aquifers is presented in [Figures 4.6.6 through 4.6.9](#). In general, counties to the northwest of the study area (Brown, Coleman, and Concho) had been using the least amount of groundwater from Cretaceous and Hickory aquifers probably because of limited supply of quality groundwater in those areas; Blanco and Burnet counties took about 2,000 acre-feet per year from the Cretaceous and Hickory aquifers; the groundwater withdrawal in Kimble, Lampasas, and Menard counties was from the Cretaceous aquifer at about 2,000 acre-feet per year or less; Llano County used about less than 2,000 acre-feet per year from the Ellenburger and Hickory aquifer; the groundwater withdrawal in Gillespie, Kerr, McCulloch, and San Saba counties had been relatively stable ranging from 3,000 to 7,000 acre-feet per year; Hays, Kendall, Mills, and Travis counties had seen a significant increase of groundwater use in recent years, while Mason and Williamson counties experienced a reduction of groundwater withdrawal. In comparison with other counties in/near the study area, Gillespie, Mason, McCulloch, and Travis counties used the most groundwater in recent years.

In addition to the aquifer-based total groundwater use as described above, the groundwater use in 2011 by category for each county associated with the study area is presented in [Table 4.6.2](#). The groundwater use in 2011 was mainly related to municipal and irrigation for all counties except McCulloch County where mining also used about 3,000 acre-feet of groundwater.

Pumping location and aquifer association for the municipal and manufacturing-mining groundwater uses will be mainly determined using the TWDB groundwater database and specific well locations. If no wells for a category are located in the TWDB groundwater database then other approaches will be explored; for example, land cover data from the National Land Cover Dataset (Fry and others, 2011) for locations of mining operations. Distribution of livestock pumping will be based on land cover data from the National Land Cover Dataset (Fry and others, 2011). Distribution of irrigation pumping will be based on the irrigation farmland distribution (U.S. Department of Agriculture, 2014) and the locations of irrigation wells.

Domestic groundwater use is not included in the TWDB water use survey. However, the domestic groundwater use can be estimated from population density. The population density in the study area is shown in [Figure 4.6.10](#). The domestic groundwater use will be estimated solely based on population in the rural areas where public water system is not available. Domestic well locations will be based on the TWDB groundwater database.

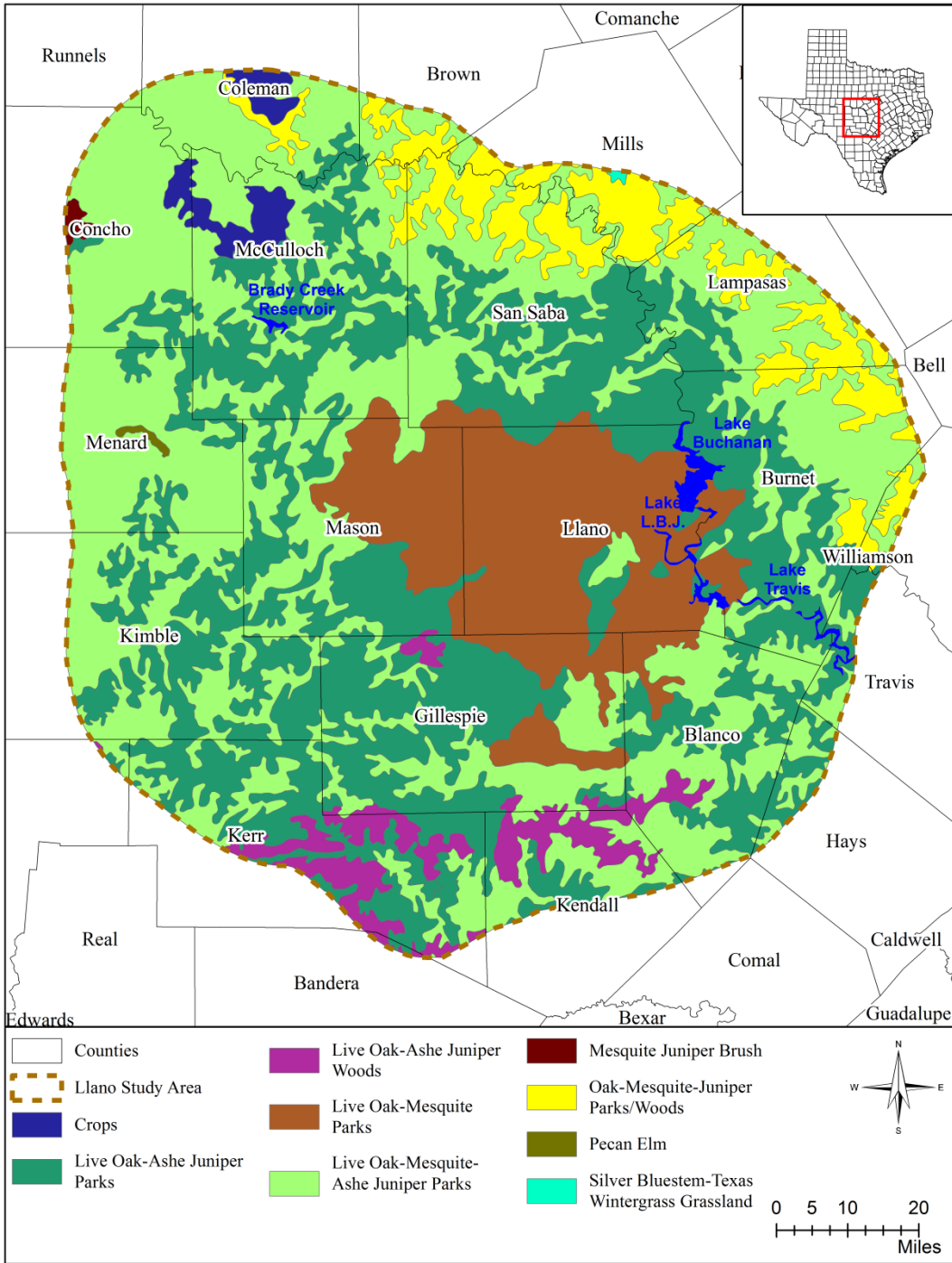


Figure 4.6.1 Vegetation type in study area (McMahan and others, 1984).

Table 4.6.1 Depth of plant roots (Schenk and Jackson, 2003).

Vegetation	Root Depth (feet)	Location	Soil Type
American Elm	23	Edwards Plateau, Texas, USA	shallow, calcareous overlaying fractured limestone
Ashe Juniper	26	Edwards Plateau, Texas, USA	shallow, calcareous overlaying fractured limestone
Cedar Elm	29	Edwards Plateau, Texas, USA	shallow, calcareous overlaying fractured limestone
Crops	6.9	various	various
Grassland	3.1	Texas, USA	various
Grassland	2.1	Texas, USA	various
Grassland	2	Texas, USA	various
Honey Mesquite	6.6	Texas, USA	Nuvalde clay loam
Live Oak	60	Edwards Plateau, Texas, USA	shallow, calcareous overlaying fractured limestone
open shrubland	19.7	Texas, USA	various
open shrubland	9.2	Texas, USA	various
open shrubland	8.6	Texas, USA	various
Sugarberry	19	Edwards Plateau, Texas, USA	shallow, calcareous overlaying fractured limestone
White Shin Oak	23	Edwards Plateau, Texas, USA	shallow, calcareous overlaying fractured limestone
Wooded grassland	7.6	Texas, USA	various
Wooded grassland	7.4	Texas, USA	various
Wooded grassland	7.4	Texas, USA	various
Wooded grassland	5.9	Texas, USA	various
Wooded grassland	5.8	Texas, USA	various
Wooded grassland	3.6	Texas, USA	various

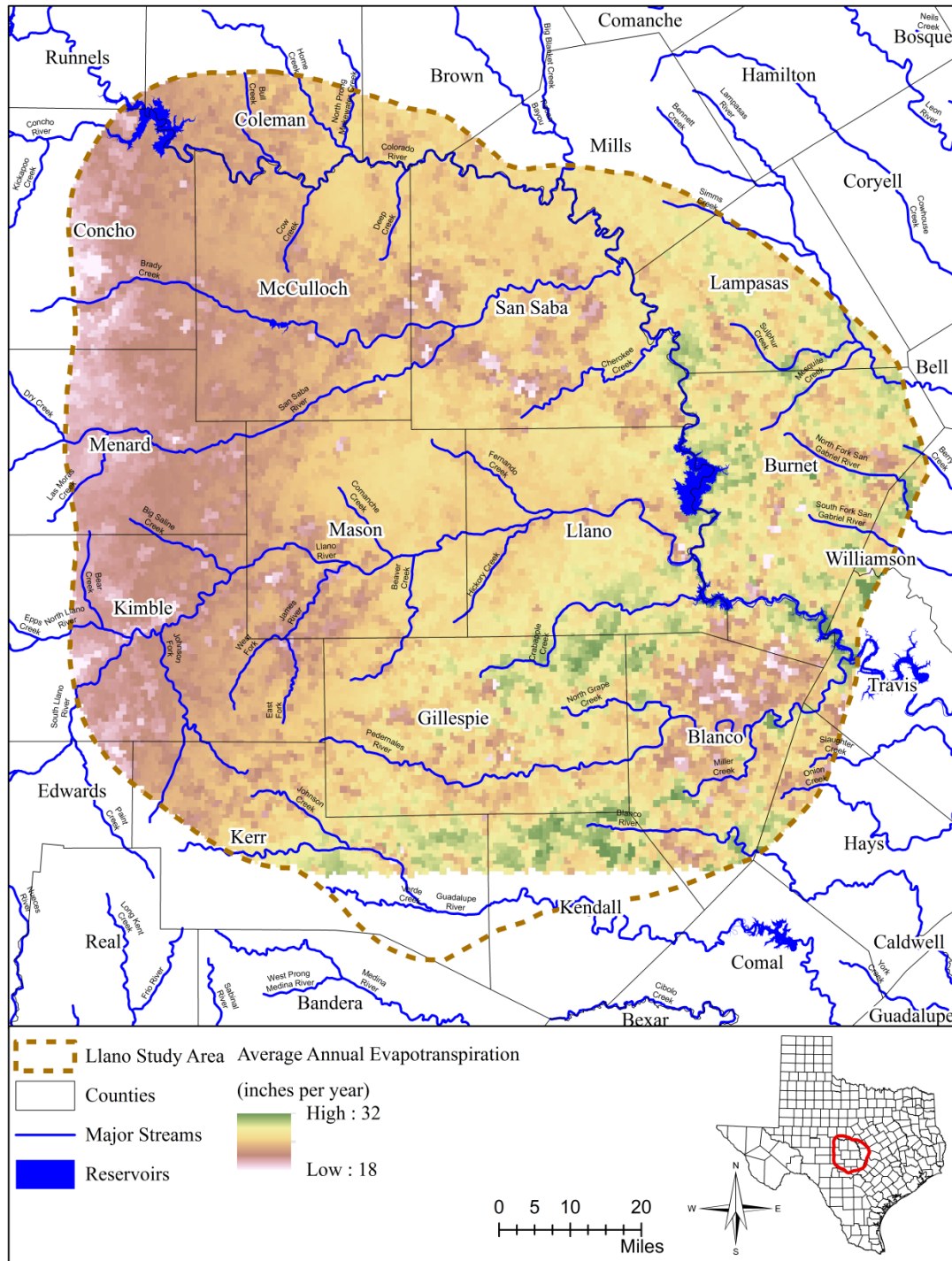


Figure 4.6.2 Estimated average annual groundwater evapotranspiration distribution between 1960 and 2009 in study area (annual evapotranspiration rates from Kirk and others (2012)).

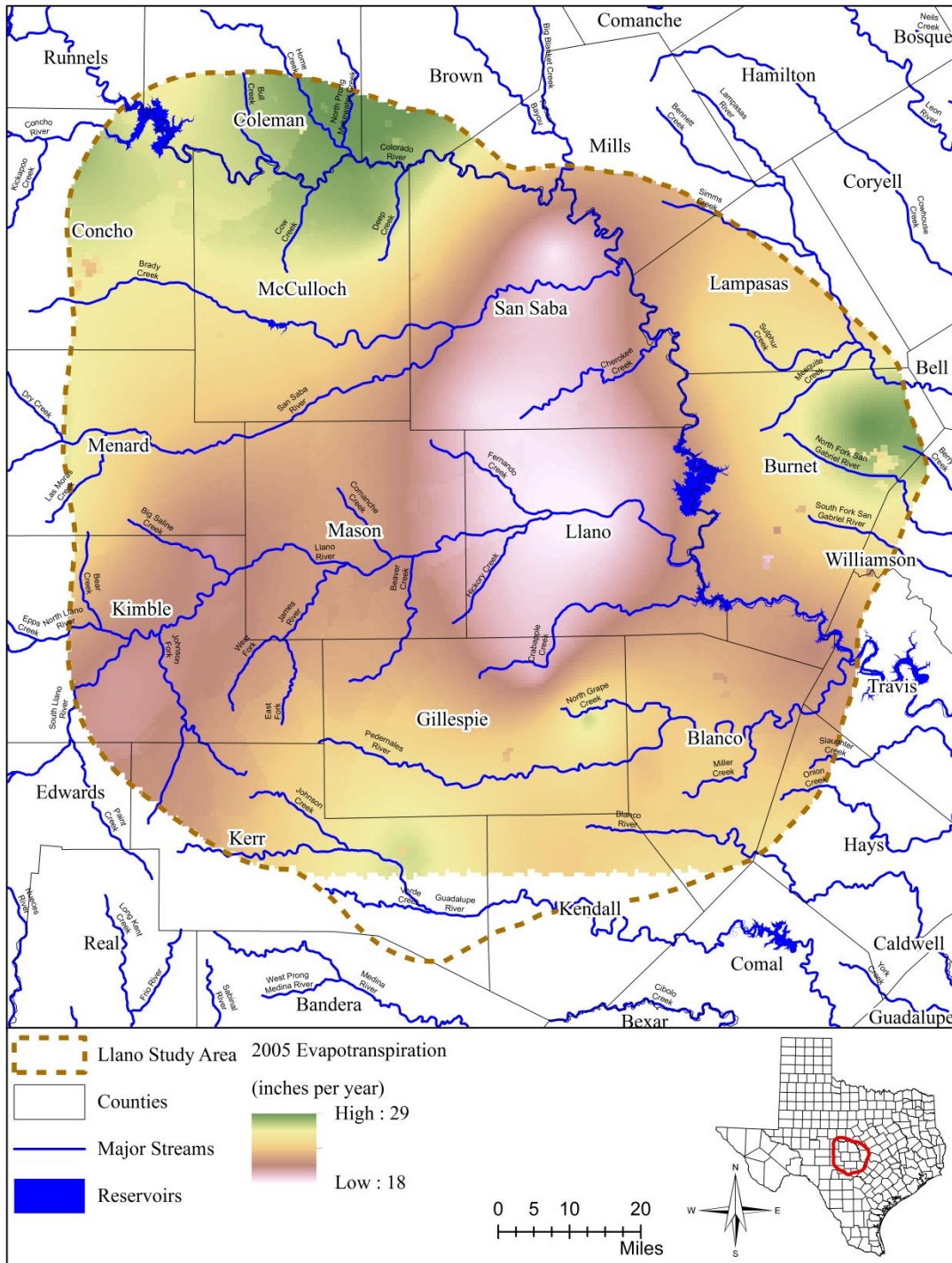


Figure 4.6.3 Estimated annual groundwater evapotranspiration distribution for 2005, a dry year with low precipitation (data from Kirk and others (2012)).

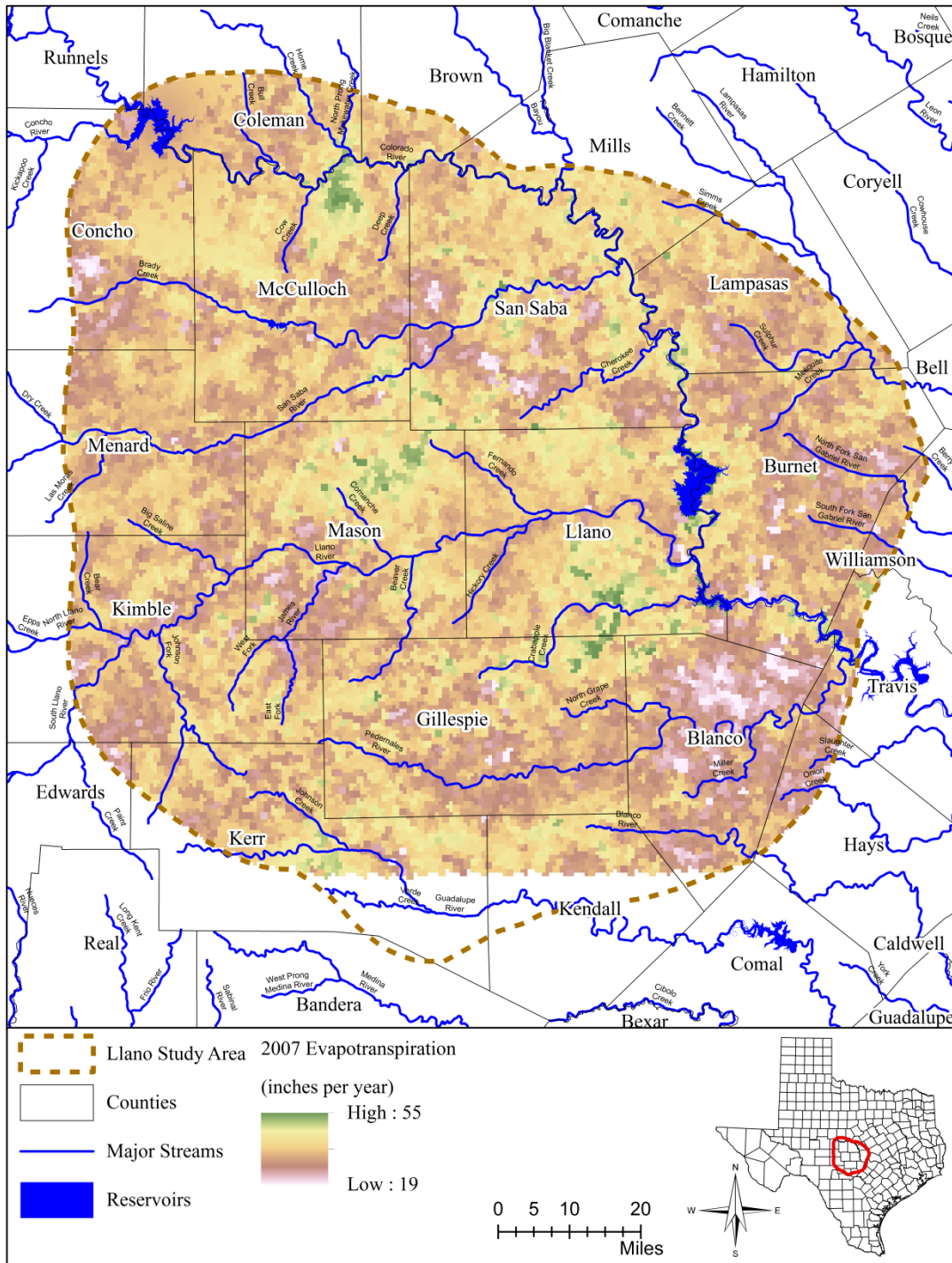


Figure 4.6.4 Estimated annual groundwater evapotranspiration distribution for 2007, a wet year with high precipitation (data from Kirk and others (2012)).

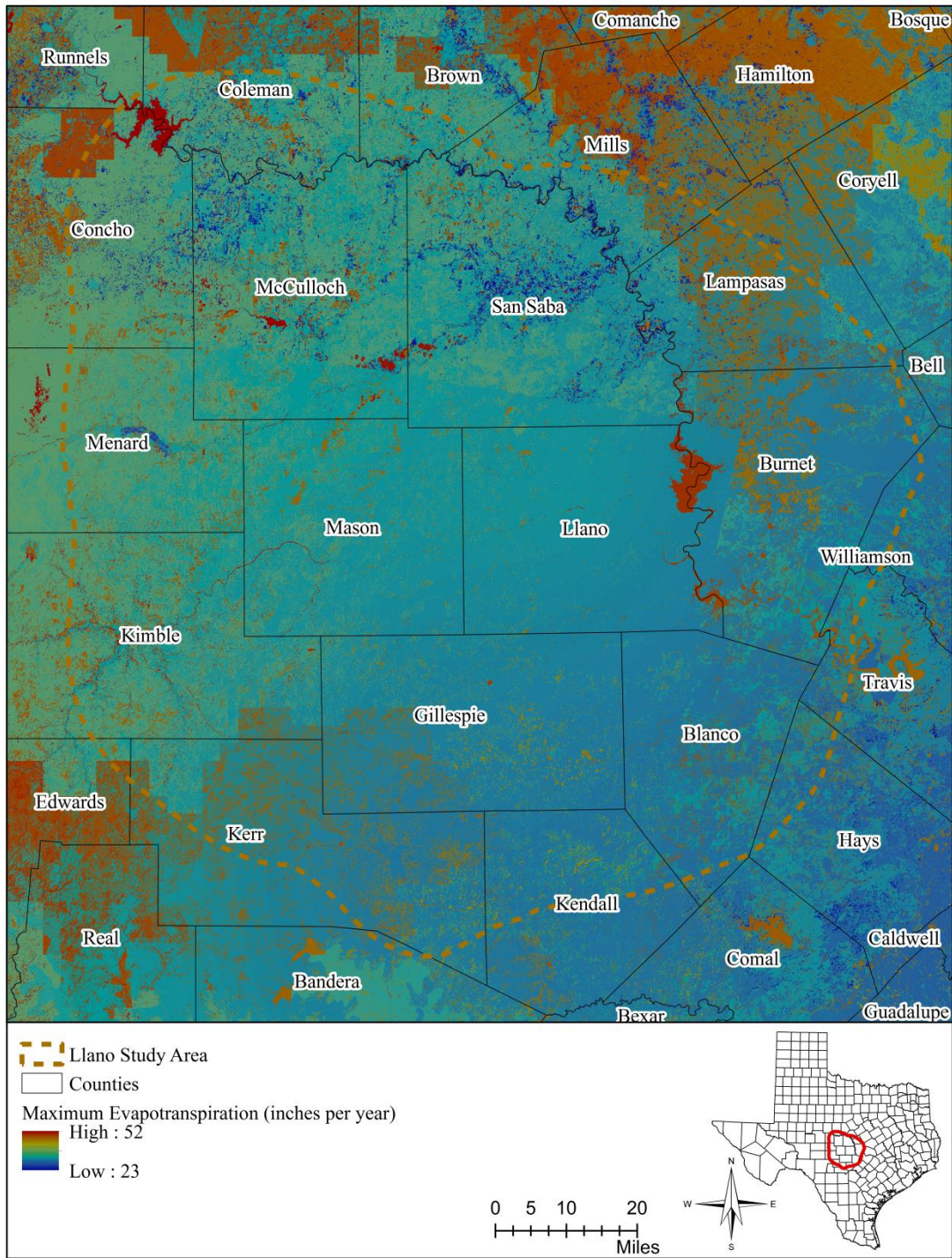


Figure 4.6.5 Maximum groundwater evapotranspiration distribution (data from Deeds and Kelley in Scanlon and others (2005)).

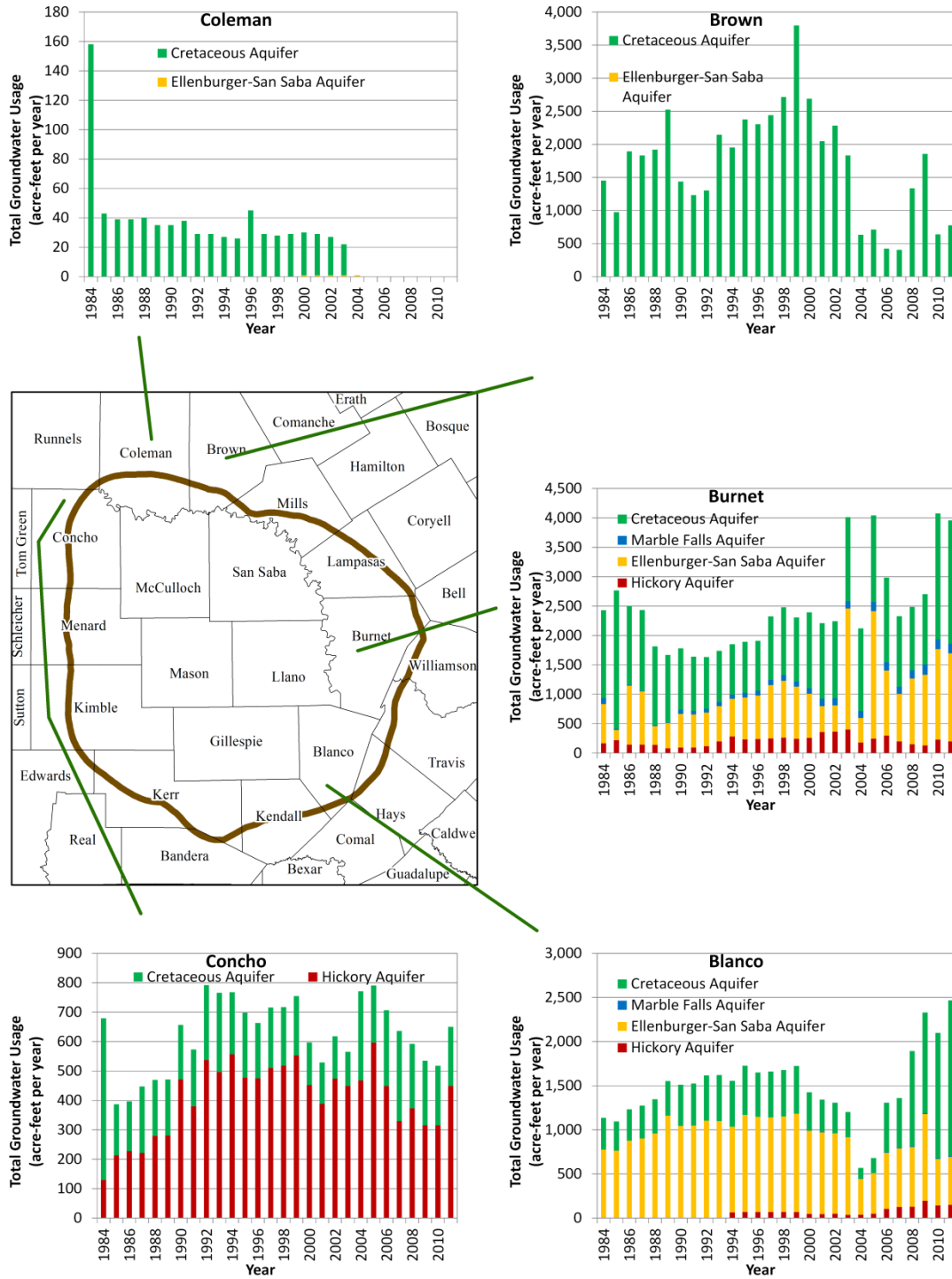


Figure 4.6.6 Annual groundwater pumping between 1984 and 2011 in Blanco, Brown, Burnet, Coleman, and Concho counties (pumping data from TWDB water use survey).

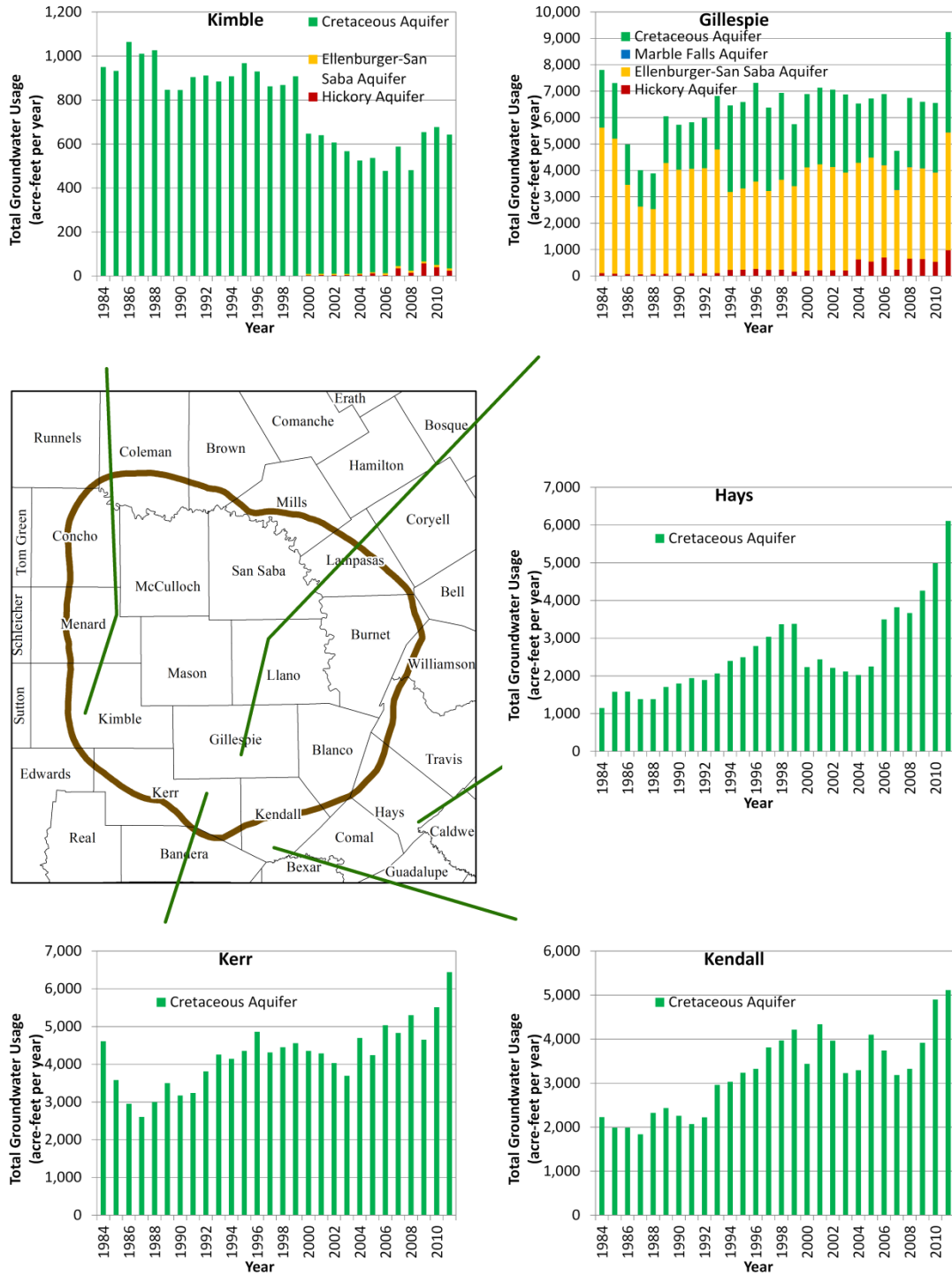


Figure 4.6.7 Annual groundwater pumping between 1984 and 2011 in Gillespie, Hays, Kendall, Kerr, and Kimble counties (pumping data from TWDB water use survey).

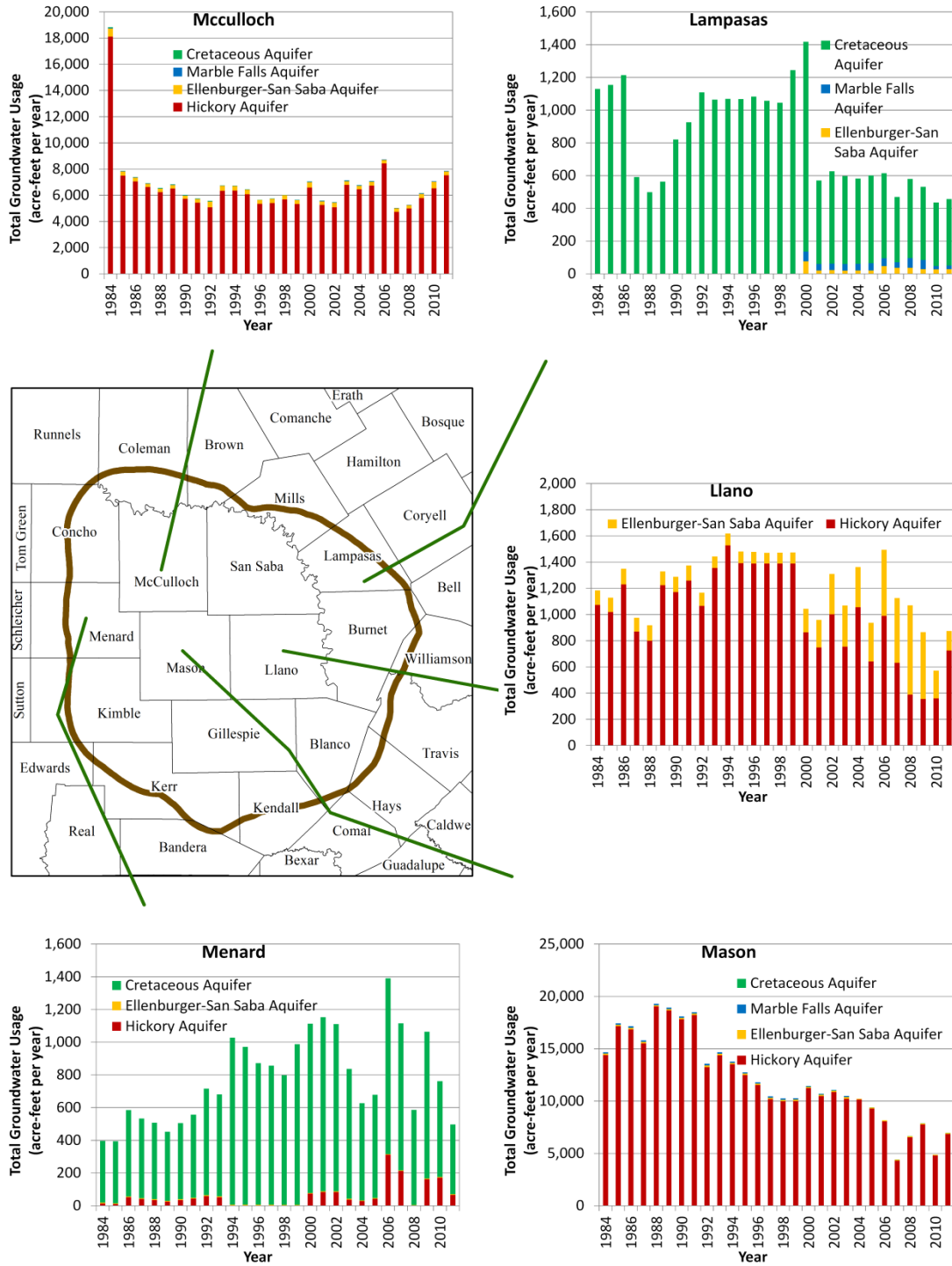


Figure 4.6.8 Annual groundwater pumping between 1984 and 2011 in Lampasas, Llano, Mason, McCulloch, and Menard counties (pumping data from TWDB water use survey).

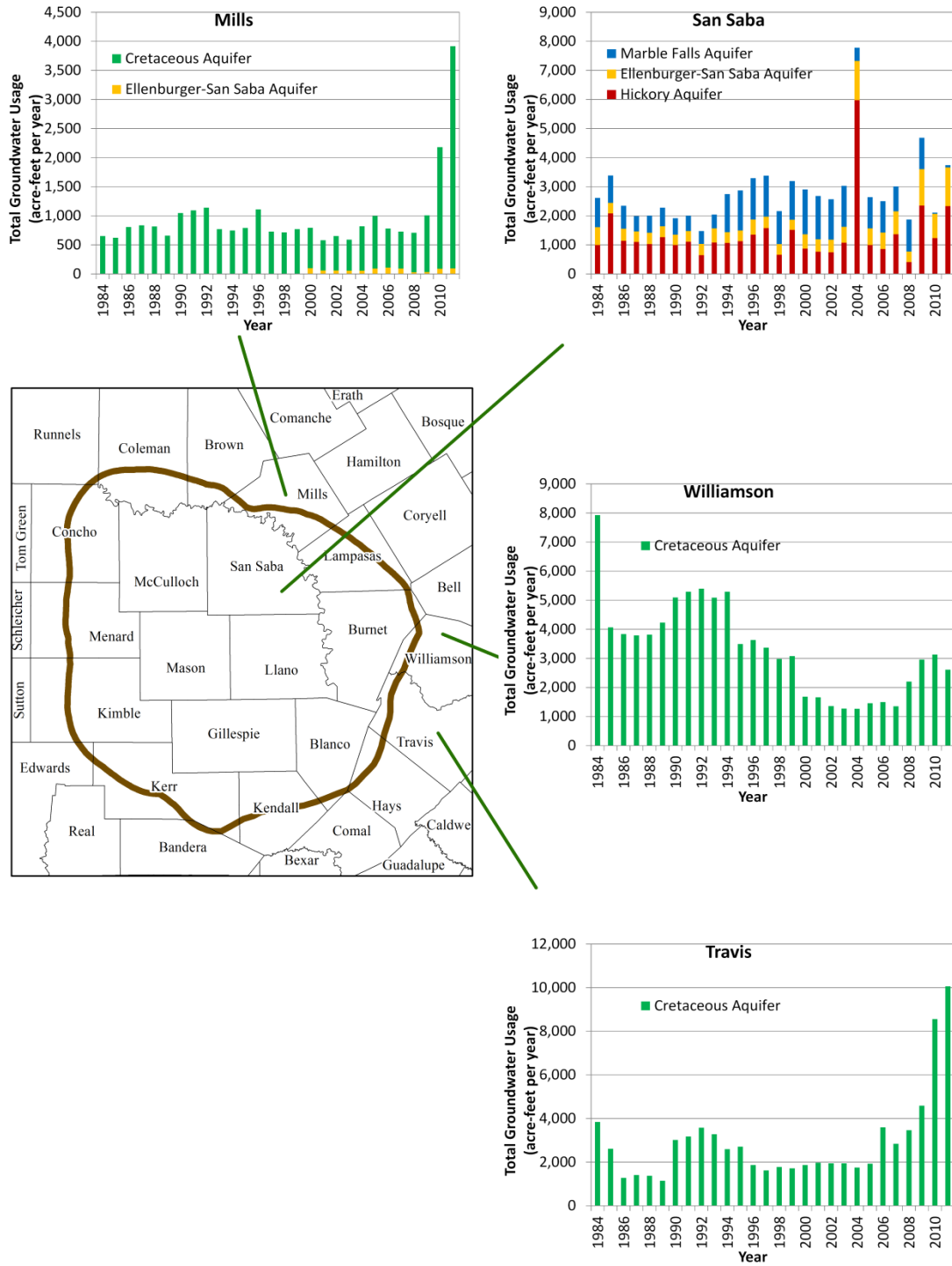


Figure 4.6.9 Annual groundwater pumping between 1984 and 2011 in Mills, San Saba, Travis, and Williamson counties (pumping data from TWDB water use survey).

Table 4.6.2 Groundwater use in 2011 by category.

County	Municipal	Manufacturing	Mining	Steam- Electric Power	Irrigation	Livestock	Total
Blanco	1,849	0	0	0	357	261	2,467
Brown	341	0	0	0	295	140	776
Burnet	2,640	9	4	0	633	671	3,957
Coleman	0	0	0	0	0	0	0
Concho	464	0	0	0	0	186	650
Gillespie	4,881	14	0	0	3,099	1,240	9,234
Hays	5,528	0	0	0	559	26	6,113
Kendall	3,881	0	0	0	824	410	5,115
Kerr	5,715	8	0	0	293	427	6,443
Kimble	240	2	0	0	88	313	643
Lampasas	108	0	0	0	71	278	457
Llano	271	3	0	0	400	200	874
Mason	912	0	0	0	5,496	561	6,969
McCulloch	2,188	0	2,788	0	2,442	444	7,862
Menard	83	0	0	0	166	248	497
Mills	324	0	0	0	3,160	431	3,915
San Saba	453	0	4	0	2,971	318	3,746
Travis	9,151	41	0	0	800	73	10,065
Williamson	2,256	3	0	0	97	257	2,613

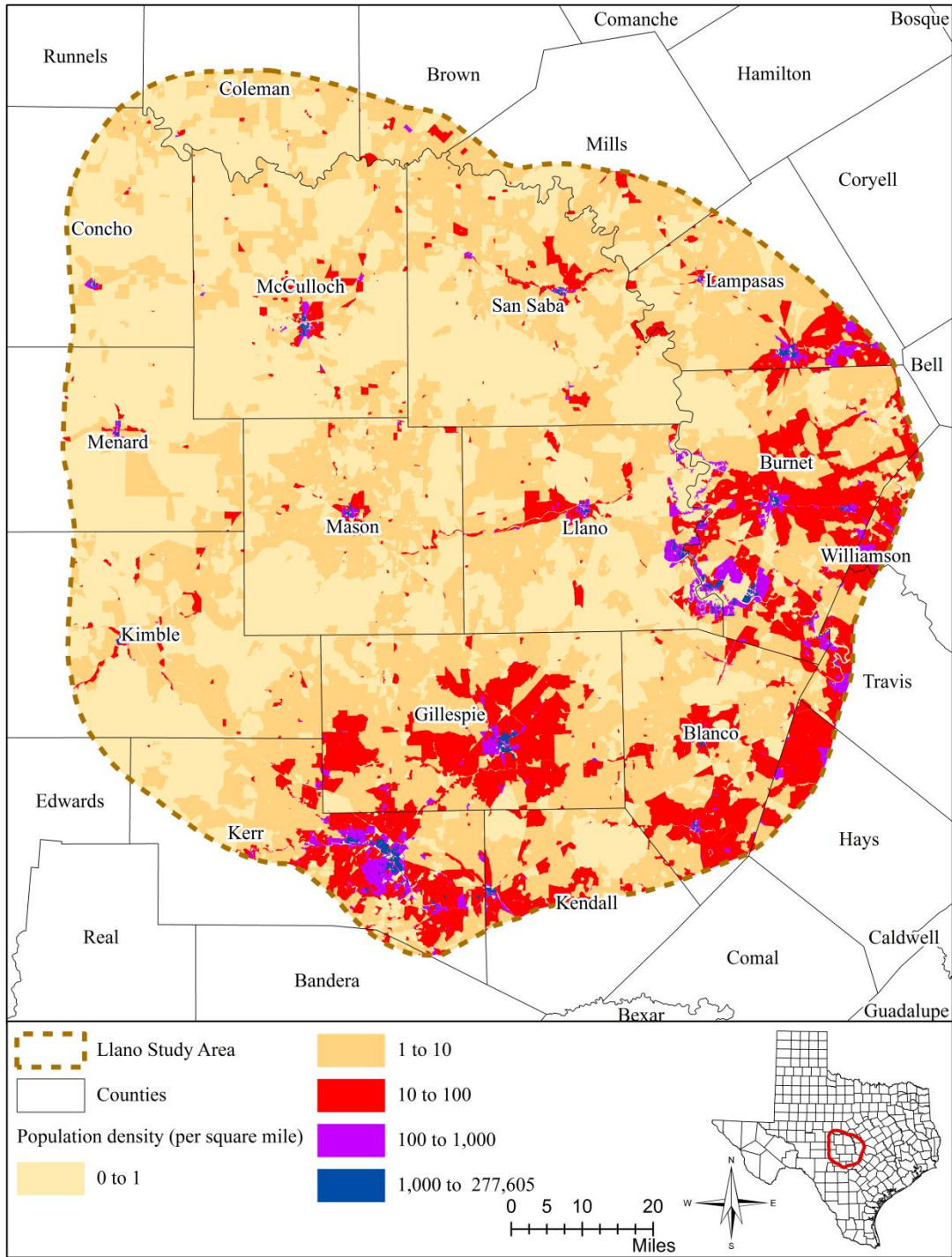


Figure 4.6.10 Population density in study area (data from the U. S. Census Bureau (2010)).

4.7 Groundwater Quality

An early regional study by the U.S. Geological Survey listed the chemical composition of groundwater at water utilities in the study area (Sundstrom and others, 1949). The U.S. Geological Survey also published countywide water quality reports (Mason, 1961; Walker, 1967; Baker and others, 1965; Follett, 1973). These studies compared the groundwater composition with the drinking water standards and evaluated the suitability of groundwater for irrigation, public water supply, and industrial uses. Later on, Bluntzer (1992) and Preston and others (1996) discovered high levels of nitrate, fluoride, and radioactivity in the groundwater from the Llano Uplift aquifers. Using the chemical and isotope data, Kreitler and others (2013) examined the groundwater origins and evolution of the groundwater flow in the Hickory and Ellenburger-San Saba aquifers. Their study suggests that faults may have separated the aquifers into hydraulically isolated sub aquifers. Kreitler and others (2013) further proposed that two flow regimes exist in the aquifers: one at the outcrop area with active recharge and the other at the downdip with a stagnant flow system.

For this conceptual model report, the groundwater quality data from the TWDB groundwater database (TWDB, 2014a) was used for the analysis. The analysis includes the evaluation of the groundwater recharge area, age, mixing, and pathways as well as comparison with the drinking water standards. In Texas, the drinking water standards (30 TAC Chapter 290, Subchapter F) govern the drinking water quality and reporting requirements for the public water systems. The drinking water standards in Texas, enforced by the Texas Commission on Environmental Quality, are based on the U.S. Environmental Protection Agency's Primary and Secondary Drinking Water Regulations. Water with any chemical constituents over the drinking water standards is considered unsafe for human consumption. The Texas Commission on Environmental Quality also prescribes secondary standards for drinking water quality. The secondary standards are non-enforceable recommendations related to the olfactory and aesthetic appearance of the water.

4.7.1 Marble Falls Aquifer

Out of 37 groundwater samples collected from the Marble Falls Aquifer, two samples (one in Burnet County and one in Lampasas County) exceed the Texas Commission on Environmental Quality's maximum contaminant level for nitrate (Figure 4.7.1). Groundwater in the Marble Falls Aquifer was mostly fresh with five samples exceeding the secondary standard for total dissolved solids concentration in McCulloch, Lampasas, and San Saba counties (Figure 4.7.2), three samples for chloride in Lampasas County (Figure 4.7.3), and one sample for sulfate in San Saba County well (Figure 4.7.4).

The elevated nitrate concentrations could be attributed to lawn fertilizers in urban areas, animal waste, and septic tank leakage in rural areas (Preston and others, 1996). The depths of the wells with the high nitrate levels (457 feet and 205 feet below ground surface) indicate that recharge to the Marble Falls Aquifer could be focused, at least locally, by fractures and other conduits. The Piper diagram shows the groundwater in the Marble Falls Aquifer was of a mixed anion-bicarbonate facies with a trend of enrichment in sodium and chloride in some of the more saline samples (Figure 4.7.5).

Carbon-14 and tritium are two radiogenic isotopes commonly used to estimate groundwater ages. Provided that initial activity and radioactive decay rate are known, one can estimate the age of the groundwater by measuring present-day activity of a radioactive element. Carbon-14 is a useful dating tool for waters up to 30,000 years old (Clark and Fritz, 1997). Thermonuclear tests performed from 1951 to 1980 had added tritium to groundwater by precipitation infiltration. Thus,

cosmogenic tritium has been used to date younger groundwater which recharged aquifers in 1952 or later (Clark and Fritz, 1997). In general, the age of groundwater increases with decreasing carbon-14 and tritium activities. Measurable tritium (greater than 1 tritium unit) in groundwater also indicates active recharge.

One sample collected at a public water supply well from the Rochelle Water Supply Corporation yielded the only carbon-14 and tritium data available for the Marble Falls Aquifer (Figure 4.7.6). The well is located on the south bank of Brady Creek near the confluence with the San Saba River. The sample with a 1.006 fraction modern carbon and 2.17 tritium units strongly indicates that the groundwater at the location was very young. The presence of modern groundwater in a well this deep suggests the existence of preferential pathway(s) that can quickly transmit recharge to this part of Marble Falls Aquifer. In this particular case, it is believed that the well and the nearby streams may be in communication.

4.7.2 *Ellenburger-San Saba Aquifer*

Out of 347 groundwater samples from the Ellenburger-San Saba Aquifer, nitrate concentration exceeds the maximum contaminant level at 19 wells in Blanco, Burnet, San Saba, and Kimble counties (Figure 4.7.7); fluoride at eight wells in San Saba, Mills, and Coleman counties (Figure 4.7.8); and gross alpha radiation at 11 wells in McCulloch, Coleman, Mills, San Saba, and Lampasas (Figure 4.7.9).

Groundwater in the Ellenburger-San Saba Aquifer was mostly fresh with 312 out of 347 samples having total dissolved solids concentrations of 1,000 milligrams per liter or less. Among the samples, the total dissolved solids concentration ranges from 178 to 51,155 milligrams per liter and exceeds the secondary standard at 35 wells in Blanco, Lampasas, San Saba, Mills, and Coleman counties (Figure 4.7.10). Chloride concentration ranges from 4.38 to 25,690 milligrams per liter and exceeds the secondary standard at 20 wells (many of them also surpass the secondary standard for total dissolved solids) (Figure 4.7.11). The groundwater in the Ellenburger-San Saba Aquifer was of a calcium-magnesium-bicarbonate facies with a trend of enrichment in sodium and chloride in some of the more saline samples (Figure 4.7.12).

The elevated nitrate concentrations could be caused by lawn fertilizer, animal waste, and septic tank leakage (Preston and others, 1996). The source of excess fluoride and alpha radiation could be in-situ or allochthonous. Goldich and Parmlee (1947) described the presence of fluoride-bearing apatite and feldspar in insoluble residues from limestones and dolomites of the Ellenburger Group in Llano County. Alternately, possible sources for the elevated fluoride could be the amphiboles and micas (Hem, 1985) in igneous and metamorphic rocks such as those comprising the Llano Uplift core. Some of the radioactivity could be imparted by uranium- and thorium-bearing minerals in the Paleozoic shale strata in the study area, such as the black, slightly fissile Smithwick shale (Kier and others, 1979). The high nitrate concentrations were restricted to the outcrop or near-outcrop areas, while the elevated fluoride and radioactivity were located in or near the outcrop and farther downdip. If the source for fluoride and alpha radiation is allochthonous, it would imply contributions to the Ellenburger-San Saba Aquifer from adjacent water-bearing units through cross-formational flow.

Carbon-14 activities measured in 46 groundwater samples in the Ellenburger-San Saba Aquifer range from 0.0187 to 1.082 fraction modern carbon and tritium activities in 36 samples range from zero to 2.81 tritium units, indicating the presence of both old and young groundwater. Areal

distribution of carbon-14 and tritium for the Ellenburger-San Saba Aquifer is presented in [Figures 4.7.13](#) and [4.7.14](#). The figures show younger groundwater (carbon-14 greater than 0.8 fraction modern carbon and tritium between 0.8 and 4 tritium units) and mixture of old and young groundwater (carbon-14 from 0.6 to 0.8 fraction modern carbon and tritium greater than 0.8 tritium units) near the aquifer recharge zone and slightly downdip in San Saba, Blanco, and southern Burnet counties. Older groundwater (carbon-14 below 0.2 fraction modern carbon and submodern tritium) is found at downdip in McCulloch County. This distribution pattern indicates that the Ellenburger-San-Saba Aquifer receives more recharge in the outcrop areas to the north and east than the northwest. The very low carbon-14 and tritium activities at the wells in McCulloch County suggest a relative long groundwater residence time in the downdip portion of the aquifer. A cluster of six carbon-14 samples from the downdip portion in southeast Gillespie County showed a large variation in radiocarbon activities from less than 0.2 fraction modern carbon (older groundwater) to greater than 0.8 fraction modern (younger groundwater). Completion intervals for these wells were inferred from well total depths ranging from 171 to 345 feet below ground surface. No correlation was found between well depth and carbon-14 activities. This could be due to the preferential flow through fractures in the aquifer in this area.

4.7.3 Hickory Aquifer

Out of 458 groundwater samples collected from the Hickory Aquifer for the water quality analysis, some exceed the maximum contaminant levels, including 40 samples for nitrate ([Figure 4.7.15](#)), four samples for fluoride ([Figure 4.7.16](#)), 40 samples for radium-226/228 ([Figure 4.7.17](#)), and 27 samples for gross alpha radiation ([Figure 4.7.18](#)). The high nitrate concentrations could be attributed to the use of agricultural fertilizers, animal waste, and septic tank leakage. The most likely source for the elevated fluoride and radioactivity (radium, alpha radiation) are the feldspars in the igneous rocks (Kreitler and others, 2013). The groundwater from the Hickory Aquifer also contains relatively high uranium and thorium. The uranium likely came from the granite-derived Hickory sandstone and thorium from the Precambrian igneous and metamorphic rocks (Preston, 1996).

Among the samples, the total dissolved solids concentration ranges from 117 to 21,813 milligrams per liter with 14 samples exceeding the 1,000 milligram per liter secondary standard for total dissolved solids ([Figure 4.7.19](#)), two samples also slightly exceed the secondary drinking water standard for chloride ([Figure 4.7.20](#)), and two samples for sulfate ([Figure 4.7.21](#)). In general, the fresh water occurred near the outcrop areas and the more saline groundwater in the downdip.

The Piper diagram shows that the groundwater from the Hickory Aquifer is predominantly of calcium-magnesium-bicarbonate-chloride facies ([Figure 4.7.22](#)). Deeper wells display a shift towards higher chloride relative to the other ions, possibly suggesting upwelling groundwater from deeper strata (Kreitler and others, 2013). The lack of clear correlation between calcium and sodium (see the cation triangle in the Piper diagram) indicates that the groundwater in the Hickory Aquifer has not fully evolved along flowpaths through ion exchange mechanisms. This may suggest that the groundwater in the deeper portion of the Hickory Aquifer be stagnant (Kreitler and others, 2013).

Out of 41 groundwater samples in the Hickory Aquifer, carbon-14 activity ranges from 0.0316 to 1.119 fraction modern carbon and tritium from zero to 3.11 tritium units, both indicating the presence of old and young groundwater. As shown in [Figures 4.7.23](#) and [24](#), relative young groundwater (carbon-14 activity greater than 0.8 fraction modern carbon and tritium between 0.8

and 4 tritium units) and mixture of old and young groundwater (carbon-14 activity from 0.4 to 0.8 fraction modern carbon and tritium greater than 0.8 tritium units) were found near the aquifer recharge zone and slightly downdip in Gillespie, Mason, and McCulloch counties. Several wells near the outcrop and slightly downdip in San Saba, Burnet, and Blanco counties, and downdip in McCulloch County showed older groundwater with carbon-14 below 0.4 fraction modern and submodern (relatively old) tritium. This distribution indicates Hickory Aquifer recharging more actively in the outcrop areas on the west and south than the north of the Llano Uplift region. The downdip wells in McCulloch County have very low radiocarbon activities ([Figure 4.7.23](#)), suggesting long groundwater residence time.

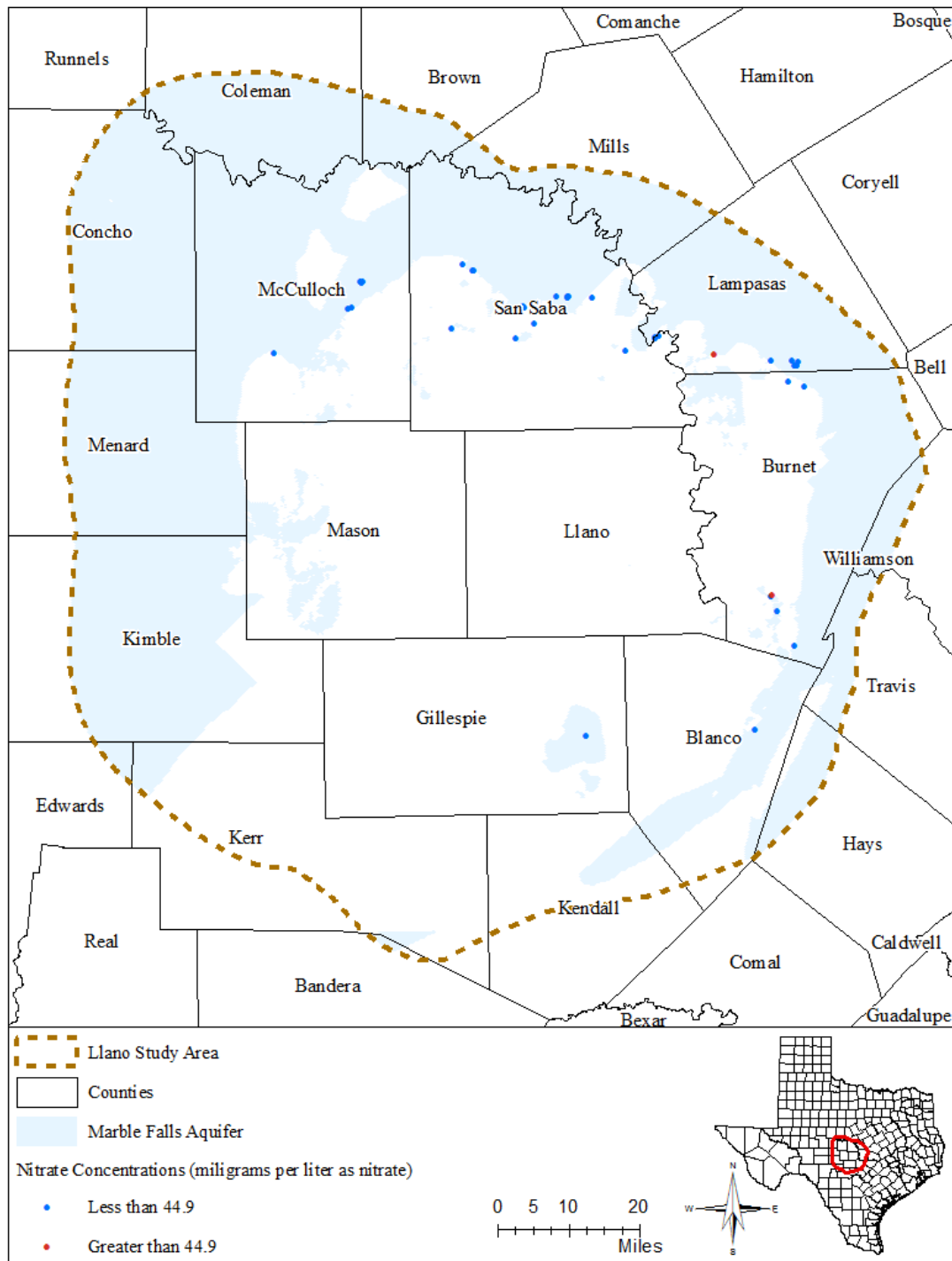


Figure 4.7.1 Nitrate concentrations in groundwater samples collected from Marble Falls Aquifer.

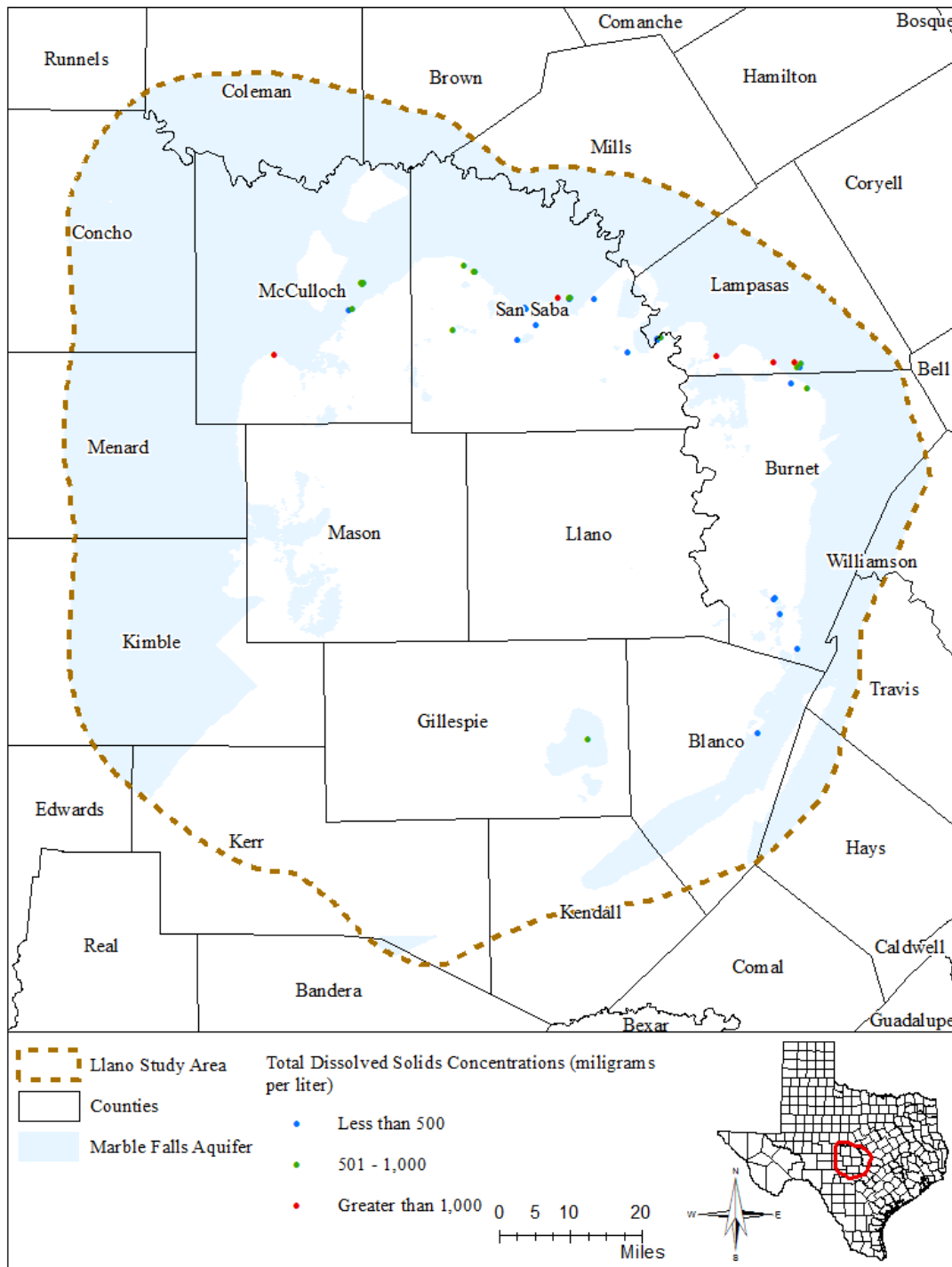


Figure 4.7.2 Total dissolved solids concentrations in groundwater samples collected from Marble Falls Aquifer.

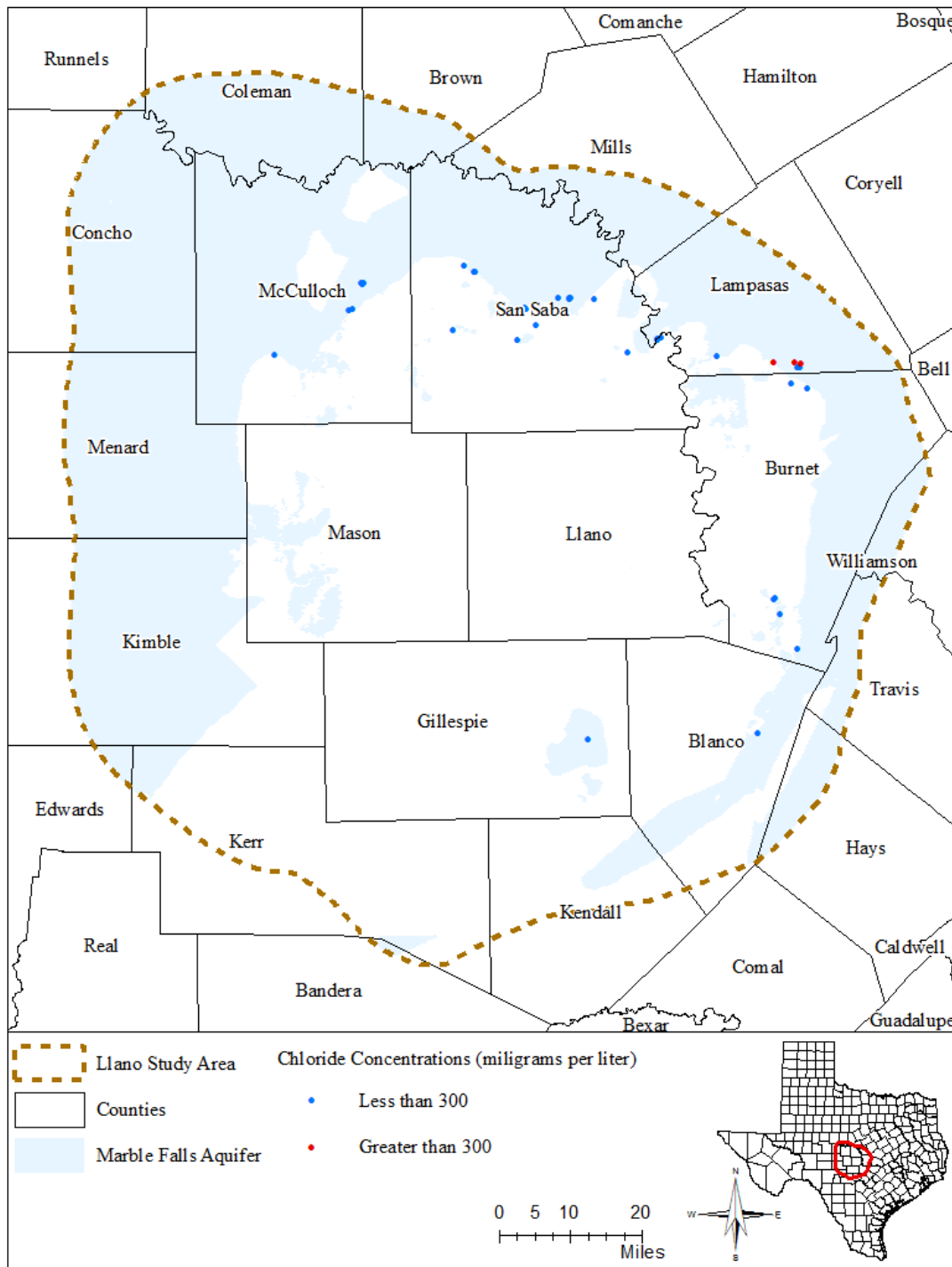


Figure 4.7.3 Chloride concentrations in groundwater samples collected from Marble Falls Aquifer.

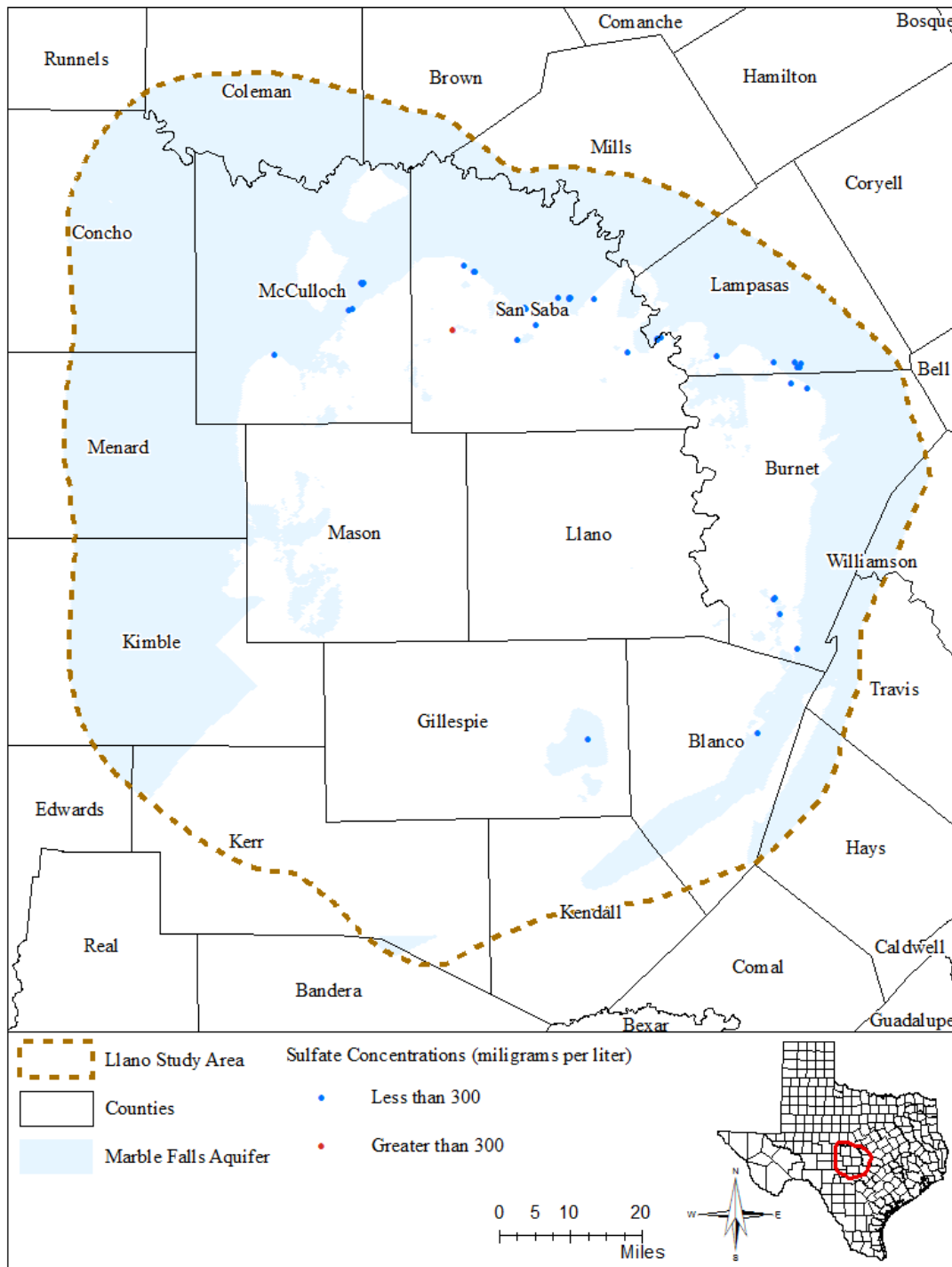


Figure 4.7.4 Sulfate concentrations in groundwater samples collected from Marble Falls Aquifer.

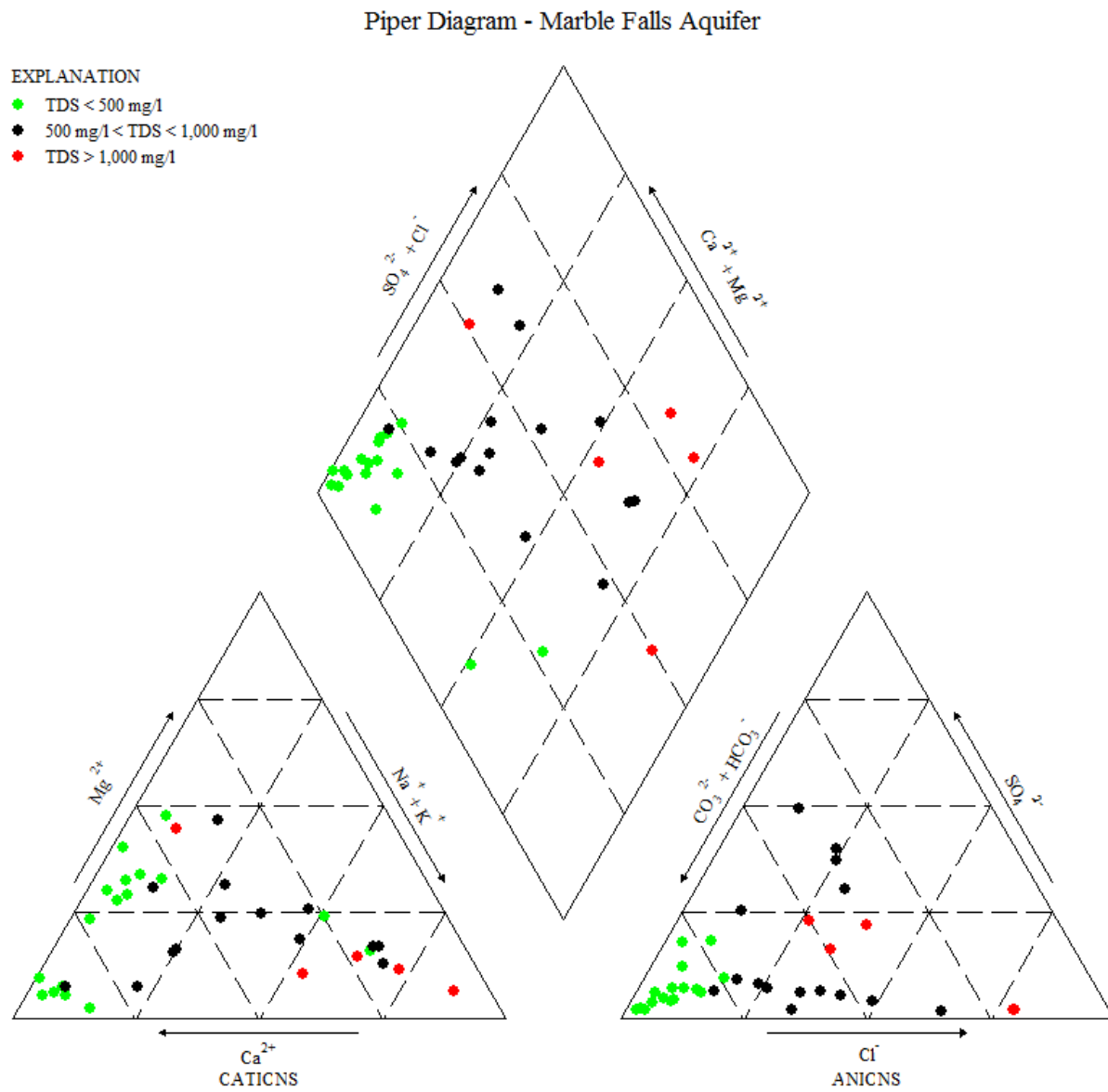


Figure 4.7.5 Piper diagram of groundwater samples collected from Marble Falls Aquifer (TDS = Total Dissolved Solids and mg/l = milligrams per liter).

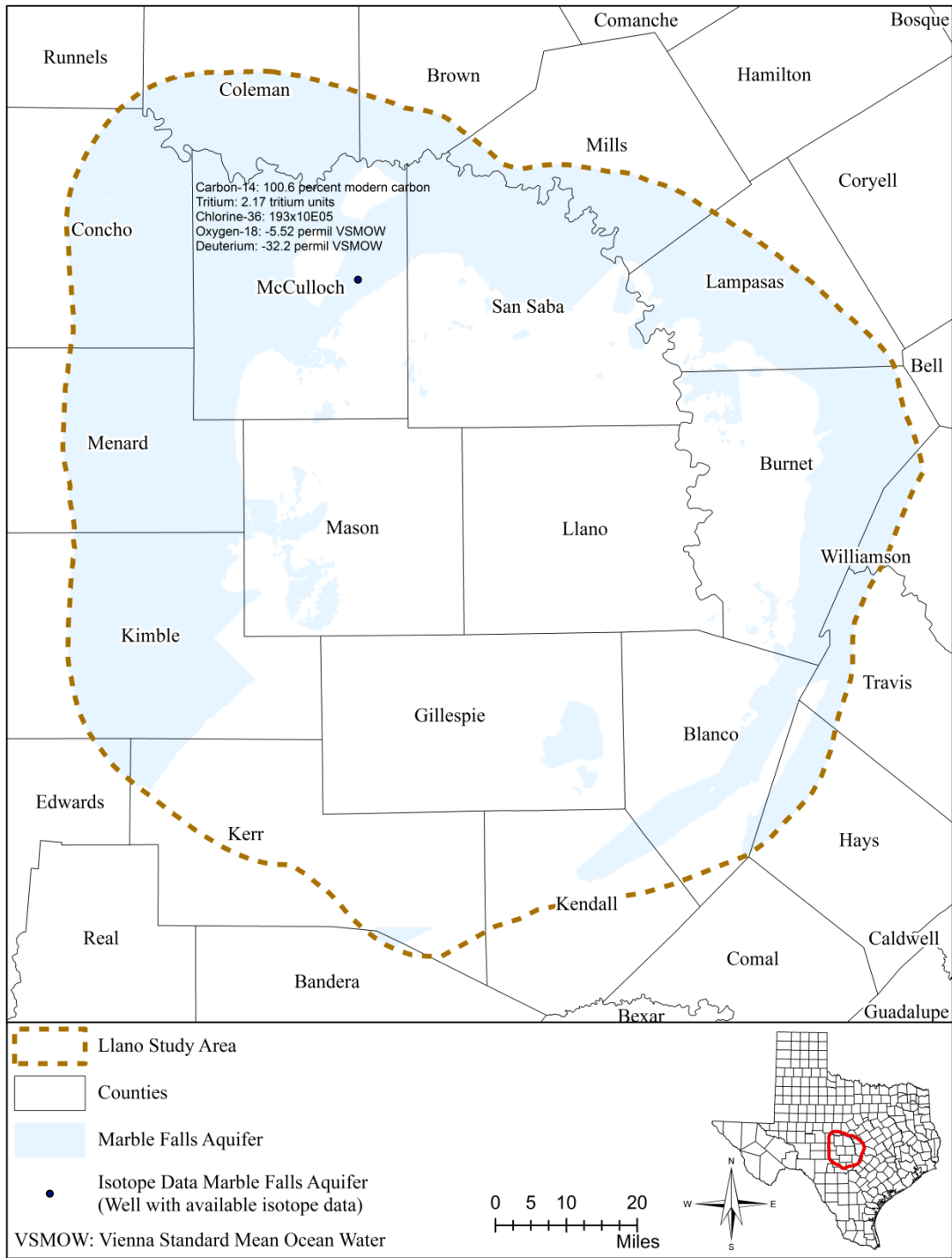


Figure 4.7.6 Stable and radiogenic isotopes in a groundwater sample collected from Marble Falls Aquifer.

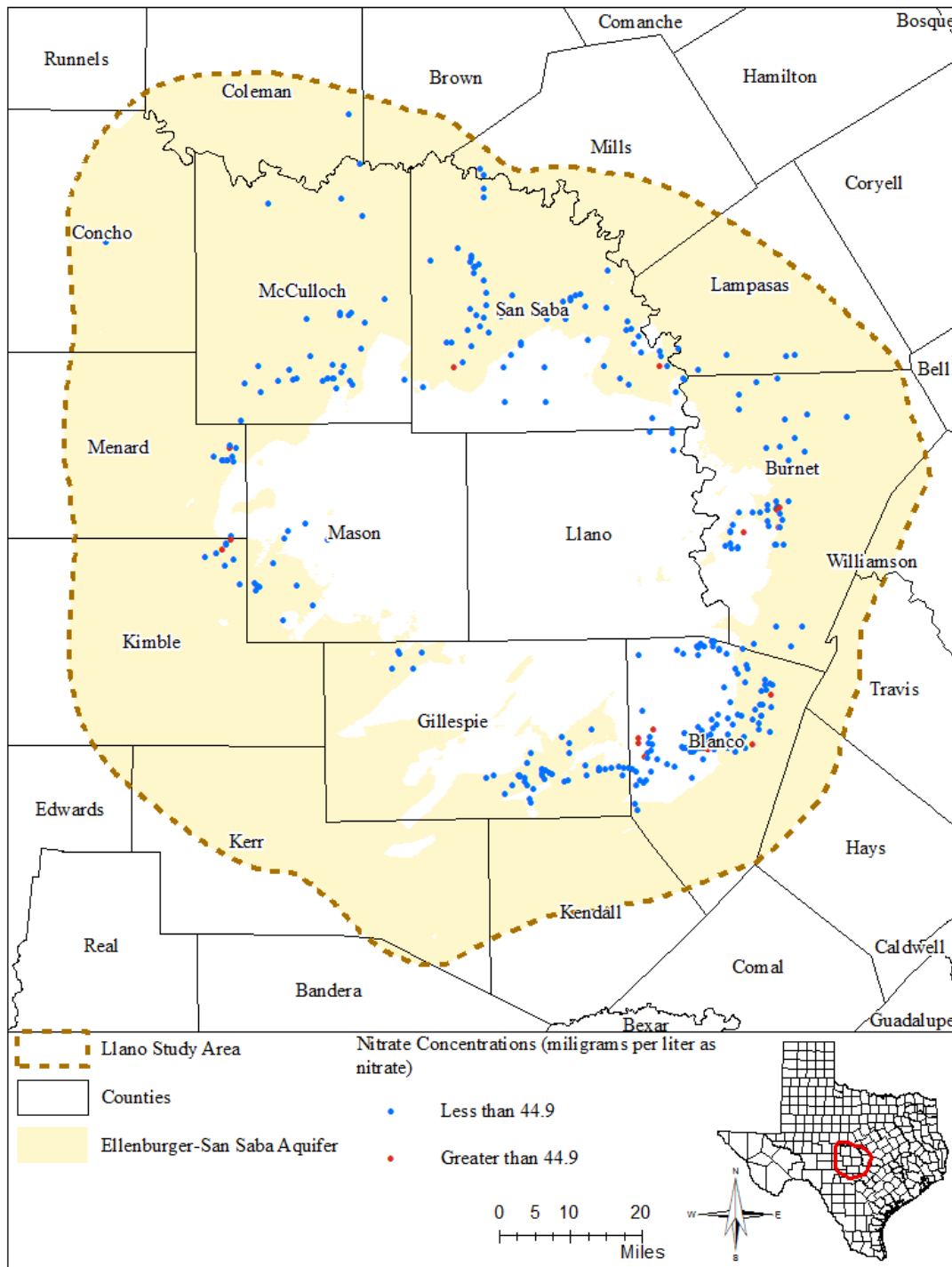


Figure 4.7.7 Nitrate concentrations in groundwater samples collected from Ellenburger-San Saba Aquifer.

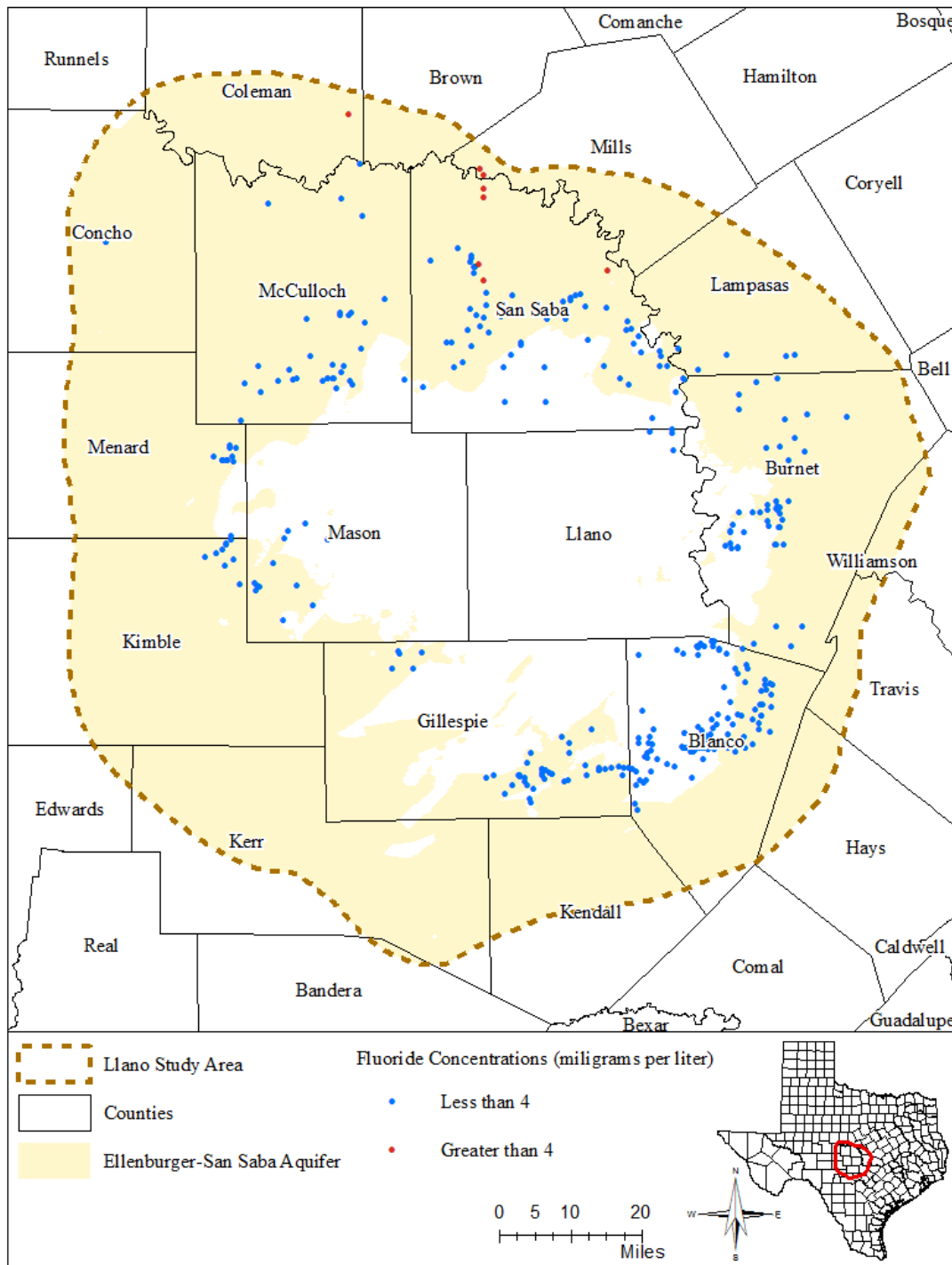


Figure 4.7.8 Fluoride concentrations in groundwater samples collected from Ellenburger-San Saba Aquifer.

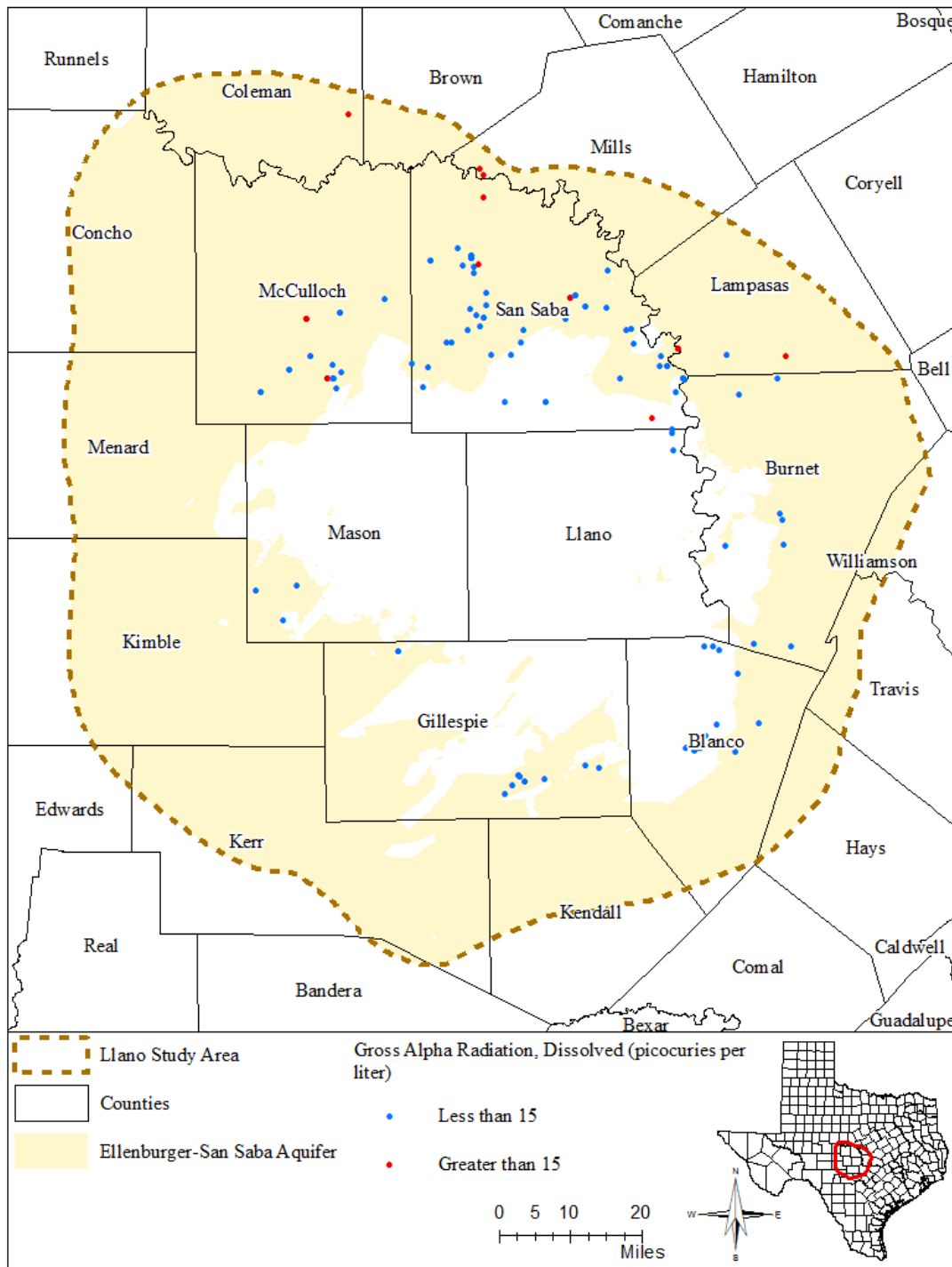


Figure 4.7.9 Gross alpha radiation in groundwater samples collected from Ellenburger-San Saba Aquifer.

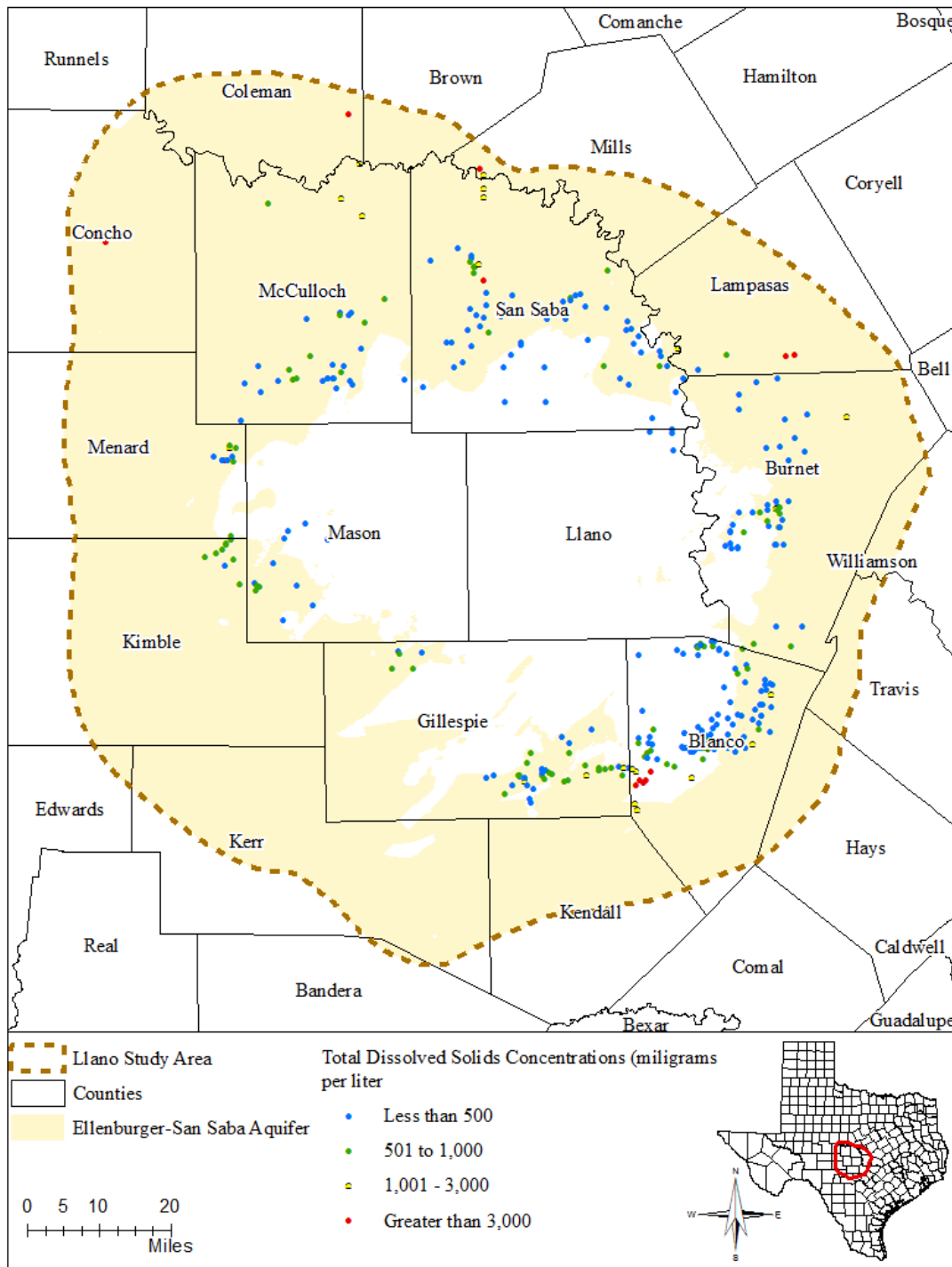


Figure 4.7.10 Total dissolved solids concentrations in groundwater samples collected from Ellenburger-San Saba Aquifer.

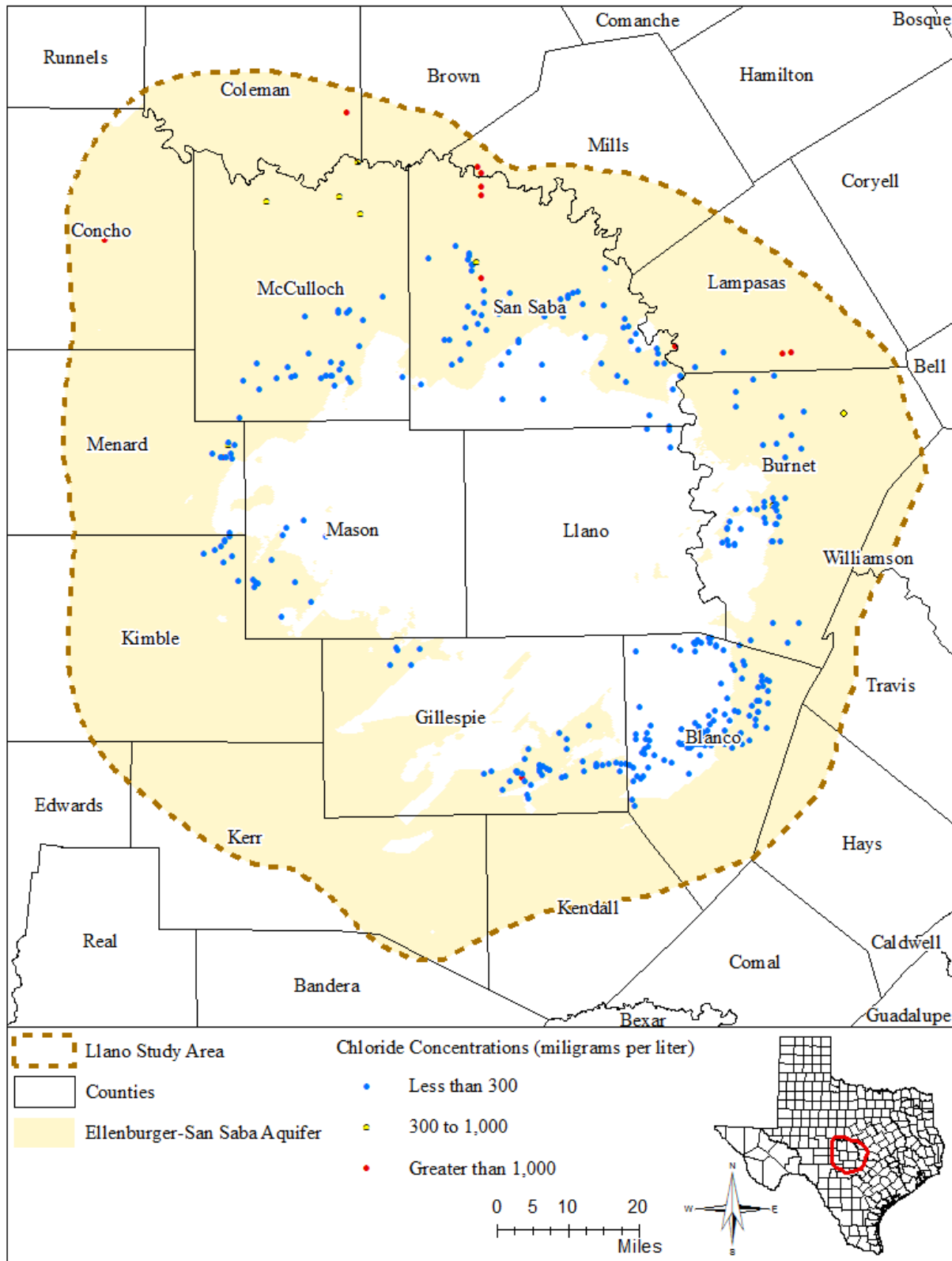


Figure 4.7.11 Chloride concentrations in groundwater samples collected from Ellenburger-San Saba Aquifer.

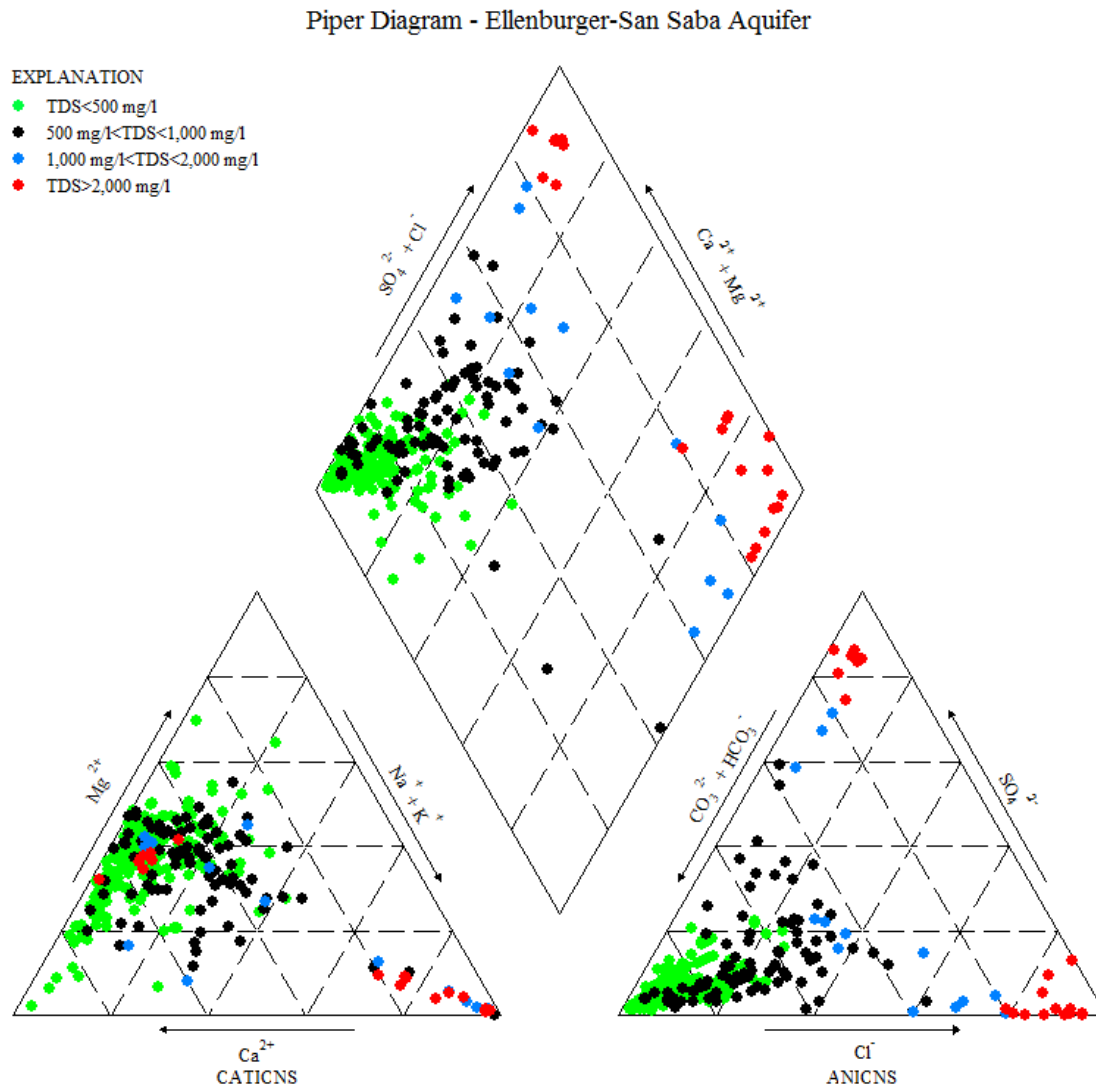


Figure 4.7.12 Piper diagram of groundwater samples collected from Ellenburger-San Saba Aquifer (TDS = Total Dissolved Solids and mg/l = milligrams per liter).

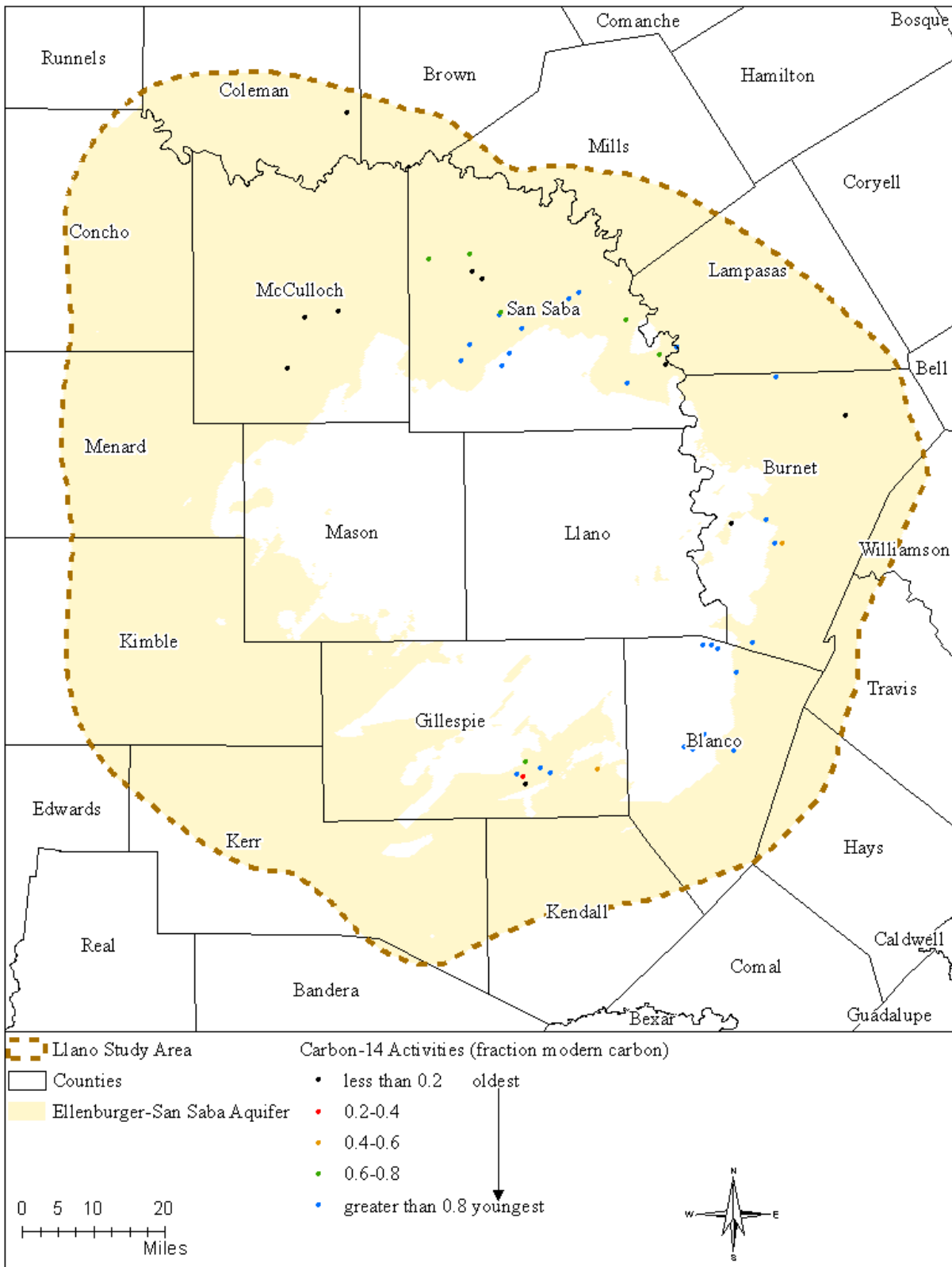


Figure 4.7.13 Carbon-14 activities in groundwater samples collected from Ellenburger-San Saba Aquifer.

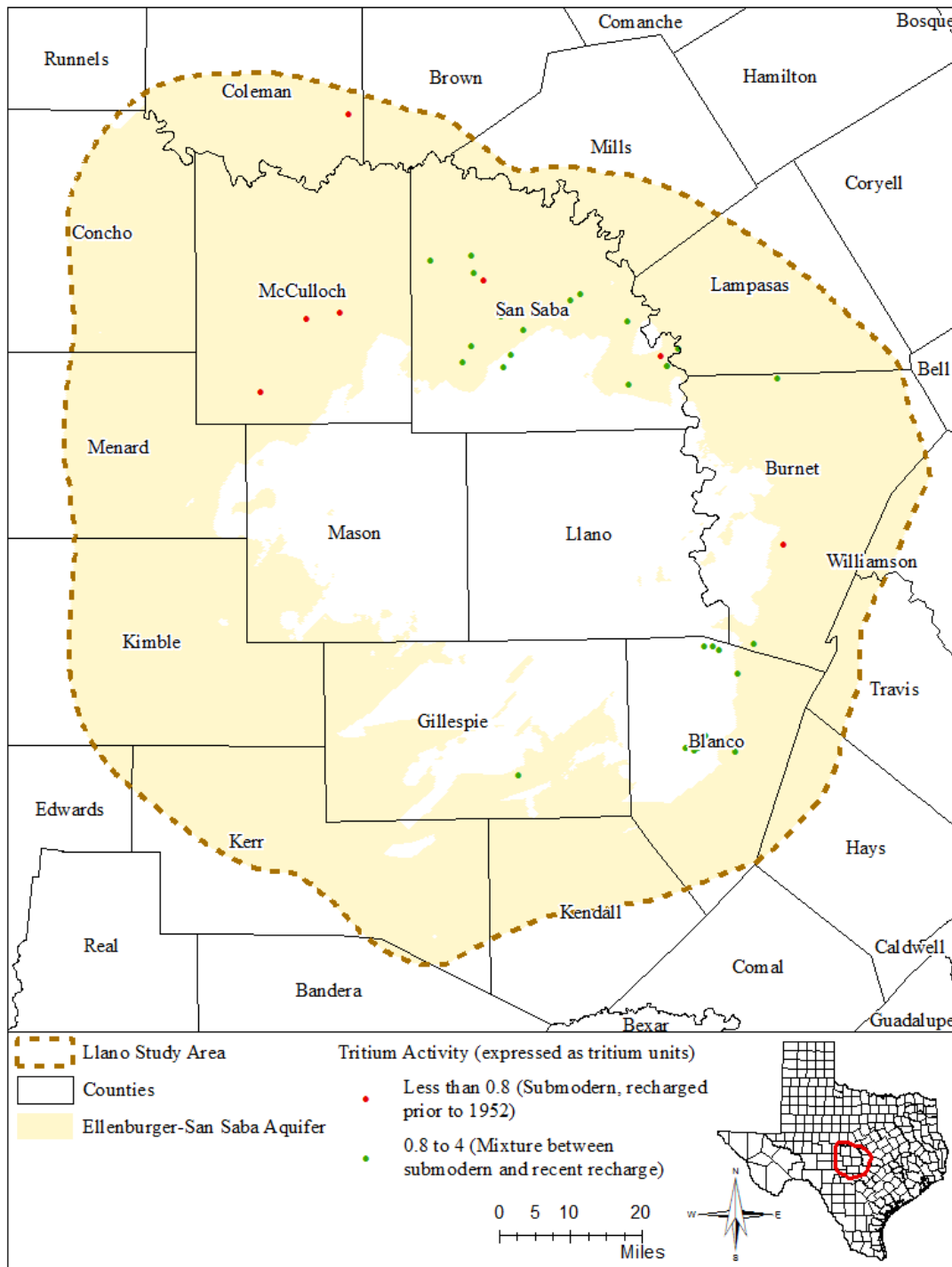


Figure 4.7.14 Tritium activities in groundwater samples collected from Ellenburger-San Saba Aquifer.

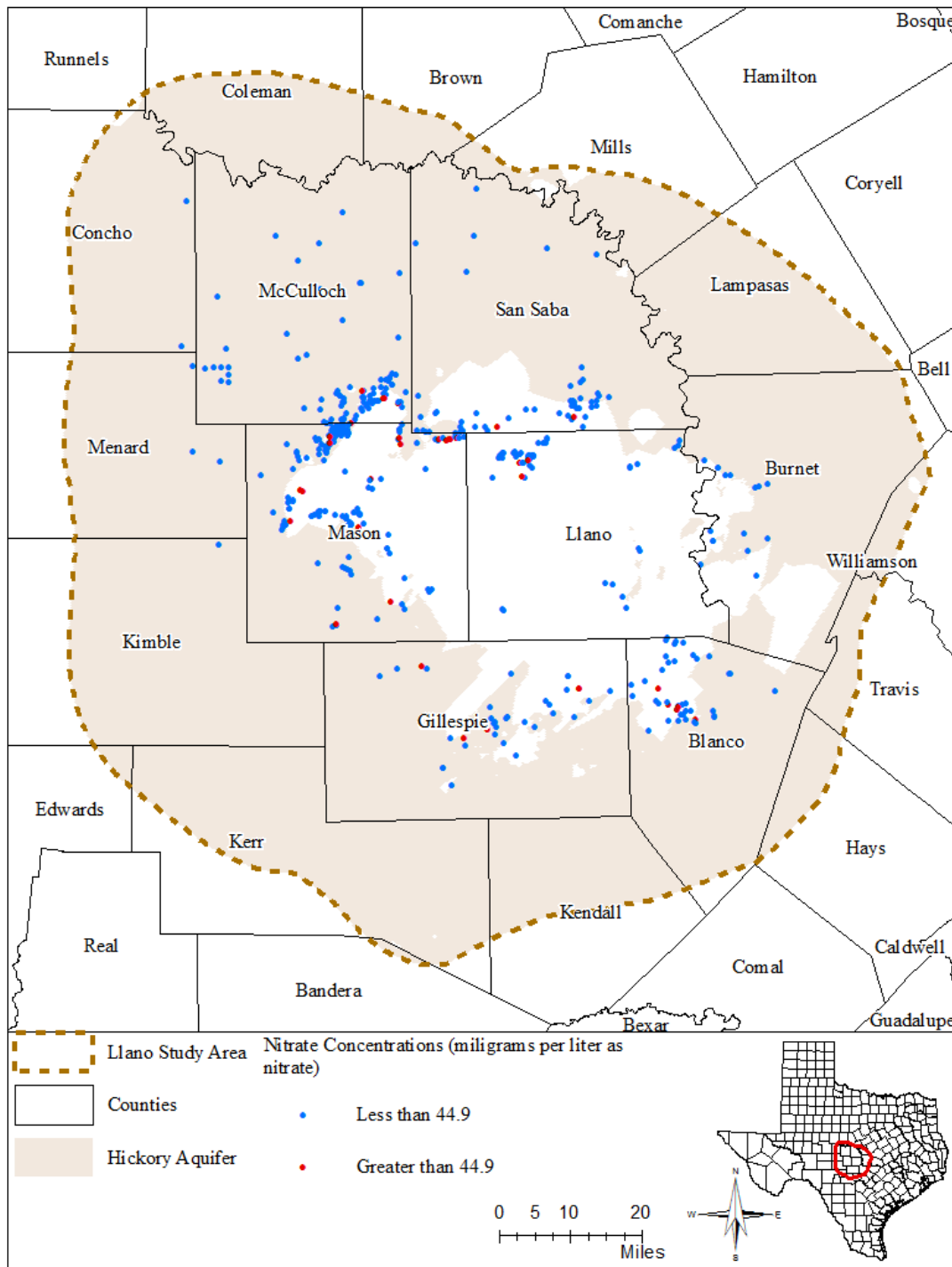


Figure 4.7.15 Nitrate concentrations of groundwater samples collected from Hickory Aquifer.

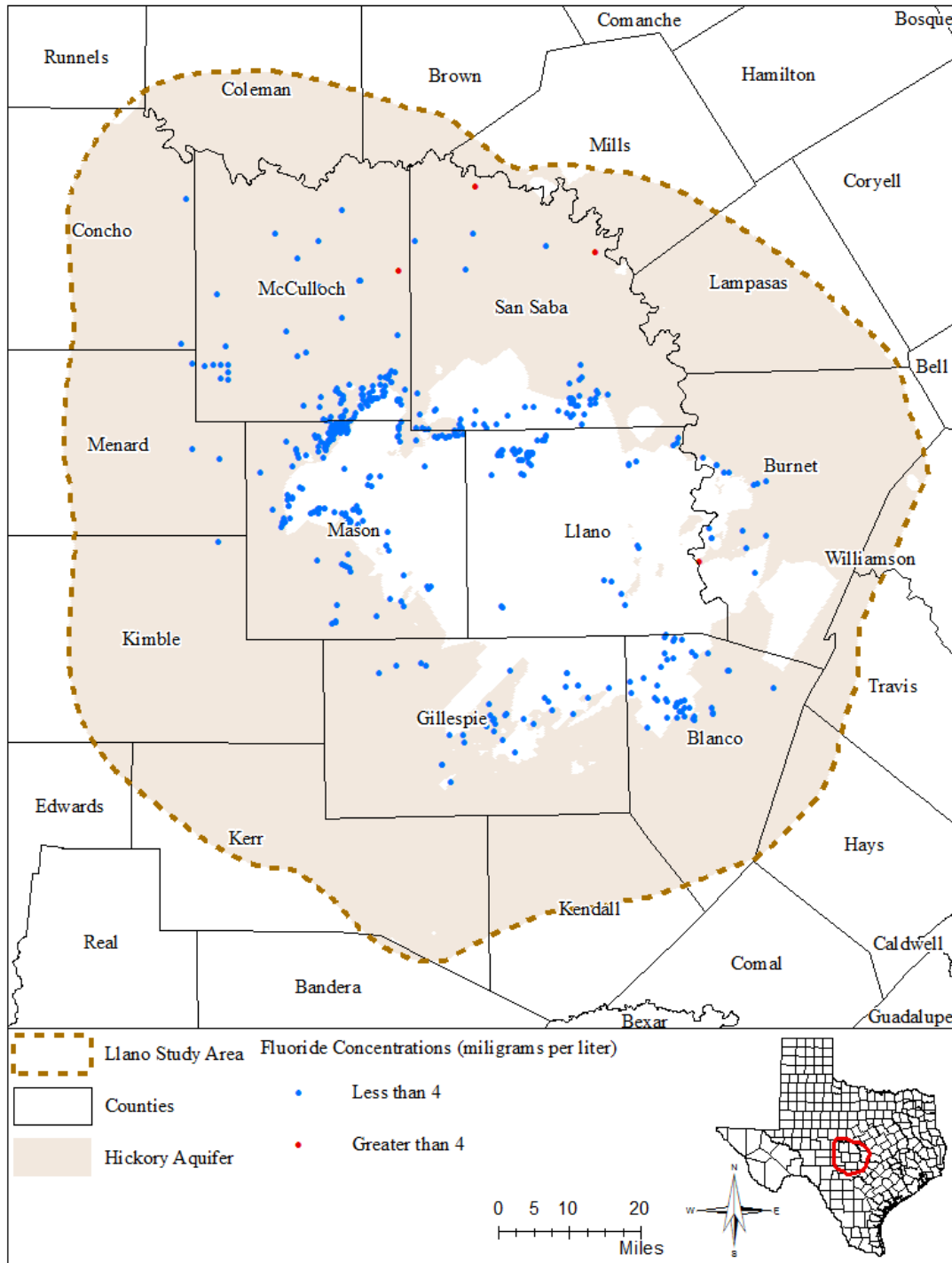


Figure 4.7.16 Fluoride concentrations of groundwater samples collected from Hickory Aquifer.

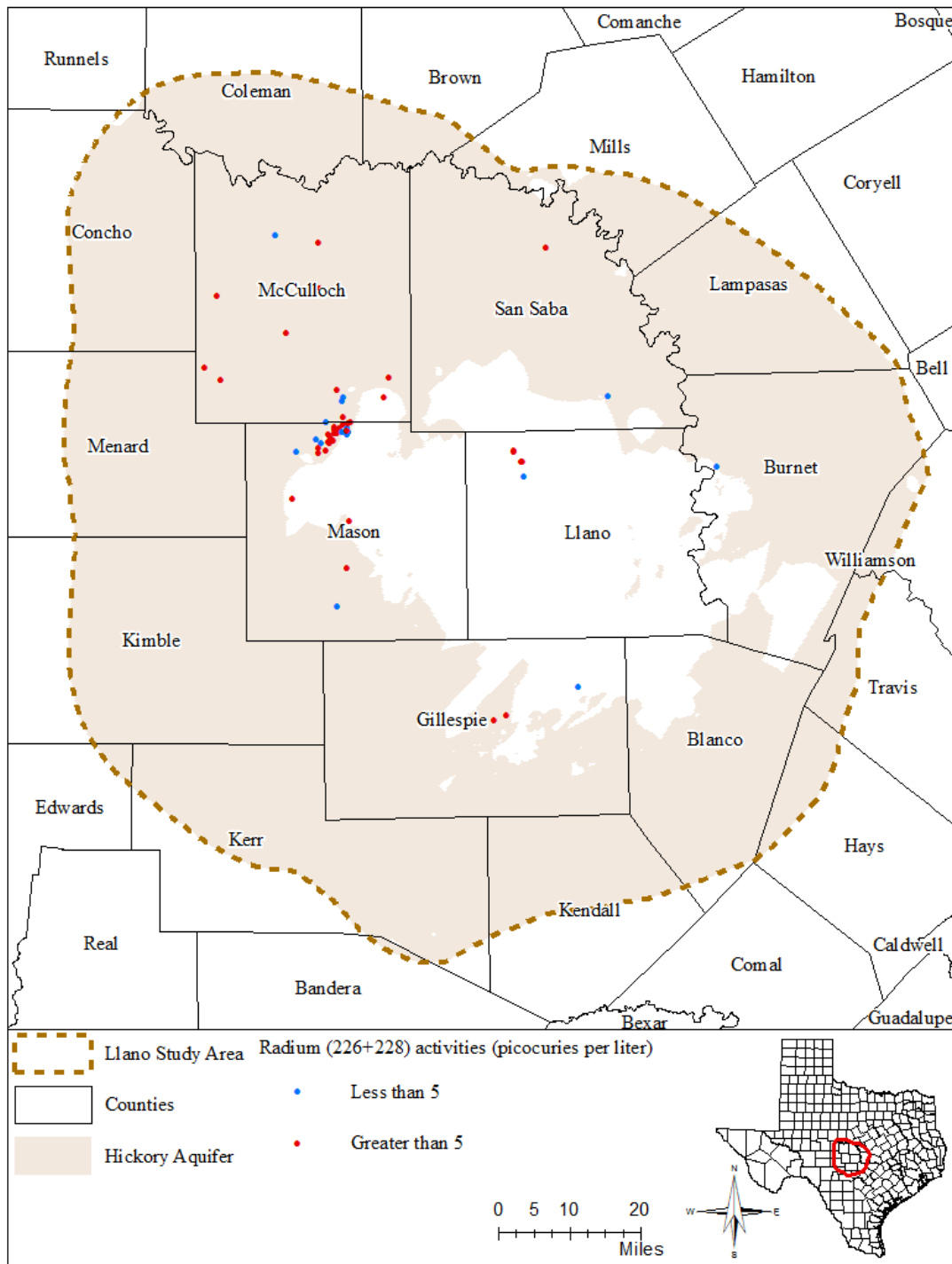


Figure 4.7.17 Radium 226/228 activities of groundwater samples collected from Hickory Aquifer.

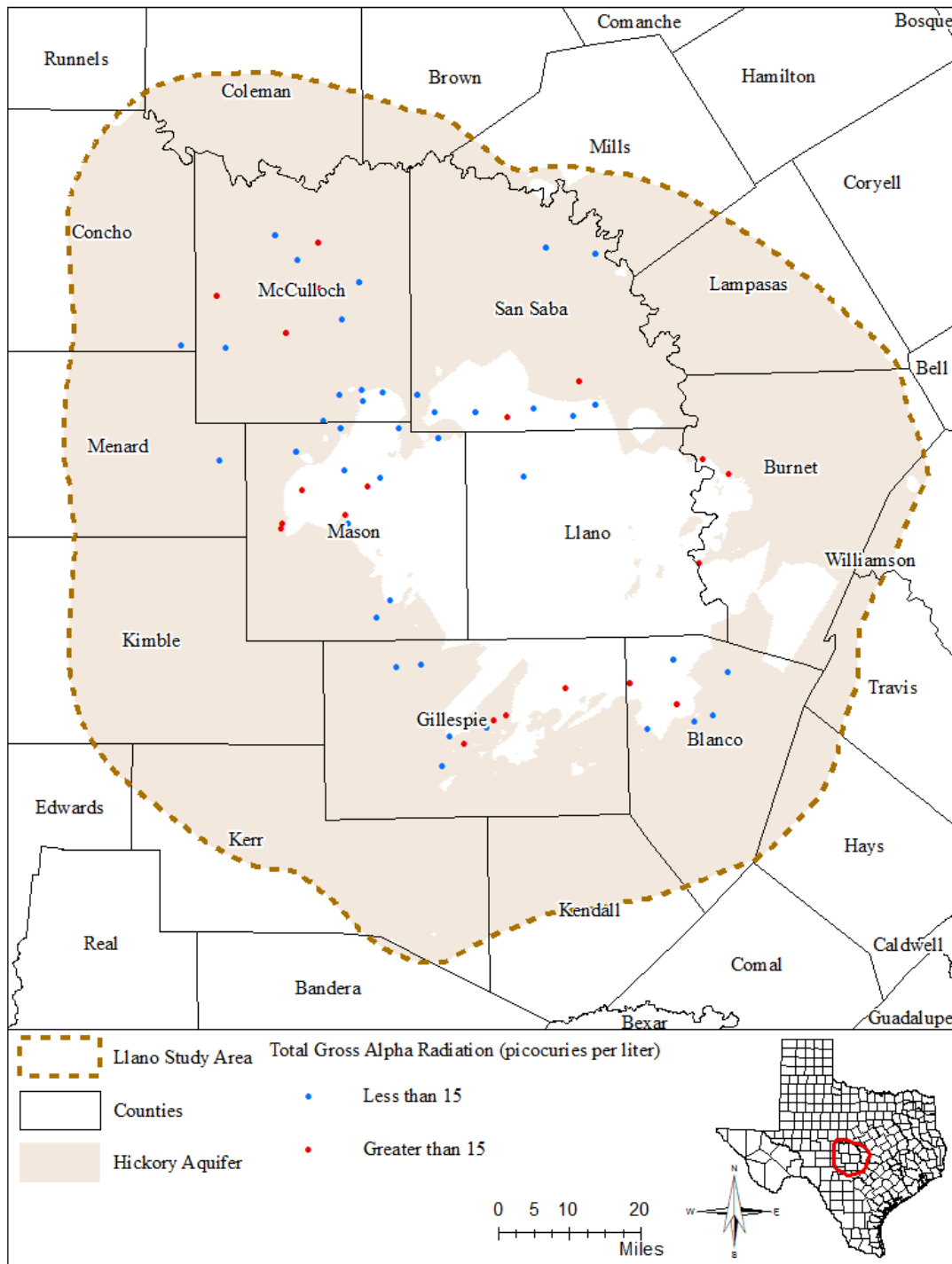


Figure 4.7.18 Gross alpha radiation of groundwater samples collected from Hickory Aquifer.

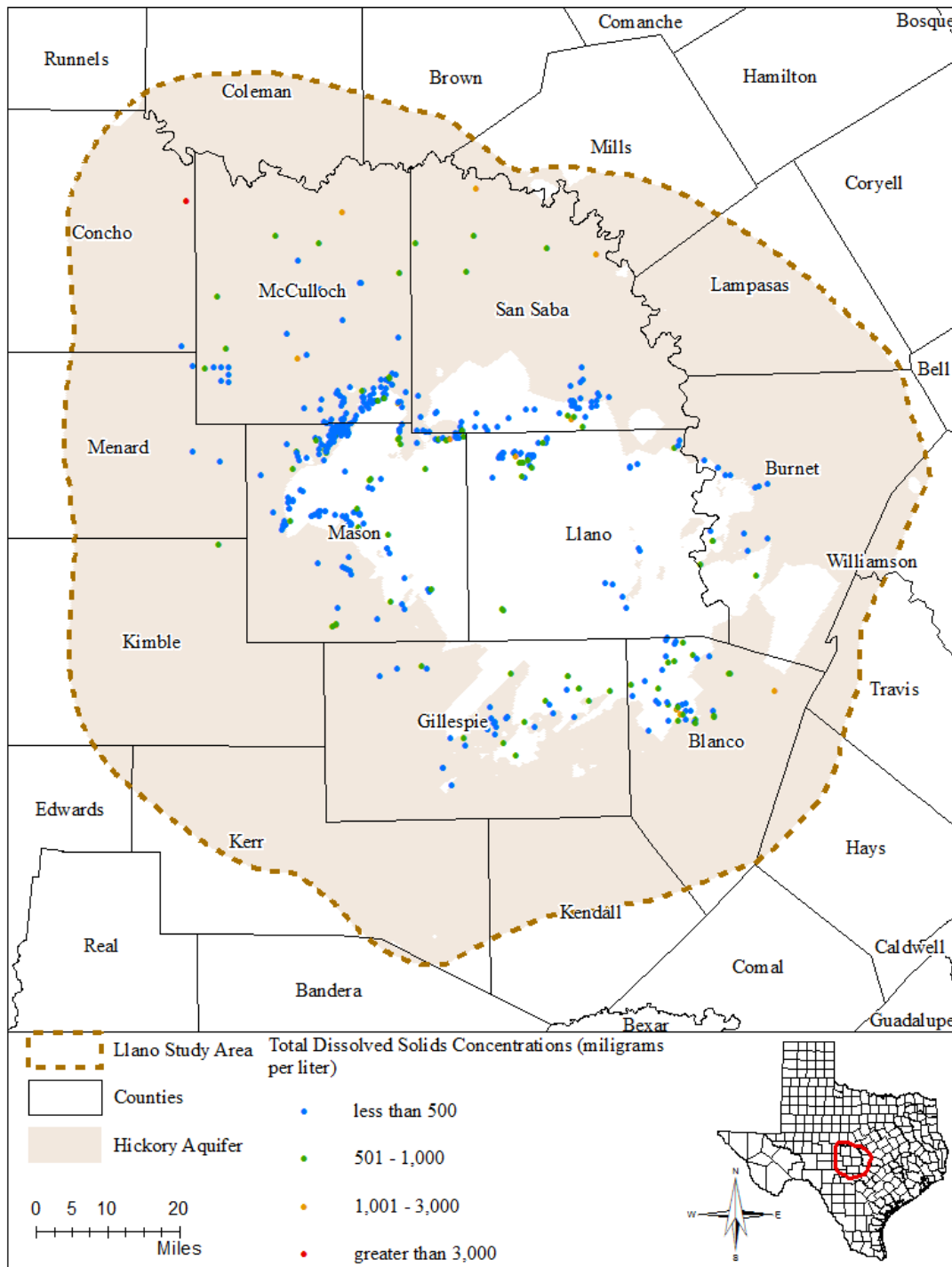


Figure 4.7.19 Total dissolved solids concentrations in groundwater samples collected from Hickory Aquifer.

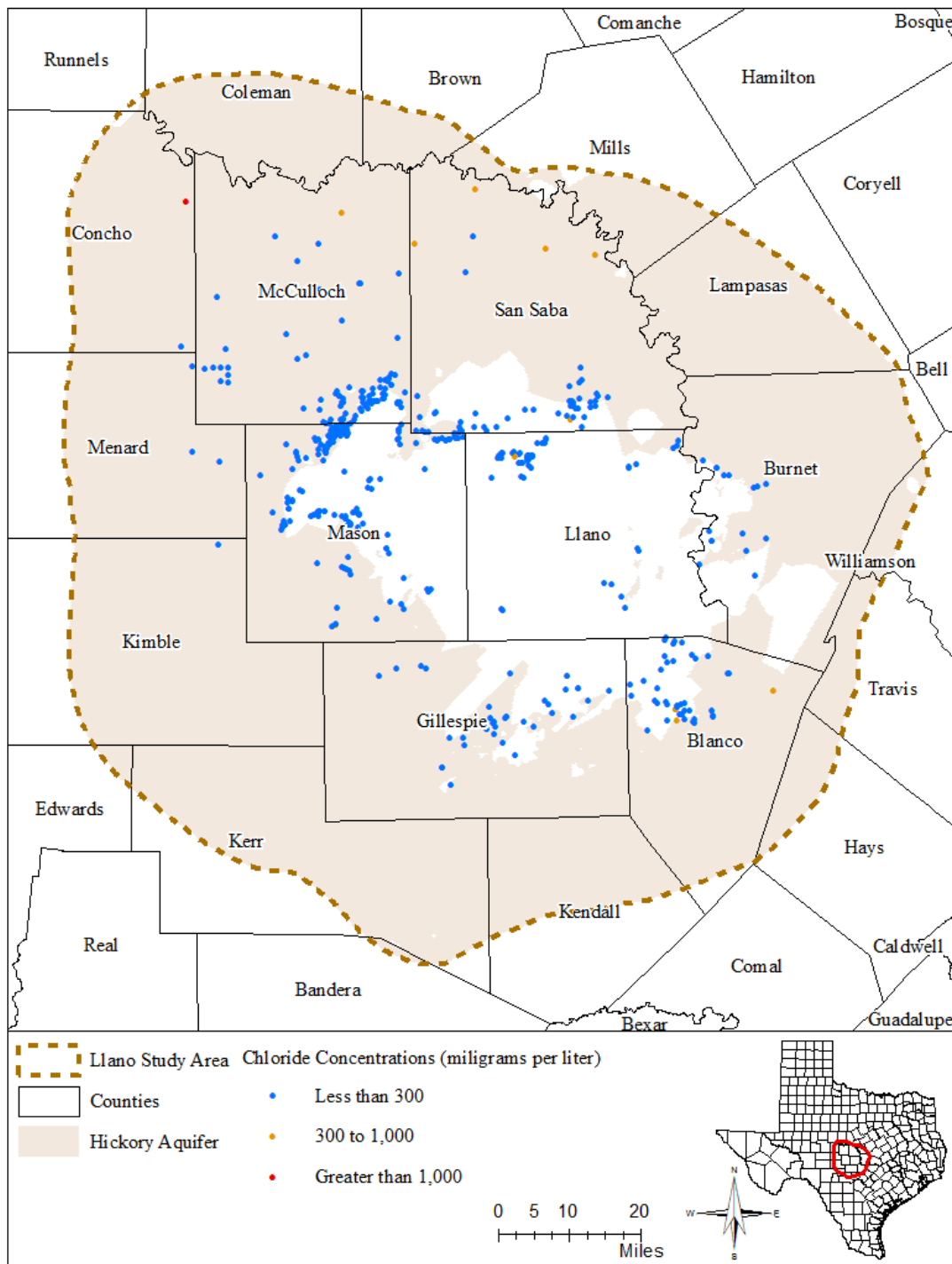


Figure 4.7.20 Chloride concentrations in groundwater samples collected from Hickory Aquifer.

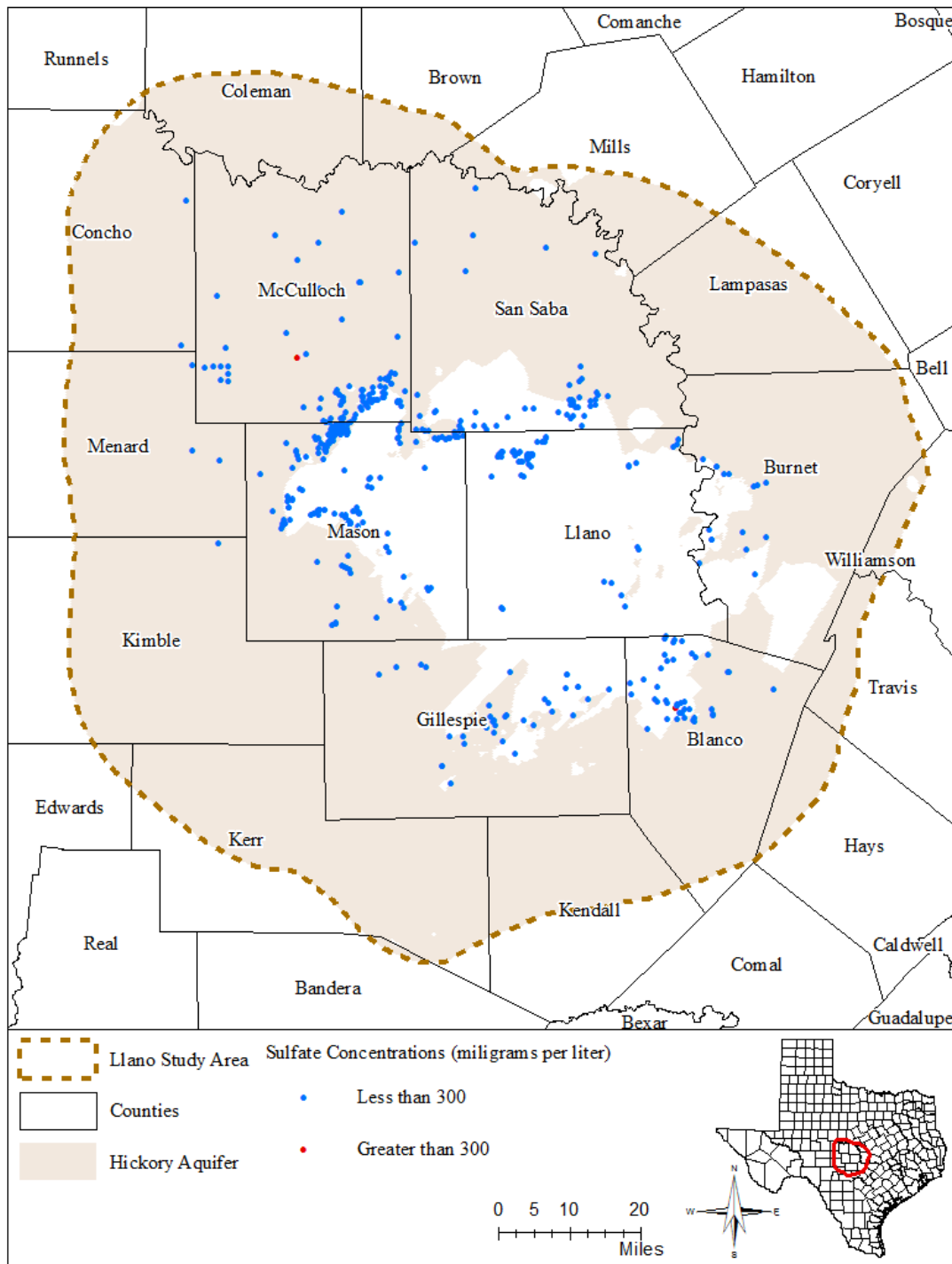


Figure 4.7.21 Sulfate concentrations in groundwater samples collected from Hickory Aquifer.

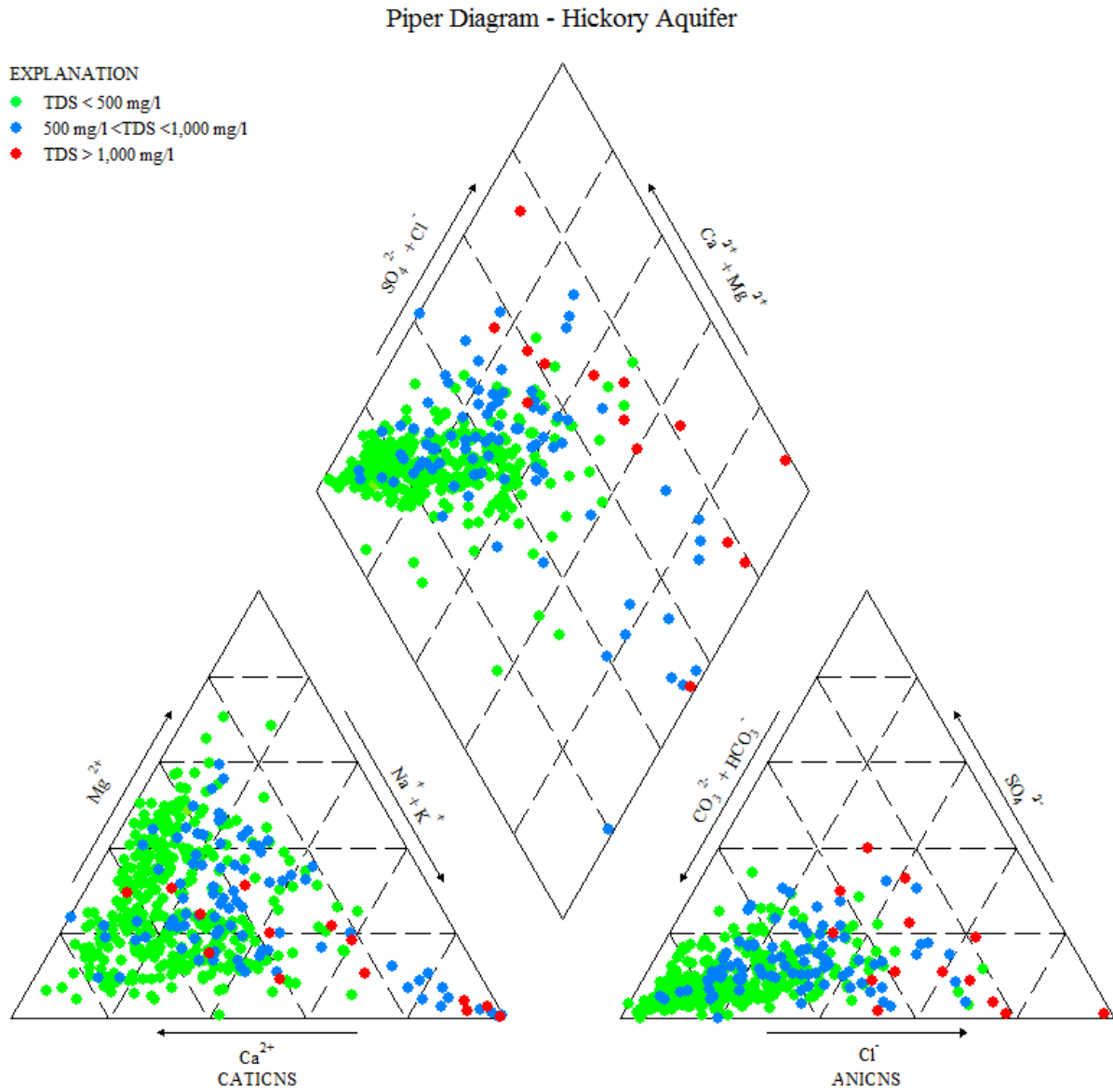


Figure 4.7.22 Piper diagram of groundwater samples collected from Hickory Aquifer (TDS = Total Dissolved Solids and mg/l = milligrams per liter).

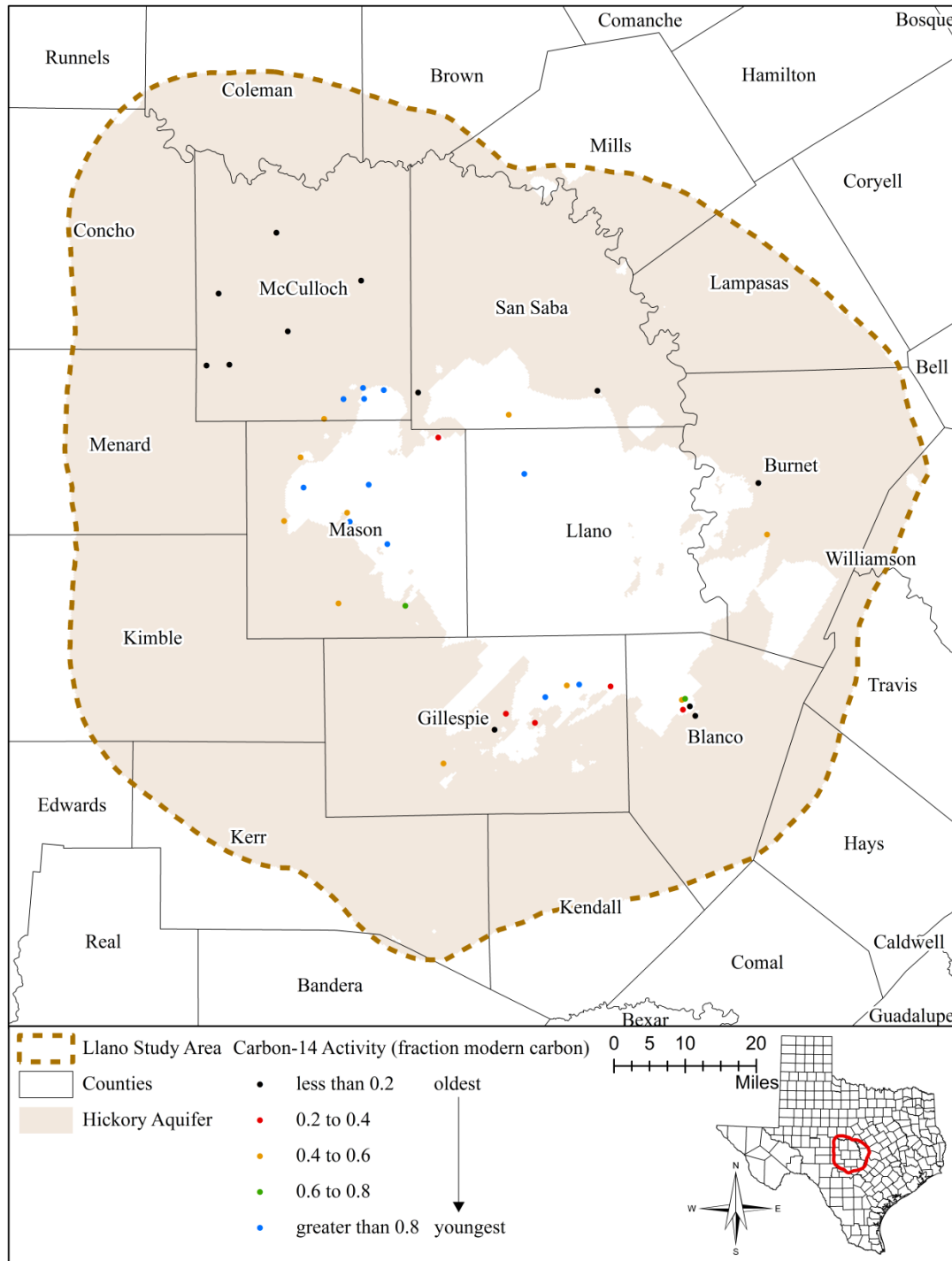


Figure 4.7.23 Carbon-14 activities in groundwater samples collected from Hickory Aquifer.

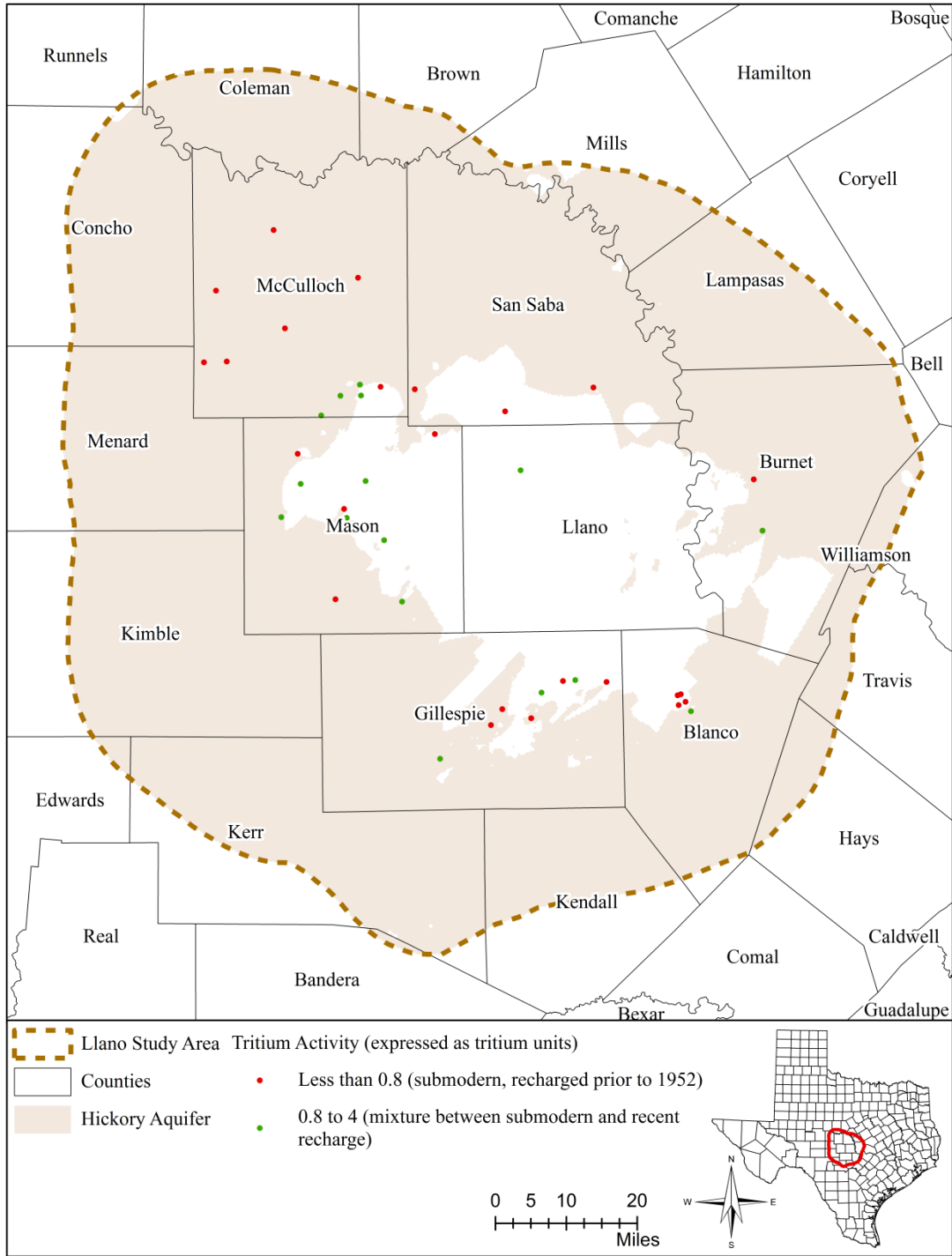


Figure 4.7.24 Tritium activities in groundwater samples collected from Hickory Aquifer.

5.0 Conceptual Groundwater Flow Model for the Llano Uplift Minor Aquifers

A groundwater conceptual flow model is a simplified version of the real groundwater flow system. A conceptual model includes identifying unique hydrostratigraphic units that host the groundwater, characteristics of the groundwater flow, and factors that control the flow.

First, the characteristics of the geologic units must be investigated and simplified to unique hydrostratigraphic units. Each hydrostratigraphic unit shares similar hydrogeologic properties and can be distinguished from adjacent hydrostratigraphic units. This step involves understanding the geologic history and using field data (such as geophysical logs and pumping tests) to determine the lateral and vertical extension of each of the hydrostratigraphic units. The result of this step is a simplified, intuitive hydrogeologic framework that can be handled using a computer code during the numerical model development.

The characteristics of the groundwater flow, such as flow direction/quantity and recharge/discharge zones are then identified using the hydrostratigraphic framework, precipitation data, water levels, stream baseflow, reservoir information, spring flow, and hydrogeologic properties of the hydrostratigraphic units.

Many factors influence the groundwater flow. Some of the processes are natural such as the infiltration of recharge due to precipitation. Others may be associated with anthropogenic activities such as groundwater pumping. The dominant processes (inflow and outflow components) must be identified and, if possible, quantified so that a numerical model can realistically simulate the flow system and minimize the uncertainty during model calibration and prediction.

The conceptual flow model for the Llano Uplift region consists of seven hydrostratigraphic units including four aquifers (from top to bottom): the Cretaceous aquifers, Marble Falls Aquifer, Ellenburger-San Saba Aquifer, and Hickory Aquifer. The Cretaceous aquifers are the uppermost layer and the Hickory Aquifer is the lowest layer. Separating the aquifers are three confining units. All seven units are discontinuous. The top and bottom of the conceptual model domain are the ground surface and the top of the Precambrian strata, respectively. In this model domain, the interaction with the underlying Precambrian units is assumed zero due to the low permeability of the unweathered portions of the Precambrian units in the study area. The lateral extent of the conceptual flow model is bounded by the Ouachita Thrust Fault to the east and southeast and the official Hickory Aquifer boundary plus five miles for the rest. The groundwater flow through the lateral boundary is also assumed zero. This assumption is based on the following reasoning: the fault wall may act as a flow barrier; the groundwater along the rest of the model domain lateral boundary may very likely be brackish which may hinder the groundwater movement due to high density. Thus, a no-flow condition is likely justified and can be maintained as long as no significant groundwater withdrawal occurs near the lateral boundary.

Aquifers are more permeable than confining units. Groundwater flow and storage occur mainly in aquifers. Cross formation flow between aquifers can happen when water levels are different between the aquifers. This cross formation flow can occur directly where a confining unit is absent or through the confining unit.

The conceptual flow model includes two hydrogeologic conditions: steady state and transient state. The steady state represents the pre-development conditions prior to 1950 when the groundwater

use was very limited in the study area. The steady state represents a time when inflows and outflows are balanced and the system is at equilibrium. As long as groundwater was withdrawn from the aquifers, either by pumping or flowing wells, the aquifer system was not at steady state anymore. Thus, the hydraulic conditions prior to 1950 were a “pseudo” steady state. In general, the real steady state should have a higher water level and greater natural discharge to streams and springs. The transient state represents the time period after 1950 when the groundwater use was significant.

5.1 Pre-Development Conditions (Steady State)

Because of limited groundwater withdrawal prior to 1950, the aquifers in the Llano Uplift region were under long-term dynamic equilibrium. Groundwater levels and flows fluctuated over time due to seasonal and annual changes in precipitation. However, the total discharge was balanced by the total recharge. As a result, the water levels and storage in the aquifers showed little long-term variation. [Figure 5.1.1](#) shows the schematic west-east hydrogeologic cross section and groundwater flow under pre-development conditions. Under pre-development conditions, recharge through precipitation infiltration is the main groundwater inflow component with minor contributions from other surface water features. The outflow components include discharges to rivers, springs, and seeps and groundwater loss by evapotranspiration.

The infiltration recharge was primarily located at the aquifer outcrop areas and, in a lesser degree, the shallow confined portion where the infiltration can trickle down through the confining unit. Once the water reached the aquifer, part of it likely took the preferential pathways to return to the ground surface as river baseflow, springs, or/and seeps. This flow system is shallow and short with relatively fast groundwater flow. The groundwater under such a flow system was often young and fresh with very low total dissolved solids.

Groundwater loss to evapotranspiration also occurred at places with shallow water tables, dense vegetation with long roots, and void-rich soils or rocks. Under certain circumstances, some of the infiltration recharge may move downdip into the deep aquifer system. This is often controlled by the aquifer transmissivity and existence of discharging points. A thick, permeable aquifer is able to transfer more water. The groundwater also needs discharging point(s) to flow out or leave the system. To make that happen, the discharging point(s) must have a lower elevation than the recharge area.

As described in Section 4 ([Figure 4.4.16](#)), almost all of the springs associated with the Paleozoic aquifers are located at the outcrop areas. This indicates that most of the recharge at the outcrop areas returned to the ground surface after traveling a relatively short distance. The lack of discharging points to the west, northwest, and north of the study area may suggest stagnant groundwater systems for the Paleozoic aquifers in the far downdip areas. The most promising areas where limited discharge could happen in the far downdip areas were along the Ouachita Thrust Fault and major rivers to the east of the study area. These areas have lower elevation than the recharge areas and may also contain fractures that provided preferential pathways. The groundwater from the deep aquifers often had poor quality due to long-residence time which allowed ion-exchange to happen between the water and aquifer matrix.

5.2 Post-Development Conditions (Transient State)

After 1950, the groundwater pumping had changed the aquifer system in the study area. These changes included falling water level or aquifer storage, reducing discharge to rivers and springs, and increasing groundwater recharge.

The initial response to pumping is a lowering of the groundwater level or a “cone of depression” around the well, which results in a decline in storage. The cone of depression deepens and extends radially with time. As the cone of depression expands, it causes groundwater to move toward the well thereby increasing the inflow to the area around the well.

The cone of depression can also cause a decrease of natural groundwater outflow from the area adjacent to the well and acts to “capture” this natural outflow. If the cone of depression causes water levels to decline in an area of shallow groundwater, evapotranspiration is reduced and the pumping is said to capture the evapotranspiration. At some point, the induced inflow and captured outflow (collectively the capture of the well) can cause the cone of depression to stabilize or equilibrate. The time to reach this new steady state conditions is mainly determined by the pumping rate and aquifer property. It takes much less time if the pumping rate is low and the aquifer transmissivity is high.

If pumping were to increase after this new near steady-state condition was established, the system inflow increases again, the natural outflow decreases again, and groundwater storage is further decreased (Alley and others, 1999). In response to this new increase in pumping, inflow would continue to increase, outflow would continue to decrease, and storage would continue to decrease as the system is equilibrating. If the pumping is relatively constant, it is possible for a groundwater basin to exhibit stable groundwater levels at a lower level than had been previously observed. Stable groundwater levels are an indication that a new near steady-state condition has been reached.

Pumping can increase to the point where no new near steady state condition is possible. In this situation, inflow can be induced no further and/or natural outflow can be decreased no further. From an outflow perspective, this condition would be reached once all springs have ceased to flow or the water table has declined to the point that shallow groundwater evapotranspiration has ceased.

Groundwater withdrawal in the study area has been primarily from the shallow system including the Cretaceous aquifers and the outcrop or near the outcrop of the Paleozoic aquifers. Aquifers in these areas are often unconfined (water table aquifers) and could be quickly replenished by rainfall. However, aquifer overdraft could happen during dry season. This can cause water level decline and reduction of stream and spring flows. This also diminishes the deep recharge to the downdip portions of the aquifers.

As discussed in Section 4.5, the confined portion of an aquifer produces much less groundwater than its unconfined portion with the same drawdown, in other words, pumping the same amount of water in the confined portion will cause much greater water level decline than the unconfined portion or outcrop area. The large water level decline can significantly change the deep flow system. First, it will enhance the groundwater flow from the hydraulic upgradient. It may also reduce or even reverse the downgradient or cross formation flows. As a result, farther downdip groundwater flow may stop; the deep aquifer system may become stagnant; and deep springs may

cease flow. Pumping may also remobilize a stagnant system and induce brackish water movement. [Figure 5.1.2](#) shows the schematic flow system under post-development conditions in the study area.

In comparison with the pre-development conditions, the widespread groundwater withdrawal after 1950 has also enhanced the effective groundwater recharge. This was the result of the lower water table in the recharge area which reduced the evapotranspiration and, in certain areas, due to irrigation return flow.

The post-development conditions are not only different from the pre-development conditions. The post-development conditions also varied over time. This variation could be due to the change of pumping, landscape, or/and climate. However, in general, the post-development conditions involved increasing groundwater withdrawal, increasing recharge, and decreasing discharge to surface water bodies.

5.3 Implementation of Groundwater Recharge and Faults

Section 4 presents the precipitation infiltration rates and groundwater recharge rates estimated from stream baseflow. On the one hand, the precipitation infiltration values are the high end of the actual groundwater recharge because these values include water retained in the unsaturated zone. On the other hand, the groundwater recharge values based on stream baseflow measurements collected primarily after 1950 are likely close to the low end of the actual groundwater recharge. This is partially due to the groundwater withdrawal that has depleted the aquifer storage. As a result, part of the precipitation recharge must replenish the aquifers first before discharging to rivers and streams as baseflow. Stream bank storage also reduces the baseflow. Therefore, the groundwater recharge rates calculated using the baseflow data are lower than the actual effective recharge values. In addition, these recharge values are average values over aquifers and confining units, though the aquifers should have much higher effective recharge values than the confining units.

The faults could act as groundwater flow preferential pathways (along the fault wall face) or barriers (perpendicular to the fault wall face) in the study area. Previous studies have shown that the groundwater flow in the study area was compartmentalized. Studies by Preston and others (1996) showed that faulting had compartmentalized the Paleozoic aquifers especially near the outcrop area, which, in turn, restricted the lateral flow. Special cases do exist when one fault(s) crosses another one(s). In this case, the fault joints may act as preferential pathways. This should be implemented correctly in the numerical model.

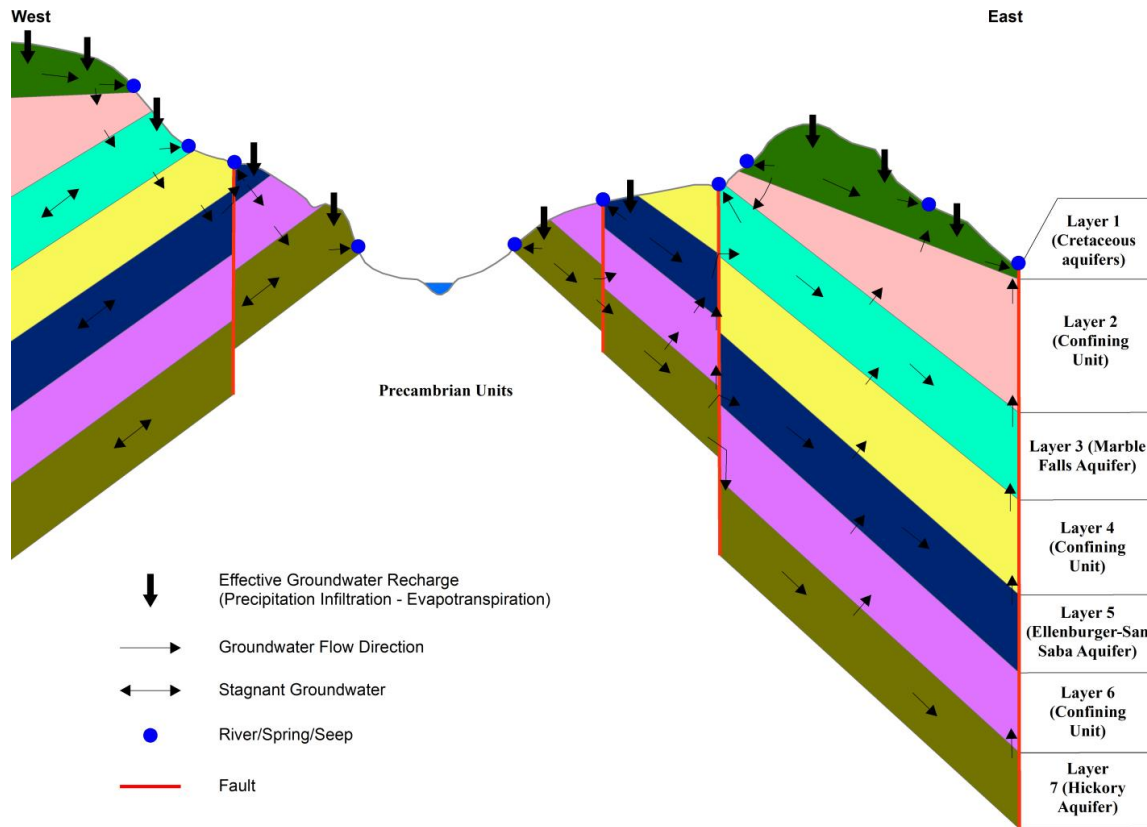


Figure 5.1.1 Schematic hydrogeologic cross section and groundwater flow of pre-development conditions.

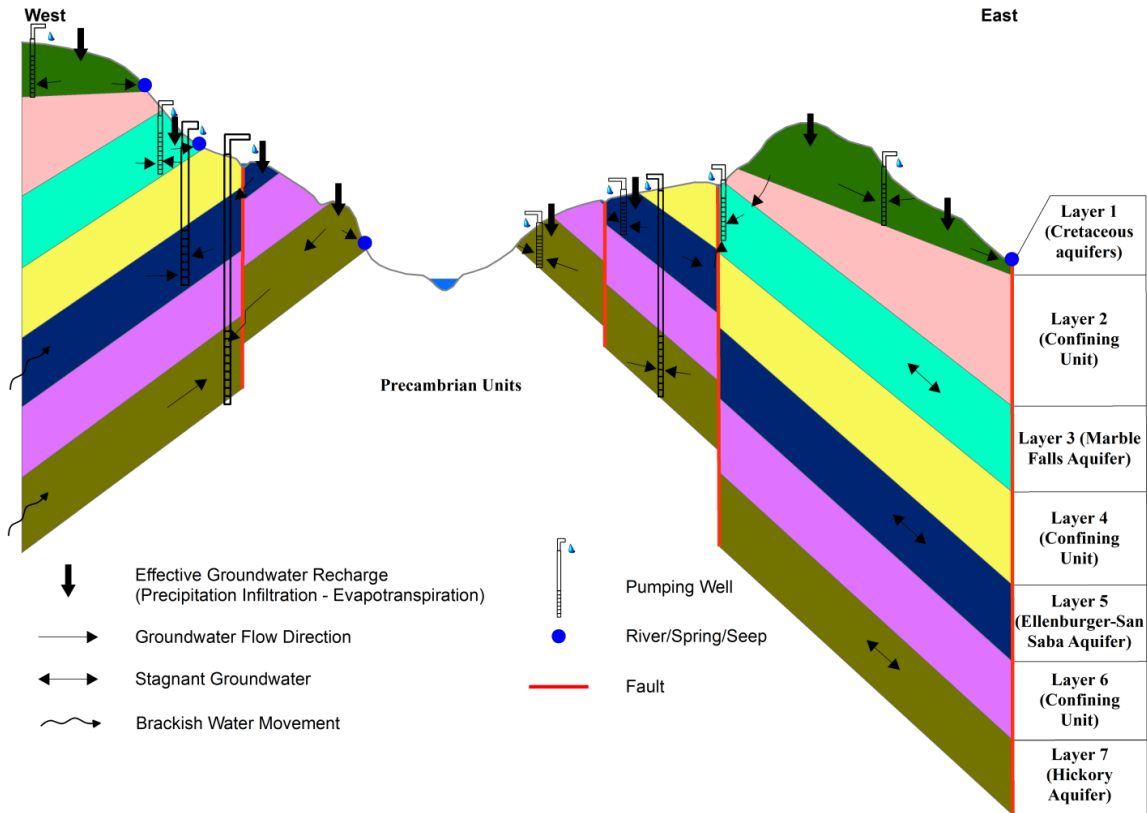


Figure 5.1.2 Schematic hydrogeologic cross section and groundwater flow of post-development conditions.

6.0 Future Improvements

Uncertainties exist due to the lack of data for certain areas and the complexity of the study area. These uncertainties are especially obvious to the east and downdip areas. Over the last year or so, more water well logs and driller reports have been collected and stored in the TWDB groundwater database. These wells are often shallow and can be used to minimize the uncertainties near the outcrop areas. More geophysical logs can be explored for the downdip areas so that the geologic structure and water quality can be better defined in the deep portion.

The interaction between the groundwater and lakes/reservoirs can be quantified using a mass balance approach. This approach requires the inflow and outflow components of a lake/reservoir to be known, such as flow from upstream, surface runoff, discharge to downstream, loss due to evaporation, and water withdrawal.

The characteristics of faults can be evaluated using tracer test and pump test. Tracer test can tell how fast groundwater flows along a fault and its connection with other faults. Pump test can be used to assess if a fault acts as a barrier by placing pumping well on one side and the observation well(s) on the other of the fault.

The TWDB will update the conceptual model if warranted by additional information through the continued stakeholder process and the development of the numerical model. If this occurs, the TWDB will inform the stakeholders.

Acknowledgements

This conceptual model cannot be done without the stakeholder participation. Many stakeholders provided valuable suggestions. These suggestions had been evaluated and incorporated into the conceptual model. The Llano Uplift groundwater availability model team would like to thank all of the stakeholders for your contributions to the development of this conceptual groundwater flow model.

Special thanks go to Mr. Paul Tybor of the Hill Country Underground Water Conservation District, Mr. Ron Fieseler of the Blanco-Pedernales Groundwater Conservation District, and Mr. Charles Schell and Mr. Mitchell Sodek of the Central Texas Groundwater Conservation District, who provided all the help they could during the data collection and the field trip. These data include water well logs, groundwater levels, and hydraulic test results, among others. In addition, we appreciate the cooperation and support from the Hickory Underground Water Conservation District No. 1 for providing funding for Dr. William Hutchison to participate directly with TWDB staff in the conceptualization and modeling phases of the project.

Mr. Roberto Anaya (TWDB) has been very helpful in the Cretaceous geology. His ideas certainly have made that part more readable. Last but not least, the appreciations go to our groundwater availability model section manager, Ms. Cindy Ridgeway, for her leadership and continuous supports (both technically and administratively) through the whole process.

References

- Alexander, Jr., W.H., Myers, B.N., Dale, O.C., 1964, Reconnaissance Investigation of the Ground-Water Resources of the Guadalupe, San Antonio, and Nueces River Basins, Texas. Texas Water Commission Bulletin 6409.
- Alexander, Jr., W.H. and Patman, J.H., 1969, Ground-Water Resources of Kimble County, Texas. Texas Water Development Board Report 95
- Alley, W.M., Reilly, T.E., and Franke, O.L., 1999, Sustainability of Groundwater Resources. U.S. Geological Survey Circular 1186.=
- Anaya, R., and Jones, I., 2009, Groundwater Availability Model for the Edwards-Trinity (Plateau) and Pecos Valley Aquifers of Texas. Texas Water Development Board Report 373, 113 p.
- Ardis, A.F. and Barker, R.A., 1993, Historical Saturated Thickness of the Edwards-Trinity Aquifer System and Selected Contiguous Hydraulically Connected Units, West-Central Texas. U.S. Geological Survey Water-Resources Investigation Report 92-4125.
- Ashworth, J.B., 1983, Ground-Water Availability of the Lower Cretaceous Formations in the Hill Country of South-Central Texas. Texas Department of Water Resources Report 273.
- Ashworth, J.B., Stein, W.G., Donnelly, A.C.A., Persky, K., and Jones, J.P., 2001, The Lower Trinity Aquifer of Bandera and Kerr Counties, Texas.
- Baker, R.C., Dale, O.C., and Baum, G.H., 1965, Ground-Water Conditions in Menard County, Texas. Texas Water Commission Bulletin 6519.
- Baker, B., Duffin, G., Flores, R., and Lynch, T., 1990, Evaluation of Water Resources in Part of Central Texas. Texas Water Development Board Report 319, 67 p.
- Barker, R.A. and Ardis, A.F., 1996, Hydrogeologic Framework of the Edwards-Trinity Aquifer System, West-Central Texas. U.S. Geological Survey Professional Paper 1421-B.
- Barker, R.A. and Ardis, A.F., 1992, Configuration of the Base of the Edwards-Trinity Aquifer System and Hydrogeology of the Underlying Pre-Cretaceous Rocks, West-Central Texas. U.S. Geological Survey Water-Resources Investigation Report 91-4071.
- Barker, R.A., Bush, P.W., and Baker, Jr., E.T., 1994, Geologic History and Hydrogeologic Setting of the Edwards-Trinity Aquifer System, West-Central Texas. U.S. Geological Survey Water-Resources Investigation Report 94-4039.
- Barnes, V.E., 1963, Correlation of Cambrian rocks in central Texas. The University of Texas at Austin, Bureau of Economic Geology, MM-6.
- Barnes, V.E. 1959, Stratigraphy of Pre-Simpson Paleozoic Subsurface Rocks of Texas and Southeast New Mexico. The University of Texas at Austin, Pub. 5924, 837 p.
- Barnes, V.E. and C. Bell, 1977, The Moore Hollow Group of Central Texas, The University of Texas at Austin, Bureau of Economic Geology Report of Investigation #88.
- Barnes, V.E., Cloud, P.E., Duncan, H., 1953, Upper Ordovician of Central Texas. Bulletin of American Association of Petroleum Geologists, Vol. 37, p. 1030-1043.

- Black, C.W., 1988, Hydrogeology of the Hickory Sandstone Aquifer, Upper Cambrian Riley Formation, Mason and McCulloch Counties, Texas. Thesis, The University of Texas at Austin, 195 p.
- Bluntzer, R.L., 1992, Evaluation of the Ground-Water Resources of the Paleozoic and Cretaceous Aquifers in the Hill Country of Central Texas. Texas Water Development Board Report 339, p. 183.
- Bradbury, K.R. and Rothschild, E.R., 1985, A Computerized Technique for Estimating the Hydraulic Conductivity of Aquifers from Specific Capacity Data. *Ground Water*, Vol. 23, Issue 2, p 240-246.
- Brown, J.B., 1980, Mesozoic History of the Llano Region, Texas. Guidebook to the Annual Field Trip of the West Texas Geological Society (October 19-21, 1980), Publication No. 80-73.
- Brune, G. and Duffin, G., 1983, Occurrence, Availability, and Quality of Ground Water in Travis County, Texas. Texas Department of Water Resources Report 276.
- Bruner, K.R. and Smosna, R., 2011, A Comparative Study of the Mississippian Barnett Shale, Fort Worth Basin, and Devonian Marcellus Shale, Appalachian Basin. U.S. Department of Energy DOE/NETL-2011/1478.
- Bureau of Economic Geology, 2013, Geologic Atlas of Texas.
- Bush, P.W., Ardis, A.F., and Wynn, K.H., 1993, Historical Potentiometric Surface of the Edwards-Trinity Aquifer System and Contiguous Hydraulically Connected Units, West-Central Texas. U.S. Geological Survey Water-Resources Investigation Report 92-4055.
- Bush, O.W., Ulery, R.L., and Rittmaster, R.L., 1994, Map Showing Dissolved Solids Concentrations and Hydrochemical Facies in Water of the Edwards-Trinity Aquifer System, West-Central Texas. U.S. Geological Survey Water-Resources Investigation Report 93-4126.
- Carrell, C.L. 2000, Structural influences on the North Hickory Aquifer, San Saba County, Texas. Thesis, Baylor University.
- Caughey, C.A., 1977, Deposition Systems in the Paluxy Formation (Lower Cretaceous), Northeast Texas-Oil, Gas, and Grounwater Resources. The University of Texas at Austin, Bureau of Economic Geology Geological Circular 77-8, 59 p.
- Christian, B. and Wuerch, D., 2012, Compilation of Results of Aquifer Tests in Texas. Texas Water Development Board Report 381, 106 p.
- Clark, I.D. and Fritz, P., 1997, Environmental Isotopes in Hydrogeology, Lewis Publishers and CRC Press, 328 p.
- Clement, T., Eshelman, D., King, J., Shaw, G., and Sneed, M., 1985, Analysis of the San Saba River Basin on the Hickory Sandstone Outcrop in Southeastern McCulloch County, Texas.
- Cornish, F.G., 1975, Tidally influenced deposits of the Hickory Sandstone, Cambrian, central Texas. Thesis, Univerisity of Texas at Austin.
- Cronin, J.G., Follett, C.R., Shafer, G.H., and Rettman, P.L., 1973, Reconnaissance Investigation of the Ground-Water Resources of the Brazos River Basin, Texas. Texas Water Commission Bulletin 6310.

- Damon, H.G., 1940, Cretaceous Conglomerate on the East Side of the Llano Uplift. Thesis, The State University of Iowa.
- Daniel B. Stephens & Associates, Inc., 2006, Aquifer Tests from County Availability Studies. Contract Report Prepared for TWDB under Contract Number 2005-483-554.
- Daniel B. Stephens & Associates, Inc., 2005, San Angelo Hickory Well Field Hydrogeologic Evaluation. Prepared for the City of San Angelo.
- DeCook, K.J., 1960, Geology and Ground-Water Resources of Hays County, Texas. Texas Board of Water Engineers Bulletin 6004.
- Dekker, F.E., 1966, Sedimentology of the Upper Cambrian Lion Mountain and Welge Sandstones, Central Texas. Thesis, The University of Texas at Austin, 135 p.
- DOMENICO, P. A. AND SCHWARTZ, F. W., 1997, Physical and Chemical Hydrogeology: John Wiley & Sons, New York, 506 p.
- Drapper, D.C., 1959, Hickory Sandstone Reservoir in Parts of Llano, Mason, San Saba, and McCulloch Counties, Texas.
- Duffin, G. and Musick, S.P., 1991, Evaluation of Water Resources in Bell, Burnet, Travis, Williamson and Parts of Adjacent Counties, Texas. Texas Water Development Board Report 326.
- Evans, D.S., 1974, Quality of Groundwater in Cretaceous Rocks of Williamson and Eastern Burnet Counties, Texas. Thesis, The University of Texas at Austin, 103 p.
- Ewing, T.E., 2004, Phanerozoic development of the Llano Uplift. pp. 25-37 in Tectonic history of southern Laurentia: A look at Mesoproterozoic, late-Paleozoic, and Cenozoic structures in central Texas. Austin Geological Society Field Trip Guidebook.
- Fisher, W.L. and Rodda, P.U., 1966, Nomenclature Revision of Basal Cretaceous Rocks between the Colorado and Red Rivers, Texas. The University of Texas at Austin, Bureau of Economic Geology Report of Investigations No. 58, 20p.
- Follett, C.R., 1973, Ground-Water Resources of Blanco County, Texas. Texas Water Development Board Report 174.
- Follett, C.R., 1956, Records of Water-Level Measurements in Hays, Travis, and Williamson Counties, Texas. Texas Board of Water Engineers Bulletin 5612.
- Fry, J., Xian, G., Jin, S., Dewitz, J., Homer, C., Yang, L., Barnes, C., Herold, N., and Wickham, J., 2011, Completion of the 2006 National Land Cover Database for the Conterminous United States, PE&RS, Vol. 77(9):858-864.
- George, P.G., Mace, R.E., and Rima P., 2011, Aquifers of Texas. Texas Water Development Board Report 380, p. 172.
- George, W.O., 1947, Ground-Water Conditions in the Vicinity of Mason, Mason County, Texas. U.S. Geological Survey Open-File Report 47-39.
- George, W.O., 1944, Water Supply for the City of San Saba, Texas. Texas Board of Water Engineers Miscellaneous Publication 244.

- Ging, P.B., Judd, L.J., and Wynn, K.H., 1997, Water-Quality Assessment of South-Central Texas – Occurrence and Distribution of Volatile Organic Compounds in Surface water and Ground water, 1983-94, and Implications for Future Monitoring. U.S. Geological Survey Water-Resources Investigation Report 97-4028.
- Goldich, S. and Parmelee, E., 1947, Physical and Chemical Properties of Ellenburger Rocks, Llano County, Texas. AAPG Bulletin Volume: 31 (1947), Issue: 11, p. 1982-2020.
- Heitmuller, F.T., and Reece, B.D., 2003, Database of Historical Documented Springs and Spring Flow Measurements in Texas. U.S. Geological Survey, Open-File Report 03-315.
- Hem, J.D., 1985, Study and Interpretation of the Chemical Characteristics of Natural Water. U.S. Geological Survey Water-Supply Paper 2254, 263 p.
- Hill, R.T., 1901, Geography and geology of the Black and Grand Prairies, Texas. U.S. Geological Survey, 21st Annual Report, pt. 7, 666 p.
- Hoh, A. and Hunt, B., 2004, Tectonic History of Southern Laurentia: A look at Mesoproterozoic, Late-Paleozoic and Cenozoic Structures in Central Texas. AGS Field Trip Guidebook 24.
- Holland, P.H. and Mendieta, H.B., 1965, Base-Flow Studies, Llano River, Texas: Quality and Quantity. Texas Water Commission Bulletin 6505.
- Hutchison, W.R., Jones, I.C., and Anaya, R., 2011, Update of the Groundwater Availability Model for the Edwards-Trinity (Plateau) and Pecos Valley Aquifers of Texas. Texas Water Development Board Report, 61 p.
- Hunt, B.B., Smith, B.A., Kromann, J., Wierman D.A., and Mikels, J.K., 2010, Compilation of pumping tests in Travis and Hays Counties, Central Texas. BSEACD Data Series Report 2010-0701, 86p.
- INTERA, Inc., Bureau of Economic Geology, and LBG-Guyton Associates, 2014, Updated Groundwater Availability Model of the Northern Trinity and Woodbine Aquifers Final Model Report, 990 p (August 2014).
- Kelley, V.A., Ewing, J., Jones, T.L., Young, S.C., Deeds, N., and Hamlin, S., 2014, Updated Groundwater Availability Model of the Northern Trinity and Woodbine Aquifers – Draft Final Model Report (May 2014), 984 p.
- Kier, R.S., 1988, Paleozoic Strata of the Llano region, Central Texas, pp. 351-360 in Hayward, O.T., eds., *Centennial Field Guide Volume 4: South-Central Section of the Geological Society of America*.
- Kier, R.S., 1980, Depositional History of the Marble Falls Formation of the Llano Region, Central Texas. Guidebook to the Annual Field Trip of the West Texas Geological Society (October 19-21, 1980), Publication No. 80-73.
- Kier, R.S., Brown, L.F., Jr., and McBride, E.F., 1979, The Mississippian and Pennsylvanian (Carboniferous) systems in the United States-Texas. U.S. Geological Survey Prof. Paper 1110-S, 45 p.
- Kirk, A., Groeneveld, D., Barz, D., Herring, J., and Murray, S., 2012, Groundwater Recharge Model: Calibration and Validation for Remote-Sensed Dual Coefficient (RDC) GMA 8 ET Estimation. TWDB Contract No. 1004831114, 164 p.

- Klemt, W.B., Perkins, R.D., and Alvarez, H.J., 1975, Ground-Water Resources of Part of Central Texas with Emphasis on the Antlers and Travis Peak Formations (Vol. 1). Texas Water Development Board Report 195, 26 p.
- Krause, S.J., 1996, Stratigraphic Framework, Facies Analysis, and Depositional History of the Middle to Late Cambrian Riley Formation, Central Texas. Thesis, The University of Texas at Austin, 172 p.
- Kreitler, C.W., Beach, J.A., O'Rourke, D., Symank, L., Bassett, R., Ewing, J., Kelley, V., 2013, Evaluation of Hydrochemical and Isotopic Data in Groundwater Management Areas 3 and 7. TWDB Contract Report.
- Kuniansky, E.L. and Holligan, K.Q., 1994, Simulations of Flow in the Edwards-Trinity Aquifer System and Contiguous Hydraulically Connected Units, West-Central Texas. U.S. Geological Survey Water-Resources Investigation Report 93-4039.
- Kuniansky, E. L., 1989, Precipitation, Streamflow, and Baseflow, in West-Central Texas, December 1974 through March 1977. U.S. Geological Survey Water-Resources Investigations Report 89-4208.
- Johnson, B., 2004, The Llano Uplift and Associated Pennsylvanian-Age Faults: an Overview And a Field Example of Faults Exposed at Hoover Point In the Backbone Ridge Graben. Pp. 62-91 in *Tectonic History of Southern Laurentia: a Look at Mesoproterozoic, Late-Paleozoic, and Cenozoic Structures in Central Texas*. Austin Geological Society Field Trip Guidebook.
- Jones, I.C., Anaya, R., and Wade, S.C., 2009, Groundwater Availability Model: Hill Country Portion of the Trinity Aquifer of Texas. Texas Water Development Board Report 377.
- Larkin T.J., and Bomar, G.W., 1983, Climatic atlas of Texas. Texas Department of Water Resources Report LP-192.
- LBG-Guyton Associates, 2007, Groundwater Availability Model for the Ellenburger Aquifer in Southeast Gillespie County, Texas. Prepared for Hill Country Underground Water Conservation District and the City of Fredericksburg, 67 p.
- Ledbetter, H.J., Jr., 1976, Stratigraphy of the Sycamore Formation, Central Texas. Thesis, Baylor University, 85 p.
- Long, L.E., 2004, Middle to Late Cambrian Nonconformity in the Llano Uplift. Pp. 59-61 in *Tectonic history of southern Laurentia: A look at Mesoproterozoic, late-Paleozoic, and Cenozoic structures in Central Texas*. Austin Geological Society Field Trip Guidebook.
- Lower Colorado River Authority, 1992, Water Supply and Demand Assessment of Burnet County, 103 p.
- Lurry, D.L. and Pavlicek, D.J., 1991, Withdrawals from the Edwards-Trinity Aquifer System and Contiguous Hydraulically Connected Units, West-Central Texas, December 1974 through March 1977. U.S. Geological Survey Water-Resources Investigation Report 91-4021.
- Mace, R.E., Angle, E.S., and Mullican, III, W.F., 2004, Aquifers of the Edwards Plateau. Texas Water Development Board Report 360.
- Mace, R.E., Chowdhury, A.H., Anaya, R., and Way, S.C., 2000, Groundwater Availability of the Trinity Aquifer, Hill Country Area, Texas: Numerical Simulations through 2050. Texas Water Development Board Report 353.

- Mason, C.C., 1961, Ground-Water Geology of the Hickory Sandstone Member of the Riley Formation, McCulloch County, Texas. Texas Board of Water Engineers Bulletin 6017.
- McBride, E.F., Abdel-Wahab, A.A., and Milliken, K.L., 2002, Petrography and Diagenesis of Half-Billion-Year-Old Cratonic Sandstone (Hickory) Llano Region, Texas: The University of Texas at Austin, Bureau of Economic Geology, Report of Investigation, No. 264, 74 p.
- McFarland, G.J., 1984, The Structure of Carboniferous Rocks on the Llano Uplift. Thesis, Baylor University, 144 p.
- McGhee, R.V., 1963, PreCambrian Geology of the Southeastern Llano Uplift, Texas. Dissertation, The University of Texas at Austin.
- McMahan, C. A., Frye, R.G., and Brown, K.L., 1984, The Vegetation Type of Texas including Cropland (http://www.tpwd.texas.gov/publications/pwdpubs/media/pwd_bn_w7000_0120_01.pdf).
- Morey, P.S., 1955, Post-Ellenburger Beds, Brown, Coke, Coleman and Runnels Counties, Texas. The University of Texas at Austin, Bureau of Economic Geology, MM-26.
- Mosher, S., 2004, Tectonic History of the Llano Uplift. pp. 38-46 in Tectonic History of Southern Laurentia: A look at Mesoproterozoic, Late-Paleozoic, and Cenozoic Structures in Central Texas. Austin Geological Society Field Trip Guidebook.
- Mount, J.R., 1963, Investigation of Ground-Water Resources near Fredericksburg, Texas. Texas Water Commission Memorandum Report 63-03.
- Mount, J.R., 1962, Ground-Water Conditions in the Vicinity of Burnet, Texas. Texas Water Commission Memorandum Report No. 62-01.
- Mount, J.R., Rayner, F.A., Shamburger, Jr., V.M., Peckham, R.C., and Osborne, Jr., F.L., 1967, Reconnaissance Investigation of the Ground-Water Resources of the Colorado River Basin, Texas. Texas Water Development Board Report 51.
- Myers, B.N., 1969, Compilation of Results of Aquifer Tests in Texas. Texas Water Development Board Report 98, 532 p. Namy, J.M., 1969, Stratigraphy of the Marble Falls Group, Southeast Burnet County, Texas. Dissertation, The University of Texas at Austin, 385 p.
- National Climatic Data Center, 2014, Monthly Observational Data at <http://gis.ncdc.noaa.gov/map/viewer/#app=cdo&cfg=cdo&theme=monthly&layers=1>.
- National Weather Service, 2013, Texas Climate Divisions (http://www.nass.usda.gov/Statistics_by_State/Texas/Charts_&_Maps/cwmap1.htm). Climate Division Map can be downloaded at http://www.nass.usda.gov/Statistics_by_State/Texas/Charts_&_Maps/cwmap.htm.
- Paige, S., 1912, Description of the Llano and Burnet Quadrangles. U.S. Geological Survey Geologic Atlas, Llano-Burnet Folio, No. 183, 16 p.
- Pettigrew, Jr., R.J., 1991, Geology and Flow Systems of Hickory Aquifer, San Saba County, Texas. Baylor Geological Studies Bulletin No. 51, 51 p.
- Plummer, F.B., 1950, The Carboniferous Rocks of the Llano Region of Central Texas. The University of Texas at Austin, Bureau of Economic Geology, Pub. 4329, 236 p.

- Preston, R.D., Pavilcek, D.J., Bluntzer, R.L., and Derton, J., 1996, The Paleozoic and Related Aquifers of Central Texas. Texas Water Development Board Report 346, p. 97.
- PRISM Climate Group, 2013, Oregon State University, <http://prism.oregonstate.edu>.
- Reeves, R.D., 1969, Ground-Water Resources of Kerr County, Texas. Texas Water Development Board Report 102.
- Reeves, R.D., 1967, Ground-Water Resources of Kendall County, Texas. Texas Water Development Board Report 60.
- Reeves, R.D. and Lee, F.C., 1962, Ground-Water Geology of Bandera County, Texas. Texas Water Commission Bulletin 6210.
- Ridgeway, C. and Petrini, H., 1999, Changes in Groundwater Conditions in the Edwards and Trinity Aquifers, 1987-1997, for the Portions of Bastrop, Bell, Burnet, Lee, Milam, Travis, and Williamson Counties, Texas. Texas Water Development Board Report 350.
- Ruggiero, R., 2014, Gillespie County 3D Structural Model and Sub-regional Area Structure Model at <http://www.hcuwcd.org/Gillespie%20County%203D%20Structural%20Model.htm>.
- R.W. Harden & Associates, Inc., Freese & Nichols, Inc., HDR Engineering, Inc., L.B.G. Guyton Associates, U.S. Geological Survey, and Dr. Joe Yelderman, Jr., 2004. Northern Trinity / Woodbine Aquifer Groundwater Availability Model: Contract report to the Texas Water Development Board, 192 p.
- Scanlon, B., Keese, K., Bonal, N., Deeds, N., Kelley, V., and Litvak, M., 2005, Evapotranspiration estimates with emphasis on groundwater evapotranspiration in Texas: prepared for the TWDB.
- Schenk, H.J. and Jackson, R.B., 2003, A Global Database of Ecosystem Root Profiles (ERP).
- Sellards, E.H., Adkins, W.S., and Plummer, F.B., 1932, The Geology of Texas, Vol. 1, Stratigraphy: The University of Texas Bulletin No. 3232, 1007 p.
- Sharp, J., Baker, T, Black, J., LaFare, J., Morton, S., Snyder, F., and Tomich, H., 1985, Potential Recharge to the Hickory Sandstone from the Katemcy Creek Watershed.
- Slade, Jr., R.M., Bentley, J.T., and Michaud, D., 2002, Results of Streamflow Gain-Loss Studies in Texas, with Emphasis on Gains from and Losses to Major and Minor Aquifers, Texas, 2000. U.S. Geological Survey, Open-File Report 02-068.
- Smith, G.E., 1974, Depositional Systems, San Angelo Formation (Permian), North Texas; Facies Control of Red-Bed Copper Mineralization. The University of Texas at Austin, Bureau of Economic Geology Report Investigation 80, 74 p.
- Standen, A. and Ruggiero, R., 2007, Llano Uplift Aquifers Structure and Stratigraphy, Prepared for Texas Water Development Board Contract Number 0604830614 (November 5, 2007), p. 78.
- Sundstrom, R.W., Broadhurst, W.L., and Dwyer, B.C., 1949, Public Water Supplies in Central and North-Central Texas. The U.S. Geological Survey Water-Supply Paper 1069.
- Sundstrom, R.W. and George, W.O., 1942, Water Resources in the Vicinity of Melvin, McCulloch County, and Menard, Menard County, Texas. U.S. Geological Survey Open File Report.

- Thornthwaite, C. W., 1931, The Climates of North America According to a New Classification: Geographical Review, 21, p. 633–635.
- TNRIS, 2014, Maps & Data at http://www.tnris.org/get-data?quicktabs_maps_data=1#quicktabs_maps_data.
- TWDB, 2014a, Well Information/Groundwater Data at http://wiid.twdb.state.tx.us/ims/wwm_drl/viewer.htm, (accessed February 2014).
- TWDB, 2014b, Geologic Atlas of Texas from the Bureau of Economic Geology of the University of Texas at Austin at <http://www.twdb.state.tx.us/groundwater/aquifer/gat/> (accessed in January 2014).
- TWDB, 2013a, Maps & GIS data, GIS data, Major aquifers at <http://www.twdb.texas.gov/mapping/gisdata.asp>.
- TWDB, 2013b, Maps & GIS data, GIS data, Minor aquifers at <http://www.twdb.texas.gov/mapping/gisdata.asp>.
- TWDB, 2013c, Maps & GIS data, GIS data, River Authorities and Special Law Districts at <http://www.twdb.texas.gov/mapping/gisdata.asp>.
- TWDB, 2013d, Maps & GIS data, GIS data, Regional Water Planning Areas at <http://www.twdb.texas.gov/mapping/gisdata.asp>.
- TWDB, 2013e, Maps & GIS data, GIS data, Groundwater Conservation Districts at <http://www.twdb.texas.gov/mapping/gisdata.asp>.
- TWDB, 2013f, Maps & GIS data, GIS data, Groundwater Management Areas at <http://www.twdb.texas.gov/mapping/gisdata.asp>.
- TWDB, 2013g, Maps & GIS data, GIS data, Priority Groundwater Management Areas - PGMA at <http://www.twdb.texas.gov/mapping/gisdata.asp>.
- TWDB, 2013h, Precipitation & Evaporation Data at <https://www.twdb.texas.gov/surfacewater/conditions/evaporation/index.asp>, (accessed December 2013).
- TWDB, 2012a, 2012 State Water Plan at <http://www.twdb.texas.gov/waterplanning/swp/2012/>.
- TWDB, 2012b, Brackish Resources Aquifer Characterization System (BRACS) Database at <http://www.twdb.texas.gov/innovativewater/bracs/database.asp>. (accessed December 2012)
- Tybor, P. 1993. Cross section A - A', Gillespie County.
- U.S. Census Bureau, 2010, TIGER/Line® Shapefiles Pre-joined with Demographic Data at <https://www.census.gov/geo/maps-data/data/tiger-line.html>.
- U.S. Department of Agriculture, 2014, National Agricultural Statistics Service, 2013 CropScape-Cropland Data Layer. <http://nassgeodata.gmu.edu/CropScape/>.
- U.S. Environmental Protection Agency, 2013, Primary Distinguishing Characteristics of Level III Ecoregions of the Continental United States. http://www.epa.gov/wed/pages/ecoregions/na_eco.htm#Level III.

- U.S. Geological Survey, 2014, USGS Surface-Water Historical Instantaneous Data for the Nation: Build Time Series at http://waterdata.usgs.gov/nwis/uv/?referred_module=sw.
- Walker, E.L., 1967, Occurrence and Quality of Groundwater in Coleman county, Texas. TWDB Report 57.
- Watson, W.G., 1980, Paleozoic Stratigraphy of the Llano Uplift Area: a Review in Geology of the Llano Region, Central. Guidebook to the Annual Field Trip of the West Texas Geological Society (October 19-21, 1980), Publication No. 80-73.
- Wermund, 1996, Physiography of Texas: The University of Texas at Austin, Bureau of Economic Geology. <http://www.beg.utexas.edu/UTopia/images/pagesizemaps/physiography.pdf>.
- Wet Rock Groundwater Services, L.L.C., 2013, Vistas at Round Mountain Subdivision: Blanco County Groundwater Availability Certification for Platting (for Lone Start Land Partners).
- Wierman, D.A., Broun, A.S., and Hunt, B.B., 2010, Hydrogeologic Atlas of the Hill Country Trinity Aquifer, Blanco, Hays and Travis Counties, Central Texas.
- Wilson, W.F., 2008, Hydrogeology of Kerr County.
- Wilson, W.F., 1962, Sedimentary Petrology and Sedimentary Structures of the Cambrian Hickory Sandstone Member, Central Texas. Dissertation, The University of Texas at Austin, 344 p.
- Winston, B.A. II, 1963, Stratigraphy and Carbonate Petrology of the Marble Falls Formation, Mason and Kimble Counties, Texas. Dissertation, The University of Texas at Austin, p. 120 p.
- Young, S.C., Meng, J., Pinkard J., and Lupton, D., 2012, Aquifer Tests and Related Well Information from Public Water Supply Wells in Groundwater Management Area 8. Contract Report Prepared by INTERA for TWDB under Contract Number 1004831116.
- Young, S.C., Doherty, J., Budge, T., and Deeds, N., 2010, Application of PEST to Re-Calibrate the Groundwater Availability Model for the Edwards-Trinity (Plateau) and Pecos Valley Aquifers, 229 p (April 2010).

Appendix A

Table A.1 Summary of springs in study area with at least one measurement (based on Heitmuller and Reece (2003)).

County	State Well Number	Maximum Flow (gallon per minute)	Date of Maximum Flow	Minimum Flow (gallon per minute)	Date of Minimum Flow	Number of Measurements	Geologic Formation
Blanco	5761802	1	8/19/1968	1	8/19/1968	1	Cretaceous Units
Blanco	5761604	2	6/6/1938	2	6/6/1938	1	Cretaceous Units
Blanco	5761304	15	1/1/1938	15	1/1/1938	1	Cretaceous Units
Blanco	5761201	84	1/1/1941	84	1/1/1941	1	Cretaceous Units
Blanco	5760303	84	1/1/1941	84	1/1/1941	1	Cretaceous Units
Blanco	5761225	426	3/7/1962	256	9/8/1952	2	Unknown
Blanco	5762209	50	5/20/1969	50	5/20/1969	1	Cretaceous Units
Blanco	5753802	20	1/1/1961	20	1/1/1961	1	Cretaceous Units
Blanco	5753709	2	1/1/1941	2	1/1/1941	1	Cretaceous Units
Blanco	5754401	18	1/1/1938	18	1/1/1938	1	Cretaceous Units
Blanco	5755103	0.5	1/1/1938	0.5	1/1/1938	1	Cretaceous Units
Blanco	5753106	4	1/1/1968	4	1/1/1968	1	Cretaceous Units
Blanco	5753215	50	5/21/1969	50	5/21/1969	1	Cretaceous Units
Blanco	5753304	10	1/1/1968	10	1/1/1968	1	Cretaceous Units
Blanco	5753318	4	1/1/1993	4	1/1/1993	1	Cretaceous Units
Blanco	5755107	25	1/1/1969	25	1/1/1969	1	Cretaceous Units
Blanco	5752319	1	9/1/1992	1	9/1/1992	1	Elleburger-San Saba
Blanco	5753317	3	---	3	---	1	Cretaceous Units
Blanco	5745601	1,661	5/28/1968	58.3	8/4/1938	2	Elleburger-San Saba
Blanco	5746101	10	1/1/1938	10	1/1/1938	1	Elleburger-San Saba
Blanco	5745303	6	1/1/1941	6	1/1/1941	1	Cretaceous Units
Blanco	5737904	2	1/1/1941	2	1/1/1941	1	Cretaceous Units
Blanco	5737703	15	1/1/1941	15	1/1/1968	2	Cretaceous Units
Blanco	5738407	5	1/1/1941	5	1/1/1941	1	Cretaceous Units
Burnet	5738302	790.9	7/25/1940	790.9	7/25/1940	1	Unknown
Burnet	5738303	26.9	6/7/1938	9	7/25/1940	2	Unknown
Burnet	5730801	200	---	200	---	1	Elleburger-San Saba
Burnet	5730908	80.8	7/25/1940	80.8	7/25/1940	1	Unknown
Burnet	5721605	150	1/1/1987	150	1/1/1987	1	Elleburger-San Saba
Burnet	5722202	5	1/1/1961	5	1/1/1961	1	Elleburger-San Saba
Burnet	5723103	60	1/1/1961	60	1/1/1961	1	Elleburger-San Saba

Table A.1 Summary of springs in study area with at least one measurement (based on Heitmuller and Reece (2003)).

County	State Well Number	Maximum Flow (gallon per minute)	Date of Maximum Flow	Minimum Flow (gallon per minute)	Date of Minimum Flow	Number of Measurements	Geologic Formation
Burnet	5723102	401	1/1/1961	401	1/1/1961	1	Elleburger-San Saba
Burnet	5722301	310	1/1/1961	310	1/1/1961	1	Elleburger-San Saba
Burnet	5714902	40	1/1/1961	40	1/1/1961	1	Elleburger-San Saba
Burnet	5714801	10	1/1/1961	10	1/1/1961	1	Elleburger-San Saba
Burnet	5714911	435	1/1/1961	435	1/1/1961	1	Elleburger-San Saba
Burnet	5715709	1	1/1/1961	1	1/1/1961	1	Elleburger-San Saba
Burnet	5714903	5	1/1/1961	5	1/1/1961	1	Elleburger-San Saba
Coleman	4238502	5	11/14/1933	5	11/14/1933	1	Unknown
Coleman	4236201	4	10/22/1933	4	10/22/1933	1	Unknown
Gillespie	5656803	480	1/1/1970	480	1/1/1970	1	Cretaceous Units
Gillespie	5656903	3	3/27/1936	3	3/27/1936	1	Unknown
Gillespie	5656403	5	1/1/1969	5	1/1/1969	1	Cretaceous Units
Gillespie	5655108	20	1/1/1960	20	1/1/1960	1	Cretaceous Units
Gillespie	5655110	50	3/17/1936	50	3/17/1936	1	Unknown
Gillespie	5655101	310	1/1/1969	310	1/1/1969	1	Cretaceous Units
Gillespie	5647701	1,000	2/13/1936	900	1/1/1960	2	Cretaceous Units
Gillespie	5648406	2.5	1/1/1969	2.5	1/1/1969	1	Cretaceous Units
Gillespie	5648405	12.5	1/1/1969	12.5	1/1/1969	1	Cretaceous Units
Gillespie	5646610	3	2/19/1936	3	2/19/1936	1	Unknown
Gillespie	5742309	4	2/20/1936	4	2/20/1936	1	Unknown
Gillespie	5742103	18	---	18	---	1	Cretaceous Units
Gillespie	5734102	10	1/1/1989	10	1/1/1989	1	Unknown
Gillespie	5734101	2	1/1/1989	2	1/1/1989	1	Unknown
Gillespie	5639304	400	1/1/1984	300	3/4/1936	2	Elleburger-San Saba
Gillespie	5640202	300	3/6/1936	300	3/6/1936	1	Unknown
Hays	5755703	1	1/20/1954	1	1/20/1954	1	Unknown
Hays	5755503	1	11/22/1950	1	11/22/1950	1	Unknown
Hays	5755502	3	11/20/1950	3	11/20/1950	1	Unknown
Hays	5755302	7	12/19/1950	7	12/19/1950	1	Unknown
Kendall	6804203	25	1/1/1964	25	1/1/1964	1	Cretaceous Units
Kendall	6804201	25	1/1/1964	15	1/1/1975	2	Cretaceous Units

Table A.1 Summary of springs in study area with at least one measurement (based on Heitmuller and Reece (2003)).

County	State Well Number	Maximum Flow (gallon per minute)	Date of Maximum Flow	Minimum Flow (gallon per minute)	Date of Minimum Flow	Number of Measurements	Geologic Formation
Kendall	5760802	50	1/1/1964	50	1/1/1964	1	Cretaceous Units
Kendall	5760903	5	1/1/1964	5	1/1/1964	1	Cretaceous Units
Kendall	5760902	2	1/1/1964	2	1/1/1964	1	Cretaceous Units
Kendall	5760901	10	1/1/1965	10	1/1/1965	1	Cretaceous Units
Kendall	5760604	40	1/1/1975	20	1/1/1965	2	Cretaceous Units
Kendall	5759401	10	8/4/1965	10	8/25/1965	3	Cretaceous Units
Kendall	5757303	2	2/7/1940	2	4/1/1964	2	Cretaceous Units
Kendall	5757302	45	4/1/1965	35	8/1/1965	2	Cretaceous Units
Kendall	5758101	8	1/1/1965	8	1/1/1965	1	Cretaceous Units
Kerr	5654402	1,113	5/29/2002	500	1/1/1966	13	Cretaceous Units
Kerr	5654703	2,863	5/29/2002	2,149.75	6/6/2001	13	Unknown
Kerr	6907801	15	3/15/1967	15	3/15/1967	1	Cretaceous Units
Kerr	6907501	3	3/15/1967	3	3/15/1967	1	Cretaceous Units
Kerr	6907401	55	3/15/1967	55	3/15/1967	1	Cretaceous Units
Kerr	6907105	30	9/15/1966	30	9/15/1966	1	Unknown
Kerr	6907104	10	9/15/1966	10	9/15/1966	1	Cretaceous Units
Kerr	6907201	15	9/15/1966	15	9/15/1966	1	Cretaceous Units
Kerr	5662803	30	5/4/1966	30	5/4/1966	1	Cretaceous Units
Kerr	5662802	50	5/4/1966	50	5/4/1966	1	Cretaceous Units
Kerr	5663406	6	12/2/1966	6	12/2/1966	1	Cretaceous Units
Kerr	5662603	50	12/1/1966	50	12/1/1966	1	Cretaceous Units
Kerr	5661504	25	4/12/1967	25	4/12/1967	1	Cretaceous Units
Kerr	5661402	25	4/12/1976	25	4/12/1976	1	Cretaceous Units
Kerr	5664501	15	6/15/1966	15	6/15/1966	1	Cretaceous Units
Kerr	5664502	100	6/15/1966	100	6/15/1966	1	Cretaceous Units
Kerr	5757502	50	2/23/1967	50	2/23/1967	1	Cretaceous Units
Kerr	5757501	50	2/23/1967	50	2/23/1967	1	Cretaceous Units
Kerr	5662106	10	4/11/1967	10	4/11/1967	1	Cretaceous Units
Kerr	5757206	20	---	20	---	1	Unknown
Kerr	5757204	1	2/23/1967	1	2/23/1967	1	Cretaceous Units
Kerr	5662103	75	4/11/1967	75	4/11/1967	1	Cretaceous Units
Kerr	5662102	3	4/11/1967	3	4/11/1967	1	Cretaceous Units
Kerr	5662105	75	4/11/1967	75	4/11/1967	1	Cretaceous Units
Kerr	5662101	150	4/11/1967	150	4/11/1967	1	Cretaceous Units
Kerr	5664107	9	11/10/1966	9	11/10/1966	1	Cretaceous Units
Kerr	5664106	15	11/10/1966	15	11/10/1966	1	Cretaceous Units

Table A.1 Summary of springs in study area with at least one measurement (based on Heitmuller and Reece (2003)).

County	State Well Number	Maximum Flow (gallon per minute)	Date of Maximum Flow	Minimum Flow (gallon per minute)	Date of Minimum Flow	Number of Measurements	Geologic Formation
Kerr	5664108	200	10/10/1966	200	10/10/1966	1	Cretaceous Units
Kerr	5757203	5	2/23/1967	5	2/23/1967	1	Cretaceous Units
Kerr	5664105	2	11/10/1966	2	11/10/1966	1	Cretaceous Units
Kerr	5757101	65	2/23/1967	Dry	1/1/1956	11	Cretaceous Units
Kerr	5664103	18	11/10/1966	18	11/10/1966	1	Cretaceous Units
Kerr	5664104	100	11/10/1966	100	11/10/1966	1	Cretaceous Units
Kerr	5664102	90	11/10/1966	90	11/10/1966	1	Cretaceous Units
Kerr	5656802	10	11/8/1966	10	11/8/1966	1	Cretaceous Units
Kerr	5654701	15	3/2/1967	15	3/2/1967	1	Cretaceous Units
Kerr	5654802	10	8/31/1966	10	8/31/1966	1	Cretaceous Units
Kerr	5654403	2,500	1/1/1966	2,500	1/1/1966	1	Cretaceous Units
Kimble	5643602	3,800	4/21/1966	3,800	4/21/1966	1	Cretaceous Units
Kimble	5643603	1,000	4/21/1966	1,000	4/21/1966	1	Cretaceous Units
Kimble	5643305	25	4/26/1966	25	4/26/1966	1	Cretaceous Units
Kimble	5645302	290	7/25/1966	290	7/25/1966	1	Cretaceous Units
Kimble	5644103	600	4/25/1966	600	4/25/1966	1	Cretaceous Units
Kimble	5644104	75	4/25/1966	75	4/25/1966	1	Cretaceous Units
Kimble	5645303	3	7/25/1966	3	7/25/1966	1	Cretaceous Units
Kimble	5634806	25	8/2/1966	25	8/2/1966	1	Cretaceous Units
Kimble	5634705	25	8/2/1966	25	8/2/1966	1	Cretaceous Units
Kimble	5638502	10.5	---	1.5	7/26/1966	2	Cretaceous Units
Kimble	5628901	2	12/9/1965	2	12/9/1965	1	Cretaceous Units
Kimble	5626602	1	3/17/1966	1	3/17/1966	1	Cretaceous Units
Kimble	5626601	3	3/17/1966	3	3/17/1966	1	Cretaceous Units
Kimble	5626504	5	4/14/1966	5	4/14/1966	1	Cretaceous Units
Kimble	5626305	25	4/16/1966	25	4/16/1966	1	Cretaceous Units
Kimble	5626304	10	3/23/1966	10	3/23/1966	1	Cretaceous Units
Kimble	5625303	1	8/1/1966	1	8/1/1966	1	Cretaceous Units
Kimble	5626113	5	4/16/1966	5	4/16/1966	1	Cretaceous Units
Kimble	5628302	15	10/15/1965	15	10/15/1965	1	Elleburger-San Saba
Kimble	5618901	25	3/23/1966	25	3/23/1966	1	Cretaceous Units
Kimble	5621701	15	7/29/1966	15	7/29/1966	1	Elleburger-San Saba
Kimble	5618903	10	5/16/1966	10	5/16/1966	1	Cretaceous Units
Kimble	5619805	2	---	2	---	1	Cretaceous Units
Kimble	5619501	25	3/21/1966	25	3/21/1966	1	Cretaceous Units

Table A.1 Summary of springs in study area with at least one measurement (based on Heitmuller and Reece (2003)).

County	State Well Number	Maximum Flow (gallon per minute)	Date of Maximum Flow	Minimum Flow (gallon per minute)	Date of Minimum Flow	Number of Measurements	Geologic Formation
Kimble	5619503	600	7/13/1966	600	7/13/1966	1	Cretaceous Units
Lampasas	4163510	1,661	12/1/1909	89.76	1/17/1973	82	Cretaceous Units
Lampasas	4161603	600	1/1/1970	600	1/1/1970	1	Elleburger-San Saba
Lampasas	4163505	3,321.12	12/1/1909	1,184.83	9/24/1931	2	Marble Falls
Lampasas	4163521	107.7	9/24/1931	107.7	9/24/1931	1	Unknown
Lampasas	4163501	3,096.72	1/21/1924	600	1/1/1970	2	Cretaceous Units
Llano	5727601	3	1/1/1961	3	1/1/1961	1	Hickory
Llano	5727602	10	1/1/1961	10	1/1/1961	1	Hickory and other cambrian
Llano	5725502	7.5	1/1/1993	7.5	1/1/1993	1	Unknown
Llano	5720801	2	1/1/1961	2	1/1/1961	1	Marble Falls
Llano	5702712	12.5	1/1/1987	12.5	1/1/1987	1	Hickory
Llano	5704701	188.5	7/23/1940	188.5	7/23/1940	1	Unknown
Llano	5702713	8.5	1/1/1987	8.5	1/1/1987	1	Elleburger-San Saba
Llano	5705705	250	1/1/1989	250	1/1/1989	1	Elleburger-San Saba
Mason	5631901	30	---	30	---	1	Unknown
Mason	5629901	5	---	5	---	1	Elleburger-San Saba
Mason	5629504	3	---	3	---	1	Unknown
Mason	5630401	3	---	3	---	1	Unknown
Mason	5630201	300	---	300	---	1	Other
Mason	5630301	5	---	5	---	1	Unknown
Mason	5630101	619	1/1/1961	619	1/1/1961	1	Elleburger-San Saba
Mason	5622804	2	---	2	---	1	Unknown
Mason	5622501	3	---	3	---	1	Unknown
Mason	5622301	30	---	30	---	1	Unknown
Mason	5623122	13.5	---	13.5	---	1	Unknown
Mason	5613805	20	---	20	---	1	Unknown
Mason	5616401	10	---	10	---	1	Unknown
Mason	5615308	15	---	15	---	1	Unknown
Mason	5616103	20	---	20	---	1	Unknown
Mason	5608905	40	1/1/1939	40	11/7/1939	2	Hickory
Mason	5608910	10	---	10	---	1	Unknown
Mason	5701713	40	---	40	---	1	Unknown
Mason	5608417	4	---	4	---	1	Unknown

Table A.1 Summary of springs in study area with at least one measurement (based on Heitmuller and Reece (2003)).

County	State Well Number	Maximum Flow (gallon per minute)	Date of Maximum Flow	Minimum Flow (gallon per minute)	Date of Minimum Flow	Number of Measurements	Geologic Formation
McCulloch	5606320	Dry	1/1/1987	Dry	1/1/1987	1	Other
McCulloch	5606309	15	1/1/1987	15	1/1/1987	1	Hickory
McCulloch	5606310	Dry	1/1/1987	Dry	1/1/1987	1	Hickory
McCulloch	4262904	1,000	1/1/1987	1,000	1/1/1987	1	Elleburger-San Saba
McCulloch	4262806	150	1/1/1987	150	1/1/1987	1	Elleburger-San Saba
McCulloch	4263710	450	1/1/1987	450	1/1/1987	1	Elleburger-San Saba
McCulloch	4262906	650	1/1/1987	650	1/1/1987	1	Elleburger-San Saba
McCulloch	4262908	805	1/1/1987	805	1/1/1987	1	Elleburger-San Saba
Menard	5619106	15	---	15	---	1	Cretaceous Units
Menard	5612910	2	1/1/1990	2	1/1/1990	1	Cretaceous Units
Menard	5611602	20	---	20	---	1	Cretaceous Units
Menard	5611402	30	---	30	---	1	Cretaceous Units
Menard	5611401	10	---	10	---	1	Cretaceous Units
Menard	5611202	15	---	15	---	1	Cretaceous Units
Menard	5601603	15	---	15	---	1	Cretaceous Units
Menard	5602404	5	---	5	---	1	Cretaceous Units
Menard	5602207	40	---	40	---	1	Cretaceous Units
San Saba	4151401	9,245	8/13/2002	2,150	1/1/1989	138	Marble Falls/ Ellenburger-San Saba
San Saba	5701509	2	11/7/1934	2	11/7/1934	1	Unknown
San Saba	5705401	1,943.30	2/26/1939	1588.75	4/25/1962	4	Elleburger-San Saba
San Saba	5703603	4	9/21/1934	4	9/21/1934	1	Unknown
San Saba	5701303	1.5	12/8/1934	1.5	12/8/1934	1	Unknown
San Saba	5703312	4.5	1/2/1935	4.5	1/2/1935	1	Unknown
San Saba	5702304	1,153.40	10/29/1934	71.8	2/12/1957	5	Unknown
San Saba	5703308	1	9/20/1934	1	9/20/1934	1	Hickory
San Saba	5608201	13.5	3/9/1935	13.5	3/9/1935	1	Other
San Saba	5705101	664.2	2/26/1939	135	1/1/1989	3	Elleburger-San Saba
San Saba	4161701	480.2	2/26/1939	12	1/1/1989	3	Elleburger-San Saba
San Saba	4264802	175	3/9/1935	Dry	1/1/1989	2	Elleburger-San Saba
San Saba	4161702	12	1/1/1989	12	1/1/1989	1	Elleburger-San

Table A.1 Summary of springs in study area with at least one measurement (based on Heitmuller and Reece (2003)).

County	State Well Number	Maximum Flow (gallon per minute)	Date of Maximum Flow	Minimum Flow (gallon per minute)	Date of Minimum Flow	Number of Measurements	Geologic Formation
							Saba
San Saba	4264804	17.5	3/9/1935	11	1/1/1989	2	Elleburger-San Saba
San Saba	4161704	250	2/25/1935	17.95	3/9/1933	12	Elleburger-San Saba
San Saba	4161803	13	7/1/1993	10	7/22/1993	2	Elleburger-San Saba
San Saba	4161703	50	1/5/1935	20	1/1/1989	2	Elleburger-San Saba
San Saba	4161802	22	7/1/1993	19	7/22/1993	2	Elleburger-San Saba
San Saba	4161801	87	7/1/1993	80	7/22/1993	2	Elleburger-San Saba
San Saba	4160701	200	12/27/1934	60	1/1/1989	2	Marble Falls/ Elleburger-San Saba
San Saba	4264901	Dry	1/1/1989	Dry	1/1/1989	1	Elleburger-San Saba
San Saba	4159901	2.5	12/29/1934	2.5	12/29/1934	1	Unknown
San Saba	4264803	Dry	1/1/1989	Dry	1/1/1989	1	Elleburger-San Saba
San Saba	4159810	3	12/29/1934	3	12/29/1934	1	Unknown
San Saba	4159503	5	12/29/1934	5	12/29/1934	1	Unknown
San Saba	4161401	3,960	6/29/1993	900	10/28/1934	6	Elleburger-San Saba
San Saba	4160605	25	3/2/1935	25	3/2/1935	1	Unknown
San Saba	4160506	5	2/28/1935	5	2/28/1935	1	Unknown
San Saba	4160504	100	3/1/1935	25	1/1/1989	2	Marble Falls
San Saba	4160203	55	3/2/1935	Dry	1/1/1989	2	Marble Falls
San Saba	4161202	2,321	1/1/1989	650	3/5/1935	2	Elleburger-San Saba
San Saba	4158204	185	10/3/1934	185	10/3/1934	1	Unknown
San Saba	4158203	30	1/1/1987	Dry	1/1/1989	3	Elleburger-San Saba
San Saba	4160204	72.5	8/30/1934	30	1/1/1989	3	Marble Falls/ Elleburger-San Saba
San Saba	4159301	220	2/21/1935	220	2/21/1935	1	Unknown
San Saba	4264301	652	1/1/1989	Dry	2/7/1957	4	Elleburger-San Saba
San Saba	4264303	40	11/28/1934	40	1/1/1989	2	Elleburger-San Saba
San Saba	4157101	1,890	1/1/1989	152.6	2/7/1957	5	Marble Falls/

Table A.1 Summary of springs in study area with at least one measurement (based on Heitmuller and Reece (2003)).

County	State Well Number	Maximum Flow (gallon per minute)	Date of Maximum Flow	Minimum Flow (gallon per minute)	Date of Minimum Flow	Number of Measurements	Geologic Formation
							Ellenburger-San Saba
San Saba	4158101	1,600	10/2/1934	27.5	1/1/1989	2	Marble Falls
San Saba	4157102	550	11/28/1934	550	11/28/1934	1	Marble Falls/ Ellenburger-San Saba
San Saba	4158205	93	1/24/1935	93	1/24/1935	1	Unknown
San Saba	4152802	650	8/28/1934	576	1/1/1989	2	Marble Falls/ Ellenburger-San Saba
San Saba	4152801	834.8	10/29/1938	107.7	2/12/1957	7	Marble Falls/ Ellenburger-San Saba
San Saba	4149806	3.5	12/15/1934	2.5	1/1/1989	2	Marble Falls/ Ellenburger-San Saba
San Saba	4149705	100	12/13/1934	100	12/13/1934	1	Unknown
San Saba	4149803	125	12/18/1934	30	1/1/1989	2	Marble Falls/ Ellenburger-San Saba
San Saba	4149805	20	1/1/1989	20	1/1/1989	1	Marble Falls/ Ellenburger-San Saba
San Saba	4149706	90	12/15/1934	90	12/15/1934	1	Unknown
San Saba	4152702	4.5	8/29/1934	4.5	8/29/1934	1	Marble Falls
San Saba	4149703	45	12/13/1934	3.5	1/1/1989	2	Marble Falls/ Ellenburger-San Saba
San Saba	4152805	38	8/28/1934	38	8/28/1934	1	Unknown
San Saba	4149804	2,380	2/24/1935	863	1/1/1989	2	Marble Falls/ Ellenburger-San Saba
San Saba	4150801	7.5	9/4/1934	Dry	1/1/1989	3	Marble Falls
San Saba	4150804	24	10/3/1934	24	10/3/1934	1	Unknown
San Saba	4149801	4,450	1/1/1989	1,386.80	2/7/1957	7	Marble Falls/ Ellenburger-San Saba
San Saba	4256901	0.5	11/16/1934	0.5	11/16/1934	1	Unknown
San Saba	4150701	1	12/1/1934	1	12/1/1934	1	Unknown
San Saba	4150602	1	12/20/1934	1	12/20/1934	1	Unknown
San Saba	4151507	2,676	---	300	7/18/1934	2	Ellenburger-San Saba
San Saba	4149605	1,129	1/1/1989	305.2	2/7/1957	4	Marble Falls/

Table A.1 Summary of springs in study area with at least one measurement (based on Heitmuller and Reece (2003)).

County	State Well Number	Maximum Flow (gallon per minute)	Date of Maximum Flow	Minimum Flow (gallon per minute)	Date of Minimum Flow	Number of Measurements	Geologic Formation
							Ellenburger-San Saba
San Saba	4149604	485	2/24/1935	Dry	1/1/1988	4	Marble Falls/ Ellenburger-San Saba
San Saba	4150603	5.5	12/20/1934	5.5	12/20/1934	1	Unknown
San Saba	4149603	1,638.12	5/3/1962	335	2/24/1935	4	Marble Falls/ Ellenburger-San Saba
San Saba	4149503	2,042.04	2/25/1939	152.59	9/8/1952	4	Unknown
San Saba	4151601	405	10/6/1934	215.424	2/12/1957	4	Marble Falls
San Saba	4149607	15	10/4/1934	15	10/4/1934	1	Unknown
San Saba	4149602	1,714.42	10/28/1938	448.8	2/11/1957	7	Ellenburger-San Saba
San Saba	4149606	5.5	10/4/1934	5.5	10/4/1934	1	Unknown
San Saba	4150405	11	2/26/1935	11	2/26/1935	1	Unknown
San Saba	4149101	987.36	6/16/1931	852.72	6/16/1931	2	Unknown
San Saba	4151201	0.5	9/13/1934	0.5	9/13/1934	1	Unknown
San Saba	4151302	7.5	9/5/1934	7.5	9/5/1934	1	Unknown
San Saba	4141901	1.5	10/30/1934	1.5	10/30/1934	1	Unknown
San Saba	4141810	1,539.38	10/28/1938	Dry	2/7/1957	5	Marble Falls/ Ellenburger-San Saba
San Saba	4248901	1,130.98	10/28/1938	Dry	1/1/1983	7	Marble Falls
San Saba	4240902	1	10/17/1934	1	10/17/1934	1	Unknown
Travis	5748404	50	---	50	---	1	Cretaceous Units
Travis	5747304	10	9/3/1972	3	3/5/1955	2	Cretaceous Units
Travis	5748105	10	9/3/1972	10	9/3/1972	1	Cretaceous Units
Travis	5740203	5	8/25/1972	5	8/25/1972	1	Cretaceous Units
Travis	5732805	5	8/25/1972	5	8/25/1972	1	Cretaceous Units

Note: Additional information such as coordinates of wells can be found in the geodatabase.

Table A.2 Summary of aquifer transmissivity and horizontal hydraulic conductivity values for Cretaceous, Marble Falls, Ellenburger-San Saba, and Hickory aquifers in study area.

Well	County	Aquifer	Specific Capacity (gallon per minute per foot)	Transmissivity (square feet per day)	Horizontal Hydraulic Conductivity (feet per day)	Source	Note
6908501	Kerr	Cretaceous	0.03	4	0.02	calculated from well specific capacity test data obtained from TWDB (2014a)	Single well test
4162104	Lampasas	Cretaceous	0.04	5	0.03	calculated from well specific capacity test data obtained from TWDB (2014a)	Single well test
5753613	Blanco	Cretaceous	0.06	4	0.04	Christian and David Wuerch (2012)	Single well test
5753614	Blanco	Cretaceous		4	0.04	Christian and David Wuerch (2012)	Multi-well hydraulic test
5760605	Kendall	Cretaceous	0.03	6	0.06	calculated from well specific capacity test data obtained from TWDB (2014a)	Single well test
6801308	Kendall	Cretaceous	0.07	12	0.06	calculated from well specific capacity test data obtained from TWDB (2014a)	Single well test
5653502	Kerr	Cretaceous	0.08	16	0.06	calculated from well specific capacity test data obtained from TWDB (2014a)	Single well test
5761219	Blanco	Cretaceous	0.25	23	0.08	Christian and	Multi-well

Table A.2 Summary of aquifer transmissivity and horizontal hydraulic conductivity values for Cretaceous, Marble Falls, Ellenburger-San Saba, and Hickory aquifers in study area.

Well	County	Aquifer	Specific Capacity (gallon per minute per foot)	Transmissivity (square feet per day)	Horizontal Hydraulic Conductivity (feet per day)	Source	Note
						David Wuerch (2012)	hydraulic test
CWR-2A	Gillespie	Cretaceous		15	0.08	Daniel B. Stephens & Associates (2006)	Multi-well hydraulic test
6801603	Kendall	Cretaceous	0.08	13	0.08	calculated from well specific capacity test data obtained from TWDB (2014a)	Single well test
6802402	Kendall	Cretaceous	0.14	24	0.08	calculated from well specific capacity test data obtained from TWDB (2014a)	Single well test
5653305	Kerr	Cretaceous	0.10	22	0.08	calculated from well specific capacity test data obtained from TWDB (2014a)	Single well test
6908513	Kerr	Cretaceous	0.05	10	0.08	calculated from well specific capacity test data obtained from TWDB (2014a)	Single well test
5748701	Hays	Cretaceous	0.04	9	0.09	calculated from well specific capacity test data obtained from TWDB (2014a)	Single well test
5653602	Kerr	Cretaceous	0.10	22	0.09	calculated	Single well

Table A.2 Summary of aquifer transmissivity and horizontal hydraulic conductivity values for Cretaceous, Marble Falls, Ellenburger-San Saba, and Hickory aquifers in study area.

Well	County	Aquifer	Specific Capacity (gallon per minute per foot)	Transmissivity (square feet per day)	Horizontal Hydraulic Conductivity (feet per day)	Source	Note
						from well specific capacity test data obtained from TWDB (2014a)	test
4146801	Lampasas	Cretaceous	0.02	3	0.09	calculated from well specific capacity test data obtained from TWDB (2014a)	Single well test
5757903	Kendall	Cretaceous	0.13	24	0.10	calculated from well specific capacity test data obtained from TWDB (2014a)	Single well test
6802602	Kendall	Cretaceous	0.11	18	0.10	calculated from well specific capacity test data obtained from TWDB (2014a)	Single well test
5619208	Menard	Cretaceous	0.09	19	0.10	calculated from well specific capacity test data obtained from TWDB (2014a)	Single well test
5750513	Gillespie	Cretaceous	0.12	20	0.11	calculated from well specific capacity test data obtained from TWDB (2014a)	Single well test
6801306	Kendall	Cretaceous	0.17	27	0.11	calculated	Single well

Table A.2 Summary of aquifer transmissivity and horizontal hydraulic conductivity values for Cretaceous, Marble Falls, Ellenburger-San Saba, and Hickory aquifers in study area.

Well	County	Aquifer	Specific Capacity (gallon per minute per foot)	Transmissivity (square feet per day)	Horizontal Hydraulic Conductivity (feet per day)	Source	Note
						from well specific capacity test data obtained from TWDB (2014a)	test
4162102	Lampasas	Cretaceous	0.05	7	0.11	calculated from well specific capacity test data obtained from TWDB (2014a)	Single well test
5753613	Blanco	Cretaceous	0.06	12	0.12	calculated from well specific capacity test data obtained from TWDB (2014a)	Single well test
5760602	Kendall	Cretaceous	0.08	17	0.12	calculated from well specific capacity test data obtained from TWDB (2014a)	Single well test
6802403	Kendall	Cretaceous	0.22	40	0.13	calculated from well specific capacity test data obtained from TWDB (2014a)	Single well test
5761218	Blanco	Cretaceous	0.16	37	0.14	calculated from well specific capacity test data obtained from TWDB (2014a)	Single well test
5809902	Williamson	Cretaceous	0.36	68	0.14	calculated	Single well

Table A.2 Summary of aquifer transmissivity and horizontal hydraulic conductivity values for Cretaceous, Marble Falls, Ellenburger-San Saba, and Hickory aquifers in study area.

Well	County	Aquifer	Specific Capacity (gallon per minute per foot)	Transmissivity (square feet per day)	Horizontal Hydraulic Conductivity (feet per day)	Source	Note
						from well specific capacity test data obtained from TWDB (2014a)	test
4153325	Lampasas	Cretaceous	0.15	23	0.15	calculated from well specific capacity test data obtained from TWDB (2014a)	Single well test
5758202	Kendall	Cretaceous	0.08	12	0.17	calculated from well specific capacity test data obtained from TWDB (2014a)	Single well test
6801409	Kerr	Cretaceous	0.10	23	0.19	calculated from well specific capacity test data obtained from TWDB (2014a)	Single well test
5761219	Blanco	Cretaceous	0.25	59	0.20	calculated from well specific capacity test data obtained from TWDB (2014a)	Single well test
5761904	Blanco	Cretaceous	0.21	41	0.20	calculated from well specific capacity test data obtained from TWDB (2014a)	Single well test
Well #1	Hays	Cretaceous	0.04	16	0.20	Daniel B.	Multi-well

Table A.2 Summary of aquifer transmissivity and horizontal hydraulic conductivity values for Cretaceous, Marble Falls, Ellenburger-San Saba, and Hickory aquifers in study area.

Well	County	Aquifer	Specific Capacity (gallon per minute per foot)	Transmissivity (square feet per day)	Horizontal Hydraulic Conductivity (feet per day)	Source	Note
						Stephens & Associates (2006)	hydraulic test
6801902	Kendall	Cretaceous	0.13	22	0.20	calculated from well specific capacity test data obtained from TWDB (2014a)	Single well test
6803106	Kendall	Cretaceous	0.10	16	0.22	calculated from well specific capacity test data obtained from TWDB (2014a)	Single well test
BT-3	Blanco	Cretaceous	0.15	14	0.24	Daniel B. Stephens & Associates (2006)	Single well test
5760101	Kendall	Cretaceous	0.06	12	0.24	calculated from well specific capacity test data obtained from TWDB (2014a)	Single well test
5740102	Travis	Cretaceous	0.27	49	0.24	calculated from well specific capacity test data obtained from TWDB (2014a)	Single well test
Well #2	Kerr	Cretaceous	1.20	15	0.25	Daniel B. Stephens & Associates (2006)	Single well test
5729304	Llano	Cretaceous	0.26	62	0.25	calculated from well specific	Single well test

Table A.2 Summary of aquifer transmissivity and horizontal hydraulic conductivity values for Cretaceous, Marble Falls, Ellenburger-San Saba, and Hickory aquifers in study area.

Well	County	Aquifer	Specific Capacity (gallon per minute per foot)	Transmissivity (square feet per day)	Horizontal Hydraulic Conductivity (feet per day)	Source	Note
						capacity test data obtained from TWDB (2014a)	
6801407	Kerr	Cretaceous	0.20	33	0.27	calculated from well specific capacity test data obtained from TWDB (2014a)	Single well test
4153324	Lampasas	Cretaceous	0.10	16	0.27	calculated from well specific capacity test data obtained from TWDB (2014a)	Single well test
5817203	Williamson	Cretaceous	0.51	102	0.27	calculated from well specific capacity test data obtained from TWDB (2014a)	Single well test
5724901	Williamson	Cretaceous	0.69	144	0.28	calculated from well specific capacity test data obtained from TWDB (2014a)	Single well test
5663105	Kerr	Cretaceous	0.25	57	0.30	calculated from well specific capacity test data obtained from TWDB (2014a)	Single well test
5652801	Kimble	Cretaceous	0.40	97	0.30	calculated from well specific	Single well test

Table A.2 Summary of aquifer transmissivity and horizontal hydraulic conductivity values for Cretaceous, Marble Falls, Ellenburger-San Saba, and Hickory aquifers in study area.

Well	County	Aquifer	Specific Capacity (gallon per minute per foot)	Transmissivity (square feet per day)	Horizontal Hydraulic Conductivity (feet per day)	Source	Note
						capacity test data obtained from TWDB (2014a)	
5762411	Blanco	Cretaceous	0.25	58	0.32	calculated from well specific capacity test data obtained from TWDB (2014a)	Single well test
5724208	Burnet	Cretaceous	0.25	56	0.35	calculated from well specific capacity test data obtained from TWDB (2014a)	Single well test
5761217	Blanco	Cretaceous		67	0.37	Christian and David Wuerch (2012)	Multi-well hydraulic test
6801310	Kendall	Cretaceous	0.82	176	0.38	calculated from well specific capacity test data obtained from TWDB (2014a)	Single well test
Sect. 2	Blanco	Cretaceous	0.46	43	0.39	Daniel B. Stephens & Associates (2006)	Multi-well hydraulic test
5654404	Kerr	Cretaceous	0.30	19	0.39	Christian and David Wuerch (2012)	Single well test
5751704	Gillespie	Cretaceous	0.21	45	0.41	calculated from well specific capacity test data obtained from TWDB (2014a)	Single well test

Table A.2 Summary of aquifer transmissivity and horizontal hydraulic conductivity values for Cretaceous, Marble Falls, Ellenburger-San Saba, and Hickory aquifers in study area.

Well	County	Aquifer	Specific Capacity (gallon per minute per foot)	Transmissivity (square feet per day)	Horizontal Hydraulic Conductivity (feet per day)	Source	Note
G0270012 J	Burnet	Cretaceous		17	0.43	Young et al., (2012)	Single well test
5752406	Gillespie	Cretaceous	0.09	20	0.43	calculated from well specific capacity test data obtained from TWDB (2014a)	Single well test
5757904	Kendall	Cretaceous	0.14	25	0.45	calculated from well specific capacity test data obtained from TWDB (2014a)	Single well test
5740408	Travis	Cretaceous	0.22	51	0.46	calculated from well specific capacity test data obtained from TWDB (2014a)	Single well test
5747903	Hays	Cretaceous	0.63	159	0.47	calculated from well specific capacity test data obtained from TWDB (2014a)	Single well test
5753908	Blanco	Cretaceous	0.15	29	0.48	calculated from well specific capacity test data obtained from TWDB (2014a)	Single well test
5759802	Kendall	Cretaceous	0.74	197	0.49	calculated from well specific capacity test data obtained	Single well test

Table A.2 Summary of aquifer transmissivity and horizontal hydraulic conductivity values for Cretaceous, Marble Falls, Ellenburger-San Saba, and Hickory aquifers in study area.

Well	County	Aquifer	Specific Capacity (gallon per minute per foot)	Transmissivity (square feet per day)	Horizontal Hydraulic Conductivity (feet per day)	Source	Note
						from TWDB (2014a)	
5752510	Blanco	Cretaceous	0.75	158	0.52	calculated from well specific capacity test data obtained from TWDB (2014a)	Single well test
5656801	Kerr	Cretaceous	0.09	20	0.53	calculated from well specific capacity test data obtained from TWDB (2014a)	Single well test
G0270012I	Burnet	Cretaceous		31	0.56	Young et al., (2012)	Single well test
5664605	Kerr	Cretaceous	1.46	332	0.58	calculated from well specific capacity test data obtained from TWDB (2014a)	Single well test
5809301	Williamson	Cretaceous	0.57	119	0.59	calculated from well specific capacity test data obtained from TWDB (2014a)	Single well test
5724101	Burnet	Cretaceous	1.00	630	0.60	Myers (1969)	Recovery of pumped well
6803103	Kendall	Cretaceous	0.38	74	0.61	calculated from well specific capacity test data obtained from TWDB (2014a)	Single well test

Table A.2 Summary of aquifer transmissivity and horizontal hydraulic conductivity values for Cretaceous, Marble Falls, Ellenburger-San Saba, and Hickory aquifers in study area.

Well	County	Aquifer	Specific Capacity (gallon per minute per foot)	Transmissivity (square feet per day)	Horizontal Hydraulic Conductivity (feet per day)	Source	Note
6908511	Kerr	Cretaceous	0.74	152	0.63	calculated from well specific capacity test data obtained from TWDB (2014a)	Single well test
6803403	Kendall	Cretaceous	0.53	101	0.64	calculated from well specific capacity test data obtained from TWDB (2014a)	Single well test
EMS Well 1	Hays	Cretaceous		136	0.68	Hunt and others (2010)	Single well test
6908202	Kerr	Cretaceous	0.15	28	0.68	calculated from well specific capacity test data obtained from TWDB (2014a)	Single well test
6908303	Kerr	Cretaceous	0.46	85	0.71	calculated from well specific capacity test data obtained from TWDB (2014a)	Single well test
6908601	Kerr	Cretaceous	0.89	186	0.74	calculated from well specific capacity test data obtained from TWDB (2014a)	Single well test
5741902	Gillespie	Cretaceous	0.60	950	0.75	Myers (1969)	Single well test
5742720	Gillespie	Cretaceous	0.40	89	0.75	calculated from well specific	Single well test

Table A.2 Summary of aquifer transmissivity and horizontal hydraulic conductivity values for Cretaceous, Marble Falls, Ellenburger-San Saba, and Hickory aquifers in study area.

Well	County	Aquifer	Specific Capacity (gallon per minute per foot)	Transmissivity (square feet per day)	Horizontal Hydraulic Conductivity (feet per day)	Source	Note
						capacity test data obtained from TWDB (2014a)	
5760905	Kendall	Cretaceous	0.19	34	0.75	calculated from well specific capacity test data obtained from TWDB (2014a)	Single well test
5739309	Burnet	Cretaceous	0.25	47	0.78	calculated from well specific capacity test data obtained from TWDB (2014a)	Single well test
4154101	Lampasas	Cretaceous	0.20	39	0.81	calculated from well specific capacity test data obtained from TWDB (2014a)	Single well test
5759702	Kendall	Cretaceous	0.51	98	0.82	calculated from well specific capacity test data obtained from TWDB (2014a)	Single well test
5741903	Gillespie	Cretaceous	0.71	155	0.83	calculated from well specific capacity test data obtained from TWDB (2014a)	Single well test
6803105	Kendall	Cretaceous	0.29	67	0.84	calculated from well specific	Single well test

Table A.2 Summary of aquifer transmissivity and horizontal hydraulic conductivity values for Cretaceous, Marble Falls, Ellenburger-San Saba, and Hickory aquifers in study area.

Well	County	Aquifer	Specific Capacity (gallon per minute per foot)	Transmissivity (square feet per day)	Horizontal Hydraulic Conductivity (feet per day)	Source	Note
						capacity test data obtained from TWDB (2014a)	
6803104	Kendall	Cretaceous	0.56	109	0.87	calculated from well specific capacity test data obtained from TWDB (2014a)	Single well test
6802107	Kendall	Cretaceous	0.59	105	0.90	calculated from well specific capacity test data obtained from TWDB (2014a)	Single well test
5757304	Kendall	Cretaceous	0.21	40	0.92	calculated from well specific capacity test data obtained from TWDB (2014a)	Single well test
5754706	Blanco	Cretaceous	0.11	19	0.95	calculated from well specific capacity test data obtained from TWDB (2014a)	Single well test
6802204	Kendall	Cretaceous	0.29	54	0.96	calculated from well specific capacity test data obtained from TWDB (2014a)	Single well test
5635508	Kimble	Cretaceous	1.01	237	0.99	calculated from well specific	Single well test

Table A.2 Summary of aquifer transmissivity and horizontal hydraulic conductivity values for Cretaceous, Marble Falls, Ellenburger-San Saba, and Hickory aquifers in study area.

Well	County	Aquifer	Specific Capacity (gallon per minute per foot)	Transmissivity (square feet per day)	Horizontal Hydraulic Conductivity (feet per day)	Source	Note
						capacity test data obtained from TWDB (2014a)	
6908617	Kerr	Cretaceous	0.50	102	1.02	calculated from well specific capacity test data obtained from TWDB (2014a)	Single well test
5663920	Kerr	Cretaceous	0.54	114	1.04	calculated from well specific capacity test data obtained from TWDB (2014a)	Single well test
5759404	Kendall	Cretaceous	0.71	138	1.10	calculated from well specific capacity test data obtained from TWDB (2014a)	Single well test
6802501	Kendall	Cretaceous	0.52	104	1.13	calculated from well specific capacity test data obtained from TWDB (2014a)	Single well test
5739308	Burnet	Cretaceous	0.34	69	1.15	calculated from well specific capacity test data obtained from TWDB (2014a)	Single well test
5759101	Kendall	Cretaceous	0.17	29	1.15	calculated from well specific	Single well test

Table A.2 Summary of aquifer transmissivity and horizontal hydraulic conductivity values for Cretaceous, Marble Falls, Ellenburger-San Saba, and Hickory aquifers in study area.

Well	County	Aquifer	Specific Capacity (gallon per minute per foot)	Transmissivity (square feet per day)	Horizontal Hydraulic Conductivity (feet per day)	Source	Note
						capacity test data obtained from TWDB (2014a)	
6908306	Kerr	Cretaceous	1.42	339	1.17	calculated from well specific capacity test data obtained from TWDB (2014a)	Single well test
5663501	Kerr	Cretaceous	0.61	127	1.19	calculated from well specific capacity test data obtained from TWDB (2014a)	Single well test
6801301	Kendall	Cretaceous		1,130	1.23	Myers (1969)	Recovery of pumped well
5663208	Kerr	Cretaceous	0.30	61	1.26	calculated from well specific capacity test data obtained from TWDB (2014a)	Single well test
5724207	Burnet	Cretaceous	0.63	156	1.28	calculated from well specific capacity test data obtained from TWDB (2014a)	Single well test
6908622	Kerr	Cretaceous	1.32	220	1.29	calculated from well specific capacity test data obtained from TWDB (2014a)	Single well test

Table A.2 Summary of aquifer transmissivity and horizontal hydraulic conductivity values for Cretaceous, Marble Falls, Ellenburger-San Saba, and Hickory aquifers in study area.

Well	County	Aquifer	Specific Capacity (gallon per minute per foot)	Transmissivity (square feet per day)	Horizontal Hydraulic Conductivity (feet per day)	Source	Note
6802603	Kendall	Cretaceous	0.83	153	1.31	calculated from well specific capacity test data obtained from TWDB (2014a)	Single well test
6801506	Kerr	Cretaceous	0.44	79	1.31	calculated from well specific capacity test data obtained from TWDB (2014a)	Single well test
5762103	Blanco	Cretaceous	1.00	199	1.33	calculated from well specific capacity test data obtained from TWDB (2014a)	Single well test
6908510	Kerr	Cretaceous	1.67	319	1.33	calculated from well specific capacity test data obtained from TWDB (2014a)	Single well test
5663913	Kerr	Cretaceous	2.08	444	1.39	calculated from well specific capacity test data obtained from TWDB (2014a)	Single well test
5750315	Gillespie	Cretaceous	0.43	81	1.40	calculated from well specific capacity test data obtained from TWDB (2014a)	Single well test

Table A.2 Summary of aquifer transmissivity and horizontal hydraulic conductivity values for Cretaceous, Marble Falls, Ellenburger-San Saba, and Hickory aquifers in study area.

Well	County	Aquifer	Specific Capacity (gallon per minute per foot)	Transmissivity (square feet per day)	Horizontal Hydraulic Conductivity (feet per day)	Source	Note
5757504	Kerr	Cretaceous	0.81	210	1.40	calculated from well specific capacity test data obtained from TWDB (2014a)	Single well test
6802102	Kendall	Cretaceous	0.60	149	1.42	calculated from well specific capacity test data obtained from TWDB (2014a)	Single well test
6801303	Kendall	Cretaceous	1.02	194	1.43	calculated from well specific capacity test data obtained from TWDB (2014a)	Single well test
6801307	Kendall	Cretaceous	1.20	242	1.44	calculated from well specific capacity test data obtained from TWDB (2014a)	Single well test
5655505	Gillespie	Cretaceous	2.10	105	1.47	Christian and David Wuerch (2012)	Single well test
6802106	Kendall	Cretaceous	1.16	243	1.50	calculated from well specific capacity test data obtained from TWDB (2014a)	Single well test
PW-3	Gillespie	Cretaceous	2.00	419	1.55	Daniel B. Stephens & Associates (2006)	Multi-well hydraulic test

Table A.2 Summary of aquifer transmissivity and horizontal hydraulic conductivity values for Cretaceous, Marble Falls, Ellenburger-San Saba, and Hickory aquifers in study area.

Well	County	Aquifer	Specific Capacity (gallon per minute per foot)	Transmissivity (square feet per day)	Horizontal Hydraulic Conductivity (feet per day)	Source	Note
5663414	Kerr	Cretaceous	1.67	365	1.65	calculated from well specific capacity test data obtained from TWDB (2014a)	Single well test
4153329	Lampasas	Cretaceous	0.29	52	1.72	calculated from well specific capacity test data obtained from TWDB (2014a)	Single well test
5741915	Gillespie	Cretaceous	0.79	150	1.85	calculated from well specific capacity test data obtained from TWDB (2014a)	Single well test
5654801	Kerr	Cretaceous	1.10	233	1.86	calculated from well specific capacity test data obtained from TWDB (2014a)	Single well test
Kennedy Ranch	Hays	Cretaceous		301	1.88	Hunt and others (2010)	Multi-well hydraulic test
Venado Ranch	Blanco	Cretaceous		1,130	1.99	Hunt and others (2010)	Single well test
6908619	Kerr	Cretaceous	1.00	204	2.04	calculated from well specific capacity test data obtained from TWDB (2014a)	Single well test
5749204	Gillespie	Cretaceous	1.00	196	2.13	calculated from well	Single well test

Table A.2 Summary of aquifer transmissivity and horizontal hydraulic conductivity values for Cretaceous, Marble Falls, Ellenburger-San Saba, and Hickory aquifers in study area.

Well	County	Aquifer	Specific Capacity (gallon per minute per foot)	Transmissivity (square feet per day)	Horizontal Hydraulic Conductivity (feet per day)	Source	Note
						specific capacity test data obtained from TWDB (2014a)	
5817401	Williamson	Cretaceous	0.29	64	2.13	calculated from well specific capacity test data obtained from TWDB (2014a)	Single well test
5753617	Blanco	Cretaceous	2.32	520	2.36	calculated from well specific capacity test data obtained from TWDB (2014a)	Single well test
Westridge	Hays	Cretaceous		179	2.38	Hunt and others (2010)	Multi-well hydraulic test
5750901	Gillespie	Cretaceous	0.64	146	2.44	calculated from well specific capacity test data obtained from TWDB (2014a)	Single well test
4153328	Lampasas	Cretaceous	0.50	129	2.58	calculated from well specific capacity test data obtained from TWDB (2014a)	Single well test
5801503	Burnet	Cretaceous	1.50	274	2.61	calculated from well specific capacity test data obtained from TWDB	Single well test

Table A.2 Summary of aquifer transmissivity and horizontal hydraulic conductivity values for Cretaceous, Marble Falls, Ellenburger-San Saba, and Hickory aquifers in study area.

Well	County	Aquifer	Specific Capacity (gallon per minute per foot)	Transmissivity (square feet per day)	Horizontal Hydraulic Conductivity (feet per day)	Source	Note
						(2014a)	
5748703	Hays	Cretaceous	1.00	262	2.62	calculated from well specific capacity test data obtained from TWDB (2014a)	Single well test
5757703	Kerr	Cretaceous	0.88	220	2.65	calculated from well specific capacity test data obtained from TWDB (2014a)	Single well test
6907207	Kerr	Cretaceous	2.45	640	2.72	calculated from well specific capacity test data obtained from TWDB (2014a)	Single well test
"Pumping Well"	Hays	Cretaceous	5.90	294	2.79	Daniel B. Stephens & Associates (2006)	Multi-well hydraulic test
5663912	Kerr	Cretaceous	2.00	450	2.82	calculated from well specific capacity test data obtained from TWDB (2014a)	Single well test
5757804	Kerr	Cretaceous	1.44	287	2.87	calculated from well specific capacity test data obtained from TWDB (2014a)	Single well test
Valley Verde	Hays	Cretaceous		293	2.93	Hunt and others (2010)	Multi-well hydraulic

Table A.2 Summary of aquifer transmissivity and horizontal hydraulic conductivity values for Cretaceous, Marble Falls, Ellenburger-San Saba, and Hickory aquifers in study area.

Well	County	Aquifer	Specific Capacity (gallon per minute per foot)	Transmissivity (square feet per day)	Horizontal Hydraulic Conductivity (feet per day)	Source	Note
							test
5750805	Gillespie	Cretaceous	1.80	375	3.32	calculated from well specific capacity test data obtained from TWDB (2014a)	Single well test
5741909	Gillespie	Cretaceous	1.05	255	3.35	calculated from well specific capacity test data obtained from TWDB (2014a)	Single well test
5663410	Kerr	Cretaceous	3.33	893	3.47	calculated from well specific capacity test data obtained from TWDB (2014a)	Single well test
5664206	Kerr	Cretaceous	1.33	279	3.66	calculated from well specific capacity test data obtained from TWDB (2014a)	Single well test
6907208	Kerr	Cretaceous	3.38	906	3.77	calculated from well specific capacity test data obtained from TWDB (2014a)	Single well test
5663309	Kerr	Cretaceous	0.65	155	3.87	calculated from well specific capacity test data obtained from TWDB	Single well test

Table A.2 Summary of aquifer transmissivity and horizontal hydraulic conductivity values for Cretaceous, Marble Falls, Ellenburger-San Saba, and Hickory aquifers in study area.

Well	County	Aquifer	Specific Capacity (gallon per minute per foot)	Transmissivity (square feet per day)	Horizontal Hydraulic Conductivity (feet per day)	Source	Note
						(2014a)	
6801207	Kerr	Cretaceous	2.67	574	3.88	calculated from well specific capacity test data obtained from TWDB (2014a)	Single well test
5663917	Kerr	Cretaceous	5.00	1,049	3.91	calculated from well specific capacity test data obtained from TWDB (2014a)	Single well test
6802507	Kendall	Cretaceous	2.47	489	3.92	calculated from well specific capacity test data obtained from TWDB (2014a)	Single well test
5739102	Burnet	Cretaceous	0.62	158	3.95	calculated from well specific capacity test data obtained from TWDB (2014a)	Single well test
Lot 12	Gillespie	Cretaceous	1.54	821	4.09	Daniel B. Stephens & Associates (2006)	Multi-well hydraulic test
Walking W	Hays	Cretaceous		307	4.10	Hunt and others (2010)	Multi-well hydraulic test
PW-1	Hays	Cretaceous	1.00	307	4.14	Daniel B. Stephens & Associates (2006)	Multi-well hydraulic test
5724902	Williamson	Cretaceous	1.50	333	4.17	calculated from well	Single well test

Table A.2 Summary of aquifer transmissivity and horizontal hydraulic conductivity values for Cretaceous, Marble Falls, Ellenburger-San Saba, and Hickory aquifers in study area.

Well	County	Aquifer	Specific Capacity (gallon per minute per foot)	Transmissivity (square feet per day)	Horizontal Hydraulic Conductivity (feet per day)	Source	Note
						specific capacity test data obtained from TWDB (2014a)	
5748212	Travis	Cretaceous	4.80	1,412	4.22	calculated from well specific capacity test data obtained from TWDB (2014a)	Single well test
5724206	Burnet	Cretaceous	2.33	578	4.25	calculated from well specific capacity test data obtained from TWDB (2014a)	Single well test
5662410	Kerr	Cretaceous	1.80	364	4.34	calculated from well specific capacity test data obtained from TWDB (2014a)	Single well test
5740409	Travis	Cretaceous	4.44	1,218	4.43	calculated from well specific capacity test data obtained from TWDB (2014a)	Single well test
5755705	Hays	Cretaceous	1.67	453	4.53	calculated from well specific capacity test data obtained from TWDB (2014a)	Single well test
5664301	Kerr	Cretaceous	3.56	986	4.54	calculated from well	Single well test

Table A.2 Summary of aquifer transmissivity and horizontal hydraulic conductivity values for Cretaceous, Marble Falls, Ellenburger-San Saba, and Hickory aquifers in study area.

Well	County	Aquifer	Specific Capacity (gallon per minute per foot)	Transmissivity (square feet per day)	Horizontal Hydraulic Conductivity (feet per day)	Source	Note
						specific capacity test data obtained from TWDB (2014a)	
5801501	Burnet	Cretaceous	2.21	498	4.57	calculated from well specific capacity test data obtained from TWDB (2014a)	Single well test
5757503	Kerr	Cretaceous	0.57	140	4.66	calculated from well specific capacity test data obtained from TWDB (2014a)	Single well test
5752407	Gillespie	Cretaceous	1.50	298	4.73	calculated from well specific capacity test data obtained from TWDB (2014a)	Single well test
G2460038 C	Williamson	Cretaceous		576	4.80	Young et al., (2012)	Single well test
5757707	Kerr	Cretaceous	1.30	324	5.06	calculated from well specific capacity test data obtained from TWDB (2014a)	Single well test
5656602	Gillespie	Cretaceous	0.52	114	5.72	calculated from well specific capacity test data obtained from TWDB (2014a)	Single well test

Table A.2 Summary of aquifer transmissivity and horizontal hydraulic conductivity values for Cretaceous, Marble Falls, Ellenburger-San Saba, and Hickory aquifers in study area.

Well	County	Aquifer	Specific Capacity (gallon per minute per foot)	Transmissivity (square feet per day)	Horizontal Hydraulic Conductivity (feet per day)	Source	Note
5741622	Gillespie	Cretaceous	0.52	117	5.83	calculated from well specific capacity test data obtained from TWDB (2014a)	Single well test
6908606	Kerr	Cretaceous	0.63	117	5.84	calculated from well specific capacity test data obtained from TWDB (2014a)	Single well test
5663512	Kerr	Cretaceous	8.33	1,950	6.09	calculated from well specific capacity test data obtained from TWDB (2014a)	Single well test
6802108	Kendall	Cretaceous	3.50	808	6.31	calculated from well specific capacity test data obtained from TWDB (2014a)	Single well test
5663909	Kerr	Cretaceous	2.20	538	6.60	calculated from well specific capacity test data obtained from TWDB (2014a)	Single well test
5758702	Kendall	Cretaceous	1.33	279	6.96	calculated from well specific capacity test data obtained from TWDB (2014a)	Single well test

Table A.2 Summary of aquifer transmissivity and horizontal hydraulic conductivity values for Cretaceous, Marble Falls, Ellenburger-San Saba, and Hickory aquifers in study area.

Well	County	Aquifer	Specific Capacity (gallon per minute per foot)	Transmissivity (square feet per day)	Horizontal Hydraulic Conductivity (feet per day)	Source	Note
5662605	Kerr	Cretaceous	4.00	888	6.99	calculated from well specific capacity test data obtained from TWDB (2014a)	Single well test
6801205	Kerr	Cretaceous	2.00	431	7.19	calculated from well specific capacity test data obtained from TWDB (2014a)	Single well test
5647903	Gillespie	Cretaceous	8.57	2,126	7.33	calculated from well specific capacity test data obtained from TWDB (2014a)	Single well test
5663405	Kerr	Cretaceous	2.27	447	7.84	calculated from well specific capacity test data obtained from TWDB (2014a)	Single well test
5663614	Kerr	Cretaceous	2.47	604	8.51	calculated from well specific capacity test data obtained from TWDB (2014a)	Single well test
Well #1	Kerr	Cretaceous	1.00	157	8.69	Daniel B. Stephens & Associates (2006)	Single well test
5663407	Kerr	Cretaceous	6.00	1,506	8.96	calculated from well specific	Single well test

Table A.2 Summary of aquifer transmissivity and horizontal hydraulic conductivity values for Cretaceous, Marble Falls, Ellenburger-San Saba, and Hickory aquifers in study area.

Well	County	Aquifer	Specific Capacity (gallon per minute per foot)	Transmissivity (square feet per day)	Horizontal Hydraulic Conductivity (feet per day)	Source	Note
						capacity test data obtained from TWDB (2014a)	
6908514	Kerr	Cretaceous	1.41	369	9.23	calculated from well specific capacity test data obtained from TWDB (2014a)	Single well test
5731904	Burnet	Cretaceous	0.58	115	9.55	calculated from well specific capacity test data obtained from TWDB (2014a)	Single well test
PW-1	Blanco	Cretaceous	82.90	46,120	11.08	Daniel B. Stephens & Associates (2006)	Multi-well hydraulic test
6801505	Kerr	Cretaceous	6.00	1,345	11.12	calculated from well specific capacity test data obtained from TWDB (2014a)	Single well test
5750104	Gillespie	Cretaceous	6.30	1,603	11.70	calculated from well specific capacity test data obtained from TWDB (2014a)	Single well test
5742505	Gillespie	Cretaceous	5.00	1,096	11.92	calculated from well specific capacity test data obtained from TWDB	Single well test

Table A.2 Summary of aquifer transmissivity and horizontal hydraulic conductivity values for Cretaceous, Marble Falls, Ellenburger-San Saba, and Hickory aquifers in study area.

Well	County	Aquifer	Specific Capacity (gallon per minute per foot)	Transmissivity (square feet per day)	Horizontal Hydraulic Conductivity (feet per day)	Source	Note
						(2014a)	
5738412	Blanco	Cretaceous	0.83	183	12.18	calculated from well specific capacity test data obtained from TWDB (2014a)	Single well test
5729309	Llano	Cretaceous	1.50	379	12.64	calculated from well specific capacity test data obtained from TWDB (2014a)	Single well test
5749504	Gillespie	Cretaceous	1.07	255	12.75	calculated from well specific capacity test data obtained from TWDB (2014a)	Single well test
5757902	Kendall	Cretaceous	5.00	1,183	13.29	calculated from well specific capacity test data obtained from TWDB (2014a)	Single well test
5761222	Blanco	Cretaceous	3.95	1,061	13.96	calculated from well specific capacity test data obtained from TWDB (2014a)	Single well test
5817503	Williamson	Cretaceous	3.17	864	14.41	calculated from well specific capacity test data obtained from TWDB	Single well test

Table A.2 Summary of aquifer transmissivity and horizontal hydraulic conductivity values for Cretaceous, Marble Falls, Ellenburger-San Saba, and Hickory aquifers in study area.

Well	County	Aquifer	Specific Capacity (gallon per minute per foot)	Transmissivity (square feet per day)	Horizontal Hydraulic Conductivity (feet per day)	Source	Note
						(2014a)	
5758705	Kendall	Cretaceous	5.20	1,084	15.27	calculated from well specific capacity test data obtained from TWDB (2014a)	Single well test
5741911	Gillespie	Cretaceous	5.00	1,096	16.12	calculated from well specific capacity test data obtained from TWDB (2014a)	Single well test
5663804	Kerr	Cretaceous	7.00	1,978	16.48	calculated from well specific capacity test data obtained from TWDB (2014a)	Single well test
6907205	Kerr	Cretaceous	4.40	911	16.56	calculated from well specific capacity test data obtained from TWDB (2014a)	Single well test
5663607	Kerr	Cretaceous		20,400	17.11	Myers (1969)	Recharging well
5663608	Kerr	Cretaceous		23,200	17.51	Myers (1969)	Recovery of pumped well
Well 1	Gillespie	Cretaceous		1,450	18.19	Daniel B. Stephens & Associates (2006)	Multi-well hydraulic test
5729308	Llano	Cretaceous	2.15	556	18.55	calculated from well specific capacity test	Single well test

Table A.2 Summary of aquifer transmissivity and horizontal hydraulic conductivity values for Cretaceous, Marble Falls, Ellenburger-San Saba, and Hickory aquifers in study area.

Well	County	Aquifer	Specific Capacity (gallon per minute per foot)	Transmissivity (square feet per day)	Horizontal Hydraulic Conductivity (feet per day)	Source	Note
						data obtained from TWDB (2014a)	
5755604	Hays	Cretaceous		1,604	20.05	Hunt and others (2010)	Multi-well hydraulic test
5755402	Hays	Cretaceous	6.00	1,748	20.56	calculated from well specific capacity test data obtained from TWDB (2014a)	Single well test
5749401	Gillespie	Cretaceous	1.54	416	20.79	calculated from well specific capacity test data obtained from TWDB (2014a)	Single well test
6908705	Kerr	Cretaceous	8.85	2,408	24.08	calculated from well specific capacity test data obtained from TWDB (2014a)	Single well test
5647908	Gillespie	Cretaceous	1.97	489	24.45	calculated from well specific capacity test data obtained from TWDB (2014a)	Single well test
6908104	Kerr	Cretaceous	4.84	1,231	24.62	calculated from well specific capacity test data obtained from TWDB (2014a)	Single well test
5664701	Kerr	Cretaceous	10.31	2,827	25.70	calculated	Single well

Table A.2 Summary of aquifer transmissivity and horizontal hydraulic conductivity values for Cretaceous, Marble Falls, Ellenburger-San Saba, and Hickory aquifers in study area.

Well	County	Aquifer	Specific Capacity (gallon per minute per foot)	Transmissivity (square feet per day)	Horizontal Hydraulic Conductivity (feet per day)	Source	Note
						from well specific capacity test data obtained from TWDB (2014a)	test
5663906	Kerr	Cretaceous		1,798	27.27	Christian and David Wuerch (2012)	Multi-well hydraulic test
5663611	Kerr	Cretaceous	9.90	2,227	31.82	calculated from well specific capacity test data obtained from TWDB (2014a)	Single well test
5663909	Kerr	Cretaceous	2.20	3,187	39.30	Christian and David Wuerch (2012)	Multi-well hydraulic test
5663604	Kerr	Cretaceous	22.33	6,414	47.16	calculated from well specific capacity test data obtained from TWDB (2014a)	Single well test
5761210	Blanco	Cretaceous	10.28	2,964	50.24	calculated from well specific capacity test data obtained from TWDB (2014a)	Single well test
PW2&3(P W-4)	Hays	Cretaceous		1,337	53.47	Hunt and others (2010)	Multi-well hydraulic test
5742506	Gillespie	Cretaceous	25.00	5,798	55.22	calculated from well specific capacity test data obtained from TWDB	Single well test

Table A.2 Summary of aquifer transmissivity and horizontal hydraulic conductivity values for Cretaceous, Marble Falls, Ellenburger-San Saba, and Hickory aquifers in study area.

Well	County	Aquifer	Specific Capacity (gallon per minute per foot)	Transmissivity (square feet per day)	Horizontal Hydraulic Conductivity (feet per day)	Source	Note
						(2014a)	
5749108	Gillespie	Cretaceous	4.00	859	61.36	calculated from well specific capacity test data obtained from TWDB (2014a)	Single well test
5663619	Kerr	Cretaceous	27.63	7,098	66.96	calculated from well specific capacity test data obtained from TWDB (2014a)	Single well test
5741907	Gillespie	Cretaceous	11.00	2,621	68.97	calculated from well specific capacity test data obtained from TWDB (2014a)	Single well test
5761620	Blanco	Cretaceous	82.89	27,291	165.40	calculated from well specific capacity test data obtained from TWDB (2014a)	Single well test
5809502	Williamson	Cretaceous	100.00	29,559	492.65	calculated from well specific capacity test data obtained from TWDB (2014a)	Single well test
5741917	Gillespie	Cretaceous	42.00	13,070	653.50	calculated from well specific capacity test data obtained from TWDB	Single well test

Table A.2 Summary of aquifer transmissivity and horizontal hydraulic conductivity values for Cretaceous, Marble Falls, Ellenburger-San Saba, and Hickory aquifers in study area.

Well	County	Aquifer	Specific Capacity (gallon per minute per foot)	Transmissivity (square feet per day)	Horizontal Hydraulic Conductivity (feet per day)	Source	Note
						(2014a)	
5741801	Gillespie	Cretaceous	65.00	17,102	684.08	calculated from well specific capacity test data obtained from TWDB (2014a)	Single well test
PW-2	Blanco	Cretaceous	201.40	79,540	884.97	Daniel B. Stephens & Associates (2006)	Multi-well hydraulic test
5763616	Blanco	Cretaceous		5		Christian and David Wuerch (2012)	Multi-well hydraulic test
Sect. 3	Blanco	Cretaceous	0.18	59		Daniel B. Stephens & Associates (2006)	Multi-well hydraulic test
PW 2&3	Blanco/Hays	Cretaceous	21.90	1,958		Daniel B. Stephens & Associates (2006)	Multi-well hydraulic test
PW-4	Blanco/Hays	Cretaceous	15.90	1,660		Daniel B. Stephens & Associates (2006)	Multi-well hydraulic test
5724103	Burnet	Cretaceous		1,060		Myers (1969)	Multi-well hydraulic test
4251702	Concho	Cretaceous	0.07	6		Christian and David Wuerch (2012)	Single well test
5741903	Gillespie	Cretaceous		700		Myers (1969)	Single well test
5663604	Kerr	Cretaceous		23,700		Myers (1969)	Recharging well
5663614	Kerr	Cretaceous		18,900		Myers (1969)	Single well test
5663901	Kerr	Cretaceous		15,100		Myers (1969)	Multi-well hydraulic

Table A.2 Summary of aquifer transmissivity and horizontal hydraulic conductivity values for Cretaceous, Marble Falls, Ellenburger-San Saba, and Hickory aquifers in study area.

Well	County	Aquifer	Specific Capacity (gallon per minute per foot)	Transmissivity (square feet per day)	Horizontal Hydraulic Conductivity (feet per day)	Source	Note
							test
4254301	McCulloch	Cretaceous	0.55	11		Christian and David Wuerch (2012)	Single well test
Minimum				3	0.02		
Maximum				79,540	884.97		
Geometric Mean				193	1.70		
G0270045 F	Burnet	Marble Falls		63	6.29	Young et al., (2012)	Single well test
G0270011 E	Burnet	Marble Falls		2,366	197.20	Young et al., (2012)	Single well test
Minimum				63	6.29		
Maximum				2,366	197.20		
Geometric Mean				386	35.22		
4262909	McCulloch	Ellenburger -San Saba	0.08	14	0.01	calculated from well specific capacity test data obtained from TWDB (2014a)	Single well test
5745515	Blanco	Ellenburger -San Saba	0.03	7	0.02	calculated from well specific capacity test data obtained from TWDB (2014a)	Single well test
5745926	Blanco	Ellenburger -San Saba	0.05	11	0.02	calculated from well specific capacity test data obtained from TWDB (2014a)	Single well test
5715708	Burnet	Ellenburger -San Saba	0.22	35	0.03	calculated from well specific	Single well test

Table A.2 Summary of aquifer transmissivity and horizontal hydraulic conductivity values for Cretaceous, Marble Falls, Ellenburger-San Saba, and Hickory aquifers in study area.

Well	County	Aquifer	Specific Capacity (gallon per minute per foot)	Transmissivity (square feet per day)	Horizontal Hydraulic Conductivity (feet per day)	Source	Note
						capacity test data obtained from TWDB (2014a)	
5745823	Blanco	Ellenburger -San Saba	0.08	17	0.06	calculated from well specific capacity test data obtained from TWDB (2014a)	Single well test
5622602	Mason	Ellenburger -San Saba	0.08	12	0.06	calculated from well specific capacity test data obtained from TWDB (2014a)	Single well test
5738423	Blanco	Ellenburger -San Saba	0.20	48	0.10	calculated from well specific capacity test data obtained from TWDB (2014a)	Single well test
5753222	Blanco	Ellenburger -San Saba	0.13	22	0.11	calculated from well specific capacity test data obtained from TWDB (2014a)	Single well test
5745514	Blanco	Ellenburger -San Saba	0.27	64	0.19	calculated from well specific capacity test data obtained from TWDB (2014a)	Single well test
4262910	McCulloch	Ellenburger -San Saba	3.26	717	0.51	calculated from well specific	Single well test

Table A.2 Summary of aquifer transmissivity and horizontal hydraulic conductivity values for Cretaceous, Marble Falls, Ellenburger-San Saba, and Hickory aquifers in study area.

Well	County	Aquifer	Specific Capacity (gallon per minute per foot)	Transmissivity (square feet per day)	Horizontal Hydraulic Conductivity (feet per day)	Source	Note
						capacity test data obtained from TWDB (2014a)	
5745925	Blanco	Ellenburger -San Saba	1.25	320	0.60	calculated from well specific capacity test data obtained from TWDB (2014a)	Single well test
5753219	Blanco	Ellenburger -San Saba	0.19	36	0.73	calculated from well specific capacity test data obtained from TWDB (2014a)	Single well test
5750206	Gillespie	Ellenburger -San Saba	1.50	354	1.04	calculated from well specific capacity test data obtained from TWDB (2014a)	Single well test
5731703	Burnet	Ellenburger -San Saba	2.00	449	1.21	calculated from well specific capacity test data obtained from TWDB (2014a)	Single well test
5738106	Blanco	Ellenburger -San Saba	2.32	639	1.64	calculated from well specific capacity test data obtained from TWDB (2014a)	Single well test
5743207	Gillespie	Ellenburger -San Saba	0.25	49	1.64	calculated from well specific	Single well test

Table A.2 Summary of aquifer transmissivity and horizontal hydraulic conductivity values for Cretaceous, Marble Falls, Ellenburger-San Saba, and Hickory aquifers in study area.

Well	County	Aquifer	Specific Capacity (gallon per minute per foot)	Transmissivity (square feet per day)	Horizontal Hydraulic Conductivity (feet per day)	Source	Note
						capacity test data obtained from TWDB (2014a)	
5750215	Gillespie	Ellenburger -San Saba	1.74	423	1.81	calculated from well specific capacity test data obtained from TWDB (2014a)	Single well test
5750210	Gillespie	Ellenburger -San Saba	1.82	432	2.25	calculated from well specific capacity test data obtained from TWDB (2014a)	Single well test
5750512	Gillespie	Ellenburger -San Saba	1.56	337	2.85	calculated from well specific capacity test data obtained from TWDB (2014a)	Single well test
5743903	Gillespie	Ellenburger -San Saba	4.00	864	2.94	calculated from well specific capacity test data obtained from TWDB (2014a)	Single well test
5751107	Gillespie	Ellenburger -San Saba	0.75	147	3.63	calculated from well specific capacity test data obtained from TWDB (2014a)	Single well test
5640402	Gillespie	Ellenburger -San Saba	4.00	864	4.41	calculated from well specific	Single well test

Table A.2 Summary of aquifer transmissivity and horizontal hydraulic conductivity values for Cretaceous, Marble Falls, Ellenburger-San Saba, and Hickory aquifers in study area.

Well	County	Aquifer	Specific Capacity (gallon per minute per foot)	Transmissivity (square feet per day)	Horizontal Hydraulic Conductivity (feet per day)	Source	Note
						capacity test data obtained from TWDB (2014a)	
5750107	Gillespie	Ellenburger -San Saba	4.13	950	4.49	calculated from well specific capacity test data obtained from TWDB (2014a)	Single well test
5752103	Gillespie	Ellenburger -San Saba	1.67	397	4.75	calculated from well specific capacity test data obtained from TWDB (2014a)	Single well test
4261604	McCulloch	Ellenburger -San Saba	7.50	1,728	5.27	calculated from well specific capacity test data obtained from TWDB (2014a)	Single well test
5750229	Gillespie	Ellenburger -San Saba	1.00	207	7.26	calculated from well specific capacity test data obtained from TWDB (2014a)	Single well test
5750218	Gillespie	Ellenburger -San Saba	5.80	1,555	7.43	calculated from well specific capacity test data obtained from TWDB (2014a)	Single well test
5620525	Menard	Ellenburger -San Saba	4.07	1,123	11.23	calculated from well specific	Single well test

Table A.2 Summary of aquifer transmissivity and horizontal hydraulic conductivity values for Cretaceous, Marble Falls, Ellenburger-San Saba, and Hickory aquifers in study area.

Well	County	Aquifer	Specific Capacity (gallon per minute per foot)	Transmissivity (square feet per day)	Horizontal Hydraulic Conductivity (feet per day)	Source	Note
						capacity test data obtained from TWDB (2014a)	
5753111	Blanco	Ellenburger -San Saba	4.55	1,296	12.10	calculated from well specific capacity test data obtained from TWDB (2014a)	Single well test
5723101	Burnet	Ellenburger -San Saba	4.55	950	12.10	calculated from well specific capacity test data obtained from TWDB (2014a)	Single well test
5739103	Burnet	Ellenburger -San Saba	4.65	1,296	18.14	calculated from well specific capacity test data obtained from TWDB (2014a)	Single well test
5745801	Blanco	Ellenburger -San Saba	9.67	2,765	22.46	calculated from well specific capacity test data obtained from TWDB (2014a)	Single well test
5715743	Burnet	Ellenburger -San Saba	10.00	2,592	25.06	calculated from well specific capacity test data obtained from TWDB (2014a)	Single well test
5750325	Gillespie	Ellenburger -San Saba	24.35	7,776	35.42	calculated from well specific	Single well test

Table A.2 Summary of aquifer transmissivity and horizontal hydraulic conductivity values for Cretaceous, Marble Falls, Ellenburger-San Saba, and Hickory aquifers in study area.

Well	County	Aquifer	Specific Capacity (gallon per minute per foot)	Transmissivity (square feet per day)	Horizontal Hydraulic Conductivity (feet per day)	Source	Note
						capacity test data obtained from TWDB (2014a)	
5750326	Gillespie	Ellenburger -San Saba	27.30	7,862	36.29	calculated from well specific capacity test data obtained from TWDB (2014a)	Single well test
5730603	Burnet	Ellenburger -San Saba	95.81	31,968	58.75	calculated from well specific capacity test data obtained from TWDB (2014a)	Single well test
5750204	Gillespie	Ellenburger -San Saba	34.09	10,368	61.34	calculated from well specific capacity test data obtained from TWDB (2014a)	Single well test
G0270012 H	Burnet	Ellenburger -San Saba		5,553	61.70	Young et al., (2012)	Single well test
5723112	Burnet	Ellenburger -San Saba	33.33	9,504	103.68	calculated from well specific capacity test data obtained from TWDB (2014a)	Single well test
5750106	Gillespie	Ellenburger -San Saba	50.25	14,688	155.52	calculated from well specific capacity test data obtained from TWDB (2014a)	Single well test
5723107	Burnet	Ellenburger	25.00	6,566	172.80	calculated	Single well

Table A.2 Summary of aquifer transmissivity and horizontal hydraulic conductivity values for Cretaceous, Marble Falls, Ellenburger-San Saba, and Hickory aquifers in study area.

Well	County	Aquifer	Specific Capacity (gallon per minute per foot)	Transmissivity (square feet per day)	Horizontal Hydraulic Conductivity (feet per day)	Source	Note
		-San Saba				from well specific capacity test data obtained from TWDB (2014a)	test
5751302	Gillespie	Ellenburger -San Saba	9.57	2,678	224.64	calculated from well specific capacity test data obtained from TWDB (2014a)	Single well test
1(P)	Blanco	Ellenburger -San Saba	0.07	84		Daniel B. Stephens & Associates (2006)	Multi-well hydraulic test
1A	Blanco	Ellenburger -San Saba	0.20	24		Daniel B. Stephens & Associates (2006)	Multi-well hydraulic test
1-P	Blanco	Ellenburger -San Saba	4.50	576		Daniel B. Stephens & Associates (2006)	Multi-well hydraulic test
2(P)	Blanco	Ellenburger -San Saba	0.05	13		Daniel B. Stephens & Associates (2006)	Multi-well hydraulic test
2(P)	Blanco	Ellenburger -San Saba	0.27	29		Daniel B. Stephens & Associates (2006)	Multi-well hydraulic test
3(P)	Blanco	Ellenburger -San Saba	0.03	216		Daniel B. Stephens & Associates (2006)	Multi-well hydraulic test
4A	Blanco	Ellenburger -San Saba	3.10	1,065		Daniel B. Stephens & Associates (2006)	Multi-well hydraulic test
4254704	McCulloch	Ellenburger	7.90	2,373		Christian and	Single well

Table A.2 Summary of aquifer transmissivity and horizontal hydraulic conductivity values for Cretaceous, Marble Falls, Ellenburger-San Saba, and Hickory aquifers in study area.

Well	County	Aquifer	Specific Capacity (gallon per minute per foot)	Transmissivity (square feet per day)	Horizontal Hydraulic Conductivity (feet per day)	Source	Note
		-San Saba				David Wuerch (2012)	test
5750101	Gillespie	Ellenburger	47.80	12,205		Myers (1969)	Single well test
5750102	Gillespie	Ellenburger		12,780		Myers (1969)	Single well test
5715701	Burnet	San Saba		16,844		Myers (1969)	Multi-well hydraulic test
Minimum				7	0.01		
Maximum				31,968	224.64		
Geometric Mean				495	2.81		
5606505	McCulloch	Hickory	0.10	15	0.03	calculated from well specific capacity test data obtained from TWDB (2014a)	Single well test
5743201	Gillespie	Hickory	0.21	37	0.16	calculated from well specific capacity test data obtained from TWDB (2014a)	Single well test
4255103	McCulloch	Hickory	0.42	95	0.27	calculated from well specific capacity test data obtained from TWDB (2014a)	Single well test
4142602	San Saba	Hickory	0.36	81	0.31	calculated from well specific capacity test data obtained from TWDB (2014a)	Single well test

Table A.2 Summary of aquifer transmissivity and horizontal hydraulic conductivity values for Cretaceous, Marble Falls, Ellenburger-San Saba, and Hickory aquifers in study area.

Well	County	Aquifer	Specific Capacity (gallon per minute per foot)	Transmissivity (square feet per day)	Horizontal Hydraulic Conductivity (feet per day)	Source	Note
5612210	McCulloch	Hickory	2.05	467	0.48	calculated from well specific capacity test data obtained from TWDB (2014a)	Single well test
4253201	McCulloch	Hickory	4.25	1,037	0.50	calculated from well specific capacity test data obtained from TWDB (2014a)	Single well test
5606708	Mason	Hickory	1.33	242	0.56	calculated from well specific capacity test data obtained from TWDB (2014a)	Single well test
5623304	McCulloch	Hickory	0.84	173	0.58	calculated from well specific capacity test data obtained from TWDB (2014a)	Single well test
4259301	Concho	Hickory	4.03	1,123	0.95	calculated from well specific capacity test data obtained from TWDB (2014a)	Single well test
5607211	McCulloch	Hickory	1.26	216	1.04	calculated from well specific capacity test data obtained from TWDB (2014a)	Single well test

Table A.2 Summary of aquifer transmissivity and horizontal hydraulic conductivity values for Cretaceous, Marble Falls, Ellenburger-San Saba, and Hickory aquifers in study area.

Well	County	Aquifer	Specific Capacity (gallon per minute per foot)	Transmissivity (square feet per day)	Horizontal Hydraulic Conductivity (feet per day)	Source	Note
5623303	McCulloch	Hickory	1.49	320	1.04	calculated from well specific capacity test data obtained from TWDB (2014a)	Single well test
5741702	Gillespie	Hickory	0.70	181	1.12	calculated from well specific capacity test data obtained from TWDB (2014a)	Single well test
5606940	Mason	Hickory	0.67	121	1.56	calculated from well specific capacity test data obtained from TWDB (2014a)	Single well test
4252504	McCulloch	Hickory	2.35	605	1.90	calculated from well specific capacity test data obtained from TWDB (2014a)	Single well test
4260901	McCulloch	Hickory	2.46	631	1.90	calculated from well specific capacity test data obtained from TWDB (2014a)	Single well test
5734403	Gillespie	Hickory	2.07	423	2.16	calculated from well specific capacity test data obtained from TWDB (2014a)	Single well test

Table A.2 Summary of aquifer transmissivity and horizontal hydraulic conductivity values for Cretaceous, Marble Falls, Ellenburger-San Saba, and Hickory aquifers in study area.

Well	County	Aquifer	Specific Capacity (gallon per minute per foot)	Transmissivity (square feet per day)	Horizontal Hydraulic Conductivity (feet per day)	Source	Note
5606660	Mason	Hickory	2.00	389	2.25	calculated from well specific capacity test data obtained from TWDB (2014a)	Single well test
4252702	McCulloch	Hickory	3.88	1,037	2.51	calculated from well specific capacity test data obtained from TWDB (2014a)	Single well test
4263815	McCulloch	Hickory	3.00	544	2.76	calculated from well specific capacity test data obtained from TWDB (2014a)	Single well test
310829992 030	McCulloch	Hickory		2,674	2.90	Myers (1969)	Multi-well hydraulic test
4254703	McCulloch	Hickory		2,527	2.94	Myers (1969)	Multi-well hydraulic test
310803992 032	McCulloch	Hickory		2,527	2.94	Myers (1969)	Recovery of obs. well
5742101	Gillespie	Hickory	3.27	778	3.02	calculated from well specific capacity test data obtained from TWDB (2014a)	Single well test
5623102	McCulloch	Hickory	2.86	734	3.20	calculated from well specific capacity test data obtained from TWDB	Single well test

Table A.2 Summary of aquifer transmissivity and horizontal hydraulic conductivity values for Cretaceous, Marble Falls, Ellenburger-San Saba, and Hickory aquifers in study area.

Well	County	Aquifer	Specific Capacity (gallon per minute per foot)	Transmissivity (square feet per day)	Horizontal Hydraulic Conductivity (feet per day)	Source	Note
						(2014a)	
5607207	McCulloch	Hickory	2.16	441	3.72	calculated from well specific capacity test data obtained from TWDB (2014a)	Single well test
4260902	McCulloch	Hickory	5.93	1,555	4.23	calculated from well specific capacity test data obtained from TWDB (2014a)	Single well test
4260603	McCulloch	Hickory	4.75	1,210	4.32	calculated from well specific capacity test data obtained from TWDB (2014a)	Single well test
310806992 031	McCulloch	Hickory	6.30	2,433	4.34	Myers (1969)	Single well test
5703217	Lampasas	Hickory	2.80	588	4.41	calculated from well specific capacity test data obtained from TWDB (2014a)	Single well test
4260503	McCulloch	Hickory	5.53	1,469	4.49	calculated from well specific capacity test data obtained from TWDB (2014a)	Single well test
4260502	McCulloch	Hickory	5.95	1,728	4.67	calculated from well specific capacity test	Single well test

Table A.2 Summary of aquifer transmissivity and horizontal hydraulic conductivity values for Cretaceous, Marble Falls, Ellenburger-San Saba, and Hickory aquifers in study area.

Well	County	Aquifer	Specific Capacity (gallon per minute per foot)	Transmissivity (square feet per day)	Horizontal Hydraulic Conductivity (feet per day)	Source	Note
						data obtained from TWDB (2014a)	
5606601	McCulloch	Hickory	15.25	3,802	4.84	calculated from well specific capacity test data obtained from TWDB (2014a)	Single well test
4260602	McCulloch	Hickory	7.28	1,901	5.01	calculated from well specific capacity test data obtained from TWDB (2014a)	Single well test
5613901	McCulloch	Hickory	8.63	1,987	5.01	calculated from well specific capacity test data obtained from TWDB (2014a)	Single well test
4254202	McCulloch	Hickory	3.86	1,037	5.10	calculated from well specific capacity test data obtained from TWDB (2014a)	Single well test
4261303	McCulloch	Hickory	6.85	1,814	5.44	calculated from well specific capacity test data obtained from TWDB (2014a)	Single well test
5607301	McCulloch	Hickory	2.80	622	5.53	calculated from well specific capacity test	Single well test

Table A.2 Summary of aquifer transmissivity and horizontal hydraulic conductivity values for Cretaceous, Marble Falls, Ellenburger-San Saba, and Hickory aquifers in study area.

Well	County	Aquifer	Specific Capacity (gallon per minute per foot)	Transmissivity (square feet per day)	Horizontal Hydraulic Conductivity (feet per day)	Source	Note
						data obtained from TWDB (2014a)	
5606908	Mason	Hickory	5.05	1,037	6.39	calculated from well specific capacity test data obtained from TWDB (2014a)	Single well test
5741301	Gillespie	Hickory	4.00	779	6.82	Myers (1969)	Single well test
5623121	McCulloch	Hickory	6.87	1,728	6.91	calculated from well specific capacity test data obtained from TWDB (2014a)	Single well test
4263916	McCulloch	Hickory	9.64	2,419	7.52	calculated from well specific capacity test data obtained from TWDB (2014a)	Single well test
5703409	Lampasas	Hickory	2.50	536	7.69	calculated from well specific capacity test data obtained from TWDB (2014a)	Single well test
5606905	Mason	Hickory	6.00	1,296	10.37	calculated from well specific capacity test data obtained from TWDB (2014a)	Single well test
5606601	McCulloch	Hickory	15.10	4,853	12.16	Myers (1969)	Recovery of pumped

Table A.2 Summary of aquifer transmissivity and horizontal hydraulic conductivity values for Cretaceous, Marble Falls, Ellenburger-San Saba, and Hickory aquifers in study area.

Well	County	Aquifer	Specific Capacity (gallon per minute per foot)	Transmissivity (square feet per day)	Horizontal Hydraulic Conductivity (feet per day)	Source	Note
							well
5741604	Gillespie	Hickory		668	13.64	Myers (1969)	Recovery of pumped well
4260401	Menard	Hickory	21.27	6,048	18.14	calculated from well specific capacity test data obtained from TWDB (2014a)	Single well test
5606901	Mason	Hickory	12.50	2,765	23.33	calculated from well specific capacity test data obtained from TWDB (2014a)	Single well test
5741306	Gillespie	Hickory	14.37	4,147	41.47	calculated from well specific capacity test data obtained from TWDB (2014a)	Single well test
5741613	Gillespie	Hickory	16.67	4,061	44.93	calculated from well specific capacity test data obtained from TWDB (2014a)	Single well test
5742104	Gillespie	Hickory	35.86	10,368	155.52	calculated from well specific capacity test data obtained from TWDB (2014a)	Single well test
5606605	Mason	Hickory	16.70	5,882		Myers (1969)	Multi-well hydraulic test

Table A.2 Summary of aquifer transmissivity and horizontal hydraulic conductivity values for Cretaceous, Marble Falls, Ellenburger-San Saba, and Hickory aquifers in study area.

Well	County	Aquifer	Specific Capacity (gallon per minute per foot)	Transmissivity (square feet per day)	Horizontal Hydraulic Conductivity (feet per day)	Source	Note
5613902	Mason	Hickory	8.66	1,778		Myers (1969)	Multi-well hydraulic test
4263801	McCulloch	Hickory		4,077		Myers (1969)	Recovery of pumped well
5607211	McCulloch	Hickory		4,786		Myers (1969)	Recovery of pumped well
5607301	McCulloch	Hickory	2.70	3,636		Myers (1969)	Recovery of pumped well
310801992 032	McCulloch	Hickory		1,965		Myers (1969)	Single well test
Minimum				15	0.03		
Maximum				10,368	155.52		
Geometric Mean				957	3.09		

Note: Additional information such as coordinates of wells can be found in the geodatabase.

Table A.3 Summary of aquifer storativity values from hydraulic tests.

Well	County	Aquifer	Storativity	Source	Comments
5741903	Gillespie	Cretaceous aquifers	0.0000008	Myers (1969)	Single well test
PW-1	Hays	Cretaceous aquifers	0.00001	Daniel B. Stephens & Associates, Inc. (2006)	Single well test
PW-1	Hays	Cretaceous aquifers	0.0000103	Daniel B. Stephens & Associates, Inc. (2006)	Multi-well hydraulic test
RMR Testwell	Hays	Cretaceous aquifers	0.000012	Daniel B. Stephens & Associates, Inc. (2006)	Multi-well hydraulic test
No. 1 Well	Hays	Cretaceous aquifers	0.000013	Daniel B. Stephens & Associates, Inc. (2006)	Multi-well hydraulic test
Lot 12	Gillespie	Cretaceous aquifers	0.000018	Daniel B. Stephens & Associates, Inc. (2006)	Multi-well hydraulic test
PW-1	Hays	Cretaceous aquifers	0.0000186	Daniel B. Stephens & Associates, Inc. (2006)	Multi-well hydraulic test
P, Lot 23	Hays	Cretaceous aquifers	0.00002	Daniel B. Stephens & Associates, Inc. (2006)	Multi-well hydraulic test
5663607	Kerr	Cretaceous aquifers	0.00002	Myers (1969)	Recharging well
No. 2 Well	Hays	Cretaceous aquifers	0.000025	Daniel B. Stephens & Associates, Inc. (2006)	Multi-well hydraulic test
5663901	Kerr	Cretaceous aquifers	0.00003	Myers (1969)	Multi-well hydraulic test
BT-3	Blanco	Cretaceous aquifers	0.0000388	Daniel B. Stephens & Associates, Inc. (2006)	Single well test
5761217	Blanco	Cretaceous aquifers	0.00004	Christian and Wuerch (2012)	Multi-well hydraulic test
Dunn TW-1	Hays	Cretaceous aquifers	0.00004	Daniel B. Stephens & Associates, Inc. (2006)	Multi-well hydraulic test
Sect. 2	Blanco	Cretaceous aquifers	0.00005	Daniel B. Stephens & Associates, Inc. (2006)	Multi-well hydraulic test
5724101	Burnet	Cretaceous aquifers	0.00005	Myers (1969)	Recovery test
PW-1	Hays	Cretaceous aquifers	0.00005	Daniel B. Stephens & Associates, Inc. (2006)	Multi-well hydraulic test
5663614	Kerr	Cretaceous aquifers	0.00005	Myers (1969)	Single well test
New Well	Hays	Cretaceous aquifers	0.00007	Daniel B. Stephens & Associates, Inc. (2006)	Multi-well hydraulic test
PW-1	Hays	Cretaceous aquifers	0.0000734	Daniel B. Stephens & Associates, Inc. (2006)	Multi-well hydraulic test
Sect. 3	Blanco	Cretaceous aquifers	0.000099	Daniel B. Stephens & Associates, Inc. (2006)	Multi-well hydraulic test
PW-4	Blanco/Hays	Cretaceous aquifers	0.0001	Daniel B. Stephens & Associates, Inc. (2006)	Multi-well hydraulic test
Test Well #1	Hays	Cretaceous aquifers	0.0001	Daniel B. Stephens & Associates, Inc. (2006)	Multi-well hydraulic test
West #5	Kendall	Cretaceous aquifers	0.00011	Daniel B. Stephens & Associates, Inc. (2006)	Multi-well hydraulic test

Table A.3 Summary of aquifer storativity values from hydraulic tests.

Well	County	Aquifer	Storativity	Source	Comments
PW-3	Gillespie	Cretaceous aquifers	0.000155	Daniel B. Stephens & Associates, Inc. (2006)	Multi-well hydraulic test
West #6	Kendall	Cretaceous aquifers	0.00018	Daniel B. Stephens & Associates, Inc. (2006)	Multi-well hydraulic test
Well #2	Kerr	Cretaceous aquifers	0.000189	Daniel B. Stephens & Associates, Inc. (2006)	Single well test
Horseshoe Bend	Kendall	Cretaceous aquifers	0.00024	Daniel B. Stephens & Associates, Inc. (2006)	Multi-well hydraulic test
TW-1	Hays	Cretaceous aquifers	0.00025	Daniel B. Stephens & Associates, Inc. (2006)	Multi-well hydraulic test
Waterstone #3	Kendall	Cretaceous aquifers	0.00025	Daniel B. Stephens & Associates, Inc. (2006)	Multi-well hydraulic test
Kreutzberg	Kendall	Cretaceous aquifers	0.00026	Daniel B. Stephens & Associates, Inc. (2006)	Multi-well hydraulic test
Well #1	Hays	Cretaceous aquifers	0.0003	Daniel B. Stephens & Associates, Inc. (2006)	Multi-well hydraulic test
Gas Line (Telephone Building)	Kendall	Cretaceous aquifers	0.00032	Daniel B. Stephens & Associates, Inc. (2006)	Multi-well hydraulic test
Well 1	Travis	Cretaceous aquifers	0.00038	Daniel B. Stephens & Associates, Inc. (2006)	Multi-well hydraulic test
5753614	Blanco	Cretaceous aquifers	0.0004	Christian and Wuerch (2012)	Multi-well hydraulic test
5763616	Blanco	Cretaceous aquifers	0.0006	Christian and Wuerch (2012)	Multi-well hydraulic test
5663906	Kerr	Cretaceous aquifers	0.0008	Christian and Wuerch (2012)	Multi-well hydraulic test
Well 3	Hays	Cretaceous aquifers	0.00095	Daniel B. Stephens & Associates, Inc. (2006)	Multi-well hydraulic test
PW-1	Blanco	Cretaceous aquifers	0.001	Daniel B. Stephens & Associates, Inc. (2006)	Multi-well hydraulic test
PW-2	Blanco	Cretaceous aquifers	0.001	Daniel B. Stephens & Associates, Inc. (2006)	Multi-well hydraulic test
PW-1	Hays	Cretaceous aquifers	0.001	Daniel B. Stephens & Associates, Inc. (2006)	Multi-well hydraulic test
West #9	Kendall	Cretaceous aquifers	0.0021	Daniel B. Stephens & Associates, Inc. (2006)	Multi-well hydraulic test
5663603	Kerr	Cretaceous aquifers	0.003	Myers (1969)	Single well test
PW2&3	Blanco/Hays	Cretaceous aquifers	0.004	Daniel B. Stephens & Associates, Inc. (2006)	Multi-well hydraulic test
PW-1/Well 5	Hays	Cretaceous aquifers	0.005	Daniel B. Stephens & Associates, Inc. (2006)	Multi-well hydraulic test
Well 1	Gillespie	Cretaceous aquifers	0.00784	Daniel B. Stephens & Associates, Inc. (2006)	Multi-well hydraulic test
Pumping Well	Hays	Cretaceous aquifers	0.008	Daniel B. Stephens & Associates, Inc. (2006)	Multi-well hydraulic test
CWR-2A	Gillespie	Cretaceous	0.041	Daniel B. Stephens &	Multi-well hydraulic test

Table A.3 Summary of aquifer storativity values from hydraulic tests.

Well	County	Aquifer	Storativity	Source	Comments
		aquifers		Associates, Inc. (2006)	
Well #1	Kerr	Cretaceous aquifers	0.055	Daniel B. Stephens & Associates, Inc. (2006)	Single well test
Minimum			0.000008		
Maximum			0.055		
Geometric Mean			0.00018		
2(P)	Blanco	Ellenburger-San Saba	0.00008	Daniel B. Stephens & Associates, Inc. (2006)	Multi-well hydraulic test
1-P	Blanco	Ellenburger-San Saba	0.00009	Daniel B. Stephens & Associates, Inc. (2006)	Multi-well hydraulic test
1A	Blanco	Ellenburger-San Saba	0.00014	Daniel B. Stephens & Associates, Inc. (2006)	Multi-well hydraulic test
2(P)	Blanco	Ellenburger-San Saba	0.0002	Daniel B. Stephens & Associates, Inc. (2006)	Multi-well hydraulic test
1(P)	Blanco	Ellenburger-San Saba	0.00027	Daniel B. Stephens & Associates, Inc. (2006)	Multi-well hydraulic test
3(P)	Blanco	Ellenburger-San Saba	0.0004	Daniel B. Stephens & Associates, Inc. (2006)	Multi-well hydraulic test
4A	Blanco	Ellenburger-San Saba	0.0017	Daniel B. Stephens & Associates, Inc. (2006)	Multi-well hydraulic test
Minimum			0.00008		
Maximum			0.0017		
Geometric Mean			0.00023		
5741604	Gillespie	Hickory	0.000037	Myers (1969)	Recovery test
Not Available	McCulloch	Hickory	0.00009	Myers (1969)	
4254703	McCulloch	Hickory	0.0001	Myers (1969)	Multi-well hydraulic test
Minimum			0.000037		
Maximum			0.0001		
Geometric Mean			0.000069		

Note: Additional information such as coordinates of wells can be found in the geodatabase.